



The Impact of Fluoride on the Corrosivity of Brackish Water on Mild Steel in Industrial Cooling Water Systems

**A thesis submitted in fulfilment of the requirements for the degree of
Doctor of Philosophy**

Prepared by

Alfonso Palazzo (702559)

Submitted to

School of Chemical and Metallurgical Engineering, Faculty of Engineering and
the Built Environment, University of the Witwatersrand, Johannesburg

Supervisors: Dr Josias van der Merwe, Greg A. Combrink

October 2015

DECLARATION

The experimental work described in this thesis was carried out in the various laboratories either owned or managed by Buckman Africa (Pty) Ltd, as well as in the School of Chemical and Metallurgical Engineering, Faculty of Engineering and the Built Environment, University of the Witwatersrand, Johannesburg, South Africa.

These studies represent original work by the author and have not been submitted in any form for any degree or diploma at any other University. Where use has been made of the work of others it, is duly acknowledged in the text.

A handwritten signature in black ink, appearing to be 'M. M. M.', is written over a horizontal dotted line.

.....19..... day of,.....October....., 2015.....

ABSTRACT

Ecological considerations compelled a steel mill in Southern Africa to pursue Zero Effluent Discharge which led to the use of substandard influent water to their open recirculating cooling systems. This resulted in severe corrosion of the mild steel equipment which impacted on the cost and risk of doing business. Extensive research has been done over the last century, particularly for potable water systems, to develop reliable mathematical models to predict the impact of various factors on corrosion. However, the application of these indices on the steel mill brackish cooling water proved unsatisfactory and all excluded the impact of fluoride.

The primary objectives of this thesis were to establish the individual and joint impacts of calcium carbonate saturation and the varying levels of the anions, particularly fluoride, at up to 90 mg/l, on the corrosion of mild steel at 45°C. Laboratory tests were performed with synthetic solutions, in accordance with ASTM methods, and on experimental design approaches. Laboratory and field data were used to construct several statistically sound and relatively accurate models and a set of hypothetical guidelines for the water chemistry parameters pertinent to fluoride-containing brackish water. SEM and EDS of the mild steel coupons confirmed the increase in uniform corrosion with increasing fluoride concentration and the tendency for micro-pitting corrosion.

An initial equation formulated solely on the calcium concentration and total alkalinity yielded superior correlation with field data than the indices produced by previous authors. It accounted for 90% of the variations in the laboratory data. Laboratory investigations into the impact of the chloride and sulphate ions indicated they differed from the indices developed for drinking water systems. The chloride ion actually decreased corrosion, similar to what was found with saline waters. The impact of the fluoride confirmed the work of previous authors performed under considerably different physical or chemical test conditions. A linear model based on fluoride, pH, calcium hardness and total alkalinity resulted in an R^2 (adj) of 88%. At above approximately 100 mg/l fluoride mild steel corrosion reached a plateau.

ACKNOWLEDGEMENTS

Firstly, I would like to thank God, Creator of the universe, abounding in wisdom and love.

I would like to give special thanks to my advisors, Dr Josias van der Merwe and Mr. Greg A. Combrink, for their guidance, insight and their confidence in me. I also want to thank the many employees of Buckman Africa (Pty) Ltd in particular: Mr. Peter Wheeler, for his advice, Mr. Frikkie van Heerden and Regardt Vreeswijk, for their assistance in terms of the field laboratory work, and Khensani Angel Ndlovu and Sabelo Sithole for their assistance in the Hammarsdale laboratory.

Finally, a huge thanks to Ornella, Cristina, Rosaria, and late dad Gaetano, as well as family and friends for their patience, care and support through the good and demanding times in these three years.

TABLE OF CONTENTS

DECLARATION	ii
ABSTRACT	iii
ACKNOWLEDGEMENTS	iv
TABLE OF CONTENTS	v
LIST OF FIGURES	ix
LIST OF TABLES	xviii
LIST OF ABBREVIATIONS AND SYMBOLS	xxiii
CHAPTER 1: INTRODUCTION	1
1.1 Background	1
1.2 Aims and Research Objectives.....	3
1.2.1 Aims.....	3
1.2.2 Hypothesis and research objectives.....	3
CHAPTER 2: LITERATURE REVIEW	5
2.1 Overview of the Iron and Steel Manufacturing Process	5
2.2 Water Use in the Iron and Steel Industry	7
2.3 Continuous Casting and its Specific Cooling Requirements	8
2.4 Types of Cooling Systems	10
2.4.1 Once through cooling systems	11
2.4.2 Closed recirculating cooling systems.....	11
2.4.3 Open recirculating cooling systems	12
2.5 Impact of High Salinity Cooling Water in Iron and Steel Mills	14
2.5.1 The use of brackish water or sea-water as cooling tower makeup	14
2.5.2 Striving for Zero Liquid Discharge (ZLD)	16
2.6 Two Cooling System Scenarios at a Southern African Steel Mill.....	16
2.6.1 System One.....	20
2.6.2 System Two	20
2.7 Corrosion Prediction	21
2.8 Impact of Fluoride.....	30
2.9 Summary of Factors Potentially Affecting Mild Steel Corrosion or Passivation	36
2.9.1 Temperature.....	36
2.9.2 Flow velocity.....	37

2.9.3	Oxygen.....	37
2.9.4	pH, calcium, carbonate, buffer capacity and humic substances.....	38
2.9.5	Magnesium.....	39
2.9.6	Chloride and sulphate	39
2.9.7	Fluoride.....	40
2.9.8	Conductivity.....	40
2.9.9	Suspended solids.....	40
2.9.10	Microbial population and the potential for Microbiologically Induced Corrosion (MIC)	41
2.9.11	Disinfectant residual.....	42
2.9.12	Heavy metals (e.g. dissolved copper).....	42
2.9.13	Corrosion inhibitors.....	42
CHAPTER 3: FIELD STUDIES.....		49
3.1	Introduction	49
3.2	Materials and Methods.....	49
3.3	Results.....	52
3.4	Discussion	70
CHAPTER 4: LABORATORY EXPERIMENTS		74
4.1	Introduction	74
4.2	Laboratories and Materials Common to the Laboratory Corrosion Tests	76
4.3	Methodology Common to the Laboratory Corrosion Tests	78
4.3.1	Water analyses	78
4.3.2	Test solution preparation.....	79
4.3.3	Corrosion set up	80
4.3.4	Monitoring during the corrosion test.....	80
4.3.5	Coupon cleaning and corrosion rate calculation.....	81
4.3.6	Minitab statistical software package	81
4.4	Experiments Performed According to Classical Design.....	82
4.4.1	Varying calcium hardness and total alkalinity.....	82
4.4.2	Impact of chloride in synthetic brackish water on mild steel	122
4.4.3	Impact of sulphate in synthetic brackish water on mild steel	128
4.4.4	Impact of fluoride in synthetic brackish water on mild steel.....	137
4.4.5	Impact of magnesium in synthetic brackish water on mild steel.....	152

4.5	Fractional Factorial Experiments	158
4.6	Evaluation of Corrosion Inhibitors	170
4.7	Regression Analysis of All the Laboratory Data	176
4.8	Extending the Investigation on Fluoride to beyond Brackish Water ...	183
4.8.1	Series 1 - Deionized water only	185
4.8.2	Series 2 - Low alkalinity	194
4.8.3	Series 3 - High alkalinity	203
4.8.4	Series 4 - Low calcium	211
4.8.5	Series 5 - High calcium.....	219
4.8.6	Series 6 - Low alkalinity and low calcium	225
4.8.7	Series 7 - High alkalinity and high calcium	231
4.8.8	Series 8 - Low alkalinity and low calcium with high chloride and high sulphate	241
4.8.9	Series 9 - High alkalinity and calcium with high chloride and high sulphate	247
4.8.10	Regression analysis of the laboratory data generated in section 4.8 (series 1-9)	254
4.9	Microscopic, Chemical and Electrochemical Studies into the Corrosive Effect of Fluoride on Mild Steel	267
4.9.1	Weight loss measurement of the effect of higher fluoride concentrations	268
4.9.2	Macroscopic appearance and low magnification light microscopy	274
4.9.3	Scanning electron microscopy and energy dispersive X-ray analysis	280
4.9.4	Electrochemical studies.....	293
CHAPTER 5: APPICATION OF THE MODELS TO PLANT CONDITIONS.		305
5.1	Open System One.....	305
5.2	Open System Two	306
CHAPTER 6: GENERAL DISCUSSION		316
6.1	Field Data	316
6.2	Laboratory Data	319
6.2.1	Synthetic brackish water experiments	319
6.2.2	Further experimentation with fluoride	328
6.2.3	Microscopic, chemical and electrochemical studies into the effect of fluoride on mild steel corrosion	329
6.2.4	Application of the models to plant conditions.....	331

CHAPTER 7: CONCLUSIONS	335
CHAPTER 8: RECOMMENDATIONS.....	342
REFERENCES.....	343
APPENDIX A: COOLING WATER CHEMISTRY FOR OPEN COOLING SYSTEM ONE FOR THE PERIOD 3 MARCH 2009 TO 25 MARCH 2011.....	355
APPENDIX B: COOLING WATER CHEMISTRY FOR OPEN COOLLING SYSTEM TWO FOR THE PERIOD 3 MARCH 2009 TO 25 MARCH 2011.....	365
APPENDIX C: CORROSION RATES FOR OPEN COOLING SYSTEM ONE AND TWO FOR THE PERIOD JUNE 2009 TO FEBRUARY 2011 ..	375
APPENDIX D: CALCULATED INDICES FOR THE OPEN SYSTEM ONE COOLING WATER CHEMISTRY FOR THE PERIOD MARCH 2009 to MARCH 2011	376
APPENDIX E: CALCULATED INDICES FOR THE OPEN SYSTEM TWO COOLING WATER CHEMISTRY FOR THE PERIOD JUNE 2009 to FEBRUARY 2011	380
APPENDIX F: MATHEMATICAL MODELS USED FOR PREDICTING THE CORROSION RATE OF MILD STEEL.....	383
APPENDIX G: MINITAB® RESULTS	392
Varying Calcium Hardness and Total Alkalinity.....	392
Varying calcium at the low range of alkalinities (Section 4.4.1).....	392
Varying calcium for the full range of total alkalinities (Section 4.4.2).....	402
Varying Chloride.....	404
Varying Sulphate.....	406
Varying Fluoride	408
Varying Magnesium.....	410
Factorial Design Experiments	411
APPENDIX H: COMPARISON OF OPEN SYSTEM ONE AND OPEN SYSTEM TWO COOLING WATER CHEMISTRY	412

LIST OF FIGURES

Figure 2-1: Process flow diagram of an integrated mill illustrating the production of molten iron followed immediately by steel production (Abt Associates <i>et al.</i> , 1995)	5
Figure 2-2: Steel making by either the BOF or EAF process (After Abt Associates <i>et al.</i> , 1995).....	6
Figure 2-3: Continuous casting cooling circuit (Flynn and Nalco Company, 2009).....	10
Figure 2-4: Once through cooling system (Buckman, 1981).....	11
Figure 2-5: Closed recirculating cooling system (Buckman, 1981)	12
Figure 2-6: Open recirculating cooling system (Buckman, 1981).....	13
Figure 2-7: Recirculating cooling system with cooling tower (Buckman, 1981)..	14
Figure 2-8: (Left) Corroded open system return pump due to salt deposits (Buckman, 2012b).....	19
Figure 2-9: (Right) Cooling tower gearboxes – one year in service (Buckman, 2012b).....	19
Figure 2-10: (Left) Evapco cooling towers, to be replaced with new cooling towers due to structural damage (Buckman, 2012b).....	19
Figure 2-11: (Right) Chemical attack on cooling towers showing spalling due to corrosion of the reinforcing bars (Buckman, 2012b)	19
Figure 2-12: Corroded cooling tower structure (Buckman, 2012b).....	19
Figure 2-13: Corroded sandfilters – total replacement of steel fabrication (Buckman, 2012b).....	20
Figure 3-1: Time series plot of Open System One and Open System Two monthly coupon corrosion rates (Buckman, 2012b)	56
Figure 3-2: Histograms of: a) Open System One monthly coupon corrosion rate and b) Open System Two monthly coupon corrosion rate.....	57
Figure 3-3: Scatterplot of Open System One versus Open System Two with regression line ($R^2 = 19\%$)	57
Figure 3-4: Scatterplots of Open System One coupon corrosion rates versus test parameters	59
Figure 3-5: Scatterplots of Open System Two coupon corrosion rates versus test parameters (Removed brushed value at July 2010: 1.11 mmpa and single high value outliers for : Ca, Fe and PO_4).....	60
Figure 3-6: Scatterplots of calculated indices versus the Open System One coupon corrosion data	61
Figure 3-7: Scatterplots of calculated indices versus the Open System Two coupon corrosion data with main outliers removed	62
Figure 4-1: Schematic diagram of Laboratory Scale and Corrosion Tester Station.....	76
Figure 4-2: Matrix plot of parameters while varying calcium and alkalinity at the low range of alkalinity levels at 35°C (Cubic model regression fit), showing the average corrosion rate versus the initial test solution parameters	90

Figure 4-3: Scatterplots of the average mild steel coupon corrosion rates versus pertinent final test solution parameters, at 35°C	91
Figure 4-4: Impact of increasing calcium hardness and decreasing total alkalinity on mild steel corrosion at 35°C (with 5% error bars on the calcium and alkalinity and ± 0.04 mmpa error bars on the corrosion rate)	93
Figure 4-5: Matrix plot of parameters while varying calcium and alkalinity at the low range of alkalinity levels at 45°C (Cubic model regression)	94
Figure 4-6: Regression analysis for the average coupon corrosion rate versus the final test solution total alkalinity at 45°C	97
Figure 4-7: Comparison of mild steel coupon data for the two temperatures (35°C versus 45°C) at the same target calcium hardnesses and similar low range of alkalinities (with ± 0.04 mmpa error bars on the corrosion rate)	98
Figure 4-8: Minitab® contour plot showing the correlation of initial calcium hardness and initial low alkalinity on mild steel coupon corrosion at 45°C	99
Figure 4-9: Minitab® report on the 2-sample t test for the mean of the coupon 1 results and coupon 2 results for 35°C	107
Figure 4-10: Minitab® report on the 2-sample t test for the mean of the coupon 1 results and coupon 2 results for 45°C	107
Figure 4-11: Comparison of mild steel coupon data for the two temperatures (35°C versus 45°C) at the same calcium hardnesses and the similar range of alkalinities (with ± 0.04 mmpa error bars on the corrosion rate)	108
Figure 4-12: Scatterplots of the average mild steel coupon corrosion rates versus pertinent parameters at 35°C (excluding outlier of results for run 60 with low pH)	109
Figure 4-13: Scatterplots of the average mild steel coupon corrosion rates versus pertinent parameters at 45°C	110
Figure 4-14: (Left) Correlation of initial calcium hardness and initial total alkalinity on mild steel coupon corrosion at 35°C	111
Figure 4-15: (Right) Correlation of final calcium hardness and final total alkalinity on mild steel coupon corrosion at 35°C	111
Figure 4-16: (Left) Correlation of initial calcium hardness and initial total alkalinity on mild steel coupon corrosion at 45°C	112
Figure 4-17: (Right) Correlation of final calcium hardness and final total alkalinity on mild steel coupon corrosion at 45°C	112
Figure 4-18: Regression analysis for the derived non-linear regression equation versus the average corrosion rate (Avg coup)	114
Figure 4-19: Scatterplot correlations of the calculated corrosion rate based on the non-linear regression equation versus the established indices	116
Figure 4-20: (Left) Results of the multivariate non-linear equation versus the targeted calcium (Ca) and total alkalinity concentrations (TOT Alk (SGO))	117
Figure 4-21: (Right) Results of the C4 model (Pisigan and Singley, 1984) versus the targeted calcium (Ca) and total alkalinity concentrations (TOT Alk (SGO))	117

Figure 4-22: (Left) Results of the Oddo and Tomson model (Oddo and Tomson, 1982) versus the targeted calcium (Ca) and total alkalinity concentrations (TOT Alk (SGO))	117
Figure 4-23: (Right) Results of the Stiff and Davis Index (Stiff and Davis, 1952) versus the targeted calcium (Ca) and total alkalinity concentrations (TOT Alk (SGO)).....	117
Figure 4-24: (Left) Results of the Langelier Saturation Index (Langelier, 1936) versus the targeted calcium (Ca) and total alkalinity concentrations (TOT Alk (SGO)).....	118
Figure 4-25: (Right) Results of the Ryznar Stability Index (Ryznar, 1944) versus the targeted calcium (Ca) and total alkalinity concentrations (TOT Alk (SGO)).....	118
Figure 4-26: (Left) Results of the Practical Scaling Index (Puckorius and Brooke, 1990) versus the targeted calcium (Ca) and total alkalinity concentrations (TOT Alk (SGO))	118
Figure 4-27: (Right) Results of the Larson Skold Index ((Larson and Skold, 1957) versus the targeted calcium (Ca) and total alkalinity concentrations (TOT Alk (SGO)).....	118
Figure 4-28: Average mild steel corrosion rate (Avg Coup), average initial chloride (Cl(i)) and average initial conductivity (Cond(i)) versus the target chloride concentration (Tgt Cl), at 45°C. Error bars: $\pm 0.05\text{mmpa}$, $\pm 50\text{ mg/l Cl}$ and $209\mu\text{S/cm}$	126
Figure 4-29: Scatterplot of average corrosion rates in mmpa (Avg Coup) versus initial chloride concentrations in mg/l as Cl^- (Cl(i)), at 45°C	127
Figure 4-30: Average mild steel corrosion rate (Avg Coup), average initial sulphate ($\text{SO}_4(\text{i})$) and average initial conductivity (Cl(i)) versus the target sulphate concentration (Tgt SO_4), at 45°C. Error bars: $\pm 0.04\text{mmpa}$, $\pm 83\text{ mg/l SO}_4$ and $101\mu\text{S/cm}$	134
Figure 4-31: Fitted line for the correlation between the average coupon corrosion rate in mmpa (Avg coup) versus the initial sulphate concentration in mg/l SO_4^{2-} ($\text{SO}_4(\text{i})$)	135
Figure 4-32: Average mild steel corrosion rate (Avg Coup), average initial calcium (Ca(i)) and average initial fluoride (F(i)) versus the target fluoride concentration (Tgt F), at 45°C, with trend lines. Error bars: $\pm 0.03\text{mmpa}$, $\pm 8.6\text{ mg/l Ca}$, and $\pm 2.4\text{ mg/l F}$	145
Figure 4-33: Scatterplots of parameters with varying initial fluoride concentration (F(i)), including best fit cubic regression lines	146
Figure 4-34: Regression analysis for the initial fluoride concentration versus the target fluoride concentration, where the quadratic model provided the closest fit	148
Figure 4-35: Regression analysis for the average coupon corrosion rate versus the test solution initial fluoride concentration, where both the linear and quadratic models were statistically significant with the linear model providing the closest fit	149
Figure 4-36: Main effects plots for the average corrosion rate demonstrating the individual impacts of the: initial pH (pH(i)), initial calcium concentration in mg/l Ca^{2+} (Ca(i)), initial total alkalinity (T alk (i))	

and initial fluoride concentration in mg/l F ⁻ (F(i)) on the resulting average corrosion rate in mmpa (Avg Coup)	150
Figure 4-37: Mild steel corrosion rate and initial magnesium concentration versus the target magnesium concentration, at 45°C. Error bars: ± 0.05mmpa.....	156
Figure 4-38: Regression analysis for the individual coupon corrosion rates versus the test solution initial magnesium concentration.	157
Figure 4-39: Scatterplots of the average corrosion rate versus various parameters measured at the commencement of the corrosion tests at 45°C.....	165
Figure 4-40: Scatterplots of parameters comparing the test initial value against the test final value at 45°C	166
Figure 4-41: Multiple regression for the average corrosion rate versus the parameters with the highest correlations demonstrating the values corresponding to the lowest corrosion rate	167
Figure 4-42: Interaction plot demonstrating the effects of the initial chloride (Cl(i)) and initial sulphate concentration (SO ₄ (i)) on the average corrosion rate (Avg Coup).....	168
Figure 4-43: Scatterplot of the calculated corrosion rate versus the average corrosion rate (R-Sq = 70.9% R-Sq(adj) = 38.2%)	169
Figure 4-44: Corrosion inhibition tests with error bars at 5% of the mean.....	175
Figure 4-45: 2-Sample t test report to ascertain the impact of temperature on the coupon corrosion rates	178
Figure 4-46: Scatterplot comparison of the initial and final parameters to examine the change in water chemistry as a result of corrosion	179
Figure 4-47: Scatterplots of the average corrosion rate versus various parameters measured at the commencement of the corrosion tests ..	180
Figure 4-48: Mild steel corrosion rate versus the initial chloride concentration for the various fluoride concentration ranges at 45°C. Error bars: ± 0.03mmpa.....	181
Figure 4-49: Average initial pH (pH(i)) and average initial total alkalinity (T alk(i)) versus the target fluoride concentration (Tgt F), at 45°C. Error bars: ± 0.23 pH and ± 3.13 mg/l CaCO ₃	190
Figure 4-50: Average mild steel corrosion rate (Avg Coup) and average initial fluoride (F(i)) versus the target fluoride concentration (Tgt F), at 45°C. Error bars: ± 0.04 mmpa and ± 2.5 mg/l F.....	191
Figure 4-51: Average initial calcium (Ca(i)) and average initial conductivity (Cond(i)) versus the target fluoride concentration (Tgt F), at 45°C. Error bars: ± 0.60 mg/l Ca ²⁺ and ± 9 µS/cm	192
Figure 4-52: Interaction plot demonstrating the effects of the initial calcium (Ca(i)) and initial magnesium (Mg(i)) and initial fluoride (F(i)) on the average corrosion rate (Avg Coup)	193
Figure 4-53: Scatterplots of the key variables versus the initial fluoride concentration (F(i)) at a total alkalinity of 55 mg/l as CaCO ₃	199
Figure 4-54: Regression summary report of the average corrosion rate (Avg coup) versus the initial fluoride concentration (F(i)) for a total alkalinity of 55 mg/l as CaCO ₃	200

Figure 4-55: Scatterplots of the key variables versus the initial fluoride concentration (F(i)) at a total alkalinity of 220 mg/l as CaCO_3 . The triangles represent a high pH data set.....	208
Figure 4-56: Regression for the average corrosion rate (Avg coup) versus the initial fluoride concentration (F(i)) at a total alkalinity of 220 mg/l as CaCO_3 (all three data sets).....	209
Figure 4-57: Repeat scatterplots of the key variables versus the initial fluoride concentration (F(i)) at a total alkalinity of 220 mg/l as CaCO_3 for data with pH values < 9	210
Figure 4-58: Scatterplots of the key variables versus the initial fluoride concentration (F(i)) at a calcium hardness of 50 mg/l as Ca^{2+}	216
Figure 4-59: Regression for the average coupon (Avg coup) versus the initial fluoride concentration (F(i)) at a calcium hardness of 50 mg/l as Ca^{2+}	217
Figure 4-60: Regression for the average coupon (Avg coup) versus the initial pH(i) at a calcium hardness of 50 mg/l as Ca^{2+}	218
Figure 4-61: Scatterplots of the key variables versus the initial fluoride concentration (F(i)) at a calcium hardness of 120 mg/l as Ca^{2+}	223
Figure 4-62: Scatterplot of initial fluoride (F(i)), initial calcium (Ca(i)) and initial total alkalinity (M alk(i)) versus target fluoride (Tgt F)(also indicated on graph as line without markers)	224
Figure 4-63: Scatterplots of the key variables versus the initial fluoride concentration (F(i)) at a calcium hardness of 50 mg/l as Ca^{2+} and a total alkalinity of 55 mg/l as CaCO_3	229
Figure 4-64: Incremental impact bar graph of variables on corrosion rate of steel for calcium at 50 mg/l as Ca^{2+} and total alkalinity at 55 mg/l as CaCO_3	230
Figure 4-65: Scatterplots of the key variables versus the initial fluoride concentration (F(i)) at a calcium hardness of 120 mg/l as Ca^{2+} and a total alkalinity of 220 mg/l as CaCO_3	236
Figure 4-66: Scatterplots of the average corrosion rate (Avg coup) versus the key variables at a calcium hardness of 120 mg/l as Ca^{2+} and a total alkalinity of 220 mg/l as CaCO_3	237
Figure 4-67: Regression for average corrosion rate (Avg coup) versus the initial sodium concentration (Na(i))	238
Figure 4-68: Scatterplots of the key variables versus the target fluoride concentration (Tgt F) at a calcium hardness of 120 mg/l as Ca^{2+} and a total alkalinity of 220 mg/l as CaCO_3	239
Figure 4-69: Scatterplots of the key variables versus the initial fluoride concentration (F(i)) at a calcium hardness of 50 mg/l as Ca^{2+} , total alkalinity of 55 mg/l as CaCO_3 , initial chloride concentration of 1000 mg/l as Cl^- and initial sulphate concentration of 1500 mg/l as SO_4^{2-}	245
Figure 4-70: Fitted line plot for the average corrosion rate (Avg coup) versus the initial fluoride concentration (F(i)) at a calcium hardness of 50 mg/l as Ca^{2+} , total alkalinity of 55 mg/l as CaCO_3 , initial chloride concentration of 1000 mg/l as Cl^- and initial sulphate concentration of 1500 mg/l as SO_4^{2-}	246

Figure 4-71: First matrix plot of the key variables at a calcium hardness of 120 mg/l as Ca^{2+} , total alkalinity of 220 mg/l as CaCO_3 , initial chloride concentration of 1000 mg/l as Cl^- and initial sulphate concentration of 1500 mg/l as SO_4^{2-}	252
Figure 4-72: Second matrix plot of the key variables at a calcium hardness of 120 mg/l as Ca^{2+} , total alkalinity of 220 mg/l as CaCO_3 , initial chloride concentration of 1000 mg/l as Cl^- and initial sulphate concentration of 1500 mg/l as SO_4^{2-}	252
Figure 4-73: Photographs of test solutions illustrating larger volumes of precipitate (calcium fluoride and corrosion products) with increasing fluoride addition (scale bar: 100 mm)	253
Figure 4-74: Scatterplots of average corrosion rate (Avg coup) in mmpa versus the various parameters at the start-up of the corrosion tests indicating the corresponding clusters	259
Figure 4-75: Box plot of the average corrosion rate (Avg coup) for the different series	260
Figure 4-76: Individual value plot of the average corrosion rate (Avg coup) versus the target fluoride concentration (Tgt F) for the series	261
Figure 4-77: Individual value plot of the average corrosion rate (Avg coup) versus the initial fluoride concentration (F(i)) for the series	261
Figure 4-78: Box plot of the initial pH (pH(i)) for the different series	262
Figure 4-79: Box plot of the initial calcium (Ca^{2+} (i)) for the different series	262
Figure 4-80: Box plot of the initial total alkalinity (M Alk(i)) for the different series	263
Figure 4-81: Box plot of the initial fluoride (F^- (i)) for the different series	263
Figure 4-82: Box plot of the initial conductivity (Cond(i)) for the different series	264
Figure 4-83: Box plot of the initial sodium (Na^+ (i)) for the different series	264
Figure 4-84: Initial calcium (Ca (i)), initial total alkalinity (Talk (i)), initial fluoride (F (i)) and the final turbidity (Turb(f)) versus the target fluoride concentration. Error bars: ± 4.2 Ca mg/l, ± 4.3 mg/l CaCO_3 , ± 1.2 NTU and ± 3.4 mg/l	271
Figure 4-85: Final total iron concentration (Fe (f)) and average coupon corrosion rate (mmpa) versus the target fluoride concentration. Error bars: ± 0.8 mg/l Fe and ± 0.06 mmpa	272
Figure 4-86: Initial pH (pH(i)) and average coupon corrosion rate (mmpa) versus the target fluoride concentration. Error bars: ± 0.07 pH and ± 0.06 mmpa	273
Figure 4-87: Photograph of cleaned mild steel corrosion coupons removed after a 3 day corrosion test performed at 45°C at varying fluoride concentrations in a solution containing 50 mg/l Ca^{2+} and a total alkalinity of 55 mg/l CaCO_3 (scale bar: 1.27 cm)	275
Figure 4-88: Photograph of coupon 1 (0 mg/l F^-) showing: a) dark apparently unaffected areas, b) uniformly corroded zones and c) “calcium deposit” as indicated by EDS (scale bar: 1.27 cm)	275
Figure 4-89: Macrograph of coupon 1 (0 mg/l F^-) showing: a) Shiny etched zones neighbouring b) the darker less corroded zones on coupon 1 (0 mg/l F^-) (scale bar: 1 mm)	276

Figure 4-90: Macrograph of coupon 1 (0 mg/l F ⁻) showing calcium carbonate crystals deposited on the tip of the coupon (i.e. zone c). Up to 30% of the coupon was covered in crystals (scale bar: 1mm).....	276
Figure 4-91: Photograph of coupon 2 (70 mg/l F ⁻) showing a mostly darkened surface with a small number of corroded areas at the edges of the coupon	277
Figure 4-92: Macrograph of coupon 2 (70 mg/l F ⁻) showing uniform corrosion zones along edge of coupon (scale bar: 1.mm)	277
Figure 4-93: Photograph of coupon 3 (100 mg/l F ⁻) with up to 45% of the surface showing zones of shallow uniform corrosion (scale bar: 1.27 cm)...	278
Figure 4-94: Macrograph of coupon 3 (100 mg/l F ⁻) showing shallow corroded zones of coupon (scale bar: 1mm).....	278
Figure 4-95: Photograph of coupon 4 (130 mg/l F ⁻) with approximately 75% uniform corrosion (scale bar: 1.27 cm)	278
Figure 4-96: Macrograph of coupon 4 (130 mg/l F ⁻) showing larger shallow corroded zones relative to the previous coupons (scale bar: 1 mm) .	279
Figure 4-97: Photograph of coupon 5 (160 mg/l F ⁻) also with approximately 75% uniform corrosion (scale bar: 1.27 cm)	279
Figure 4-98: Macrograph of coupon 5 (160 mg/l F ⁻) showing larger shallow corroded areas similar in appearance to coupon 4 (scale bar: 1 mm)	279
Figure 4-99: Photograph of coupon 6 (200 mg/l F ⁻) with approximately 50% uniform corrosion (scale bar: 1.27 cm)	280
Figure 4-100: Macrograph of coupon 6 (200 mg/l F ⁻) showing large shallow corroded areas (scale bar: 1 mm)	280
Figure 4-101: SEM image of coupon 1, spots 1-3, showing crystalline material and the areas analysed	284
Figure 4-102: SEM image of coupon 2, spots 3-5, showing a flaky particle and the areas analysed.....	284
Figure 4-103: SEM image of coupon 3, showing a crystal amongst heterogeneous material and the areas analysed , spots 7 and 8.....	285
Figure 4-104: SEM image of coupon 3, showing a small rosette aggregate and the areas analysed, spots 9-12	285
Figure 4-105: Elemental maps of the area shown in Figure 4-104 of coupon 3, calcium(blue) and fluorine (green), spots 9-12	286
Figure 4-106: SEM image of coupon 6, showing small crystals and the crystal analysed, spot 13	286
Figure 4-107: Elemental maps of the area shown in Figure 4-106 of coupon 6, spot 13, calcium(blue) and fluorine (green)	287
Figure 4-108: SEM of coupon 6, showing crystals high in calcium and fluorine, spots 14 and 15	287
Figure 4-109: SEM image of coupon 6, spot 16 “spectrum 3” showing a flaky particle without calcium and fluorine.....	288
Figure 4-110: Scanning electron micrograph of cleaned coupon 1 showing adherent and dense calcareous surface deposit surrounded by iron oxide/s and the areas analysed, spots 17-19	290

Figure 4-111: SEM image of cleaned coupon 2, showing a dark area covered in corrosion product adjacent to a shiny etched surface and the areas analysed, spots 20-22	290
Figure 4-112: SEM image of cleaned coupon 2, spectrum showing numerous micro-pitting in an area that exhibited uniform corrosion, spot 22...	291
Figure 4-113: SEM image of cleaned coupon 4 (Figures 4-95 and 4-96), showing numerous micro-pitting in an area that exhibited uniform corrosion, as apparent by the irregular surface morphology	291
Figure 4-114: SEM images of coupon 5, (Figures 4-97 and 4-98) showing areas of uniformly corroded areas adjacent to a darker area with corrosion product and the areas analysed, spots 23 and 24.....	292
Figure 4-115: SEM image of coupon 6, showing numerous micro-pitting in an area that also appeared macroscopically as uniform corrosion (Figures 4-99 and 4-100)	292
Figure 4-116: SEM image of coupon 6, showing higher magnification of micro pits in an area which exhibited uniform corrosion.....	293
Figure 4-117: Schematic diagram of heated and unaerated three electrode test cell	295
Figure 4-118: Tafel plot of test 1a (0 mg/l F ⁻)	295
Figure 4-119: Tafel plot of test 1b (0 mg/l F ⁻)	296
Figure 4-120: Tafel plot of test 2a (20 mg/l F ⁻)	297
Figure 4-121: Tafel plot of test 2b (20 mg/l F ⁻)	297
Figure 4-122: Tafel plot of test 3a (40 mg/l F ⁻)	297
Figure 4-123: Tafel plot of test 3b (40 mg/l F ⁻)	298
Figure 4-124: Tafel plot of test 4a (60 mg/l F ⁻)	298
Figure 4-125: Tafel plot of test 4b (60 mg/l F ⁻)	298
Figure 4-126: Tafel plot of test 5a (80 mg/l F ⁻)	299
Figure 4-127: Tafel plot of test 5b (80 mg/l F ⁻)	299
Figure 4-128: Tafel plot of test 6a (100 mg/l F ⁻)	299
Figure 4-129: Tafel plot of test 6b (100 mg/l F ⁻)	300
Figure 4-130: Scatterplots of potentiodynamic data versus the actual fluoride concentration	302
Figure 5-1: Scatterplot comparison of the calculated mild steel corrosion rate (mmpa), based on the BWM and the Open System One water chemistry, versus the measured plant Open System One mild steel coupon corrosion rates (mmpa).....	306
Figure 5-2: Time series plots of the mild steel corrosion rates predicted for CWS 2, based on the new model (i.e. BWM) and CWS2 water chemistry, versus the plant CWS 2 mild steel corrosion rates.....	308
Figure 5-3: Multiple regression for Open System Two showing the fluoride-New Model (i.e. BWM) interaction plot and the effect of the individual variables	311
Figure 5-4: Multiple regression for Open System Two showing the phosphate-total alkalinity interaction plot and the effect of the individual variables	313
Figure H-1: Open System One versus Open System Two - pH comparison showing a relatively low pH for Open System One for February 2010.....	412

Figure H-2: Open System One versus Open System Two – Conductivity comparison showing spikes for June and May 2010 for Open System One and two respectively	413
Figure H-3: Open System One versus Open System Two – Calcium comparison	413
Figure H-4: Open System One versus Open System Two – Total alkalinity comparison showing depressions in the Open System One alkalinity in January and February 2010 and a peak in December 2010.....	414
Figure H-5: Open System One versus Open System Two – Sodium comparison showing spikes for June and May 2010 for Open System One and two respectively.....	414
Figure H-6: Open System One versus Open System Two – Magnesium comparison showing a spike for May 2010 for Open System Two ..	415
Figure H-7: Open System One versus Open System Two – Iron comparison showing a spike for March 2010 Open System Two	415
Figure H-8: Open System One versus Open System Two – Iron phosphate comparison showing generally higher levels for Open System One	416
Figure H-9: Open System One versus Open System Two – Fluoride comparison showing generally higher levels for Open System One from November 2009	416
Figure H-10: Open System One versus Open System Two – Chloride comparison showing spikes for June and May 2010 for Open System One and two respectively.....	417
Figure H-11: Open System One versus Open System Two – Sulphate comparison showing spikes for June and May 2010 for Open System One and two respectively.....	417
Figure H-12: Open System One versus Open System Two – Oil comparison showing a spike for June 2010 Open System Two	418

LIST OF TABLES

Table 2-1: Water usage rates by steel making processes (Flynn and Nalco Company, 2009)	8
Table 2-2: Advantages and disadvantages of zero liquid discharge (Makini, 2005).....	16
Table 2-3: Estimated capital expenses incurred to repair cooling systems (Buckman, 2012b).....	17
Table 2-4: Estimated increase in annual costs to maintain the cooling systems (Buckman, 2012b).....	18
Table 2-5: Parameters considered in scale or corrosion prediction indices	44
Table 2-6: Standard corrosion inhibitors used in cooling systems (referenced mostly from: Buckman, 1981; Flynn and Nalco Company, 2009 and Frayne, 1999)	47
Table 3-1: Laboratory A equipment and software	50
Table 3-2: Statistical analysis of the cooling water chemistry from Open System One for the period June 2009 to February 2011 (Buckman, 2012b)...	54
Table 3-3: Statistical analysis of cooling water chemistry for Open System Two for the period June 2009 to February 2011 (Buckman, 2012b)	55
Table 3-4: Statistical analysis of the open system mild steel coupon corrosion rates (in mmpa) for the period June 2009 to February 2011	56
Table 3-5: Pearson correlations and p values for the Open System One coupon corrosion rate versus the calculated indices (Appendix D).....	63
Table 3-6: Pearson correlations and p values for the Open System Two coupon corrosion rate versus the calculated indices (Appendix D).....	65
Table 3-7: Minitab [®] regression analysis for Open System One	68
Table 3-8: Minitab [®] regression for Open System Two.....	69
Table 4-1: Ranges of water chemistry parameters investigated.....	75
Table 4-2: Ranges of other priority species	75
Table 4-3: Facilities and equipment utilized.....	76
Table 4-4: Laboratory equipment at Laboratory A and Laboratory C.....	77
Table 4-5: Laboratory reagents and consumables.....	78
Table 4-6: Varying calcium and alkalinity at the low range of alkalinity levels- Target and start-up concentrations	84
Table 4-7: Varying calcium and alkalinity at the low range of alkalinity levels- Cessation concentrations	86
Table 4-8: Corrosion coupon and Corratel [®] readings while varying calcium and alkalinity at the low range of alkalinity levels	88
Table 4-9: Statistically significant relationships between various parameters in the 35°C corrosion test	92
Table 4-10: Statistically significant relationships between various parameters in the 45°C corrosion test	95
Table 4-11: Varying calcium and alkalinity at the system equivalent alkalinity range- Target and start-up concentrations	102
Table 4-12: Varying calcium and alkalinity at the system equivalent alkalinity range- Cessation concentrations.....	104

Table 4-13: Corrosion coupon and Corrater [®] readings while varying calcium and alkalinity at the system equivalent alkalinity range	106
Table 4-14: Statistically significant relationships between the average coupon corrosion rate and various parameters in the 35°C and 45°C corrosion tests.....	111
Table 4-15: Regression analysis report for variables correlating with the mild steel coupon corrosion rates at 35°C and 45°C	112
Table 4-16: Statistically significant relationships between the calculated rate and the other indices	115
Table 4-17: Summary of the statistically significant correlations between the calculated corrosion rate and the established indices.....	115
Table 4-18: Varying the chloride concentration and temperature while holding the other variables constant- Target and start-up concentrations.....	123
Table 4-19: Varying the chloride concentration and temperature while holding the other variables constant- Cessation concentrations.....	124
Table 4-20: Corrosion coupon and Corrater [®] readings while varying the chloride concentration	125
Table 4-21: Statistically significant relationships between the average coupon corrosion rate and various parameters while varying the chloride concentration	127
Table 4-22: Varying the sulphate concentration and temperature while holding the other variables constant- Target and start-up concentrations.....	129
Table 4-23: Varying the sulphate concentration and temperature while holding the other variables constant- Cessation concentrations.....	131
Table 4-24: Corrosion coupon and Corrater [®] readings while varying the sulphate concentration	133
Table 4-25: Statistically significant relationships between the average coupon corrosion rate and various parameters while varying the sulphate concentration	136
Table 4-26: Varying the fluoride concentration and temperature while holding the other variables constant- Target and start-up concentrations.....	138
Table 4-27: Varying the fluoride concentration and temperature while holding the other variables constant- Cessation concentrations.....	140
Table 4-28: Corrosion coupon and Corrater [®] readings while varying the fluoride concentration	143
Table 4-29: Statistically significant linear relationships between various parameters while varying the fluoride concentration.....	147
Table 4-30: Varying the magnesium concentration and temperature while holding the other variables constant- Target and start-up concentrations.....	153
Table 4-31: Varying the magnesium concentration and temperature while holding the other variables constant- Cessation concentrations.....	154
Table 4-32: Corrosion coupon and Corrater [®] readings while varying the magnesium concentration.....	155
Table 4-33: Statistically significant relationships between the average corrosion rate and various parameters while varying the magnesium concentration	157
Table 4-34: Laboratory reagents	159
Table 4-35: Factorial design experiment at 45°C - Target concentrations.....	160

Table 4-36: Test solution concentrations for factorial design experiment at 45°C - A	162
Table 4-37: Test solution concentrations for factorial design experiment at 45°C - B	163
Table 4-38: Factorial design experiment at 45°C – Coupon and Corrat [®] results	164
Table 4-39: Regression analysis report for variables correlating with the average mild steel coupon corrosion rate according to the factorial design...	168
Table 4-40: Corrosion inhibition tests at 45°C- Target concentrations	170
Table 4-41: Corrosion inhibitors tested	171
Table 4-42: Corrosion inhibition tests at 45°C - Start-up concentrations.....	172
Table 4-43: Corrosion inhibition tests at 45°C – Cessation concentrations	173
Table 4-44: Corrosion inhibition tests at 45°C – Coupon and Corrat [®] results .	174
Table 4-45: Test series to investigate the corrosivity of fluoride on mild steel...	184
Table 4-46: Corrosion tests varying fluoride in deionized water at 45°C – Target and start-up concentrations.....	187
Table 4-47: Corrosion tests varying fluoride in deionized water at 45°C– Cessation concentrations	188
Table 4-48: Corrosion coupon results while varying the fluoride concentration in deionized water	189
Table 4-49: Corrosion tests varying fluoride in low alkalinity water at 45°C – Target and start-up concentrations	196
Table 4-50: Corrosion tests varying fluoride in low alkalinity water at 45°C – Cessation concentrations	197
Table 4-51: Corrosion coupon readings while varying fluoride in low alkalinity water at 45°C.....	198
Table 4-52: Corrosion tests varying fluoride in high alkalinity water at 45°C – Target and start-up concentrations	205
Table 4-53: Corrosion tests varying fluoride in low alkalinity water at 45°C – Cessation concentrations	206
Table 4-54: Corrosion coupon readings while varying fluoride in high alkalinity water at 45°C.....	207
Table 4-55: Corrosion tests varying fluoride in low calcium water at 45°C – Target and start-up concentrations	213
Table 4-56: Corrosion tests varying fluoride in low calcium water at 45°C – Cessation concentrations	214
Table 4-57: Corrosion coupon readings while varying fluoride in low calcium water at 45°C.....	215
Table 4-58: Corrosion tests varying fluoride in high calcium water at 45°C – Target and start-up concentrations	220
Table 4-59: Corrosion tests varying fluoride in high calcium water at 45°C – Cessation concentrations	221
Table 4-60: Corrosion coupon readings while varying fluoride in high calcium water at 45°C	222
Table 4-61: Corrosion tests varying fluoride in low calcium and alkalinity water at 45°C – Target and start-up concentrations.....	226
Table 4-62: Corrosion tests varying fluoride in low calcium and alkalinity water at 45°C – Cessation concentrations.....	227

Table 4-63: Corrosion coupon readings while varying fluoride in low calcium and alkalinity water at 45°C	228
Table 4-64: Corrosion tests varying fluoride in high calcium and alkalinity water at 45°C – Target and start-up concentrations	233
Table 4-65: Corrosion tests varying fluoride in high calcium and alkalinity water at 45°C – Cessation concentrations	234
Table 4-66: Corrosion coupon readings while varying fluoride in high calcium and alkalinity water at 45°C	235
Table 4-67: Corrosion tests varying fluoride in low calcium and alkalinity water with high chloride and sulphate concentrations at 45°C – Target and start-up concentrations	242
Table 4-68: Corrosion tests varying fluoride in low calcium and alkalinity water with high chloride and sulphate concentrations at 45°C – Cessation concentrations.....	243
Table 4-69: Corrosion coupon readings while varying fluoride in low calcium and alkalinity water with high chloride and sulphate concentrations at 45°C.....	244
Table 4-70: Corrosion tests varying fluoride in high calcium and alkalinity water with high chloride and sulphate concentrations at 45°C – Target and start-up concentrations	249
Table 4-71: Corrosion tests varying fluoride in low calcium and alkalinity water with high chloride and sulphate concentrations at 45°C – Cessation concentrations.....	250
Table 4-72: Corrosion coupon readings while varying fluoride in high calcium and alkalinity water with high chloride and sulphate concentrations at 45°C.....	251
Table 4-73: Summary of the outcomes of Section 4.8.....	256
Table 4-74: Scatterplots of the clusters and their relative positions	258
Table 4-75: Grouping of the series based on the range of their corrosion rates ..	260
Table 4-76: Statistically significant Spearman rho correlations between the average corrosion rate (Avg coup) and the various initial test parameters	265
Table 4-77: Statistically significant Pearson correlations between the average corrosion rate (Avg coup) and the various initial test parameters.....	266
Table 4-78: Corrosion tests varying fluoride in deionized water with 50 mg/l Ca ²⁺ and 55 mg/l CaCO ₃ at 45°C – Target, start-up and ending concentrations.....	269
Table 4-79: Corrosion coupon results while varying fluoride in deionized water with 50 mg/l Ca ²⁺ and 55 mg/l CaCO ₃ at 45°C	269
Table 4-80: SEM and EDS equipment, software and operating conditions (Location: University of the Witwatersrand)	281
Table 4-81: SEM and EDS of coupon surfaces prior to cleaning.....	283
Table 4-82: SEM and EDS of coupon surfaces post cleaning	289
Table 4-83: Tafel plots results and calculated corrosion rates in mmpa.....	296
Table 5-1: The inclusion of various extraneous variables to improve or supersede the new brackish water model for Open System Two mild steel corrosion prediction.....	309
Table 5-2: Application of the models to Open Systems One and Two.....	314

Table A-1: Cooling water chemistry (raw data) for Open System One for the period 3 March 2009 to 25 March 2011 (Buckman, 2012b)	356
Table A-2: Statistical analysis of the Open System One data.....	364
Table B-1: Cooling water chemistry (raw data) and statistical analysis for Open System Two for the period 1 June 2009 to 28 February 2011 (Buckman, 2012b).....	366
Table C-1 Mild steel coupon corrosion rates for Open Systems One and Two for the period June 2009 to February 2011	375
Table D-1: Indices calculated for Open System One at 45°C for comparison with the mild steel coupon corrosion rates.....	377
Table D-2: Additional indices calculated using WaterCycle™ software (from FrenchCreek Software)	379
Table E-1: Indices calculated for Open System Two at 45°C for comparison with the mild steel coupon corrosion rates.....	381
Table E-2: Additional indices calculated using WaterCycle™ software (from French Creek Software)	382
Table F-1: Equations from literature.....	383
Table F-2: Units of equations referred to in Table F-1	390
Table G-1: Minitab® correlations at the low range of alkalinities between parameters at 35°C	392
Table G-2: Minitab® correlations at the low range of alkalinities between parameters at 45°C	397
Table G-3: Varying calcium and alkalinity for the full range of total alkalinities at 35°C.....	402
Table G-4: Varying calcium and alkalinity for the full range of total alkalinities at 45°C.....	403
Table G-5: Minitab® correlations of the average coupon corrosion with chloride and other parameters	404
Table G-6: Minitab® correlations of the average coupon corrosion with sulphate and other parameters	406
Table G-7: Minitab® correlations of the average coupon corrosion with fluoride and other parameters	408
Table G-8: Minitab® correlations of the average coupon corrosion with magnesium and other parameters.....	410
Table G-9: Minitab® correlations of the average coupon corrosion with the other parameters based on data obtained per factorial experimental design	411

LIST OF ABBREVIATIONS AND SYMBOLS

a	Area of coupon (cm ²)
A	Feigenbaum constant
A _{lk}	HCO ₃ ⁻ in moles per litre
Alk	Total alkalinity (mg/l as CaCO ₃)
(aq)	Aqueous form
ASTM	American Society for Testing and Materials
ATMP	Aminotri (methylenephosphonic acid)
Avg Coup	Average corrosion rate of 2 or 3 coupons
AWWA	American Water Works Association
BD	Blowdown rate from the cooling system
β	Buffer capacity (mg/l as CaCO ₃)
ba	Anodic Tafel constant
bc	Cathodic Tafel constant
BWM	“Brackish Water Model”
BOF	Basic Oxygen Furnace
COC	Cycles-of-concentration
CCPP	Calcium carbonate precipitation potential
CI	Corrosivity Index or Larson-Skold or Larson Ratio
CIn	Cassil Index
CPU or ΔC	Apparent colour in chloroplatinate units
CR	Pisigan and Singley index (e.g. CR4)
d	Density of the metal (g/cm ³)
DO	Dissolved oxygen
E	Evaporation rate
EAF	Electric Arc Furnace
E _{corr} (calc)	Calculated corrosion potential

E_{corr} (obs)	Observed corrosion potential
EDS	Energy Dispersive Spectroscopy
epm	Equivalents per million
eq/l	Equivalents per litre
(f)	Final
FIME	Free Ion Momentary Excess or Momentary Excess
HEDP	Hydroxyethylidene-1, 1-diphosphonic acid
HRT	Hydraulic Retention Time
HPA	Hydroxyphosphonoacetic acid
(i)	Initial
I	Ionic strength (moles/litre)
i_{corr}	Corrosion current
ICP-OES	Inductively Coupled Plasma Optical Emission Spectrometry
ISM	Ion speciation modelling
I_s	Oddo-Tomson index
j_{corr}	Corrosion current density
K	Constant based on the total ionic strength and temperature, used in the Stiff-Davis Index calculation
K1 and K2	First and second acidity constants for the carbonate system
K_{sp}	Solubility product constant
log	Logarithm to base 10
LR	Larson-Skold or Larson Ratio or Corrosivity Index (CI)
LRM	Modified Larson Ratio
LSI	Langelier Saturation Index
M	Makeup rate to the cooling system

M Alk	Total alkalinity (mg/l as CaCO ₃)
m ³ /h	Cubic meters per hour
m ³ /tonne	Cubic meters per metric ton
mdd	Milligrams per decimetre squared per day
[]	meq/litre
ME	Momentary Excess or Free Ion Momentary Excess (FIME)
meq/l	Milliequivalents per litre
MIC	Microbiologically induced or influenced corrosion
m/m	Mass-by-mass
m/v	Mass-by-volume
μS/cm	Micro Siemen per centimetre
NACE	National Association of Corrosion Engineers (USA)
nt	Not tested
NTU	Nephelometric turbidity units
OCP	Open circuit potential
OFAT	One-factor-at-a-time
PBTC	2-Phosphonobutane-1, 2, 4-Tricarboxylic Acid
PCA	Phosphonic carboxylic acid
Palk	-log (M alkalinity), M alkalinity (mg/l as CaCO ₃)
pCa	-log (Ca), Ca = calcium (mg/l as Ca ²⁺)
p value	The probability of being wrong or making a Type 1 error or the critical alpha value at which the null hypothesis is rejected
pH	-log[H ⁺]
pH _e	pH of equilibrium
pH _s	pH of calcium carbonate saturation
ppm	Parts per million
PSI	Puckorius or Practical Scaling Index
R ²	percent variation explained by the regression analysis model

R^2 (adj) or	
R-Sq (adj)	Percent variation explained by the regression analysis model after being adjusted for the number of variables and sample size (used in place of R^2 for multiple regression analysis)
r value	Pearson correlation coefficient
rho	Spearman correlation coefficient
RSI	Ryznar Stability Index
SANAS	South African National Accreditation System
Satn	Saturation
SDI	Stiff-Davis Index
SEM	Scanning electron microscopy
SHMP	Sodium hexametaphosphate
SI	Langelier Saturation Index
t	Time, in various units
T _{Ca}	Calcium in moles per litre
Tonne	Metric ton (t)
TT	Tolyltriazole
US EPA	United States of America Environmental Protection Agency
V/dec	Volts per decade of current
WC	WaterCycle™
Y	Yahalom Index
ZED	Zero Effluent Discharge
ZLD	Zero Liquid Discharge

CHAPTER 1: INTRODUCTION

1.1 Background

In their pursuit of Zero Effluent Discharge (ZED), industrial plants are reducing fresh water intake and limiting the volume of water released back into the environment. As a result of this and the cascading reuse of water, industry is often forced to utilise inferior water quality for lower risk applications. For example: the washing of equipment or shop floors, as cooling medium, and when possible, in direct contact with the intermediate or finished product, or as a component of the finished product. The utilization of substandard water as makeup to open recirculating cooling systems can often render these complex water systems susceptible to increased fouling and corrosion. This of course can severely hamper production, threaten both plant and process integrity, and ultimately add to company cost and risk of doing business.

Water-borne constituents responsible for fouling or corrosion may be either microbiological or chemical in nature. When an available water source is more saline than fresh water, but not as high in dissolved solids as sea water, then such water may be considered brackish. In nature, brackish surface waters can vary significantly in salinity, either spatially and/or over time (Nielsen *et al.*, 2003). The same applies to a Southern African steel mill where water conductivities ranged from 2500 $\mu\text{S}/\text{cm}$ to as high as 5000 $\mu\text{S}/\text{cm}$ (Buckman, 2010, 2011, 2012a, 2012b), with the principal anions consisting mostly of chloride (200 to 800 mg/l), sulphate (400 to 1000 mg/l) and varying levels of fluoride (2 to 100 mg/l).

Fluoride rich rocks (for example, fluorite, cryolite, and fluorapatite) are the main source of fluoride in groundwater (Brindha and Elango, 2011). Groundwater low in calcium and high in sodium and bicarbonate typically contains higher fluoride levels (Brindha and Elango, 2011). The other key sources of fluoride include: volcanic ash, combustion of coal, infiltration of agricultural runoff containing chemical fertilisers and effluent from industries. Examples of industries producing effluent high in fluoride are the aluminium smelters, cement production, and

ceramic and brick firing (Brindha and Elango, 2011). Effluent streams high in fluorides are also common in steel mills. In steel mills, fluorspar (CaF_2) has been used for centuries in the fluxing of ores and is the primary reason for high levels of fluoride in their water systems.

The corrosion of carbon steel exposed to these environments is important since it is by far the most widespread material of choice in the fabrication of industrial cooling circuits, particularly in steel mills. It is therefore necessary for steel mills, and similarly for the chemical industry at large, to improve its understanding of the corrosivity of brackish water used in their water circuits. Such an endeavour will ultimately assist in the design, operation, maintenance and chemical treatment of such water systems and thereby predict and possibly extend the life expectancy of equipment.

Early work done to improve the understanding and prediction of the corrosivity of water to mild steel extends back to Tillmans and Heublein (1912), Baylis (1926) and Langelier (1936). Some of the indices, including those inadvertently used to predict corrosion, that have gained acceptance in the chemical industry world-wide now include the following: Langelier Saturation Index (Langelier, 1936), CCPP (Calcium Carbonate Precipitation Potential) (Merrill and Sanks, 1978), Ryznar Stability Index (Ryznar, 1944), Puckorius or Practical Scaling Index (Puckorius and Brooke, 1990), Larson-Skold Index (Larson and Skold, 1957) and the more recent eight-variable empirical model constructed by Pisigan and Singley (1984). The former indices were designed primarily for the drinking water industry and were mostly indicative of the tendency of a surface water to precipitate calcium carbonate, rather than predict the absolute corrosivity of specific waters. It is only since the introduction of the Practical Scaling Index (PSI) that continuing attention is being given specifically to the prediction of corrosion in industrial cooling systems.

Nevertheless, it has become obvious that the calcium content and alkalinity of the brackish water used as a cooling medium tend to decrease the corrosivity of mild

steel at typical cooling system pH and temperatures (Pisigan and Singley, 1984). In contrast to this, the increasing levels of chloride or sulphate (Feigenbaum *et al.*, 1978) have tended to increase the corrosivity of brackish water on mild steel. In addition to the favourable impact of the calcium hardness and total alkalinity, there are the various commonly utilized cooling water corrosion inhibitors which may further deter the corrosivity of brackish water.

1.2 Aims and Research Objectives

1.2.1 Aims

The primary purpose of this thesis is to develop an improved understanding of the corrosivity of a specific industrial brackish water stream, by determining the impact of calcium carbonate saturation and the varying levels of: magnesium, chloride, sulphate and particularly fluoride on the corrosion of steel at 45°C. The secondary purpose is to develop mathematical models that can be relied on to accurately predict the corrosivity of the brackish water on mild steel, based on the chemical analysis of the water.

1.2.2 Hypothesis and research objectives

It is hypothesised that the calcium content and alkalinity of a brackish water used as a cooling medium will tend to decrease the corrosivity on mild steel at typical cooling system pH and temperatures. In contrast to this, the increasing levels of: chloride, sulphate or fluoride will increase the corrosivity of brackish water on mild steel. Various commonly utilized cooling water corrosion inhibitors may be considered to further deter the corrosivity of brackish water. The objectives below outline the steps necessary to address the main purposes of the thesis and the hypothesis.

Objective 1: To determine the relationship between the various common water chemistry parameters and the corrosion rate of mild steel in brackish water at elevated temperatures (35 and 45°C).

Objective 2: To develop mathematical/computer models that will allow for an accurate estimation of the corrosion of mild steel utilizing brackish water in their industrial cooling systems at typical operation temperatures.

Objective 3: Assess the nature and impact of varying levels of fluoride on mild steel corrosion in brackish water.

Objective 4: To develop additional mathematical/computer models that will allow for an accurate estimation of the impact of fluoride on mild steel in a representative raw water and brackish water at temperatures typical of industrial cooling systems.

Objective 5: To draw comparisons between the developed model and actual plant data. The model will be applied to at least two industrial cooling water systems utilizing brackish water as a cooling medium.

Objective 6: To use the data and models to establish a set of hypothetical guideline values for a range of water quality parameters to guide prospective users of brackish waters as cooling water.

Objective 7: To research and evaluate commercially viable options which will minimize the corrosion of mild steel in contact with such aggressive electrolytes at elevated temperatures.

CHAPTER 2: LITERATURE REVIEW

2.1 Overview of the Iron and Steel Manufacturing Process

The steel manufacturing process occurs in several steps, commencing either with the production of molten steel from iron ore using the basic oxygen furnace (BOF), as depicted in the integrated steel making process in Figure 2-1, or from scrap with the electric arc furnace (EAF). The BOF input materials include molten iron, 30% steel scrap and high-purity oxygen whereas in the EAF the primary inputs are: graphite electrodes, electricity and steel scrap (Figure 2-2) (Kent, 2008).

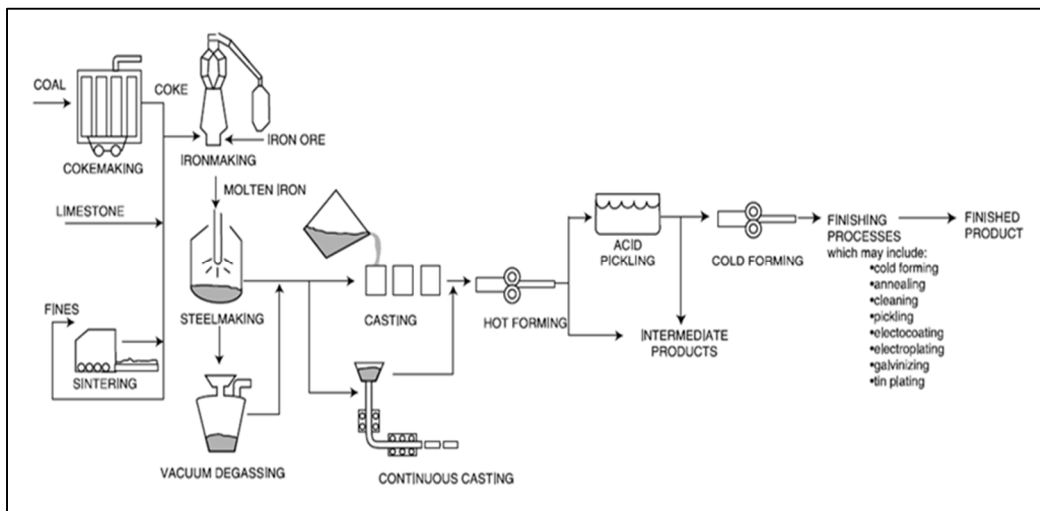


Figure 2-1: Process flow diagram of an integrated mill illustrating the production of molten iron followed immediately by steel production (Abt Associates *et al.*, 1995)

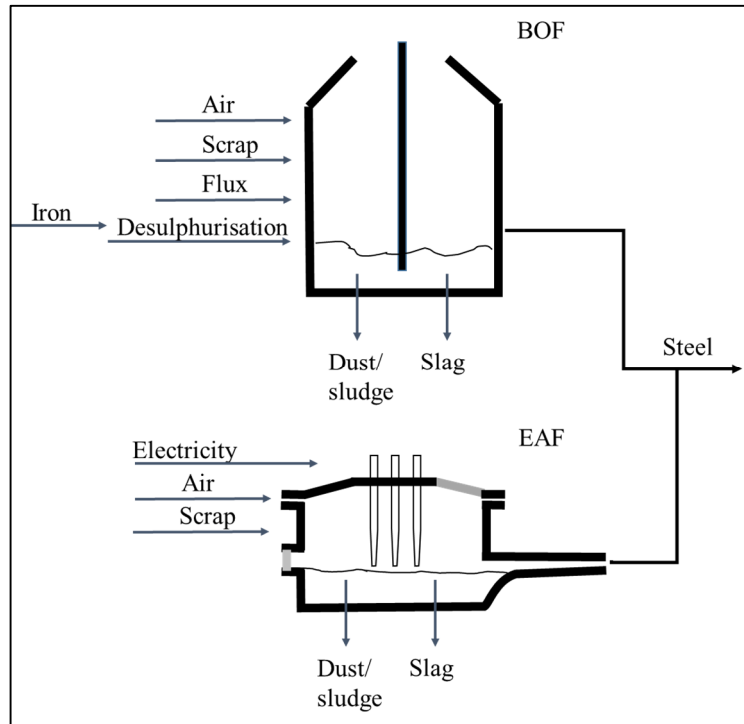


Figure 2-2: Steel making by either the BOF or EAF process (After Abt Associates *et al.*, 1995)

EAFs, also known as minimills, have modernized existing mills by increasing capacity and efficiency, while reducing man-hours and energy needed per ton of steel (Kent, 2008). Kent reported that the 50% decline in USA's iron and steel sector water withdrawals were attributed to the advent of the EAFs and the stricter effluent discharge regulations. Minimills emerged more or less simultaneously in the United States, Southern Europe, and Japan in the 1950s (Schorsch, 1996).

During steelmaking both the BOF and EAF processes require the addition of certain alloys and fluxes: fluorspar, dolomite, and alloying agents (aluminium etc.). The outputs from the two processes include: slag, metal dust, gasses and the molten steel (Flynn and Nalco Company, 2009).

Once the molten steel is produced using a BOF or an EAF, it needs to be converted into a product, and therefore has to be solidified into shapes and finished. Traditionally, forming was performed by pouring the molten metal into ingot moulds and allowed to cool and solidify. The more modern and the currently

preferred method of forming is continuous casting (Abt Associates *et al.*, 1995) and it accounts for over 86% of raw steel produced in the USA. Continuous casting is the process of continuously pouring molten metal from a ladle, emerging at over 1500°C (Flynn and Nalco Company, 2009) and passing into casting machines, which then allows it to descend and cool, and later be cut into the required shapes shown in Figure 2-1. Further forming is performed either by hot rolling, to produce: slabs, strips, bars, or plates, or by cold rolling which generally produce wires, tubes, sheet, and strip steel. Cold forming results in a product that has improved mechanical properties, better machinability, special size accuracy, and of a thinner gauge (McGannon, 1971). The product from a cold rolling process is hard and brittle and therefore requires an annealing furnace to make it more ductile.

2.2 Water Use in the Iron and Steel Industry

Having revealed the energy intensive nature of the steel manufacturing process, it is now possible to elaborate on the process chemistries and the enormous water dependency of this industry. The iron and steel industry has historically always been a high water consumer in various processes, for example, as a coolant for furnaces, equipment, and the intermediate product itself (Christophersen, 2008). The management of water at specific plants varies greatly, due to local aspects such as water availability, water quality, plant configuration and legislation. Water usage varies with these factors, and therefore, ranges broadly from 0.63 to 27.5 m³/tonne (Flynn and Nalco Company, 2009). The steel industry uses saltwater, brackish water and freshwater and it is used in mainly two ways: indirect cooling or direct cooling.

In indirect cooling, the water may require some pre-treatment as it is often heated to high temperatures and sometimes entails the use of closed systems. Water used in direct cooling, for example, for the scrubbing of gases or for descaling, results in a slightly more contaminated effluent stream, thereby demanding continuous treatment (Degrémont, 1991). These commonly encountered open recirculating systems comprise: coke plants, blast furnace gas scrubbing, oxygen converter gas scrubbing and the continuous casting and hot rolling mills. The main contaminants

present in the high volumes of water used to quench or cool the steel are the high levels of suspended solids and mill scale with oil and grease (Christophersen, 2008). Table 2-1 summarizes the water usages by process type.

Table 2-1: Water usage rates by steel making processes (Flynn and Nalco Company, 2009)

Technology	Water usage (m ³ /tonne)
Blast Furnace	1.5
Basic Oxygen Furnace	8.8
Direct Reduction	1.2
Electric Arc Furnace	1.0
Continuous Casting	4.2
Hot Strip Mill	13

In addition to the contaminated water from open recirculating cooling systems, integrated iron and steel mills generally also have to treat specific highly polluted effluent from the coke plant, acid pickling effluents and cold rolling mills (Degrémont, 1991).

According to the 2011 World Steel by Zhang (World Steel Chairman) and Basson (World Steel Director General), a recent survey showed that the average water consumption for an integrated steel plant is 28.6 m³/tonne steel. For the electric arc furnace, the average is 28.1 m³/tonne steel. It was also declared that the water consumption and discharge were close to each other, indicating an overall efficient use of water. In most cases, water loss is caused by evaporation. The application of advanced technologies has allowed steel plants to recycle and reuse around 98% of their water (WorldSteel, 2011).

2.3 Continuous Casting and its Specific Cooling Requirements

As mentioned before, the development of the continuous casting process was a significant breakthrough in the steel making process. This consequently led to steel mills developing into a more continuous process with cooling becoming a critically integral component of the continuous casting system. Consequently, the continuous

facility became reliant on at least three main types of cooling water systems (Degrémont, 1991):

- **Mould cooling.** This is usually a closed recirculating cooling circuit for cooling of the ingot mould and it generally makes use of high quality water. The closed circuit is cooled by an open recirculating system (Figure 2-3).
- **Machine cooling.** An open recirculating cooling system for machine cooling.
- **Spray cooling.** The casting machine, and the bloom or billets is cooled by means of direct spraying through spray nozzles and the runoff is then collected in basins along with oil, grease, and mill scale. The scale that settles or is filtered out is recycled for sintering operations, if the mill has a Sinter Plant. Waste treatment plant sludge is also generated from this water circuit (American Iron and Steel Institute, 1992). The filtrate is then reused in spray cooling and receives makeup to compensate for the water lost due to evaporation and blowdown.

Chemical treatment of these systems have usually included: scale inhibitors, biocides and corrosion inhibitors, and their purpose is to minimize the fouling of heat transfer surfaces and reduce plugging of spray nozzles that could lead to loss in production.

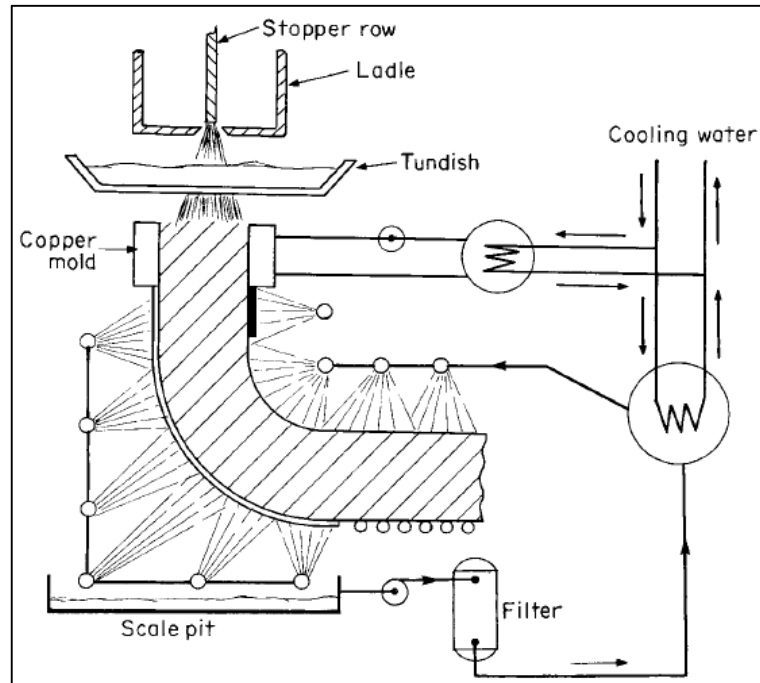


Figure 2-3: Continuous casting cooling circuit (Flynn and Nalco Company, 2009)

2.4 Types of Cooling Systems

As mentioned before, the cooling in iron and steel mills can either be direct or indirect. Indirect cooling in industrial plants is generally used to cool process fluids (liquids and gasses), whereas the use of direct cooling is for cooling of solid products and is applied through the use of spray nozzles.

During the use of direct cooling, the water becomes contaminated with whatever process chemicals it may be exposed to, and in the case of steel mills this includes: gases, oil and grease, suspended iron oxide particles and dissolved species, for example fluoride (arising from the use of casting powders). To remove heat from process or equipment, three main types of cooling systems are considered: once through, open recirculating and closed systems (Buckman, 1981). Each of these systems is appropriate for different purposes.

2.4.1 Once through cooling systems

In once through systems, the cooling water passes through the heat transfer equipment only once and is then discharged back to the environment. Unless required before discharge, there is no evaporative cooling of the water and therefore these systems require large volumes of water and must be located near a large river or lake (Figure 2-4) (Buckman, 1981).

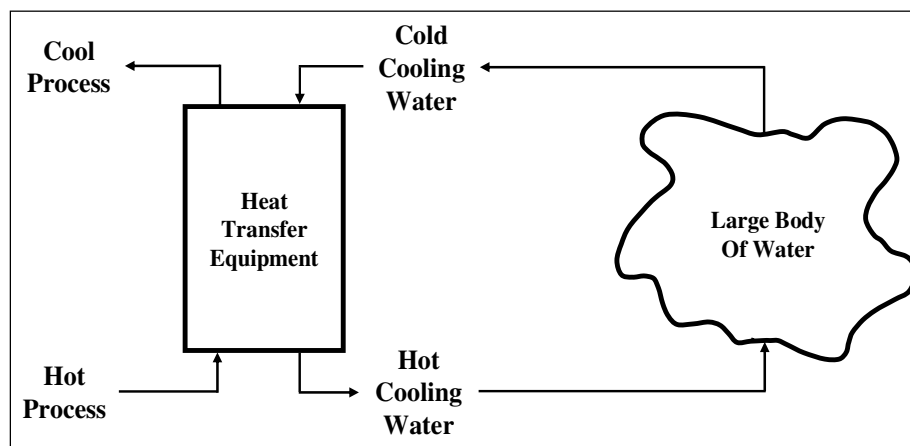


Figure 2-4: Once through cooling system (Buckman, 1981)

2.4.2 Closed recirculating cooling systems

In closed recirculating cooling systems, heat is transferred to the cooling water from the hot process, but is then transferred out of the cooling water by conduction through the use of additional heat transfer equipment and then reused. No water is evaporated and closed loops do not concentrate salts as an open system does. An example of a closed system is the engine cooling system in a vehicle. The radiator serves as the heat transfer device to reject heat into the atmosphere (Figure 2-5) (Buckman, 1981).

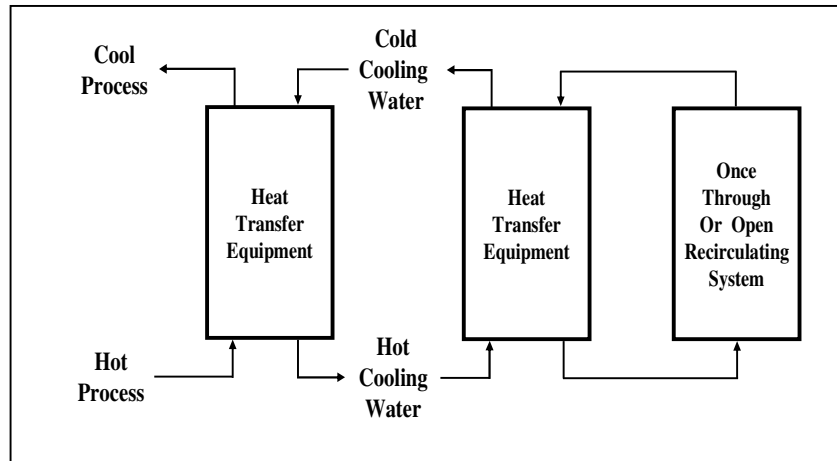


Figure 2-5: Closed recirculating cooling system (Buckman, 1981)

2.4.3 Open recirculating cooling systems

In open recirculating cooling systems, the heat that is transferred from a process, via heat transfer equipment, into the cooling water where it is rejected into the atmosphere by evaporation. The remaining cooled water, supplemented by additional water taken into the system, referred to as makeup, is then recirculated for additional heat removal. This heat rejection usually occurs in an evaporative cooling tower, or infrequently using spray ponds. Since the cooling water evaporates to remove heat that it has picked up, the dissolved solids in the circulating water concentrate in the water and if excessive, can lead to fouling and corrosion of the heat transfer equipment, the pipework and the cooling tower. The water system is also open to the atmosphere, so contaminants from the air can be scrubbed into the cooling water which could exacerbate the above mentioned problems (Figure 2-6) (Buckman, 1981).

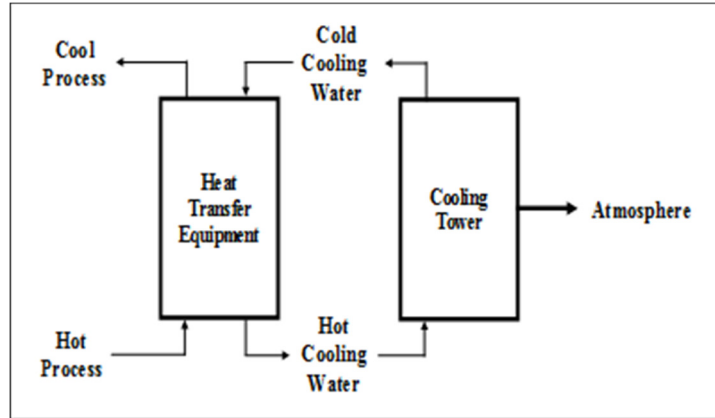


Figure 2-6: Open recirculating cooling system
(Buckman, 1981)

The concentration of dissolved materials in an open recirculating system and the loss of treatment chemicals dosed in the system are related to the total volume of the system and the makeup rate, evaporation rate and the bleed-off or blowdown rate (Figure 2-7). The material balance of water is expressed by Equation 2.1:

$$M = E + BD \dots\dots\dots [2.1]$$

where: M = makeup rate (m³/h),
E = evaporation rate (m³/h),
BD = blowdown rate (m³/h).

Since dissolved materials are only removed from the cooling system by blowdown, leaks or windage, these materials become more concentrated with the continued evaporation. The makeup required to keep the system full, also continually introduces more dissolved materials. The concentration factor or cycles-of-concentration is the ratio of the total water added to the system divided by the total water lost due to the drift and blowdown; that is Equation 2.2:

$$COC = M / BD \dots\dots\dots [2.2]$$

where: COC = cycles-of-concentration.

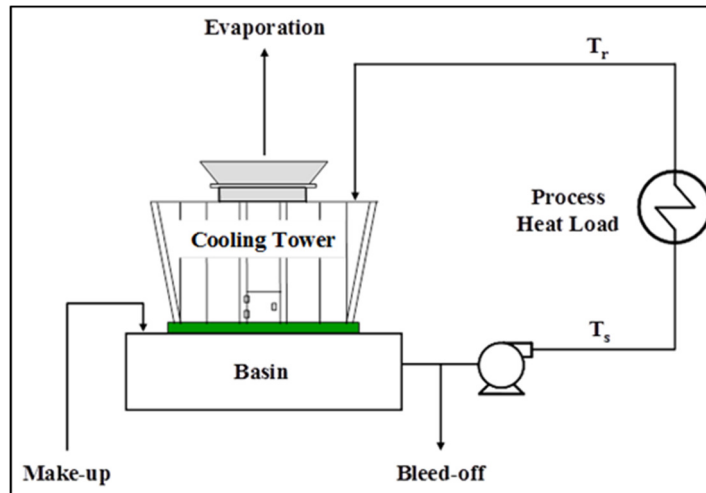


Figure 2-7: Recirculating cooling system with cooling tower (Buckman, 1981)

Increasing the cycles-of-concentration decreases the makeup water requirement and the rate of blow-down. However, there is a diminishing return in terms of the water savings with increasing cycles-of-concentration and eventually there is a limit on the cycles-of-concentration due to the increased scaling tendency with increased dissolved solids.

Increasing the cycles-of-concentration increases the likelihood of calcium carbonate precipitation, which in turn increases the risk of impeding heat transfer, resulting in possible equipment damage and production losses.

2.5 Impact of High Salinity Cooling Water in Iron and Steel Mills

The use of more saline water types in cooling systems provide certain advantages and disadvantages. It is important to consider the motives and precautions taken for industrial applications. The use of brackish water or sea-water or embracing a Zero Liquid Discharge (ZLD) philosophy are some of the reasons for the use of a high salinity water in the cooling systems.

2.5.1 The use of brackish water or sea-water as cooling tower makeup

The limited availability of fresh water at many locations around the world has led to the expansion of industrial and commercial activity around lakes and rivers

(Wallis and Aull, 2009). Alternatives to the use of fresh water makeup to the open recirculating cooling water have been the use of sea-water, brackish estuarine or ground water, or high salinity reclaimed water.

The provision and operation of high salinity cooling towers would not have been possible without the special design requirements associated with such water types. Maulbetsch and Di Fillippo, (2010) considered the thermal performance, cooling system cost, environmental impact and operational and maintenance costs and from their report it was clear that for high salinity cooling water:

- A 5 to 10 percent larger cooling tower was required, due to the reduced vapour pressure and reduced cooling tower performance;
- The materials of construction for the structures, tower fill, drift eliminators, piping, fasteners, railings and access stairways all needed to be suitable for sea-water or high salinity exposure and are significantly more expensive. The deposition of salts attributed to windage or drift leads to the corrosion of equipment in the immediate vicinity of the cooling tower. Just in terms of the differential costs of materials the salt or brackish water system is deemed between 35 and 50% more expensive than the fresh water towers;
- Even the tower or basin, sometimes constructed of concrete, may have deteriorated and required regular maintenance;
- The cooling system had to be operated at low cycles-of-concentration to minimize the risk of scale on heat exchanger surfaces.

According to Maulbetsch and Di Fillippo (2010), there were installations with towers operating on salt or brackish water at power plants and industrial facilities, and the makeup waters ranged from: brackish waters (from groundwater) with salinities of a hundred ppm to estuarine or bay waters with salinities of a few thousand to seawater concentration, and seawater with a salinity of 35,000 ppm. Cooling systems taking in seawater are reported to have operated at between 1.5 and 2.0 cycles-of-concentration resulting in the circulation water containing total dissolved solids of up to 70,000 ppm (Maulbetsch and Di Fillippo, 2010).

In 2001, Fleming provided a list of 25 facilities where Marley Cooling Tower, then one of the largest manufacturers of cooling towers in the USA, had installed cooling towers that had or were utilizing either sea-water, brackish water or high salinity water as makeup (Marley, 2001). Fleming reported the earliest of these cooling towers were constructed in 1953 and estimated there were over 90 worldwide.

2.5.2 Striving for Zero Liquid Discharge (ZLD)

Instead of taking in either sea-water, brackish water or high salinity for use as cooling water it is also possible that industrial facilities may, for various reasons, be utilizing their own high salinity effluent streams as cooling tower makeup. A working example of this scenario will be discussed later where the facility is striving towards Zero Liquid Discharge (ZLD). “Zero Liquid Discharge is a process that is beneficial to industrial and municipal organizations as well as the environment because money is being saved and no effluent, or discharge, is left over. ZLD systems employ the most advanced wastewater treatment technologies to purify and recycle virtually all of the wastewater produced” (Siemens, 2012). Table 2-2 lists the reasons for and against zero liquid discharge.

Table 2-2: Advantages and disadvantages of zero liquid discharge (Makini, 2005)

Advantages	Disadvantages
Reduction in water/energy demand	Possibility of product contamination
Zero pollution	Solid/concentrated brine effluent
Bottom line savings	Higher capital or retrofitting costs
Improved reliability; reduced downtime	Community distrust of water quality
No concern about US EPA compliances	Engineering concerns
Community acceptance and trust	

2.6 Two Cooling System Scenarios at a Southern African Steel Mill

In the recent decade, one of the largest suppliers of steel products in sub-Saharan Africa committed to achieving zero liquid discharge (ZLD) in order to reduce the environmental impact of its operation, produce higher grade products and reduce the cost of production. The unique combination of technologies employed to

accomplish this objective included: clarification, filtration, reverse osmosis, evaporation and crystallization. The waste sludge generated by the process has been dewatered and sent to landfill.

The main intentions of the upgrade of the effluent treatment plant were to remove suspended solids and hardness from the main process water circuit and remove salts from the various unit processes within the steel mill, for example the cooling towers. However, subsequent to the introduction of the desalination technologies it became evident that the cooling water had significantly increased in salinity leading to corrosion and scaling problems being reported by the various users. Some of the problems identified are given in Tables 2-3 and 2-4 and illustrated in Figures 2-8 to 2-13 (Buckman, 2012b).

Table 2-3: Estimated capital expenses incurred to repair cooling systems (Buckman, 2012b)

Capex	Rand Value (millions)
Hydraulic pipes	3.5
Spray chamber structural repairs (Chamber 1)	20.0
Spray chamber major repairs (Chamber 2)	26.5
Dewatering tank	0.6
Self cleaning strainers	2.5
Cooling tower civils	6.0
Stainless steel welded bearings	2.6 once-off
Total capex (Rand, million)	55.6

Table 2-4: Estimated increase in annual costs to maintain the cooling systems (Buckman, 2012b)

Increased Maintenance Costs	Rand Value (thousands)
Stainless steel grating	315 once-off
Spray chamber walkways	650 once-off
Cooling tower gearboxes	90 per annum
Evapco cooling towers	150 once-off
Sand filters	300
Plate heat exchangers	500
Water pipes	220
Other (cylinders, mould oscillation equipment, strainer, roll life, segment refurbishment)	8,157
Total for increased maintenance cost (Rand, thousand)	10,742

During the site inspections, it became obvious that the corrosion in question originated from the waterside of the pipes or equipment. Where external corrosion was encountered, it was ascribed to either water leaking from the equipment, for example, the pipes or pump, or due to salt drift deposition (Buckman, 2012b). Photographs of the damage to the cooling tower return pump, its metal base and concrete floor (Figure 2-8), the gearbox (Figure 2-9) and the Evapco cooling tower (Figure 2-10) support this position. Figures 2-11 and 2-12 were more indicative of the waterside corrosion damage to both the metal and concrete components of the larger cooling towers (Buckman, 2012b). Internal and external corrosion of the sand filters (Figure 2-13) required that they also be replaced.



Figure 2-8: (Left) Corroded open system return pump due to salt deposits (Buckman, 2012b)

Figure 2-9: (Right) Cooling tower gearboxes – one year in service (Buckman, 2012b)



Figure 2-10: (Left) Evapco cooling towers, to be replaced with new cooling towers due to structural damage (Buckman, 2012b)

Figure 2-11: (Right) Chemical attack on cooling towers showing spalling due to corrosion of the reinforcing bars (Buckman, 2012b)



Figure 2-12: Corroded cooling tower structure (Buckman, 2012b)



Figure 2-13: Corroded sandfilters – total replacement of steel fabrication (Buckman, 2012b)

Although this particular steel mill contains several open systems utilizing the brackish water of concern, the focus was primarily on the two open recirculating cooling water systems described below (Buckman, 2012b).

2.6.1 System One

This open recirculating system cools the plate heat exchangers of a closed primary system by means of evaporative cooling and 10% of the recirculation is filtered through a side-stream filter in order to keep the suspended solids below 10 mg/l. The capacity of this system is 900 m³ and the circulation rate is approximately 1100 m³/h. The hot water temperature reaches 40°C whereas the cold water temperature is at approximately 30°C. Mild steel and stainless steel are the main materials of construction (Buckman, 2012b).

2.6.2 System Two

This system provides slab cooling, as well as machine cooling for a continuous casting machine. Water is pumped from the cooling tower basin to the machines where it is split before proceeding to the two machines. Due to the contamination with scale and oil, this water is pumped into scale pits where the scale is first

removed, followed by oil removal by means of sand filtration. Fluoride continually contaminates this water due to the addition of fluoride containing casting powder. Fluoride and iron are the major components found in deposits in pipes (Buckman, 2012b).

The capacity of this system is 2300 m³ and the circulation rate is approximately 1360 m³/h. the hot water temperature can reach 45°C, whereas the cold water temperature is at approximately 30°C. Mild steel and stainless steel were the main materials of construction (Buckman, 2012b).

Both systems required chemical treatment with corrosion inhibitors, biocides, scale inhibitors and biodispersants in order to reduce the potential detrimental impact of the various contaminants on the plant equipment.

2.7 Corrosion Prediction

The operation of industrial cooling systems is complicated by the presence of impurities in the cooling water. The various impurities could lead to corrosion, scale, and fouling, and the net effect is an increased cost of production or reduced production capacity. For these reasons, it is imperative that the plant scientist or engineer is able to accurately predict the optimum system conditions in order to at least minimize these potential impacts. In terms of corrosion predictions, the indices that have gained wide acceptance in the corrosion community include the following:

- Langelier Saturation Index (LSI);
- Ryznar Stability Index (RSI);
- Puckorius or Practical Scaling Index (PSI);
- Larson-Skold or Larson ratio (LR) or Corrosivity Index (CI);
- Oddo-Tomson Index (Oddo and Tomson, 1982, 1992).

The first three indices are based on the calculation of the pH at which calcium carbonate reaches saturation (pH_s), as derived by Langelier (1936). This pH of saturation (pH_s) is a function of a number of water chemistry parameters, which

include: total dissolved solids (TDS), temperature, calcium concentration, total alkalinity, magnesium and sulphate concentrations. Increases in the values for: temperature, calcium and/or alkalinity and/or decreases in TDS, magnesium and sulphate would result in decreased values for the calculated pH_s . Therefore, according to any of the three equations (Equations 2.3, 2.4, 2.5) as the value of pH_s is decreased, so the measured pH or pH_e (Equation 2.6) of the water is more likely able to exceed the pH_s , and thereby result in an increased scaling tendency.

$$\text{Langelier equation: } LSI = pH - pH_s \dots\dots\dots [2.3]$$

$$\text{Ryznar equation: } RSI = 2 \times pH_s - pH \dots\dots\dots [2.4]$$

$$\text{PSI calculation: } PSI = 2 \times pH_s - pH_e \dots\dots\dots [2.5]$$

$$\text{where: } pH_e = \text{equilibrium pH } (pH_e = 1.485 \times \log_{10} \times (Alk) + 4.54)) \dots\dots [2.6]$$

Alk = total alkalinity (mg/l as $CaCO_3$).

The Langelier Saturation Index indicates the tendency of a water sample to either deposit calcium carbonate or be under-saturated with respect to calcium carbonate saturation. When water is under-saturated with respect to calcium carbonate, it can be assumed to be corrosive and the prediction is occasionally reliable when applied in potable water treatment (Langelier, 1936).

However, it has also been established that there are many other chemical and physical factors that influence the corrosion of mild steel in water (Pisigan and Singley, 1987) (Imran *et al.*, Nov 2005). Water-borne species or related factors that have been identified are: chloride, sulphate, dissolved oxygen, temperature, pressure (due to the solubility of gases such as carbon dioxide and oxygen), flow velocity (as it influences the supply of species that may either encourage or inhibit reactions at the metal surface), the Hydraulic Retention Time (HRT), oxidizing or reducing substances and organic matter. Further to this, there are also the significant influences that micro-organisms and biological matter can have either directly or indirectly in terms microbiologically induced or influenced corrosion.

The Langelier Saturation Index (LSI) (Langelier, 1936) was originally developed as a guide to indicate the tendency of the water in municipal water systems to either deposit or dissolve calcium carbonate. Although a misnomer of corrosion prediction, it has stood the test of time to the point where it has become the universal corrosion predictive tool in water systems, including industrial water systems. Industrial systems are generally operated at elevated temperatures due to heat exchange processes. Heat exchanger skin temperatures can be as much as 10 to 20°C hotter than the hot water exiting a condenser. According to Langelier (1936) the index is only applicable within the 7.0 to 9.5 pH range and for water containing less than 800 mg/l total dissolved solids. It was already at an early stage that Langelier became aware that “calcium carbonate is 500-fold more soluble in sea than fresh water” (Langelier, 1936) and therefore imposed a limit in terms of the accuracy of the salinity correction factor. As the index is based on thermodynamic principles, it only predicts the directional tendency and driving force, and not the rate, nor the capacity for precipitation or corrosion inhibition. Another factor influencing the rate of precipitation is the flow rate of the water over the surface receiving the “self-healing or natural protective coating” (Langelier, 1936).

In 1944, Ryznar endeavoured to eliminate the possible misinterpretation that water with a positive LSI would not be corrosive by his introduction of the Ryznar Stability Index (RSI) (Ryznar, 1944). This index was to provide a quantitative measure of the scaling tendency. It proved to be significantly more accurate than the Langelier Index. Most of his laboratory work was performed between 50°C and 90°C. In terms of the applicability of the RSI, it was found that it approximated the LSI over the range of normal cooling water operations, but as with the LSI, it becomes questionable under highly scaling conditions.

In 1960, Stumm demonstrated that the role calcium carbonate in preventing the corrosion of iron is not as simple as described by Langelier (1936), whereby a protective coating or “eggshell lining” is formed (Stumm, 1960). Stumm concluded that the surface scale was modified and the anodic surface area was reduced.

Langelier (1936) had never intended for his index, or the various modifications of the index, to become the universally applicable tool for predicting the corrosivity of water. However, it was between 1960 until the mid-nineties that the LSI attracted a strong negative commentary within the municipal potable water arena. It was stated that the LSI had no correlation with corrosion rate (Stumm, 1960; Larson and Sollo, 1967; Singley, 1981; Schock, 1984; Piron *et al.*, 1986; Pisigan Jr. and Singley, 1987), and based on the empirical evidence the use of the LSI for corrosion prediction should be abandoned (AWWARF and DVGW, 1996). The same sentiment applied to the RSI and the various other “corrosion prediction indices” listed below:

- Aggressiveness Index (AI) (Millette *et al.*, 1980);
- Momentary Excess (ME) (Dye, 1958);
- Calcium Carbonate Precipitation Potential (CCPP) (Merrill and Sanks, 1978); and
- Driving Force Index (DFI) (Rossum and Merrill, 1983).

A review of the above calcium carbonate based indices by Rossum and Merrill (1983) concluded that the LSI, RSI and AI did not appear to correlate with the CCPP. It was reported the LSI and DFI were only satisfactory in terms of indicating saturation level, in terms of calcium carbonate precipitation, and shown not to be useful for any other purpose. Rossum and Merrill also stated there was redundancy in the DFI, AI and LSI. The CCPP was recommended as the index that was most representative of a water’s state of calcium carbonate saturation in order to provide a measure of the capacity and rate of calcium carbonate precipitation or dissolution.

The Puckorius Index (PSI) (Puckorius and Brooke, 1990) is a refinement of the RSI, in which an empirical alkalinity function is derived to modify the calculated pH_s . In both large industrial and power station cooling systems, either the LSI or PSI is still used to control acid feed for calcium carbonate scale control.

Early research already confirmed that the precipitation/dissolution of calcium carbonate was not the only water quality parameter relevant to the corrosion of

distribution systems (Langelier, 1936). Other factors such as ratios of anions, velocity, pH and calcium concentration were also correlated with corrosion rates, but perhaps the best researched is the Larson and Skold Index also known as the Larson Ratio (LR) (Larson and Skold, 1957, 1958). Pipe loop corrosion studies were conducted at The Illinois State Water Survey which eventually culminated in the index becoming an ASTM standard. The LR is defined in Equation 2.7 as:

$$\text{Larson Ratio} = ([\text{Cl}^-] + [\text{SO}_4^{2-}]) / ([\text{HCO}_3^-]) \dots\dots\dots [2.7]$$

where: [] = meq/litre,

Cl^- = chloride (meq/litre as Cl^-),

SO_4^{2-} = sulphate (meq/litre as SO_4^{2-}),

HCO_3^- = bicarbonate alkalinity (meq/litre as CaCO_3).

Values above 0.5 are considered corrosive, but the index remains a qualitative measure and cannot predict the capacity to dissolve metal from the inside of a pipe. It does not take into account the effects of: calcium, ionic strength, temperature, Holding Retention Time (HRT), dissolved oxygen and, for steel mills, the impact of the fluoride concentration.

Feigenbaum *et al.* (1978) showed poor correlation between the already-mentioned calcium carbonate based indices and the saline waters of the Negev Desert, and Feigenbaum therefore developed an empirical index (Equations 2.8 and 2.9) which included the effect of calcium carbonate solubility and the ions of the Larson Ratio:

$$Y = A \times H + 0.34 \times (\text{Cl}^- + \text{SO}_4^{2-})^{(-1 / (A \times H))} + 19 \dots\dots\dots [2.8]$$

where: $Y < 200$ = indicative of severe corrosion, $200-500$ = intermediate corrosion, and > 500 = minimal corrosion,

$A = 3.5 \times 10^{-4}$;

$H = ([\text{Ca}] \times [\text{HCO}_3^-]^2) / [\text{CO}_2] \dots\dots\dots [2.9]$

Cl^- = chloride (mg/l as Cl^-),

SO_4^{2-} = sulphate (mg/l as SO_4^{2-}).

The reported lack of a definite correlation between the Langelier Saturation Index and corrosion rates evident in both the drinking water industry and laboratory scale closed loop experiments prompted Pisigan and Singley (1985) to embark on a series of jar tests. The results of the laboratory tests permitted them to empirically derive an eight-variable model (Equation 2.10) that could account for 98% of the variations in corrosion rate under the experimental conditions explored (Pisigan and Singley, 1985). The equation hypothesized indicated that the corrosion rate of mild steel was in fact influenced by factors beyond just precipitation or dissolution of calcium carbonate:

$$\text{Corrosion Rate (mpy)} = ((\text{Cl}^-)^{0.509} \times (\text{SO}_4^{2-})^{0.025} \times (\text{Alk})^{0.423} \times (\text{DO})^{0.799}) / ((\text{Ca})^{0.676} \times (\beta)^{0.030} \times (10^{\text{SI}})^{0.107} \times (\text{Day})^{0.381}) \dots\dots\dots [2.10]$$

where: DO = dissolved oxygen (mg/l as O_2),

Ca = calcium (mg/l as Ca^{2+})

β = buffer capacity (mg/l as CaCO_3),

SI = Langelier Saturation Index,

Day = days.

The model (Pisigan and Singley, 1985) suggested that increasing chloride, sulphate, alkalinity, and dissolved oxygen would accelerate corrosion, whereas increases in calcium, buffer capacity, saturation index, and exposure time would lead to a decrease in corrosion rate. In this hypothetical equation, the alkalinity was declared to accelerate rather than reduce corrosion, as is commonly known. The authors attributed this contradiction to the overwhelming influence of the increased ionic strength over the effect of alkalinity, with increasing dosages of NaHCO_3 while attempting to raise the alkalinity during the laboratory experiments.

The first use of the buffer capacity (β) appeared in literature pertaining to the subject of corrosion prediction in the work by Stumm (1960). Laboratory tests with

synthetic solutions helped explain the mutual interaction of corrosion stimulating and inhibiting factors of natural waters, namely: pH, buffer capacity, CaCO₃ deposition and alkalinity. This study was thought to at least have partially explained the increase in corrosion rates with increasing pH between the values of 7.0 and 8.5. The buffer capacity equation (Equation 2.11) is given as:

$$\beta = 2.3 \times [((H^+) \times (Alk) / ((H^+) + 2 \times K_2) \times ((H^+) / ((H^+) + K_1) + (K_2 / ((H^+) + K_2)) + (H^+) - (OH^-))] \dots\dots\dots [1.11]$$

where: K1 and K2 = first and second acidity constants for the carbonate system,
 Alk = total alkalinity (eq/l),
 β = buffer capacity (eq/l),
 H⁺ and OH⁻ = hydronium and hydroxide (moles/litre).

Stumm (1960) found that as the pH approaches 8.4, either from a higher or lower pH value, the corrosion rate of cast iron increased with decreasing buffer intensity. It is presumed this effect occurs as a result of there being fewer but larger cathodic and anodic areas, thereby enhancing the electrochemical cell.

Based on the independent studies reported by Pisigan and Singley (1987) and Imran *et al.* (Nov 2005), it was possible to propose a modified Larson ratio (LRM) (Equation 2.12) which would compensate for the increase in total dissolved solids with the addition of alkalinity by the inclusion of the sodium ion concentration:

$$LRM = (((Cl^- + SO_4^{2-} + Na^+)^{1/2} / Alk) \times (T / 25) \times (HRT) \dots\dots\dots [2.12]$$

where: Na⁺ = sodium (mg/l as Na⁺),
 Alk = total alkalinity (mg/l as CaCO₃),
 T = temperature (°C),
 HRT = Hydraulic Retention Time (days).

Imran *et al.* continued their work on potable water distribution systems and in September of 2005 published an article (Imran *et al.*, Sept 2005) which included a wider range of parameters in an empirically derived non-linear model (Equation 2.13):

$$\Delta C = ((Cl^-)^{0.485} \times (Na)^{0.561} \times (SO_4^{2-})^{0.118} \times (DO)^{0.967} \times (T)^{0.813} \times (HRT)^{0.836}) / 10^{1.321} \times (Alk)^{0.912} \dots\dots\dots [2.13]$$

where: Cl = chloride (mg/l as Cl⁻),
Na⁺ = sodium (mg/l as Na⁺),
SO₄²⁻ = sulphate (mg/l as SO₄²⁻),
DO = dissolved oxygen (mg/l as O₂),
T = temperature (°C),
HRT = Hydraulic Retention Time (days),
Alk = total alkalinity (mg/l as CaCO₃).

The model is based on the change in apparent colour (ΔC in chloroplatinate units (CPU)) as a measure of corrosion in distribution lines as it was found to be a reliable surrogate measurement of total iron. Calcium and pH were not deemed significant during the statistical modelling, because all tests were performed in waters stabilized for CaCO₃ solubility. Alkalinity was the only variable that could be effectively controlled by chemical addition.

In the arena of oil-field brines, where the high salinity affects the ionic strength and influences the calcium carbonate solubility the Stiff-Davis Index (SDI) has been used (Stiff and Davis, 1952) in place of the Langelier Index. Waters with total dissolved solids levels higher than 4000 mg/l require that the SDI (Equation 2.14) is used:

$$SDI = pH - pCa - pAlk - K \dots\dots\dots [2.14]$$

where: SDI = Stiff-Davis Index (positive value indicates scale formation
 whereas a negative value indicates corrosion),
 pH = measured pH,
 $pCa = -\log (Ca)$, Ca = calcium (mg/l as Ca^{2+}), and
 $pAlk = -\log (M \text{ alkalinity})$, M alkalinity (mg/l as $CaCO_3$),
 K = constant based on the total ionic strength and temperature.

The Stiff-Davis (Stiff and Davis, 1952) method is one of the easiest ways to calculate calcium carbonate scaling tendencies (Calcite Saturation Index) in brines and it is valid for temperatures from 0–90°C and ionic strengths from 0–4. This index does not take into account the pressure and carbon dioxide concentration. It requires that the pH is measured on a fresh sample to avoid inaccuracies. As ionic strength or the temperature increase, so the K value decreases, resulting in a higher SDI, indicating a higher calcium carbonate scaling tendency. Higher concentrations of calcium or alkalinity would also lead to higher SDI values, also resulting in increased scaling tendencies. Calculating the SDI requires a calculation of the ionic strength, knowing the temperature of the operation and looking up the K value in a K versus ionic strength graph.

The Oddo-Tomson (1982) equation (Equation 2.15) is an alternative index applicable to high ionic strength waters for predicting the formation of calcium carbonate and various sulphate scales. It is valid between temperatures of 0–200°C, ionic strengths of 0–4.0, and pressures of 1–1380 bar (0-20000 psig).

$$I_s = \log (T_{Ca} \times A_{lk}) + pH - 2.78 + 1.143 \times 10^{-2} \times T - 4.72 \times 10^{-6} \times T^2 - 4.37 \times 10^{-5} \times P - 2.05 \times I^{1/2} + 0.727 \times I \dots\dots\dots [2.15]$$

where: I_s = Oddo-Tomson index (positive value indicates scale formation
 whereas a negative value indicates corrosion),
 T_{Ca} = calcium (mg/l as Ca^{2+}),
 A_{lk} = bicarbonate (mg/l),
 T = temperature (°F),

pH = measured pH,
P = pressure (psi),
I = ionic strength (moles /litre).

The calculation was reported by Oddo and Tomson (1982) to be accurate at high and low temperatures and pressures. The calculation can be easily performed in the field and is said to work well when applied to geopressured wells.

The prediction of the corrosivity of underground minewaters towards mild steel was also explored by White and Higginson (1985). It was reported that the corrosion took place under cathodic control, with the metal acting as a substrate for the cathodic reaction. Thus the corrosivity of minewaters is largely dependent upon on the oxygen concentration and the pH of the water. This is of course without consideration to localized corrosion such as differential corrosion or microbiologically-induced corrosion.

2.8 Impact of Fluoride

The remaining parameter relevant to steel mill brackish water that has not been dealt with thus far is the fluoride concentration. The following is a review of the literature pertaining to the impact of fluoride on corrosion of mild steel in aqueous environments.

The Cartledge electrostatic hypothesis as confirmed by Rostron (1979a) provided an approximate correlation between molecular structure and the tendency of the molecule to sustain or destroy the passive state of mild steel. The passivity destroying efficacy of monatomic anions was found to correlate with the charge density of the anions, provided there is no hydrogen bonding or chromic oxide film. The tests were done with various aqueous solutions at 18°C to 20°C. Contrary to the expected order of passivity destruction: $S^{2-} > F^- >> Cl^- > Br^- > I^-$, it was revealed that due to the strong hydrogen bonding between fluoride and water the attraction between fluoride and the passive iron surface was weakened relative to the other halides (Rostron, 1979b). The redox potential, influenced by the addition of various

oxidants, for example ferricyanide, was also found to influence the passivity destruction which was particularly noticeable with chloride at the higher potentials (0.4 V to 0.7 V). The impact decreased with a lowering of the potential (0.15 V to 0.35 V).

Electrochemical and surface analytical studies performed by Strehblow, Titze and Löchel (Strehblow *et al.*, 1979) (Löchel and Strehblow, 1983) showed that, in the presence of fluoride (0.1 M HF) at 25°C, the breakdown of passivity of iron (99.98%) occurred in the presence of both weakly acidic solutions ($\text{pH} \geq 5.5$) and alkaline solutions buffered to pH 8 (0.05 M H_3BO_3 + 0.039 M KOH) but homogenous attack occurred on the surface in strongly acidic solutions ($\text{pH} < 5.5$). It was proposed that with increasing pH, the effect of fluoride on the dissolution of the passive layer was less pronounced. Ring-disc electrode tests were performed to give insight into the electrochemical reactions and their mechanisms by detection of intermediate and reaction products occurring during the fluoride attack of passive iron in non-stagnant conditions. It was found that the fluoride attack occurred in possibly three stages. In the first stage the fluoride increased the passive current density and the production of Fe^{3+} ions. In the latter two stages, there was a temporary breakdown of the passive layer, releasing Fe^{2+} ions, followed by a “decisive change” in the physical or chemical structure of the passive layer causing permanent general Fe^{2+} dissolution resulting in high current densities and severe surface attack.

According to Singh *et al.* (1981), small amplitude cyclic voltammetry produced fairly good agreement with the weight loss technique in terms of corrosion rates and corrosion inhibition. The corrosion tests were performed with sodium fluoride solutions on mild steel (ASTM 212 steel) for concentrations up to 2%, in contact with air and the resulting corrosion rates ranged between 0.09 mmpa and 0.16 mmpa. The maximum corrosion rate of 0.16 mmpa was recorded at a fluoride concentration of 1%. In oxygen saturated solutions the corrosion rates increased to as high as 1.27 mmpa and when the solutions were saturated with nitrogen the corrosion rates decreased to approximately 0.02 mmpa. Sodium chromate was

found to effectively inhibit mild steel corrosion. Up to nearly 90% inhibition could be attained with 800 ppm of sodium chromate.

Mayer *et al.* (1984) demonstrated that fluoride containing solutions were only slightly less aggressive towards mild steel than equivalent chloride containing solutions, which implies that the fluoride ion may be considered to be relatively corrosive. The relative corrosiveness of the anions in aqueous solutions at 300°C followed the same sequence as the pH of the solutions at 25°C: $\text{HCl} = \text{FeCl}_3 \geq \text{HF} \geq \text{FeF}_3 \geq \text{NiCl} > \text{NiF}_2$. Even when fluoride concentrations in boiler water may be as low as 0.01 ppm it was found that concentrations in the boiler internal porous magnetite deposits reached levels as high as 4000 ppm. Preventing narrow crevices at poor tube-to-tube contact and removing porous deposits as well as preventing low pH levels was proposed to avert the fluoride accelerated acid-type corrosion of boilers.

Potentiostatic and potentiodynamic tests performed with mild steel in neutral buffered solutions at 25°C showed that the fluoride ion was able to produce pitting at potential values lower than other halides and that the presence of fluoride ions completely destroyed the passivity of mild steel (1020 SAE Steel) due to the formation of a soluble complex between the ferric and fluoride ions (Moll *et al.*, 1985). The breakdown potential depended linearly on the logarithm of the NaF concentration.

Tests performed by Vasil'eva *et al.* (1986) with a water containing: 610 mg/l Ca^{2+} , 15.2 mg/l F^- , 480mg/l SO_4^{2-} , 16.4 mg/l PO_4^{3-} (as P_2O_5), pH 8.6, demonstrated a reduction in corrosion rate of mild steel (St. 3) when the temperature was raised from 30°C to 70°C. The reduction in corrosion rate was reported to be due to the deposition of calcium fluoride and phosphate. A second stage of testing, performed at 30°C with varying sulphate concentrations, showed that higher sulphate concentrations resulted in higher mild steel corrosion rates. At 7.2 mg/l P_2O_5 and 11.3 mg/l F^- , the increase in sulphate concentration from 1212 mg/l to 2592 mg/l, as SO_4^{2-} , resulted in a doubling of the corrosion rate from 0.02 mmpa to 0.04 mmpa

in the presence of agitation. It was also found that the agitated test solutions resulted in significantly lower mild steel corrosion rates. A test solution without agitation produced a corrosion rate of 0.07 mmpa, whereas an agitated solution resulted in a mild steel corrosion rate of 0.02 mmpa.

A statistical model was proposed by Raingevars *et al.* (1989) based on the corrosive behaviour of carbon steel (St. 3) in ammonium fluoride. A polynomial equation (Equation 2.16) was found, by multifactor regression analysis, to provide the best approximating function for the variables: pH, ammonium fluoride concentration and time. The range of conditions investigated were for pH: 5.8 to 6.9, an ammonium fluoride concentration of between 0.2 M and 10 M, at 20°C, and a period of 20 hours to 700 hours. In summary then, as the ammonium fluoride concentration increased so the pH of the solution increased and the corrosion rate decreased. The mean deviation between the calculated corrosion rate and the experimental results was 8%.

$$Y^{\text{theor}} = b_0 + b_1x_1 + b_2x_2 + b_3/x_3 + b_4x_1x_2 + \dots \dots \dots [2.16]$$

where: Y^{theor} = St. 3 corrosion rate in g/(m³.h),

x_1 = measured pH,

x_2 = ammonium fluoride concentration (moles /litre),

x_3 = time (hours)

$b_0 = 0.0324 \pm 0.0170$

$b_1 = 7.809 \pm 3.840$

$b_2 = -0.00114 \pm 0.00029$

$b_3 = -332.6 \pm 224.6$

$b_4 = 4208 \pm 3529$

It has been established that fluoride anions can cause pitting of corrugated reinforced steel in alkaline media of high pH (Macias and Escudero, 1994). Saturated lime solutions can precipitate CaF₂ to lower the fluoride concentration to below the minimum level that can promote pitting. In the absence of sufficient

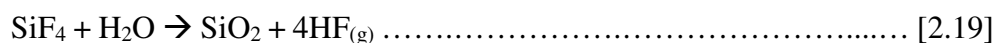
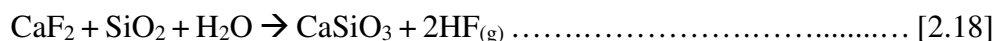
Ca(OH)₂ the residual fluoride can increase passive film dissolution and corrosion rates. The K_{sp} for CaF₂ is 4.0×10^{-11} (Benfield and Morgan, 1990). In addition to the increase in passive film dissolution with fluoride concentration, pitting corrosion was observed at fluoride concentrations higher than 1900 mg/l.

Dillon and Waltman (1995) studied the impact of by-products from certain mould powders on the reduction of the spray water alkalinity with the production of acids. Mould powders generally consist mostly of calcium oxide and silica, with the balance typically including: sodium oxide, fluoride compounds, alumina, and minor quantities of magnesium oxide and carbon. Given that chemical treatment could not be controlled based on the choice and quantity of mould powder used, a preliminary laboratory test procedure was devised to evaluate the effect of mould powders on bulk water alkalinity and corrosivity. It was proposed that raising the alkalinity and pH of the bulk water with: caustic, soda ash or magnesium hydroxide could serve as a method of corrosion control but this treatment option was not substantiated.

In a study on the fluoride induced corrosion of mild steel rebar in contact with alkaline solutions (0.01 N NaOH), Singh *et al.* (2002) found that at less than 25 ppm fluoride had a deleterious effect on the corrosion of steel, whereas at above 100 ppm it had an inhibitory effect on the corrosion rate. At higher concentrations, the ion is expected to react with calcium and form calcium fluoride, which is a sparingly soluble salt.

In 2003, Brell *et al.* identified two types of corrosion damage in the casting chamber. The first was a localized metal loss in the wetted areas of the upper spray chamber, whereas the second showed exfoliation in the humid environment, where there the metal was not in contact with the spray water. They proposed that the pH was lowered when fluoride and silica dissolved into the spray water directly below the mould. The possible high temperature mechanisms of acid production are as given in Equations 2.17 to 2.19.





Since the alkaline species are sparingly soluble and the acidic species (e.g. HF) very soluble, the alkalinity and pH decreased substantially if there was insufficient alkalinity to neutralize the HF (Brell *et al.*, 2003). They proposed that the mould powders affected the quantity of acid generated by:

- Basicity of the mould powder (determined by the ratio of CaO to SiO₂ and which influences the tendency to produce a crystalline structure);
- Solidification temperature of the mould powder (which determines the ratio of solid and liquid slag between the mould and steel); and
- The rate of consumption of the mould powder.

Sodium carbonate was said to be preferable over caustic soda in order to raise alkalinity without excessive increases to the pH (Brell *et al.*, 2003). A minimum total alkalinity of 80 mg/l as CaCO₃ was found to be ideal to minimize acid corrosion. Corrosion rates were seen to decrease from 6.25 mmpa down to between 0.13 mmpa and 0.25 mmpa.

Chemical treatment of the cooling water could therefore be achieved with the addition of either calcium or alkalinity, but preferably with soda ash (Brell *et al.*, 2003). The addition of sufficiently high levels of calcium, with increased temperatures could abate corrosion by removing the fluoride from solution by its precipitation as calcium fluoride (Macias and Escudero, 1994; Brell *et al.*, 2003). According to Brell *et al.* a minimum alkalinity of 80 mg/l as CaCO₃ would be necessary to significantly reduce corrosion.

In the above review of articles pertaining to the role of fluoride in corrosion, it was evident that fluoride impacted on either the general corrosion rate or pitting corrosion (Moll *et al.*, 1985, Macias and Escudero, 1994, Dillon and Waltman, 1995) of mild steel. Mayer *et al.* (1984) confirmed the presence of fluoride in

crevices. It was generally found that the higher the fluoride concentration, the lower the resulting alkalinity and pH, and the higher the corrosion rate.

In summary, it is apparent that although much has been done to attain reasonably accurate predictive tools for the corrosion rates of mild steel in potable water, there are differences in opinion, and more work is needed to predict the corrosivity of fluoride in fresh and brackish water. The key components of a corrosion index applicable to a fluoride containing brackish cooling water are:

- Varying ionicity of the solution;
- Elevated temperatures (i.e. 40°C to 60°C);
- Capacity to dissolve metal from the inside of pipes (i.e. not just the driving force); and
- Impact of fluoride over the concentration range given earlier.

It is envisioned that this investigation will culminate in an index that will contain the above attributes and possibly resemble Imran's multi variable empirical equation (Imran *et al.*, Sept 2005). The index will be required to predict the corrosivity of brackish water in a steel mill mild steel cooling system.

2.9 Summary of Factors Potentially Affecting Mild Steel Corrosion or Passivation

A summary of the factors and water quality parameters commonly understood to impact on the corrosion of mild steel in cooling water systems include: pH, temperature, flow velocity, dissolved oxygen, calcium hardness, alkalinity, the buffer capacity, organic substances, chloride, sulphate, fluoride, conductivity and suspended solids.

2.9.1 Temperature

As a general rule the rate of most chemical reactions increases with temperature (Flynn and Nalco Company, 2009) however, there are exceptions (Atkinson and Van Droffellar, 1995). Although the diffusion rate of oxygen increases with temperature, thereby further increasing the corrosion rate, due to the reduced

solubility of oxygen in water at elevated temperature the corrosion rate may decrease. Species inversely soluble with temperature, for example calcium carbonate and calcium phosphate, could also lead to a decrease in the corrosion rate with increased temperature.

2.9.2 Flow velocity

The flow velocity of the water affects the oxygen concentration. When oxygen becomes limiting, it results in a decrease in the corrosion rate. The calcium and carbonate ions may also become limiting, thereby also slowing down the precipitation of calcium carbonate at the cathode. Miller and Loewenthal (1982) compared the passivation potential of two water samples with approximately similar chemical compositions and varying flow rates and it was found that only the higher flow rate resulted in passivation after 30 days. According to Brits *et al.* (1998), if there is an adequate supply of calcium, oxygen and alkalinity, higher bulk water flow velocities are likely to lead to higher corrosion rates and increased calcium carbonate precipitation. It was indicated that an increase in the rate of carbonate precipitation improved the likelihood of an impermeable protective layer. At lower flow rates, the calcium carbonate layer consists of larger crystals causing it to be more permeable and therefore less likely to inhibit corrosion. It should however be noted that supersaturation does not ensure passivation and neither does undersaturation necessarily enhance corrosion.

2.9.3 Oxygen

Dissolved oxygen is known to influence the electrochemical cell in primarily two ways. At the anode as the metal is oxidised, it reacts with the oxygen to form passivating oxides, whereas at the cathode it accepts electrons thereby sustaining corrosion. The acceptance of electrons at the cathode results in an increase in the pH due to the formation of hydroxide ions. This elevated pH converts the bicarbonate ions into carbonate ions, facilitating an increase in the carbonate concentration, which in turn increases the rate of calcium carbonate precipitation (Brits *et al.*, 1998).

2.9.4 pH, calcium, carbonate, buffer capacity and humic substances

Baylis (1926) demonstrated the practical benefit of calcium carbonate protection by controlling the pH to values greater than 8. As already known to the water works personnel at the time, there were factors other than pH and the dissolved oxygen concentration that influenced corrosion (Baylis, 1926). At near-neutral pH conditions ($5 < \text{pH} < 9$) the pH does not have the same direct impact it has on the oxide and hydroxide layers as at low pH (< 5), but it can still affect these layers by impacting on the anions present in the solution, such as sequestering agents. The reduction of oxygen is the most important reaction resulting in the passivation of the iron as magnetite (Silverman and Puyear, 1987).

An increase in alkalinity generally results in a lowering in the mild steel corrosion rate (Hedberg and Johansson, 1987). Together with high concentrations of calcium, the carbonate at the cathode will tend to form an impermeable microcrystalline monolayer. At the anode, there are three ways in which the carbonates are involved: a) Dissolved carbonate reduces the impact of aggressive anions (i.e. chloride and sulphate) (Evans, 1981), b) Bicarbonate and carbonate ions act as a reservoir of hydroxide ions to facilitate the formation of ferrous and ferric hydroxides and oxides, and c) carbonate can react with ferric ions to form ferric carbonate which can form the protective calcium carbonate or magnetite film with time (Stumm, 1960).

Stumm (1960) related the passivation of iron to the buffer capacity (β) which was described as the moles/l of strong base required to effect a unit change in pH. The higher the buffer capacity, the smaller the pH difference between the anode and cathode and the larger the number of small cathodic and anodic regions, thereby resulting in passivation. Poor passivation would result due to a lower buffer capacity wherein there is a small number of large cathodic and anodic regions. The opposite to this effect was found in the study by Sander *et al.* (1997), who found that under stagnant conditions the iron coupons showed higher weight losses with increasing buffer capacity.

Additional factors affecting the formation of calcium carbonate on the metal surface were investigated by various authors: Larson (1975), Campbell (1980) Sontheimer *et al.* (1981) and Campbell and Turner (1983). It was found that the presence of certain humic substances, at greater than 0.6 mg/l, lead to the precipitation of calcium carbonate at the cathode resulting in a decrease in the size of the cathodic area and polarization of the cathode.

2.9.5 Magnesium

Magnesium carbonate, like calcium carbonate deposits, form part of the corrosion product layer which regulates the supply of oxygen to the corroding surface (Uhlig, 1963).

2.9.6 Chloride and sulphate

Evans (1981) explained the generally accepted behaviour of chloride and sulphate ions on mild steel. It was stated by Evans (1981) that these aggressive ions are adsorbed onto the anodic surface displacing water, oxygen and hydroxide species and allowing for the release of ferrous ions into the bulk solution and therefore preventing the development of an oxide film and passivation of the metal surface. As early as 1927 it was observed that bicarbonate and carbonate species reduce the corrosive impact of chloride and sulphate (Evans, 1981) by displacing them in the anodic areas.

According to Degrémont (1991), the high concentration of chloride ion in a low pH anodic zone prevents the local precipitation of iron hydroxide by forming hydrochloric acid, thereby resulting in severe corrosion. In the absence of oxygen a chloride containing water may only be mildly corrosive if the water has sufficient alkalinity, as with sea water (Degrémont, 1991). In the presence of oxygen, such water may become extremely corrosive with increasing chloride concentration. Sulphates are also known to increase corrosion directly through the increase in conductivity (Degrémont, 1991).

2.9.7 Fluoride

As discussed in the earlier sections, fluoride can concentrate in and therefore accelerate under-deposit or crevice corrosion, especially under acidic conditions (Mayer *et al.*, 1984; Moll *et al.*, 1985; Dillon and Waltman, 1995). It will generally be more corrosive in oxygen/aerated water (Singh *et al.*, 1981). Deoxygenating the bulk water will decrease the corrosivity of the fluorides. The higher the fluoride concentration the higher the resulting mild steel corrosion rates (Moll *et al.*, 1985). Fluoride levels can be decreased in the presence of sufficiently high levels of calcium due to the precipitation of calcium fluoride, which is reported to inhibit corrosion (Macias and Escudero, 1994). Chromate has also been reported to successfully inhibit fluoride induced corrosion (Singh *et al.*, 1981).

2.9.8 Conductivity

The impact of conductivity on corrosion is complicated, for it depends on the species involved. Higher levels of bicarbonate and carbonate tend to decrease the corrosion rate, while higher concentrations of the aggressive ions tend to increase corrosion (Flynn and Nalco Company, 2009). Mineralisation of water with as little as 1 mg/l of chloride or sulphate can promote corrosion. Other ions also capable of stimulating corrosion include bromide and nitrate. On the other hand silicate and chromate ions tend to enhance the formation of protective layers (Degrémont, 1991).

2.9.9 Suspended solids

Suspended solids in the cooling water can settle out to form porous deposits, which increase the risk of a localised corrosion in the form of "under-deposit corrosion", as well as provide sites for microbes to colonize, which in turn can lead to elevated corrosion rates (Buckman, 1981). Table 2-5 provides additional support, summarizing water quality parameters considered by the various authors in their compilation of the various scale and/or corrosion prediction indices over the last 77 years.

In addition to the water chemistry parameter discussed and the indices listed in Table 2-5 there are still several additional factors to consider, namely the impact of micro-organisms, disinfectant residual, heavy metals and the use of corrosion inhibitors.

2.9.10 Microbial population and the potential for Microbiologically Induced Corrosion (MIC)

Micro-organisms responsible for Microbiologically Induced Corrosion (MIC) in open recirculating cooling systems include: algae, bacteria and fungi. Their continued reinfection of cooling systems is attributed to their ingress from the air, as airborne spores, or with the makeup water from the usual water sources.

The on-going growth of micro-organisms and their resultant negative impacts on cooling systems depend on the prevailing conditions, namely the water temperatures and pH, and the continued replenishment of the nutrients (Frayne, 1999). In general, most micro-organisms require specific favourable ecologies for optimum growth and survival, and usually cooling systems provide the range of suitable environments, such as aerobic or anaerobic, sunlight or no sunlight, a midrange pH (7.0 - 9.5) and temperature (20 - 45°C). There are numerous ways in which micro-organisms can influence corrosion:

- Creation of differential aeration cells, leading to localized corrosion (Lee *et al.*, 1980);
- Biofilms may take up corrosion by-products (Tuovinen *et al.*, 1980);
- Oxidation of ferrous or reduce ferric ions (Shair, 1975; Okereke *et al.*, 1991);
- Reduction of oxygen by autotrophic nitrification (conversion of ammonia to nitrite) and continued nitrification (conversion of nitrite to nitrate) thereby creating oxygen concentration cells (Larson, 1939);
- Reduction of the localized pH and/or produce corrosive metabolites (Tuovinen *et al.*, 1980).

2.9.11 Disinfectant residual

The use of biocides in cooling systems is a common practice, as it most certainly decreases the tendency for MIC. However, chlorine residuals usually do lead to increased corrosion rates (Pisigan and Singley, 1987; Hoyt *et al.*, 1979) and the impact is greater than that of monochloramine (Treweek *et al.*, 1985). It was found by Pisigan and Singley (1987) that the chlorination of hard water (1.5 mg/l free chlorine) on mild steel after 5 and 11 day tests resulted in corrosion rates that were higher than in the absence of any free chlorine. The tests also suggested that the dissolved chlorine species (HOCl and OCl^-) were more powerful cathodic depolarizers than dissolved oxygen.

2.9.12 Heavy metals (e.g. dissolved copper)

Dissolved copper at concentrations as low as 0.01 mg/l is known to catalyse the corrosion of iron (Hatch, 1955; Cruse, 1971). Hatch reported on the deposition of copper onto ferrous components which resulted in galvanic cells and the increased tendency toward pitting corrosion. It was proposed that the formation of copper deposits from water with low concentrations of dissolved copper was a cumulative process.

2.9.13 Corrosion inhibitors

Corrosion control requires either a change in the metal or a change in the environment of the metal. Changing the metal may sometimes be impractical due to excessive costs or other operational problems. Changing the environment is a widely accepted method of controlling the corrosion in cooling systems.

Controlling the corrosion in a cooling system is usually performed in one of three ways. The first entails the laying down of a protective layer of calcium carbonate by relying on the inherent calcium hardness and alkalinity of the water. This is the approach considered in the use of most of the saturation indices discussed thus far, that is by Langelier (1936), Ryznar (1944), Puckorius and Brooke (1990) etc. The second common method is by removing the oxygen from the water either mechanically or chemically, but this would be impractical for open cooling systems

as they continually receive oxygen from the atmosphere via the cooling towers. The third approach is the addition of corrosion inhibitors.

Table 2-6 lists the various commercially available corrosion inhibitors considered in the treatment of cooling systems. Their typical usage concentrations, as well as their advantages and disadvantages are shown. Corrosion inhibitors are organic or inorganic substances added to water at low concentrations, at milligram per litre dosages, to prevent the corrosion of the metals. The inhibitors are broadly grouped into three categories (Buckman, 1981; Flynn and Nalco Company, 2009): anodic/passivation/reactive inhibitors; cathodic/precipitation inhibitors; and filming inhibitors.

The anodic inhibitors are further grouped into the oxidizers and non-oxidizers. The oxidizers (for example: nitrite and chromate) promote the rapid oxidation of the metal surface, leading to the formation of a protective iron oxide layer and do not require the presence of dissolved oxygen (Buckman, 1981; Flynn and Nalco Company, 2009). The second sub-group of anodic inhibitors is the non-oxidizers (for example orthophosphate), and they function by reacting with a corrosion product, such as Fe^{2+} , to form an insoluble precipitate. Cathodic corrosion inhibitors generally reduce the corrosion rate by forming a barrier or film at the cathode, thereby preventing oxygen diffusion to the cathodic surface, slowing down the cathodic reaction and ultimately the corrosion rate. The third category form a barrier of some kind and it is mostly by adsorption of the inhibitor onto the metal surface. Azoles fall into this category.

continuation of Table 2-5														
Other	Time	F	SO ₄	Cl	Press	Temp	Mg	DO	TDS or Ionicity strength)	M alk	Ca	pH	Index	
						✓			✓	✓	✓	✓	Calcium Carbonate Precipitation Potential (CCPP), (Merrill and Sanks, 1978)	
CO ₂ ⁽⁴⁾			✓	✓						✓	✓	✓	Yahalom Index (Y), (Feigenbaum <i>et al.</i> ,1978)	
					✓	✓			✓	✓	✓	✓	O & T scaling Index (I _s), (Oddo and Tomson, 1982)	
pH _s			θ			θ			θ ⁽¹⁾	✓	✓		Puckorius index (PSI), (Puckorius and Brooke, 1990)	
pH _s , β ⁽⁶⁾	✓							✓			✓		CR (Pisigan and Singley, 1984).	
LSI ⁽⁷⁾	✓		θ			θ		✓	✓	θ	θ	θ	CR4 (Pisigan and Singley, 1984).	
β ⁽⁶⁾ , LSI ⁽⁷⁾	✓		✓	✓		θ		✓	θ	✓	✓	θ	CR8 (Pisigan and Singley, 1984).	
Na, β ⁽⁶⁾ , pH _s , LSI ⁽⁷⁾	✓		✓	✓		θ	✓	✓	✓	✓	✓	✓	CR13 (Pisigan and Singley, 1984).	
	✓		✓	✓		✓			✓ (Na)	✓			Modified Larsons Ratio (LRM) (Imran <i>et al.</i> , 2005)	
ISM ⁽⁸⁾	θ	θ	θ	θ		θ	θ		θ	✓	✓	θ	Calcium carbonate saturation	
ISM ⁽⁸⁾	θ	✓	θ	θ		θ	θ	θ	θ	θ	✓	θ	Calcium fluoride saturation	
Iron, ISM ⁽⁸⁾	θ	θ	θ	θ		θ	θ	θ	θ	✓	θ	θ	Iron carbonate saturation	
ISM ⁽⁸⁾ , PO ₄ , Fe.	θ	θ	θ	θ		θ	θ		θ	θ	θ	θ	Iron phosphate saturation	
ISM ⁽⁸⁾	θ	θ	θ	θ		θ	θ		θ	✓	✓	θ	Calcium carbonate FIME	
ISM ⁽⁸⁾	θ	✓	θ	θ		θ	θ		θ	θ	✓	θ	Calcium fluoride FIME	

continuation of Table 2-5

Notes:

- ø. Light shaded “ø”: A parameter forming part of a calculated parameter declared in the column labeled “Other”.
- ✓. Dark shaded tick: A parameter directly involved in the index indicated.
- 1. Includes a pH of saturation (pH_s) calculation which is based on:
 - a. Temperature adjusted dissociation and equilibrium constants
 - b. Ionic strength corrected calcium and alkalinity concentrations.
- 2. Non-carbonate hardness.
- 3. Temperature corrected.
- 4. CO₂ concentration may be calculated from the total alkalinity and pH. CO₂, total alkalinity, carbonate alkalinity and pH can be calculated on the basis of any two of the four defining a carbonate system.
- 5. P Alkalinity may be extrapolated from a nomograph if the pH and M alkalinity are known.
- 6. Includes a buffer capacity calculation.
- 7. Involves calculating the LSI
- 8. Ion speciation modelling with WaterCycle™ (A product French Creek Software) (WaterCycle, 2012)
- 9. FIME = Free ion momentary excess value calculated using French Creek WaterCycle™ software (WaterCycle, 2012). It is a measure of the capacity for precipitation.
- 10. ISM = Ion speciation modelling

Table 2-6: Standard corrosion inhibitors used in cooling systems (referenced mostly from: Buckman, 1981; Flynn and Nalco Company, 2009 and Frayne, 1999)

Corrosion Inhibitor	pH Range	Concentrations (mg/l)	Advantages	Disadvantages
Amines/Amides (e.g. fatty amines/amides, diamine)	Variable	1-10, 0.01 to 0.1% (m/v) in mineral acid cleaning solutions	Can offer biostat and surfactant properties	Continuous dosing required Can be a nutrient source for biofilm growth
Azole (e.g. Tolyltriazole)	6.0 – 9.0	1 - 3	Protection of various metal	Toxicity to aquatic organisms
Chromate (as CrO_4^{2-})		30- 500	Extremely effective	Highly toxic. No longer used by major treatment companies
Molybdate (as MoO_4^{2-})	7.0 – 8.5	50 – 150, 1.5 - 10 (with phosphonates)	Inhibits pitting corrosion	Costly
Nitrite (as NO_3^-)	9.0 – 9.5	200 – 1000, High dosages with high chloride or sulphate	Low cost relative to molybdate	Oxidized by nitrifying bacteria and therefore only used in closed systems
Orthophosphate (as PO_4^{3-})	6.5 – 8.5 Less effective at below pH 7.5	5 - 20	Low cost	Can promote eutrophication, Overdosing can precipitate calcium phosphate or iron phosphate Needs divalent cations (Ca, Zn)

continuation of Table 2-6				
Corrosion Inhibitor	pH Range	Concentrations (mg/l)	Advantages	Disadvantages
Phosphonate	7.0 – 9.0	10- 20 Hydroxyphosphonoacetic acid (HPA): 8 -12 as active	Also functions as a scale inhibitor	Some reversion possible
Polyphosphates	6.5 – 8.5	10 - 20	Reversion to orthophosphate can provide corrosion inhibition	Prone to reversion at extreme pH, high temperature or in oxidizing conditions Needs ≥ 50 mg/l calcium hardness
Silicates	6.0 – 9.0	8-15 Higher SiO ₂ to Na ratio required for higher pH.	Low cost.	Continuous dosing necessary
Zinc (as Zn)	6.5 – 7.5, Higher pH if with polymeric stabilizers.	0.5 – 5.0	Low cost.	Prone to precipitation at elevated pH (> 7.5) or in high suspended solids containing water

CHAPTER 3: FIELD STUDIES

3.1 Introduction

Before commencing the laboratory evaluations, it was necessary to collate and analyse the industrial cooling water quality data from a steel manufacturer in Southern Africa. A study of the brackish cooling water yielded the most appropriate median water quality data relevant for the test work. These data also revealed the operating ranges of the key parameters suspected to have had an impact on the corrosion of mild steel as monitored by means of corrosion coupons. The initial analytical work was performed by a Buckman Africa operated customer based laboratory, Laboratory A, for which the materials and equipment is listed in Table 3-1. The two licensed software programs are held by Buckman on behalf of the author. The cooling water computer modelling program used to predict the various saturation and engineering indices, WaterCycleTM was obtained from French Creek Software, Inc., USA. The statistical software program, Minitab[®] is licensed from Minitab Inc.

3.2 Materials and Methods

In order to first understand the corrosivity of the brackish water in the two open recirculating cooling water systems at the steel manufacturer, it was necessary to first examine the water chemistry data provided by Laboratory A, the onsite customer based laboratory. These data are shown in Appendices A and B for Open Cooling Systems One and Two respectively. The data was collated for the period 3 March 2009 to 25 March 2011, and the tests were performed four times per week for each cooling system. In order to correlate the water chemistry with the corrosion rate, the monthly mean for each water chemistry parameter was compared against the corresponding monthly mild steel corrosion coupon result. The mean of the parameter was chosen over the median as it was more representative of any outliers that may have impacted the coupon corrosion rate during its 30 days in the cooling

system. Table 3-1 lists the equipment used to analyse for the various water chemistry parameters.

Table 3-1: Laboratory A equipment and software

Materials and Software	Tests parameters
1. Inductively Coupled Plasma Optical Emission Spectrometry (ICP-OES) (Perkin Elmer Thermo iCap 3300) (ISO 17025:2005 accredited))	Aluminium, calcium, iron, magnesium, ortho phosphate, potassium, sodium, sulphate, silica, zinc
2. Potentiometric titrator (Metrohm 785 DMP Titrino) extended with an 856 Conductivity module and an 8567 pH module	pH, phenolphthalein alkalinity, total alkalinity, conductivity
3. Photometric (Aquakem™ 250 Photometric Analyser) Test methods: a) Ammonia: Salicylate and Dichloroisocyanurate b) Chloride: Mercuric thiocyanate and ferric nitrate c) Fluoride: Alizarin fluorine blue, acetate buffer and ferrous nitrate d) Nitrate and nitrite: sulphanilamide and N-1-naphthylethylenediamine dichloride	Ammonia, chloride, fluoride, nitrate, nitrite
4. Gravimetric. Labcon forced circulation oven and Ohaus GA 200D or Shimadzu AY120 electronic balances	Suspended solids, oil
5. Mild steel corrosion coupons (C1010) and corrosion coupon rack (ASTM D2688-90, 2011) Cleaning solutions: a) Inhibited hydrochloric acid (1% (m/v) Armohib 28) b) Sodium carbonate (5% (m/v)) c) Ethanol (absolute)	General corrosion rate
6. WaterCycle™ (Version 7.00W2) (French Creek Software, Inc., USA). Cooling water computer modelling software	Computer modelling of indices, saturation rates and free ion momentary excess values
8. Minitab 16® (Version 16.2.3) and later Minitab 17.0® (Licensed from Minitab Inc.) Statistical analysis software	Statistical analysis of data

Laboratory A employed its own in-house methods (Table 3-1) of which only the ICP method was ISO/IEC 17025:2005 accredited. The inductively coupled plasma spectrometer was used for detecting the concentrations of aluminium, calcium, iron, magnesium, ortho phosphate, potassium, sodium, sulphate, silica, and zinc in the routine cooling tower samples. Potentiometric titrations were performed to determine the total and phenolphthalein alkalinities with a 0.05N nitric acid as the titrant.

The test for suspended solids was performed by filtering a suitable volume of the water sample, between 100 and 500 ml, using a pre-weighed Whatman grade 1 filter paper (or equivalent). The filter paper and the solids were then oven dried, at 105°C for an hour, allowed to cool to ambient temperature in a desiccator, and weighed on the four digit laboratory balance. The mass of the solids was determined by difference and expressed on the basis of the sample volume.

The oil content was determined by extracting a given volume of a water sample with 100 ml of petroleum ether (40-60°C, Analytical Reagent grade) and the oven dried solvent extractable matter determined gravimetrically, similar to the oven drying, cooling and weighing procedure performed in the suspended solids analysis.

The relative corrosivity of the cooling water of the two open recirculating cooling systems was determined using mild steel (C1010) coupons supplied by Metal Samples in the USA. These mild steel coupons were similar in composition to the piping metallurgy (API 5L Gr B and SABS 719 Gr A) of the cooling systems. The corrosion coupons were located in the middle of the flow in cooling water piping at the same velocity as is common in the cooling system. ASTM D2688-90 (2011) was followed. The coupon rack fluid velocity was kept at approximately 1.5 m/s by means of a suitable flow control device installed on the leaving side of the test rack. Corrosion coupon racks were installed on the hot water return to the cooling towers where they were used to house the coupons for the duration of their 30 day exposure. Thereafter, the coupons were then removed, cleaned and weighed and the corrosion rates calculated based on their weight loss. The coupon cleaning method

followed was in accordance with ASTM G1-90 (1999): Standard Practice for Preparing, Cleaning, and Evaluating Corrosion Test Specimens. The cleaning procedure entailed an initial light brushing followed by a chemical cleaning with three chemical cleaning solutions (Table 3-1). The coupons were sequentially immersed into each cleaning solution for 30 seconds prior to oven drying at 105°C for 30 minutes and then weighed once cooled to room temperature.

WaterCycle™ (Version 7.00W2) was used to calculate the various indices, saturation rates and free ion momentary excess values for the two cooling systems based on their respective water chemistries, Appendices A and B for Open Cooling Systems One and Two respectively. The additional indices were calculated based on the equations given in Appendix F and the results of the modelling for each cooling system are reported in Appendices D and E.

A licenced statistical analysis software, Minitab 16® (Version 16.2.3), was used to statistically correlate the monthly averaged water chemistry and indices against the monthly cooling system corrosion coupon data.

3.3 Results

Tables 3-2, 3-3 and 3-4 provide a statistical overview of the cooling system water chemistry common to both open recirculating cooling systems and the monthly mild steel coupon corrosion rates for each system respectively. A comparison of detailed statistics of the two system (Tables 3-2 and 3-3) showed that Open System One generally had relatively higher values, except for the iron concentration. Figure 3-1 depicts the correlation in the corrosion rates of the two systems and the seasonal fluctuations. Figure 3-2 are the histograms of the monthly mild steel coupon corrosion rates in mmpa from the two open systems. Both Figures 3-1 and 3-2 demonstrated moderately positive correlations between the corrosion rates of the two systems.

The Spearman rho for Open System One (CWS 1 (mmpa)) and Open System Two (CWS 2 (mmpa)) was 0.460 with a p value of 0.041. A regression analysis of the two sets of corrosion data produced an R^2 of 19% (Figure 3-3).

The histograms Figure 3-2 tended towards normal distributions with either one or two outliers, thereby resulting them in being slightly right skewed. Both the mean and median coupon corrosion rates of Open System One were significantly higher than those of Open System Two. The data presented for Open System Two would have been a tighter cluster if it was not for Open System Two's outlier value of 1.11 mmpa recorded for July 2010 which was deemed to be due to a process related contamination, possibly oil or high fluoride levels.

Table 3-2: Statistical analysis of the cooling water chemistry from Open System One for the period June 2009 to February 2011 (Buckman, 2012b)

Variable	Units	Mean	Standard Deviation	Minimum	First quartile	Median	Third quartile	Maximum
pH		7.8	0.3	7.4	7.6	7.8	8.0	8.3
Conductivity	μS/cm	4886	924	3000	4295	4935	5468	7412
Ionic Strength	molarity	0.066	0.014	0.039	0.057	0.065	0.075	0.102
Sodium	mg/l as Na	1006	205	638	870	1007	1111	1632
Calcium	mg/l as Ca	81	20	47	66	75	95	120
Magnesium	mg/l as Mg	27	9	17	21	24	34	46
Iron	mg/l as Fe	0.37	0.11	0.20	0.28	0.34	0.48	0.57
Total alkalinity	mg/l as CaCO ₃	124	38	68	92	119	151	204
Chloride	mg/l as Cl	794	202	417	627	796	935	1312
Sulphate	mg/l as SO ₄	1143	277	618	952	1141	1400	1776
Fluoride	mg/l as F	72	16	41	61	74	83	97
Phosphate	mg/l as PO ₄	4.5	2.4	0.7	2.7	4.7	6.0	9.2
Zinc	mg/l as Zn	1.0	0.5	0.3	0.6	0.9	1.2	2.4
Silica	mg/l as SiO ₂	19	5	9	17	19	20	28
Aluminium	mg/l as Al	0.4	0.2	0.1	0.2	0.4	0.6	1.0
Oil	mg/l	1.3	0.5	0.7	0.9	1.2	1.6	2.8

Table 3-3: Statistical analysis of cooling water chemistry for Open System Two for the period June 2009 to February 2011 (Buckman, 2012b)

Variable	Units	Mean	Standard Deviation	Minimum	First quartile	Median	Third quartile	Maximum
pH		7.5	0.3	6.9	7.3	7.6	7.6	8.2
Conductivity	μS/cm	4229	877	2804	3546	4267	4990	5813
Ionic Strength	molarity	0.0557	0.0117	0.0374	0.0455	1.149	1.614	2.818
Sodium	mg/l as Na	821	182.1	501.8	674.2	795.8	967.4	1184.4
Calcium	mg/l as Ca	66	16	45	55	62	72	104
Magnesium	mg/l as Mg	25	7	13	20	23	29	44
Iron	mg/l as Fe	0.64	0.41	0.16	0.34	0.49	0.88	1.54
Total alkalinity	mg/l as CaCO ₃	115	41	35	102	114	135	219
Chloride	mg/l as Cl	722	196	400	569	762	894	1020
Sulphate	mg/l as SO ₄	955	226	674	747	896	1130	1367
Fluoride	mg/l as F	42	17.2	6.2	30.7	38.2	59.0	70.2
Phosphate	mg/l as PO ₄	1.6	0.8	0.6	0.9	1.4	2.3	3.4
Silica	mg/l as SiO ₂	19	5	9	16	19	20	28
Aluminium	mg/l as Al	0.5	0.2	0.1	0.2	0.4	0.6	1.0
Oil	mg/l	1.3	0.5	0.7	1.0	1.1	1.6	2.8

Table 3-4: Statistical analysis of the open system mild steel coupon corrosion rates (in mmpa) for the period June 2009 to February 2011

Variable	Open System One	Open System Two
Mean	0.42	0.30
Standard Deviation	0.22	0.22
Minimum	0.10	0.08
First quartile	0.24	0.15
Median	0.40	0.27
Third quartile	0.56	0.36
Maximum	0.80	1.11
Range	0.70	1.03

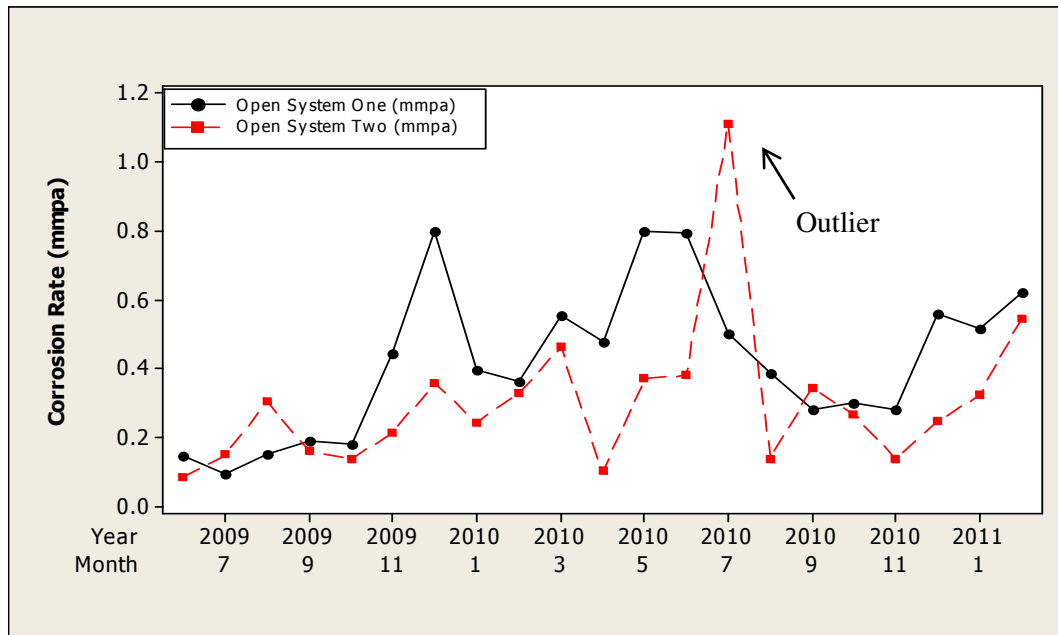


Figure 3-1: Time series plot of Open System One and Open System Two monthly coupon corrosion rates (Buckman, 2012b)

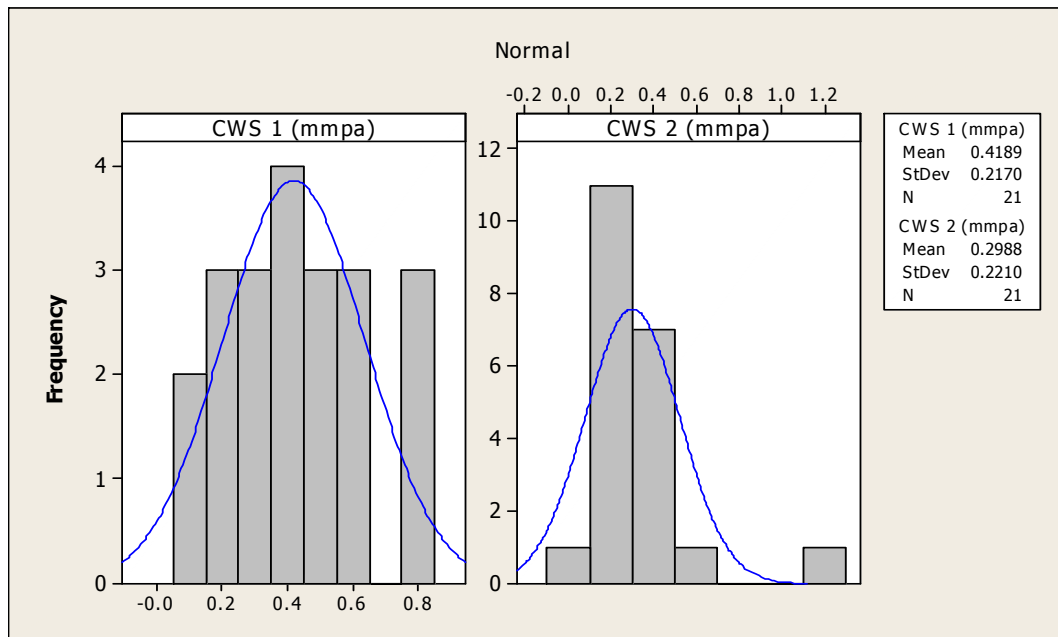


Figure 3-2: Histograms of: a) Open System One monthly coupon corrosion rate and b) Open System Two monthly coupon corrosion rate

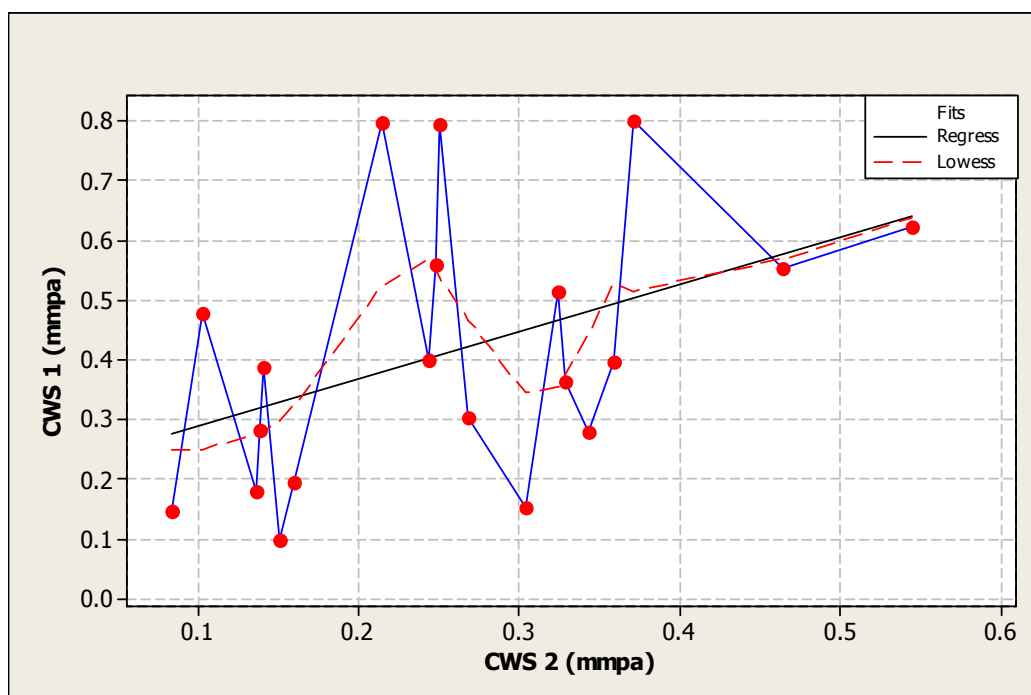


Figure 3-3: Scatterplot of Open System One versus Open System Two with regression line ($R^2= 19\%$)

Figure 3-4, the scatterplots of the coupon corrosion data for Open System One versus the parameters monitored, illustrates the lack of correlations that may have existed. Figure 3-5 is a similar correlation matrix for Open System Two (without the outlier). Mild steel corrosion coupon data taken from the Open System One cooling system was then compared against various predicted corrosion rates or corrosion tendencies on the basis of the water chemistries reported.

The literature derived indices (Tables: D-1 and D-2) (Appendix D) considered in this survey included the following relevant to corrosion, at slightly elevated temperature (45°C) and pressure (4 bar):

- Langelier Saturation Index
- Buffer Capacity
- Calcium Carbonate Precipitation Potential (CCPP)
- Oddo and Tomson Index (O&T)
- Stiff and Davis Index
- Ryznar Stability Index
- Practical(Puckorius) Scaling Index
- Larson-Skold Index
- pH_s (pH of saturation)
- C4 and C8 (4 and 8 variable corrosion rate equations)
- Saturation levels and Free Ion Momentary Excess (FIME) for various scale forming species, e.g. calcium carbonate.

Figure 3-6 is a scatterplot matrix for Open System One where the coupon corrosion data was correlated against the commonly used indices (Tables C-1 and C-2). Pearson correlations and p values were then calculated, using Minitab[®] to determine if there were any linear relationships between the calculated indices and the corrosion rates for each system (Tables 3-5 and 3-6). Regression equations, Equations 3.1 and 3.2 were then formulated for the two systems based on their respective water chemistries (Tables 3-7 and 3-8). Figure 3-7 is a scatterplot matrix for Open System Two.

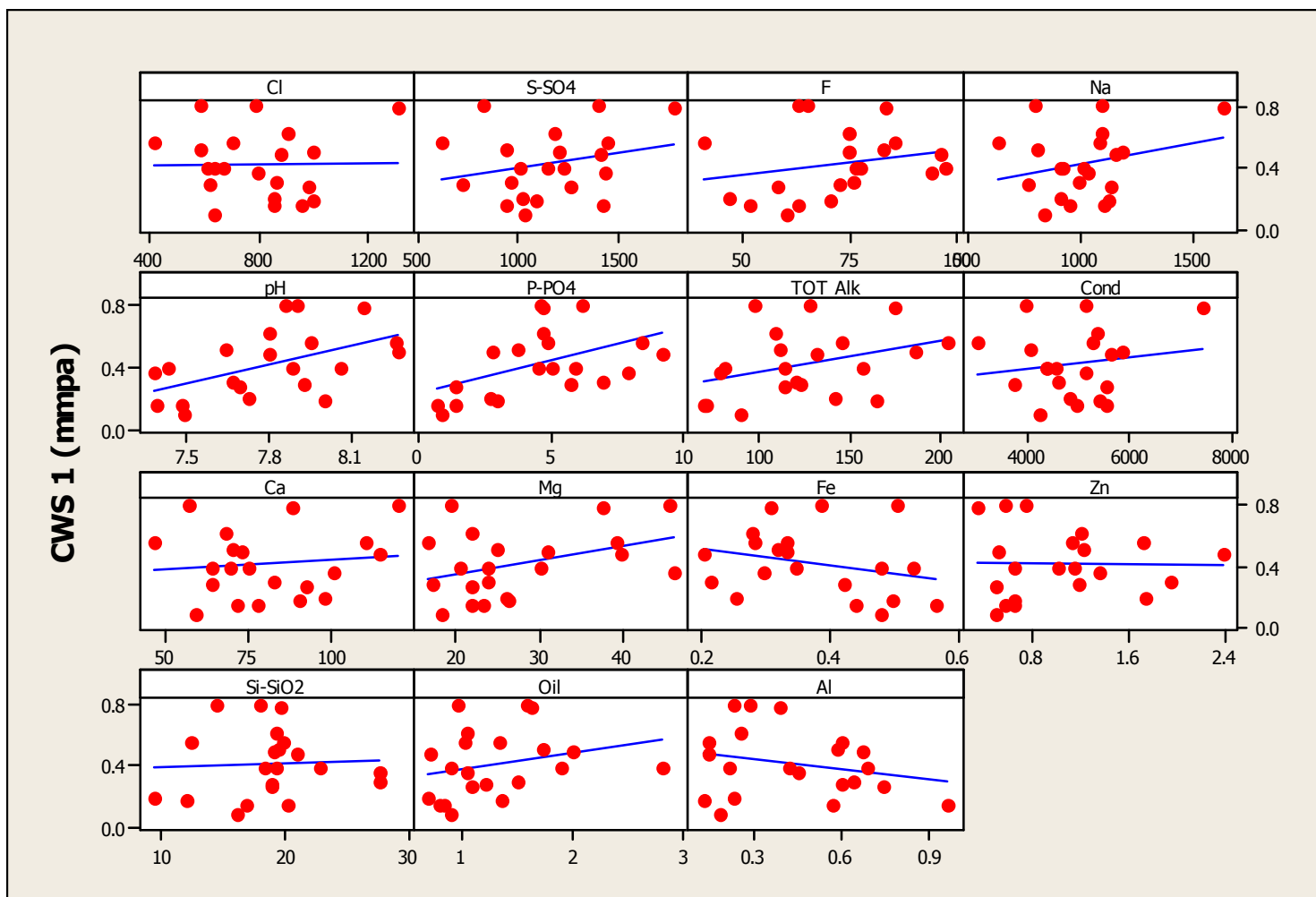


Figure 3-4: Scatterplots of Open System One coupon corrosion rates versus test parameters

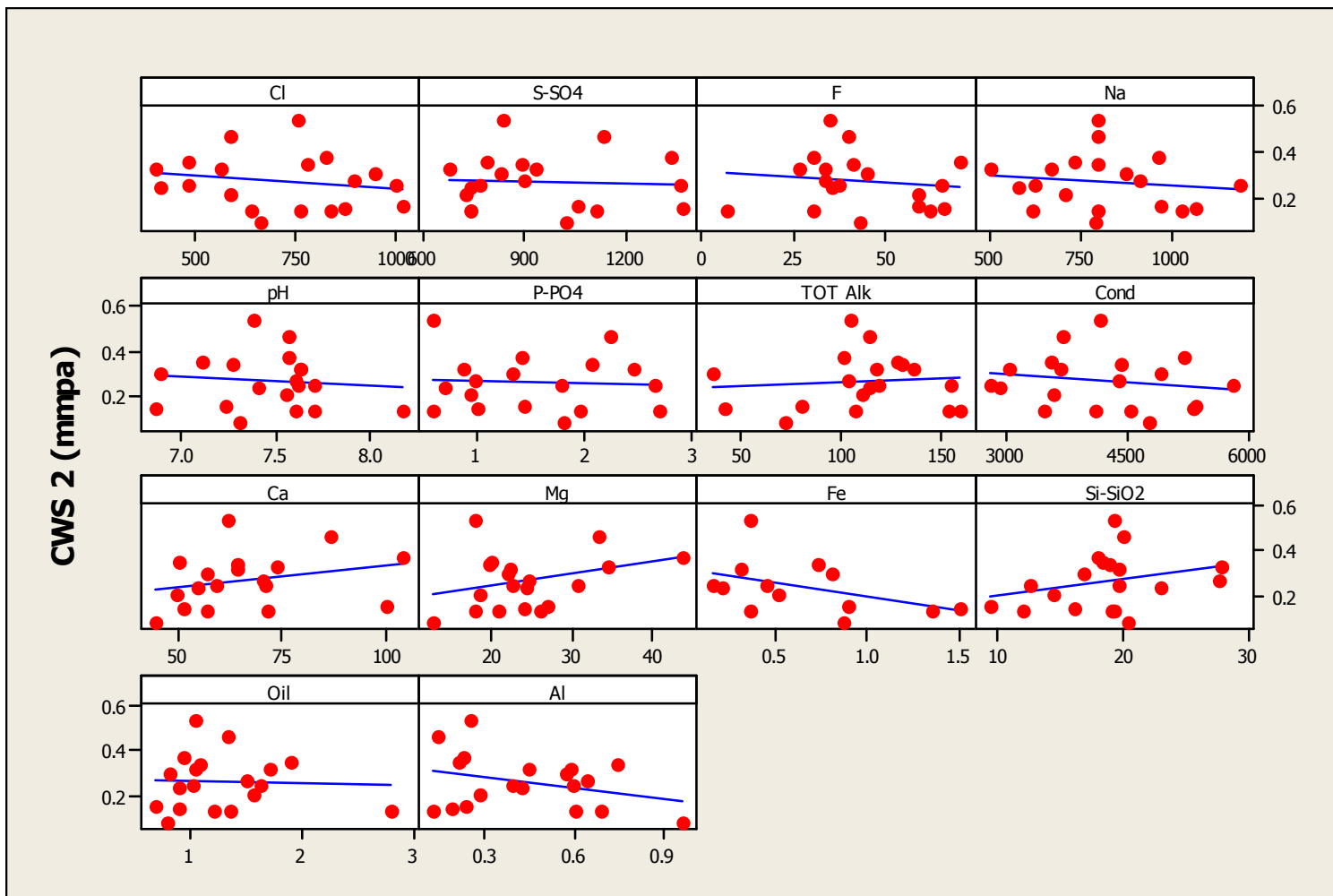


Figure 3-5: Scatterplots of Open System Two coupon corrosion rates versus test parameters (Removed brushed value at July 2010: 1.11 mmpa and single high value outliers for : Ca, Fe and PO₄)

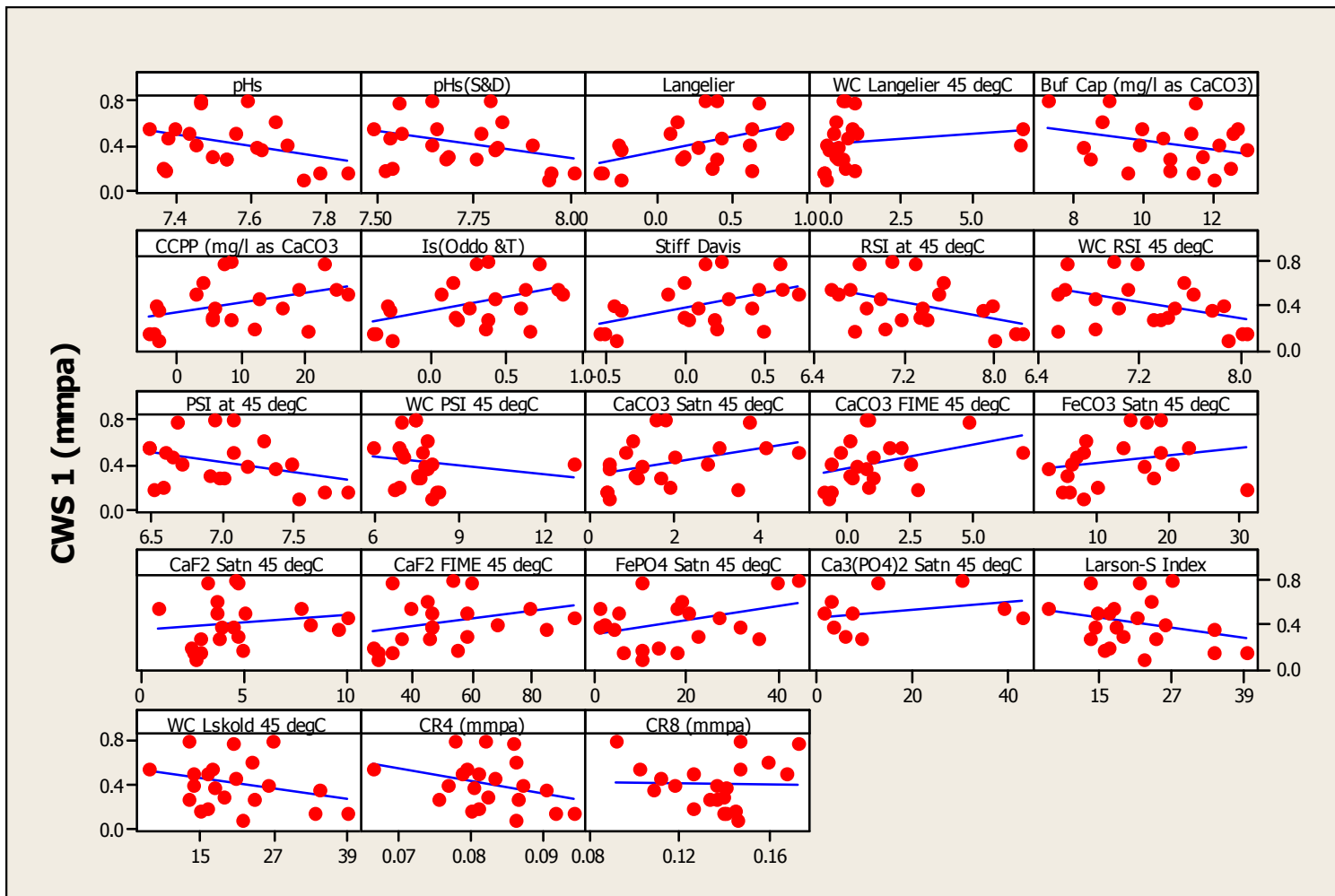


Figure 3-6: Scatterplots of calculated indices versus the Open System One coupon corrosion data

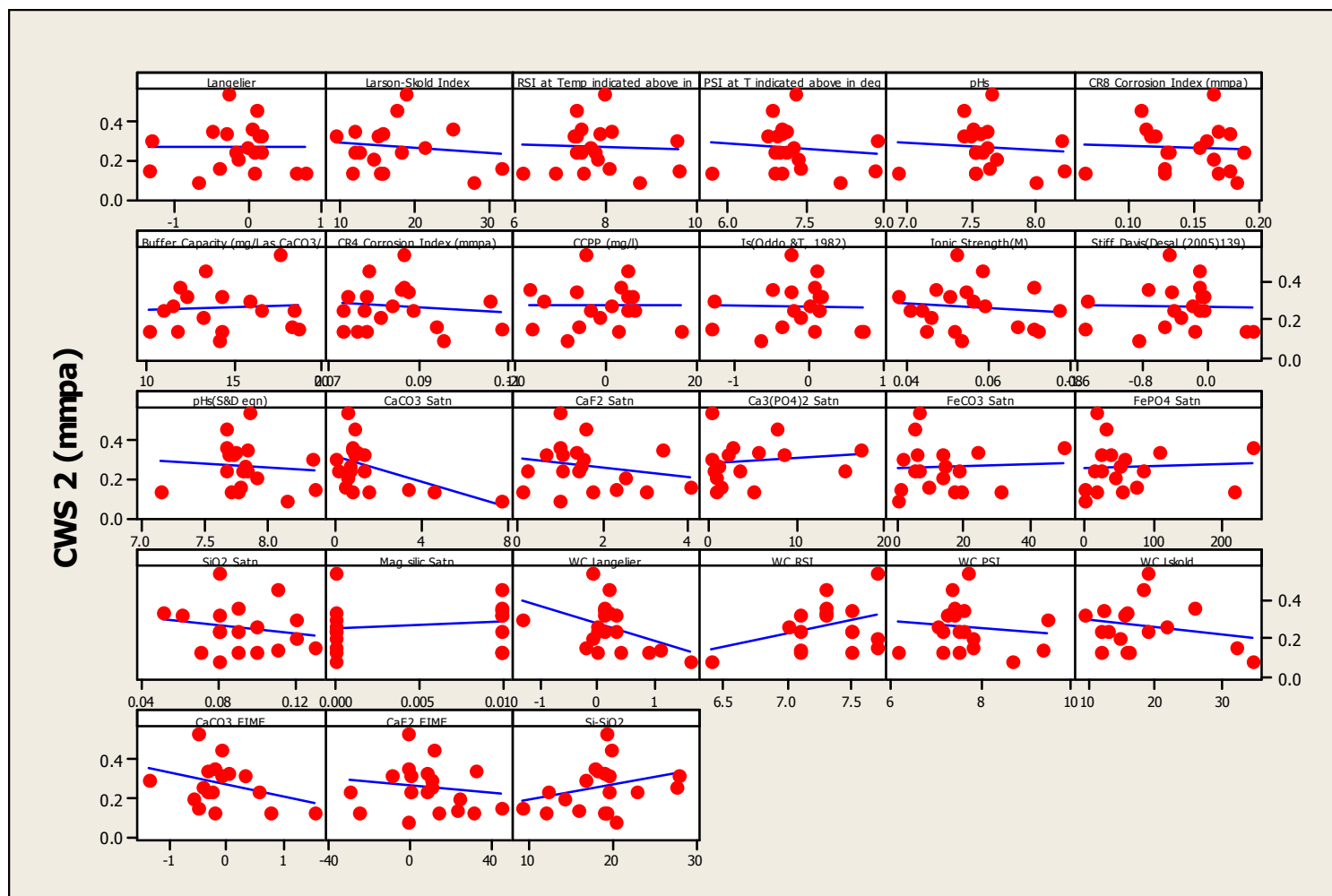


Figure 3-7: Scatterplots of calculated indices versus the Open System Two coupon corrosion data with main outliers removed

Table 3-5: Pearson correlations and p values for the Open System One coupon corrosion rate versus the calculated indices (Appendix D)

Index	<u>First value:</u> Pearson correlation coefficient (r value) <u>Second value:</u> p value	Comments regarding the direction and strength of the correlation
pHs	-0.337	Weakly negative
	0.135	Significantly different (i.e. > 0.05)
pHs (S&D)	-0.339	Weakly negative
	0.133	Significantly different
Langelier	0.482	Moderately positive
	0.027	Not significantly different (i.e. < 0.05)
WC Langelier	0.172	Weakly positive
	0.456	Significantly different
Buffer Capacity	-0.319	Weakly negative
	0.159	Significantly different
CCPP	0.407	Moderately positive
	0.067	Significantly different
Is (Oddo)	0.478	Moderately positive
	0.028	Not significantly different
Stiff Davis	0.484	Moderately positive
	0.026	Not significantly different
RSI	-0.453	Moderately negative
	0.039	Not significantly different
WC RSI	-0.424	Moderately negative
	0.055	Slightly significantly different
PSI	-0.361	Weakly negative
	0.107	Significantly different
WC PSI	-0.166	Weakly negative
	0.472	Significantly different
WC CaCO ₃ Satn	0.379	Weakly positive
	0.091	Significantly different

continuation of Table 3-5		
Index	r value p value	Comments
WC CaCO ₃ FIME	0.374	Weakly positive
	0.095	Significantly different
WC FeCO ₃ Satn	0.230	Weakly positive
	0.329	Significantly different
WC CaF ₂ Satn	0.150	Weakly positive
	0.518	Significantly different
WC CaF ₂ FIME	0.295	Weakly positive
	0.195	Significantly different
WC FePO ₄ Satn	0.357	Weakly positive
	0.122	Significantly different
WC Ca ₃ (PO ₄) ₂ Satn	0.281	Weakly positive
	0.431	Significantly different
WC Silica Satn	Not determined	Not determined
WC Magnesium silicate Satn	Not determined	Not determined
Larson-Skold	-0.282	Weakly negative
	0.216	Significantly different
WC Larson Skold	-0.283	Weakly negative
	0.214	Significantly different
CR4	-0.332	Weakly negative
	0.142	Significantly different
CR8	-0.006	Weakly negative
	0.979	Significantly different

Notes:

1. WC = WaterCycle™ derived values for comparison to the MS Excel based calculations.
2. Large p value (i.e. > 0.05) indicating the observed correlation is a chance finding.
3. Small p value (i.e. < 0.05) indicating the observed value is not by chance and there is a statistically significant effect by the factor on the response.
4. The Pearson correlation coefficient assesses whether two continuous variables are linearly related. The coefficient will fall between -1 and +1. The closer the absolute correlation is to 1 the more tightly the data points fall on a line. A correlation close to 0 indicates no linear relationship.

Table 3-6: Pearson correlations and p values for the Open System Two coupon corrosion rate versus the calculated indices (Appendix D)

Index	Including Outliers		Excluding Outliers	
	r value p value	Comments	r value p value	Comments
pHs	-0.161	Weakly negative	-0.109	Weakly negative
	0.498	Significantly different (i.e. > 0.05)	0.657	Significantly different
pHs (S&D)	-0.133	Weakly negative	-0.087	Weakly negative
	0.577	Significantly different	0.723	Significantly different
Langelier	0.098	Weakly positive	-0.001	Weakly negative
	0.681	Significantly different	0.996	Significantly different
WC Langelier	-0.334	Weakly negative	-0.434	Weakly negative
	0.150	Significantly different	0.064	Significantly different
Buffer Capacity	0.029	Weakly positive	0.067	Weakly positive
	0.902	Significantly different	0.797	Significantly different
CCPP	-0.030	Weakly negative	-0.004	Weakly negative
	0.900	Significantly different	0.988	Significantly different
Is (Oddo)	0.094	Weakly positive	-0.012	Weakly negative
	0.693	Significantly different	0.960	Significantly different
Stiff Davis	0.082	Weakly positive	-0.016	Weakly negative
	0.731	Significantly different	0.947	Significantly different
RSI	-0.122	Weakly negative	-0.037	Weakly negative
	0.610	Significantly different	0.880	Significantly different

continuation of Table 3-6				
Index	Including Outliers		Excluding Outliers	
	r value p value	Comments	r value p value	Comments
WC RSI	0.222	Weakly positive	0.369	Weakly positive
	0.347	Significantly different	0.145	Significantly different
PSI	-0.168	Weakly negative	-0.118	Weakly negative
	0.478	Significantly different	0.631	Significantly different
WC PSI	-0.166	Weakly negative	-0.117	Weakly negative
	0.484	Significantly different	0.632	Moderately positive
WC CaCO ₃ Satn	-0.445	Moderately negative	-0.521	Moderately negative
	0.049	Not significantly different	0.022	Not significantly different
WC CaCO ₃ FIME	-0.404	Moderately negative	-0.338	Weakly negative
	0.078	Significantly different	0.184	Significantly different
WC FeCO ₃ Satn	0.182	Weakly positive	0.052	Weakly positive
	0.443	Significantly different	0.832	Significantly different
WC CaF ₂ Satn	-0.301	Weakly negative	-0.191	Weakly negative
	0.196	Significantly different	0.434	Significantly different
WC CaF ₂ FIME	-0.245	Weakly negative	-0.132	Weakly negative
	0.298	Significantly different	0.590	Significantly different
WC FePO ₄ Satn	0.140	Weakly positive	0.047	Weakly positive
	0.557	Significantly different	0.852	Significantly different

continuation of Table 3-6				
Index	Including Outliers		Excluding Outliers	
	r value p value	Comments	r value p value	Comments
WC $\text{Ca}_3(\text{PO}_4)_2$ Satn	-0.409	Moderately negative	0.143	Weakly positive
	0.074	Significantly different	0.598	Significantly different
Larson-Skold	-0.305	Weakly negative	-0.156	Weakly negative
	0.190	Significantly different	0.551	Significantly different
WC Larson Skold	-0.328	Weakly negative	-0.218	Weakly negative
	0.159	Significantly different	0.400	Significantly different
CR4	-0.236	Weakly negative	-0.097	Weakly negative
	0.317	Significantly different	0.692	Significantly different
CR8	-0.204	Weakly negative	-0.057	Weakly negative
	0.388	Significantly different	0.817	Significantly different
WC Ionic Strength	-0.315	Weakly negative	-0.120	Weakly negative
	0.176	Significantly different	0.625	Significantly different
WC Silica Satn	0.139	Weakly positive	-0.174	Weakly negative
	0.559	Significantly different	0.491	Significantly different
WC Magnesium silicate Satn	-0.206	Weakly negative	0.177	Weakly negative
	0.384	Significantly different	0.482	Significantly different

Minitab[®] regression analyses were then performed for both Open System One and Two and the respective equations (Equations 3.1 and 3.2) and the statistical data shown in Tables 3-7 and 3-8.

Table 3-7: Minitab® regression analysis for Open System One

CWS 1 (mmpa) = 1.69 - 0.00497 Cl - 0.00371 S-SO4 - 0.00975 F + 0.00618 Na + 0.013 pH + 0.0244 P-PO4 - 0.00879 TOT Alk + 0.000583 Cond - 0.00806 Ca + 0.0457 Mg - 1.72 Fe - 0.047 Zn - 0.0307 Si-SiO2 + 0.0519 Oil - 0.012 Al[3.1]					
where: All the ions are in mg/l except conductivity in µS/cm and total alkalinity in mg/l as CaCO₃.					
Predictor	Coef	SE Coef	T	P	
Constant	1.694	2.448	0.69	0.527	
Cl	-0.004970	0.001084	-4.58	0.010	
S-SO4	-0.0037076	0.0006971	-5.32	0.006	
F	-0.009750	0.003743	-2.61	0.060	
Na	0.006180	0.001256	4.92	0.008	
pH	0.0133	0.3619	0.04	0.972	
P-PO4	0.02444	0.03569	0.68	0.531	
TOT Alk	-0.008792	0.002052	-4.28	0.013	
Cond	0.0005829	0.0003497	1.67	0.171	
Ca	-0.008061	0.004216	-1.91	0.128	
Mg	0.04570	0.01126	4.06	0.015	
Fe	-1.7192	0.3756	-4.58	0.010	
Zn	-0.0471	0.1406	-0.34	0.754	
Si-SiO2	-0.03069	0.01319	-2.33	0.081	
Oil	0.05188	0.05802	0.89	0.422	
Al	-0.0119	0.1492	-0.08	0.940	
S = 0.0764516 R-Sq = 97.5% R-Sq(adj) = 87.9%					
Analysis of Variance					
Source	DF	SS	MS	F	P
Regression	15	0.898182	0.059879	10.24	0.018
Residual Error	4	0.023379	0.005845		
Total	19	0.921561			

Table 3-8: Minitab® regression for Open System Two

CWS 2 (mmpa) = 3.21 - 0.00160 Cl - 0.00132 S-SO4 - 0.0170 F + 0.00259 Na - 0.326 pH + 0.128 P-PO4 + 0.00131 TOT Alk + 0.000149 Cond - 0.00058 Ca - 0.00218 Mg - 0.00433 Si-SiO2 + 0.025 Oil - 0.611 Al [3.2]					
where: All the ions are in mg/l except conductivity in μS/cm and total alkalinity in mg/l as CaCO₃.					
Predictor	Coef	SE Coef	T	P	
Constant	3.207	1.128	2.84	0.065	
Cl	-0.001595	0.001230	-1.30	0.285	
S-SO4	-0.0013172	0.0008221	-1.60	0.207	
F	-0.016993	0.005145	-3.30	0.046	
Na	0.002592	0.001577	1.64	0.199	
pH	-0.3264	0.1555	-2.10	0.127	
P-PO4	0.12791	0.07105	1.80	0.170	
TOT Alk	0.001312	0.001708	0.77	0.498	
Cond	0.0001494	0.0001384	1.08	0.359	
Ca	-0.000584	0.004455	-0.13	0.904	
Mg	-0.002180	0.007782	-0.28	0.798	
Si-SiO2	-0.004333	0.007850	-0.55	0.619	
Oil	0.0249	0.1121	0.22	0.838	
Al	-0.6113	0.2177	-2.81	0.067	
S = 0.0938073 R-Sq = 88.9% R-Sq(adj) = 40.6%					
Analysis of Variance					
Source	DF	SS	MS	F	P
Regression	13	0.210678	0.016206	1.84	0.339
Residual Error	3	0.026399	0.008800		
Total	16	0.237077			
Source	DF	Seq SS			
Cl	1	0.002655			
S-SO4	1	0.002851			

continuation of Table 3-8

F	1	0.058125
Na	1	0.024272
pH	1	0.001446
P-PO4	1	0.000099
TOT Alk	1	0.021584
Cond	1	0.009206
Ca	1	0.013552
Mg	1	0.004811
Si-SiO2	1	0.002314
Oil	1	0.000385
Al	1	0.069378

Unusual Observations

CWS 2						
Obs	C1	(mmpa)	Fit	SE Fit	Residual	St Resid
1	664	0.0830	0.0714	0.0935	0.0116	1.60 X
2	877	0.1504	0.1412	0.0936	0.0092	1.37 X
14	902	*	1.0691	0.2844	*	* X

X denotes an observation whose X value gives it large leverage.

3.4 Discussion

Although Open System One and Open System Two received the same brackish makeup there were significant differences in their operating conditions and chemical treatment. Over the extended period of 30 days, the coupons would have also been subjected to varying degrees of fouling and multiple forms of corrosion, including possibly: microbiologically induced corrosion. The significant differences noted between the two open systems were: volumes, operating temperatures, cycles-of-concentration, side-stream sand filter efficiencies and particularly oil removal rates.

The matrix scatterplots of the Open System coupon data against the measured parameters (Figure 3-4) clearly indicated unacceptable trends due to the widely scattered data and the lack of any observable relationships between the corrosion rate and the individual variables. The pH and phosphate concentrations appeared to be weak positively related to the corrosion rate.

In reviewing the Open System Two matrix scatterplots (Figure 3-5) it was found that only higher levels of calcium, magnesium and silica correlated with higher corrosion rates. These correlations also appeared weak due to the dispersed nature of the scatterplots. All the other water chemistry parameters demonstrated the opposite tendencies, including those noted to be positively related to corrosion in the Open System One scatterplots.

Due to numerous unaccounted factors that could potentially have affected the coupon corrosion rates, it was virtually impossible to derive any statistically significant correlations between each individually monitored water chemistry parameter and the coupon corrosion data. This was evident of both cooling systems over the period of a year and eight months. Since the previous exercise proved largely futile at identifying the key factors responsible for the mild steel corrosion it was necessary to investigate the possible combined effect/s and interdependency of the various factors.

Mild steel corrosion coupon data taken from both cooling systems were then compared against various predicted corrosion rates. Pearson correlations and p-values were then calculated, using Minitab[®], to determine if there were any relationships between the calculated indices and the corrosion rates. A study of the results indicated the following pertinent points for Open System One (Table 3-5):

- Low p values, indicative of statistically significant effects by the factors on the response were noted for the: LSI (Langelier Saturation Index), I_s (O & T scaling Index), SDI (Stiff and Davis Index), and RSI (Ryznar Stability Index).

However, the Pearson correlation coefficients (r values) for these four factors does however contradict what was expected, should it be understood that higher calcium carbonate scaling tendencies will lead to reduced mild steel corrosion. According to literature this phenomenon has been disproved before.

- It was noted though that there was a correlation between the buffer capacity and the corrosion rate, as confirmed by Stumm (1960), that increases in the former could decrease mild steel corrosion. However, the p value for this factor was significantly high indicating that the relationship could be attributed to chance as opposed to being statistically significant.

A similar study was performed on Open System Two where correlations between corrosion data and indices were done both with outliers and without the outliers and the findings reported (Table 3-6):

- With all the correlations performed, it was found that only the calcium carbonate saturation level produced a statistically significant correlation (i.e. p value < 0.05). The directional tendency of the correlation was in line with what was expected, for a water under-saturated with respect to calcium carbonate is deemed to be corrosive in nature (Langelier, 1936).
- Similar correlations to the calcium carbonate saturation, but with highly probable chance findings (i.e. high p values) were noted for the following: calcium carbonate FIME (Free Ion Momentary Excess), CCPP (Calcium Carbonate Precipitation Potential), RSI (Ryznar Stability Index), I_s (O & T scaling Index), and SDI (Stiff and Davis Index).

Minitab[®] regression analyses of the time plotted corrosion data versus the water quality parameters monitored produced Equations 3.1 and 3.2, one for each cooling system (Tables 3-7 and 3-8).

For Open System One, the following variables appeared to increase corrosion: sodium, pH, magnesium, phosphate, conductivity and oil, whereas the following appeared to decrease corrosion: chloride, sulphate, fluoride, alkalinity, calcium, iron, zinc silica and aluminium. In a closer examination of the coefficients derived in the regression analysis, it was evident that the p value (0.018) in the analysis of variance recorded in Table 3-7 indicated that the relationship between the corrosion rate and the variables listed was statistically significant at an α -level of 0.05. The R^2 value adjusted for the number of terms in the model (R-Sq (adj)) showed that the variable incorporated in the regression equation explained 88% of the variance in the corrosion rate, indicating that the model fits the data extremely well. The following variables incorporated in Equation 3.1 were found to be statistically significant: chloride, sulphate, sodium, alkalinity, magnesium and iron whereas the following were not statistically significant: fluoride, pH, phosphate, conductivity, calcium, zinc, silica oil and aluminium.

For Open System Two, the following variables appeared to increase corrosion: sodium, pH, phosphate, alkalinity, conductivity and oil, whereas the following appeared to decrease corrosion: magnesium, chloride, sulphate, fluoride, calcium, iron, zinc silica and aluminium. In a closer examination of the coefficients derived in the regression analysis it was evident that the p value (0.339) in the analysis of variance recorded in Table 3-8 indicated that the relationship between the corrosion rate and the variables listed was not statistically significant at an α -level of 0.05. The R^2 value adjusted for the number of terms in the model (R-Sq (adj)) showed that the variables included in the regression equation (Equation 3.2) explained 41% of the variance in the corrosion rate, indicating that the model does not fit the data well. The only variable found to be statistically significant was fluoride.

CHAPTER 4: LABORATORY EXPERIMENTS

4.1 Introduction

In determining the relationship between the various water chemistry parameters and the corrosion rate of mild steel in brackish water at elevated temperatures (35 - 45 °C), numerous laboratory tests were conducted with various different synthetic solutions and according to different experimental designs. Two laboratories (Laboratories B and C) were relied on for a comprehensive set of chemical analyses. The corrosion tests were all performed in Laboratory B (Table 4-3).

In the first round of corrosion tests a classical experimental design was followed. This entailed varying a single parameter at a time, while holding all the other parameters constant. The reason for not adopting a higher fluoride concentration was to avoid excessive calcium fluoride precipitation, which would completely alter the residual calcium hardness levels during the investigations, Table 4-1. The following parameters were varied one at a time: calcium, magnesium, alkalinity, sulphate, chloride and fluoride. The coupon corrosion rates, Corratel[®] readings and iron levels were recorded to quantify the corrosivity of the synthetic solutions on mild steel. Other water quality parameters such as: pH, conductivity, sodium and the oxygen concentrations were also monitored.

In the second round of tests, a fractional factorial experimental design approach was explored. The same parameters were varied and monitored as in round one. The purpose of this study was to examine the combined effect of all the variables and a broader range of chemistries to the experiments performed in the classical design.

In the third round of tests, various corrosion inhibitors were evaluated in a worst case synthetic solution in order to find the most effective commercially viable solution at inhibiting the corrosion attributable to high fluoride containing brackish waters. A second and equally important reason for this round was to assess the potential impact of zinc and phosphate, on the mild steel coupon corrosion rate, as these two

corrosion inhibitors were already employed in the steel mill cooling systems evaluated.

The fourth round of corrosion tests entailed a more comprehensive investigation into the influence of fluoride on corrosivity of mild steel. This round is divided into a number of series, each with its intended purpose and each series performed in triplicate with duplicate mild steel (C1010) corrosion coupons. The fluoride concentrations were raised incrementally at the following concentrations: 0, 10, 20, 40, 70 and 90 mg/l as F⁻, and the temperature was held constant at 45°C.

The fifth round investigated the visual, chemical and electrochemical examination of the effects exhibited during the exposure of mild steel to solutions containing 50 mg/l Ca²⁺ and 55 mg/l CaCO₃ with varying concentrations of fluoride at 45°C. The investigation was expanded beyond 90 mg/l fluoride.

Based on the data provided in Tables A-1, A-2 and B-1 a list of the ranges for each water chemistry parameter is given in Tables 4-1 and 4-2.

Table 4-1: Ranges of water chemistry parameters investigated

Data (units)		Minimum	Maximum
pH		6.86	8.3
Calcium	mg/l as Ca ²⁺	44	120
Magnesium	mg/l as Mg ²⁺	12	46
Total alkalinity	mg/l as CaCO ₃	35	220
Chloride	mg/l as Cl ⁻	400	1312
Sulphate	mg/l as SO ₄ ²⁻	618	1776
Fluoride	mg/l as F ⁻	6	97
Conductivity	µS/cm	2804	7412

Table 4-2: Ranges of other priority species

Data (units)	Phosphate	Silica	Zinc	Oil	Sodium
	mg/l as PO ₄ ³⁻	mg/l as SiO ₂	mg/l as Zn ²⁺	mg/l	mg/l as Na ⁺
Minimum	0.6	19	0.5	0.5	500
Maximum	9.2	28	2.5	3.0	1632

4.2 Laboratories and Materials Common to the Laboratory Corrosion Tests

The preparation of the synthetic solutions, the method and reagents used in the water analyses, and the corrosion test equipment and procedure are outlined below. Tables 4-4 and 4-5 list the analytical equipment, laboratory reagents and consumables, while Figure 4-1 shows the corrosion test set up.

Table 4-3: Facilities and equipment utilized

Equipment	Location
Laboratory chemical analyses	Buckman Africa on-site laboratory (Laboratory A), Buckman Africa (Hammarisdale) (Laboratory B), and Buckman Africa on-site laboratory (Laboratory C)
Laboratory Scale and Corrosion Tester	Buckman Africa, Hammarisdale (Laboratory B)
Corrater [®] , probes and electrode tips	
Electrochemical Techniques	

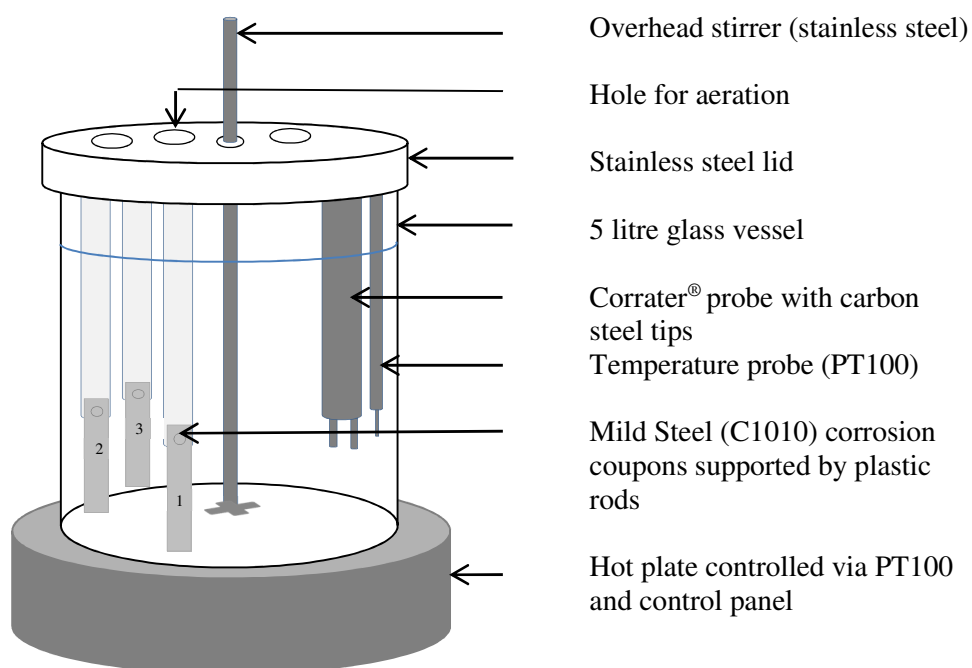


Figure 4-1: Schematic diagram of Laboratory Scale and Corrosion Tester Station

Table 4-4: Laboratory equipment at Laboratory A and Laboratory C

Equipment	Test parameters
1. Atomic Absorption Spectrophotometer (Spectra-AA-600) and Inductively Coupled Plasma (Arcos 165 Radial View ICP (ISO 17025:2005 accredited))	Sodium, iron, calcium and magnesium
2. Automatic Titrator (Metrohm 785 DMP Titrino, 760 SC, 712 Conductivity meter)	pH, conductivity and alkalinity
3. UV-Visible Spectrophotometer (Hach DR/2000 direct reading spectrometer) and Ion Chromatograph 761 Compact IC with the Metrohm.838 Advantage sample processor	Sulphate
4. UV-Visible Spectrophotometer (Hach DR/890 colorimeter) and Ion Chromatograph (761 Compact IC with the Metrohm.838 Advantage sample processor)	Fluoride
5. UV-Visible Spectrophotometer (Hach DR/890 colorimeter)	Oxygen
6. Automatic Titrator (785 DMP Titrino, 760 SC, 712 Conductivity meter) and Ion Chromatograph (761 Compact IC with the Metrohm.838 Advantage sample processor)	Chloride
7. Balance (Mettler EA 200)	Weighing of reagents
8. Oven (Mettmert oven (F.A. code 750)	Oven drying of reagents
9. Six place “Laboratory Scale and Corrosion Tester”	Corrosion tests
10. Corratel [®] RCS 9000 and 7012-0-0 two electrode adjustable insertion probe with ¾” NPT tube fitting (Rohrback Cosasco Systems)	General corrosion and pitting

Table 4-5: Laboratory reagents and consumables

Reagent or consumable	Supplier
Mild Steel corrosion coupons (C1010). 120 glass bead grit finish. P/N: CO100; Size: 12.7mm X 76.2mm X 1.59mm ; Hole: 4.76mm ; Hole Location: 6.35mm from end; Area.: 1946.5 mm ² C1010 nominal chemical composition: plain carbon steel with 0.10% carbon content. C 0.08 - 0.13, Mn 0.30 - 0.60, P 0.03 - 0.04, S 0.05.	Metal Samples, Munford, AL. USA.
Corrater® mild steel electrode kits – 060814-K03005	Rohrback Cosasco Systems, USA
Fluoride reagent, For DR 890: cat. no. 444-49 Oxygen reagent, For DR 890: HRDO cat. no. 25150-25	Hach Company
Calcium chloride, Assay min 99.5% as CaCl ₂ .2H ₂ O	Associated Chemical Enterprises, Johannesburg, South Africa.
Ethanol, 99.9% as C ₂ H ₅ OH	
Hydrochloric acid, 32% as HCl	
Magnesium chloride, Assay min 99-101% as MgCl ₂ .6H ₂ O	
Sodium chloride, Assay min 99.5% as NaCl	
Sodium fluoride, Assay min 98.5% as NaF	
Sodium hydrogen carbonate, Assay min 99.5% as NaHCO ₃	
Sodium hydroxide, Assay min 98% as NaOH	
Sodium sulphate, Assay min 99% as Na ₂ SO ₄	
Sulphuric acid, 99.5% as H ₂ SO ₄	

4.3 Methodology Common to the Laboratory Corrosion Tests

The methodology detailed below is applicable throughout Chapter 4, unless there is specific mention of alternative or supplementary equipment, procedures or reagents.

4.3.1 Water analyses

Laboratories B and C employed their own in-house methods (Table 4-4) of which only the ICP method used by Laboratory C was ISO/IEC 17025:2005 accredited. The inductively coupled plasma spectrometer was used for detecting the concentrations of calcium, magnesium and sodium in the samples collected during the corrosion tests. Additional water analyses performed by Laboratory C included

chloride and sulphate and they were tested by means of an ion chromatograph. This form of chromatography measures concentrations of ionic species by separating them based on their interaction with a resin. Ionic species separate differently depending on species type and size.

The pH, total alkalinity and conductivity measurements were performed on the water samples, in Laboratory B, using an automatic titrator (Table 4-4) fitted with pH and conductivity probes, and the tests performed within an hour of their removal from the corrosion test solutions.

The fluoride and oxygen concentrations were tested by means of a spectrophotometer and the reagents supplied by the supplier of the spectrophotometer (Tables 4-4 and 4-5).

Testing for the total iron concentrations also required immediate processing of the test solution samples as well as an acid digestion. 50 ml samples were acidified with 2 ml of concentrated hydrochloric acid (Table 4-5) for 10 minutes, followed by cooling. The digested samples were then made up to volume prior to testing on the Atomic Absorption Spectrophotometer (Table 4-4).

4.3.2 Test solution preparation

Reagents required at a uniform concentration for the batch of six tests were weighed out using the four-digit balance. The weights required of these reagents were calculated using MS Excel. This excluded the reagent/s required at varying concentrations for the set of six tests. The reagents were dissolved into 25 litres of distilled water, excluding the reagents required at differing concentrations, and additional distilled water added taking up the volume to 29 litres. The 29 litres was then divided equally (4833 ml) into six 5 litre corrosion test vessels. The outstanding reagent/s, that is those required at the different concentrations, were then dissolved into the volumes contained in the glass corrosion test vessel and test volumes made up to exactly five litres with distilled water. If pH adjustment was

necessary, it was done prior to making the final volumes up to five litres. pH adjustments were made with drop wise addition of 2% (m/v) sulphuric acid.

4.3.3 Corrosion set up

The corrosivities of the corrosion test solutions were determined by both the direct weight technique, using mild steel (C1010) corrosion coupons, and by means of a Corrater[®] RCS 9000 fitted with mild steel electrode kits (Table 4-4 and 4-5) and these were compared against the total iron concentrations. Each set of tests was performed in a batch of six tests, according to Figures 4-1.

Mild steel (C1010) corrosion coupons were placed into the plastic coupon holders suspended in the glass corrosion test vessels and the Corrater[®] probes (with mild steel tips) are inserted into the vessels. Each corrosion test vessel also supported a PT 100 temperature probe, an overhead stirrer and bottom heating plate. The contents of the vessel were stirred at 100-110 rpm and the temperature of each test vessel set independently at the control panel.

C1010 (mild steel) corrosion coupons were subjected to synthetic test solutions (4000 ml) and the coupons then removed, cleaned and weighed and the corrosion rates calculated based on their weight loss. The method followed was in accordance with ASTM methods:

- G31-72 (1999): Standard Practice for Laboratory Immersion Corrosion Testing of Metals; and
- G1-90 (1999): Standard Practice for Preparing, Cleaning, and Evaluating Corrosion Test Specimens.

4.3.4 Monitoring during the corrosion test

At the start of the test, one litre of each test solution was removed and submitted for laboratory analyses to both Laboratory A, the Buckman, Hammarsdale laboratory as well as Laboratory C.

- Laboratory A tests for: pH, conductivity, total alkalinity, sulphate, fluoride, and total iron, whereas
- Laboratory C performs the following analyses: calcium, magnesium, chloride, sulphate, sodium, as well as some of the ions analysed by the Hammarsdale laboratory.

Corrater[®] readings were recorded daily (general corrosion rate in mpy) for the duration of the three day corrosion tests. Upon ending the corrosion tests after a period of 72 hours, additional samples were removed from the test solutions and submitted to the above laboratories for the same analyses. The corrosion coupons were removed and submitted to the Hammarsdale laboratory for cleaning and corrosion rate calculation.

4.3.5 Coupon cleaning and corrosion rate calculation

The coupons were first hand washed under a running tap (i.e. using municipal water) removing only the loose corrosion by-products and then gently rubbed with ethanol soaked hand roll paper, followed by oven drying at 105°C for 30 minutes. The dried coupons were then allowed to cool in a desiccator and weighed to four decimal places. The final coupon and initial coupon masses were then used to calculate the total mass loss using the Equation 4.1:

$$\text{Corrosion rate (mmpa)} = (144.23 \times w) / (d \times a \times t) \dots\dots\dots [4.1]$$

where: w = mass loss due to corrosion (mg),

d = density of the metal (7.85 g/cm³),

a = exposed area of the coupon (cm²) (19.465 cm²),

t = time in days.

4.3.6 Minitab statistical software package

Minitab 16[®] (Version 16.2.3) and Minitab 17.0[®] (Licensed from Minitab Inc.) statistical analysis software were used throughout to assist in the analysis and

interpretation of the laboratory results. The software was typically used to perform basic statistics calculations (for example: calculating the mean, median, standard deviation and range) (Section 3.3), drawing graphs (for example: scatterplots, matrix plots, histograms, 3D plots, time series plots and effects plots), the fractional factorial design of experiments, as explained in Section 4.5, and performing regression analyses (linear and non-linear multivariate regression) as apparent in Section 4.7.

4.4 Experiments Performed According to Classical Design

In each group of six tests, five of the tests were performed at 45°C and one at 35°C. The 35°C test was performed with a synthetic solution that was identical to the intermediate of the five synthetic solutions performed at 45°C. This was done to investigate the effect of a 10°C difference in temperature over the range typically found in the cooling system circuits being investigated.

4.4.1 Varying calcium hardness and total alkalinity

4.4.1.1 Low alkalinity investigation

Varying levels of calcium hardness and total alkalinity were first considered. Corrosion rates were obtained for at least five different concentrations for each variable, e.g. calcium hardness: 50, 62.5, 75, 87.5 and 100. Table 4-6 outlines the target concentrations for each run for the initial investigation conducted at relatively low alkalinities compared to the ranges initially listed in Table 4-1. In Table 4-1 the total alkalinity common to the two open cooling systems utilizing brackish water ranged from 35 to 220 mg/l as CaCO₃ whereas the range for this study was from 19 and 67.5 mg/l as CaCO₃. This was done to first explore the impact of lower alkalinity on corrosion in order to assemble a more comprehensive model in terms of what was believed to be a critical parameter in the prevention of mild steel corrosion of a brackish water. The target concentrations for the other species included were: magnesium 27 mg/l as Mg²⁺, chloride: 750 mg/l as Cl⁻, sulphate: 1125 mg/l as SO₄²⁻, and fluoride: 10 mg/l as F⁻. A low fluoride concentration

targeted in order to avoid calcium fluoride precipitation which more than likely alter the residual hardness of the brackish water.

In addition to the target concentrations and temperatures Table 4-6 also reports on the chemical analyses of the test solutions prior to the corrosion tests. The same chemical analyses are then repeated upon culmination of the three day tests. These results are given in Table 4-7 together with the coupon and Corrater[®] results in Table 4-8.

Figures 4-2 and 4-3 are the scatterplots of the average coupon corrosion data versus the test solution initial and final water chemistry parameters. These corrosion tests were performed at 35°C and they indicate a decrease in the corrosion rate with an increase in the total alkalinity. Table 4-9 shows the strength and direction of the correlations between the various parameters for the corrosion tests performed at this temperature. A strong negative linear correlation was found between the final total alkalinity and the corrosion rate. As the 35°C tests were all performed at the same target total alkalinity of 37 mg/l, Figure 4-4 therefore illustrates the impact of the calcium hardness on the total alkalinity and corrosion rate. The corrosion rate appeared to increase until it reached a turning point at target calcium concentration of approximately 87.5 mg/l. The figure also shows close correlations between the initial and final values for both the calcium and total alkalinity, with the exception of the single total alkalinity outlier at the target calcium concentration of 100 mg/l.

In Figures 4-5 and 4-6 and Table 4-10, the total alkalinity is indicated to be strongly correlated with the corrosion rate at 45°C. Figure 4-7 demonstrates the impact of the calcium concentration at three different values of the target alkalinity, showing a similar trend to the results obtained at 35°C. A contour plot of the corrosion rate versus the initial calcium and total alkalinity values, for the results obtained at 45°C (Figure 4-8) illustrates the joint impact of the two parameters. High corrosion rates were evident in the zone with low total alkalinity and low calcium hardness. Higher corrosion rates were noticed at relatively high calcium concentrations, particularly at a low total alkalinity.

Table 4-6: Varying calcium and alkalinity at the low range of alkalinity levels- Target and start-up concentrations

Run	Target concentrations / conditions			Test solution concentrations at start-up									
	Calcium (mg/l as Ca ²⁺)	Total alkalinity (mg/l as CaCO ₃)	Temperature (°C)	Calcium ⁽²⁾ (mg/l as Ca ²⁺)	Total alkalinity ⁽¹⁾ (mg/l as CaCO ₃)	pH ⁽¹⁾	Magnesium ⁽²⁾ (mg/l as Mg ²⁺)	Chloride ⁽²⁾ (mg/l as Cl ⁻)	Sulphate (mg/l as SO ₄ ²⁻)	Fluoride (mg/l as F ⁻)	Conductivity ⁽¹⁾ (µS/cm)	Total iron ⁽¹⁾ (mg/l as Fe ³⁺ (total))	Oxygen ⁽¹⁾ (mg/l as O ₂)
1	50.0	18	45	51.1	27.6	7.53	26.1	779	1.4	9.3	4564	< 0.01	5.3
2	50.0	28	45	50.6	35.6	7.20	26.5	765	1.4	9.1	4216	< 0.01	6.6
3	50.0	37	45	49.4	45.3	7.41	25.6	739	1.4	9.6	4408	< 0.01	5.9
4	50.0	55	45	49.4	51.7	7.65	24.9	800	1.4	9.0	4384	< 0.01	5.8
5	50.0	73	45	49.3	61.7	7.77	26.0	765	1.3	9.2	4288	< 0.01	5.9
7	62.5	18	45	60.1	20.1	7.51	26.3	732	1.2	9.5	4296	< 0.01	5.3
8	62.5	28	45	63.4	26.4	7.46	27.6	763	1.3	9.5	4352	< 0.01	6.2
9	62.5	37	45	66.2	24.3	7.62	28.7	752	1.3	8.3	3420	< 0.01	5.8
10	62.5	55	45	60.1	45.4	7.86	26.2	717	1.3	8.3	4176	< 0.01	5.9
11	62.5	73	45	61.1	57.9	7.99	26.5	927	1.4	8.5	4348	< 0.01	5.8
13	75.0	18	45	61.5	20.3	7.38	22.4	-	1.1	9.0	3972	< 0.01	6.9

14	75.0	28	45	63.0	27.6	7.46	22.9	741	1.1	9.0	4024	< 0.01	5.7
15	75.0	37	45	62.3	31.9	7.52	22.7	758	1.1	8.4	3988	< 0.01	6.7
16	75.0	55	45	63.5	47.3	8.10	22.5	750	1.1	8.3	3964	< 0.01	6.5
17	75.0	73	45	62.9	58.0	7.93	22.8	760	1.2	9.9	4120	< 0.01	6.6
19	87.5	18	45	83.6	19.0	7.25	27.0	2972	1.2	9.3	4320	< 0.01	6.6
20	87.5	28	45	82.9	24.9	7.34	26.7	822	1.3	8.6	4376	< 0.01	5.9
21	87.5	37	45	83.6	30.5	7.49	26.6	780	1.2	9.0	4340	< 0.01	6.3
22	87.5	55	45	84.4	42.6	7.71	26.8	777	1.2	8.0	4348	< 0.01	6.5
23	87.5	73	45	83.7	55.3	7.89	27.2	805	1.3	9.7	4376	< 0.01	6.9
25	100.0	18	45	94.1	23.5	6.93	26.8	790	1.2	8.9	4292	< 0.01	6.5
26	100.0	28	45	93.6	29.5	7.28	26.2	790	1.3	9.9	4224	< 0.01	6.8
27	100.0	37	45	92.5	37.5	7.52	26.2	805	1.3	9.4	4148	< 0.01	6.5
28	100.0	55	45	-	53.7	7.75	-	-	1.3	9.8	4176	< 0.01	5.9
29	100.0	73	45	89.1	67.5	7.86	25.1	769	1.2	9.1	4284	< 0.01	6.6
6	50.0	37	35	49.9	38.8	7.32	26.1	772	1.4	9.3	4180	< 0.01	6.2
12	62.5	37	35	59.5	32.6	7.58	25.9	1188	1.4	8.3	4208	< 0.01	6.1
18	75.0	37	35	62.9	30.8	7.51	22.7	725	1.1	9.6	4004	< 0.01	6.3
24	87.5	37	35	-	26.6	7.33	-	-	1.3	9.7	4216	< 0.01	6.1
30	100.0	37	35	90.1	38.6	7.55	24.7	781	1.2	9.9	4232	< 0.01	6.1

Notes: 1. Test conducted in Laboratory B, 2. Test conducted in Laboratory C, nt = not tested.

Table 4-7: Varying calcium and alkalinity at the low range of alkalinity levels- Cessation concentrations

Run	Target concentrations / conditions			Test solution concentrations upon cessation of corrosion tests									
	Calcium (mg/l as Ca ²⁺)	Total alkalinity (mg/l as CaCO ₃)	Temperature (°C)	Calcium ⁽²⁾ (mg/l as Ca ²⁺)	Total alkalinity ⁽¹⁾ (mg/l as CaCO ₃)	pH ⁽¹⁾	Magnesium ⁽²⁾ (mg/l as Mg ²⁺)	Chloride ⁽²⁾ (mg/l as Cl ⁻)	Sulphate (mg/l as SO ₄ ²⁻)	Fluoride (mg/l as F ⁻)	Conductivity ⁽¹⁾ (µS/cm)	Total iron ⁽¹⁾ (mg/l as Fe ³⁺ (total))	Oxygen ⁽¹⁾ (mg/l as O ₂)
1	50.0	18	45	55.7	28.2	7.45	28.5	835	1.33	9.5	4572	8.9	4.1
2	50.0	28	45	53.6	36.2	7.41	28.0	806	1.27	9.5	4472	8.4	4.6
3	50.0	37	45	53.6	47.8	7.65	27.6	826	1.39	9.3	4544	6.5	3.9
4	50.0	55	45	52.6	51.0	7.86	28.3	881	1.36	9.4	4448	6.4	5.1
5	50.0	73	45	50.9	65.1	8.00	27.7	838	1.30	9.4	4552	6.1	5.2
7	62.5	18	45	63.4	21.8	7.51	27.5	735	1.26	9.5	4172	12.7	5.0
8	62.5	28	45	68.0	27.6	7.54	30.0	825	1.36	8.8	4756	10.1	4.8
9	62.5	37	45	61.8	32.1	7.62	26.9	723	1.23	9.0	4280	10.7	4.9
10	62.5	55	45	60.0	41.5	7.83	26.8	782	1.26	9.0	4328	9.7	5.1
11	62.5	73	45	59.6	50.2	7.94	27.5	796	1.29	8.8	4416	12.9	5.1
13	75.0	18	45	66.4	21.8	7.39	24.1	779	1.28	8.6	4208	14.3	4.5
14	75.0	28	45	67.8	28.1	7.48	23.3	783	1.26	9.0	4272	16.4	3.8

15	75.0	37	45	63.6	30.9	7.52	23.3	696	1.27	8.6	4368	15.1	3.7
16	75.0	55	45	62.0	48.9	8.14	23.3	777	1.27	8.0	4448	15.0	4.0
17	75.0	73	45	61.9	59.1	7.98	24.0	782	1.29	9.1	4376	15.1	3.9
19	87.5	18	45	90.4	20.0	7.2	29.1	860	1.37	9.6	4620	12.8	nt
20	87.5	28	45	88.8	26.1	7.42	28.4	829	1.38	8.8	4608	12.5	nt
21	87.5	37	45	87.2	28.6	7.43	28.5	827	1.33	7.6	4532	11.6	nt
22	87.5	55	45	85.1	34.9	7.66	28.4	849	1.35	9.8	4620	15.9	nt
23	87.5	73	45	84.1	43.3	7.75	28.5	823	1.36	9.0	4664	12.9	nt
25	100.0	18	45	103.0	22.7	7.29	28.9	900	1.35	9.4	4568	38.8	3.9
26	100.0	28	45	99.2	26.1	7.44	28.8	849	1.31	9.9	4460	23.4	4.6
27	100.0	37	45	94.3	29.8	7.51	27.7	826	1.34	9.6	4544	18.6	4.4
28	100.0	55	45	91.2	42.0	7.58	27.5	810	1.30	9.6	4256	40.0	3.7
29	100.0	73	45	89.0	53.1	7.98	26.3	806	1.33	9.6	4500	26.0	5.1
6	50.0	37	35	51.8	43.8	7.58	27.5	792	1.27	9.8	4376	7.6	4.2
12	62.5	37	35	60.8	31.1	7.55	26.3	727	1.22	9.0	4352	10.0	5.6
18	75.0	37	35	63.5	31.4	7.56	23.6	755	1.28	10.1	4508	13.7	4.7
24	87.5	37	35	86.6	27.3	7.34	28.3	809	1.31	8.0	4608	11.6	nt
30	100.0	37	35	89.2	30.7	7.47	25.8	770	1.21	9.9	4296	16.8	3.9

Table 4-8: Corrosion coupon and Corrater® readings while varying calcium and alkalinity at the low range of alkalinity levels

Run	Target concentrations / conditions			Corrosion Coupon Results			Corrater® readings			
	Calcium (mg/l as Ca ²⁺)	Total alkalinity	Temperature (°C)	Coupon 1 (mmpa)	Coupon 2 (mmpa)	Average (mmpa)	Day 1 (mmpa)	Day 2 (mmpa)	Day 3 (mmpa)	Day 4 (mmpa)
1	50.0	18	45	0.53	0.57	0.55	0.92	1.25	0.99	0.89
2	50.0	28	45	0.34	0.32	0.33	0.99	0.96	0.94	0.97
3	50.0	37	45	0.20	0.34	0.27	0.98	1.11	1.01	0.99
4	50.0	55	45	0.28	0.33	0.30	0.92	1.02	0.85	0.82
5	50.0	73	45	0.26	0.27	0.26	0.92	0.74	0.73	0.63
7	62.5	18	45	0.62	0.74	0.68	0.86	0.84	0.92	1.06
8	62.5	28	45	0.54	0.58	0.56	0.79	0.80	0.80	0.97
9	62.5	37	45	0.56	0.65	0.61	1.05	0.59	0.62	0.72
10	62.5	55	45	0.48	0.56	0.52	1.39	0.53	0.64	0.69
11	62.5	73	45	0.41	0.45	0.43	1.12	0.40	0.55	0.66
13	75.0	18	45	0.78	0.70	0.74	0.76	0.81	0.76	0.82
14	75.0	28	45	0.70	0.67	0.68	0.18	0.18	0.22	0.25
15	75.0	37	45	0.51	0.61	0.56	0.74	0.78	0.74	0.78

16	75.0	55	45	0.43	0.48	0.46	0.67	0.64	0.65	0.65
17	75.0	73	45	0.47	0.42	0.44	0.79	0.82	0.79	0.75
19	87.5	18	45	0.81	0.84	0.82	0.84	0.90	nt	nt
20	87.5	28	45	0.84	0.92	0.88	0.85	0.87	nt	nt
21	87.5	37	45	0.74	0.76	0.75	1.04	0.99	nt	nt
22	87.5	55	45	0.60	0.65	0.63	0.73	0.74	nt	nt
23	87.5	73	45	0.37	0.51	0.44	0.91	1.04	nt	nt
25	100	18	45	0.75	0.71	0.73	0.77	0.84	0.86	0.98
26	100	28	45	0.51	0.58	0.54	0.84	0.86	0.74	0.76
27	100	37	45	0.36	0.60	0.48	1.04	1.10	1.06	1.00
28	100	55	45	0.48	0.32	0.40	0.75	0.79	0.77	0.69
29	100	73	45	0.23	0.45	0.34	0.84	0.53	0.51	0.54
6	50.0	37	35	0.24	0.36	0.30	0.88	1.19	1.03	1.02
12	62.5	37	35	0.54	0.56	0.55	0.65	0.60	0.72	0.73
18	75.0	37	35	0.67	0.67	0.67	0.96	0.92	0.97	0.95
24	87.5	37	35	0.73	0.68	0.71	0.98	1.00	nt	nt
30	100	37	35	0.45	0.70	0.58	0.64	0.67	0.64	0.63

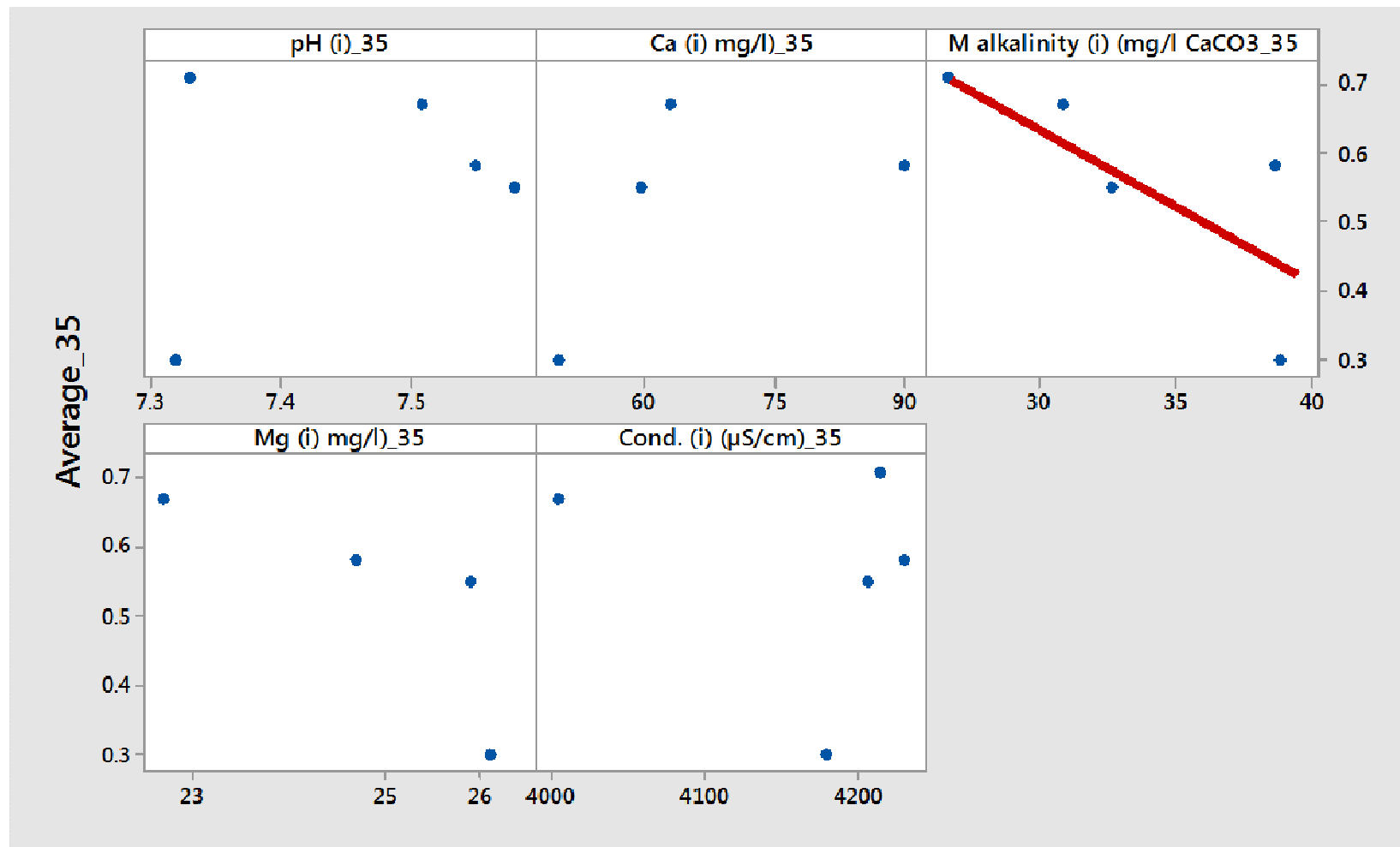


Figure 4-2: Matrix plot of parameters while varying calcium and alkalinity at the low range of alkalinity levels at 35°C (Cubic model regression fit), showing the average corrosion rate versus the initial test solution parameters

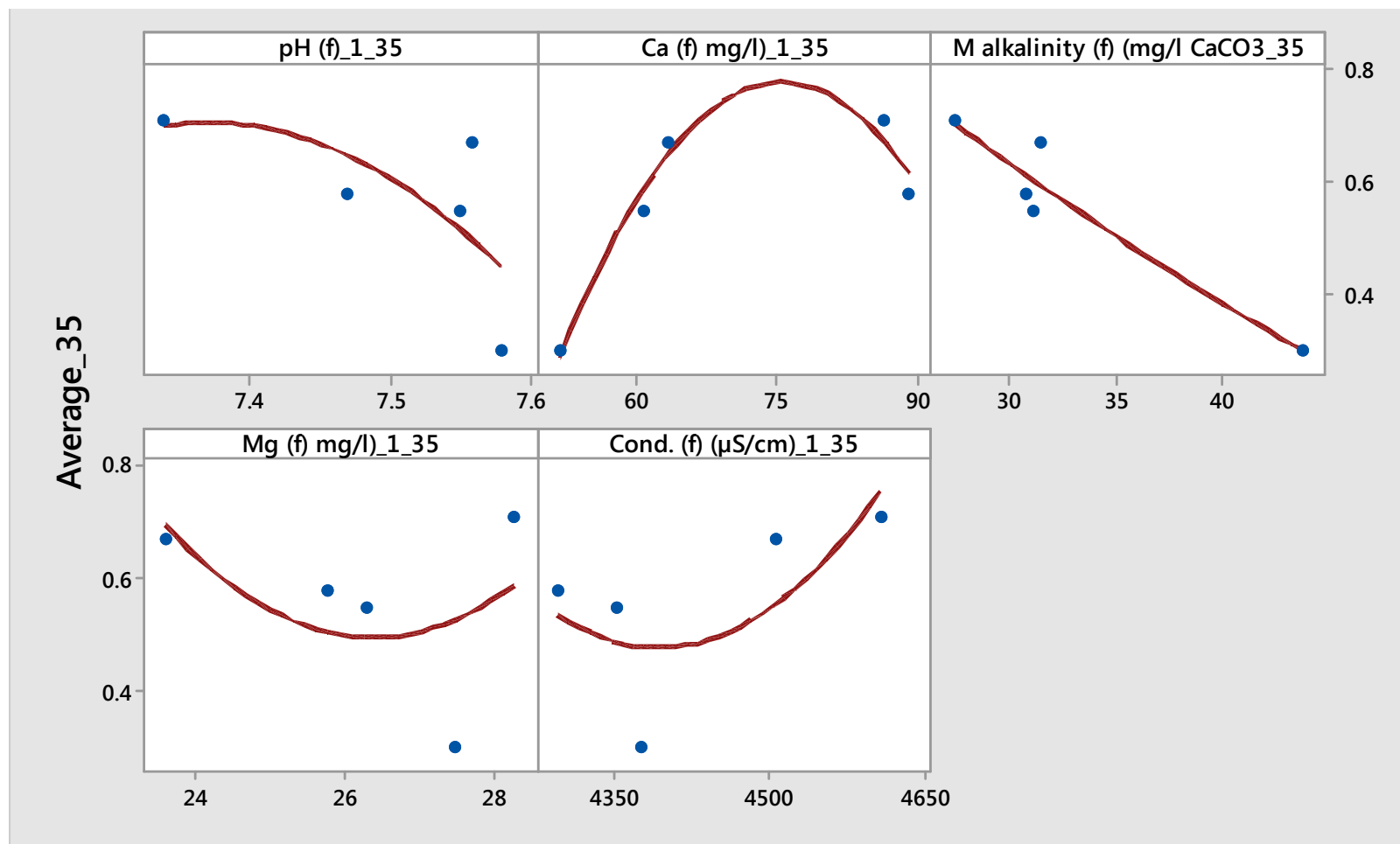


Figure 4-3: Scatterplots of the average mild steel coupon corrosion rates versus pertinent final test solution parameters, at 35°C

Table 4-9: Statistically significant relationships between various parameters in the 35°C corrosion test

#	Parameter 1	Parameter 2	Strength and direction of relationship
1	pH (initial)	Day 2 coupon corrosion (mmpa)	Strongly negative
2	Chloride (initial)	Fluoride (final)	Strongly negative
3	Oxygen (initial)	Conductivity (initial)	Strongly negative
4	pH (final)	Calcium (final)	Strongly negative
5	Total alkalinity (final)	Coupon position 1 (mmpa)	Strongly negative
6	Total alkalinity (final)	Coupon position 2 (mmpa)	Strongly negative
7	Total alkalinity (final)	Average of Coupon 1 and 2 (mmpa)	Strongly negative
8	Sulphate (final)	Day 1 (mmpa)	Strongly positive
9	Sulphate (final)	Conductivity (final)	Strongly positive
10	Conductivity (final)	Day 1 (mmpa)	Strongly positive
11	Coupon position 1 (mmpa)	Average of Coupon 1 and 2 (mmpa)	Strongly positive
12	Coupon position 2 (mmpa)	Average of Coupon 1 and 2 (mmpa)	Strongly positive

Note: Further details are shown in Table G-1 of Appendix G.

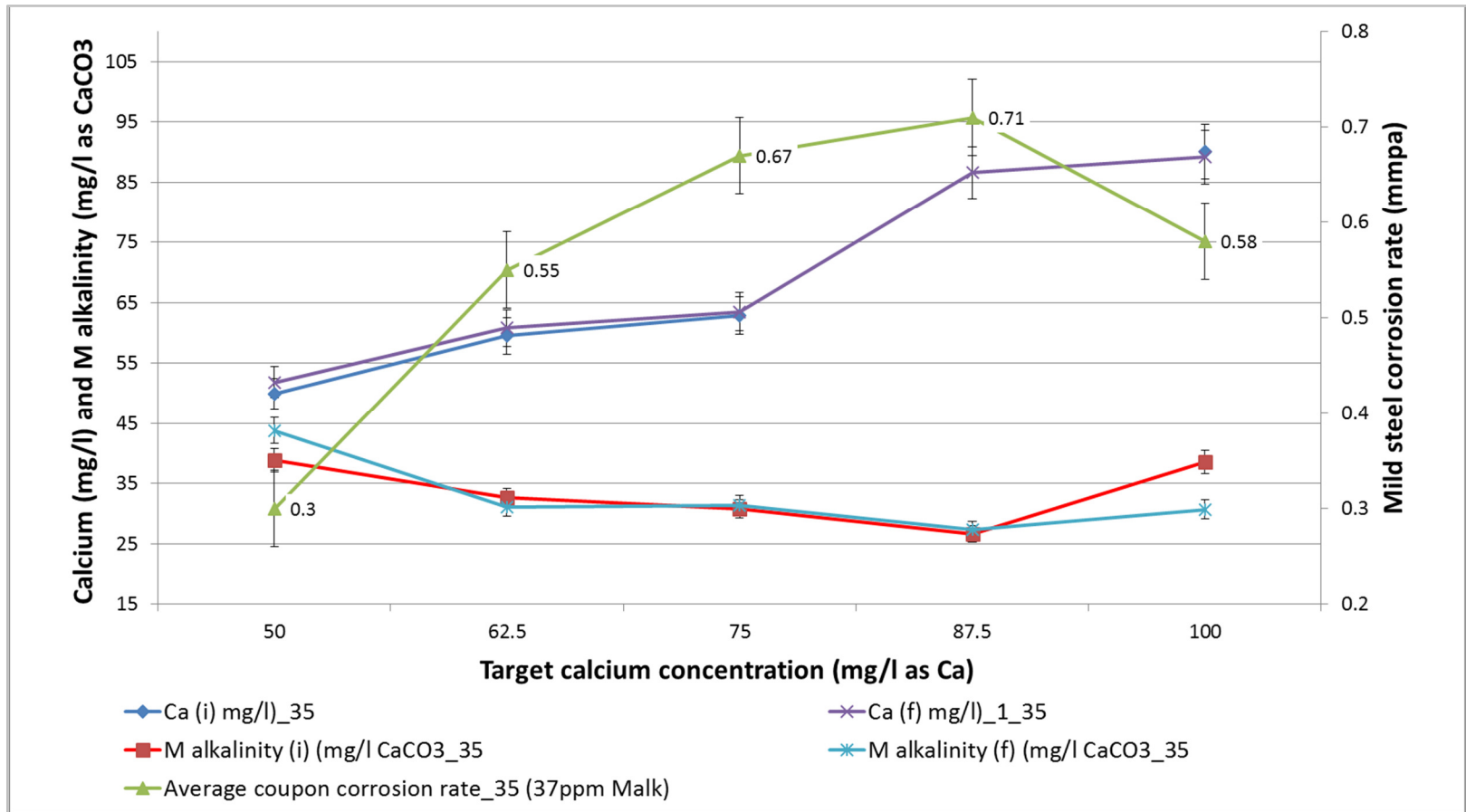


Figure 4-4: Impact of increasing calcium hardness and decreasing total alkalinity on mild steel corrosion at 35°C (with 5% error bars on the calcium and alkalinity and ± 0.04 mmpa error bars on the corrosion rate)

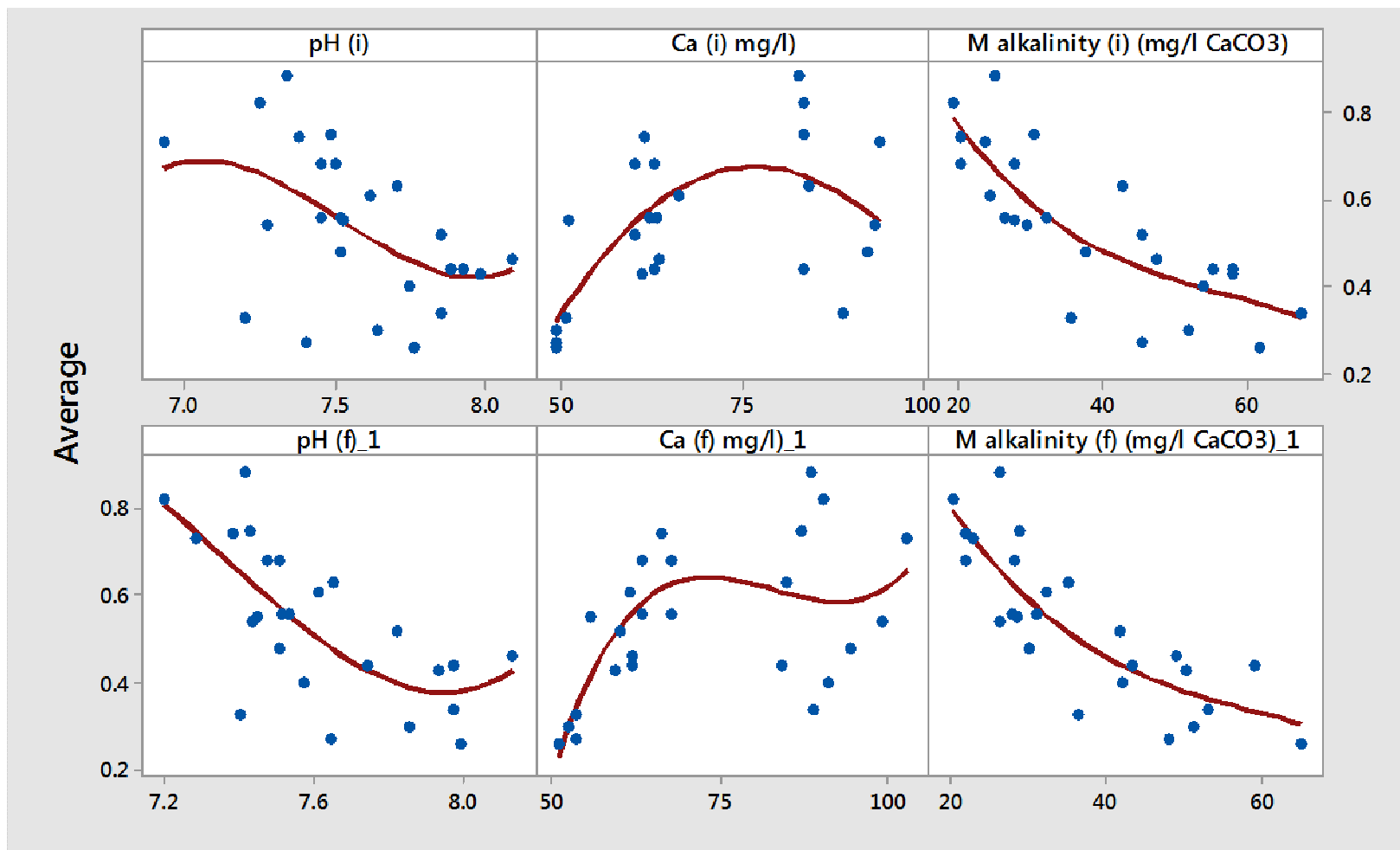


Figure 4-5: Matrix plot of parameters while varying calcium and alkalinity at the low range of alkalinity levels at 45°C (Cubic model regression)

Table 4-10: Statistically significant relationships between various parameters in the 45°C corrosion test

#	Parameter 1	Parameter 2	Strength and direction of relationship
1	pH (initial)	Total alkalinity (initial)	Moderately positive
2	Sulphate (initial)	Magnesium (initial)	Moderately positive
3	Calcium(initial)	Oxygen (initial)	Moderately positive
4	Total alkalinity (initial)	pH (initial)	Moderately positive
5	Calcium(initial)	Total Iron (initial)	Moderately positive
6	pH (initial)	Coupon position 2 (mmpa)	Moderately negative
7	Calcium(initial)	Coupon position 2 (mmpa)	Moderately positive
8	pH (initial)	Average of Coupon 1 and 2 (mmpa)	Moderately negative
9	Calcium(initial)	Average of Coupon 1 and 2 (mmpa)	Moderately positive
10	Magnesium (initial)	Day 1 (mmpa)	Moderately positive
11	Sulphate (initial)	Conductivity (initial)	Moderately positive
12	Total alkalinity (initial)	pH (final)	Strongly positive
13	Sulphate (initial)	Magnesium (final)	Moderately positive
14	Total alkalinity (initial)	Coupon position 1 (mmpa)	Moderately negative
15	Total alkalinity (initial)	Coupon position 2 (mmpa)	Moderately negative
16	Total alkalinity (initial)	Average of Coupon 1 and 2 (mmpa)	Moderately negative
17	Sulphate (initial)	Coupon position 1 (mmpa)	Moderately negative
18	Sulphate (initial)	Coupon position 2 (mmpa)	Moderately negative
19	Sulphate (initial)	Average of Coupon 1 and 2 (mmpa)	Moderately negative
20	Sulphate (initial)	Day 3 (mmpa)	Moderately negative
21	Conductivity (initial)	Magnesium (final)	Moderately negative
22	Conductivity (initial)	Chloride (final)	Moderately positive
23	Conductivity (initial)	Sulphate (final)	Moderately positive
24	Conductivity (initial)	Conductivity (final)	Moderately positive
25	Conductivity (initial)	Day 2 (mmpa)	Moderately positive
26	Fluoride (initial)	Day 2 (mmpa)	Moderately positive
27	Oxygen (initial)	Calcium(final)	Moderately positive
28	pH (final)	Calcium(final)	Moderately negative
29	pH (final)	Total alkalinity (final)	Strongly positive

continuation of Table 4-10			
#	Parameter 1	Parameter 2	Strength and direction of relationship
30	Calcium(final)	Total alkalinity (final)	Moderately negative
31	Calcium(final)	Sulphate (final)	Moderately positive
32	pH (final)	Coupon position 1 (mmpa)	Moderately negative
33	pH (final)	Coupon position 2 (mmpa)	Moderately negative
34	pH (final)	Average of Coupon 1 and 2 (mmpa)	Moderately negative
35	Calcium(final)	Coupon position 1 (mmpa)	Moderately positive
36	Calcium(final)	Coupon position 2 (mmpa)	Moderately positive
37	Calcium(final)	Average of Coupon 1 and 2 (mmpa)	Moderately positive
38	Magnesium (final)	Chloride (final)	Moderately positive
39	Magnesium (final)	Sulphate (final)	Moderately positive
40	Magnesium (final)	Conductivity (final)	Moderately positive
41	Magnesium (final)	Day 1 (mmpa)	Moderately positive
42	Magnesium (final)	Day 2 (mmpa)	Moderately positive
43	Magnesium (final)	Day 3 (mmpa)	Moderately positive
44	Total alkalinity (final)	Coupon position 1 (mmpa)	Moderately negative
45	Total alkalinity (final)	Coupon position 2 (mmpa)	Strongly negative
46	Total alkalinity (final)	Average of Coupon 1 and 2 (mmpa)	Strongly negative
47	Chloride (final)	Sulphate (final)	Moderately positive
48	Chloride (final)	Conductivity (final)	Moderately positive
49	Sulphate (final)	Day 2 (mmpa)	Moderately positive
50	Sulphate (final)	Day 3 (mmpa)	Moderately positive
51	Chloride (final)	Coupon position 2 (mmpa)	Strongly positive
52	Chloride (final)	Average of Coupon 1 and 2 (mmpa)	Strongly positive
53	Coupon position 2 (mmpa)	Average of Coupon 1 and 2 (mmpa)	Strongly positive
54	Day 2 (mmpa)	Day 3 (mmpa)	Strongly positive

Note: Further details are shown in Table G-2 of Appendix G.

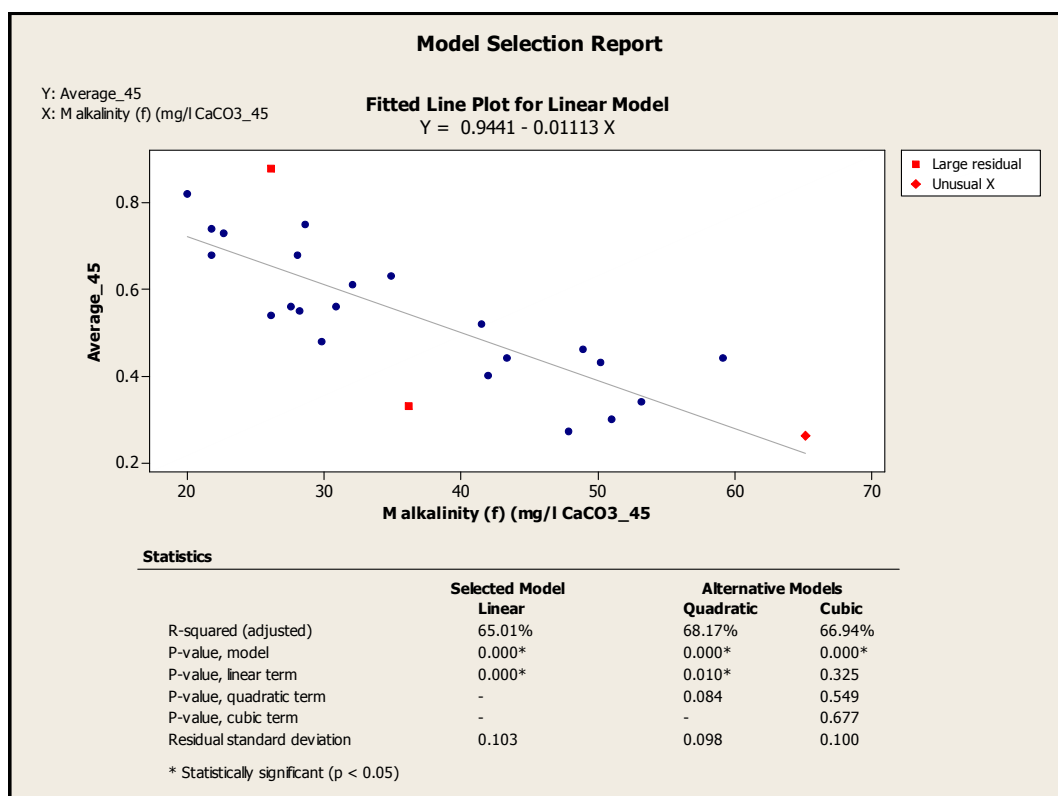


Figure 4-6: Regression analysis for the average coupon corrosion rate versus the final test solution total alkalinity at 45°C

Amongst the response variables used on as indicators of mild steel corrosion at 35°C, namely: the mild steel coupon corrosion rates, the Corrat[®] measurements using mild steel tips, the test solution final total iron levels and the residual oxygen concentrations, the only response variable to consistently produce statistically significant strong correlations was the average coupon corrosion rate. Due to the lack of correlations between the various corrosion indicator parameters, evident in Table 4-9, it was decided to eliminate the measurement of the oxygen concentration, while focusing predominantly on the average corrosion rate. The correlations demonstrated strongly negative relationships between the average and individual coupon corrosion rates and the total alkalinity in solution at the end of the corrosion test (i.e. Total alkalinity (final)). The relationship between the corrosion rate and the total alkalinity is supported by Table 4-9 and Figures 4-2 and 4-3.

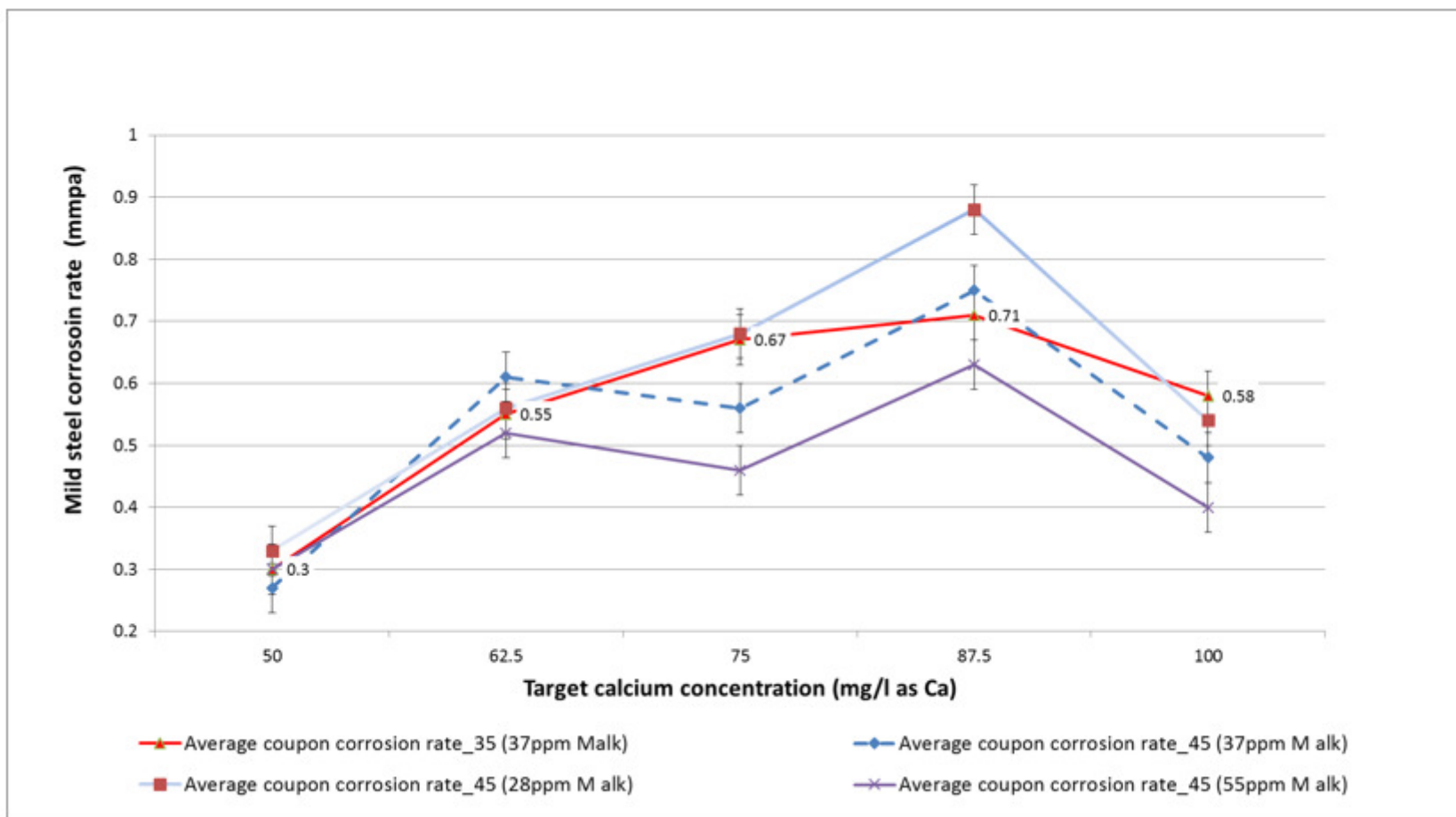


Figure 4-7: Comparison of mild steel coupon data for the two temperatures (35°C versus 45°C) at the same target calcium hardnesses and similar low range of alkalinities (with ± 0.04 mmpa error bars on the corrosion rate)

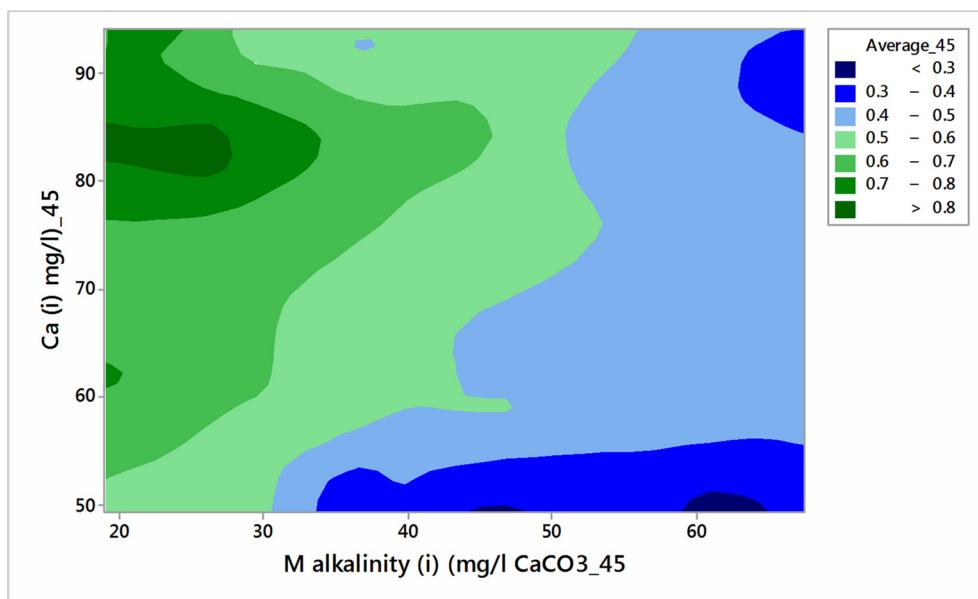


Figure 4-8: Minitab® contour plot showing the correlation of initial calcium hardness and initial low alkalinity on mild steel coupon corrosion at 45°C

Although the intention in this experiment was to hold the total alkalinity constant, it appears the increasing calcium hardness may have been the cause of the decreased total alkalinity, which in turn could possibly have led to the increased mild steel corrosion rates. Various other corrosion indicator response variables also produced strong correlations with their expected outcomes, and they are given in bold text in Table 4-9.

An analysis of the results of corrosion tests at 45°C again shows a statistically significant relationship between the average mild steel coupon corrosion rates and the final total alkalinity of the test solutions. It is also apparent that there were equally strongly positive correlations between the average coupon data and the final chloride, as well as between the average coupon data and the Corrater® corrosion results (Table 4-10). Figure 4-6 illustrates a good cubic model regression analysis fit between the final total alkalinity and the average corrosion rate, but the linear regression produced the best fit over the quadratic and cubic models. The linear model accounts for 65.01% of the variances in the average coupon corrosion rate (Figure 4-6).

A comparison between the coupon data of the corrosion tests performed at 35°C versus those at 45°C showed that the two sets were very similar for the range of temperatures, calcium hardness and total alkalinities considered in the experiments (Figure 4-7). Due to the limited number of tests and the relative inaccuracy of the coupon results, it would be necessary to conduct a more detailed investigation in order to accurately quantify the impact of the temperature difference of 10°C.

Figure 4-8 indicates the different regions of corrosivity for the range of initial calcium and initial total alkalinity at 45°C. As in Figure 4-7, an increase in the initial total alkalinity caused a lowering of the corrosion rate. The role of the calcium hardness was again evident, similarly to Figure 4-7.

4.4.1.2 At system equivalent alkalinity

The previous section focused on the impact low alkalinity brackish water has on the corrosion of mild steel. This section focuses on obtaining a more comprehensive understanding of the impact of the broader range of alkalinity typical of cooling systems. All the other synthetic water target concentrations were kept the same.

Before attempting to address several questions in terms of the impact the water quality and temperature have on the corrosivity of mild steel this set of tests also serves to check whether the :

- Two independent coupon populations were significantly similar by applying the 2-sample t test. The purpose of this test was to calculate the average difference between the two coupon corrosion rates, using the Minitab® software, in order to determine any discrepancies (Figure 4-9);
- Coupon-based corrosion rates correlated with the Corrat® and total iron levels as indicators of the corrosivity of the water on mild steel corrosion.

The main points in this section were to determine:

- The effect of an increase in temperature from 35°C to 45°C together with an increase in calcium hardness from 50 to 100 mg/l , as Ca^{2+}

- The effect of independently increasing the calcium hardness from 50 mg/l to 100 mg/l as Ca^{2+}
- The effect of independently increasing the total alkalinity from 55 to 220 mg/l as CaCO_3
- The combined effect of increasing both the water hardness and total alkalinity.

Table 4-11 summarizes the target water qualities and the test start-up concentrations. The same laboratories, equipment, reagents and consumables were employed following the same procedures in this set of experiments (sub-sections 4.2 and 4.3).

As well as the target concentrations and temperatures Table 4-11 also reports the chemical analyses of the test solutions prior to the corrosion tests. The same chemical analyses were then repeated upon culmination of the three day tests. These results are given in Table 4-12, together with the coupon and Corrat[®] results of Table 4-13.

Figures 4-9 and 4-10 are the Minitab[®] 2-sample t tests for the coupon results for 35 °C and 45 °C respectively.

Figure 4-11 shows the impact of a 10 °C change in temperature on the corrosion rates as well as the impact of higher and lower alkalinity.

Figures 4-12 and 4-13, the scatterplots for 35 °C and 45 °C, show the strength and duration of the correlations between the average coupon corrosion data and the other variables. Table 4-12 provides the statistical linear model correlation data for these relationships.

In Figures 4-14 to 4-17 the contour plots illustrate the potential combined impact of the calcium hardness and total alkalinity.

Table 4-11: Varying calcium and alkalinity at the system equivalent alkalinity range- Target and start-up concentrations

Run	Target concentrations / conditions			Test solution concentrations at start-up								
	Calcium (mg/l as Ca ²⁺)	Total alkalinity (mg/l as CaCO ₃)	Temperature (°C)	Calcium ⁽²⁾ (mg/l as Ca ²⁺)	Total alkalinity ⁽¹⁾ (mg/l as CaCO ₃)	pH ⁽¹⁾	Magnesium ⁽²⁾ (mg/l as Mg ²⁺)	Chloride ⁽²⁾ (mg/l as Cl ⁻)	Sulphate (25x diln) ⁽²⁾ (mg/l as SO ₄ ²⁻ x 10 ³)	Fluoride (25x diln) ⁽¹⁾ (mg/l as F ⁻)	Conductivity ⁽¹⁾ (µS/cm)	Total iron ⁽¹⁾ (mg/l as Fe ³⁺ (total))
31	50.0	55	45	53.0	55.0	7.84	28.9	807	1.27	8.9	4440	< 0.01
22	50.0	82.5	45	53.8	72.9	7.82	29.6	837	1.26	9.0	4520	< 0.01
33	50.0	110	45	53.5	103.0	7.81	29.5	828	1.31	9.1	4584	< 0.01
34	50.0	165	45	52.2	153.3	7.83	28.5	787	1.24	9.9	4620	< 0.01
35	50.0	220	45	50.8	208.6	7.81	28.4	790	1.22	9.4	4704	< 0.01
37	62.5	55	45	60.6	56.6	7.80	27.4	760	1.19	9.6	4208	< 0.01
38	62.5	82.5	45	60.5	86.6	7.83	27.8	786	1.25	9.9	4640	< 0.01
39	62.5	110	45	59.7	113.0	7.85	27.3	811	1.22	9.7	4656	< 0.01
40	62.5	165	45	60.1	170.0	7.88	27.4	771	1.25	8.4	4740	< 0.01
41	62.5	220	45	59.1	218.0	7.89	27.3	785	1.24	8.9	4520	< 0.01
43	75.0	55	45	73.9	66.4	7.99	27.9	772	1.20	8.5	4312	< 0.01

44	75.0	82.5	45	71.4	94.3	7.89	28.1	773	1.20	9.5	4352	< 0.01
45	75.0	110	45	73.1	123.2	7.98	28.0	771	1.23	9.8	4408	< 0.01
46	75.0	165	45	71.8	182.7	7.86	27.8	804	1.21	9.0	4476	< 0.01
47	75.0	220	45	71.1	228.0	7.94	27.8	783	1.25	9.3	4540	< 0.01
49	87.5	55	45	86.5	61.4	7.62	25.1	736	1.24	9.8	4424	< 0.01
50	87.5	82.5	45	85.1	81.0	7.67	24.9	765	1.25	10.2	4436	< 0.01
51	87.5	110	45	87.1	113.5	7.77	25.3	753	1.27	10.1	4433	< 0.01
52	87.5	165	45	86.6	170.6	7.80	25.1	755	1.27	10.1	4660	< 0.01
53	87.5	220	45	85.6	219.9	7.83	25.0	794	1.24	10.0	4568	< 0.01
55	100.0	55	45	96.7	62.9	7.70	24.7	787	1.26	8.9	4672	< 0.01
56	100.0	82.5	45	96.5	87.7	7.73	24.8	787	1.24	9.9	4556	< 0.01
57	100.0	110	45	96.6	119.4	7.74	24.7	810	1.24	9.8	4680	< 0.01
58	100.0	165	45	97.4	176.3	7.76	24.6	778	1.24	9.4	4672	< 0.01
59	100.0	220	45	92.2	225.2	7.78	24.2	809	1.28	9.6	4732	< 0.01
36	50.0	110	35	51.7	109.9	7.84	28.6	823	1.24	9.6	4569	< 0.01
42	62.5	110	35	59.3	118.0	7.84	27.9	806	1.26	9.2	4676	< 0.01
48	75.0	110	35	73.2	100.4	7.91	28.7	815	1.27	9.5	4388	< 0.01
54	87.5	110	35	86.5	113.1	7.76	25.2	801	1.30	10.1	4444	< 0.01
60	100.0	110	35	95.1	18.9	6.02	23.9	797	1.26	9.9	4452	< 0.01

Notes: 1. Test conducted in Laboratory B, 2. Test conducted in Laboratory C, nt = not tested.

Table 4-12: Varying calcium and alkalinity at the system equivalent alkalinity range- Cessation concentrations

Run	Target concentrations / conditions			Test solution concentrations upon cessation of corrosion tests								
	Calcium (mg/l as Ca ²⁺)	Total alkalinity (mg/l as CaCO ₃)	Temperature (°C)	Calcium ⁽²⁾ (mg/l as Ca ²⁺)	Total alkalinity ⁽¹⁾ (mg/l as CaCO ₃)	pH ⁽¹⁾	Magnesium ⁽²⁾ (mg/l as Mg ²⁺)	Chloride ⁽²⁾ (mg/l as Cl ⁻)	Sulphate (25x diln) ⁽²⁾ (mg/l as SO ₄ ²⁻) x 10 ³	Fluoride (25x diln) ⁽¹⁾ (mg/l as F ⁻)	Conductivity ⁽¹⁾ (µS/cm)	Total iron ⁽¹⁾ (mg/l as Fe ³⁺ (total))
31	50.0	55	45	55.3	53.9	8.10	31.1	888	1.33	8.8	4668	6.4
22	50.0	82.5	45	51.9	72.9	8.32	30.4	853	1.34	9.1	4716	3.9
33	50.0	110	45	50.6	96.9	8.46	30.6	847	1.35	9.4	4784	4.3
34	50.0	165	45	47.2	141.0	8.61	29.3	826	1.28	8.9	4784	2.9
35	50.0	220	45	39.1	174.2	8.69	29.5	852	1.31	8.9	4900	2.7
37	62.5	55	45	58.0	48.8	8.15	28.2	807	1.26	9.4	4640	6.1
38	62.5	82.5	45	58.3	75.5	8.34	29.3	829	1.31	9.3	4828	3.5
39	62.5	110	45	56.2	93.3	8.48	28.7	807	1.27	8.9	4832	3.0
40	62.5	165	45	52.3	144.0	8.56	28.2	827	1.25	9.9	4892	2.1
41	62.5	220	45	43.6	172.0	8.62	29.5	860	1.34	9.5	4880	2.0
43	75.0	55	45	70.7	54.5	8.23	29.6	798	1.26	9.8	4548	1.7
44	75.0	82.5	45	69.6	76.1	8.37	29.2	797	1.26	9.5	4520	1.4

continuation of Table 4-12												
45	75.0	110	45	65.8	100.2	8.49	29.0	808	1.26	9.3	4584	1.2
46	75.0	165	45	58.3	136.2	8.54	28.9	804	1.25	9.8	4636	0.8
47	75.0	220	45	46.2	155.4	8.59	28.1	797	1.24	9.5	4664	1.4
49	87.5	55	45	87.4	52.3	8.3	26.9	791	1.44	10.1	4776	3.3
50	87.5	82.5	45	83.4	67.3	8.37	26.8	797	1.35	10.1	4544	0.5
51	87.5	110	45	80.2	87.8	8.5	26.3	796	1.34	9.9	4680	2.9
52	87.5	165	45	70.7	115.8	8.51	25.8	787	1.33	9.9	4668	1.4
53	87.5	220	45	55.6	143.5	8.57	25.8	831	1.40	10.1	4788	0.7
55	100.0	55	45	94.8	46.9	8.11	26.0	845	1.32	10	4764	2.8
56	100.0	82.5	45	92.3	65.6	8.25	26.2	828	1.31	9.2	4820	0.4
57	100.0	110	45	88.6	91.9	8.3	25.8	863	1.30	9.6	4812	2.0
58	100.0	165	45	76	120.1	8.35	25.5	833	1.32	9.9	4840	0.0
59	100.0	220	45	59.7	138.2	8.37	24.2	832	1.31	9.8	4844	0.0
36	50.0	110	35	49.3	101.8	8.38	29.3	815	1.27	9.1	4620	4.0
42	62.5	110	35	56.1	94.8	8.41	28.3	816	1.32	9.5	4916	4.3
48	75.0	110	35	68.8	76.9	8.27	27.3	793	1.19	8.8	4456	1.8
54	87.5	110	35	79.6	95.7	8.37	25.6	822	1.34	10.0	4480	2.0
60	100.0	110	35	98.6	10.9	6.84	24.5	816	1.29	9.8	4556	36.4

Table 4-13: Corrosion coupon and Corrat[®] readings while varying calcium and alkalinity at the system equivalent alkalinity range

Run	Target concentrations / conditions			Corrosion Coupon Results			Corrat [®] readings			
	Calcium (mg/l as Ca ²⁺)	Total alkalinity (mg/l as CaCO ₃)	Temperature (°C)	Coupon 1 (mmpa)	Coupon 2 (mmpa)	Average (mmpa)	Day 1 (mmpa)	Day 2 (mmpa)	Day 3 (mmpa)	Day 4 (mmpa)
31	50	55	45	0.45	0.48	0.46	0.92	0.90	0.85	0.89
22	50	82.5	45	0.31	0.38	0.35	0.39	0.34	0.32	0.30
33	50	110	45	0.25	0.32	0.28	0.35	0.36	0.28	0.27
34	50	165	45	0.16	0.25	0.21	0.22	0.21	0.21	0.23
35	50	220	45	0.16	0.24	0.20	0.25	0.22	0.22	0.22
37	62.5	55	45	0.41	0.50	0.46	0.92	0.85	0.86	0.84
38	62.5	82.5	45	0.37	0.39	0.38	0.72	0.66	0.53	0.57
39	62.5	110	45	0.29	0.30	0.29	0.76	0.73	0.75	0.52
40	62.5	165	45	0.10	0.28	0.19	0.48	0.51	0.53	0.49
41	62.5	220	45	0.16	0.32	0.24	0.54	0.50	0.50	0.49
43	75	55	45	0.30	0.37	0.34	0.75	0.79	0.76	0.76
44	75	82.5	45	0.23	0.26	0.25	0.20	0.20	0.23	0.30
45	75	110	45	0.22	0.19	0.20	0.72	0.74	0.79	0.81
46	75	165	45	0.21	0.14	0.18	0.64	0.71	0.76	0.84
47	75	220	45	0.22	0.25	0.24	0.79	0.76	0.75	0.84
49	87.5	55	45	0.24	0.34	0.29	0.32	0.25	0.29	0.36
50	87.5	82.5	45	0.21	0.23	0.22	0.39	0.35	0.37	0.38
51	87.5	110	45	0.13	0.16	0.15	0.25	0.27	0.26	0.20
52	87.5	165	45	0.17	0.22	0.20	0.24	0.21	0.19	0.19
53	87.5	220	45	0.21	0.29	0.25	0.31	0.25	0.27	0.24
55	100	55	45	0.23	0.26	0.24	0.25	0.22	0.16	nt
56	100	82.5	45	0.13	0.13	0.13	0.12	0.14	0.12	nt
57	100	110	45	0.14	0.14	0.14	0.21	0.21	0.19	nt
58	100	165	45	0.19	0.22	0.21	0.13	0.11	0.10	nt
59	100	220	45	0.33	0.37	0.35	0.19	0.20	0.22	nt
36	50	110	35	0.23	0.30	0.26	0.33	0.36	0.25	0.26
42	62.5	110	35	0.19	0.34	0.26	0.43	0.42	0.45	0.44
48	75	110	35	0.15	0.25	0.20	0.96	0.94	0.99	0.97
54	87.5	110	35	0.14	0.16	0.15	0.56	0.47	0.48	0.42
60	100	110	35	0.61	0.69	0.65	0.11	0.34	0.39	nt

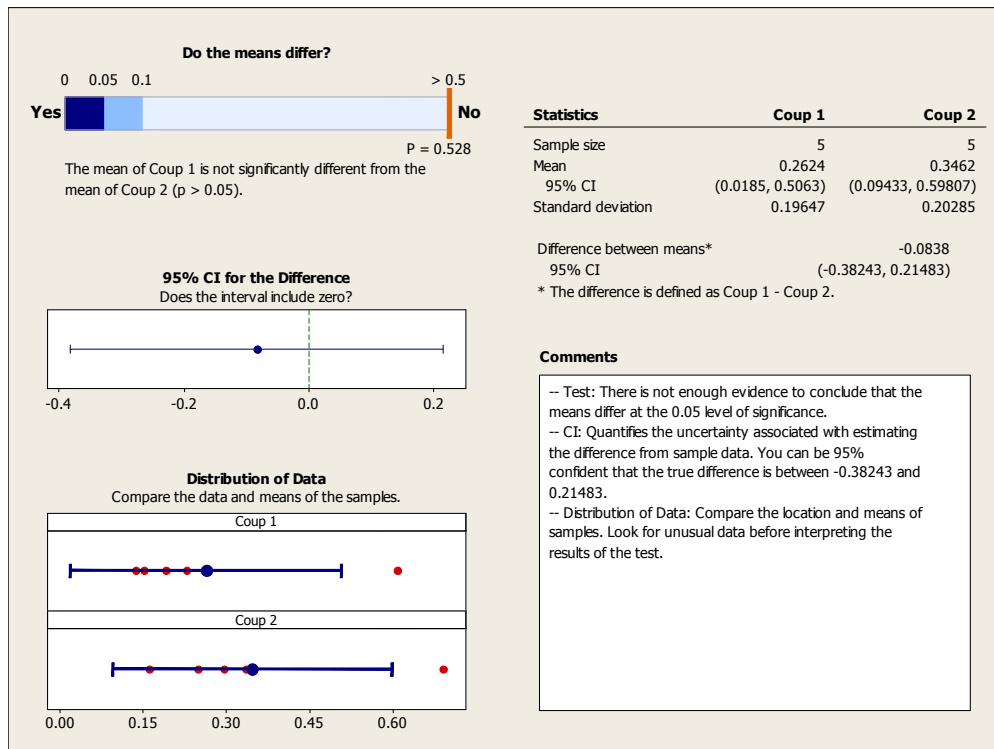


Figure 4-9: Minitab[®] report on the 2-sample t test for the mean of the coupon 1 results and coupon 2 results for 35°C

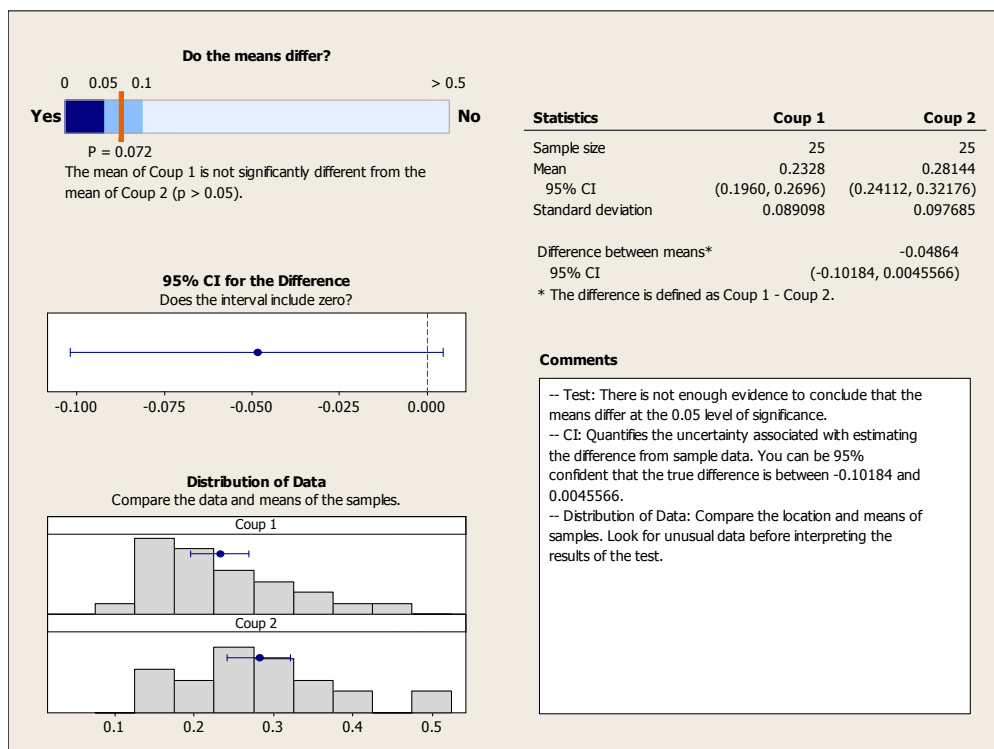


Figure 4-10: Minitab[®] report on the 2-sample t test for the mean of the coupon 1 results and coupon 2 results for 45°C

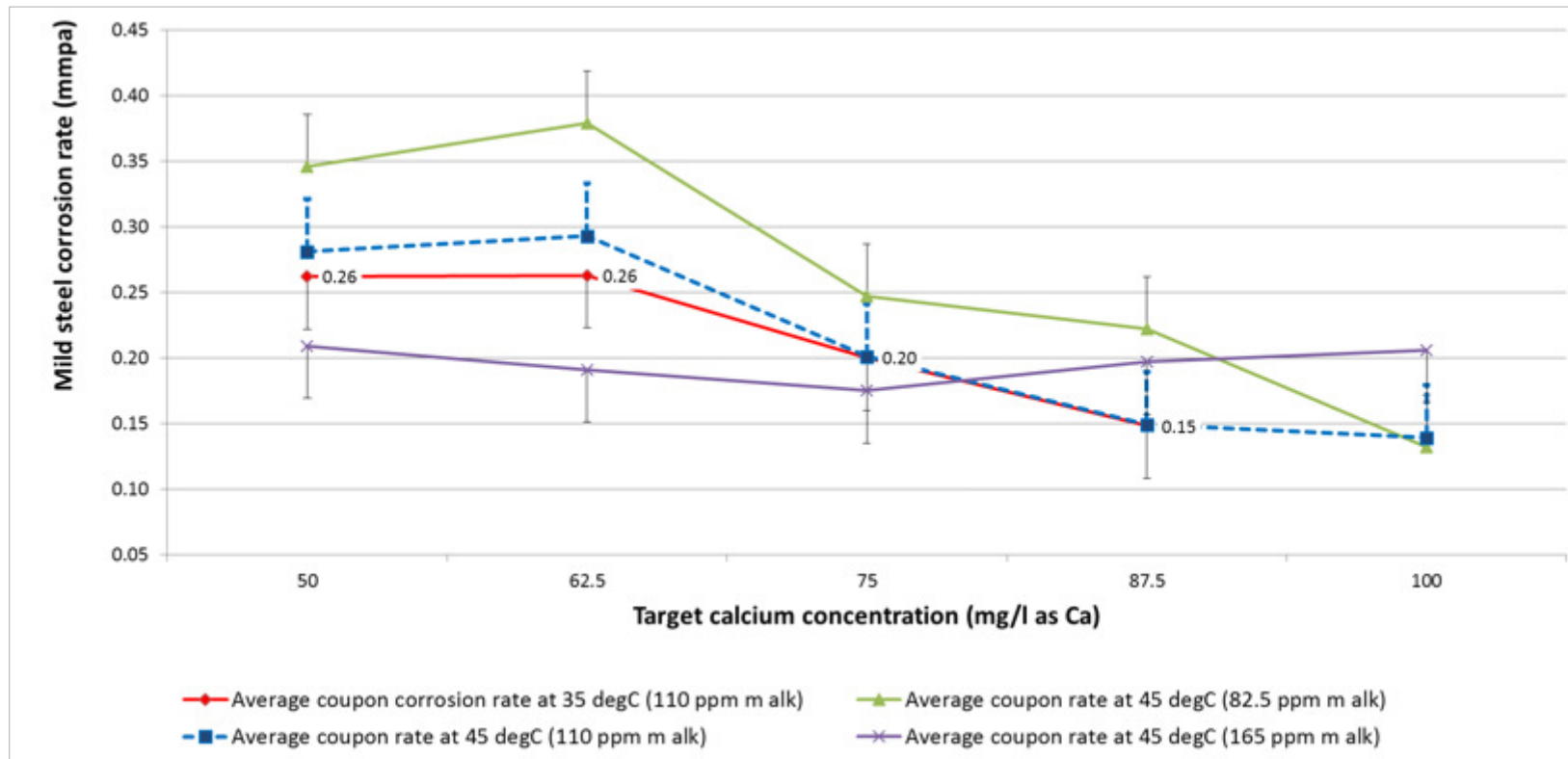


Figure 4-11: Comparison of mild steel coupon data for the two temperatures (35°C versus 45°C) at the same calcium hardnesses and the similar range of alkalinities (with ± 0.04 mmpa error bars on the corrosion rate)

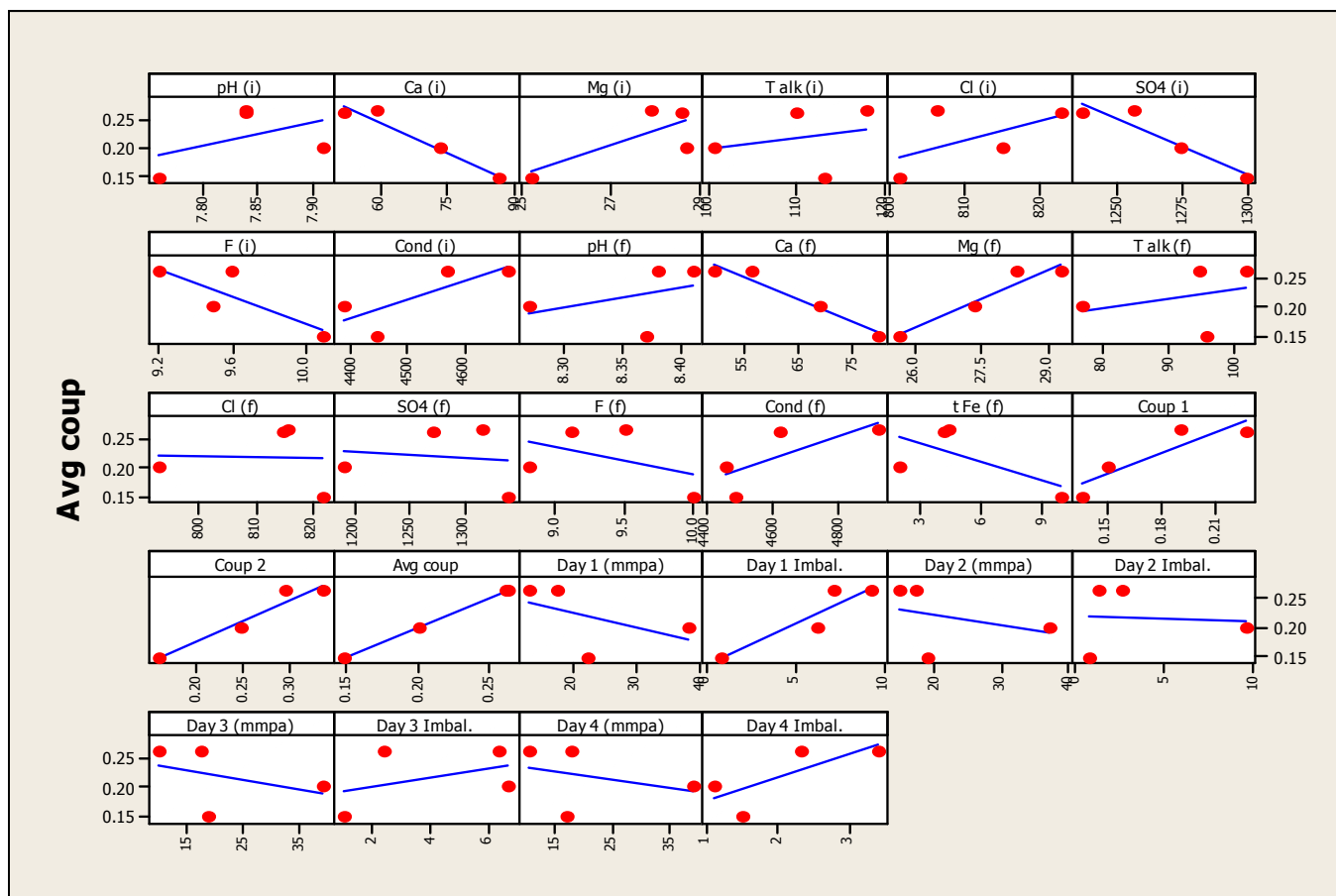


Figure 4-12: Scatterplots of the average mild steel coupon corrosion rates versus pertinent parameters at 35°C (excluding outlier of results for run 60 with low pH)

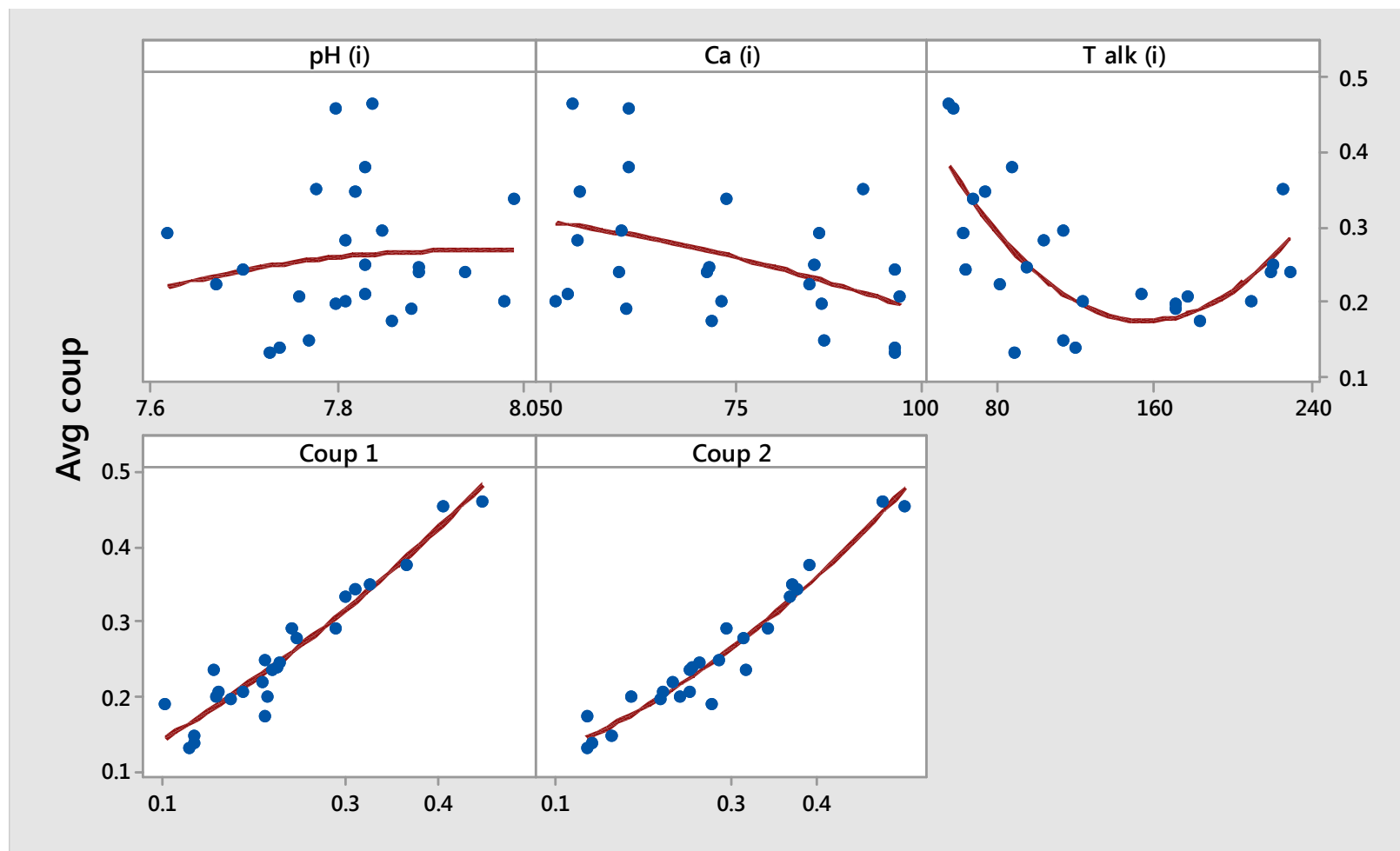


Figure 4-13: Scatterplots of the average mild steel coupon corrosion rates versus pertinent parameters at 45°C

Table 4-14: Statistically significant relationships between the average coupon corrosion rate and various parameters in the 35°C and 45°C corrosion tests

35°C		45°C	
Parameter	Strength and direction of relationship	Parameter	Strength and direction of relationship
Calcium (initial)	Strongly	Day 1 (mmpa)	Moderately positive
Sulphate (initial)	Strongly	Day 2 (mmpa)	Moderately positive
Magnesium (final)	Strongly	Day 3 (mmpa)	Moderately positive
Calcium (final)	Strongly	Day 4 (mmpa)	Moderately positive
Coupon position 2	Strongly	Calcium (initial)	Moderately
		Total alkalinity	Weakly negative
		pH (final)	Moderately
		Coupon position 1	Strongly positive
		Coupon position 2	Strongly positive

Note: Detailed statistical correlation data are shown in Tables G-3 and G-4.

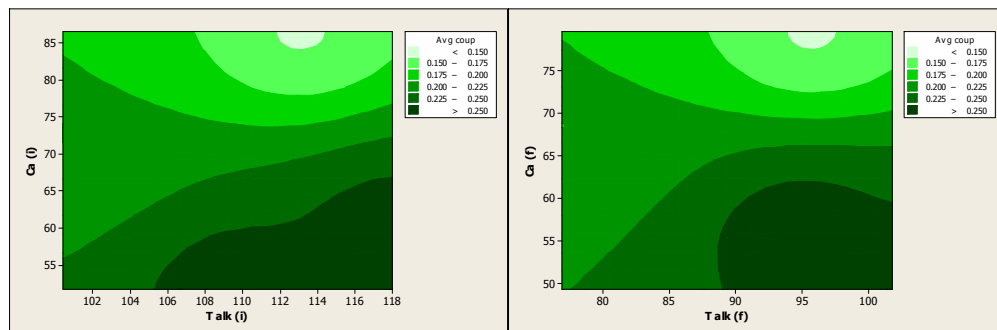


Figure 4-14: (Left) Correlation of initial calcium hardness and initial total alkalinity on mild steel coupon corrosion at 35°C

Figure 4-15: (Right) Correlation of final calcium hardness and final total alkalinity on mild steel coupon corrosion at 35°C

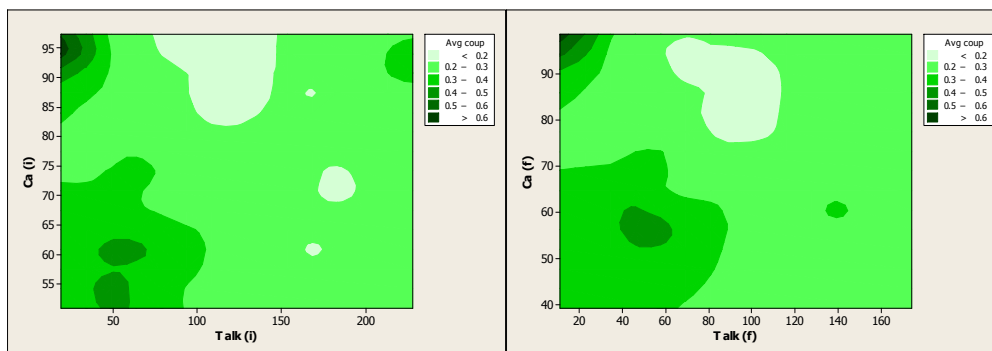


Figure 4-16: (Left) Correlation of initial calcium hardness and initial total alkalinity on mild steel coupon corrosion at 45°C

Figure 4-17: (Right) Correlation of final calcium hardness and final total alkalinity on mild steel coupon corrosion at 45°C

A linear regression analysis was conducted to predict the linear relationship between coupon corrosion rate and various predictors in order to determine how the response variable changes as the particular predictor variables change (Equation 4.2). This was done taking into account any impact the 10°C temperature difference might also have on mild steel corrosivity (Table 4-15).

Table 4-15: Regression analysis report for variables correlating with the mild steel coupon corrosion rates at 35°C and 45°C

Regression Analysis: Avg coup versus pH (i), Ca (i), ...				
The regression equation is				
Avg coup = 3.93 - 0.219 pH (i) - 0.00559 Ca (i) - 0.0390 Mg (i)				
- 0.000329 T alk (i) + 0.000987 Cl (i) + 0.000151 SO4 (i)				
- 0.0470 F (i) - 0.000283 Cond (i) + 0.00666 Target T				
Predictor	Coef	SE Coef	T	P
Constant	3.934	1.319	2.98	0.007
pH (i)	-0.21915	0.05851	-3.75	0.001
Ca (i)	-0.005591	0.002376	-2.35	0.029
Mg (i)	-0.03896	0.02640	-1.48	0.156
T alk (i)	-0.0003294	0.0003101	-1.06	0.301
Cl (i)	0.0009867	0.0008458	1.17	0.257
SO4 (i)	0.0001513	0.0006146	0.25	0.808
F (i)	-0.04699	0.03448	-1.36	0.188
Cond (i)	-0.0002828	0.0001533	-1.84	0.080
Target T degC	0.006660	0.004637	1.44	0.166
S = 0.0751701 R-Sq = 68.6% R-Sq(adj) = 54.4%				

continuation of Table 4-15						
Analysis of Variance						
Source	DF	SS	MS	F	P	
Regression	9	0.246539	0.027393	4.85	0.002	
Residual Error	20	0.113011	0.005651			
Total	29	0.359549				
Source	DF	Seq SS				
pH (i)	1	0.133768				
Ca (i)	1	0.058011				
Mg (i)	1	0.000155				
T alk (i)	1	0.017679				
Cl (i)	1	0.000002				
SO4 (i)	1	0.001643				
F (i)	1	0.009261				
Cond (i)	1	0.014364				
Target T degC	1	0.011656				
Unusual Observations						
Obs	pH (i)	Avg coup	Fit	SE Fit	Residual	St Resid
29	7.78	0.3500	0.1992	0.0436	0.1508	2.46R

Note: R = an observation with a large standardized residual.

A non-linear multivariate regression analysis was performed to determine how the response variable changes as the particular predictor variables change. This was done without taking into account the impact the 10°C temperature difference, Equation 4.3:

$$\text{Corrosion (mmpa)} = 4.58\text{E-}6 \text{ Ca}^2 - 8.85\text{E-}3 \text{ Ca} + 4.64\text{E-}5 (\text{Ca} \times \text{M alk}) - 9.30\text{E-}3 \times \text{M alk} + 1.90\text{E-}5 \text{ M alk}^2 + 1.26\text{.....} [4.3]$$

where: Ca = calcium (mg/l as Ca²⁺),

M alk = total alkalinity (mg/l as CaCO₃).

Figure 4-18 confirms the accuracy of the empirically derived non-linear regression equation by comparing it to the laboratory coupon corrosion data. An R² (adj) value of 90% was obtained. The graph also indicates where large residuals and an unusual result occurred, explicitly at the upper section of curve (indicated with red markers).

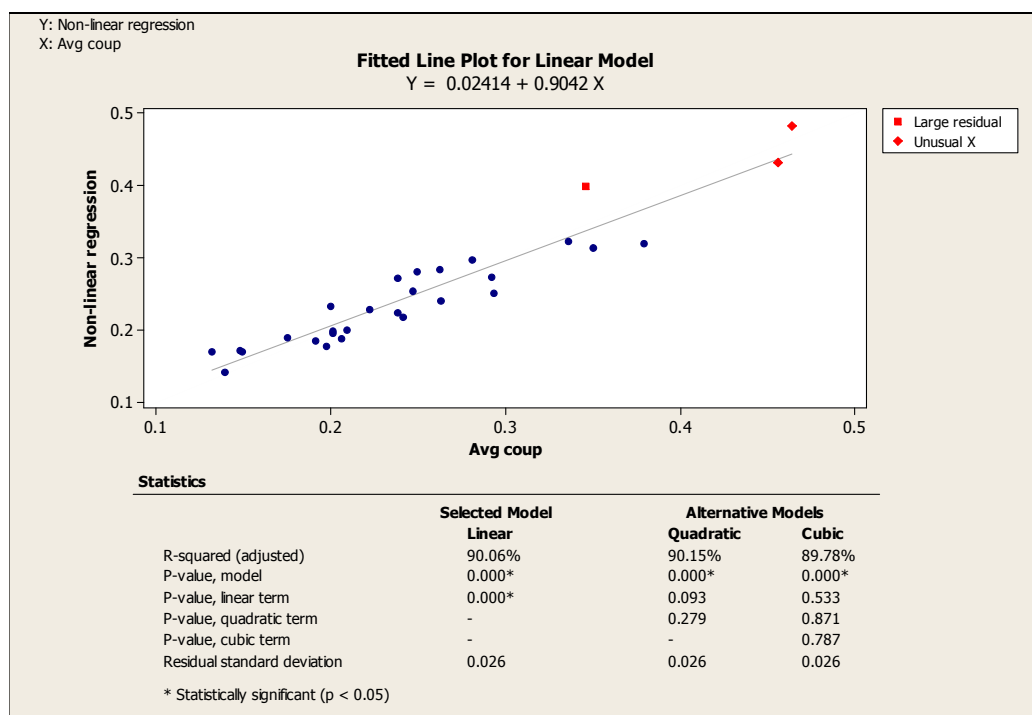


Figure 4-18: Regression analysis for the derived non-linear regression equation versus the average corrosion rate (Avg coup)

The empirically derived equation was then compared, statistically, against the predictive indices discussed in the literature survey, by using the test solution target values and the comparison performed at both 35°C and 45°C (Table 4-16). This analysis indicated the calculated rate had the following statistically significant moderately strong relationships (with Pearson coefficients in red text) at a 95% confidence level, as indicated by the p values in bold (Tables 4-16 and 4-17), and Figure 4-19.

A contour plot (Figure 4-20), of the derived multivariate non-linear regression equation, Equation 4.3, was for a visual comparison with the contour plots of the laboratory coupon corrosion data (Figures 4-16 to 4-17). Contour plots (Figures 4-21 to 4-27) of statistically significant indices taken from literature, Table 4-17, were also included for further comparisons.

Table 4-16: Statistically significant relationships between the calculated rate and the other indices

Index	Calculated rate (mmpa)	
	r value	p value
Calcium hardness (as Ca ²⁺)	-0.408	0.093
Total alkalinity (as CaCO ₃)	-0.344	0.162
CR8 Corrosion	-0.053	0.833
Buffer Capacity	-0.344	0.162
CR4 Corrosion	0.529	0.024
CR8 Corrosion	-0.053	0.833
CCPP (mg/l)	-0.259	0.300
I _s (Oddo &T, 1982)	-0.536	0.022
Ionic Strength	-0.531	0.023
Stiff & Davis	-0.570	0.013
CaCO ₃ saturation	-0.180	0.474
CaF ₂ saturation	0.176	0.485
Langelier saturation index	-0.532	0.023
RSI	0.526	0.025
PSI	0.539	0.021
Larson Skold	0.545	0.019
CaCO ₃ FIME	-0.038	0.880

Notes: The r value is the Pearson Coefficient of Correlation and indicates the direction and the intensity of the correlation. The p value (if ≤ 0.05) indicates statistical significance at the 95% confidence level.

Table 4-17: Summary of the statistically significant correlations between the calculated corrosion rate and the established indices

Negative relationships	Positive relationships
I_s (Oddo) , Oddo-Tomson (1982) method	CR4 , 4 variable model (Pisigan and Singley, 1984)
Ionic strength	RSI , Ryznar Stability Index (Ryznar, 1944)
SDI , Stiff Davis Index (Stiff and Davis, 1952)	PSI , Puckorius or Practical Scaling Index (Puckorius and Brooke, 1990)
LSI , Langelier Saturation Index (Langelier, 1936)	LR , Larson Skold Index also known as the Larson Ratio (Larson and Skold, 1957, 1958).

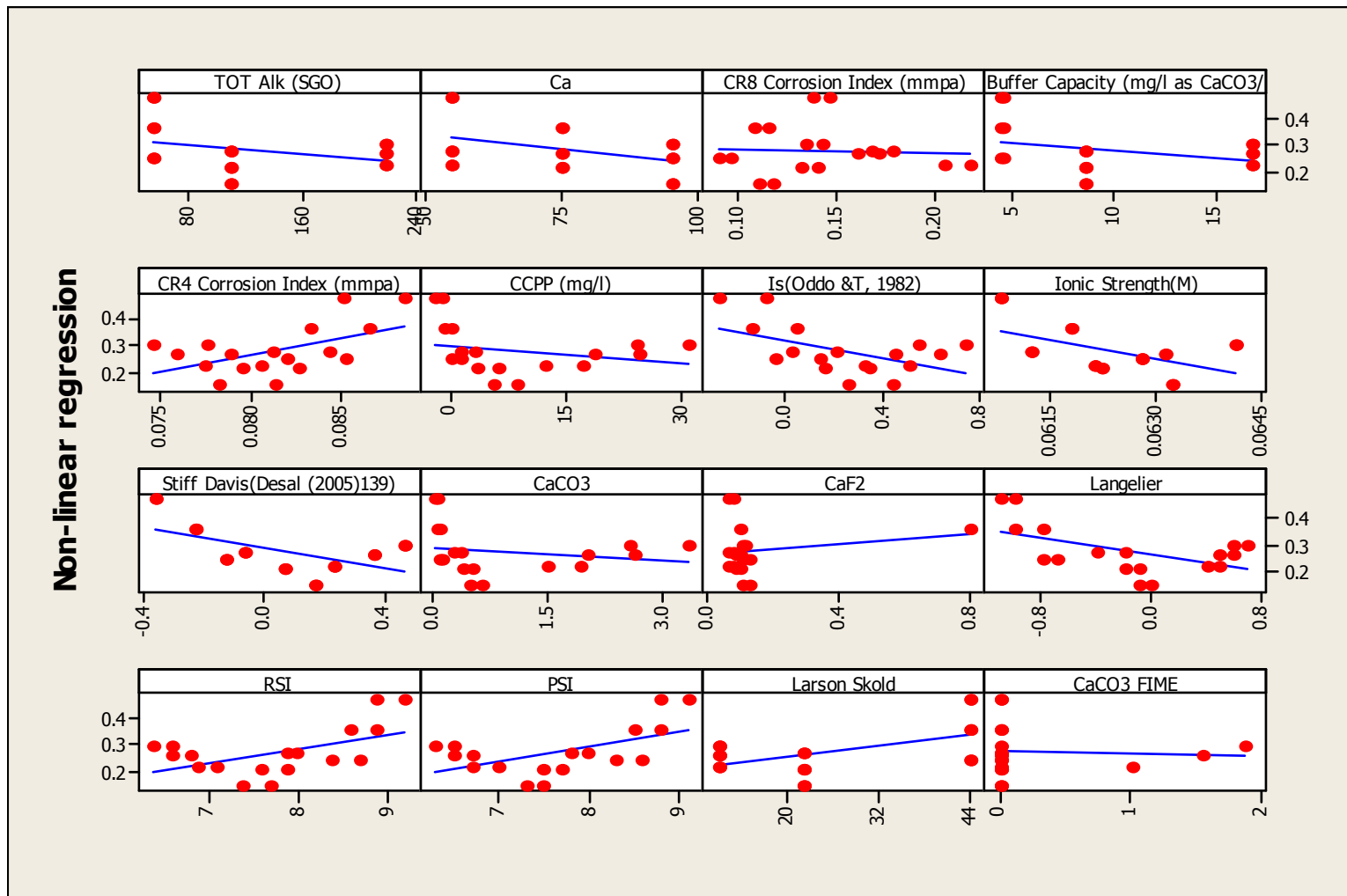


Figure 4-19: Scatterplot correlations of the calculated corrosion rate based on the non-linear regression equation versus the established indices

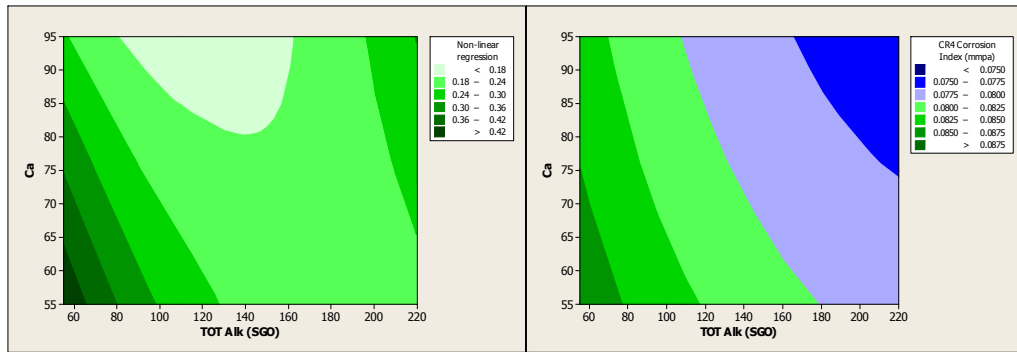


Figure 4-20: (Left) Results of the multivariate non-linear equation versus the targeted calcium (Ca) and total alkalinity concentrations (TOT Alk (SGO))

Figure 4-21: (Right) Results of the C4 model (Pisigan and Singley, 1984) versus the targeted calcium (Ca) and total alkalinity concentrations (TOT Alk (SGO))

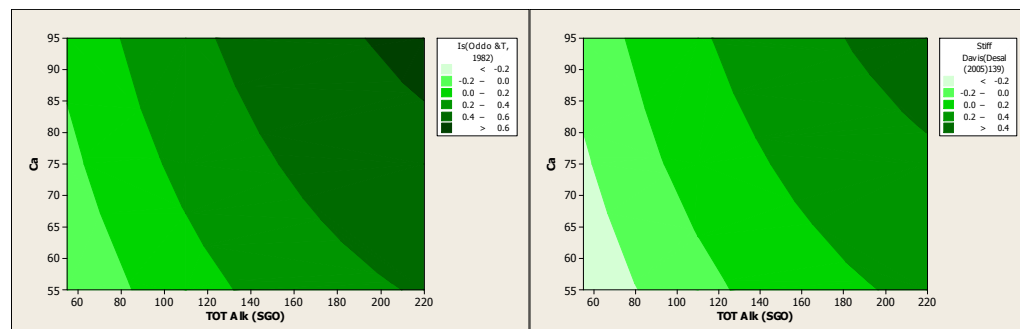


Figure 4-22: (Left) Results of the Oddo and Tomson model (Oddo and Tomson, 1982) versus the targeted calcium (Ca) and total alkalinity concentrations (TOT Alk (SGO))

Figure 4-23: (Right) Results of the Stiff and Davis Index (Stiff and Davis, 1952) versus the targeted calcium (Ca) and total alkalinity concentrations (TOT Alk (SGO))

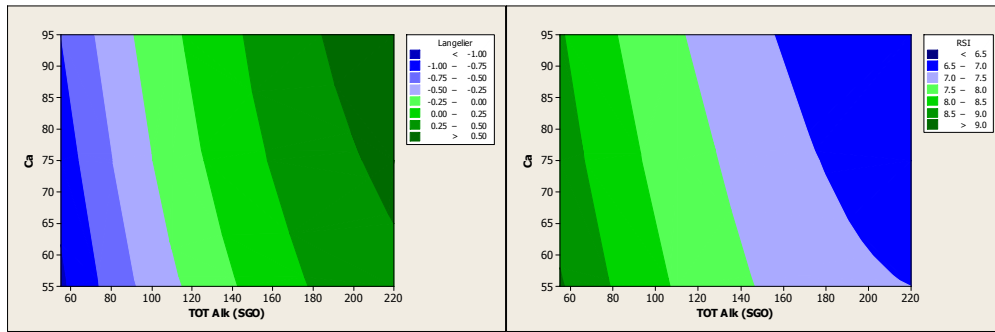


Figure 4-24: (Left) Results of the Langelier Saturation Index (Langelier, 1936) versus the targeted calcium (Ca) and total alkalinity concentrations (TOT Alk (SGO))

Figure 4-25: (Right) Results of the Ryznar Stability Index (Ryznar, 1944) versus the targeted calcium (Ca) and total alkalinity concentrations (TOT Alk (SGO))

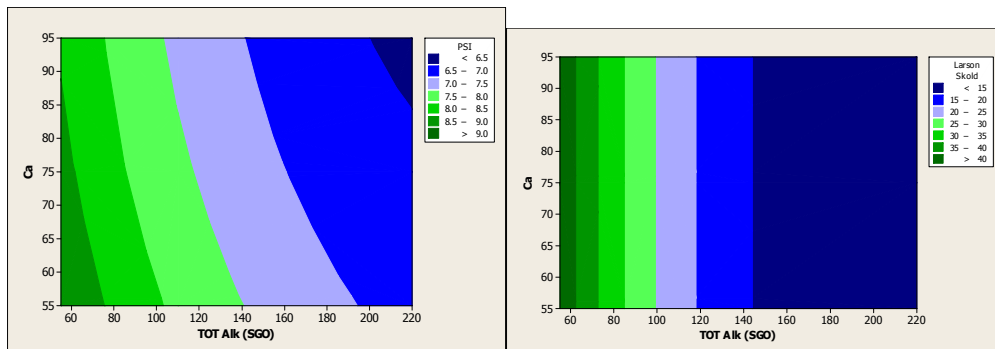


Figure 4-26: (Left) Results of the Practical Scaling Index (Puckorius and Brooke, 1990) versus the targeted calcium (Ca) and total alkalinity concentrations (TOT Alk (SGO))

Figure 4-27: (Right) Results of the Larson Skold Index ((Larson and Skold, 1957) versus the targeted calcium (Ca) and total alkalinity concentrations (TOT Alk (SGO))

Based on Figure 4-9, 2-sample t tests for the coupon results for 35°C, it appears there were insufficient data to conclude whether the means were significantly different for the two coupon positions. The 2 sample t-test for the tests performed at 45°C for the mean of coupon 1 versus the mean of coupon 2 showed that the two coupon positions were not statistically different with 25 samples and at a 95%

confidence level ($p > 0.05$) (Figure 4-10). The second tables in Figures 4-9 and 4-10 gave the confidence interval for the difference in population means. In the 35°C and 45°C cases, the 95% confidence intervals were: -0.38 and 0.21, and -0.10 and 0.00 respectively. As both intervals included zero, it was suggested that there was no difference between the coupon one and coupon two results.

Figure 4-11 shows the impact of a 10°C difference in temperature, where the higher temperature produced higher corrosion rates at the lower targeted calcium hardness values of 50 and 62.5 mg/l as Ca. At the higher calcium hardness values both temperatures produced similar corrosion rates. Figure 4-11 depicts the impact of different total alkalinities where higher alkalinity resulted in lower coupon corrosion rates, with the exception of the increased corrosion evident for the points corresponding to the combined effect of high calcium hardness (above 75 mg/l as Ca) and high alkalinity (165 mg/l as CaCO_3). The figure includes ± 0.04 mmpa error bars to indicate the uncertainty of the measurements.

The scatterplots for 35°C and 45°C, Figures 4-12 and 4-13 shows the distribution of the plots and the strength and duration of the correlations between the average coupon corrosion data and the other variables. Scatterplots of the results of the corrosion tests performed with synthetic solutions, at 35°C, for the entire range of calcium hardness and alkalinities experienced by the two open cooling systems, demonstrate that there were relatively good linear regression correlations between the average coupon corrosion rate and various parameters. Figure 4-12 illustrates these correlations for both the initial and final calcium concentrations (both strong negative relationships), the final magnesium concentration (a strong positive relationship) and the initial sulphate concentration (a strong negative relationship). The other magnesium and sulphate plots produced similar but weaker correlations than their already mentioned counterparts. A comparison of the average corrosion rate with the total iron concentrations and the Corrater® general corrosion rate readings, for the data at both 35°C and 45°C, showed it was only possible to find statistically significant linear correlations, at a 95% confidence level, between the average corrosion rate and the Corrater® general corrosion readings for the tests

performed at 45°C (Figures 4-12 and 4-13, and Table 4-14). The latter two measures of corrosion were only regarded to be moderately strong and positively correlated. The lack of correlation between the average corrosion rate and the total iron levels may be attributed to the inaccuracies associated with the laboratory wet chemical techniques employed in the total iron analysis.

According to Table 4-14, which is based on the calculated *r* and *p* values listed in Tables G-3 and G-4, only the following predictor variables produced statistically significant strong correlations with the average coupon corrosion rates at 35°C:

- The initial and final calcium, both with negative correlations,
- Initial sulphate, with a negative correlation, and
- Final magnesium and coupon at position two, with positive correlations.

At 45°C, moderate negative relationships were apparent for the:

- Initial total alkalinity
- Final pH, and
- Initial calcium.

Moderate positive relationships were apparent for the average coupon corrosion rates and Corratel[®] general corrosion rates for all four days.

The contour plots (Figures 4-14 and 4-15) for the average coupon corrosion rate versus calcium and total alkalinity for the corrosion tests performed at 35°C demonstrated that:

- Lowest corrosion rates occurred at high calcium levels (> 70 mg/l as Ca) and high total alkalinity (> 90 mg/l as CaCO₃), and the
- Highest corrosion rates at high total alkalinity (> 90 mg/l as CaCO₃) and low calcium (< 60 mg/l as Ca).

The contour plots (Figures 4-16 and 4-17) for the average coupon corrosion rate versus calcium and total alkalinity tests performed at 45°C demonstrated that:

- Lowest corrosion rates occurred at:

- high calcium levels (80-100 mg/l as Ca) and moderately high total alkalinity (65-110 mg/l as CaCO₃), as well as
- moderate calcium levels (60 – 80 mg/l as Ca) and moderate total alkalinity (150-200 mg/l as CaCO₃), and the
- Highest corrosion rates at low total alkalinity (< 50 mg/l as CaCO₃) and either low calcium levels (< 50 mg/l as Ca) or high calcium levels (> 85 mg/l as Ca).

It is apparent that the regions of either low or high corrosivity were similar for both the lower temperature of 35°C and higher temperature of 45°C. The linear regression analysis of the correlation between the average coupon corrosion rates with the various predictors showed that certain predictors had a significant impact on average coupon corrosion rate, namely: the constant in the equation, the initial pH and the initial calcium concentration (Equation 4.2 in Table 4-15). The adjusted R² (R-Sq (adj)) described the moderate variation (54%) in the observed response values that was explained by the predictors.

An empirically derived non-linear regression equation (Equation 4.3), based on only the solution's initial calcium and initial total alkalinity, was confirmed to account for 90% of the variations in the average corrosion coupon data. This equation was correlated against the various established indices and it was found that their statistically significant linear relationships were only moderately strong in nature at the 95% confidence level. These indices, listed from highest to lowest in terms of both statistical significance and the intensity of the correlation, were: SDI (Stiff Davis Index) (Stiff and Davis, 1952), LR (Larson Skold Index also known as the Larson Ratio) (Larson and Skold, 1957), PSI (Puckorius or Practical Scaling Index) (Puckorius and Brooke, 1990), I_s (Oddo) (Oddo-Tomson (1982) method, LSI (Langelier Saturation Index) (Langelier, 1936), Ionic strength, CR4 (4 variable model), and RSI (Ryznar Stability Index) (Ryznar, 1944), 1958), (Pisigan and Singley, 1984). The remainder of the indices listed in Table 4-10, namely the: Buffer Capacity (Stumm, 1960), CCPP (mg/l) (Merrill and Sanks, 1978), CaCO₃ saturation, CaF₂ saturation, CR8 Corrosion (Pisigan and Singley, 1984) and CaCO₃ FIME (Dye, 1958) were not statistically significant and weakly correlated.

A comparison of the contour plot of new model versus that of other indices, for the set of target values considered, revealed some subtle differences between them. One of the more obvious differences was the greater impact the calcium concentration had on the corrosivity, as evident by the relatively steeper diagonal contour lines (Figure 4-20).

4.4.2 Impact of chloride in synthetic brackish water on mild steel

The main aim of relevance in this section were to determine the corrosive effects on mild steel primarily due to: an increase in chloride from 500 to 1076 mg/l as Cl, and an increase in temperature by 10°C, from 35°C to 45°C. For this set of experiments, it was again decided to select the middle of the ranges for the unvaried parameters: calcium, total alkalinity, sulphate, fluoride and magnesium. The target water qualities and the test start-up concentrations are summarised in Table 4-18. The same laboratories, equipment, reagents, consumables and procedures were followed for this set of experiments (sub-sections 4.2 and 4.3).

As well as the target concentrations and temperatures, Table 4-18 also shows the chemical analyses of the test solutions prior to the commencement of the corrosion tests. The same chemical analyses were then repeated upon culmination of the three day tests. These results are reported in Table 4-19 and the coupon and Corrater® results in Table 4-20. Figures 4-28 and 4-29 show the relationship between the initial chloride concentration and the mild steel corrosion rate at 45°C. Table 4-21 provides further support for the lack of a statistically significant correlation between the average corrosion rate and the chloride concentration.

Table 4-18: Varying the chloride concentration and temperature while holding the other variables constant- Target and start-up concentrations

Run	Target concentrations / conditions		Test solution concentrations at start-up									
	Chloride (mg/l as Cl ⁻)	Temperature (°C)	Chloride ⁽²⁾ (mg/l as Cl ⁻)	pH ⁽¹⁾	Calcium ⁽²⁾ (mg/l as Ca ²⁺)	Magnesium ⁽²⁾ (mg/l as Mg ²⁺)	Total alkalinity ⁽¹⁾ (mg/l as CaCO ₃)	Sulphate diln ⁽²⁾ (mg/l as SO ₄ ²⁻) x 10 ³	Fluoride diln ⁽¹⁾ (mg/l as F ⁻) (25x)	Sodium ⁽²⁾ (mg/l as Na ⁺)	Conductivity ⁽¹⁾ (µS/cm)	Total iron ⁽¹⁾ (mg/l as Fe ³⁺ (total))
61	500	45	511	7.99	73.2	27.6	58.4	1.32	9.8	714	3992	< 0.10
62	625	45	672	7.95	73.0	27.7	54.0	1.30	8.4	799	4396	< 0.10
63	750	45	774	8.01	73.9	27.5	56.5	1.35	9.1	851	4736	< 0.10
64	875	45	825	7.83	69.7	26.0	50.4	1.33	8.9	nt	4888	< 0.10
65	1000	45	1029	7.93	64.3	25.4	51.4	1.25	9.7	971	5336	< 0.10
109	500	45	430	8.06	73.3	27.0	71.1	1.00	9.2	738	3840	< 0.10
110	644	45	532	7.91	74.0	27.0	67.0	1.01	9.4	813	4228	< 0.10
111	788	45	610	7.92	73.7	27.1	91.2	9.20	8.8	889	4620	< 0.10
112	932	45	827	8.07	76.1	27.7	68.4	1.00	9.6	992	5004	< 0.10
113	1076	45	1017	8.05	75.0	27.6	63.7	1.01	10.0	1058	5428	< 0.10
313	500	45	593	7.85	nt	nt	67.9	1.25	9.5	nt	3660	< 0.10
314	625	45	757	7.86	nt	nt	69.7	1.25	9.6	nt	4084	< 0.10
315	750	45	801	7.85	nt	nt	70.2	1.35	9.9	nt	4168	< 0.10
316	875	45	872	7.84	nt	nt	71.6	1.35	9.9	nt	4740	< 0.10
317	1000	45	1054	7.85	nt	nt	66.8	1.20	9.3	nt	5072	< 0.10
66	750	35	753	7.89	67.4	25.7	51.4	1.30	8.7	821	4424	< 0.10
114	788	35	677	8.08	74.2	27.2	61.4	9.60	9.2	914	4700	< 0.10
318	750	35	761	7.97	nt	nt	66.7	1.30	10.1	nt	4352	< 0.10

Notes: 1. Test conducted in Laboratory B, 2. Test conducted in Laboratory C, nt = not tested.

Table 4-19: Varying the chloride concentration and temperature while holding the other variables constant- Cessation concentrations

Run	Target concentrations / conditions		Test solution concentrations upon cessation of corrosion tests									
	Chloride (mg/l as Cl ⁻)	Temperature (°C)	Chloride ⁽²⁾ (mg/l as Cl ⁻)	pH ⁽¹⁾	Calcium ⁽²⁾ (mg/l as Ca ²⁺)	Magnesium ⁽²⁾ (mg/l as Mg ²⁺)	Total alkalinity ⁽¹⁾ (mg/l as CaCO ₃)	Sulphate diln ⁽²⁾ (mg/l as SO ₄ ²⁻) x 10 ³	Fluoride diln ⁽¹⁾ (mg/l as F ⁻)	Sodium ⁽²⁾ (mg/l as Na ⁺)	Conductivity ⁽¹⁾ (µS/cm)	Total iron ⁽¹⁾ (mg/l as Fe ³⁺ (total))
61	500	45	523	7.98	70.9	29.1	70.9	1.37	8.9	761	4104	1.9
62	625	45	724	8.01	70.0	28.7	70.3	1.41	9.4	820	4120	2.1
63	750	45	807	7.98	70.8	28.8	70.3	1.42	9.1	894	4468	2.1
64	875	45	934	7.85	62.3	26.0	61.1	1.31	8.7	936	4748	2.0
65	1000	45	1198	7.92	65.5	26.8	63.1	1.36	9.4	1041	5064	2.9
109	500	45	354	8.10	71.1	27.6	48.3	8.66	8.4	747	4056	6.2
110	644	45	564	7.91	73.4	28.0	50.2	1.01	9.4	841	4468	5.7
111	788	45	696	8.20	71.6	27.6	54.8	1.04	9.4	921	4944	6.1
112	932	45	910	8.13	72.1	28.8	52.8	9.84	9.4	1015	5380	4.0
113	1076	45	984	8.13	75.0	29.3	54.4	1.06	9.7	1125	5824	2.3
313	500	45	566	7.82	nt	nt	52.3	1.40	10.1	nt	4120	2.7
314	625	45	787	7.86	nt	nt	55.5	1.55	9.9	nt	4656	3.4
315	750	45	930	7.83	nt	nt	53.9	1.55	10.3	nt	4904	3.7
316	875	45	989	7.84	nt	nt	71.6	1.40	10.4	nt	4740	3.5
317	1000	45	1112	7.85	nt	nt	66.8	1.20	10.4	nt	5072	6.6
66	750	35	755	7.97	63.3	25.9	62.4	1.33	8.6	826	4292	1.9
114	788	35	718	8.02	72.7	28.1	52.3	1.08	9.3	947	4824	2.6
318	750	35	829	7.67	nt	nt	53.2	1.40	9.8	nt	4588	5.0

Table 4-20: Corrosion coupon and Corrater[®] readings while varying the chloride concentration

Run	Target concentrations / conditions		Corrosion Coupon Results				Corrater [®] readings			
	Chloride (mg/l as Cl ⁻)	Temperature (°C)	Coupon 1 (mmpa)	Coupon 2 (mmpa)	Coupon 3 (mmpa)	Average (mmpa)	Day 1 (mmpa)	Day 2 (mmpa)	Day 3 (mmpa)	Day 4 (mmpa)
61	500	45	0.38	0.44	0.44	0.42	0.36	0.35	0.34	0.34
62	625	45	0.31	0.42	0.39	0.37	0.41	0.40	0.35	0.36
63	750	45	0.34	0.44	0.45	0.41	0.32	0.30	0.28	0.26
64	875	45	0.40	0.44	0.47	0.44	0.46	0.44	0.40	0.40
65	1000	45	0.40	0.45	0.51	0.45	0.79	0.78	0.77	0.75
109	500	45	0.37	0.35	nt	0.36	nt	nt	nt	nt
110	644	45	0.43	0.44	nt	0.44	nt	nt	nt	nt
111	788	45	0.36	0.33	nt	0.35	nt	nt	nt	nt
112	932	45	0.34	0.38	nt	0.36	nt	nt	nt	nt
113	1076	45	0.32	0.47	nt	0.39	nt	nt	nt	nt
313	500	45	0.31	0.36	0.35	0.34	nt	nt	nt	nt
314	625	45	0.35	0.41	0.45	0.40	nt	nt	nt	nt
315	750	45	0.31	0.34	0.38	0.34	nt	nt	nt	nt
316	875	45	0.29	0.29	0.34	0.31	nt	nt	nt	nt
317	1000	45	0.33	0.30	0.37	0.34	nt	nt	nt	nt
66	750	35	0.35	0.35	0.45	0.38	0.49	0.48	0.46	0.45
114	788	35	0.39	0.33	nt	0.36	nt	nt	nt	nt
318	750	35	0.27	0.27	0.33	0.29	nt	nt	nt	nt

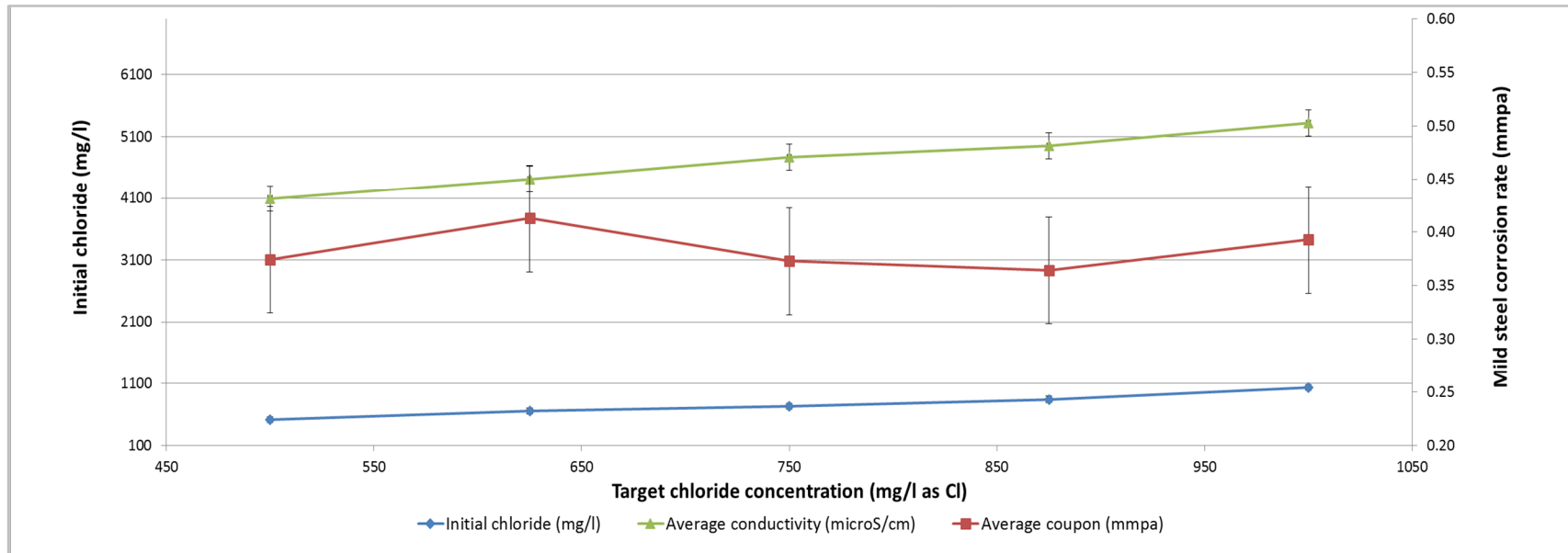


Figure 4-28: Average mild steel corrosion rate (Avg Coup), average initial chloride (Cl(i)) and average initial conductivity (Cond(i)) versus the target chloride concentration (Tgt Cl), at 45°C. Error bars: $\pm 0.05\text{mmpa}$, $\pm 50\text{ mg/l Cl}$ and $209\mu\text{S/cm}$

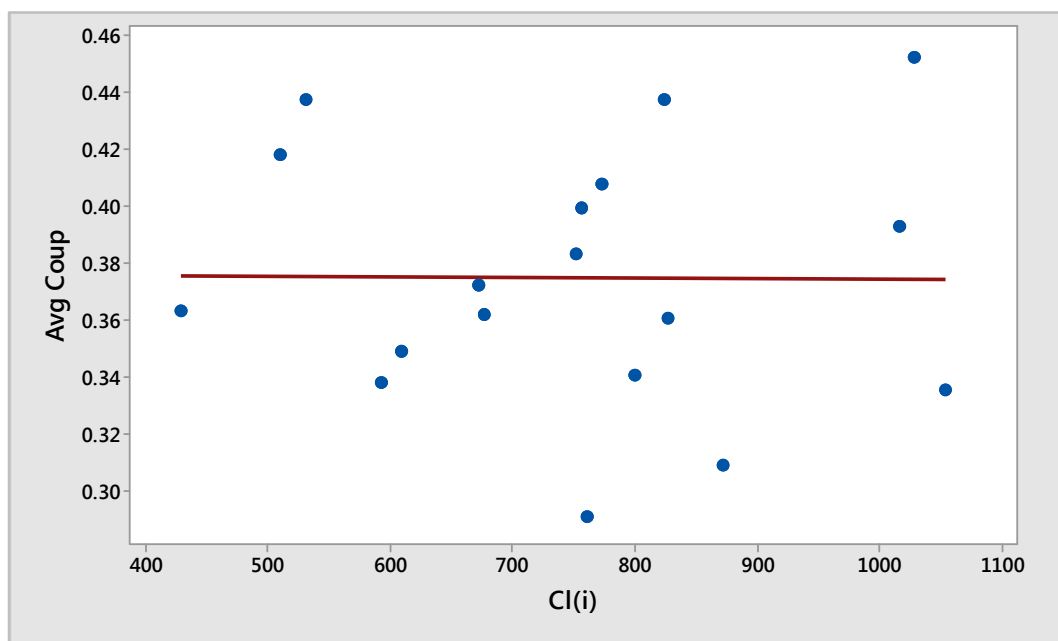


Figure 4-29: Scatterplot of average corrosion rates in mmpa (Avg Coup) versus initial chloride concentrations in mg.l as Cl^- (Cl(i)), at 45°C

Table 4-21: Statistically significant relationships between the average coupon corrosion rate and various parameters while varying the chloride concentration

Parameter	Strength and direction of relationship
Coupon 1	Strongly positive
Coupon 2	Strongly positive
Coupon 3	Strongly positive

Note: Detailed statistical correlation data are shown in Tables G-5a.

Figure 4-28 demonstrates strong positive correlations between the target, and initial chloride concentrations and the initial conductivity readings. Table 4-21 indicates statistically significant correlations between the average corrosion rate and the individual corrosion rates. The p values are given in Table G-5. Statistically significant relationships were detected between all the chloride and conductivity readings, with Pearson correlation coefficients ranging from 0.74 to 0.97 (Table G-5).

There appeared to be no statistically significant correlations between any of the chloride concentrations (namely the target, initial or final chloride concentrations) and the corrosion rates measured by either the coupon method or the Corrater[®] (Figure 4-29 and Table G-5). The complete absence of a relationship between the initial chloride concentration and the corrosion rate was demonstrated by the broad and uniform scatter of data points and almost horizontal regression line in the graph of average corrosion rate (Avg Coup) versus initial chloride concentration (Cl(i)) in Figure 4-29. Due to the small sample size (n=18), it was not possible to provide a precise estimate of the strength of the relationship.

4.4.3 Impact of sulphate in synthetic brackish water on mild steel

The main aim in this section were to determine the corrosive effects on mild steel primarily due to: an increase in sulphate from 750 to 1600 mg/l as SO_4^{2-} , and an increase in temperature by 10°C, from 35°C to 45°C. For this set of experiments it was again decided to select the middle of the ranges for the unvaried parameters: calcium, total alkalinity, chloride, fluoride and magnesium. A summary of the target water qualities and the test start-up concentrations are shown in Table 4-22.

Further to the target concentrations and temperatures, Table 4-22 also reports the chemical analyses of the test solutions prior to the commencement of the corrosion tests. The same chemical analyses were then repeated upon culmination of the three day tests. These results are reported in Table 4-23 together with the coupon and Corrater[®] results in Table 4-24.

Figure 4-30 shows the strength of the relationships between the average mild steel corrosion rate, average initial sulphate and average initial conductivity versus the target sulphate concentration. Tables 4-25 and G-6a provide the statistical linear model correlation data for these relationships. Figure 4-31 shows the relationship between the initial sulphate concentration and the average mild steel corrosion rate.

Table 4-22: Varying the sulphate concentration and temperature while holding the other variables constant- Target and start-up concentrations

Run	Target concentrations / conditions		Test solution concentrations at start-up									
	Sulphate (mg/l as SO ₄ ²⁻)	Temperature (°C)	Sulphate (25x diln) ⁽²⁾ (mg/l as SO ₄ ²⁻) x 10 ³	pH ⁽¹⁾	Calcium ⁽²⁾ (mg/l as Ca ²⁺)	Magnesium ⁽²⁾ (mg/l as Mg ²⁺)	Total alkalinity ⁽¹⁾ (mg/l as CaCO ₃)	Chloride ⁽²⁾ (mg/l as Cl ⁻)	Fluoride (25x diln) ⁽¹⁾ (mg/l as F ⁻)	Sodium ⁽²⁾ (mg/l as Na ⁺)	Conductivity ⁽¹⁾ (µS/cm)	Total iron ⁽¹⁾ (mg/l as Fe ³⁺ (total))
67	750	45	7.31	8.09	68.1	27.3	67.7	745	9.5	714	3556	< 0.10
68	937.5	45	9.27	8.10	75.7	26.6	71.7	775	9.9	727	3960	< 0.10
69	1125	45	1.10	8.09	72.0	25.6	67.4	811	9.8	nt	4260	< 0.10
70	1312	45	1.29	8.11	73.1	22.2	69.6	774	9.9	715	4536	< 0.10
71	1500	45	1.22	8.09	72.5	22.6	69.5	782	9.7	814	4832	< 0.10
211	750	45	7.12	7.68	75.0	25.7	63.1	747	12.7	717	3812	< 0.10
212	937.5	45	8.90	7.76	75.9	26.2	66.4	724	13.0	821	4136	< 0.10
213	1125	45	1.20	7.71	73.4	25.4	74.0	783	13.7	980	4484	< 0.10
214	1312.5	45	1.12	7.65	74.2	25.5	86.1	745	10.8	900	4780	< 0.10
215	1500	45	1.39	7.73	73.1	25.3	85.8	711	12.6	1060	5140	< 0.10
216	1600	45	1.27	7.73	74.5	25.7	69.3	792	13.1	1162	5504	< 0.10

continuation of Table 4-22												
	Sulphate (mg/l as SO ₄ ²⁻)	Temperature (°C)	Sulphate (25x diln) ⁽²⁾ (mg/l as SO ₄ ²⁻) x 10 ³	pH ⁽¹⁾	Calcium ⁽²⁾ (mg/l as Ca ²⁺)	Magnesium ⁽²⁾ (mg/l as Mg ²⁺)	Total alkalinity ⁽¹⁾ (mg/l as CaCO ₃)	Chloride ⁽²⁾ (mg/l as Cl ⁻)	Fluoride (25x diln) ⁽¹⁾ (mg/l as F ⁻)	Sodium ⁽²⁾ (mg/l as Na ⁺)	Conductivity ⁽¹⁾ (µS/cm)	Total iron ⁽¹⁾ (mg/l as Fe ³⁺ (total))
307	750	45	7.00	8.01	nt	nt	105.0	759	10.4	nt	3604	< 0.10
308	937.5	45	1.08	8.14	nt	nt	71.5	725	9.9	nt	4044	< 0.10
309	1125	45	1.23	7.95	nt	nt	71.6	727	9.1	nt	4304	< 0.10
310	1312	45	1.35	7.98	nt	nt	101.0	768	8.9	nt	4536	< 0.10
311	1500	45	1.73	8.12	nt	nt	76.8	774	9.8	nt	4804	< 0.10
72	1125	35	1.15	8.11	74.8	23.1	72.0	802	9.9	666	4364	< 0.10
312	1125	35	1.10	8.09	nt	nt	67.7	817	9.6	nt	4256	< 0.10

Notes: 1. Test conducted in Laboratory B, 2. Test conducted in Laboratory C, nt = not tested.

Table 4-23: Varying the sulphate concentration and temperature while holding the other variables constant- Cessation concentrations

Run	Target concentrations / conditions		Test solution concentrations upon cessation of corrosion tests									
	Sulphate (mg/l as SO ₄ ²⁻)	Temperature (°C)	Sulphate (25x diln) ⁽²⁾ (mg/l as SO ₄ ²⁻) x 10 ³	pH ⁽¹⁾	Calcium ⁽²⁾ (mg/l as Ca ²⁺)	Magnesium ⁽²⁾ (mg/l as Mg ²⁺)	Total alkalinity ⁽¹⁾ (mg/l as CaCO ₃)	Chloride ⁽²⁾ (mg/l as Cl ⁻)	Fluoride (25x diln) ⁽¹⁾ (mg/l as F ⁻)	Sodium ⁽²⁾ (mg/l as Na ⁺)	Conductivity ⁽¹⁾ (µS/cm)	Total iron ⁽¹⁾ (mg/l as Fe ³⁺ (total))
67	750	45	7.64	8.19	67.8	26.8	53.9	777	9.9	768	4068	6.1
68	937.5	45	9.52	8.22	69.1	25.7	54.8	831	10.1	741	4128	6.4
69	1125	45	1.12	8.19	70.5	22.5	54.8	824	10.0	662	4412	7.9
70	1312.5	45	1.50	8.23	67.4	24.2	59.5	807	10.3	810	4732	7.0
71	1500	45	1.59	8.26	75.0	22.1	59.3	803	9.9	780	5080	9.9
211	750	45	8.61	7.89	77.6	29.6	55.6	857	14.2	819	4416	14.2
212	937.5	45	7.85	7.89	77.7	29.3	55.8	793	14.6	892	4772	14.6
213	1125	45	1.12	7.96	74.3	27.5	61.9	860	13.2	974	5180	13.2
214	1312.5	45	1.37	7.92	73.7	27.7	67.5	833	13.8	1066	5404	13.8
215	1500	45	1.41	8.02	75.4	28.2	63.0	725	17.8	1192	5968	17.8
216	1600	45	1.69	7.96	75.8	27.9	62.7	786	15.5	1253	6192	15.5

continuation of Table 4-23												
	Sulphate (mg/l as SO ₄ ²⁻)	Temperature (°C)	Sulphate (25x diln) ⁽²⁾ (mg/l as SO ₄ ²⁻) x 10 ³	pH ⁽¹⁾	Calcium ⁽²⁾ (mg/l as Ca ²⁺)	Magnesium ⁽²⁾ (mg/l as Mg ²⁺)	Total alkalinity ⁽¹⁾ (mg/l as CaCO ₃)	Chloride ⁽²⁾ (mg/l as Cl ⁻)	Fluoride (25x diln) ⁽¹⁾ (mg/l as F ⁻)	Sodium ⁽²⁾ (mg/l as Na ⁺)	Conductivity ⁽¹⁾ (µS/cm)	Total iron ⁽¹⁾ (mg/l as Fe ³⁺ (total))
307	750	45	9.00	7.90	nt	nt	50.2	808	9.8	nt	4004	9.8
308	937.5	45	1.15	7.92	nt	nt	51.9	975	9.4	nt	4672	9.4
309	1125	45	1.40	7.92	nt	nt	53.8	877	9.5	nt	4776	9.5
310	1312.5	45	1.60	7.91	nt	nt	52.4	946	9.5	nt	4928	9.5
311	1500	45	1.75	7.92	nt	nt	56.3	827	9.7	nt	5380	9.7
72	1125	35	1.16	8.05	78.0	23.0	56.4	823	9.9	733	4452	7.4
312	1125	35	1.18	7.89	nt	nt	53.8	829	8.9	nt	4492	8.9

Table 4-24: Corrosion coupon and Corrat[®] readings while varying the sulphate concentration

Run	Target concentration s / conditions		Corrosion Coupon Results				Corrat [®] readings			
	Sulphate (mg/l as SO ₄ ²⁻)	Temperature (°C)	Coupon 1 (mmpa)	Coupon 2 (mmpa)	Coupon 3 (mmpa)	Average (mmpa)	Day 1 (mmpa)	Day 2 (mmpa)	Day 3 (mmpa)	Day 4 (mmpa)
67	750	45	0.26	0.30	nt	0.28	0.63	0.61	0.59	0.60
68	937.5	45	0.23	0.28	nt	0.26	0.93	0.91	0.90	0.91
69	1125	45	0.24	0.30	nt	0.27	0.73	0.70	0.69	0.66
70	1312.5	45	0.31	0.31	nt	0.31	0.52	0.49	0.48	0.52
71	1500	45	0.38	0.35	nt	0.37	1.38	1.37	1.28	1.29
211	750	45	0.26	0.28	nt	0.27	nt	nt	nt	nt
212	937.5	45	0.19	0.27	nt	0.23	nt	nt	nt	nt
213	1125	45	0.29	0.41	nt	0.35	nt	nt	nt	nt
214	1312.5	45	0.24	0.27	nt	0.25	nt	nt	nt	nt
215	1500	45	0.32	0.32	nt	0.32	nt	nt	nt	nt
216	1600	45	0.33	0.39	nt	0.36	nt	nt	nt	nt
307	750	45	0.35	0.33	0.35	0.34	nt	nt	nt	nt
308	937.5	45	0.28	0.27	0.33	0.29	nt	nt	nt	nt
309	1125	45	0.32	0.34	0.39	0.35	nt	nt	nt	nt
310	1312.5	45	0.35	0.43	0.46	0.41	nt	nt	nt	nt
311	1500	45	0.33	0.42	0.43	0.40	nt	nt	nt	nt
72	1125	35	0.25	0.26	nt	0.26	0.64	0.62	0.60	0.65
312	1125	35	0.31	0.35	0.37	0.34	nt	nt	nt	nt

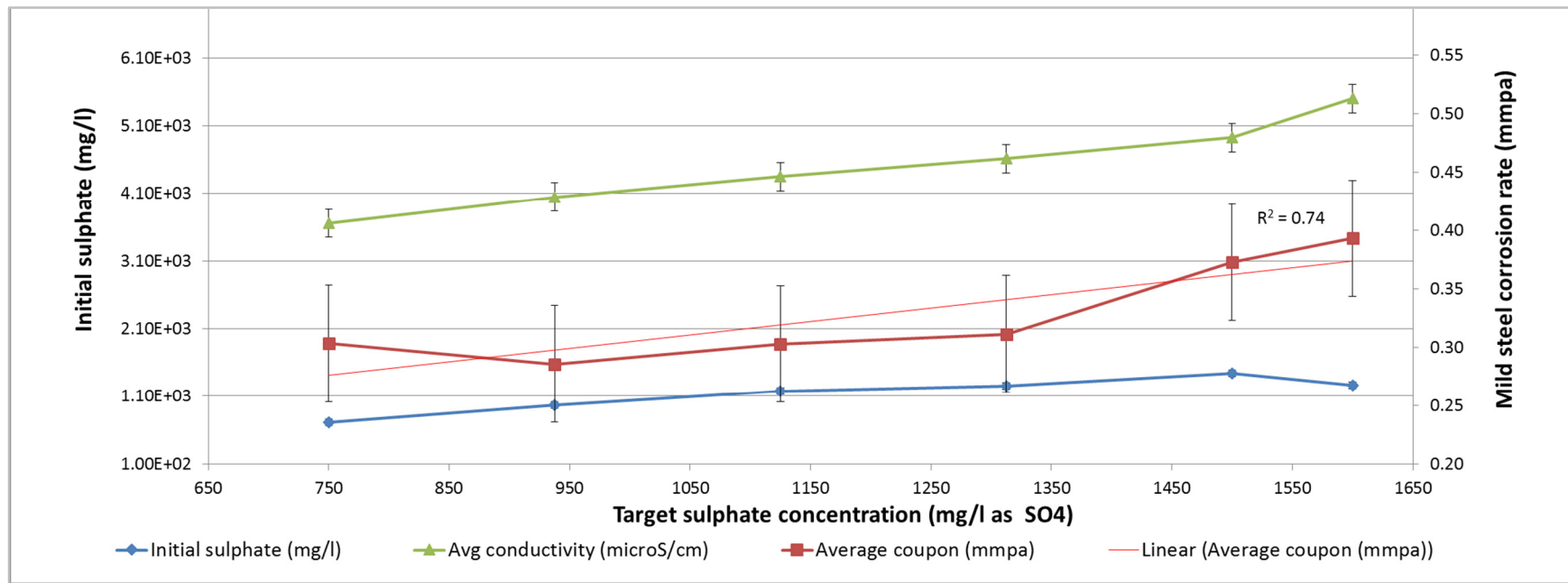


Figure 4-30: Average mild steel corrosion rate (Avg Coup), average initial sulphate (SO₄(i)) and average initial conductivity (Cl(i)) versus the target sulphate concentration (Tgt SO₄), at 45°C. Error bars: ± 0.04 mmpa, ± 83 mg/l SO₄ and 101 μ S/cm

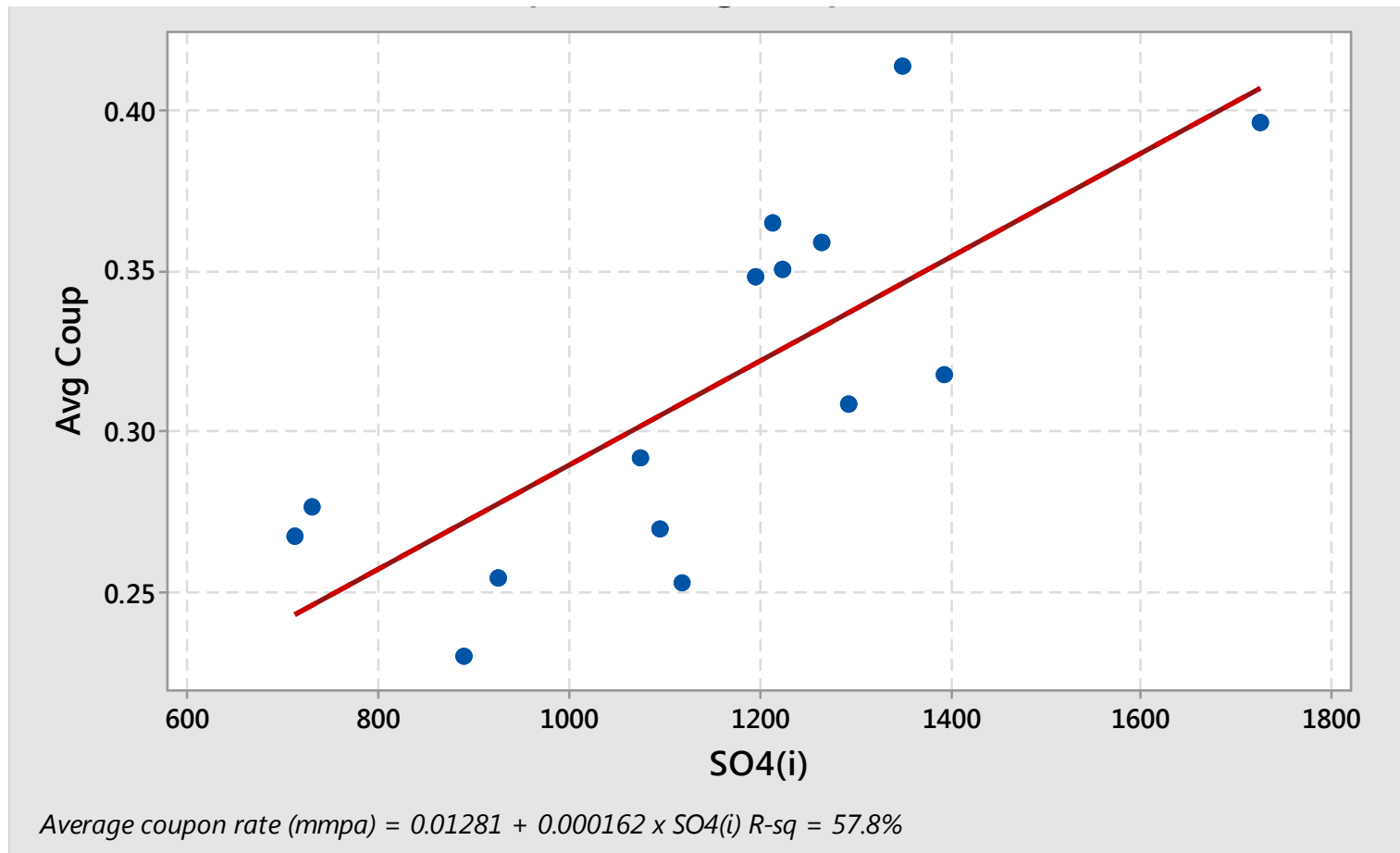


Figure 4-31: Fitted line for the correlation between the average coupon corrosion rate in mmpa (Avg coup) versus the initial sulphate concentration in mg/l SO₄²⁻ (SO4(i))

Table 4-25: Statistically significant relationships between the average coupon corrosion rate and various parameters while varying the sulphate concentration

Parameter	Strength and direction of relationship
Coupon 1	Strongly positive
Coupon 2	Strongly positive
Target sulphate	Moderately positive
Sulphate (initial)	Moderately positive
Sulphate (final)	Strongly positive

Note: Detailed statistical correlation data are shown in Tables G-6a.

A similar correlation analysis was performed between the target, initial and final sulphate concentrations and the initial and final conductivity readings and the results are summarized in Table G-6.

Figure 4-30, Table 4-25 and the Pearson correlation coefficients given in Table G-6 all confirmed statistically significant moderate strong positive linear relationships between the coupon corrosion rates (that is the coupon 1 rate, coupon 2 rate and average corrosion rate) and the sulphate concentrations (that is the target, initial or final sulphate concentrations). However, the best fit for the relationship between the average corrosion rate and initial sulphate concentration, depicted in Figure 4-31, was best represented by a linear fit with an adjusted R-square value of 57.8%.

Although statistically significant strong positive linear correlations were apparent between the sulphate concentrations and the conductivities, shown in Figure 4-30 and the Pearson correlation coefficients listed in Table G-6 between 0.69 and 0.96, there was a lack of correlation between the test solution conductivities and the average coupon corrosion rates (Table G-6). Pearson correlation coefficients obtained for the latter were between 0.39 and 0.44.

4.4.4 Impact of fluoride in synthetic brackish water on mild steel

The main points of relevance in this section were to determine the corrosive effects on mild steel primarily due to: an increase in fluoride from 0 to 90 mg/l as F^- , and an increase in temperature by $10^{\circ}C$, from $35^{\circ}C$ to $45^{\circ}C$. For this set of experiments, it was again decided to select the middle of the ranges for the unvaried parameters: calcium, total alkalinity, sulphate, chloride and magnesium. The target water qualities and the test start-up concentrations are summarised in Table 4-26.

As well as the target concentrations and temperatures Table 4-26 also reports the chemical analyses of the test solutions prior to the commencement of the corrosion tests. The same chemical analyses were then repeated upon culmination of the three day tests. These results are given in Table 4-27, with the coupon and Corratel[®] results in Table 4-28. As evident in the tables, it was essential to perform a sufficient number of test runs across the range of fluoride concentrations being investigated, in order to attain the precision required of the regression analyses.

A scatterplot is provided in Figure 4-32 of average mild steel corrosion rate (Avg Coup), initial calcium (Ca(i)) and initial total alkalinity (Talk(i)) versus the total fluoride concentration (Tgt F), at $45^{\circ}C$, with quadratic regression lines (red). The figure demonstrates the impact of the increasing fluoride concentration on the coupon corrosion rate and the resulting water chemistry. Figure 4-33 is the scatterplots of parameters versus the initial fluoride concentration (F(i)) showing the best fit cubic regression lines.

Table 4-26: Varying the fluoride concentration and temperature while holding the other variables constant- Target and start-up concentrations

Run	Target concentrations / conditions		Test solution concentrations at start-up									
	Fluoride (mg/l as F ⁻)	Temperature (°C)	Fluoride ⁽¹⁾ (25x diln) (mg/l as F ⁻)	pH ⁽¹⁾	Calcium ⁽²⁾ (mg/l as Ca2+)	Magnesium ⁽²⁾ (mg/l as Mg ²⁺)	Total alkalinity ⁽¹⁾	Chloride ⁽²⁾ (mg/l as Cl ⁻)	SO ₄ ²⁻ x 10 ³	Sulphate (25x diln) ⁽²⁾ (mg/l as SO ₄ ²⁻)	Sodium ⁽²⁾ (mg/l as Na ⁺)	Conductivity ⁽¹⁾ (µS/cm)
73	0	45	0.0	7.79	71.9	26.1	69.9	783	1.31	nt	4500	> 0.10
74	1	45	1.3	7.99	70.8	25.9	69.4	776	1.32	nt	4448	< 0.10
75	5	45	4.8	7.91	70.4	25.6	69.9	791	1.33	nt	4449	< 0.10
76	10	45	9.8	7.98	56.2	26.4	71.3	792	1.31	nt	4449	< 0.10
77	25	45	23.3	7.98	48.7	25.3	71.7	775	1.32	nt	4572	< 0.10
79	0	45	0.1	7.98	73.8	27.5	66.8	820	1.25	nt	4544	< 0.10
80	20	45	17.9	7.99	70.4	25.9	67.9	814	1.24	nt	4516	< 0.10
146	10	45	27.0	7.65	40.6	21.7	112.1	697	1.15	918	4556	< 0.10
147	20	45	24.2	7.78	36.3	23.5	67.2	688	9.90	897	4536	< 0.10
148	40	45	24.5	7.66	29.7	23.2	71.5	604	8.97	903	4568	< 0.10
149	70	45	31.2	7.64	23.8	22.4	84.1	673	9.36	915	4560	< 0.10
150	90	45	35.8	7.73	22.3	22.4	69.4	664	9.80	929	4536	< 0.10
152	1	45	0.6	7.97	73.1	25.2	70.1	72	1.07	869	4456	< 0.10
153	5	45	4.4	7.97	73.0	25.1	70.7	658	1.00	865	4456	< 0.10
154	10	45	5.8	7.94	72.7	24.8	72.0	703	1.06	870	4480	< 0.10
155	25	45	28.4	7.91	72.6	25.6	84.0	707	1.08	881	4492	< 0.10

Continuation of Table 4-26												
	Fluoride (mg/l as F ⁻)	Temperature (°C)	Fluoride ⁽¹⁾ (25x diln) (mg/l as F ⁻)	pH ⁽¹⁾	Calcium ⁽²⁾ (mg/l as Ca2+)	Magnesium ⁽²⁾ (mg/l as Mg ²⁺)	Total alkalinity ⁽¹⁾ (mg/l as	Chloride ⁽²⁾ (mg/l as Cl ⁻)	Sulphate (25x diln) ⁽²⁾ (mg/l as SO ₄ ²⁻) x 10 ³	Sodium ⁽²⁾ (mg/l as Na ⁺)	Conductivity ⁽¹⁾ (µS/cm)	Total iron ⁽¹⁾ (mg/l as Fe ³⁺ (total))
156	5	45	2.5	7.93	74.9	25.9	68.2	651	9.34	869	4468	< 0.10
319	0	45	0.1	7.98	73.8	27.5	66.8	820	1.25	nt	4544	< 0.10
320	20	45	17.9	7.99	70.4	25.9	67.9	814	1.24	nt	4516	< 0.10
325	0	45	0.1	8.09	nt	nt	77.7	902	1.15	nt	4724	< 0.10
326	1	45	1.9	8.04	nt	nt	74.1	907	1.20	nt	4372	< 0.10
327	5	45	4.5	7.80	nt	nt	73.0	897	1.30	nt	4372	< 0.10
328	10	45	11.0	7.80	nt	nt	103.0	869	1.40	nt	4384	< 0.10
329	25	45	24.3	8.03	nt	nt	70.9	829	1.30	nt	4440	< 0.01
331	0	45	0.0	8.03	nt	nt	66.0	881	1.20	nt	4168	< 0.01
332	20	45	11.0	8.05	nt	nt	69.4	870	1.35	nt	4256	< 0.01
333	50	45	26.0	8.06	nt	nt	66.5	711	1.20	nt	4256	< 0.01
337	40	45	22.9	7.86	56.5	24.4	60.3	678	9.77	nt	4264	< 0.01
338	50	45	25.9	7.85	48.0	24.4	58.7	645	9.79	nt	4204	< 0.01
339	60	45	31.5	7.87	39.9	23.3	58.3	654	9.82	nt	4296	< 0.01
340	70	45	34.1	7.86	34.3	23.0	58.6	655	1.01	nt	4252	< 0.01
341	80	45	32.2	7.83	28.6	22.7	57.9	590	9.08	nt	4204	< 0.01
342	90	45	33.7	7.83	58.5	22.4	56.8	568	8.50	nt	4200	< 0.01
78	5	35	5.0	7.93	73.6	26.0	71.7	776	1.29	nt	4524	< 0.01
84	50	35	47.1	7.92	73.5	28.9	69.6	842	1.28	nt	4588	< 0.01
324	50	35	47.1	7.92	73.5	28.9	69.6	842	1.28	nt	4588	< 0.01
330	5	35	5.4	8.01	nt	nt	73.2	847	1.25	nt	4372	< 0.01
336	50	35	31.0	8.03	nt	nt	66.4	835	1.20	nt	4332	< 0.01

Table 4-27: Varying the fluoride concentration and temperature while holding the other variables constant- Cessation concentrations

Run	Target concentrations / conditions		Test solution concentrations upon cessation of corrosion tests									
	Fluoride (mg/l as F ⁻)	Temperature (°C)	Fluoride ⁽¹⁾ (25x diln) (mg/l as F ⁻)	pH ⁽¹⁾	Calcium ⁽²⁾ (mg/l as Ca ²⁺)	Magnesium ⁽²⁾ (mg/l as Mg ²⁺)	Total alkalinity ⁽¹⁾ (mg/l as CaCO ₃)	Chloride ⁽²⁾ (mg/l as Cl ⁻)	Sulphate ⁽²⁾ (mg/l as SO ₄ ²⁻) x 10 ³	Sodium ⁽²⁾ (mg/l as Na ⁺)	Conductivity ⁽¹⁾ (µS/cm)	Total iron ⁽¹⁾ (mg/l as Fe ³⁺ (total))
73	0	45	0.0	7.99	67.6	27.7	47.3	827	1.35	nt	4832	5.9
74	1	45	1.3	8.02	68.3	27.3	50.3	832	1.36	nt	4760	6.6
75	5	45	5.0	8.02	71.5	26.3	53.9	799	1.31	nt	4710	7.0
76	10	45	10.3	8.01	55.4	26.7	57.2	800	1.32	nt	4652	7.0
77	25	45	25.0	8.10	53.9	26.5	58.3	793	1.34	nt	4752	7.9
79	0	45	0.1	7.88	72.7	29.7	48.8	908	1.38	nt	4792	4.2
80	20	45	18.6	7.97	66.5	26.3	52.1	893	1.21	nt	4824	4.4
146	10	45	22.4	8.18	36.4	22.2	74.3	628	1.12	946	4768	5.4
147	20	45	22.2	8.18	35.8	25.5	70.6	744	1.04	963	4748	7.0
148	40	45	nt	8.16	nt	nt	70.7	nt	nt	nt	4740	5.4
149	70	45	27.0	8.24	21.5	24.1	74.4	618	9.32	994	4840	6.8
150	90	45	34.3	8.20	18.0	23.2	70.1	662	9.82	980	4772	6.4
152	1	45	2.0	7.97	72.4	26.5	56.0	797	1.21	907	4652	10.1
153	5	45	3.1	7.94	70.9	26.4	66.1	731	1.10	913	4684	11.3
154	10	45	19.9	7.80	68.5	26.6	74.3	718	1.08	930	4700	11.5
155	25	45	12.5	8.04	72.2	26.2	73.5	780	1.14	908	4760	10.9

continuation of Table 4-27												
	Fluoride (mg/l as F ⁻)	Temperature (°C)	Fluoride ⁽¹⁾ (25x diln) (mg/l as F ⁻)	pH ⁽¹⁾	Calcium ⁽²⁾ (mg/l as Ca ²⁺)	Magnesium ⁽²⁾ (mg/l as Mg ²⁺)	Total alkalinity ⁽¹⁾ (mg/l as CaCO ₃)	Chloride ⁽²⁾ (mg/l as Cl ⁻)	Sulphate (25x diln) ⁽²⁾ (mg/l as SO ₄ ²⁻) x 10 ³	Sodium ⁽²⁾ (mg/l as Na ⁺)	Conductivity ⁽¹⁾ (µS/cm)	Total iron ⁽¹⁾ (mg/l as Fe ³⁺ (total))
156	5	45	6.0	7.86	72.5	26.0	60.7	701	1.08	880	4544	12.6
319	0	45	0.1	7.88	72.7	29.7	48.8	908	1.38	nt	4792	4.2
320	20	45	18.6	7.97	66.5	26.3	52.1	893	1.21	nt	4824	4.4
325	0	45	0.0	7.67	nt	nt	43.9	849	1.30	nt	4652	5.0
326	1	45	1.8	7.87	nt	nt	51.1	755	1.50	nt	5012	2.9
327	5	45	5.2	7.87	nt	nt	56.1	809	1.55	nt	4848	2.8
328	10	45	11.3	7.88	nt	nt	55.1	777	1.40	nt	4800	3.9
329	25	45	25.1	7.88	nt	nt	57.3	762	1.45	nt	4856	4.9
331	0	45	0.0	7.79	nt	nt	42.9	871	1.30	nt	4656	4.7
332	20	45	18.0	7.94	nt	nt	52.7	889	1.50	nt	4908	4.9
333	50	45	47.0	8.03	nt	nt	59.4	842	1.40	nt	4736	5.0
337	40	45	18.9	8.18	50.6	25.1	56.4	630	9.34	nt	4400	8.3
338	50	45	22.6	8.20	41.9	24.6	57.9	680	1.04	nt	4380	7.2
339	60	45	28.3	8.27	33.9	24.3	60.3	673	1.11	nt	4372	8.9

continuation of Table 4-27

	Fluoride (mg/l as F ⁻)	Temperature (°C)	Fluoride ⁽¹⁾ (25x diln) (mg/l as F ⁻)	pH ⁽¹⁾	Calcium ⁽²⁾ (mg/l as Ca2+)	Magnesium ⁽²⁾ (mg/l as Mg ²⁺)	Total alkalinity ⁽¹⁾ (mg/l as CaCO ₃)	Chloride ⁽²⁾ (mg/l as Cl ⁻)	Sulphate (25x diln) ⁽²⁾ (mg/l as SO ₄ ²⁻) x 10 ³	Sodium ⁽²⁾ (mg/l as Na ⁺)	Conductivity ⁽¹⁾ (µS/cm)	Total iron ⁽¹⁾ (mg/l as Fe ³⁺ (total))
340	70	45	24.5	8.25	28.2	23.8	59.5	555	8.65	nt	4352	9.2
341	80	45	34.0	8.31	22.0	23.1	60.2	651	1.01	nt	4412	7.9
342	90	45	39.5	8.21	18.1	21.5	58.8	586	9.28	nt	4356	8.6
78	5	35	5.1	8.02	69.1	26.7	54.1	851	1.39	nt	4646	4.7
84	50	35	46.9	7.94	73.7	28.8	54.9	855	1.31	nt	4769	3.9
324	50	35	46.9	7.94	73.7	28.8	54.9	855	1.31	nt	4769	3.9
330	5	35	5.3	7.85	nt	nt	54.3	780	1.40	nt	4568	4.8
336	50	35	43.5	7.96	nt	nt	59.7	888	1.40	nt	4520	4.8

Notes: 1. Test conducted in Laboratory B, 2. Test conducted in Laboratory C, nt = not tested.

Table 4-28: Corrosion coupon and Corrat[®] readings while varying the fluoride concentration

Run	Target concentrations / conditions		Corrosion Coupon Results				Corrat [®] readings			
	Fluoride (mg/l as F ⁻)	Temperature (°C)	Coupon 1 (mmpa)	Coupon 2 (mmpa)	Coupon 3 (mmpa)	Average (mmpa)	Day 1 (mmpa)	Day 2 (mmpa)	Day 3 (mmpa)	Day 4 (mmpa)
73	0	45	0.27	0.31	0.33	0.31	1.37	1.33	1.29	1.26
74	1	45	0.33	0.33	0.35	0.34	0.68	0.59	0.58	0.57
75	5	45	0.33	0.36	0.38	0.36	0.49	0.49	0.49	0.48
76	10	45	0.35	0.38	0.38	0.37	0.48	0.46	0.45	0.44
77	25	45	0.30	0.35	0.42	0.36	0.52	0.51	0.47	0.44
79	0	45	0.27	0.32	0.33	0.31	1.41	1.39	1.34	1.29
80	20	45	0.29	0.35	0.35	0.33	0.72	0.69	0.61	0.52
146	10	45	0.36	0.39	nt	0.38	nt	nt	nt	nt
147	20	45	0.45	0.48	nt	0.46	nt	nt	nt	nt
148	40	45	0.42	0.44	nt	0.43	nt	nt	nt	nt
149	70	45	0.45	0.42	nt	0.44	nt	nt	nt	nt
150	90	45	0.42	0.41	nt	0.42	nt	nt	nt	nt
152	1	45	0.25	0.29	nt	0.27	nt	nt	nt	nt
153	5	45	0.29	0.27	nt	0.28	nt	nt	nt	nt
154	10	45	0.36	0.27	nt	0.31	nt	nt	nt	nt

continuation of Table 4-28										
155	25	45	0.37	0.42	nt	0.40	nt	nt	nt	nt
156	5	45	0.22	0.28	nt	0.25	nt	nt	nt	nt
319	0	45	0.27	0.32	0.33	0.31	56.40	55.40	53.40	51.40
320	20	45	0.29	0.35	0.35	0.33	28.80	27.70	24.40	20.60
325	0	45	0.39	0.42	0.36	0.39	49.80	40.60	38.20	37.90
326	1	45	0.33	0.36	0.35	0.34	39.90	39.40	39.20	36.90
327	5	45	0.27	0.31	0.28	0.29	54.60	39.70	40.30	40.10
328	10	45	0.27	0.36	0.35	0.32	56.30	39.60	37.50	32.30
329	25	45	0.32	0.42	0.39	0.38	46.70	42.60	39.60	38.10
331	0	45	0.39	0.37	0.41	0.39	26.90	26.10	25.10	24.60
332	20	45	0.39	0.40	0.42	0.40	30.20	29.20	28.80	27.80
333	50	45	0.45	0.43	0.48	0.45	38.20	36.10	31.20	29.70
337	40	45	0.47	0.48	nt	0.47	nt	nt	nt	nt
338	50	45	0.50	0.50	nt	0.50	nt	nt	nt	nt
339	60	45	0.50	0.48	nt	0.49	nt	nt	nt	nt
340	70	45	0.45	0.44	nt	0.45	nt	nt	nt	nt
341	80	45	0.48	0.48	nt	0.48	nt	nt	nt	nt
342	90	45	0.48	0.45	nt	0.47	nt	nt	nt	nt
78	5	35	0.28	0.32	0.36	0.32	0.86	0.84	0.76	0.74
84	50	35	0.31	0.39	0.42	0.37	1.00	0.99	0.97	0.92
324	50	35	0.31	0.39	0.42	0.37	40.10	39.40	38.60	36.80
330	5	35	0.19	0.30	0.27	0.26	33.60	34.10	31.70	30.20
336	50	35	0.40	0.45	0.45	0.43	38.20	36.50	30.20	29.40

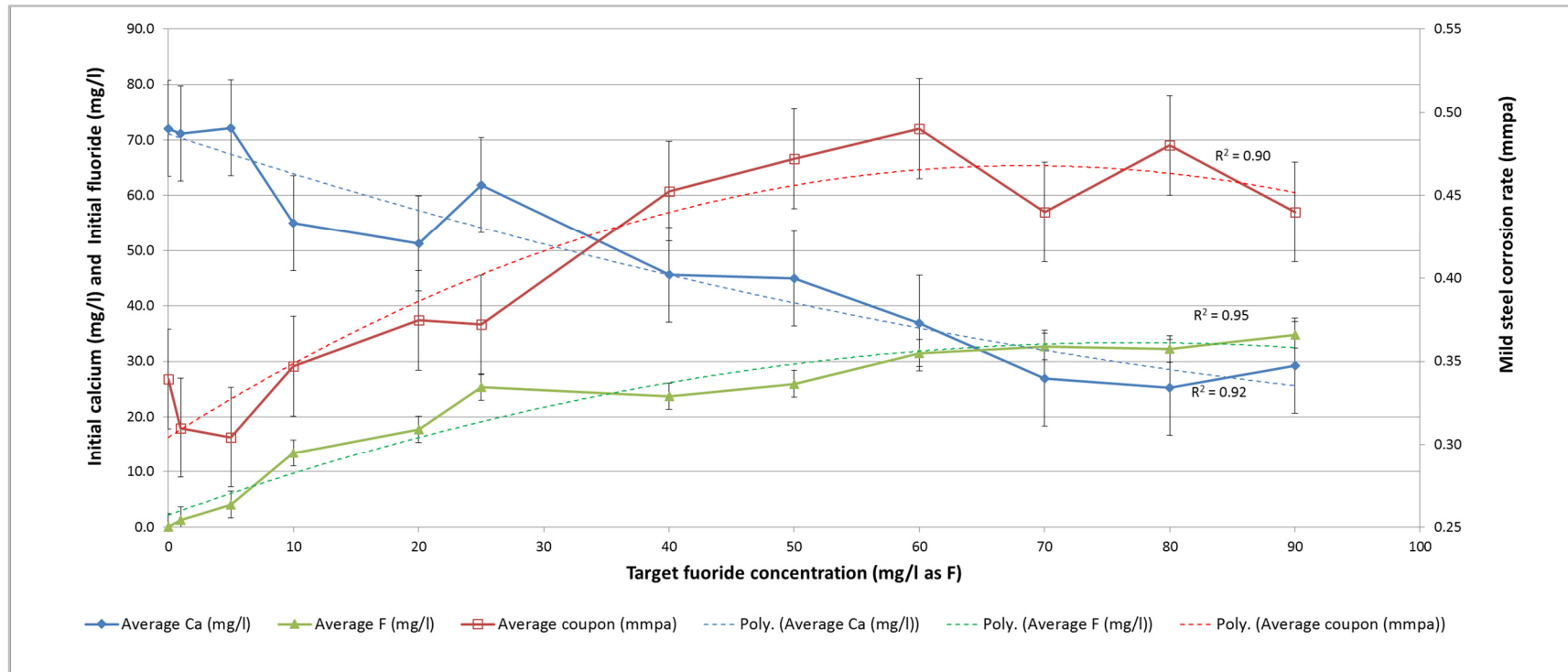


Figure 4-32: Average mild steel corrosion rate (Avg Coup), average initial calcium (Ca(i)) and average initial fluoride (F(i)) versus the target fluoride concentration (Tgt F), at 45°C, with trend lines. Error bars: $\pm 0.03\text{mmpa}$, $\pm 8.6\text{ mg/l Ca}$, and $\pm 2.4\text{ mg/l F}$

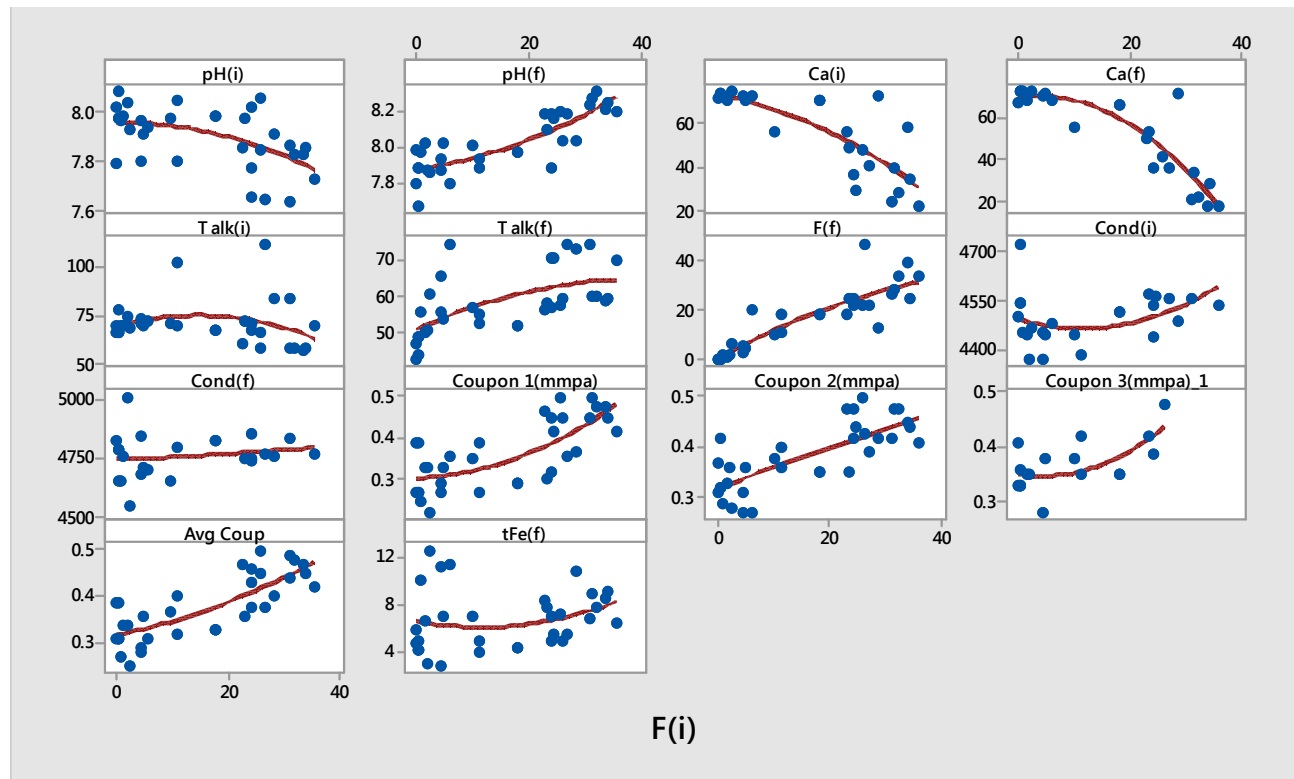


Figure 4-33: Scatterplots of parameters with varying initial fluoride concentration ($F(i)$), including best fit cubic regression lines

Table 4-29 is a summary of the intensity and directional tendency of the statistically significant linear relationships between the average coupon corrosion rate and the various parameters, as well as between the initial fluoride concentration and various parameters.

Table 4-29: Statistically significant linear relationships between various parameters while varying the fluoride concentration

Parameter 1	Parameter 2	Strength and direction of relationship
Average of Coupons 1,2 and 3	Target Fluoride	Strongly positive
	Calcium (initial) Calcium (final)	Strongly negative
	Fluoride (initial) Fluoride (final) pH (final)	Moderately positive
	Magnesium (initial) Magnesium (final) Chloride (final) Day 1 (mmpa) Day 2 (mmpa) Day 3 (mmpa) Day 4 (mmpa)	Moderately negative
	Total alkalinity (final) Conductivity (initial)	Weakly positive
	Total alkalinity (initial)	Weakly negative
Fluoride (initial)	Fluoride (final)	Strongly positive
Fluoride (initial)	Total alkalinity (final)	Weakly positive
Conductivity (initial)	Calcium (initial) Calcium (final)	Moderately negative
Conductivity (initial)	Total iron (final)	Strongly negative

Note: Detailed statistical correlation data are shown in Tables G-7.

Figure 4-34 illustrates a statistically significant quadratic model, with an R^2 (adj) value of 87%, as the best fit to the relationship between the initial actual fluoride concentrations and the targeted fluoride concentrations.

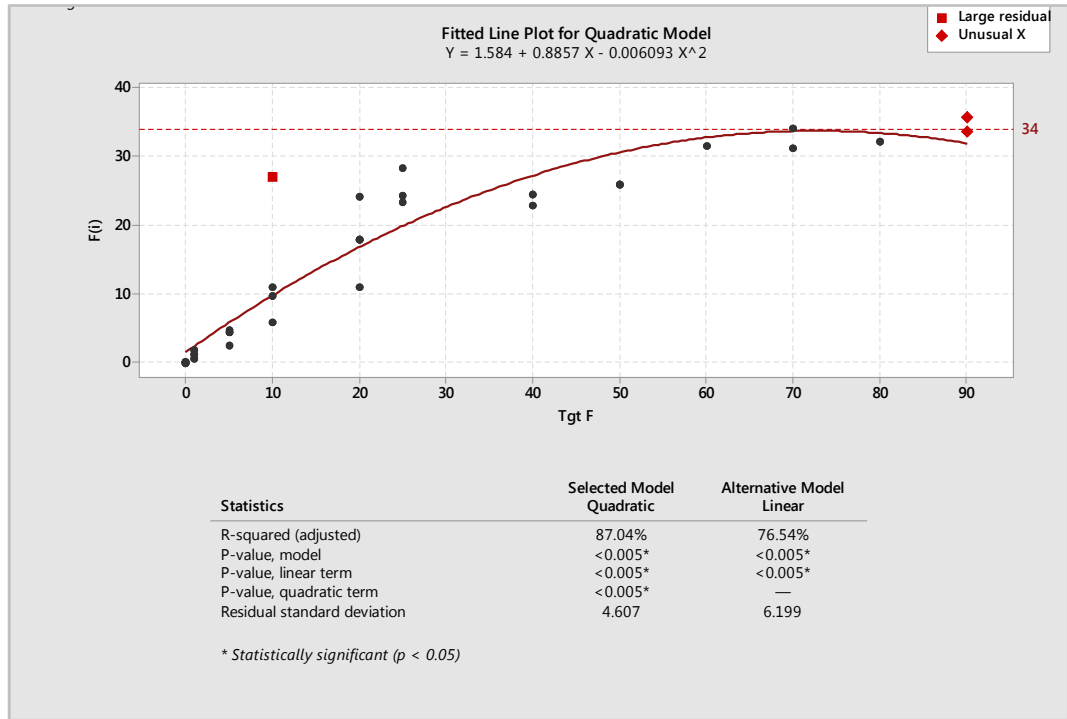


Figure 4-34: Regression analysis for the initial fluoride concentration versus the target fluoride concentration, where the quadratic model provided the closest fit

Figure 4-35 illustrates the relationship between the average corrosion rate and the initial fluoride concentration, with the preferred regression model fitted to the data. As evident, the linear model produced the closest fit with an R^2 (adj) of 60%, making it superior to the quadratic model with an R^2 (adj) of 59%. The resultant equation for the linear model is given in Equation (4.4).

$$\text{Average coupon corrosion rate} = 0.3110 + 0.004272 \times F(i) \dots \dots \dots [4.4]$$

where: Average coupon corrosion rate in millimetres per annum (mmpa),

$F(i)$ = initial fluoride concentration (mg/l as F^-).

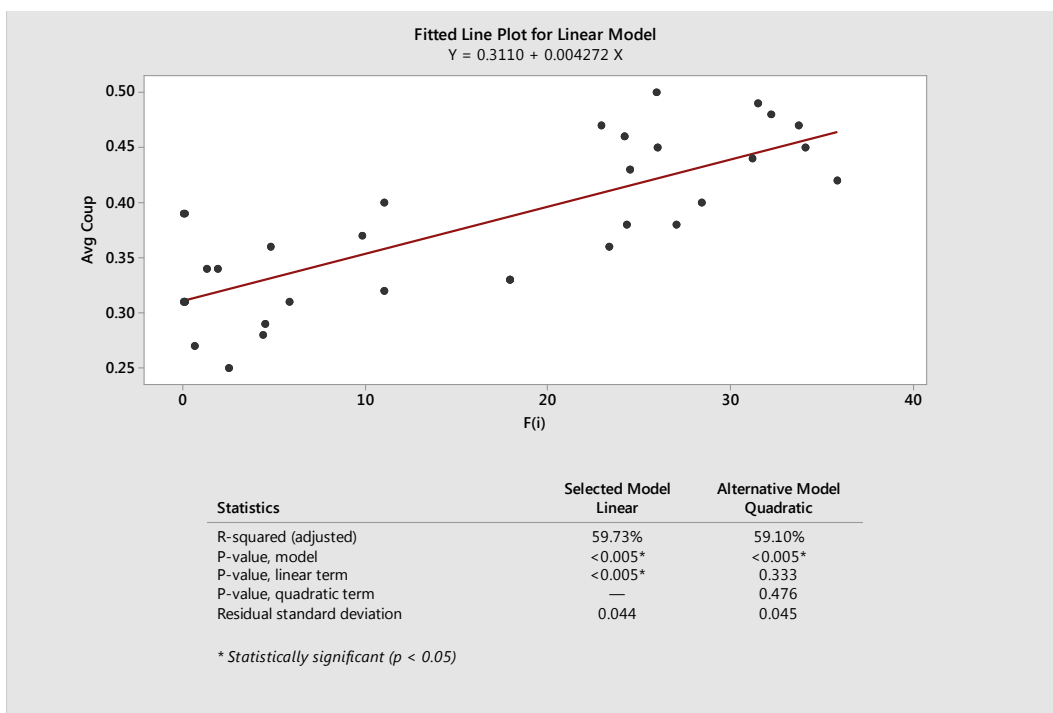


Figure 4-35: Regression analysis for the average coupon corrosion rate versus the test solution initial fluoride concentration, where both the linear and quadratic models were statistically significant with the linear model providing the closest fit

The inclusion of additional statistically significant parameters resulted in a regression model (Equation 4.5) with an R^2 (adj) of 88%.

$$\text{Average corrosion rate} = 2.021 - 0.00292 \times F(i) - 0.2180 \times \text{pH}(i) - 0.00225 \times M \text{ alk}(i) + 0.00894 \times \text{Ca}(i) - 0.00009 \text{Ca}(i)^2 \dots\dots\dots[4.5]$$

where: Average coupon corrosion rate is in millimetres per annum (mmpa),
 $\text{pH}(i)$ = initial pH,
 $M \text{ alk}(i)$ = initial total alkalinity (mg/l as CaCO_3),
 $\text{Ca}(i)$ = initial calcium concentration (mg/l as Ca^{2+}).

Figure 4-36 illustrates the effects of the main variables, namely: the initial pH ($\text{pH}(i)$), initial calcium ($\text{Ca}(i)$), initial alkalinity ($M \text{ alk}(i)$), and initial fluoride ($F(i)$) on the average coupon corrosion rate. Increases in the initial pH and initial total alkalinity appeared related to the decreases in the mild steel corrosion. The opposite

relationship was evident between the initial fluoride concentration and the average coupon corrosion rate. The initial calcium concentration first increased and then decreased relative to the mild steel corrosion rate.

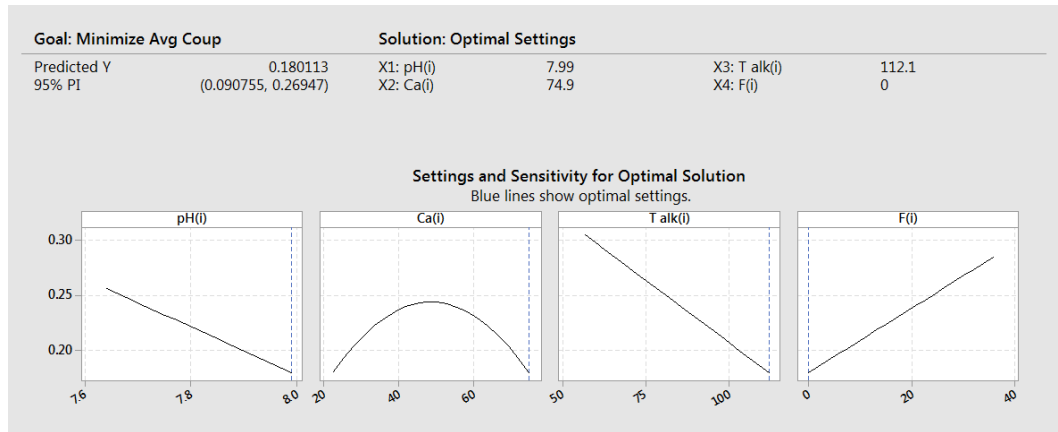


Figure 4-36: Main effects plots for the average corrosion rate demonstrating the individual impacts of the: initial pH (pH(i)), initial calcium concentration in mg/l Ca^{2+} (Ca(i)), initial total alkalinity (T alk (i)) and initial fluoride concentration in mg/l F^- (F(i)) on the resulting average corrosion rate in mmpa (Avg Coup)

In the previous series of tests, all the variables were intended to be held constant while varying the fluoride concentration. Sodium fluoride was added to chemically comparable synthetic solutions and the effects recorded for the changes in chemistry and resultant mild steel corrosion rates.

Figures 4-32 and 4-33 both reveal the following statistically significant trends with the initial or target fluoride concentration:

- Strong positive correlations with the coupon corrosion rates;
- Strong negative correlations with the initial and final calcium concentrations;
- Weak positive correlations with the final pH, final alkalinity, initial conductivity and final total iron concentrations;
- Weak negative correlations with the initial pH, initial alkalinity, and final conductivity.

Table 4-29 confirmed the following statistically significant correlations with the average corrosion rate:

- Strong correlations with the following three variables: target fluoride, initial calcium and final calcium;
- Moderate positive correlations with the following variables: initial fluoride, final fluoride and final pH;
- Moderate negative correlations with the initial and final magnesium, and final chloride;
- Weak correlations with the initial and final alkalinity, and initial conductivity.

Figure 4-34 demonstrates that although high fluoride concentrations were targeted during the series of tests (i.e. 90 mg/l as F^-), it was only possible to reach a maximum initial fluoride concentrations of approximately 34 mg/l (as F^-). This maximum fluoride solubility may be attributed to the reduced calcium fluoride solubility at 45°C and the initial calcium concentration of 75 mg/l (as Ca^{2+}). A regression analysis for the average coupon corrosion rate versus the test solution initial fluoride concentration, for the initial fluoride range of between 0 and 34 mg/l F^- , found that both the linear and quadratic models were statistically significant with the linear model providing the closest fit (R^2 (adj) of 60%) (Figure 4-35).

As apparent in Equation 4.5, with an R^2 (adj) of 88%, the average mild steel coupon corrosion rate was mostly influenced by the: initial pH, initial calcium, initial total alkalinity and initial fluoride concentrations. As apparent in the plots of the initial calcium and initial fluoride concentrations versus the target fluoride concentration, apparent in Figure 4-32, the addition of sodium fluoride immediately resulted in calcium fluoride. At the target fluoride concentration of 40 mg/l (as F^-) the initial fluoride concentration had reduced by 32% to 27 mg/l. At the target fluoride concentration of 70 mg/l the initial fluoride concentration reached its maximum solubility of 34 mg/l, for the given synthetic solution (Figure 4-34). At this stage, 51% of the initial 70 mg/l of initial fluoride had precipitated. The mild steel corrosion rate could not be measured at higher fluoride concentrations for no higher

soluble initial fluoride levels were attainable above this ceiling concentration (Figure 4-35).

4.4.5 Impact of magnesium in synthetic brackish water on mild steel

This section delves primarily into the influence of the magnesium ion, for the range: 10 to 70 mg/l as Mg^{2+} , and the impact of an increase in temperature by 10°C, from 35°C to 45°C. For this set of experiments it was again decided to select the middle of the ranges for the fixed parameters, namely: calcium, total alkalinity, sulphate, fluoride and chloride. Table 4-30 summarises the target water qualities and the test start-up concentrations.

Further to the target concentrations and temperatures, Table 4-30 also reports the chemical analyses of the test solutions prior to the commencement of the corrosion tests. The same chemical analyses were then repeated upon culmination of the three day tests and are given in Table 4-31. The coupon and Corrater[®] results are shown in Table 4-32. The relationship between the average mild steel corrosion rate and magnesium concentrations are shown in Table 4-33 and Figures 4-37 and 4-38.

Table 4-30: Varying the magnesium concentration and temperature while holding the other variables constant- Target and start-up concentrations

Run	Target concentrations / conditions		Test solution concentrations at start-up									
	Magnesium (mg/l as Mg ²⁺)	Temperature (°C)	Magnesium ⁽²⁾ (mg/l as Mg ²⁺)	pH ⁽¹⁾	Calcium ⁽²⁾ (mg/l as Ca ²⁺)	Total alkalinity ⁽¹⁾ (mg/l as CaCO ₃)	Chloride ⁽²⁾ (mg/l as Cl ⁻)	Sulphate (25x diln) ⁽²⁾ (mg/l as SO ₄ ²⁻) x 10 ³	Fluoride ⁽¹⁾ (25x diln) (mg/l as F ⁻)	Sodium ⁽²⁾ (mg/l as Na ⁺)	Conductivity ⁽¹⁾ (µS/cm)	Total iron ⁽¹⁾ (mg/l as Fe ³⁺ (total))
85	10	45	7.6	7.87	72.9	52.1	790	1.24	9.8	739	4684	< 0.01
86	15	45	nt	7.91	nt	53.0	nt	nt	9.3	nt	4668	< 0.01
87	30	45	23.7	7.89	71.0	54.5	788	1.24	9.8	672	4664	< 0.01
88	50	45	41.9	7.91	66.7	57.1	783	1.19	8.8	657	4714	< 0.01
89	70	45	52.8	7.89	73.5	59.9	767	1.22	9.3	658	4941	< 0.01
90	30	35	24.6	7.92	69.2	53.9	794	1.25	8.8	673	4436	< 0.01

Notes: 1. Test conducted in Laboratory B, 2. Test conducted in Laboratory C, nt = not tested.

Table 4-31: Varying the magnesium concentration and temperature while holding the other variables constant- Cessation concentrations

Run	Target concentrations / conditions		Test solution concentrations upon cessation of corrosion tests									
	Magnesium (mg/l as Mg ²⁺)	Temperature (°C)	Magnesium ⁽²⁾ (mg/l as Mg ²⁺)	pH ⁽¹⁾	Calcium ⁽²⁾ (mg/l as Ca ²⁺)	Total alkalinity ⁽¹⁾	Chloride ⁽²⁾ (mg/l as Cl ⁻)	Sulphate (25x diln) ⁽²⁾ (mg/l as SO ₄ ²⁻) x 10 ³	Fluoride ⁽¹⁾ (25x diln) (mg/l as F ⁻)	Sodium ⁽²⁾ (mg/l as Na ⁺)	Conductivity ⁽¹⁾ (µS/cm)	Total iron ⁽¹⁾ (mg/l as Fe ³⁺ (total))
85	10	45	7.67	8.00	66.7	53.3	832	1.33	8.3	761	4636	2.7
86	15	45	11.9	8.04	69.4	54.1	844	1.27	9.0	730	4600	4.6
87	30	45	25.3	8.17	71.4	56.8	828	1.31	9.5	nt	4511	4.4
88	50	45	41.5	8.17	68.2	58.5	813	1.21	10.0	669	4364	4.6
89	70	45	57.3	8.19	69.8	61.9	764	1.22	10.3	610	4224	4.0
90	30	35	22.9	8.10	70.6	56.4	782	1.27	10.0	705	4348	4.4

Table 4-32: Corrosion coupon and Corrater[®] readings while varying the magnesium concentration

Run	Target concentrations / conditions		Corrosion Coupon Results			Corrater [®] readings			
	Magnesium (mg/l as Mg ²⁺)	Temperature (°C)	Coupon 1 (mmpa)	Coupon 2 (mmpa)	Average (mmpa)	Day 1 (mmpa)	Day 2 (mmpa)	Day 3 (mmpa)	Day 4 (mmpa)
85	10	45	0.23	0.26	0.25	0.64	0.61	0.53	0.52
86	15	45	0.25	0.35	0.30	0.60	0.59	0.56	0.52
87	30	45	0.29	0.39	0.34	0.49	0.47	0.45	0.44
88	50	45	0.39	0.45	0.42	0.70	0.64	0.65	0.64
89	70	45	0.39	0.51	0.45	0.59	0.56	0.54	0.53
90	30	35	0.27	0.40	0.33	0.91	0.86	0.78	0.66

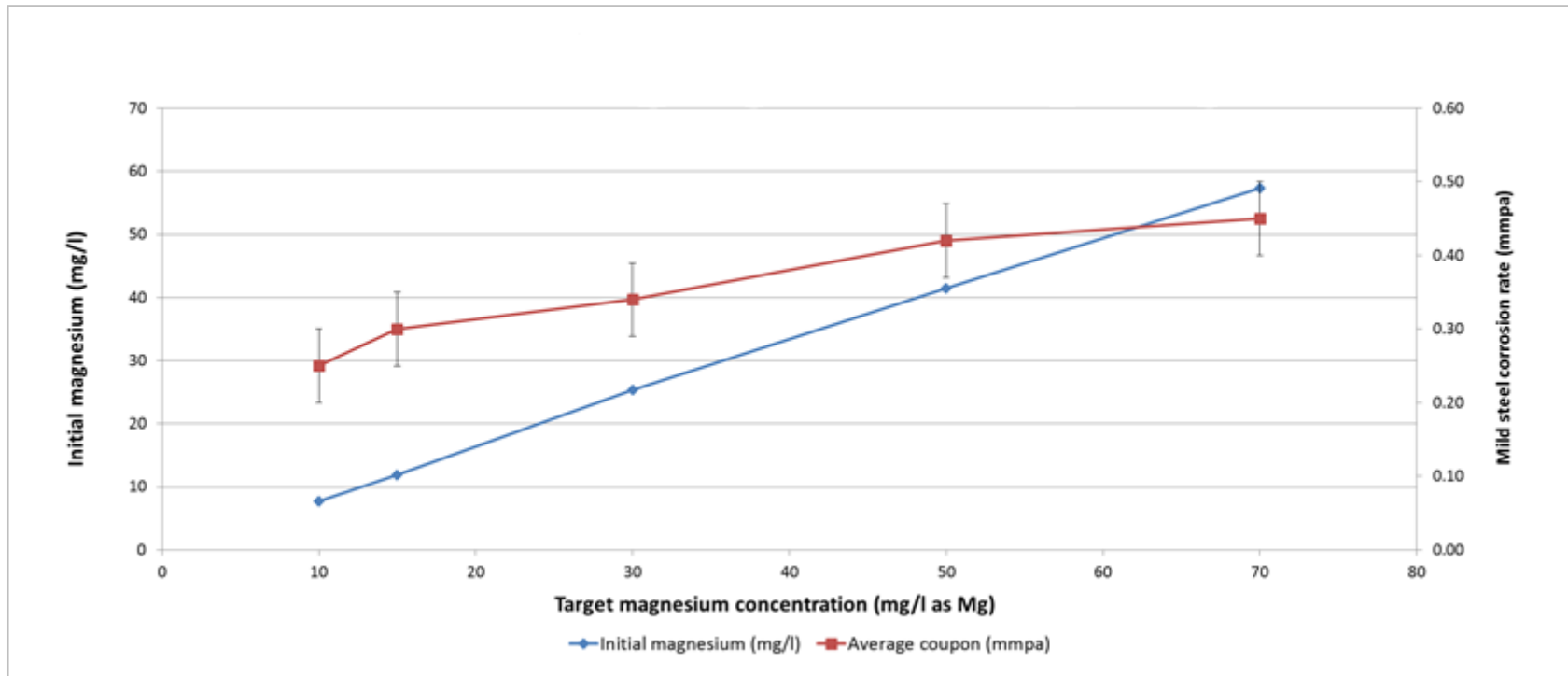


Figure 4-37: Mild steel corrosion rate and initial magnesium concentration versus the target magnesium concentration, at 45°C.
Error bars: $\pm 0.05\text{mmpa}$

Table 4-33: Statistically significant relationships between the average corrosion rate and various parameters while varying the magnesium concentration

Parameter	Strength and direction of relationship
Magnesium (initial and final)	Strongly positive
Total alkalinity (initial and final)	Strongly positive
Sulphate (final)	Strongly negative
pH (final)	Strongly positive
Fluoride (final)	Strongly positive
Conductivity (final)	Strongly negative

Note: Detailed statistical correlation data are shown in Tables G-9.

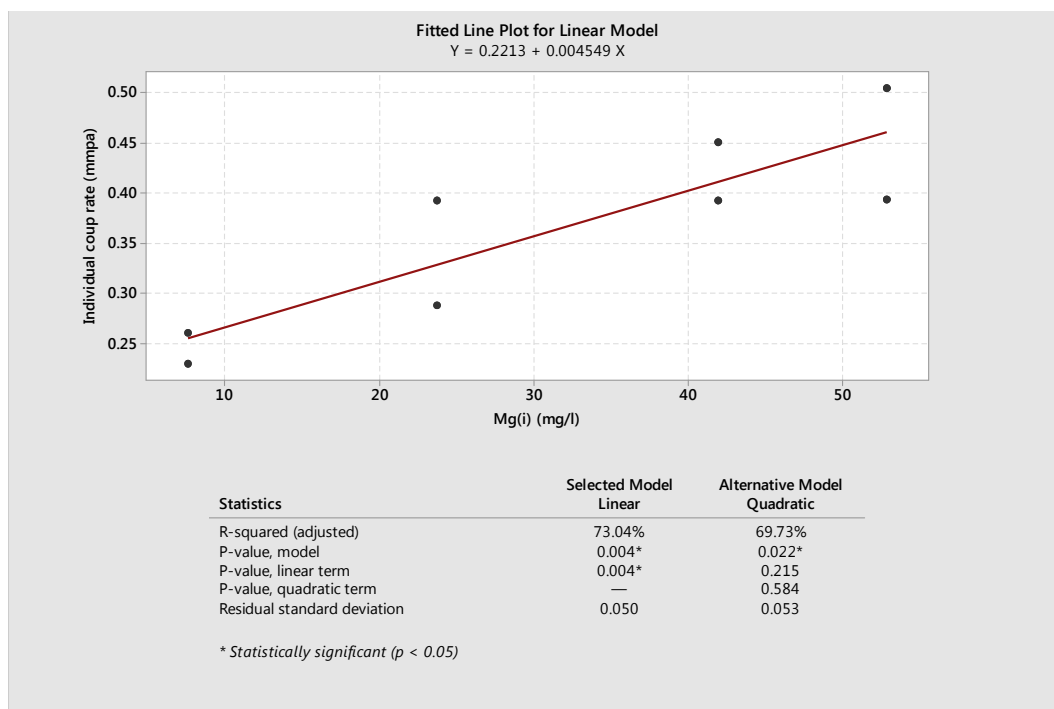


Figure 4-38: Regression analysis for the individual coupon corrosion rates versus the test solution initial magnesium concentration.

Figure 4-37 and Table 4-33 both indicate statistically significant strong positive correlations between the average corrosion rate and the magnesium (initial and final) concentrations. The impact of magnesium on the corrosion rate correlates with the directional tendencies indicated by the LSI (Langelier Saturation Index)

(Langelier, 1936), RSI (Ryznar Stability Index) (Ryznar, 1944) and PSI (Puckorius or Practical Scaling Index) (Puckorius and Brooke, 1990). The higher the magnesium concentration the higher the pH_s (pH of saturation) and, in accordance with the indices, the lower the resultant levels of calcium carbonate saturation, and the increased tendency for mild steel corrosion.

Strong positive correlations were also apparent between the average corrosion rate apparent and several other parameters, namely: the initial and final total alkalinity, the final pH and the final fluoride concentration. Strong negative correlations were apparent between the average corrosion rate and two parameters: the final conductivity and final sulphate concentration (Table 4-33). These relationships were also supported by the p values given in Table G-8.

The regression analysis for the average coupon corrosion rate versus the test solution initial magnesium concentration produced statistically significant linear regression plot (Figure 4-38). Although the model was statistically significant ($p < 0.05$), the samples were small ($n = 6$). Small samples do not provide a very precise estimate of the strength of the relationship; R^2 (adj) will vary a great deal. For a more precise estimate, larger samples (typically 40 or more in this case) should be used. R^2 (adj) obtained for the linear was 73%.

4.5 Fractional Factorial Experiments

In the second round of corrosion tests a fractional factorial experimental design approach was adopted, and Minitab® was used to perform the exercise. The variables were all varied for each run and all the tests were conducted at 45°C.

The combined effect of all the variables were studied with a wider range of chemistries than the classical design. The only exception to the equipment, procedures and consumables employed in this chapter were the reagents used to provide the calcium and magnesium ions and the method used to prepare the corrosion test solutions. Table 4-34 lists the reagents used in place of the calcium

chloride and magnesium chloride listed in Table 4-5 and Table 4-35 is the summary of the target water qualities.

In order to prepare the test solutions with the target concentrations specified in Table 4-35, it was first necessary to prepare 500 ml stock solutions for each of the main ions, namely calcium, magnesium, sulphate, chloride, fluoride and bicarbonate. For example, the calcium stock solution was prepared with calcium nitrate by dissolving 64.8149 g of calcium nitrate tetrahydrate (Table 4-34) into 500 ml of deionised water. The masses of the reagents were calculated so that the addition of: 10, 20, 40 or 80 ml of any of the stock solutions would provide any of the specified ion concentrations. The addition of a 10 ml aliquot of the 500 ml calcium stock solution to a 5 l corrosion test solution targeted a calcium concentration of 44 mg/l. The same method was followed for the remaining ions and corrosion test solutions. The masses taken for the remaining ions were as follows: 31.6490 g of magnesium nitrate hexahydrate, 14.7018 g of sodium bicarbonate, 27.6279 g of sodium fluoride, 267.8617 g of sodium chloride, and 332.6916 g of sodium sulphate (Table 4-5).

Minitab[®] was used to generate the number of runs and the concentrations to be tested for the ranges specified for the different variables. The corrosion tests were then performed in batches of six tests, as done previously. The results of the corrosion tests were analysed using Minitab[®].

Table 4-34: Laboratory reagents

Reagent	Supplier
Calcium nitrate tetrahydrate, Assay min 98% (m/m) as $\text{Ca}(\text{NO}_3)_2 \cdot 4\text{H}_2\text{O}$	Associated Chemical Enterprises, Johannesburg, South Africa
Magnesium nitrate hexahydrate, Assay min 98% (m/m) as $\text{MgN}_2\text{O}_6 \cdot 6\text{H}_2\text{O}$	

Table 4-35: Factorial design experiment at 45°C - Target concentrations

Run Order	Centre Point	Target concentrations					
		Calcium (mg/l as Ca^{2+})	Magnesium (mg/l as Mg^{2+})	Sulphate (mg/l as SO_4^{2-})	Chloride (mg/l as Cl^-)	Fluoride (mg/l as F^-)	Total alkalinity (mg/l as CaCO_3)
91	1	44	12	0	1300	0	220
92	1	120	50	1800	0	100	35
93	0	82	31	900	650	50	128
94	1	44	12	1800	0	100	220
95	1	44	50	0	1300	100	35
96	0	82	31	900	650	50	128
97	1	120	50	0	1300	0	35
98	1	120	12	1800	1300	0	35
99	1	120	12	0	0	100	35
100	1	120	12	0	1300	100	220
101	1	120	50	1800	1300	100	220
102	1	44	50	1800	1300	0	220
103	1	44	50	1800	0	0	35
104	1	44	12	0	0	0	35
105	1	120	12	1800	0	0	220
106	1	44	50	0	0	100	220
107	1	44	12	1800	1300	100	35
108	1	120	50	0	0	0	220

Table 4-36 reports the chemical analyses of the test solutions prior to the commencement of the corrosion tests. The same chemical analyses were then repeated upon culmination of the three day tests. These results are given in Table 4-37 together with the coupon and Corrater[®] results in Table 4-38.

Figure 4-39 indicates the following correlations with mild steel coupon corrosion rate:

- Increases in the initial pH, initial chloride or initial total alkalinity concentrations appeared to lead to decreasing corrosion rates approximating either linear or quadratic models
- Quadratic models were evident for the initial: calcium, fluoride and sodium concentrations.

Figure 4-40 shows that most of the variables did not change considerably during the experiments. The pH changed significantly during the experiment, but there was no observable trend between the initial and final pH values.

A Minitab® generated multiple regression analysis of the average corrosion rate versus the main effect parameters, as exhibited by Figure 4-41, revealed the potentially optimum values for the key parameters. The minimum corrosion was reported for a calcium concentration of 129 mg/l (as Ca^{2+}), sulphate concentration of 586 mg/l (SO_4^{2-}), chloride concentration of 1465 mg/l (as Cl^-), and a pH of 9.27.

Equation 4.6 models the relationship between the average corrosion rate and the main effect input variables, at 45°C, and had an R^2 value of 95%.

$$\begin{aligned} \text{Average corrosion rate} = & 2.375 - 0.003575 \times \text{Ca(i)} - 0.000372 \times \text{SO4(i)} \\ & - 0.000036 \times \text{Cl(i)} - 0.2171 \text{pH(i)} + 0.000014 \times \text{Ca(i)}^2 \dots\dots\dots[4.6] \end{aligned}$$

where: Average coupon corrosion rate in millimetres per annum (mmpa),
 SO4(i) = initial sulphate concentration (mg/l as SO_4^{2-}),
 Cl(i) = initial chloride concentration (mg/l as Cl^-).

Table 4-36: Test solution concentrations for factorial design experiment at 45°C - A

Run	Test solution concentrations									
	Initial pH ⁽¹⁾	Final pH ⁽¹⁾	Initial calcium ⁽²⁾ (mg/l as Ca ²⁺)	Final calcium ⁽²⁾ (mg/l as Ca ²⁺)	Initial magnesium ⁽²⁾ (mg/l as Mg ²⁺)	Final magnesium ⁽²⁾ (mg/l as Mg ²⁺)	Initial total alkalinity ⁽¹⁾ (mg/l as CaCO ₃)	Final total alkalinity ⁽²⁾ (mg/l as CaCO ₃)	Initial chloride ⁽²⁾ (mg/l as Cl ⁻)	Final chloride ⁽²⁾ (mg/l as Cl ⁻)
91	8.52	8.64	39.1	11.9	11.8	13.1	283.8	211.2	585	1196
92	7.49	8.18	101	96.1	43.6	48.3	37.9	40.4	9	375
93	8.10	8.62	48.1	46.6	33.9	36.8	143.8	132.2	303	683
94	8.63	9.10	5.48	6.14	10.9	11.7	283.1	304	5	0.96
95	7.50	8.17	40.8	29.6	45.5	47.5	47.1	51.1	605	1305
96	8.26	8.71	46.6	44.4	34.3	35.9	137.1	132.5	309	648
97	7.91	7.65	170	178	51.9	56.3	33.1	24.4	1423	1570
98	8.79	7.74	176	176	13.7	14.4	50.8	31.5	1465	1501
99	7.66	7.49	217	142	13.6	13.7	39.2	25.2	8	4.84
100	8.13	8.17	63.6	54.0	12.9	14.1	154.1	126.9	1331	1507
101	8.72	8.45	79.5	68.9	49.0	52.2	158.9	145.4	1408	1516
102	9.35	8.50	46.5	30.2	47.8	50.6	139.4	101.1	1302	1375
103	7.72	8.22	42	47.8	44.7	47.3	37.8	49.6	0	3.33
104	7.92	7.82	39.4	34.8	11.0	11.7	37.0	25.2	3	3.25
105	8.44	8.41	145	108	11.7	12.4	247.2	125.6	3	0
106	9.64	9.16	10.3	10.9	38.2	38.6	258	261	3	3.36
107	7.75	8.50	32.3	17.4	12.1	12.9	41.8	73.1	1143	1281
108	8.03	8.17	17.4	74.8	12.9	43.9	199	91.1	3	4.92

Notes: 1. Test conducted in Laboratory B, 2. Test conducted in Laboratory C, nt = not tested.

Table 4-37: Test solution concentrations for factorial design experiment at 45°C - B

Run	Test solution concentrations									
	Initial sulphate (25x diln) ⁽²⁾ (mg/l as SO ₄ ²⁻)	Final sulphate (25x diln) ⁽²⁾ (mg/l as SO ₄ ²⁻)	Initial fluoride (25x diln) ⁽¹⁾ (mg/l as F ⁻)	Final fluoride (25x diln) ⁽¹⁾ (mg/l as F ⁻)	Initial sodium ⁽²⁾ (mg/l as Na ⁺)	Final sodium ⁽²⁾ (mg/l as Na ⁺)	Initial conductivity ⁽¹⁾ (μS/cm)	Final conductivity ⁽¹⁾ (μS/cm)	Initial total iron ⁽¹⁾ (mg/l as Fe ³⁺ (total))	Final total iron ⁽¹⁾ (mg/l as Fe ³⁺ (total))
91	1	0	2.0	1.0	472	830	2540	4464	< 0.01	13.5
92	975	1050	87.5	83.0	492	744	2830	4184	< 0.01	15.0
93	475	475	43.5	38.5	482	910	2660	4788	< 0.01	6.1
94	950	975	80.5	78	569	960	2600	4592	< 0.01	22.4
95	0	0	80.5	61.5	485	895	2770	4940	< 0.01	19.0
96	475	450	44.5	34.0	494	889	2670	4672	< 0.01	12.9
97	3	1	0.0	0.0	842	893	5336	5860	< 0.01	21.0
98	1350	1400	2.0	2.0	1300	1370	6760	7128	< 0.01	5.4
99	1	2	84.0	79.0	121	127	1428	1476	< 0.01	25.4
100	1	1	88	86.5	884	982	5044	5528	< 0.01	43.2
101	1350	1500	86.0	84.5	1362	1460	7320	7768	< 0.01	2.0
102	1450	1400	1.5	0.5	1179	1251	6148	6568	< 0.01	3.6
103	1125	1275	1.0	0.5	932	992	4524	4880	< 0.01	9.8
104	5	1	0.0	0.0	15	17.2	420	424	< 0.01	14.7
105	975	1050	1.0	0.0	833	874	4236	4448	< 0.01	2.4
106	1	1	72.0	52.5	195	207	1260	1328	< 0.01	3.3
107	1250	1425	73.0	67.0	1642	1724	7636	8012	< 0.01	16.8
108	1	0	0.0	0.0	105	120	1540	1452	< 0.01	5.6

Table 4-38: Factorial design experiment at 45°C – Coupon and Corrat[®] results

Run	Corrosion Coupon Results				Corrat [®] readings			
	Coupon 1 (mmpa)	Coupon 2 (mmpa)	Coupon 3 (mmpa)	Average (mmpa)	Day 1 (mmpa)	Day 2 (mmpa)	Day 3 (mmpa)	Day 4 (mmpa)
91	0.32	0.37	0.44	0.38	0.62	0.58	0.54	0.51
92	0.61	0.61	0.59	0.60	0.50	0.46	0.46	0.48
93	0.27	0.32	0.32	0.30	1.00	0.99	0.88	0.86
94	0.62	0.57	0.56	0.59	0.66	0.63	0.64	0.63
95	0.48	0.48	0.46	0.47	0.97	0.95	0.94	0.88
96	0.33	0.37	0.34	0.35	0.32	0.19	0.27	0.28
97	0.35	0.39	0.38	0.38	0.57	0.52	0.49	0.48
98	0.42	0.41	0.46	0.43	0.84	0.82	0.79	0.81
99	0.61	0.56	0.59	0.59	0.35	0.28	0.27	0.25
100	0.40	0.47	0.48	0.45	0.92	0.88	0.87	0.84
101	0.36	0.39	0.38	0.38	0.75	0.67	0.63	0.60
102	0.38	0.41	0.44	0.41	0.77	0.71	0.70	0.70
103	0.75	0.84	0.79	0.79	0.66	nt	nt	nt
104	0.56	0.63	0.64	0.61	0.81	nt	nt	nt
105	0.42	0.36	0.45	0.41	0.73	nt	nt	nt
106	0.48	0.45	0.53	0.49	31.2	nt	nt	nt
107	0.73	0.68	0.61	0.67	25.2	nt	nt	nt
108	0.57	0.56	0.56	0.56	24.3	nt	nt	nt

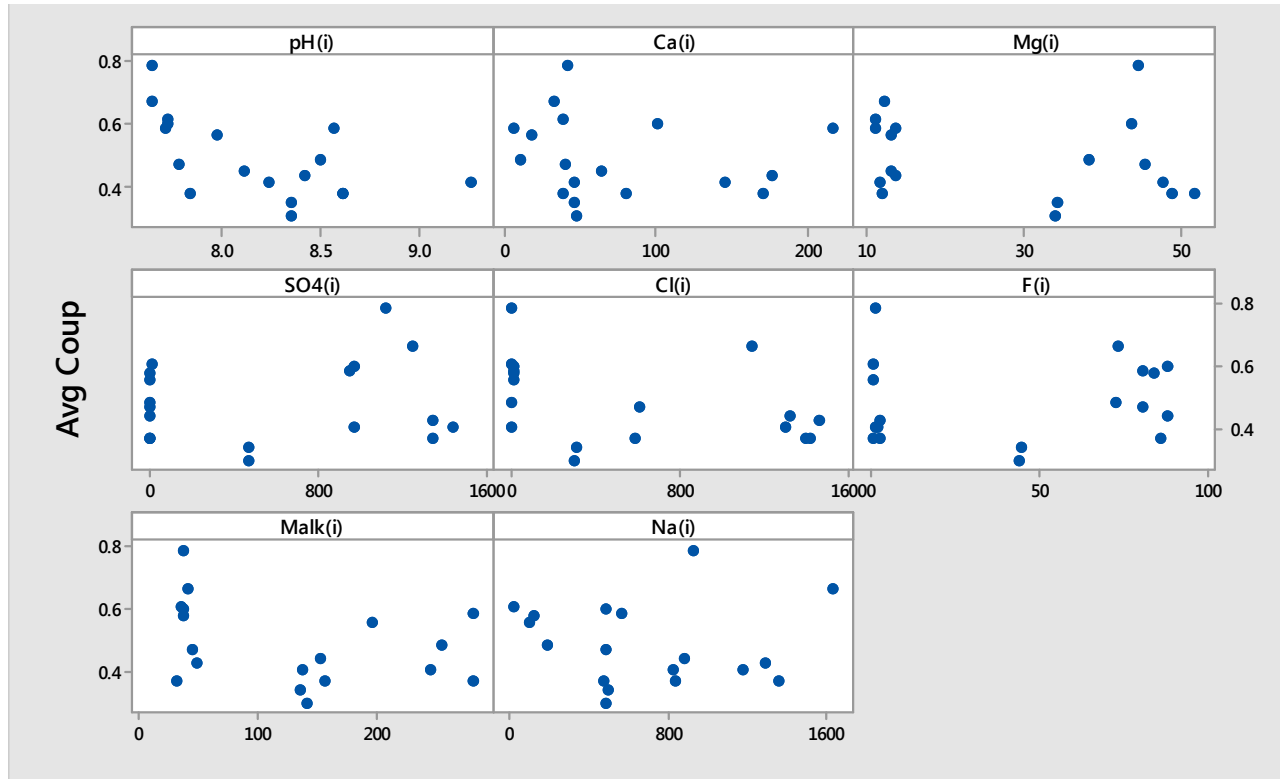


Figure 4-39: Scatterplots of the average corrosion rate versus various parameters measured at the commencement of the corrosion tests at 45°C

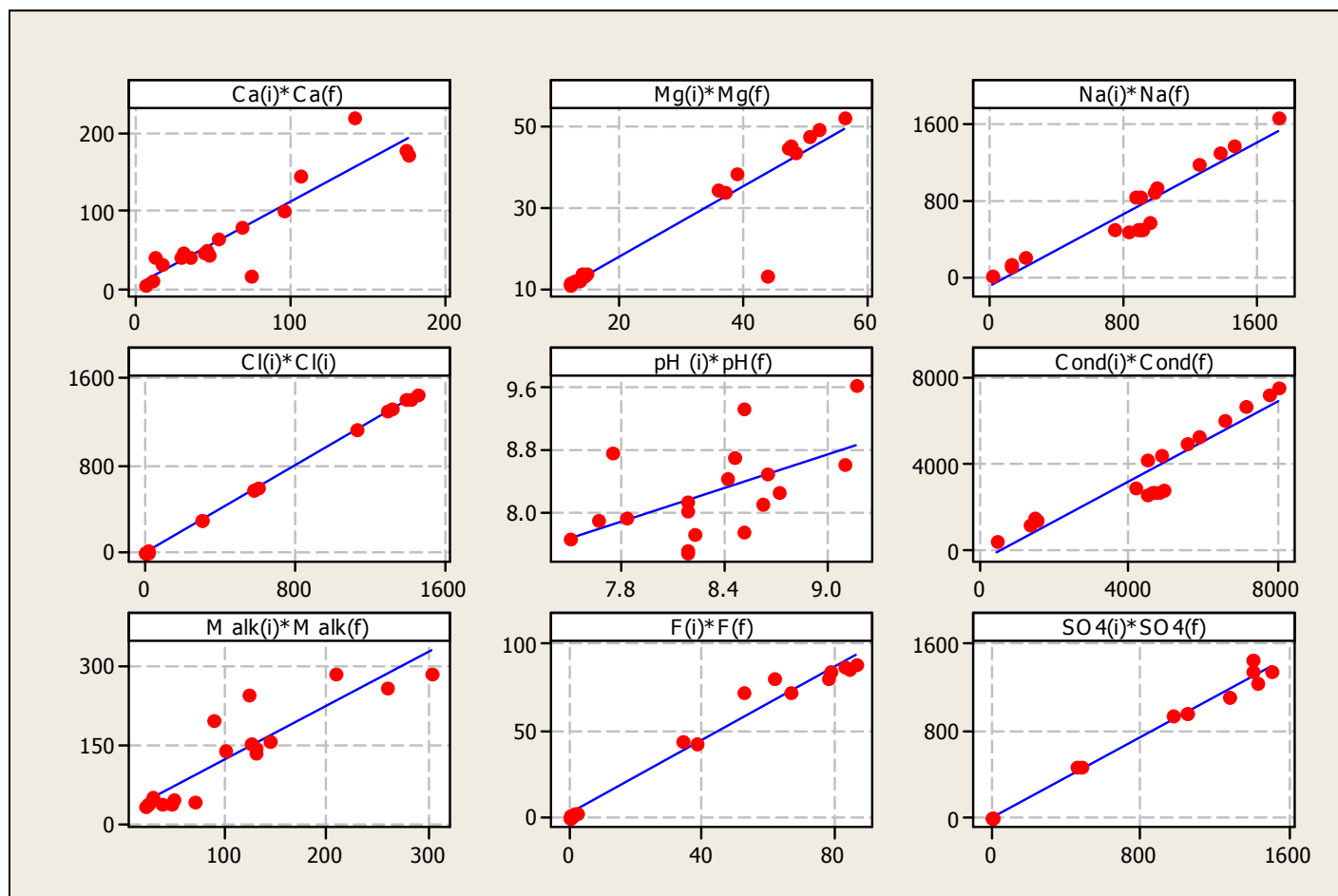


Figure 4-40: Scatterplots of parameters comparing the test initial value against the test final value at 45°C

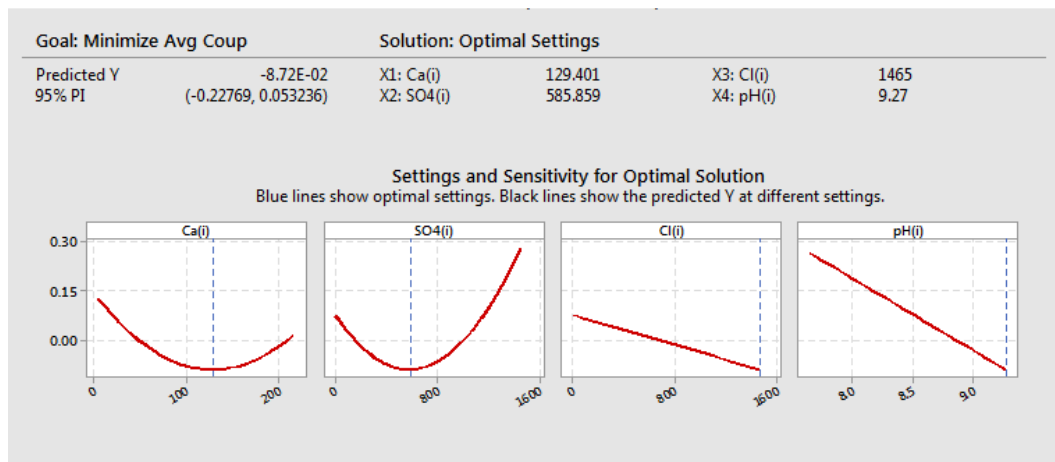


Figure 4-41: Multiple regression for the average corrosion rate versus the parameters with the highest correlations demonstrating the values corresponding to the lowest corrosion rate

The solid line shows the impact of the initial sulphate concentration on the average corrosion rate in the absence of the chloride ion (Figure 4-42). An increase in the sulphate concentration initially decreased the corrosion rate and then at above approximately 400 mg/l it was observed to increase the mild steel corrosion rate. The dotted line reflects a general reduction in the impact of the sulphate concentration at the introduction of a relatively high concentration of the chloride ion (1465 mg/l). The interaction plot of the initial chloride and initial sulphate concentration on the average corrosion rate (Figure 4-42) therefore depicts the potentially inhibitory effect of the chloride concentration on the corrosivity of the sulphate ion.

A more comprehensive multivariate model was also developed (Equation 4.7), as given in Table 4-39 and illustrated in Figure 4-43, and shown to be statistically significant ($p < 0.05$), but the number of test runs was low ($n = 18$). It was therefore not possible to obtain a very precise estimate of the strength of the relationship and consequently the adjusted R^2 value (38%) was significantly lower than the unadjusted the R^2 value (71%). A more precise estimate would require typically 40 or more test runs.

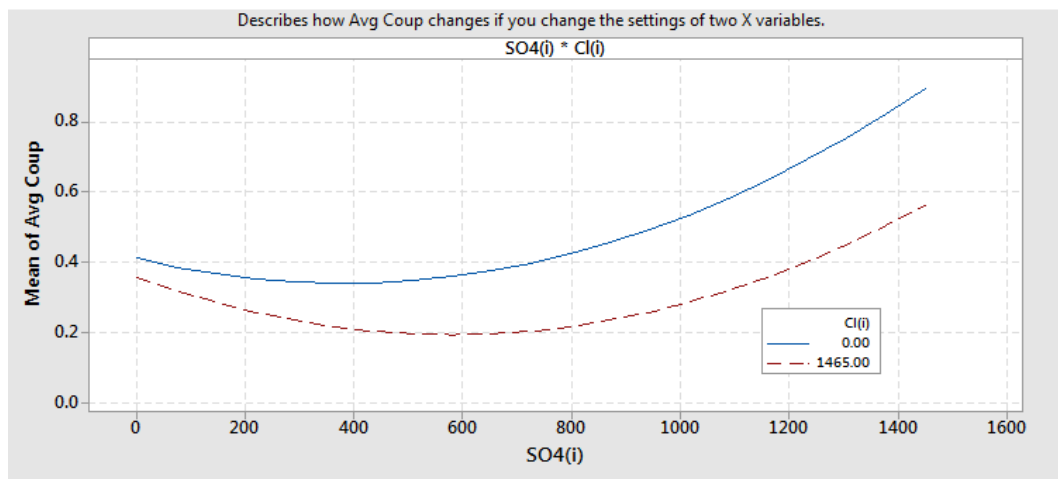


Figure 4-42: Interaction plot demonstrating the effects of the initial chloride (Cl(i)) and initial sulphate concentration (SO4(i)) on the average corrosion rate (Avg Coup)

Table 4-39: Regression analysis report for variables correlating with the average mild steel coupon corrosion rate according to the factorial design

Regression Analysis: Avg Coup versus Ca(i), Mg(i), ...					
The regression equation is					
Avg Coup = - 0.016 - 0.00110 Ca (i) - 0.00382 Mg (i) - 0.000418 Na (i) - 0.000351 Cl (i) + 0.0885 pH (i) + 0.000174 Cond(i) - 0.00141 M alk(i) + 0.000394 F (i) - 0.000082 SO4 (i) [4.7]					
Predictor	Coef	SE Coef	T	P	
Constant	-0.0157	0.6576	-0.02	0.982	
Ca (i)	-0.0011026	0.0006097	-1.81	0.108	
Mg (i)	-0.003822	0.002117	-1.80	0.109	
Na (i)	-0.0004184	0.0006067	-0.69	0.510	
Cl (i)	-0.0003509	0.0001530	-2.29	0.051	
pH (i)	0.08848	0.08348	1.06	0.320	
Cond(i)	0.0001737	0.0001536	1.13	0.291	
M alk(i)	-0.0014125	0.0005417	-2.61	0.031	
F (i)	0.0003936	0.0006646	0.59	0.570	
SO4 (i)	-0.0000821	0.0001074	-0.76	0.467	
S = 0.102312 R-Sq = 70.9% R-Sq(adj) = 38.2%					
Analysis of Variance					
Source	DF	SS	MS	F	P
Regression	9	0.20409	0.02268	2.17	0.145
Residual Error	8	0.08374	0.01047		
Total	17	0.28784			

continuation of Table 4-39		
Source	DF	Seq SS
Ca(i)	1	0.00768
Mg(i)	1	0.00994
Na(i)	1	0.00001
Cl(i)	1	0.07653
pH (i)	1	0.03767
Cond(i)	1	0.00040
M alk(i)	1	0.06235
F(i)	1	0.00341
SO ₄ (i)	1	0.00612

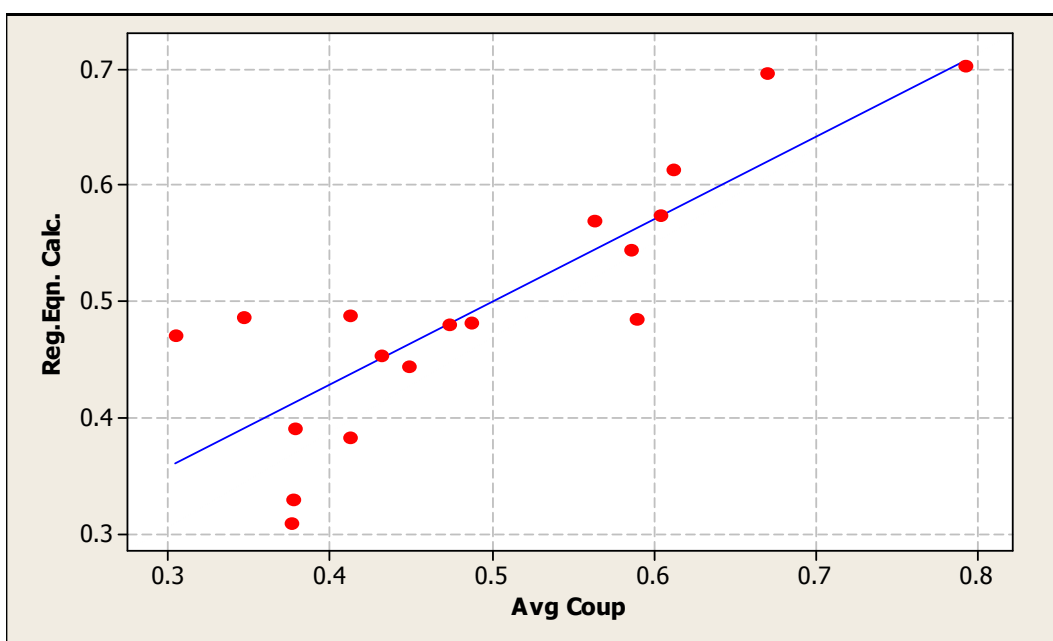


Figure 4-43: Scatterplot of the calculated corrosion rate versus the average corrosion rate ($R\text{-Sq} = 70.9\%$ $R\text{-Sq}(\text{adj}) = 38.2\%$)

Matrix plots of the variables, comparing the initial values versus the final values, (Figure 4-40) indicated that it was mostly pH and to a limited extent the total alkalinity and the calcium levels that underwent significant changes during the experiments.

A four variable main effects regression model (Equation 2.8) ($R^2 = 95\%$) was developed and it indicated that for the ranges given, the most influential initial parameters were the calcium concentration, pH, chloride concentration and sulphate

concentration. While increases in initial pH and initial chloride tended to linearly decrease the coupon corrosion rate, the initial calcium and initial sulphate concentrations, first decreased and then increased corrosion. The negative correlation between the initial chloride concentration and the corrosion rate was reflected in both a four variable equation and in the interaction plot generated between the initial chloride and initial sulphate concentrations. Chloride was noted to have reduced the corrosivity of the sulphate ion on mild steel corrosion for the range of chemistries at 45°C.

Although a more elaborate multivariate regression model was developed to include all the variables tested, it was not possible to obtain a very precise estimate of the strength of the relationship due to the low number of test runs.

4.6 Evaluation of Corrosion Inhibitors

In this third round of tests various corrosion inhibitors were evaluated in a worst case synthetic solution in order to find the most effective commercially viable solution. It was decided to evaluate potential impact of zinc and phosphate, on the mild steel corrosion rate, as these two corrosion inhibitors were already employed in the steel mill cooling systems evaluated. The purpose of this section was to quantify the effects of various commonly used corrosion inhibitors when applied to a water chemistry representing the middle of the range of calcium hardness and total alkalinity with the chloride, sulphate and fluoride at the highest levels for the range of chemistries covered in this document thus far (Table 4-40). These tests were all conducted at 45°C.

Table 4-40: Corrosion inhibition tests at 45°C- Target concentrations

Test solution target concentrations						
pH	Calcium (mg/l as Ca ²⁺)	Magnesium (mg/l as Mg ²⁺)	Total alkalinity (mg/l as CaCO ₃)	Chloride (mg/l as Cl ⁻)	Sulphate (mg/l as SO ₄ ²⁻)	Fluoride(m g/l as F ⁻)
7.8 – 8.3	75	27	110	1100	1500	90

The corrosion inhibitors considered are listed and described in Table 4-41.

Table 4-41: Corrosion inhibitors tested

Run	Corrosion inhibitor (active ingredient concentration in mg/l)	
109	Product A (10)	Phosphonic carboxylic acid (PCA)
110	Product B (5.3)	Phosphoric acid (PO_4^{3-})
111	Product C(2)	Tolyltriazole (TT)
112	Product D(10)	Aminotri (methylenephosphonic acid) (ATMP)
113	Product E (10)	2-Phosphonobutane-1,2,4-tricarboxylic acid (PBTC)
114	Control 1	-
115	Product F (5)	Sodium hexametaphosphate (SHMP)
116	Product G(2.2)	Zinc dosed as zinc chloride
117	Product H(5)	Molybdate (MoO_4^-) dosed as sodium molybdate
118	Product I(12)	Hydroxyethylidene-1, 1-diphosphonic (HEDP)
119	Product J (9.9)	Silica dosed as sodium metasilicate pentahydrate (SiO_2) $5\text{H}_2\text{O}$
120	Control 2	-

Note: The industrial grade corrosion inhibitors were sourced from Buckman Africa (Pty) Ltd, 1 Buckman Boulevard, Hammarsdale, KZN, 3700, South Africa.

Table 4-42 and 4-43 report the chemical analyses of the test solutions prior to the corrosion tests and upon culmination of the three day tests respectively. The coupon and Corrater[®] readings are given in Table 4-44 as well as in the Figure 4-44.

As evident in Figure 4-44, the two most effective commercially available corrosion inhibitors evaluated individually within their typical dosage range, appear to be phosphoric acid, at 5.3 mg/l (as PO_4^{3+}) and zinc, at 2.2 mg/l (as Zn^{2+}). The average coupon corrosion rates obtained for these two inhibitors were 0.44 and 0.47 mmpa respectively. The average mild steel coupon corrosion rates for the two control tests ranged between 0.53 and 0.60 mmpa. The use of molybdate alone appeared to result in slightly higher mild steel corrosion rates of between 0.55 and 0.61 mmpa.

Table 4-42: Corrosion inhibition tests at 45°C - Start-up concentrations

Run	Test solution concentrations at start-up								
	pH ⁽¹⁾	Calcium ⁽²⁾ (mg/l as Ca ²⁺)	Magnesium ⁽²⁾ (mg/l as Mg ²⁺)	Total alkalinity ⁽¹⁾ (mg/l as CaCO ₃)	Chloride ⁽²⁾ (mg/l as Cl ⁻)	Sulphate (25x diln) ⁽²⁾ (mg/l as SO ₄ ²⁻)	Fluoride (25x diln) ⁽¹⁾ (mg/l as F ⁻)	Conductivity ⁽¹⁾ (µS/cm)	Total iron ⁽¹⁾ (mg/l as Fe ³⁺ (total))
109	7.88	45.6	26.6	110.4	1132	2.00	79.5	5942	< 0.01
110	7.99	23.0	26.5	102.9	1068	1.75	84.5	5904	< 0.01
111	8.16	19.9	26.0	109.2	1090	1.50	82.5	5799	< 0.01
112	7.91	21.1	25.7	107.0	1087	2.00	82.0	6291	< 0.01
113	7.89	24.7	25.8	109.4	1070	1.50	82.5	6328	< 0.01
114	8.07	19.8	25.8	109.2	1080	2.00	86.0	6592	< 0.01
115	8.17	22.2	25.5	115.4	1129	2.00	87.0	6268	< 0.01
116	8.06	17.7	25.1	117.4	1128	2.00	88.5	6224	< 0.01
117	8.23	18.9	24.6	123.4	1187	1.75	87.5	6216	< 0.01
118	8.12	23.8	24.7	110.0	1163	1.75	92.5	6196	< 0.01
119	8.74	15.8	24.6	127.5	1133	2.00	89.0	6160	< 0.01
120	8.19	17.7	24.6	110.9	1126	2.00	81.5	6144	< 0.01

Notes: 1. Test conducted in Laboratory B, 2. Test conducted in Laboratory C.

Table 4-43: Corrosion inhibition tests at 45°C – Cessation concentrations

Run	Test solution concentrations at cessation of corrosion tests								
	pH ⁽¹⁾	Calcium ⁽²⁾ (mg/l as Ca ²⁺)	Magnesium ⁽²⁾ (mg/l as Mg ²⁺)	Total alkalinity ⁽¹⁾ (mg/l as CaCO ₃)	Chloride ⁽²⁾ (mg/l as Cl ⁻)	Sulphate (25x diln) ⁽²⁾ (mg/l as SO ₄ ²⁻)	Fluoride (25x diln) ⁽¹⁾ (mg/l as F ⁻)	Conductivity ⁽¹⁾ (µS/cm)	Total iron ⁽¹⁾ (mg/l as Fe ³⁺ (total))
109	8.64	20.7	27.5	93.2	1145	2.00	4.3	6185	5.3
110	8.67	21.4	27.2	109.7	1170	1.75	4.3	6182	4.3
111	8.68	24.0	27.3	118.7	1118	1.75	4.3	6197	6.3
112	8.54	21.3	26.6	111.7	1120	2.25	4.3	6642	7.1
113	8.65	26.7	26.7	115.8	1115	2.00	4.3	6279	8.9
114	5.67	21.2	26.5	3.8	1148	2.00	4.3	6235	10.4
115	8.62	20.2	26.7	126.1	1234	2.00	4.3	6684	3.3
116	8.62	17.9	26.5	118.2	1224	2.00	4.3	6600	2.8
117	8.69	14.7	26.4	123.5	1214	2.00	4.3	6604	3.7
118	8.48	25.2	25.6	112.4	1200	2.00	4.3	6524	3.6
119	8.79	14.4	26.2	140.9	1226	2.00	4.3	6668	3.0
120	8.67	15.9	26.4	124	1254	1.75	4.3	6632	4.7

Notes: 1. Test conducted in Laboratory B, 2. Test conducted in Laboratory C, nt = not tested.

Table 4-44: Corrosion inhibition tests at 45°C – Coupon and Corrater® results

Run	Corrosion Coupon Results				Corrater® readings			
	Coupon 1 (mmpa)	Coupon 2 (mmpa)	Coupon 3 (mmpa)	Average (mmpa)	Day 1 (mmpa)	Day 2 (mmpa)	Day 3 (mmpa)	Day 4 (mmpa)
109	0.46	0.47	0.51	0.48	0.97	0.95	0.95	0.93
110	0.42	0.43	0.46	0.44	0.72	0.63	0.62	0.51
111	0.45	0.45	0.50	0.47	1.25	1.12	1.11	1.10
112	0.49	0.47	0.53	0.50	0.82	0.74	0.59	0.55
113	0.51	0.53	0.55	0.53	0.62	0.59	0.49	0.45
114	0.56	0.60	nt	0.58	0.84	0.73	0.64	0.61
115	0.50	0.53	0.50	0.51	1.43	1.42	1.41	1.40
116	0.47	0.44	0.48	0.47	0.97	0.86	0.85	0.80
117	0.55	0.61	0.59	0.58	0.76	0.72	0.68	0.70
118	0.48	0.55	0.53	0.52	0.65	0.61	0.53	0.51
119	0.43	0.52	0.47	0.48	0.93	0.86	0.84	0.80
120	0.54	0.56	0.53	0.55	1.50	1.48	1.48	1.46

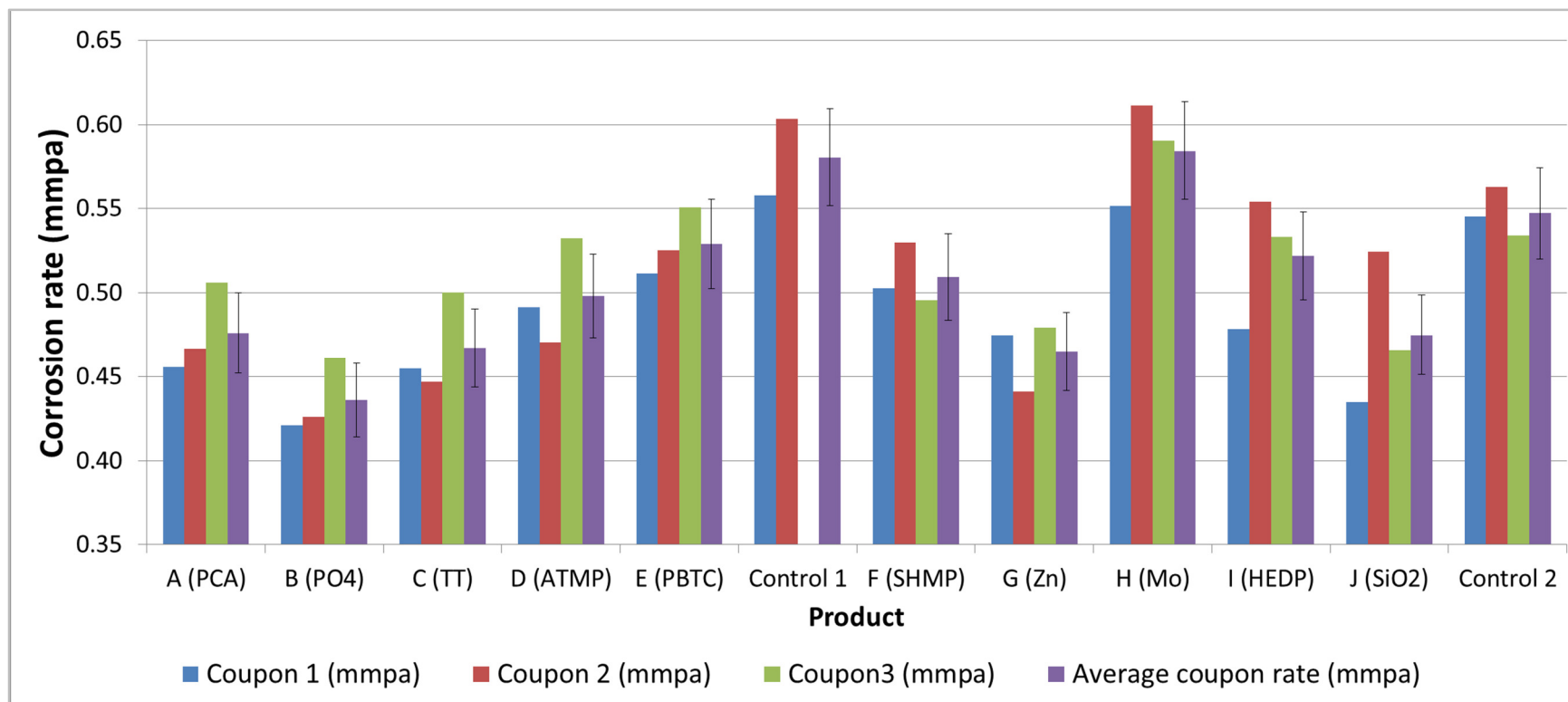


Figure 4-44: Corrosion inhibition tests with error bars at 5% of the mean

Relative to the control test averages the two corrosion inhibitors produced minor reductions in mild steel corrosion of approximately 22.7% and 9.7% respectively (Figure 4-44). Although considered minimal the reductions in corrosion would be significant in terms of the impact on the newly developed models and their comparison to the plant derived corrosion data. The use of molybdate alone appeared to have slightly increased mild steel corrosion by 3.6%. Although the tests served merely as initial screening tests they were performed without varying the concentrations of the inhibitors. The inhibitors were also not evaluated together at varying concentrations in order to seek the most optimal combinations.

4.7 Regression Analysis of All the Laboratory Data

The purpose of this section was to rely on all the laboratory data generated to this point (157 runs) in order to determine:

- The impact the additional 10°C had on the coupon corrosion rate by comparing results obtained for the corrosion tests performed at 35°C versus 45°C; and
- Evaluate all the data generated at 45°C in a multivariate non-linear regression analysis in order to establish any new trends for comparison against the outcomes of the individual sub-sections of Chapter 4.

The data used in this section was taken from both the classical and factorial design experiments. The data collated in Chapter 4 was analysed using the Minitab[®] software and the results reported below.

The data taken from all the classic and factorial design experiments did not provide sufficient evidence to conclude that the mean coupon corrosion rate of 35°C was less than 45°C. A summary report of the 2-sample t test between the average corrosion rate and temperature is depicted in Figure 4-45. This outcome may have been attributed to the small sample sizes. Based on the sample sizes, standard deviations, and α , there would have been a 90% chance of detecting a difference of 0.14737 mmpa.

Figure 4-46 compares the chemistries of the corrosion test solutions taken before and after the corrosion tests. The most obvious changes were prominent for: pH, total alkalinity, calcium and fluoride. There was a significant amount of grouping in the data points, especially in the graphs for sulphate and pH. This was obviously due to the manner in which the experiments were performed where each parameter was altered in turn while keeping the others constant.

In scatterplots of the average corrosion rate versus various parameters measured at the commencement of the corrosion tests (Figure 4-47) the following was evident:

- Weak negative linear correlations between the average corrosion rate and the following parameters: pH, calcium, total alkalinity, chloride, sulphate and conductivity;
- Weak positive linear correlation between the average corrosion rate and the fluoride concentration.

A multiple regression for the average corrosion rate (mmpa) resulted in the Equation 4.8, with an R^2 of 81%.

$$\begin{aligned} \text{Average corrosion rate} = & 7.16 - 0.006825 \times \text{M alk (i)} - 0.001882 \times \text{Cl(i)} \\ & + 0.00081 \times \text{F(i)} - 1.346 \text{ pH(i)} - 0.001462 \text{ Ca(i)} + 0.000022 \times \text{M alk(i)}^2 \\ & + 0.000000 \times \text{Cl(i)}^2 - 0.000025 \times \text{F(i)}^2 + 0.0719 \times \text{pH(i)}^2 + 0.000003 \times \text{Cl(i)} \times \\ & \text{F(i)} + 0.000180 \times \text{Cl(i)} \times \text{pH(i)} \dots\dots\dots[4.8] \end{aligned}$$

As apparent in Figure 4-48, the mild steel coupon corrosion rate appeared independent of both the initial chloride concentration and initial fluoride concentration. Although most of the low initial fluoride related coupon corrosion rates appeared generally lower than the intermediate fluoride related coupon corrosion rates, it was confirmed, by means of a 2-sample t test, that their means were not significantly different ($P = 0.89$). The observed differences between their means was 0.0073 mmpa. A 2-sample t test performed on the means of the low and high fluoride related coupon corrosion rates also found that there was no evidence to conclude that they were different at the 0.05 level of significance ($P = 0.35$). The difference between their means was 0.0590 mmpa.

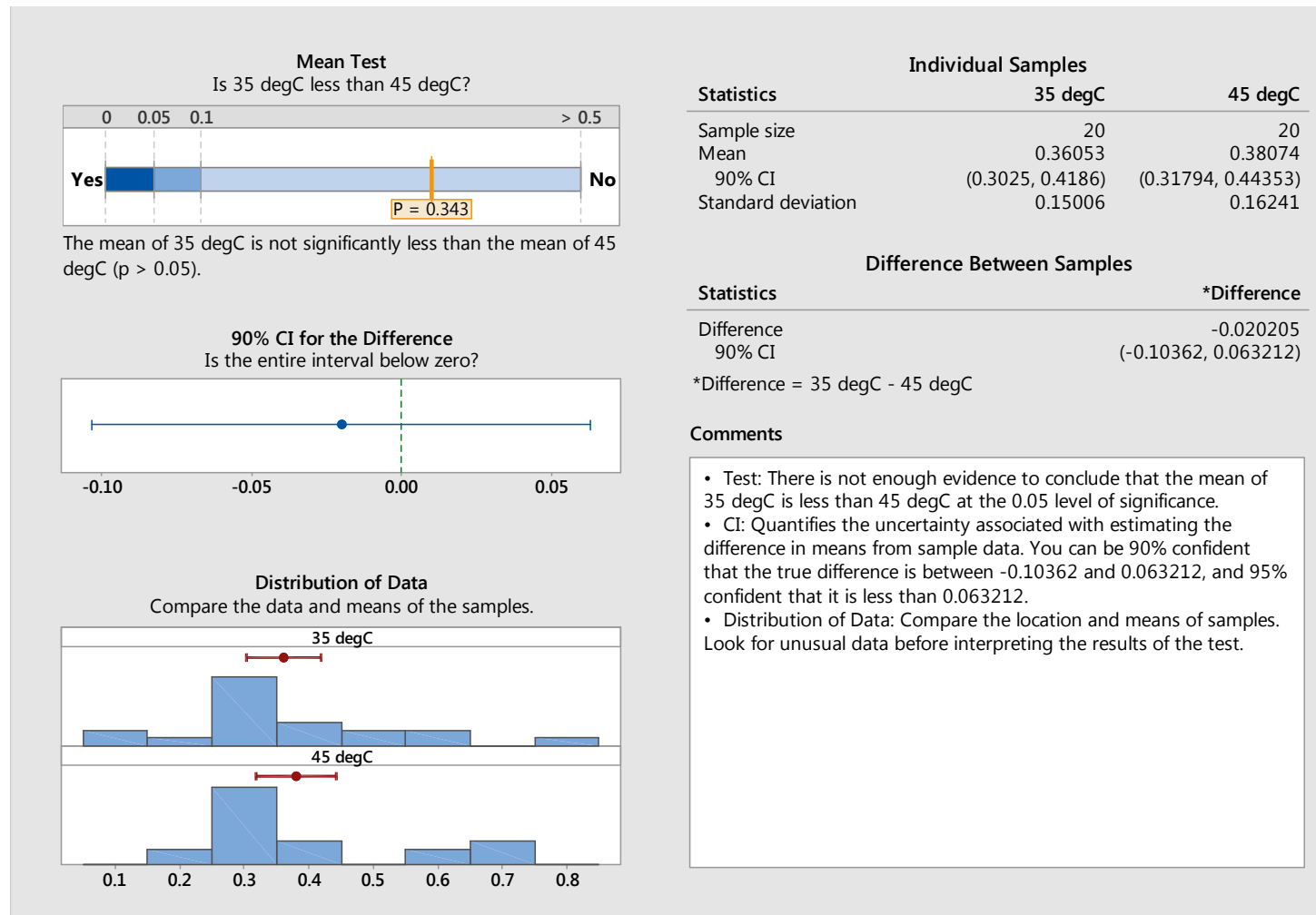


Figure 4-45: 2-Sample t test report to ascertain the impact of temperature on the coupon corrosion rates

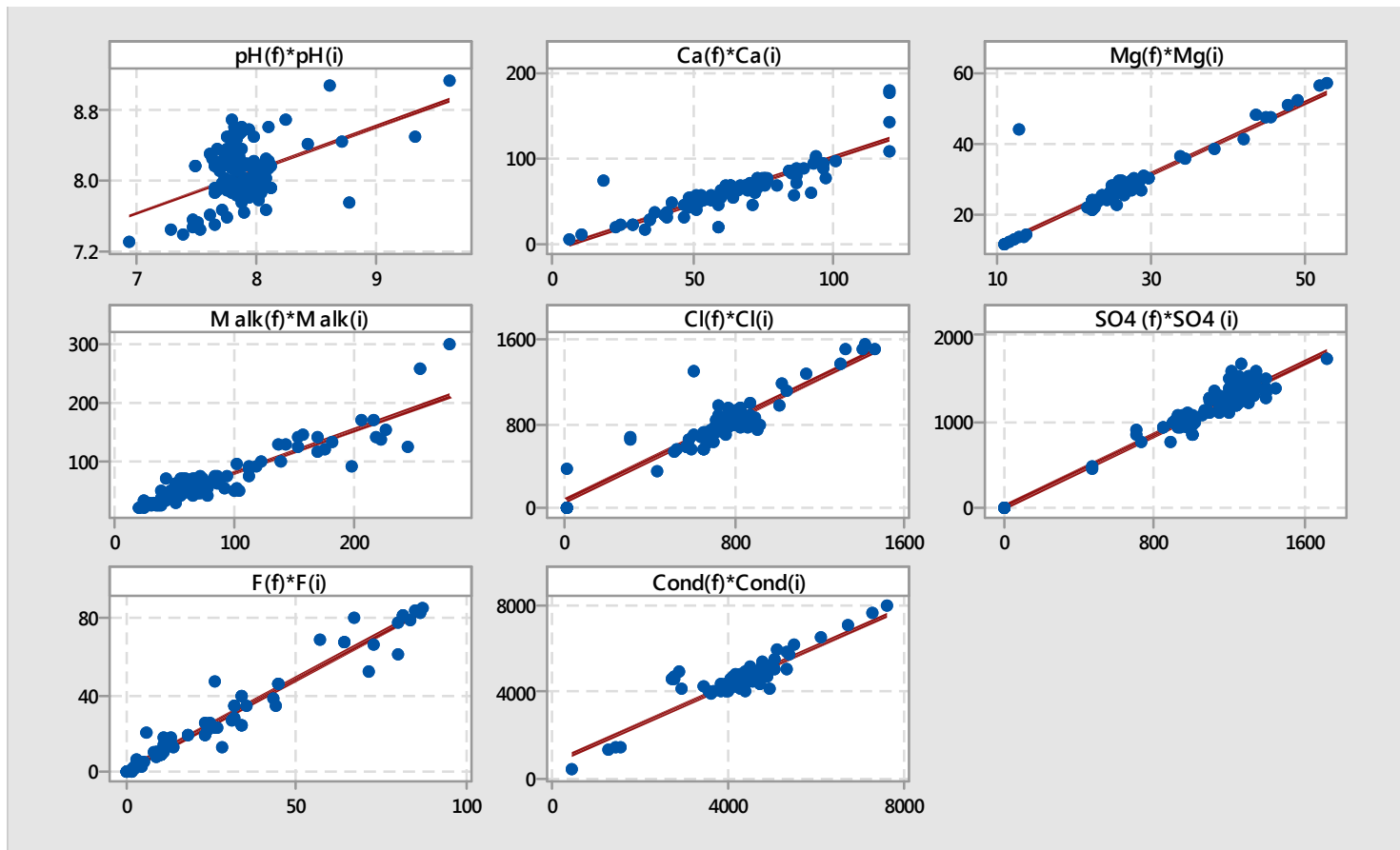


Figure 4-46: Scatterplot comparison of the initial and final parameters to examine the change in water chemistry as a result of corrosion

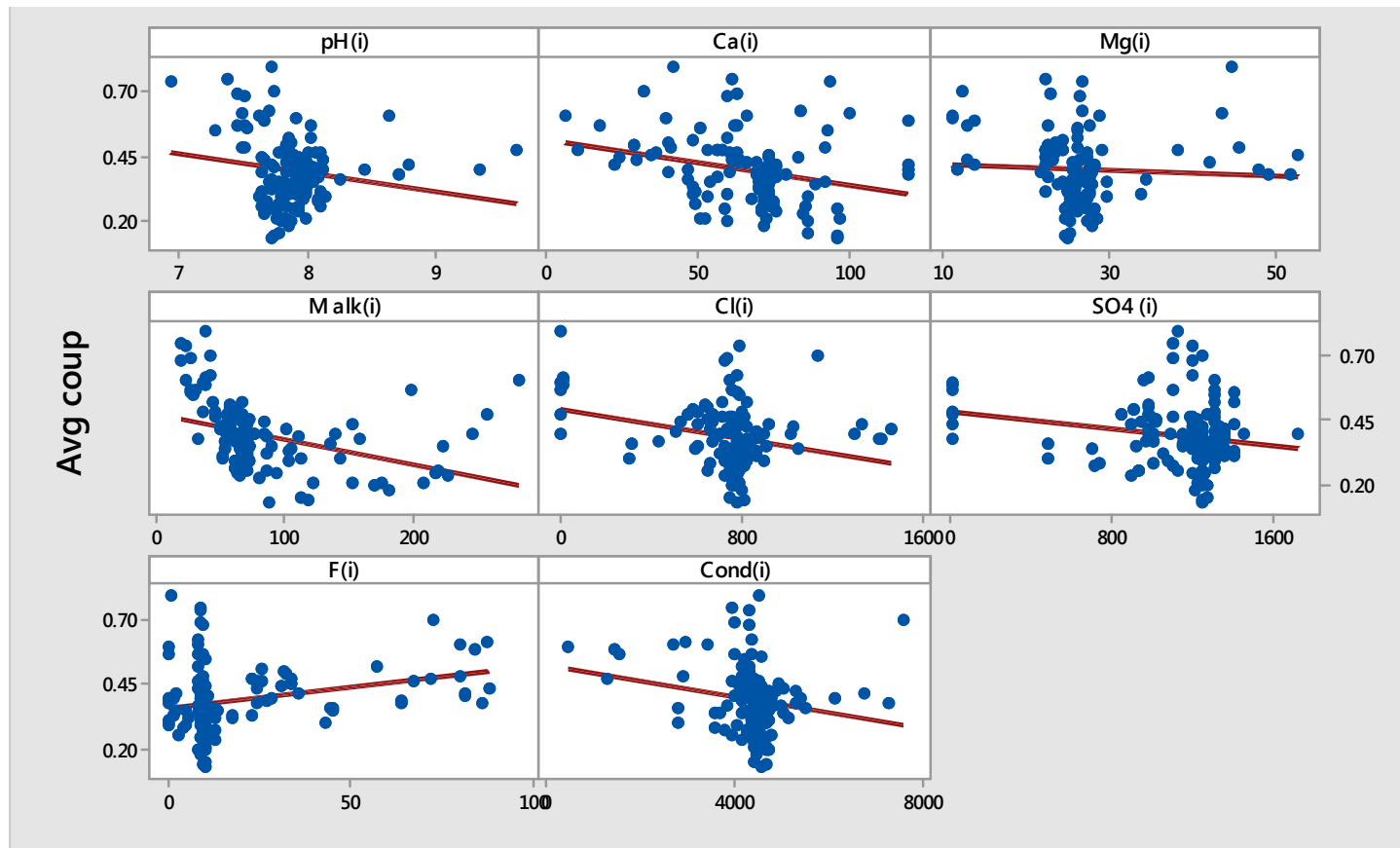


Figure 4-47: Scatterplots of of the average corrosion rate versus various parameters measured at the commencement of the corrosion tests

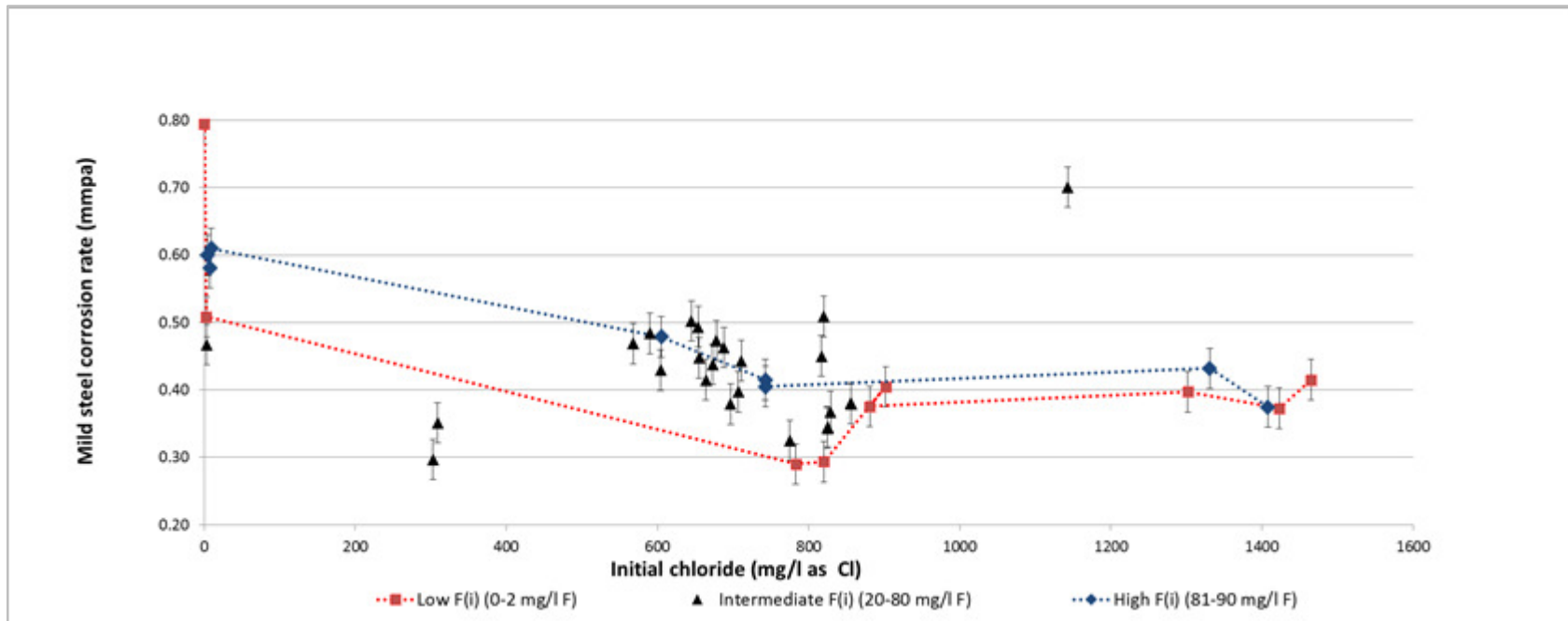


Figure 4-48: Mild steel corrosion rate versus the initial chloride concentration for the various fluoride concentration ranges at 45°C. Error bars: $\pm 0.03\text{mmpa}$

In Chapter 4 approximately one out of every six beaker tests were performed at 35°C (n = 20). There was insufficient evidence to conclude that the mean coupon corrosion rate of 35°C was statistically significantly less than 45°C.

A comparison of the chemistries of the corrosion test solutions taken before and after the corrosion tests showed that there had been noticeable changes in: pH, total alkalinity, and the calcium and fluoride concentrations due to the corrosion that had taken place in the test solutions.

Weak negative linear correlations were apparent between most of the initial test solution water quality parameters and the average corrosion rate, namely: pH, calcium, total alkalinity, chloride, sulphate and conductivity. A weak positive linear correlation was apparent between the average corrosion rate and fluoride. A multiple regression for the average corrosion rate resulted in a five variable equation (Equation 4.8) ($R^2 = 81\%$), including the following variables: pH, calcium, total alkalinity, chloride and fluoride. This supports the findings of Section 4.4.4 where the coupon corrosion rate was only moderate strongly correlated with the fluoride concentration, unless the fluoride concentration was considered together with the pH, calcium and total alkalinity, in a multivariate equation. These corroborate the findings of the field study (Chapter 3), where it was also evident that there were no statistically significant strong correlations between any of the individual water chemistry parameters and the coupon based mild corrosion rates but where a good fit was possible on the basis of a multivariate regression analysis. Although the previous authors reported the impact or roles of the individual factors, namely: pH (Rostron, 1979b, Strehblow *et al.*, 1979, Löchel and Strehblow, 1983, Mayer *et al.*, 1984), calcium (Vasil'eva *et al.*, 1986, Macias and Escudero, 1994), alkalinity (Dillon and Waltman, 1995, Brell *et al.*, 2003) and the fluoride ion (Moll *et al.*, 1985), there were no reports found of their joint impact on mild steel, particularly at 45°C.

A comparison of the means of the average mild steel coupon corrosion rates for the grouped fluoride concentration, that is: a) fluoride less than 2 mg/l, b) between 20

and 80 mg/l and c) 81 to 90 mg/l showed that they were not statistically significantly different. As revealed in Section 4.4.2 it was again evident that the chloride concentration had no detectable impact on the mild steel corrosion rate, for the range of chemistries and temperature investigated.

4.8 Extending the Investigation on Fluoride to beyond Brackish Water

The purpose of this section was to gain further insight into the impact of fluoride on the corrosion resistance of mild steel in order to obtain an enhanced understanding of the results obtained in the previous section. These corrosion tests were different from all the previous tests as they were not performed in brackish synthetic solutions. This section is divided into a series of sub-sections, each with its intended purpose and each series performed in triplicate with duplicate mild steel (C1010) corrosion coupons. Throughout this section the fluoride concentrations were raised incrementally at the following concentrations: 0, 10, 20, 40, 70 and 90 mg/l as F^- , at 45°C. This was to reproduce the conditions experienced in the steel mill cooling systems (Table 3-2).

As outlined in Table 4-45, the initial series of tests were to determine the impact of fluoride alone on mild steel at 45°C. This was accomplished by the addition of sodium fluoride to deionised water to produce the specified range of fluoride concentrations. In the second and third series two different levels of total alkalinity (55 and 220 mg/l $CaCO_3$) were introduced into the synthetic test solutions. This was to explore the impact of the range of alkalinities on the potentially corrosive nature of fluoride on mild steel. The fourth and fifth series were performed to investigate the impact of the calcium ion without the impact of the alkalinities, and it was done at 50 and 120 mg/l, as Ca^{2+} . In the sixth series, a low calcium hardness (50 mg/l Ca^{2+}) and low total alkalinity (5 mg/l $CaCO_3$) were employed whereas in the seventh series both the calcium hardness and alkalinity were taken to their maximum values of 120 mg/l Ca^{2+} and 220 mg/l as $CaCO_3$, respectively. It was only in the eighth and ninth series that the maximum chloride and sulphate concentrations were incorporated, at 1000 and 1500 mg/l. These last two series

differed in their calcium and total alkalinity, where the former was at the lowest values, similar to series 6 and the later at the highest as values, as in series seven.

Table 4-45: Test series to investigate the corrosivity of fluoride on mild steel

Test Series/ Test Conditions to which sodium fluoride was added	Purpose
1. Deionized water	To determine the impact of fluoride alone on mild steel.
2. Low alkalinity water (target total alkalinity: 55 mg/l as CaCO ₃)	To determine the impact of fluoride with minimal alkalinity versus series one in which the resultant sodium fluoride solutions were lower than pH 7 due to the pH of the deionized water.
3. High alkalinity water (target total alkalinity: 220 mg/l as CaCO ₃)	To compare the impact of high alkalinity against series 2.
4. Low calcium hardness water (target calcium hardness: 50 mg/l as CaCO ₃)	To determine the impact of low calcium on the fluoride concentration and the mild steel corrosivity.
5. High calcium hardness water (target calcium hardness: 120 mg/l as CaCO ₃)	As in series 4 above but at the high end of the calcium concentration range. To compare this to the previous series where a low calcium concentration was explored.
6. Low calcium hardness and low alkalinity water (target calcium hardness: 50 mg/l as Ca and total alkalinity: 55 mg/l as CaCO ₃)	To determine the impact of low alkalinity and low calcium hardness and to compare these results versus that of the low alkalinity and low calcium series.
7. High calcium hardness and high alkalinity water (target calcium hardness: 120 mg/l as Ca ²⁺ and total alkalinity: 220 mg/l as CaCO ₃)	To determine the impact of high alkalinity and high calcium hardness and to compare these results versus that of the high alkalinity and high calcium series, as well as the previous series (i.e. series 6).

8. As in 6 but including high chloride and high sulphate (target chloride: 1000 mg/l as Cl^- and target sulphate: 1500 mg/l as SO_4^{2-})	To compare the effect of the high chloride and sulphate concentrations versus series 6.
9. As in 7 but including high chloride and high sulphate (target chloride: 1000 mg/l as Cl^- and target sulphate: 1500 mg/l as SO_4^{2-})	To compare the effect of the high chloride and sulphate concentrations versus series 6, 7 and 8.

Sub-sections 4.2 and 4.3 outline the equipment, reagents and procedures. The salts used are listed in previous tables and included: sodium fluoride, sodium hydrogen carbonate, calcium nitrate, sodium chloride and sodium sulphate. Details of the reagents are given in Tables 4-5 and 4-34.

4.8.1 Series 1 - Deionized water only

Sodium fluoride was added to deionized water at the concentrations reported in Table 4-46 and the results of the water analyses are shown in Table 4-47. The coupon corrosion rates shown in Table 2-48.

Although the addition of sodium fluoride to deionized water appeared to affect the pH it was noticed the pH changes were within the margin of experimental error (Figure 4-49). It was therefore not possible to ascertain the effect sodium fluoride addition on deionised water. The higher sodium fluoride concentration resulted in the correspondingly higher soluble fluoride, total alkalinity, conductivities and a higher but relatively constant coupon corrosion rates (Figures 4-49, 4-50 and 4-51).

The initial fluoride concentration was found to range from slightly to moderately lower than the target fluoride concentration by between 1 to 20 mg/l (as F^-) (Figure 4-50). The largest discrepancy (20 mg/l F^-) was noted at the 70 mg/l target fluoride concentration. A graph of the average corrosion rate versus the target fluoride concentration lead to a graph which approximated a quadratic model ($R^2 = 78\%$) (Figure 4-50).

When the initial calcium and initial magnesium concentrations were included in the model then the R^2 reached 85% (Equation 4.9).

$$\text{Average corrosion rate} = 0.4338 + 0.01063 \times F(i) - 0.0627 \times Ca(i) - 0.412 \times Mg(i) - 0.000089 \times F(i)^2 + 0.676 \times Ca(i)^2 \times Mg(i) \dots [4.9]$$

where: $Mg(i)$ = initial magnesium (mg/l as Mg^{2+}).

Correlations of the average corrosion rate with: the initial sodium ($P = 0.002$, Pearson = 0.748) ($R^2 = 73\%$), initial fluoride ($P = 0.001$, Pearson = 0.625) ($R^2 = 55\%$), initial total alkalinity ($P = 0.033$, Pearson = 0.420) ($R^2 = 18\%$) and initial conductivity ($P = 0.001$, Pearson = 0.639) ($R^2 = 56\%$) revealed that they were all statistically significant positive relationships and the strongest relationship was with the initial sodium concentration, followed by the initial conductivity and only thirdly the initial fluoride concentration. Where the regression analysis based on the initial calcium, initial magnesium and initial conductivity produced an R^2 of 85% (Equation 4.9), similar regression analyses with either initial sodium or initial total alkalinity in place of the conductivity only produced R^2 values of 83% and 78% respectively.

A multivariate regression effects plot for the average corrosion rate (Figure 4-52) versus the varying initial fluoride, initial calcium and initial magnesium levels showed how the corrosion rate increased when the fluoride concentration was raised. The figure also showed a lowering of the soluble calcium and a raising of the soluble magnesium concentrations with increasing fluoride concentration. Although there were noticeable changes in the magnesium concentrations, it was decided to not make any speculations due to the limited data (14 data points) and the limited range of the values (0.0 to 0.2 mg/l). Figure 4.49 displays how both the average initial calcium and average initial conductivity vary versus the target fluoride concentration.

Table 4-46: Corrosion tests varying fluoride in deionized water at 45°C – Target and start-up concentrations

Run	Target fluoride (mg/l as F ⁻)	Test solution concentrations at start-up									
		Fluoride (25x diln) ⁽¹⁾ (mg/l as F ⁻)	pH ⁽¹⁾	Calcium ⁽²⁾ (mg/l as Ca ²⁺)	Magnesium ⁽²⁾ (mg/l as Mg ²⁺)	Total alkalinity ⁽¹⁾ (mg/l as CaCO ₃)	Chloride ⁽²⁾ (mg/l as Cl ⁻)	Sulphate (25x diln) ⁽²⁾ (mg/l as SO ₄ ²⁻)	Sodium ⁽²⁾ (mg/l as Na ⁺)	Conductivity ⁽¹⁾ (µS/cm)	Total iron ⁽¹⁾ (mg/l as Fe ³⁺ (total))
115	0	0.7	4.54	0.4	nt	0.0	nt	nt	nt	0	< 0.01
116	10	8.0	4.96	0.3	nt	1.9	nt	nt	nt	44	< 0.01
117	20	14.4	5.07	0.0	nt	3.1	nt	nt	nt	92	< 0.01
118	40	33.5	5.11	0.2	nt	5.4	nt	nt	nt	188	< 0.01
119	70	60.3	5.09	0.2	nt	9.0	nt	nt	nt	324	< 0.01
120	90	86.8	5.11	0.3	nt	13.7	nt	nt	nt	488	< 0.01
127	0	2.0	4.08	0.5	nt	0.0	nt	nt	nt	32	< 0.01
128	10	8.2	5.34	0.2	nt	4.2	nt	nt	nt	48	< 0.01
129	20	17.1	5.30	0.3	nt	5.3	nt	nt	nt	96	< 0.01
130	40	34.0	5.17	0.3	nt	7.6	nt	nt	nt	192	< 0.01
131	70	50.0	5.22	0.1	nt	11.3	nt	nt	nt	336	< 0.01
132	90	93.3	5.21	0.2	nt	14.7	nt	nt	nt	464	< 0.01
133	0	0.0	5.54	0.4	0.0	5.4	3	5.87	0	8	< 0.01
134	10	9.7	5.17	0.7	0.0	6.1	3	6.08	10	52	< 0.01
135	20	20.2	5.21	1.9	0.1	7.8	3	5.81	22	100	< 0.01
136	40	40.5	5.23	2.7	0.0	10.9	3	5.81	45	204	< 0.01
137	70	61.0	5.27	1.3	0.1	15.3	3	5.92	80	356	< 0.01
138	90	84.1	5.27	0.2	0.0	19.6	3	5.78	116	500	< 0.01
139	0	0.0	6.20	0.7	0.1	8.9	2	5.90	1	8	< 0.01
140	10	9.5	4.90	0.3	0.0	6.7	4	5.20	10	56	< 0.01
141	20	17.4	5.38	0.3	0.1	9.6	4	5.20	21	104	< 0.01
142	40	37.1	5.65	0.3	0.1	20.6	4	5.27	44	204	< 0.01
143	70	61.0	5.30	0.5	0.1	15.0	4	5.20	79	352	< 0.01
144	90	92.1	5.24	0.5	0.1	20.2	4	5.26	109	492	< 0.01
145	0	0.0	4.54	2.8	0.0	5.0	2	4.98	1	2	< 0.01
151	0	1.1	5.08	2.3	0.2	3.9	3	6.60	0	0	< 0.01

Notes: 1. Test conducted in Laboratory B, 2. Test conducted in Laboratory C, nt = not tested.

Table 4-47: Corrosion tests varying fluoride in deionized water at 45°C– Cessation concentrations

Run	Target fluoride (mg/l as F ⁻)	Test solution concentrations at cessation of corrosion tests									
		Fluoride (25x diln) ⁽¹⁾ (mg/l as F ⁻)	pH ⁽¹⁾	Calcium ⁽²⁾ (mg/l as Ca ²⁺)	Magnesium ⁽²⁾ (mg/l as Mg ²⁺)	Total alkalinity ⁽¹⁾ (mg/l as CaCO ₃)	Chloride ⁽²⁾ (mg/l as Cl ⁻)	Sulphate (25x diln) ⁽²⁾ (mg/l as SO ₄ ²⁻)	Sodium ⁽²⁾ (mg/l as Na ⁺)	Conductivity ⁽¹⁾ (µS/cm)	Total iron ⁽¹⁾ (mg/l as Fe ³⁺ (total))
115	0	1.3	4.87	1.1	nt	1.4	nt	nt	nt	10	5.7
116	10	8.0	5.67	0.4	nt	2.9	nt	nt	nt	67	7.3
117	20	18.1	6.32	0.6	nt	5.0	nt	nt	nt	126	8.5
118	40	38.4	6.52	0.8	nt	8.5	nt	nt	nt	242	13.6
119	70	70.3	5.92	0.6	nt	11.8	nt	nt	nt	405	16.7
120	90	100.0	6.12	0.4	nt	16.4	nt	nt	nt	554	13.8
127	0	3.9	6.00	1.4	nt	0.0	nt	nt	nt	12	7.0
128	10	10.5	6.63	2.0	nt	16.3	nt	nt	nt	396	6.9
129	20	nt	6.30	nt	nt	8.6	nt	nt	nt	124	24.6
130	40	42.0	6.44	1.8	nt	13.2	nt	nt	nt	240	19.2
131	70	68.5	6.23	1.1	nt	18.8	nt	nt	nt	392	25.3
132	90	94.4	5.95	1.0	nt	23.8	nt	nt	nt	544	17.5
133	0	2.9	5.82	1.1	0.1	9.3	3	6.68	1	0	5.1
134	10	10.9	5.47	2.2	0.1	9.1	3	6.00	12	56	2.3
135	20	25.3	5.25	0.6	0.1	11.3	3	6.12	25	116	4.5
136	40	41.6	5.04	2.7	0.1	20.1	3	6.08	51	120	5.2
137	70	68.2	5.38	1.0	0.1	20.8	3	6.03	90	404	7.9
138	90	91.2	5.34	0.5	0.1	27.2	3	5.94	127	556	16.6
139	0	0.0	6.59	0.7	0.1	8.7	1	5.60	2	12	9.1
140	10	9.4	6.10	0.5	0.1	6.7	4	5.25	11	64	10.8
141	20	18.0	6.41	0.5	0.1	8.7	4	5.25	22	116	17.0
142	40	32.2	6.25	1.3	0.1	11.2	4	5.25	45	224	17.1
143	70	70.2	6.31	0.7	0.1	22.4	4	5.25	84	384	20.4
144	90	96.2	6.32	0.7	0.1	20.2	4	5.25	116	532	18.5
145	0	12.2	5.94	0.6	0.2	3.9	2	5.30	3	20	6.7
151	0	1.3	5.52	2.4	0.2	4.2	4	7.39	2	48	10.6

Table 4-48: Corrosion coupon results while varying the fluoride concentration in deionized water

Run	Target fluoride (mg/l as F ⁻)	Corrosion Coupon Results		
		Coupon 1	Coupon 2	Average
		mmpa	mmpa	mmpa
115	0	0.56	0.58	0.57
116	10	0.50	0.55	0.53
117	20	0.60	0.62	0.61
118	40	0.57	0.58	0.57
119	70	0.72	0.71	0.71
120	90	0.56	0.59	0.58
127	0	0.57	0.61	0.59
128	10	0.62	0.63	0.63
129	20	0.55	0.65	0.60
130	40	0.55	0.58	0.57
131	70	0.69	0.72	0.71
132	90	0.70	0.65	0.67
133	0	0.26	0.34	0.30
134	10	0.57	0.54	0.55
135	20	0.63	0.62	0.62
136	40	0.54	0.59	0.57
137	70	0.68	0.65	0.66
138	90	0.64	0.72	0.68
139	0	0.41	0.42	0.41
140	10	0.56	0.56	0.56
141	20	0.58	0.58	0.58
142	40	0.62	0.57	0.59
143	70	0.71	0.73	0.72
144	90	0.61	0.65	0.63
145	0	0.31	0.29	0.30
151	0	0.47	0.46	0.46

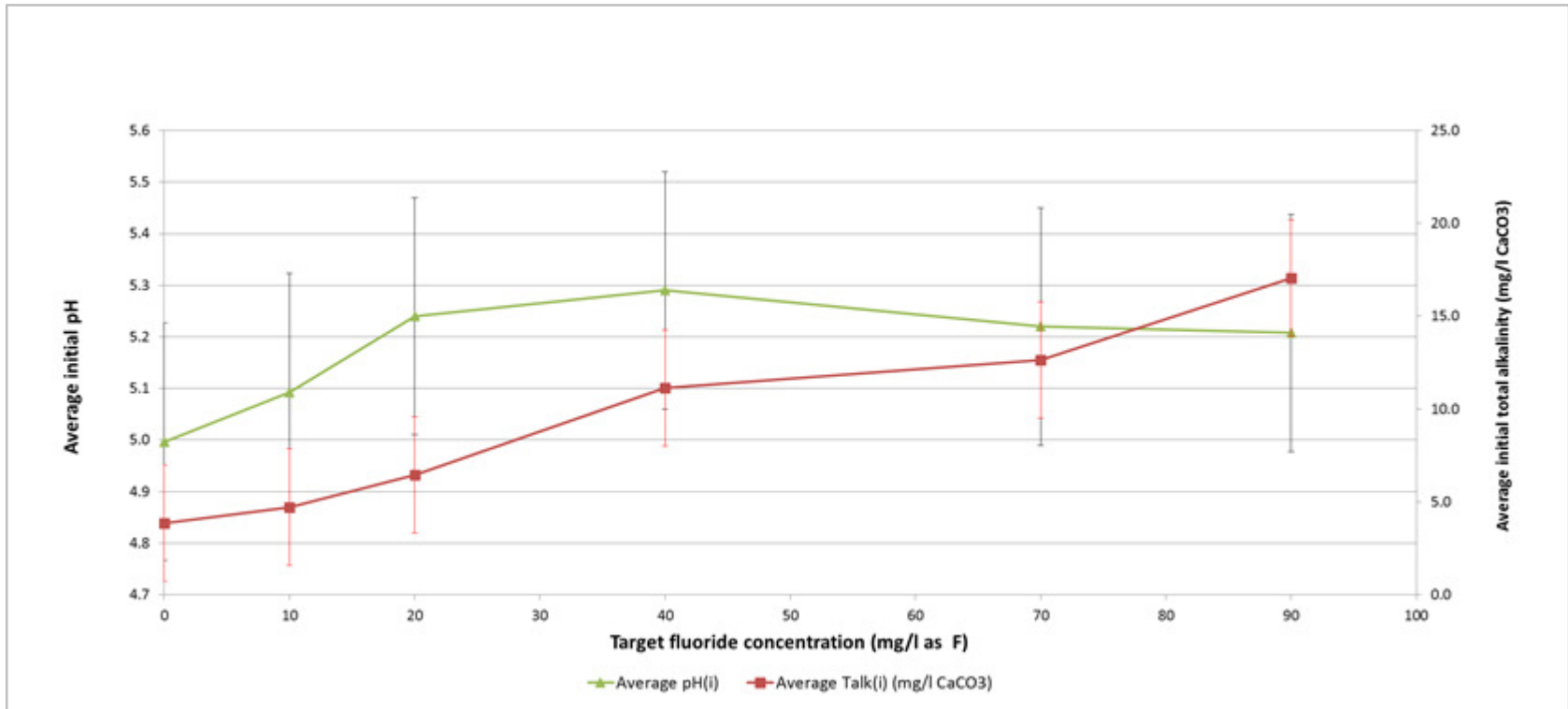


Figure 4-49: Average initial pH (pH(i)) and average initial total alkalinity (T alk(i)) versus the target fluoride concentration (Tgt F), at 45°C. Error bars: ± 0.23 pH and ± 3.13 mg/l CaCO₃

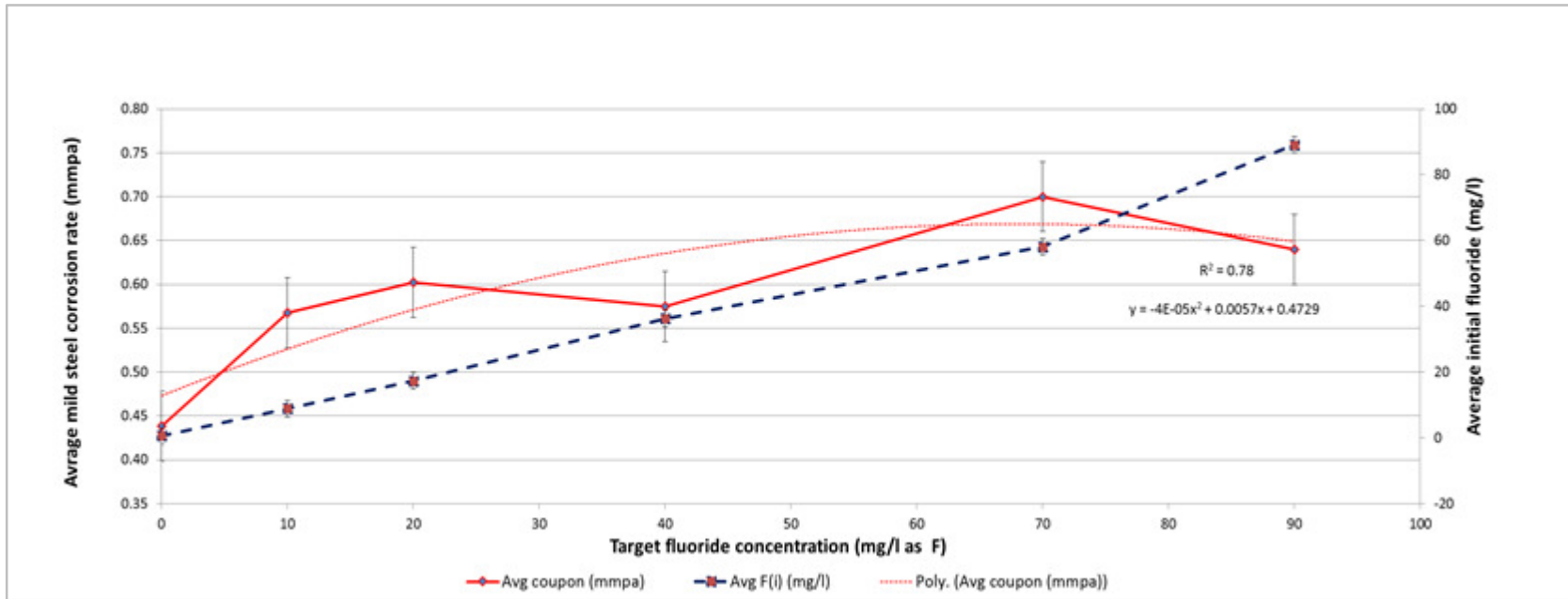


Figure 4-50: Average mild steel corrosion rate (Avg Coup) and average initial fluoride (F(i)) versus the target fluoride concentration (Tgt F), at 45°C. Error bars: ± 0.04 mmpa and ± 2.5 mg/l F

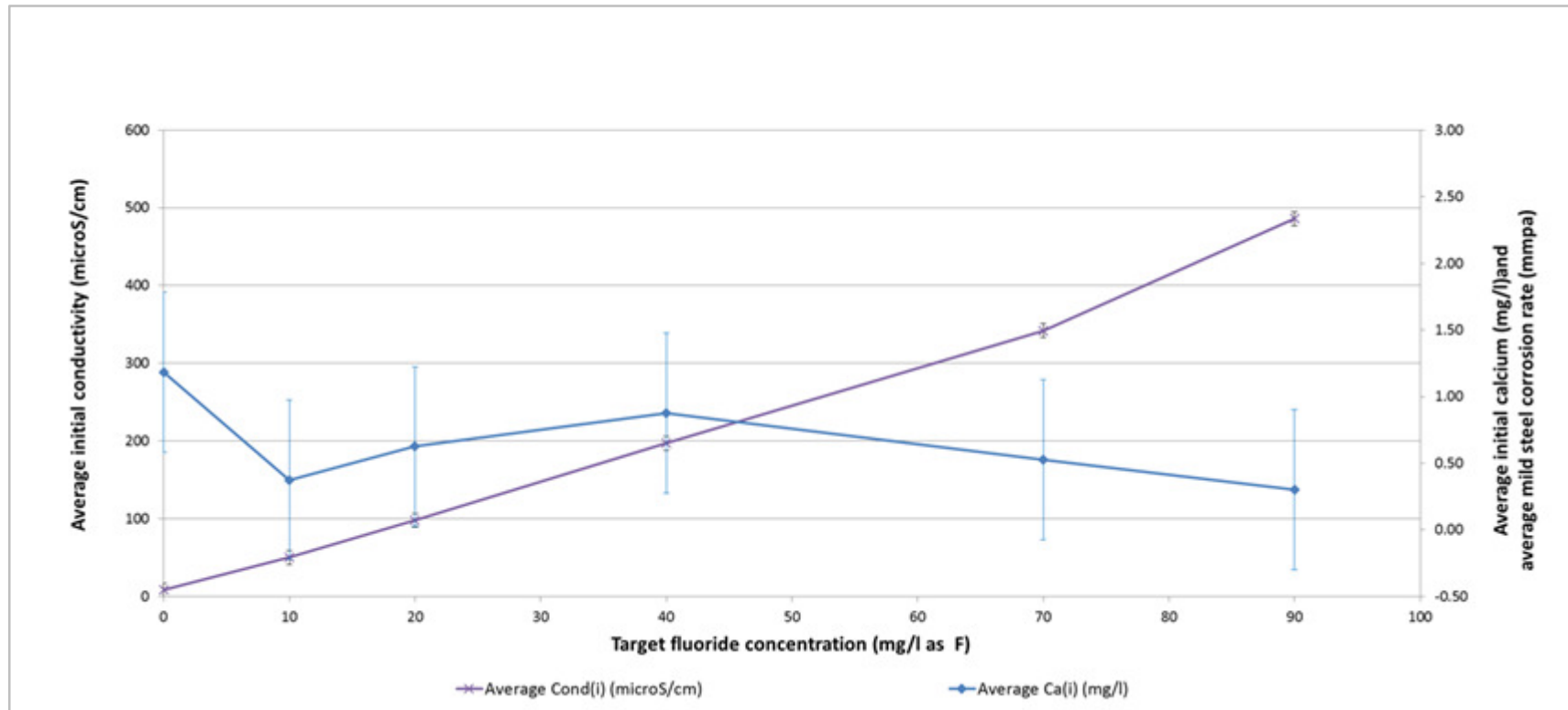


Figure 4-51: Average initial calcium (Ca(i)) and average initial conductivity (Cond(i)) versus the target fluoride concentration (Tgt F), at 45°C. Error bars: ± 0.60 mg/l Ca^{2+} and ± 9 $\mu\text{S/cm}$

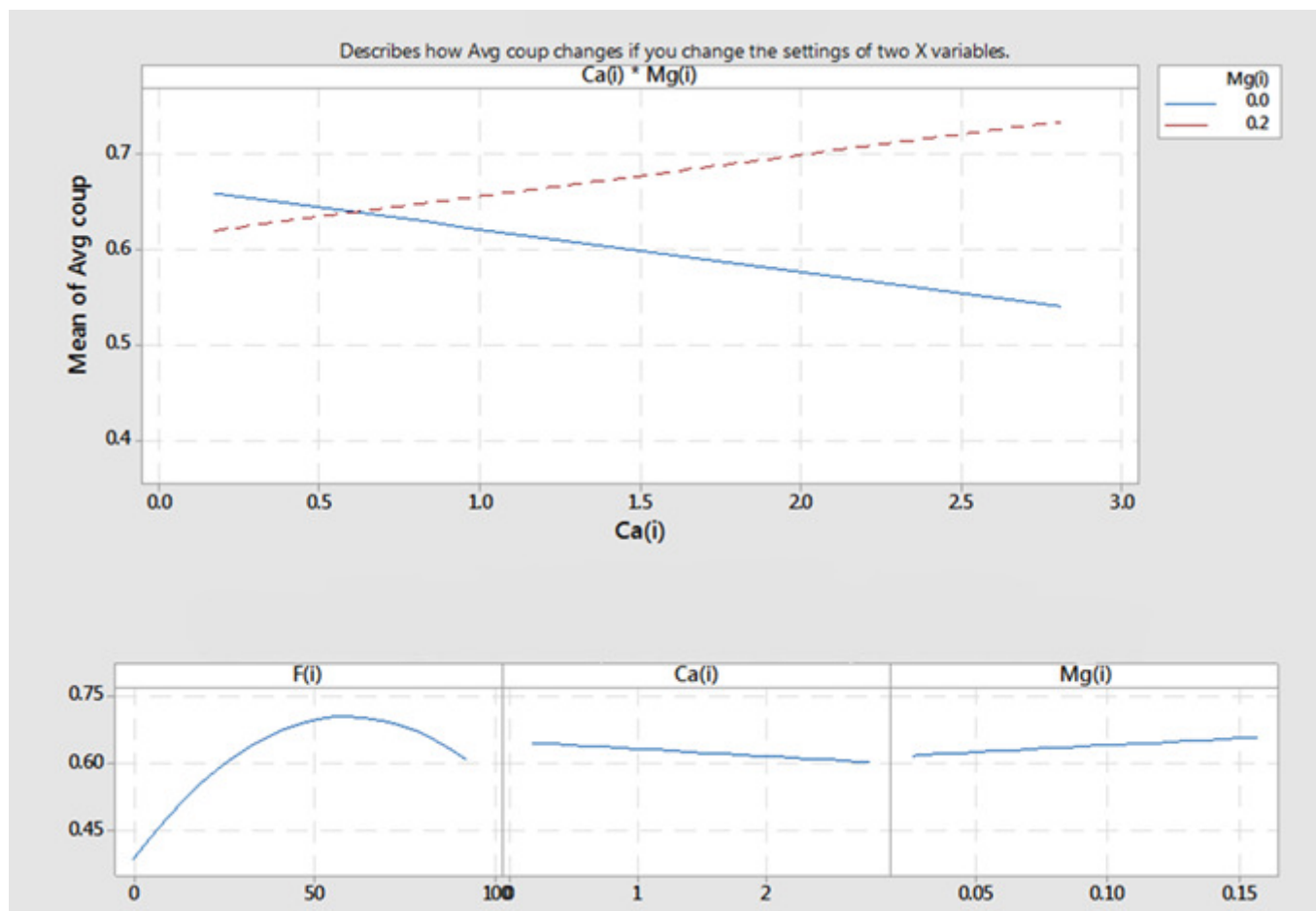


Figure 4-52: Interaction plot demonstrating the effects of the initial calcium (Ca(i)) and initial magnesium (Mg(i)) and initial fluoride (F(i)) on the average corrosion rate (Avg Coup)

A significant finding was that the addition of sodium fluoride produced a significantly elevated alkalinity, conductivity and coupon corrosion rates. The coupon corrosion rate increased dramatically between 0 and 20 mg/l fluoride and then appeared to plateau at a target fluoride concentration of approximately 78 mg/l.

At the higher sodium fluoride concentrations, the calcium and magnesium levels became confined to narrower bands at the lower ends of the ranges of values obtained where deionized water alone was used. This may have been due to trace quantities of calcium fluoride precipitation, as indicated by the slightly diminished fluoride levels, especially at the 70 mg/l target fluoride concentration. A quadratic model with R^2 equal to 78% was obtained for the correlation between the average corrosion rate (in mmpa) and the initial fluoride concentration (in mg/l as F^-). The accuracy of a quadratic model was however questionable at the 90 mg/l target fluoride concentration due to the minimal number of data points in this part of the graph. Although a more accurate model was obtained where the initial calcium and initial magnesium were included as input variables (R^2 equal to 85%), it was uncertain at this point whether these two parameters merely reflected the impact of the fluoride concentration or did indeed directly influence the coupon corrosion rate.

A comparison of the linear correlations for the average corrosion rate versus the initial sodium, initial fluoride, initial total alkalinity and initial conductivity demonstrated that the strongest correlation was with the initial sodium concentration. Multiple regression analyses based on the initial calcium, initial magnesium and initial fluoride concentration produced a higher R^2 value than for the models that employed either the initial sodium, initial alkalinity or initial conductivity in place of the initial fluoride concentration.

4.8.2 Series 2 - Low alkalinity

Sodium fluoride was added to deionized water with a target total alkalinity of 55 mg/l (as $CaCO_3$) at the concentrations given in Table 4-49 and the results of the water analyses shown in Table 4-50, along with the coupon corrosion rates in Table

4-51. The purpose of this series was to investigate the impact of low total alkalinity together while varying the fluoride concentration between 0 and 90 mg/l.

As apparent in Figure 4-53, the addition of sodium fluoride to deionized water with a total alkalinity of 55 mg/l CaCO_3 resulted in the following trends. The initial fluoride concentration correlated very closely with the target fluoride concentration and the initial conductivity. Both the initial and final pH values were not deemed to have undergone any significant changes whereas the initial and final calcium hardness values decreased from their starting trace quantities upon reaching an initial fluoride concentration of approximately 40 mg/l (as F^-). Although the initial and final alkalinities were first observed to increase, for the initial fluoride concentrations of up to approximately 50 mg/l, they both then remained relatively constant with continued fluoride addition. The average corrosion rate decreased with the increased initial fluoride concentration.

Figure 4-54, a Minitab[®] regression summary report for the average corrosion rate versus the initial fluoride concentration, indicated a statistically significant weak negative linear relationship between the corrosion rate and sodium fluoride concentration. Due to the limited sample size ($n = 18$), it was not possible to provide a very precise estimate of the strength of the relationship. An R^2 of 38% was obtained. Regression analyses performed with: conductivity, sodium and total alkalinity alone, gave the following sequence in terms of the R^2 values: total alkalinity (47%) > conductivity (36%) and sodium (36%).

Table 4-49: Corrosion tests varying fluoride in low alkalinity water at 45°C – Target and start-up concentrations

Run	Target fluoride (mg/l as F ⁻)	Test solution concentrations at start-up									
		Fluoride (25x diln) ⁽¹⁾ (mg/l as F ⁻)	pH ⁽¹⁾	Calcium ⁽²⁾ (mg/l as Ca ²⁺)	Magnesium ⁽²⁾ (mg/l as Mg ²⁺)	Total alkalinity ⁽¹⁾ (mg/l as CaCO ₃)	Chloride ⁽²⁾ (mg/l as Cl ⁻)	Sulphate (25x diln) ⁽²⁾ (mg/l as SO ₄ ²⁻)	Sodium ⁽²⁾ (mg/l as Na ⁺)	Conductivity ⁽¹⁾ (µS/cm)	Total iron ⁽¹⁾ (mg/l as Fe ³⁺ (total))
157	0	0.0	7.99	0.4	0.1	64.6	3	6.44	28	164	< 0.01
158	10	11.0	8.10	0.4	0.1	64.2	3	6.50	37	164	< 0.01
159	20	20.5	7.98	0.4	0.1	69.8	3	6.63	48	216	< 0.01
160	40	36.7	7.92	0.6	0.1	77.9	3	6.49	68	304	< 0.01
161	70	62.9	8.00	0.6	0.1	65.1	3	6.47	100	448	< 0.01
162	90	89.5	7.97	0.4	0.1	70.8	3	6.49	123	556	< 0.01
163	0	0.0	8.16	0.6	0.2	62.6	2	7.47	20	108	< 0.01
164	10	9.5	8.11	0.8	0.2	63.0	2	7.45	32	156	< 0.01
165	20	20.2	8.08	0.7	0.1	65.9	3	7.45	44	216	< 0.01
166	40	37.8	8.10	0.6	0.2	79.0	2	7.46	67	316	< 0.01
167	70	61.6	8.11	0.6	0.2	70.5	2	7.44	99	468	< 0.01
168	90	77.5	8.03	0.5	0.1	72.1	2	7.39	120	564	< 0.01
169	0	0.6	8.14	1.0	0.2	63.7	3	7.36	27	108	< 0.01
170	10	9.5	8.10	0.9	0.2	66.3	3	6.12	38	156	< 0.01
171	20	20.3	8.04	0.7	0.2	67.7	4	6.18	51	212	< 0.01
172	40	40.7	8.02	1.1	0.2	83.8	3	6.46	74	312	< 0.01
173	70	64.1	8.08	0.5	0.1	73.7	3	6.15	109	464	< 0.01
174	90	79.5	8.10	0.4	0.1	74.7	3	5.95	132	556	< 0.01

Notes: 1. Test conducted in Laboratory B, 2. Test conducted in Laboratory C, nt = not tested.

Table 4-50: Corrosion tests varying fluoride in low alkalinity water at 45°C – Cessation concentrations

Run	Target fluoride (mg/l as F ⁻)	Test solution concentrations at cessation of corrosion tests									
		Fluoride (25x diln) ⁽¹⁾ (mg/l as F ⁻)	pH ⁽¹⁾	Calcium ⁽²⁾ (mg/l as Ca ²⁺)	Magnesium ⁽²⁾ (mg/l as Mg ²⁺)	Total alkalinity ⁽¹⁾ (mg/l as CaCO ₃)	Chloride ⁽²⁾ (mg/l as Cl ⁻)	Sulphate (25x diln) ⁽²⁾ (mg/l as SO ₄ ²⁻)	Sodium ⁽²⁾ (mg/l as Na ⁺)	Conductivity ⁽¹⁾ (µS/cm)	Total iron ⁽¹⁾ (mg/l as Fe ³⁺ (total))
157	0	0.0	8.25	0.6	0.1	60.2	3	6.68	25	104	17.7
158	10	8.4	8.39	0.6	0.1	69.9	3	6.48	41	176	15.4
159	20	18.4	8.42	0.7	0.2	72.1	3	6.49	52	232	17.2
160	40	35.4	8.32	1.3	0.2	66.3	3	6.54	72	328	9.4
161	70	65.9	8.37	0.8	0.2	72.2	3	6.55	105	488	11.9
162	90	90.9	8.33	0.6	0.2	75.9	3	6.52	131	588	8.3
163	0	0.0	8.40	1.0	0.2	82.0	3	7.83	24	232	17.7
164	10	10.3	8.42	0.9	0.2	65.4	3	7.54	34	172	15.8
165	20	20.8	8.38	0.8	0.1	70.8	3	7.63	46	232	16.1
166	40	39.7	8.36	1.3	0.2	91.7	3	7.58	69	340	10.7
167	70	65.9	8.46	1.0	0.2	77.0	3	7.61	107	512	21.2
168	90	81.9	8.43	0.7	0.1	78.0	3	7.50	128	600	12.0
169	0	0.4	8.54	1.1	0.2	68.7	4	6.28	30	140	26.4
170	10	11.0	8.50	0.8	0.2	70.8	4	6.36	42	180	31.2
171	20	24.5	8.44	0.6	0.1	79.1	4	6.51	57	248	28.0
172	40	42.9	8.38	1.1	0.2	93.7	3	6.16	82	356	17.6
173	70	68.5	8.51	0.6	0.1	80.6	4	6.13	117	512	25.1
174	90	83.0	8.45	0.5	0.1	81.6	3	6.08	140	604	13.3

Table 4-51: Corrosion coupon readings while varying fluoride in low alkalinity water at 45°C

Run	Target fluoride (mg/l as F ⁻)	Corrosion Coupon Results		
		Coupon 1 (mmpa)	Coupon 2 (mmpa)	Average (mmpa)
157	0	0.84	0.83	0.84
158	10	0.75	0.76	0.75
159	20	0.81	0.81	0.72
160	40	0.69	0.68	0.78
161	70	0.78	0.79	0.78
162	90	0.63	0.66	0.65
163	0	0.72	0.80	0.76
164	10	0.64	0.74	0.69
165	20	0.87	0.84	0.85
166	40	0.65	0.62	0.64
167	70	0.70	0.63	0.66
168	90	0.63	0.67	0.65
169	0	0.80	0.82	0.81
170	10	0.74	0.79	0.77
171	20	0.88	0.79	0.83
172	40	0.61	0.66	0.63
173	70	0.79	0.70	0.75
174	90	0.67	0.67	0.67

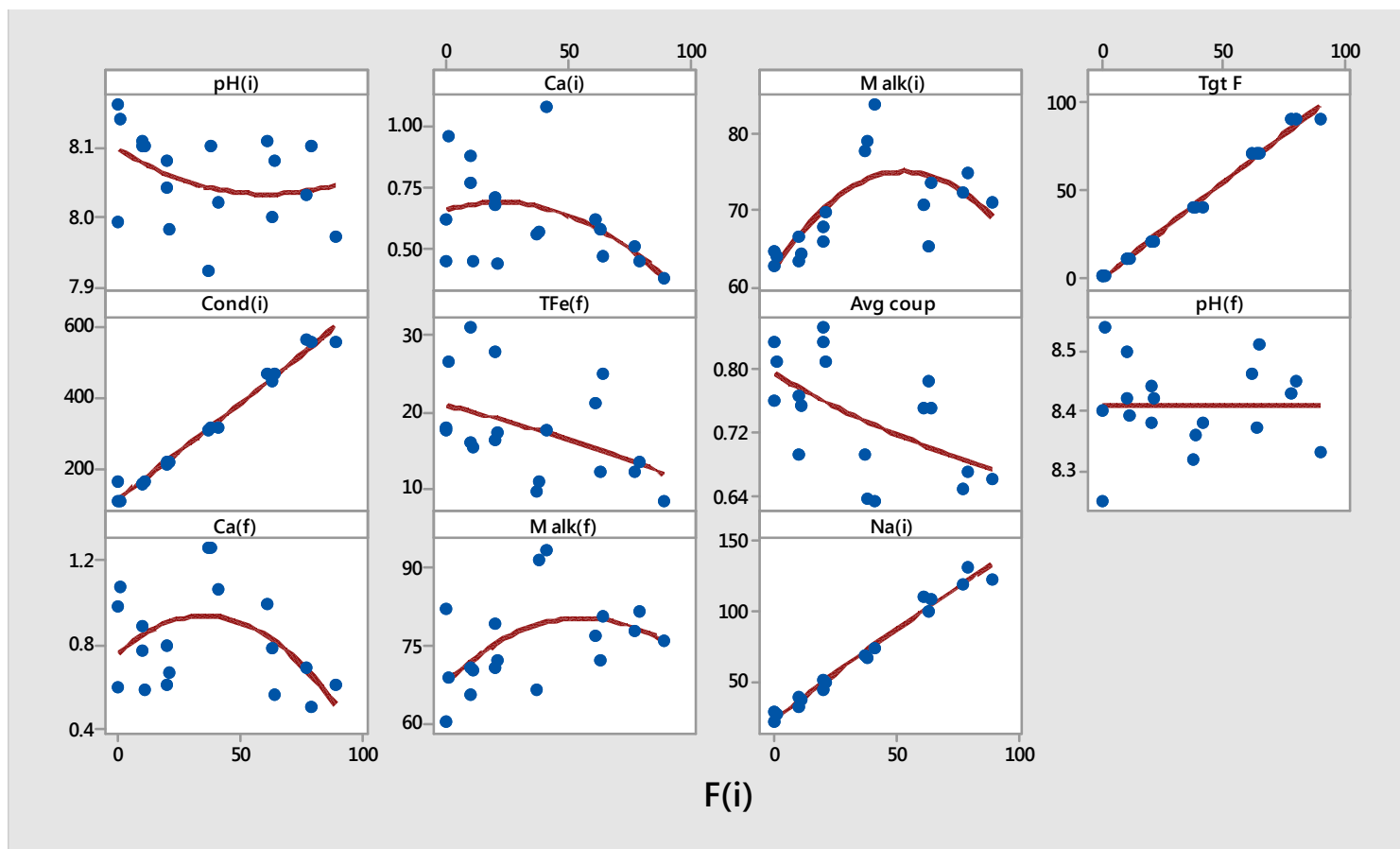


Figure 4-53: Scatterplots of the key variables versus the initial fluoride concentration ($F(i)$) at a total alkalinity of 55 mg/l as CaCO_3

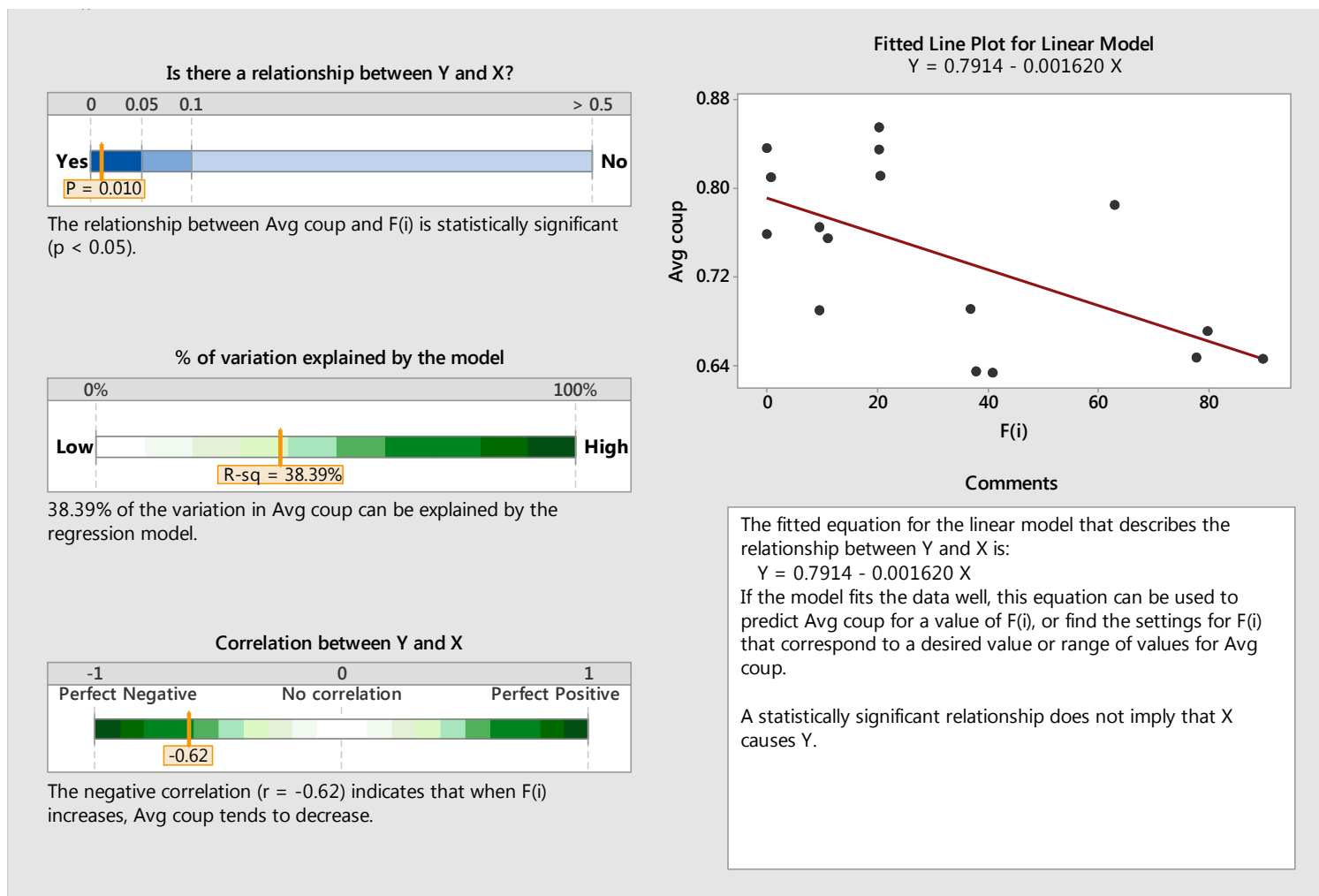


Figure 4-54: Regression summary report of the average corrosion rate (Avg coup) versus the initial fluoride concentration (F(i)) for a total alkalinity of 55 mg/l as CaCO_3

In view of the impact the sodium fluoride addition had on the total alkalinity and the strong correlation between the sodium fluoride addition and the conductivity it was decided to compare the following regression models: a) fluoride and total alkalinity versus b) conductivity and total alkalinity versus c) sodium and total alkalinity. The three models and their R^2 values are given in Equations 4.10 to 4-12.

Fluoride and total alkalinity model ($R^2 = 79.73\%$, $R^2(\text{adj}) = 74\%$):

$$\begin{aligned} \text{Average corrosion rate} = & 1.472 + 0.00276 \times F(i) - 0.01060 \times M \text{ alk}(i) \\ & - 0.000041 \times F(i)^2 \dots\dots\dots[4.10] \end{aligned}$$

Conductivity and total alkalinity model ($R^2 = 82\%$, $R^2(\text{adj}) = 76\%$):

$$\begin{aligned} \text{Average corrosion rate} = & 1.403 + 0.001065 \times \text{Cond}(i) - 0.01119 \times M \text{ alk}(i) \\ & - 0.000002 \times \text{Cond}(i)^2 \dots\dots\dots[4.11] \end{aligned}$$

where: Average coupon corrosion rate is in millimetres per annum (mmpa),
 $\text{Cond}(i)$ = initial conductivity ($\mu\text{S}/\text{cm}$).

Sodium and total alkalinity model ($R^2 = 76\%$, $R^2(\text{adj}) = 70\%$):

$$\begin{aligned} \text{Average corrosion rate} = & 1.378 + 0.00297 \times \text{Na}(i) - 0.01002 \times M \text{ alk}(i) \\ & - 0.000023 \times \text{Na}(i)^2 \dots\dots\dots[4.12] \end{aligned}$$

where: Average coupon corrosion rate is in millimetres per annum (mmpa),
 $\text{Na}(i)$ = initial calcium (mg/l as Na^+).

The conductivity-total alkalinity model produced a marginally superior data fit to the fluoride-total alkalinity and sodium-total alkalinity based models.

The addition of sodium fluoride to (deionized) water with a total alkalinity of 55 mg/l CaCO_3 resulted in a reduced corrosion rate, but with only a weak correlation with the fluoride concentration, as indicated by a relatively low R^2 of 38%. Regression analyses performed according to conductivity, sodium and total

alkalinity alone, gave the following sequence in terms of the R^2 values: total alkalinity (47%) > conductivity (36%) and sodium (36%).

The total alkalinity correlated with the increasing fluoride concentration up to a fluoride concentration of approximately 50 mg/l F^- and thereafter it experienced a significant decline. The initial increase in alkalinity was associated with the addition of the sodium fluoride but at greater than 50 mg/l fluoride the higher residual alkalinities were thought to have reacted with the soluble calcium concentration to consequently precipitate calcium carbonate. Calcium carbonate precipitation was not reported, but owing to the low calcium levels the amount of precipitate may not have been noticed. If there had been sufficient calcium in solution, there would have been a higher tendency for calcium fluoride to precipitate prior to calcium carbonate due to the known lower solubility of the latter. The solubility product constants for calcium carbonate and calcium fluoride, at near room temperature, are 8.7×10^{-9} and 4.0×10^{-11} respectively (Benfield and Morgan, 1990). A possible exception to this sequence could occur if the pH escalated to values high enough (>10) to first precipitate calcium carbonate. Such a condition could have manifested at the cathodic sites on the corroding coupon at sufficiently high corrosion rates. Further research or experimentation would be necessary to confirm this phenomenon. The subsequent reduction in both the calcium concentration and total alkalinity diminished the continued decrease in corrosion with increased sodium fluoride addition.

A comparison of three regression models confirmed the superior fit of the conductivity-alkalinity based model (Equation 4.11) (R^2 (adj) = 76%) over the fluoride-alkalinity (Equation 4.10) (R^2 (adj) = 74%) and sodium-alkalinity (Equation 4.12) (R^2 (adj) = 70%) based models at predicting the corrosivity of fluoride addition on mild steel in low alkalinity, at 45°C.

At this juncture, based on the known facts of this sub-section and the previous sub-section, it remained uncertain whether the fluoride is directly responsible for the

increased mild steel corrosion rates because of the comparable sodium ion and electrical conductivity based models.

4.8.3 Series 3 - High alkalinity

Sodium fluoride was added to deionized water with a targeted total alkalinity of 220 mg/l (as CaCO₃), at the concentrations given in Table 2-52. The results of the water analyses were shown in Table 2-53, along with the coupon corrosion rates in Table 2-54.

As apparent in Figure 4-55, there appeared a significant amount of grouping of the data, so it became necessary to distinguish the two groups by using pink triangular markers for the set of data with the distinctly higher pH values. As apparent in Figure 4-55, the lower pH related data set (i.e. < pH 9.0) were more closely correlated in terms of both their water chemistry parameters and the mild steel corrosion rates, so it was decided to only analyse the lower pH group of data. The higher pH data set did however produce comparable mild steel coupon corrosion rates to the two sets pertaining to the lower pH group of data. Based on this lower pH group of data, it was found that the regression for the average corrosion rate (Avg coup) versus the initial fluoride concentration (F(i)) was approximately similar to the low total alkalinity test work performed in the series 2, and again a statistically significant quadratic equation was produced as the best fit (R^2 (adj) of 57%). Figure 4-56 shows the regression analysis of the average coupon corrosion rate versus the initial fluoride concentration performed with all three data sets. Figure 4-57 is a repeat of the scatterplots of the key variables versus the initial fluoride concentration for only the high pH group showing slightly altered water chemistry trends when compared to Figure 4-55, due to the absence of the higher pH data set. Equations 4.13 and 4.14 were produced for this lower pH subset.

Conductivity and pH model ($R^2 = 83\%$):

$$\begin{aligned} \text{Average corrosion rate} = & 35.74 - 0.0652 \times \text{Cond(i)} - 4.06 \times \text{pH(i)} + 0.00760 \times \\ & \text{Cond(i)} \times \text{pH(i)} \dots \dots \dots [4.13] \end{aligned}$$

Conductivity, pH and fluoride model ($R^2 = 96\%$):

$$\begin{aligned} \text{Average corrosion rate} = & -2546 - 0.790 \times \text{Cond}(i) + 627 \times \text{pH}(i) + 3.796 \times \\ & \text{F}(i) - 38.4 \times \text{pH}(i)^2 + 0.0918 \times \text{Cond}(i) \times \text{pH}(i) - 0.441 \times \text{pH}(i) \times \\ & \text{F}(i) \dots\dots\dots [4.14] \end{aligned}$$

Regression models based only on conductivity and total alkalinity or only on fluoride and total alkalinity were less appropriate to the above two equations, only having produced R^2 values $< 66\%$. Regression models with only conductivity, sodium, total alkalinity and pH revealed that the relationship with the total alkalinity was not statistically significant and of the remaining variables the conductivity produced the strongest correlation ($R^2 = 62\%$), followed by sodium ($R^2 = 38\%$), and pH ($R^2 = 3\%$). The best fit regression model for this set with fluoride added to water with 220 mg/l total alkalinity was Equation 4.14.

No regression was possible with the higher pH group alone (pink triangular symbols in Figure 4-55) due to insufficient data. What was revealed regarding this high pH group was that the entire set of results were from a batch of tests that had unknowingly prepared with a slightly higher pH and lower calcium hardness deionised water. It is anticipated that this lower quality deionised water affected the outcome of this batch of tests.

Figure 4-56 presents an enlarged view of the impact of the initial fluoride concentration on the average corrosion rate of all three data sets reported on in Tables 4-52 and 4-54 showing the quadratic model as the best fit. In Figure 4-57 the high pH data set was excluded in order to permit for a comparison of the scatterplots versus that of Figure 4-55. The most noticeable differences were between the initial and final pH and total alkalinity curves of the two scatterplots.

Table 4-52: Corrosion tests varying fluoride in high alkalinity water at 45°C – Target and start-up concentrations

Run	Target fluoride (mg/l as F ⁻)	Test solution concentrations at start-up									
		Fluoride (25x diln) ⁽¹⁾ (mg/l as F ⁻)	pH ⁽¹⁾	Calcium ⁽²⁾ (mg/l as Ca ²⁺)	Magnesium ⁽²⁾ (mg/l as Mg ²⁺)	Total alkalinity ⁽¹⁾ (mg/l as CaCO ₃)	Chloride ⁽²⁾ (mg/l as Cl ⁻)	Sulphate (25x diln) ⁽²⁾ (mg/l as SO ₄ ²⁻)	Sodium ⁽²⁾ (mg/l as Na ⁺)	Conductivity ⁽¹⁾ (µS/cm)	Total iron ⁽¹⁾ (mg/l as Fe ³⁺ (total))
175	0	0.9	8.63	2.3	0.2	234.8	4	5.93	100	412	< 0.01
176	10	10.8	8.61	0.6	0.2	249.9	4	7.97	111	452	< 0.01
177	20	22.1	8.61	0.9	0.2	229.3	4	7.88	119	496	< 0.01
178	40	40.1	8.62	3.1	0.2	227.8	4	7.75	140	588	< 0.01
179	70	74.9	8.58	0.6	0.2	229.4	4	8.22	174	732	< 0.01
180	90	90.6	8.56	0.6	0.2	235.3	4	7.74	197	828	< 0.01
181	0	0.0	8.69	0.6	0.2	230.0	3	7.85	99	408	< 0.01
182	10	10.0	8.69	0.6	0.2	248.0	3	6.48	112	464	< 0.01
183	20	20.7	8.68	0.7	0.2	234.0	3	6.46	125	520	< 0.01
184	40	40.5	8.67	0.5	0.2	234.0	3	6.45	148	608	< 0.01
185	70	68.9	8.65	0.5	0.2	233.5	3	7.84	183	752	< 0.01
186	90	83.5	8.60	0.5	0.1	228.3	3	6.26	205	840	< 0.01
187	0	0.0	9.16	0.3	0.1	265.6	4	6.06	104	456	< 0.01
188	10	11.7	9.14	0.5	0.1	272.4	4	1.12	117	508	< 0.01
189	20	23.1	9.15	0.3	0.1	259.9	4	1.09	128	560	< 0.01
190	40	45.0	9.09	0.2	0.1	258.1	4	1.09	149	652	< 0.01
191	70	74.8	9.15	0.4	0.1	267.9	4	1.10	185	836	< 0.01
192	90	96.3	9.11	0.4	0.2	266.3	4	1.06	208	924	< 0.01

Notes: 1. Test conducted in Laboratory B, 2. Test conducted in Laboratory C, nt = not tested.

Table 4-53: Corrosion tests varying fluoride in low alkalinity water at 45°C –
Cessation concentrations

Run	Target fluoride (mg/l as F ⁻)	Test solution concentrations at cessation of corrosion tests									
		Fluoride (25x diln) ⁽¹⁾ (mg/l as F ⁻)	pH ⁽¹⁾	Calcium ⁽²⁾ (mg/l as Ca ²⁺)	Magnesium ⁽²⁾ (mg/l as Mg ²⁺)	Total alkalinity ⁽¹⁾ (mg/l as CaCO ₃)	Chloride ⁽²⁾ (mg/l as Cl ⁻)	Sulphate (25x diln) ⁽²⁾ (mg/l as SO ₄ ²⁻)	Sodium ⁽²⁾ (mg/l as Na ⁺)	Conductivity ⁽¹⁾ (µS/cm)	Total iron ⁽¹⁾ (mg/l as Fe ³⁺ (total))
175	0	0.4	9.15	2.0	0.2	274.5	4	8.08	113	536	24.1
176	10	0.0	9.12	2.3	0.2	285.2	2	6.63	123	524	21.6
177	20	25.4	9.12	2.1	0.2	257.2	4	8.22	134	572	23.6
178	40	45.5	9.06	1.9	0.3	256.1	4	8.35	154	664	18.3
179	70	79.2	9.12	2.5	0.2	264.6	5	8.24	203	860	23.9
180	90	94.0	9.07	1.9	0.2	265.6	4	8.00	222	952	18.4
181	0	0.0	9.11	0.9	0.2	292.1	4	6.50	119	532	21.3
182	10	11.0	9.11	0.9	0.2	289.9	4	6.67	131	544	21.0
183	20	22.2	9.13	1.0	0.2	270.9	4	6.66	146	604	23.7
184	40	44.2	9.09	1.3	0.2	265.0	3	6.38	169	704	23.1
185	70	72.1	9.15	0.9	0.2	275.0	3	6.40	219	892	23.0
186	90	108.0	9.11	0.8	0.2	262.1	4	1.10	240	976	22.6
187	0	0.0	8.67	0.7	0.2	230.7	4	1.32	119	392	19.3
188	10	12.0	8.67	0.5	0.2	239.4	4	1.14	129	440	20.0
189	20	26.8	8.67	0.5	0.2	228.6	4	1.15	140	480	20.8
190	40	59.1	8.65	1.1	0.2	230.2	3	1.07	164	580	23.5
191	70	77.8	8.63	0.8	0.2	231.1	4	1.14	210	716	19.2
192	90	102.0	8.60	0.6	0.2	230.2	4	1.13	233	796	22.2

Table 4-54: Corrosion coupon readings while varying fluoride in high alkalinity water at 45°C

Run	Target fluoride (mg/l as F ⁻)	Corrosion Coupon Results		
		Coupon 1 (mmpa)	Coupon 2 (mmpa)	Average (mmpa)
175	0	0.81	0.93	0.87
176	10	0.85	0.90	0.88
177	20	0.88	0.93	0.91
178	40	0.88	0.93	0.91
179	70	0.96	1.03	1.00
180	90	0.84	0.88	0.86
181	0	0.78	0.80	0.79
182	10	0.78	0.95	0.86
183	20	0.96	0.91	0.94
184	40	0.96	0.94	0.95
185	70	1.04	1.05	1.04
186	90	0.93	0.99	0.96
187	0	0.83	0.83	0.83
188	10	0.87	1.01	0.94
189	20	0.97	1.00	0.99
190	40	0.98	0.95	0.96
191	70	1.06	1.05	1.06
192	90	0.90	0.95	0.93

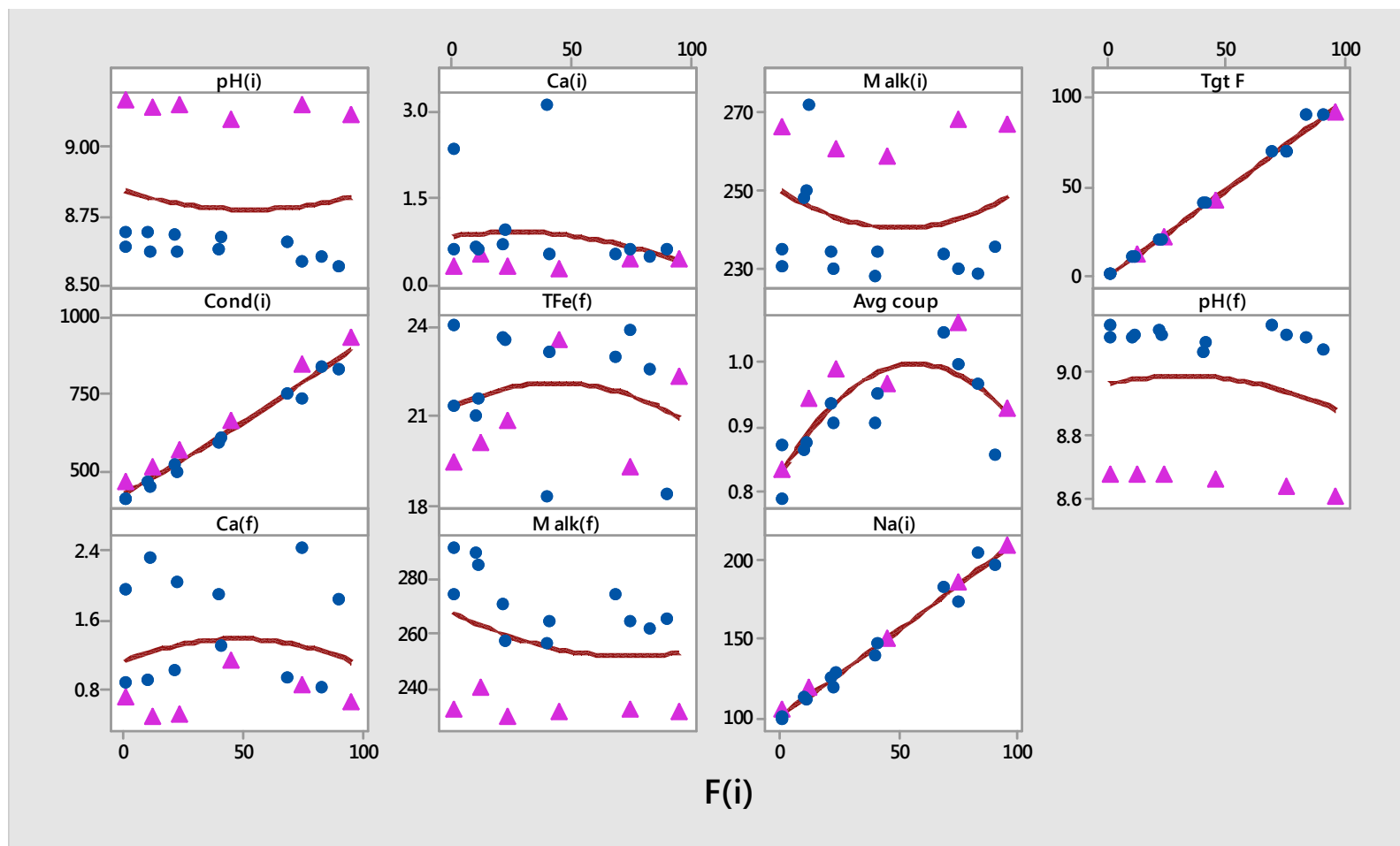


Figure 4-55: Scatterplots of the key variables versus the initial fluoride concentration ($F(i)$) at a total alkalinity of 220 mg/l as CaCO_3 . The triangles represent a high pH data set

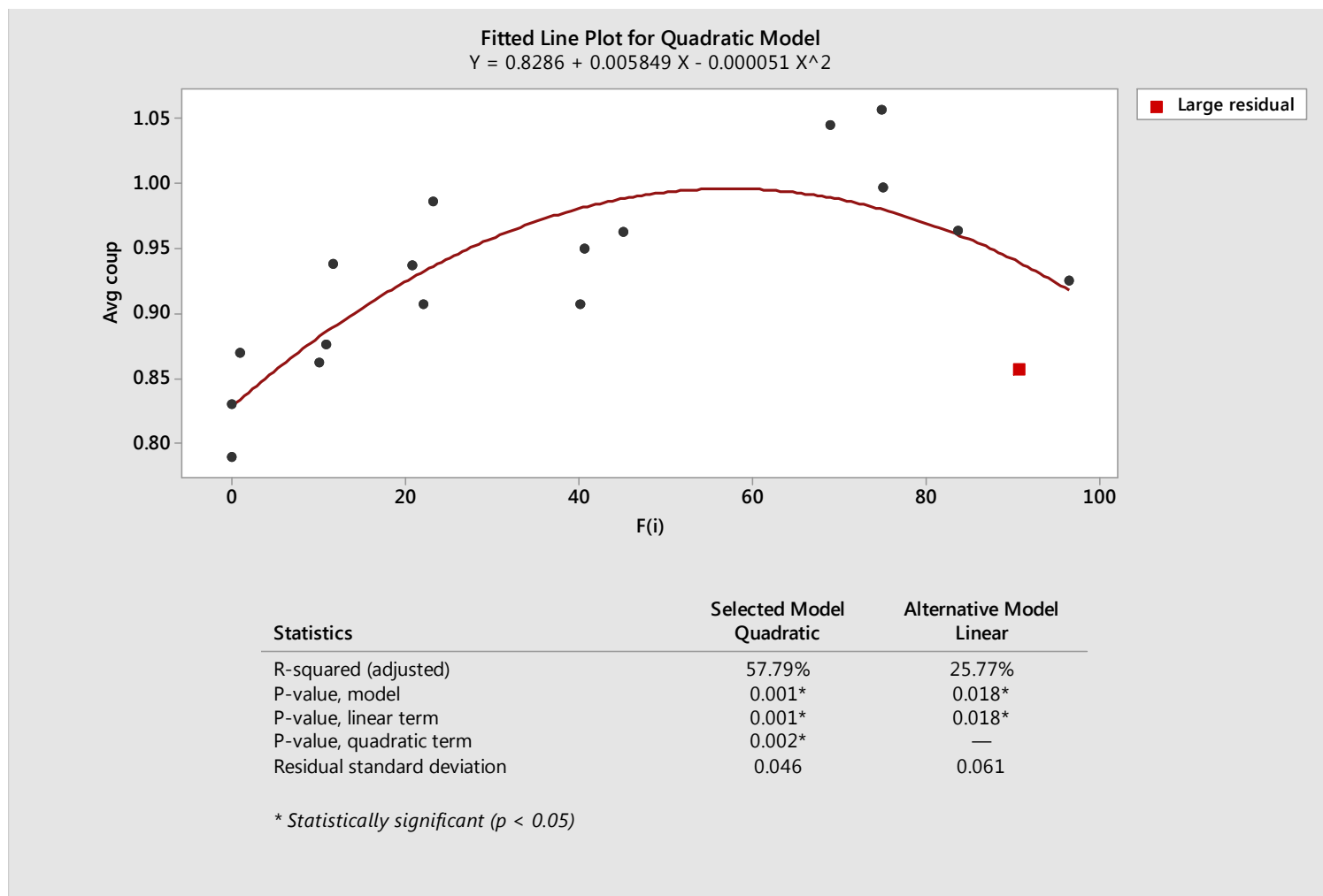


Figure 4-56: Regression for the average corrosion rate (Avg coup) versus the initial fluoride concentration (F(i)) at a total alkalinity of 220 mg/l as CaCO_3 (all three data sets)

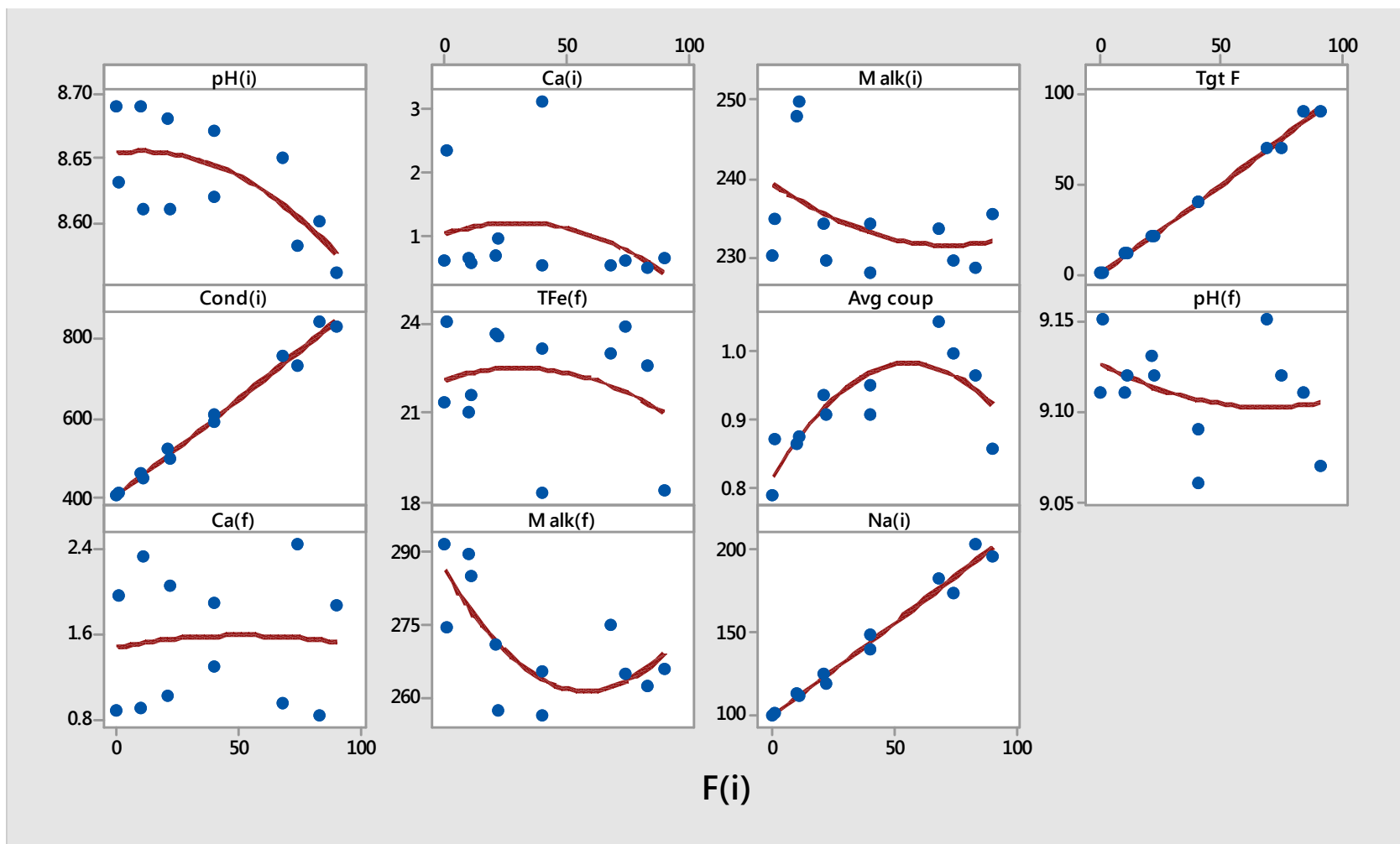


Figure 4-57: Repeat scatterplots of the key variables versus the initial fluoride concentration ($F(i)$) at a total alkalinity of 220 mg/l as CaCO_3 for data with pH values < 9

Due to the clustering of data, it was decided to only utilize the water chemistry data with initial pH values less than 9.0 in order to study the relationships of the water chemistry with the initial fluoride concentrations. A comparison of the regression for the data both with and without the high pH cluster produced approximately similar fluoride only based regression models with R^2 values of approximately 57%.

Regression analyses of the correlation of the average mild steel corrosion rate with variables individually indicated that conductivity had the strongest association ($R^2 = 62\%$), followed by fluoride, then sodium ($R^2 = 38\%$), and pH ($R^2 = 3\%$). The relationship with the total alkalinity was found to not be statistically significant ($P > 0.05$).

The inclusion of the initial conductivity and initial pH into the regression model resulted in a vastly improved regression equation (Equation 4.14) (R -square = 96%).

No regression was possible with the higher pH data set due to insufficient data. This data set was all from the same batch of experiments and was probably attributed to the slightly higher pH and total alkalinity, and lower calcium hardness batch of deionized water used (Figure 4-55). The higher pH deionised water appeared have resulted in slightly lower total iron levels and marginally higher average coupon corrosion rates but more data would be required to confirm this finding.

4.8.4 Series 4 - Low calcium

Sodium fluoride was added to deionized water with a targeted calcium hardness of 50 mg/l (as Ca^{2+}) at the concentrations given in Table 4-55. The purpose of this series was to investigate the impact of low calcium hardness with varying fluoride concentrations. The fluoride concentrations targeted ranged between 0 and 90 mg/l. The results of the water analyses were shown in Table 4-56, along with the coupon corrosion rates in Table 4-57.

The addition of sodium fluoride to the low calcium containing (deionized) water caused the pH to decrease from an initial value of 5.57 to the lowest value of 4.54, (Figure 4-58). Conversely, the total alkalinity increased over the entire target fluoride range, as did the conductivity and sodium concentrations. The average corrosion rate increased slightly until it reached the initial fluoride concentration of approximately 25-30 mg/l where after it again demonstrated a slight decline.

Among the likely factors that influenced the outcome of the trend for this series, noted for their weak correlation with the average corrosion rate were the initial (F(i)) (Figure 4-59) and to a slightly greater extent the initial pH (pH(i)) (Figure 4-60).

A regression model was attempted which resulted in Equation 4.15 with a p value of 0.162 and R² of 72%:

$$\text{Average corrosion rate} = -4.08 + 0.0832 \times \text{Ca(i)} + 0.894 \times \text{pH(i)} + 0.0470 \times \text{M alk(i)} - 0.00403 \times \text{M alk(i)}^2 - 0.01687 \times \text{Ca(i)} \times \text{pH(i)} \dots \dots \dots [4.15]$$

Table 4-55: Corrosion tests varying fluoride in low calcium water at 45°C – Target and start-up concentrations

Run	Target fluoride (mg/l as F ⁻)	Test solution concentrations at start-up									
		Fluoride (25x dln) ⁽¹⁾ (mg/l as F ⁻)	pH ⁽¹⁾	Calcium ⁽²⁾ (mg/l as Ca ²⁺)	Magnesium ⁽²⁾ (mg/l as Mg ²⁺)	Total alkalinity ⁽¹⁾ (mg/l as CaCO ₃)	Chloride ⁽²⁾ (mg/l as Cl ⁻)	Sulphate (25x dln) ⁽²⁾ (mg/l as SO ₄ ²⁻)	Sodium ⁽²⁾ (mg/l as Na ⁺)	Conductivity ⁽¹⁾ (µS/cm)	Total iron ⁽¹⁾ (mg/l as Fe ³⁺ (total))
193	0	0.3	5.57	50.2	0.1	4.9	3	9.06	0	304	< 0.01
194	10	10.8	5.46	49.8	0.1	5.6	3	9.00	12	348	< 0.01
195	20	6.3	5.25	34.3	0.1	4.8	3	9.00	22	336	< 0.01
196	40	12.0	5.05	18.4	0.1	4.3	3	9.08	47	324	< 0.01
197	70	29.9	5.00	10.2	0.1	6.2	3	9.09	86	400	< 0.01
198	90	52.0	5.02	5.0	0.1	9.0	3	9.09	111	496	< 0.01
199	0	1.4	5.41	48.9	0.1	nt	3	8.80	0	304	< 0.01
200	10	0.0	5.22	48.6	0.1	nt	2	8.90	12	352	< 0.01
201	20	6.0	5.01	33.2	0.1	nt	3	8.84	23	400	< 0.01
202	40	8.0	5.30	15.4	0.1	nt	3	6.41	47	332	< 0.01
203	70	26.9	4.96	6.0	0.1	nt	3	9.02	79	412	< 0.01
204	90	55.4	4.54	1.3	0.1	nt	3	9.13	102	508	< 0.01
205	0	0.0	5.35	49.9	0.3	nt	4	4.71	1	304	< 0.01
206	10	11.0	5.43	51.9	0.1	5.8	3	4.38	12	352	< 0.01
207	20	24.1	5.37	50.7	0.1	7.3	3	4.38	26	396	< 0.01
208	40	8.7	5.01	16.8	0.1	4.9	3	4.38	50	336	< 0.01
209	70	32.5	5.02	1.6	0.1	7.3	3	1.63	87	412	< 0.01
210	90	58.6	5.08	0.7	0.1	10.7	0	9.32	112	504	< 0.01

Notes: 1. Test conducted in Laboratory B, 2. Test conducted in Laboratory C, nt = not tested.

Table 4-56: Corrosion tests varying fluoride in low calcium water at 45°C –
Cessation concentrations

Run	Target fluoride (mg/l as F ⁻)	Test solution concentrations at cessation of corrosion tests									
		Fluoride (25x diln) ⁽¹⁾ (mg/l as F ⁻)	pH ⁽¹⁾	Calcium ⁽²⁾ (mg/l as Ca ²⁺)	Magnesium ⁽²⁾ (mg/l as Mg ²⁺)	Total alkalinity ⁽¹⁾ (mg/l as CaCO ₃)	Chloride ⁽²⁾ (mg/l as Cl ⁻)	Sulphate (25x diln) ⁽²⁾ (mg/l as SO ₄ ²⁻)	Sodium ⁽²⁾ (mg/l as Na ⁺)	Conductivity ⁽¹⁾ (µS/cm)	Total iron ⁽¹⁾ (mg/l as Fe ³⁺ (total))
193	0	2.2	7.32	48.2	0.2	9.2	3	8.34	1	356	21.0
194	10	12.9	7.39	57.3	0.2	12.1	3	9.06	14	412	26.1
195	20	11.3	7.40	41.9	0.2	12.1	3	9.11	29	392	29.1
196	40	7.8	7.25	20.0	0.1	13.7	3	9.09	56	388	20.0
197	70	40.7	6.96	4.3	0.1	17.7	3	9.05	101	492	22.5
198	90	96.0	6.60	2.3	0.1	20.9	3	9.05	126	588	20.6
199	0	0.0	5.19	55.5	0.4	nt	4	9.10	3	356	21.3
200	10	10.9	4.97	55.7	0.2	nt	3	9.29	14	408	23.3
201	20	7.1	5.03	39.7	0.2	nt	3	8.67	28	392	19.8
202	40	10.0	5.07	19.5	0.2	nt	3	8.72	53	384	19.3
203	70	29.1	4.61	4.4	0.1	nt	3	8.70	94	492	20.8
204	90	48.7	4.21	2.5	0.1	nt	3	8.68	115	584	21.1
205	0	0.0	7.53	59.5	0.2	10.3	4	4.38	1	360	26.6
206	10	10.5	7.44	43.4	0.2	13.0	4	4.38	28	412	24.7
207	20	8.0	7.40	18.8	0.1	15.3	4	4.38	57	412	27.8
208	40	35.6	7.02	4.7	0.1	17.0	3	9.32	100	308	20.2
209	70	58.3	6.70	2.6	0.1	20.7	4	4.84	121	492	27.1
210	90	51.9	6.55	2.5	0.1	21.7	4	4.38	121	596	nt

Table 4-57: Corrosion coupon readings while varying fluoride in low calcium water at 45°C

Run	Target fluoride (mg/l as F ⁻)	Corrosion Coupon Results		
		Coupon 1 (mmpa)	Coupon 2 (mmpa)	Average (mmpa)
193	0	0.47	0.48	0.47
194	10	0.52	0.53	0.53
195	20	0.55	0.57	0.56
196	40	0.52	0.51	0.51
197	70	0.56	0.49	0.53
198	90	0.49	0.47	0.48
199	0	0.47	0.47	0.47
200	10	0.47	0.56	0.52
201	20	0.50	0.46	0.48
202	40	0.47	0.51	0.49
203	70	0.56	0.52	0.54
204	90	0.43	0.46	0.44
205	0	0.48	0.53	0.51
206	10	0.45	0.52	0.48
207	20	0.45	0.46	0.46
208	40	0.52	0.52	0.52
209	70	0.53	0.53	0.53
210	90	0.50	0.52	0.51

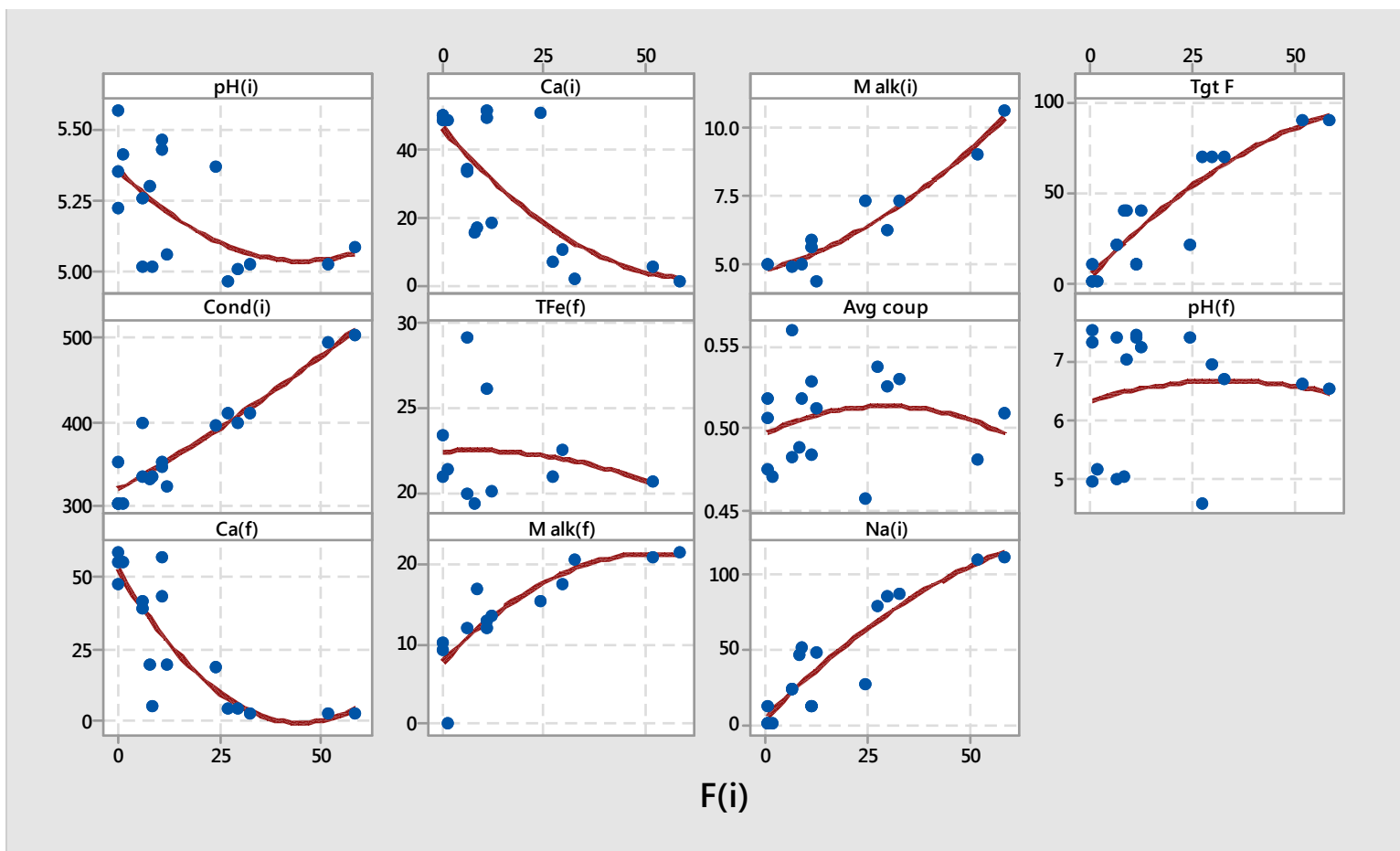


Figure 4-58: Scatterplots of the key variables versus the initial fluoride concentration ($F(i)$) at a calcium hardness of 50 mg/l as Ca^{2+}

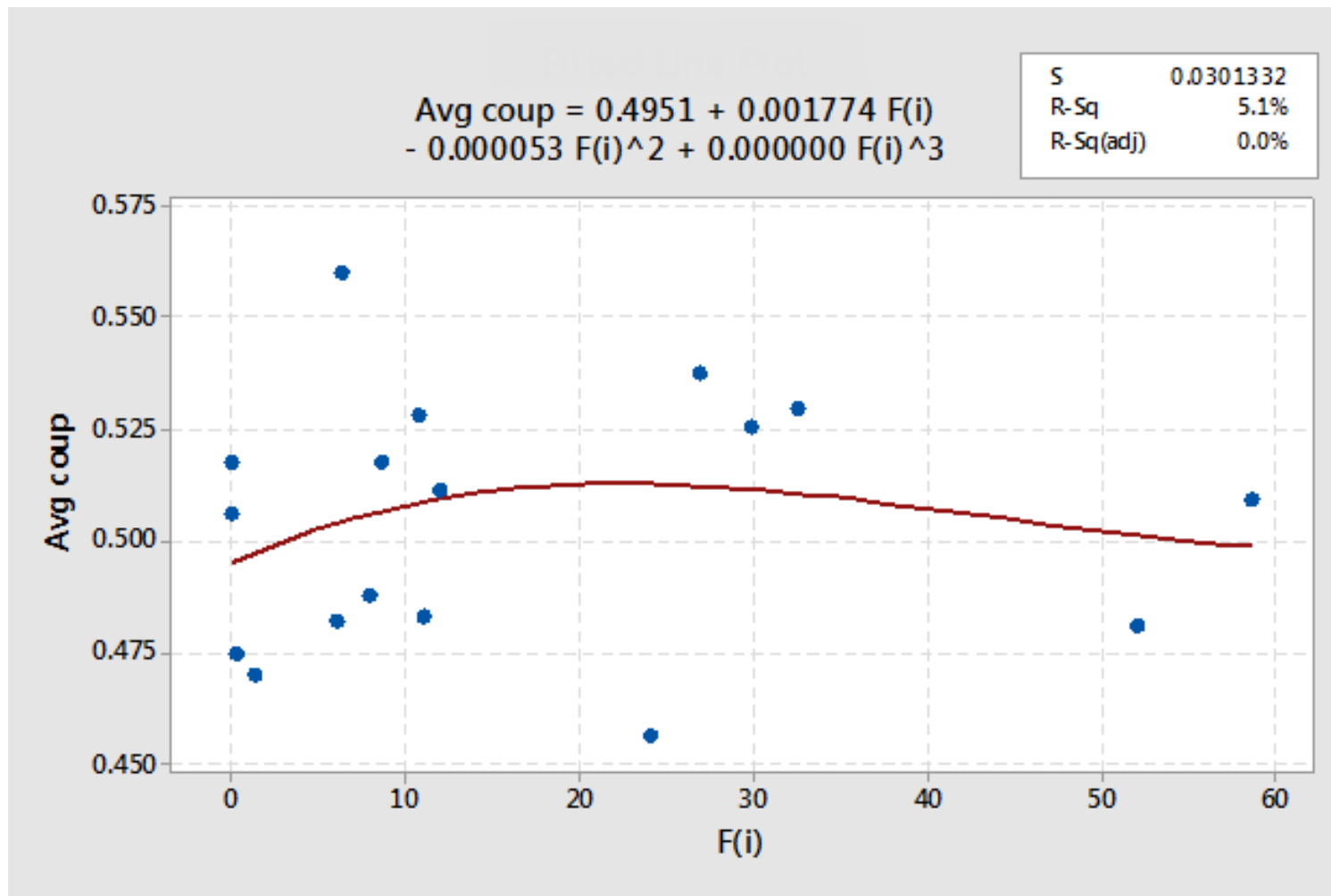


Figure 4-59: Regression for the average coupon (Avg coup) versus the initial fluoride concentration (F(i)) at a calcium hardness of 50 mg/l as Ca^{2+}

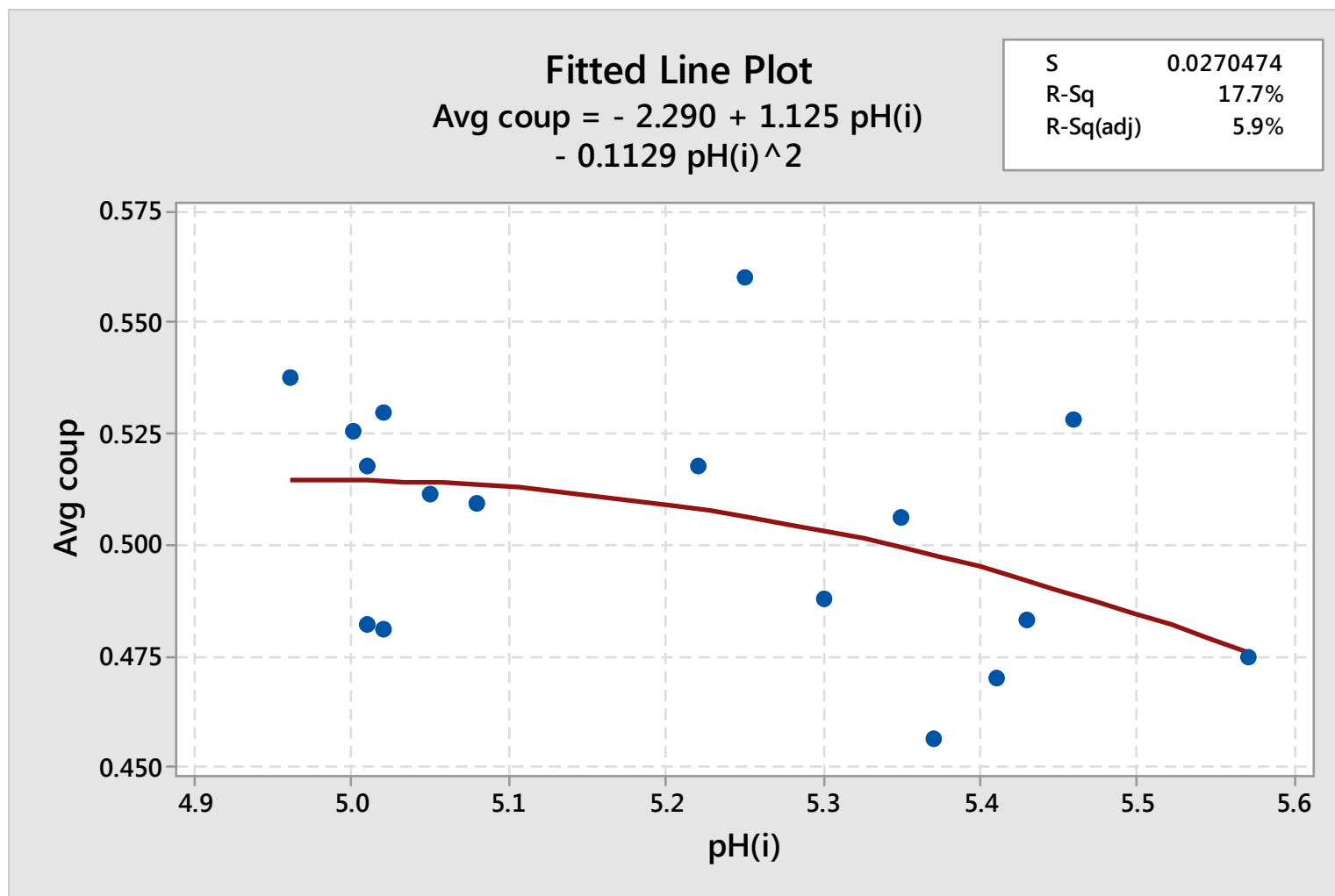


Figure 4-60: Regression for the average coupon (Avg coup) versus the initial pH(i) at a calcium hardness of 50 mg/l as Ca²⁺

The addition of sodium fluoride to deionized water with 50 mg/l of soluble calcium (as Ca^{2+}) resulted in decreases in the test solution initial pH and calcium concentrations and increases in the initial total alkalinity.

As indicated by the inadequate regression R^2 and R^2 (adj) values, it was not possible to identify statistically significant strong correlations between the average corrosion rate and either the: a) initial pH or b) initial fluoride concentration. This was mostly due to the sample size ($n = 17$) not being large enough to provide a very precise estimate of the strength of the relationship.

A relationship was obtained for the average corrosion rate based on the use of the following three variables: initial calcium, initial pH and initial total alkalinity, and although a reasonably good fit was attained, $R^2 = 72\%$, the model was however not statistically significant ($p = 0.162$).

4.8.5 Series 5 - High calcium

Sodium fluoride was added to deionized water with a target calcium hardness of 120 mg/l (as Ca^{2+}) at the concentrations given in Table 4-58 and the results of the water analyses shown in Table 4-59, along with the coupon corrosion rates in Table 4-60. The fluoride concentrations targeted ranged between 0 and 90 mg/l.

The addition of sodium fluoride to the high calcium (120 mg/l as Ca^{2+}) containing (deionized) water caused a dramatic decrease in both the initial soluble fluoride and calcium concentrations (Figures 4-61 and 4-62). The calcium and fluoride concentration decreased to lower than 20 and 8 mg/l respectively. Although the total alkalinity also decreased with increasing target fluoride concentration, as apparent in Figure 4-62, it did remain higher for higher residual fluoride concentrations (Figure 4-61). The only fitting model for the data was the regression Equation 4.16.

The regression model, Equation 4.16, was compiled based on the initial fluoride and initial alkalinity with a p value of 0.033 and an R^2 of 45%.

$$\text{Average corrosion rate} = 0.2645 - 0.01033 \times F(i) + 0.0999 \times M \text{ alk}(i) - 0.01563 \times M \text{ alk}(i)^2 \dots\dots\dots [4.16]$$

Table 4-58: Corrosion tests varying fluoride in high calcium water at 45°C – Target and start-up concentrations

Run	Target fluoride (mg/l as F ⁻)	Test solution concentrations at start-up									
		Fluoride (25x diln) ⁽¹⁾ (mg/l as F ⁻)	pH ⁽¹⁾	Calcium ⁽²⁾ (mg/l as Ca ²⁺)	Magnesium ⁽²⁾ (mg/l as Mg ²⁺)	Total alkalinity ⁽¹⁾ (mg/l as CaCO ₃)	Chloride ⁽²⁾ (mg/l as Cl ⁻)	Sulphate (25x diln) ⁽²⁾ (mg/l as SO ₄ ²⁻)	Sodium ⁽²⁾ (mg/l as Na ⁺)	Conductivity ⁽¹⁾ (µS/cm)	Total iron ⁽¹⁾ (mg/l as Fe ³⁺ (total))
217	0	0.0	4.97	120.0	0.1	2.3	3	1.45	1	696	< 0.01
218	10	0.4	5.04	109.0	0.1	2.7	3	0.92	12	704	< 0.01
219	20	0.2	4.85	101.0	0.1	2.3	4	1.06	22	728	< 0.01
220	40	0.5	4.70	79.1	0.1	2.0	3	0.96	46	716	< 0.01
221	70	0.5	4.55	48.6	0.2	1.7	3	0.92	80	704	< 0.01
222	90	0.7	4.39	25.5	0.1	1.3	3	0.92	104	684	< 0.01
223	0	0.0	5.31	114.0	0.1	3.3	3	0.55	0	708	< 0.01
224	10	4.1	5.19	113.0	0.1	3.9	3	0.55	11	740	< 0.01
225	20	0.6	5.13	103.0	0.1	3.8	1	0.47	24	720	< 0.01
226	40	3.1	4.85	79.7	0.1	3.3	3	0.55	48	712	< 0.01
227	70	3.2	4.66	47.3	0.1	3.2	1	0.47	83	708	< 0.01
228	90	5.4	4.60	27.7	0.2	3.3	1	0.47	106	700	< 0.01
229	0	1.0	5.40	118.0	0.1	3.7	3	0.54	0	700	< 0.01
230	10	3.2	5.35	113.0	0.1	4.3	3	0.56	11	716	< 0.01
231	20	3.2	5.24	102.0	0.1	4.0	3	0.57	23	720	< 0.01
232	40	3.2	5.11	87.7	0.1	4.0	3	0.55	46	708	< 0.01
233	70	3.9	4.85	51.3	0.1	3.4	3	0.55	81	708	< 0.01
234	90	5.4	4.78	26.3	0.1	3.6	3	0.55	103	700	< 0.01

Notes: 1. Test conducted in Laboratory B, 2. Test conducted in Laboratory C, nt = not tested.

Table 4-59: Corrosion tests varying fluoride in high calcium water at 45°C – Cessation concentrations

Run	Target fluoride (mg/l as F ⁻)	Test solution concentrations at cessation of corrosion tests									
		Fluoride (25x diln) ⁽¹⁾ (mg/l as F ⁻)	pH ⁽¹⁾	Calcium ⁽²⁾ (mg/l as Ca ²⁺)	Magnesium ⁽²⁾ (mg/l as Mg ²⁺)	Total alkalinity ⁽¹⁾ (mg/l as CaCO ₃)	Chloride ⁽²⁾ (mg/l as Cl ⁻)	Sulphate (25x diln) ⁽²⁾ (mg/l as SO ₄ ²⁻)	Sodium ⁽²⁾ (mg/l as Na ⁺)	Conductivity ⁽¹⁾ (µS/cm)	Total iron ⁽¹⁾ (mg/l as Fe ³⁺ (total))
217	0	0.0	7.08	130.0	0.3	9.2	3	0.93	1	82	26.9
218	10	0.6	7.02	121.0	0.3	9.0	3	0.93	14	83	24.1
219	20	0.6	7.06	113.0	0.3	9.5	3	0.93	26	84	26.5
220	40	0.0	6.94	90.3	0.2	8.1	3	0.92	52	82	23.7
221	70	7.3	7.05	57.2	0.2	11.6	3	1.08	96	82	29.3
222	90	0.7	6.89	30.3	0.2	13.0	3	0.92	121	79	22.3
223	0	0.0	7.15	139.0	0.1	16.5	14	0.46	1	85	26.0
224	10	3.8	7.19	131.0	0.2	18.0	14	0.48	14	86	25.1
225	20	6.5	7.26	118.0	0.2	18.3	14	0.47	28	84	26.5
226	40	7.4	7.02	92.2	0.2	19.6	14	0.48	56	84	24.8
227	70	4.5	6.99	57.8	0.2	22.4	14	0.47	99	83	30.5
228	90	8.0	6.69	30.6	0.2	17.2	13	0.46	122	81	19.4
229	0	0.5	7.28	135.0	0.2	10.9	3	0.55	2	83	20.5
230	10	4.5	7.28	128.0	0.1	11.1	3	0.54	13	84	16.8
231	20	4.2	7.26	116.0	0.1	10.5	3	0.56	27	84	15.5
232	40	4.0	7.15	91.3	0.2	10.8	3	0.58	52	80	14.9
233	70	4.9	7.17	57.2	0.2	12.4	3	0.54	96	81	15.7
234	90	7.1	7.02	32.4	0.2	12.3	3	0.55	121	80	14.1

Table 4-60: Corrosion coupon readings while varying fluoride in high calcium water at 45°C

Run	Target fluoride (mg/l as F ⁻)	Corrosion Coupon Results		
		Coupon 1 (mmpa)	Coupon 2 (mmpa)	Average (mmpa)
217	0	0.42	0.41	0.42
218	10	0.38	0.42	0.40
219	20	0.45	0.41	0.43
220	40	0.37	0.35	0.36
221	70	0.38	0.45	0.41
222	90	0.34	0.36	0.35
223	0	0.42	0.41	0.42
224	10	0.38	0.42	0.40
225	20	0.45	0.41	0.43
226	40	0.37	0.35	0.36
227	70	0.38	0.45	0.41
228	90	0.34	0.36	0.35
229	0	0.41	0.42	0.42
230	10	0.36	0.41	0.38
231	20	0.35	0.36	0.36
232	40	0.37	0.33	0.35
233	70	0.40	0.39	0.40
234	90	0.36	0.41	0.38

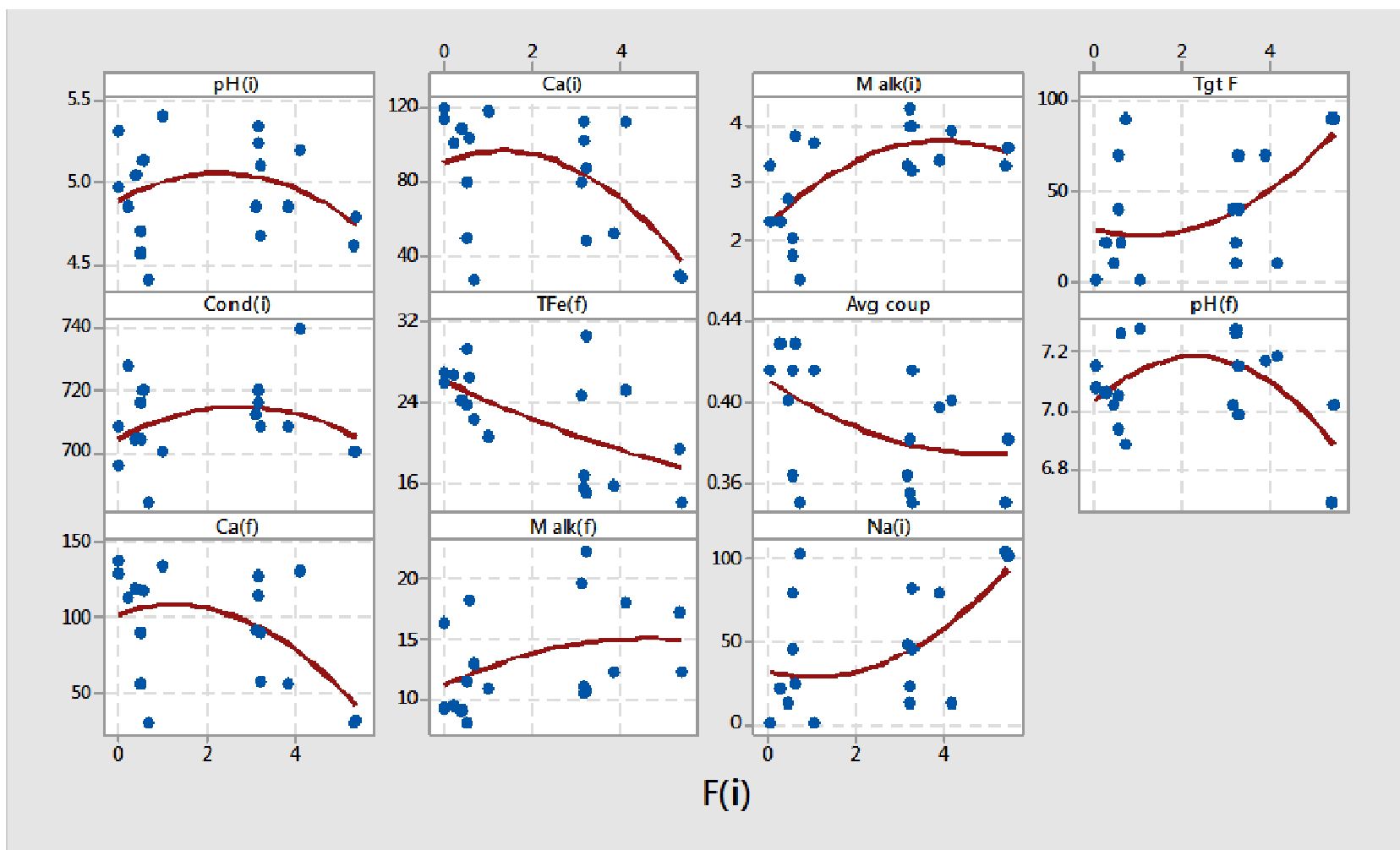


Figure 4-61: Scatterplots of the key variables versus the initial fluoride concentration ($F(i)$) at a calcium hardness of 120 mg/l as Ca^{2+}

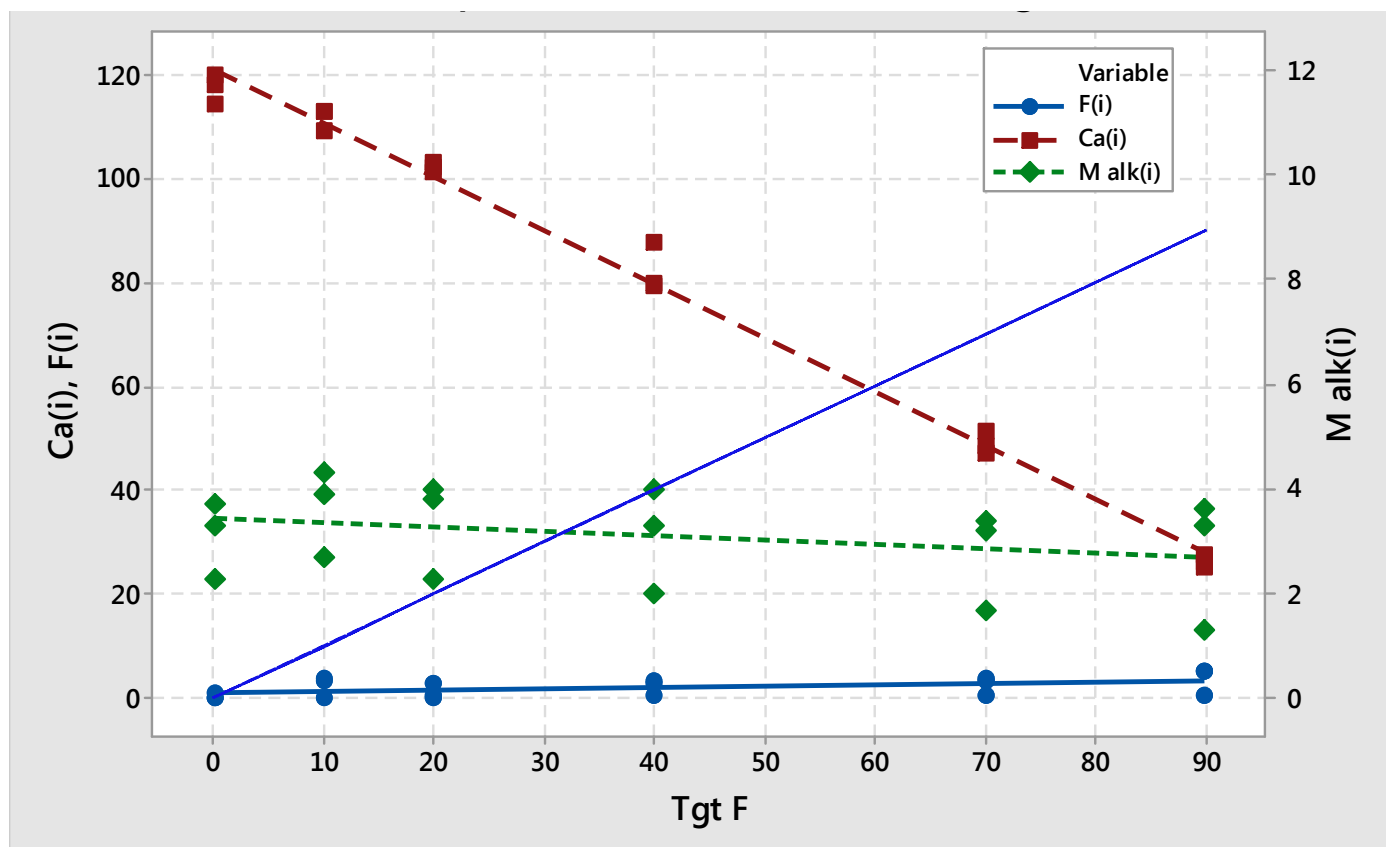


Figure 4-62: Scatterplot of initial fluoride (F(i)), initial calcium (Ca(i)) and initial total alkalinity (M alk(i)) versus target fluoride (Tgt F)(also indicated on graph as line without markers)

The high level of calcium hardness (120 mg/l as Ca^{2+}) resulted in the precipitation of calcium fluoride that lead to almost negligible concentrations of fluoride. Fluoride residuals were as low as 8 mg/l as F^- . Calcium levels also decreased with increasing fluoride addition to ~30 mg/l as Ca^{2+} . The residual soluble fluoride level contribute some alkalinity to the deionized water based test solutions but this was to a limited extent (i.e. < 5 mg/l as CaCO_3).

A statistically significant and moderately strong quadratic model (Equation 4.16) ($R^2 = 45\%$) was proposed to define the influences the initial fluoride concentration and initial total alkalinity had on the coupon corrosion rate.

4.8.6 Series 6 - Low alkalinity and low calcium

Sodium fluoride was added to deionized water with a target calcium hardness of 50 mg/l (as CaCO_3) and total alkalinity of 55 mg/l as CaCO_3 at the concentrations given in Table 4-61 and the results of the water analyses shown in Table 4-62, along with the coupon corrosion rates in Table 4-63. The fluoride concentrations targeted ranged between 0 and 90 mg/l.

Corrosion tests performed with deionized water containing low levels of calcium (50 mg/l as Ca^{2+}) and low total alkalinity (55 mg/l as CaCO_3) indicated the following trends with increasing initial fluoride concentrations (Figure 4-63): decreasing initial calcium concentration, decreasing initial pH, increasing sodium and conductivity levels, and increasing corrosion rate. The initial total alkalinity (M alk(i)) did not increase, but there was an apparent increase in the final total alkalinity with increasing fluoride.

A regression model was produced which resulted in Equation 4.17 with a p value of 0.001 and R^2 of 87%.

$$\begin{aligned} \text{Average corrosion rate} = & -11.36 - 0.00896 \times \text{M alk(i)} + 0.385 \times \text{Ca(i)} \\ & + 1.584 \times \text{pH(i)} + 0.00352 \times \text{F(i)} - 0.0490 \times \text{Ca(i)} \times \text{pH(i)} \dots\dots\dots [4.17] \end{aligned}$$

Table 4-61: Corrosion tests varying fluoride in low calcium and alkalinity water at 45°C – Target and start-up concentrations

Run	Target fluoride (mg/l as F ⁻)	Test solution concentrations at start-up									
		Fluoride (25x diln) ⁽¹⁾ (mg/l as F ⁻)	pH ⁽¹⁾	Calcium ⁽²⁾ (mg/l as Ca ²⁺)	Magnesium ⁽²⁾ (mg/l as Mg ²⁺)	Total alkalinity ⁽¹⁾ (mg/l as CaCO ₃)	Chloride ⁽²⁾ (mg/l as Cl ⁻)	Sulphate (25x diln) ⁽²⁾ (mg/l as SO ₄ ²⁻) x 10 ³	Sodium ⁽²⁾ (mg/l as Na ⁺)	Conductivity ⁽¹⁾ (µS/cm)	Total iron ⁽¹⁾ (mg/l as Fe ³⁺ (total))
235	0	0.0	8.02	48.3	0.2	54.4	3	1.01	20	428	< 0.01
236	10	9.8	8.08	47.5	0.1	58.3	3	1.01	33	452	< 0.01
237	20	20.2	8.08	48.7	0.1	60.0	3	1.02	45	504	< 0.01
238	40	11.4	7.96	20.5	0.2	63.6	3	1.08	67	436	< 0.01
239	70	28.5	7.98	21.1	0.1	54.7	3	0.93	103	512	< 0.01
240	90	45.5	7.85	10.8	0.1	62.8	4	1.00	128	612	< 0.01
241	0	0.0	7.97	49.9	0.1	70.2	3	1.10	25	428	< 0.01
242	10	12.6	7.90	48.5	0.1	61.7	3	1.10	35	456	< 0.01
243	20	26.0	7.90	48.2	0.1	92.9	3	1.10	48	504	< 0.01
244	40	12.1	7.92	16.1	0.1	69.1	3	1.09	71	440	< 0.01
245	70	35.6	7.89	1.8	0.1	52.4	3	1.09	124	516	< 0.01
246	90	58.3	7.79	0.7	0.1	56.4	3	0.99	30	608	< 0.01
247	0	0.8	8.04	46.8	0.1	57.4	4	0.69	23	424	< 0.01
248	10	10.7	8.06	47.0	0.1	58.2	4	0.69	33	444	< 0.01
249	20	23.1	8.08	47.0	0.1	58.5	4	0.98	54	492	< 0.01
250	40	17.7	7.94	21.1	0.2	70.2	4	0.69	69	492	< 0.01
251	70	30.4	7.99	4.0	0.1	62.5	3	0.87	102	500	< 0.01
252	90	47.3	7.87	1.3	0.1	54.8	3	0.87	123	596	< 0.01

Notes: 1. Test conducted in Laboratory B, 2. Test conducted in Laboratory C, nt = not tested.

Table 4-62: Corrosion tests varying fluoride in low calcium and alkalinity water at 45°C – Cessation concentrations

Run	Target fluoride (mg/l as F ⁻)	Test solution concentrations at cessation of corrosion tests									
		Fluoride (25x diln) ⁽¹⁾ (mg/l as F ⁻)	pH ⁽¹⁾	Calcium ⁽²⁾ (mg/l as Ca ²⁺)	Magnesium ⁽²⁾ (mg/l as Mg ²⁺)	Total alkalinity ⁽¹⁾ (mg/l as CaCO ₃)	Chloride ⁽²⁾ (mg/l as Cl ⁻)	Sulphate (25x diln) ⁽²⁾ (mg/l as SO ₄ ²⁻) x 10 ³	Sodium ⁽²⁾ (mg/l as Na ⁺)	Conductivity ⁽¹⁾ (µS/cm)	Total iron ⁽¹⁾ (mg/l as Fe ³⁺ (total))
235	0	0.0	8.07	44.8	0.4	38.9	4	1.04	29	432	27.3
236	10	11.5	8.08	45.3	0.2	43.4	4	1.02	41	484	21.0
237	20	11.7	8.04	31.5	0.2	39.1	4	1.04	53	484	22.7
238	40	15.1	8.33	14.9	0.2	52.1	4	1.14	78	488	20.8
239	70	33.7	8.58	3.3	0.2	68.4	4	0.93	122	616	27.8
240	90	53.1	8.57	3.9	0.2	71.3	4	0.94	149	736	25.5
241	0	0.0	8.08	43.5	0.2	42.3	3	1.18	43	432	27.6
242	10	0.6	8.00	44.2	0.2	44.3	2	1.11	43	484	32.1
243	20	15.9	8.05	33.9	0.2	43.3	3	1.14	57	484	20.2
244	40	13.9	8.34	15.4	0.2	55.8	3	1.11	82	492	17.8
245	70	40.0	8.61	2.0	0.1	67.1	3	1.12	123	612	23.0
246	90	66.8	8.56	2.6	0.2	71.8	4	1.12	147	716	17.9
247	0	0.4	8.17	44.6	0.2	42.2	5	0.80	29	420	24.5
248	10	11.3	8.08	42.4	0.2	40.9	4	0.69	39	460	20.3
249	20	13.2	8.14	15.8	0.2	40.6	4	0.69	80	468	19.7
250	40	15.1	8.35	15.0	0.2	51.7	5	0.69	77	488	17.0
251	70	32.1	8.67	3.7	0.2	66.8	4	0.69	118	600	27.0
252	90	54.9	8.60	1.1	0.1	69.0	3	0.85	143	700	23.0

Table 4-63: Corrosion coupon readings while varying fluoride in low calcium and alkalinity water at 45°C

Run	Target fluoride (mg/l as F ⁻)	Corrosion Coupon Results		
		Coupon 1 (mmpa)	Coupon 2 (mmpa)	Average (mmpa)
235	0	0.43	0.58	0.51
236	10	0.44	0.38	0.41
237	20	0.45	0.45	0.45
238	40	0.59	0.57	0.58
239	70	0.86	0.86	0.86
240	90	0.75	0.81	0.78
241	0	0.48	0.42	0.45
242	10	0.48	0.50	0.49
243	20	0.35	0.32	0.33
244	40	0.60	0.62	0.61
245	70	0.78	0.77	0.77
246	90	0.65	0.67	0.66
247	0	0.46	0.56	0.51
248	10	0.45	0.50	0.47
249	20	0.49	0.46	0.48
250	40	0.36	0.56	0.46
251	70	0.84	0.84	0.84
252	90	0.68	0.76	0.72

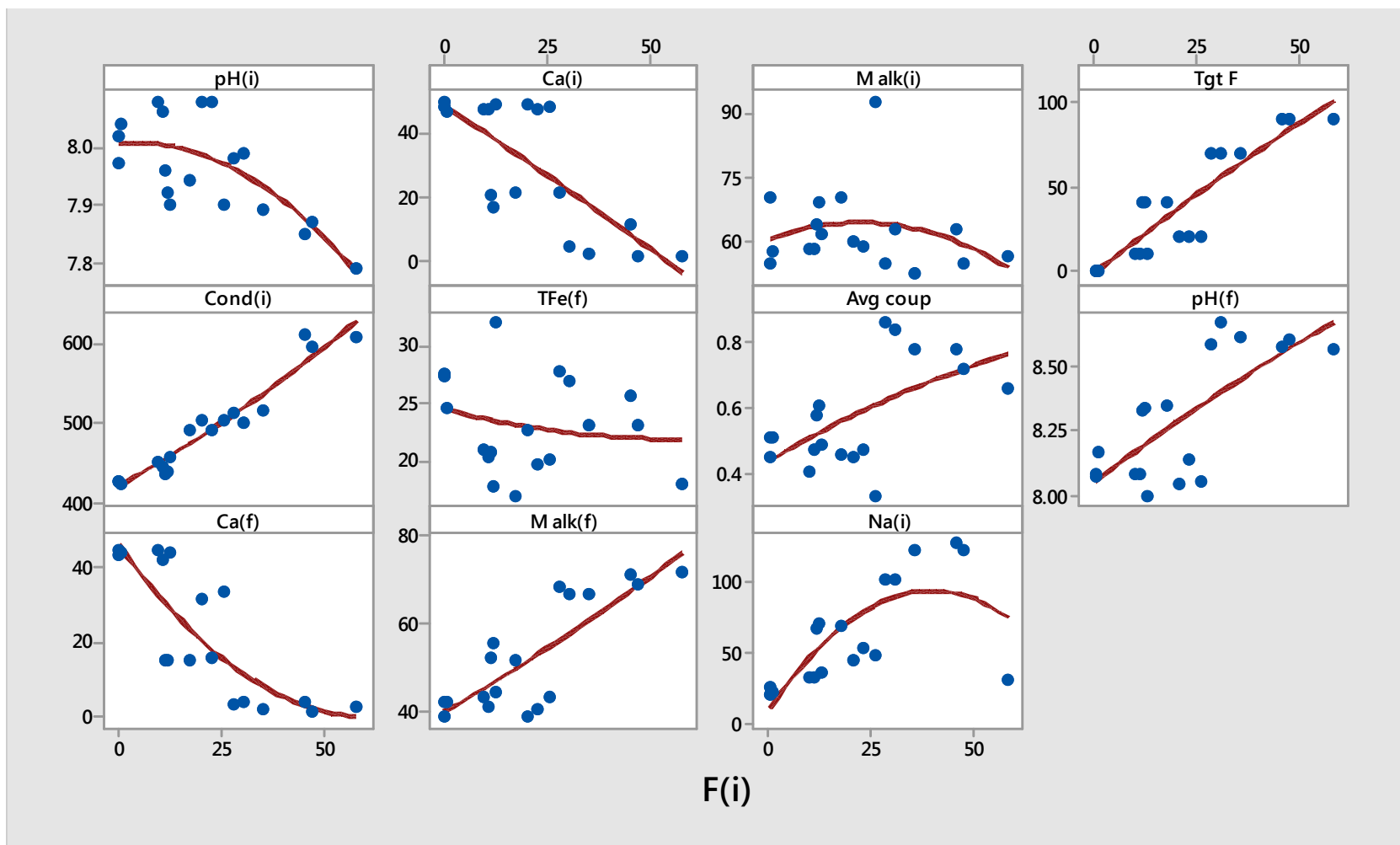


Figure 4-63: Scatterplots of the key variables versus the initial fluoride concentration ($F(i)$) at a calcium hardness of 50 mg/l as Ca^{2+} and a total alkalinity of 55 mg/l as CaCO_3

Impacts of the variables are given in Figure 4-64 where the initial pH and initial alkalinity had the largest influence on the average corrosion rate.

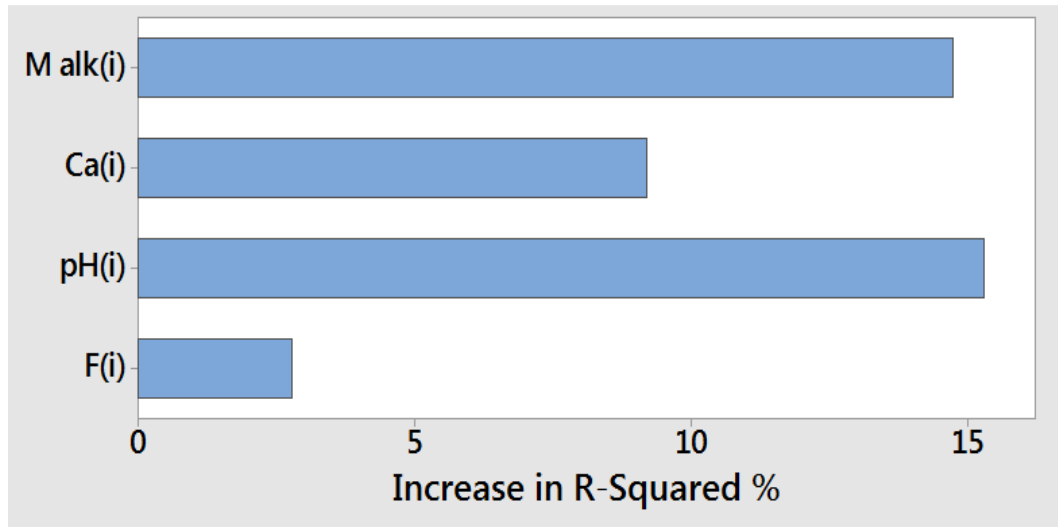


Figure 4-64: Incremental impact bar graph of variables on corrosion rate of steel for calcium at 50 mg/l as Ca^{2+} and total alkalinity at 55 mg/l as CaCO_3

The regression models were produced when the fluoride was substituted with either conductivity or sodium. Equations 4.18 and 4.19 indicate the impacts of the initial conductivity or initial sodium concentrations were significantly higher than that of the initial fluoride concentration. Equations 4.18 and 4.19, both with p values of 0.001 and R^2 values of 88 and 94% respectively.

- Conductivity instead of fluoride:

$$\text{Average corrosion rate} = -14.05 - 0.00901 \times \text{M alk(i)} + 0.436 \times \text{Ca(i)} + 1.876 \times \text{pH(i)} + 0.000940 \times \text{Cond(i)} - 0.0554 \times \text{Ca(i)} \times \text{pH(i)} \dots [4.18]$$

- Sodium instead of fluoride:

$$\text{Average corrosion rate} = -19.51 - 0.00551 \times \text{M alk(i)} + 0.499 \times \text{Ca(i)} + 2.571 \times \text{pH(i)} - 0.00247 \times \text{Na(i)} + 0.000041 \text{Na(i)}^2 - 0.0630 \times \text{Ca(i)} \times \text{pH(i)} \dots [4.19]$$

In this series of corrosion tests performed with low levels of calcium and total alkalinity, it was revealed the average coupon corrosion rate depended mostly on the initial total alkalinity, initial pH and initial calcium, but was also significantly affected by either the initial fluoride, initial conductivity or initial sodium concentrations. A reasonably good statistically significant ($p = 0.001$) fit was obtained for the first four variable model (Equation 4.17) ($R^2 = 87\%$) where fluoride was the fourth variable. Substituting the fluoride with conductivity only produced a 0.57% improvement in the regression model. However, a substitution of the fluoride with sodium lead to a significant improvement in the model resulting in an R^2 of 94% (Equation 4.19).

4.8.7 Series 7 - High alkalinity and high calcium

Sodium fluoride was added to deionized water with a target calcium hardness of 120 mg/l (as Ca^{2+}) and total alkalinity of 220 mg/l as CaCO_3 at the concentrations given in Table 4-64 and the results of the water analyses shown in Table 4-65, along with the coupon corrosion rates in Table 4-66. The fluoride concentrations targeted ranged between 0 and 90 mg/l.

There were decreases in the initial calcium concentration and initial conductivity and an increase in the average corrosion rate (Avg coup) with increasing initial fluoride concentrations (Figure 4-65). The concurrent reductions in the initial calcium and initial fluoride concentrations indicated calcium fluoride precipitation. A regression of the average coupon corrosion rate versus the initial fluoride concentration alone resulted in an R^2 (adj) value of 43% ($p = 0.006$). This was supported by higher levels of precipitation observed with increasing sodium fluoride addition. The average coupon corrosion rate was plotted against the various key variables and the following linear trends noted (Figure 4-66):

- Higher average corrosion rates with decreasing initial calcium levels ($p = 0.011$, $r = -0.611$); and
- Higher average corrosion rates with increasing initial pH ($\text{pH}(i)$) ($p = 0.012$, $r = 0.578$), initial total alkalinity ($\text{M alk}(i)$) ($p = 0.013$, $r = 0.573$) and initial sodium concentration ($\text{Na}(i)$) ($p = 0.000$, $r = 0.916$).

A regression model for the average corrosion rate versus the initial sodium concentration (Figure 4-67) demonstrated that the linear plot was statistically significant and had an R^2 (adj) value of 83%. A quadratic regression was attempted but found to not be statistically significant ($p = 0.164$).

Scatterplots of the key variables against the target fluoride concentration demonstrated the impacts that were either directly or indirectly ascribable to the sodium fluoride addition (Figure 4-68).

Regression models (Equations 4.20 ($R^2 = 94\%$) and 4.21 ($R^2 = 97\%$)) were then considered to determine the impacts of the initial sodium and initial fluoride on the initial pH and initial total alkalinity.

$$\begin{aligned} \text{Initial pH} = & 5.37 + 0.0823 \times F(i) - 0.02246 \times Na(i) + 0.02428 \times M \text{ alk}(i) \\ & + 0.0248 \times Ca(i) - 0.00798 \times F(i)^2 + 0.000074 \times Na(i)^2 - 0.000165 \times M \text{ alk}(i) \\ & \times Ca(i) \dots \dots \dots [4.20] \end{aligned}$$

$$\begin{aligned} \text{Initial total alkalinity} = & 35 - 5.10 \times F(i) + 1.148 \times Na(i) + 5.6 \times pH(i) \\ & - 7.34 \times Ca(i) + 0.424 \times F(i)^2 - 0.00337 \times Na(i)^2 + 0.968 \times pH(i) \times \\ & Ca(i) \dots \dots \dots [4.21] \end{aligned}$$

Table 4-64: Corrosion tests varying fluoride in high calcium and alkalinity water at 45°C – Target and start-up concentrations

Run	Target fluoride (mg/l as F ⁻)	Test solution concentrations at start-up									
		Fluoride (25x diln) ⁽¹⁾ (mg/l as F ⁻)	pH ⁽¹⁾	Calcium ⁽²⁾ (mg/l as Ca ²⁺)	Magnesium ⁽²⁾ (mg/l as Mg ²⁺)	Total alkalinity ⁽¹⁾ (mg/l as CaCO ₃)	Chloride ⁽²⁾ (mg/l as Cl ⁻)	Sulphate (25x diln) ⁽²⁾ (mg/l as SO ₄ ²⁻) x 10 ³	Sodium ⁽²⁾ (mg/l as Na ⁺)	Conductivity ⁽¹⁾ (µS/cm)	Total iron ⁽¹⁾ (mg/l as Fe ³⁺ (total))
253	0	0.0	7.99	67.6	0.2	187.8	3	0.72	93	1004	> 0.01
254	10	7.7	7.83	60.7	0.2	161.2	3	0.65	101	1000	< 0.01
255	20	6.6	7.91	51.2	0.1	159.8	3	0.72	110	1012	< 0.01
256	40	5.4	8.03	40.8	0.1	180.3	3	0.72	132	1016	< 0.01
257	70	0.0	8.30	32.5	0.3	199.4	13	0.94	160	1024	< 0.01
258	90	8.0	8.30	37.4	0.2	192.0	3	0.72	176	1028	< 0.01
259	0	0.0	8.08	89.1	0.3	203.1	4	0.85	98	1016	< 0.01
260	10	0.0	7.86	76.1	0.3	182.6	15	0.85	110	1008	< 0.01
261	20	7.9	7.94	69.7	0.3	180.7	4	0.87	122	1000	< 0.01
262	40	7.0	8.02	58.6	0.3	191.4	4	0.87	146	1000	< 0.01
263	70	8.8	8.24	60.4	0.4	200.8	5	1.09	182	984	< 0.01
264	90	11.1	8.17	42.6	0.3	199.7	5	0.85	196	976	< 0.01
343	0	0.0	7.65	67.3	0.4	165.5	4	0.70	99.3	980	< 0.01
344	10	nt	7.49	nt	nt	151.2	nt	nt	nt	964	< 0.01
345	20	7.5	7.45	50.2	0.2	143.4	4	0.70	120	964	< 0.01
346	40	10.6	7.54	34.4	0.2	164.9	4	0.70	141	976	< 0.01
347	70	9.3	7.80	19.6	0.2	171.3	4	0.70	172	988	< 0.01
348	90	12.5	8.01	12.9	0.1	183.6	4	0.70	192	1000	< 0.01

Notes: 1. Test conducted in Laboratory B, 2. Test conducted in Laboratory C, nt = not tested.

Table 4-65: Corrosion tests varying fluoride in high calcium and alkalinity water at 45°C – Cessation concentrations

Run	Target fluoride (mg/l)	Test solution concentrations at cessation of corrosion tests									
		Fluoride dln) ⁽¹⁾ (mg/l as F ⁻)	pH ⁽¹⁾	Calcium ⁽²⁾ (mg/l as Ca ²⁺)	Magnesium ⁽²⁾ (mg/l as Mg ²⁺)	Total alkalinity ⁽¹⁾ (mg/l as CaCO ₃)	Chloride ⁽²⁾ (mg/l as Cl ⁻)	Sulphate dln) ⁽²⁾ (mg/l as SO ₄ ²⁻) x 10 ³	Sodium ⁽²⁾ (mg/l as Na ⁺)	Conductivity ⁽¹⁾ (µS/cm)	Total iron ⁽¹⁾ (mg/l as Fe ³⁺ (total))
253	0	0.7	7.82	51.6	0.2	54.8	3	0.72	109	924	8.5
254	10	7.5	7.89	47.9	0.2	56.7	3	0.72	119	956	12.2
255	20	7.6	7.95	38.4	0.3	67.2	3	0.70	126	960	13.0
256	40	0.0	8.12	24.3	0.2	87.0	3	0.00	148	968	13.2
257	70	0.0	8.47	11.1	0.2	130.3	21	0.83	187	1060	18.7
258	90	13.7	8.68	13.9	0.2	165.2	3	0.72	206	1124	17.0
259	0	1.1	7.83	62.3	0.4	61.8	5	0.85	113	888	5.7
260	10	10.5	7.88	59.2	0.4	61.5	4	0.85	127	924	8.5
261	20	8.7	7.95	46.7	0.3	64.4	4	0.87	143	916	5.9
262	40	9.3	8.10	27.0	0.3	86.6	5	0.41	161	932	12.0
263	70	13.7	8.45	15.1	0.3	129.8	4	0.87	206	1016	16.8
264	90	nt	8.68	nt	nt	167.6	nt	nt	nt	1076	21.4
343	0	< 0.1	6.50	62.6	0.186	54	3	< 0.01	115	972	8.79
344	10	10.9	7.10	54.6	0.194	60	3	0.00	127	956	4.02
345	20	7.9	7.15	43.2	0.198	98.1	4	0.81	140	944	5.065
346	40	nt	7.38	nt	nt	89.7	nt	nt	nt	956	6.695
347	70	11.2	7.87	10.3	0.185	119.1	4	0.75	204	1044	10.86
348	90	17.5	8.20	5.97	0.162	143.1	4	0.75	231	1108	6.535

Table 4-66: Corrosion coupon readings while varying fluoride in high calcium and alkalinity water at 45°C

Run	Target fluoride (mg/l as F ⁻)	Corrosion Coupon Results		
		Coupon 1 (mmpa)	Coupon 2 (mmpa)	Average (mmpa)
253	0	0.14	0.03	0.08
254	10	0.26	0.14	0.20
255	20	0.19	-0.06	0.06
256	40	0.25	0.11	0.18
257	70	0.39	0.32	0.36
258	90	0.52	0.47	0.50
259	0	0.13	0.12	0.12
260	10	0.19	0.20	0.19
261	20	0.18	0.09	0.14
262	40	0.28	0.23	0.25
263	70	0.53	0.32	0.43
264	90	0.64	0.58	0.61
343	0	0.14	0.05	0.10
344	10	0.08	-0.14	-0.03
345	20	0.04	0.06	0.05
346	40	0.38	0.38	0.38
347	70	0.53	0.17	0.35
348	90	0.46	0.49	0.48

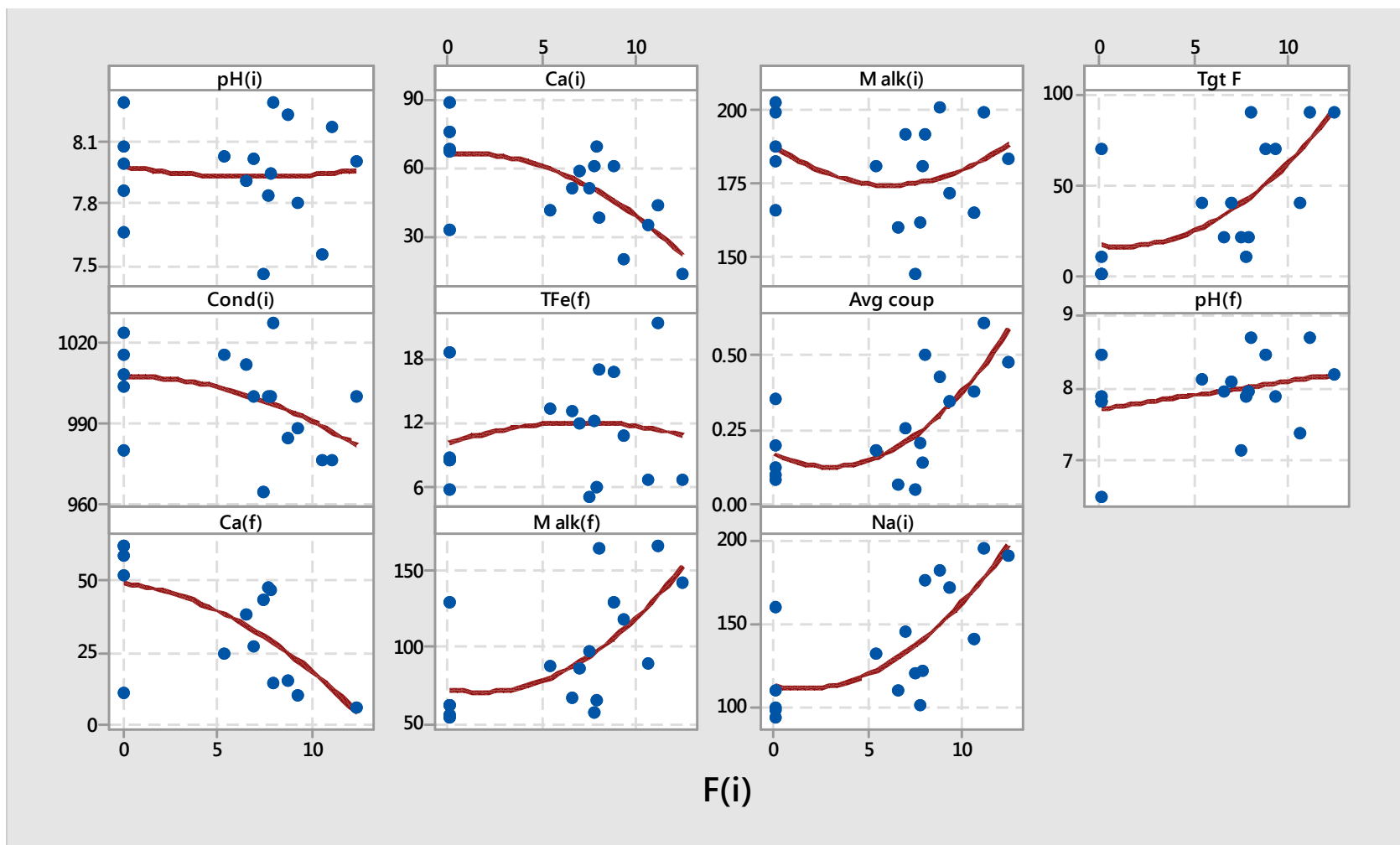


Figure 4-65: Scatterplots of the key variables versus the initial fluoride concentration ($F(i)$) at a calcium hardness of 120 mg/l as Ca^{2+} and a total alkalinity of 220 mg/l as $CaCO_3$

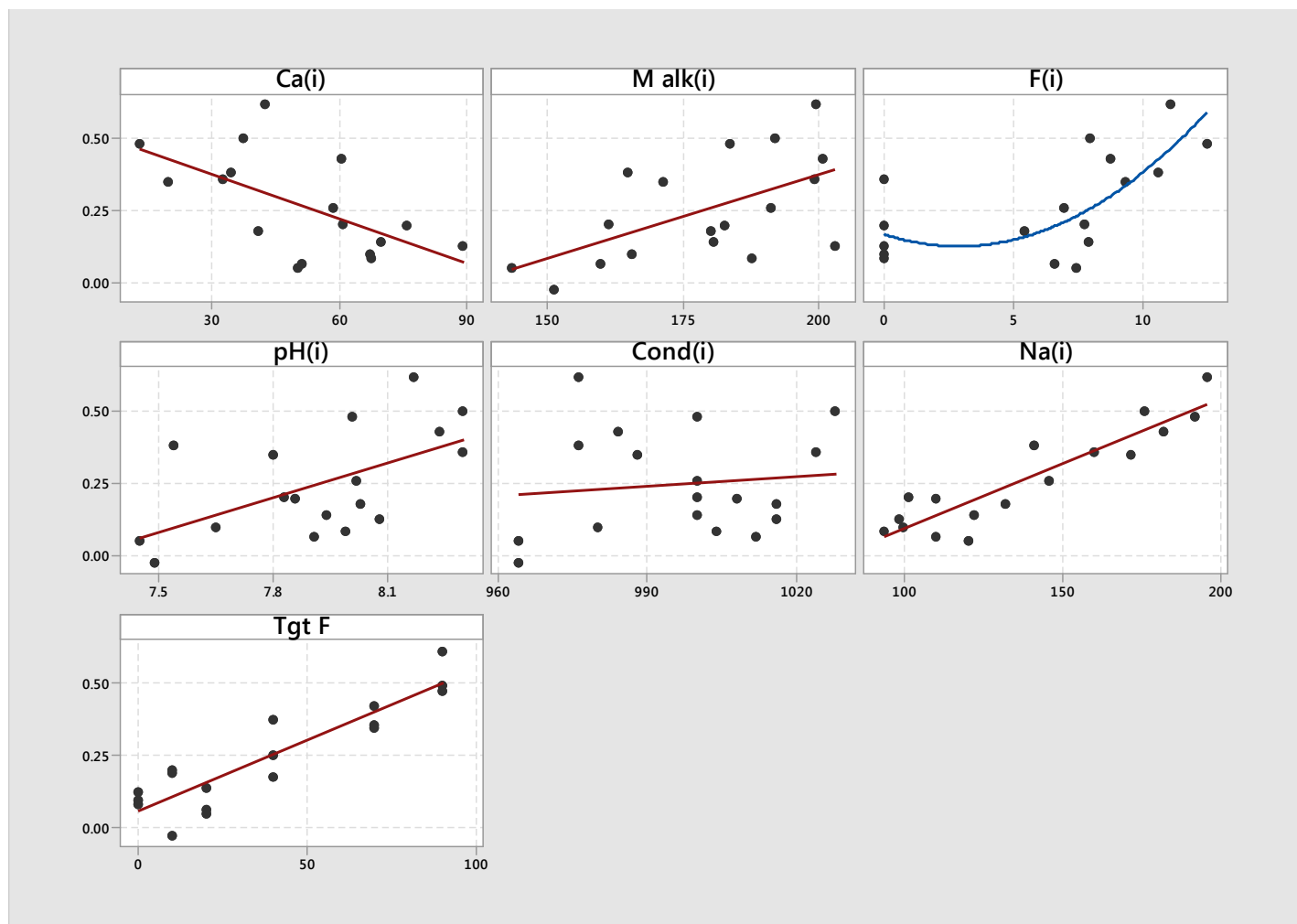


Figure 4-66: Scatterplots of the average corrosion rate (Avg coup) versus the key variables at a calcium hardness of 120 mg/l as Ca^{2+} and a total alkalinity of 220 mg/l as CaCO_3

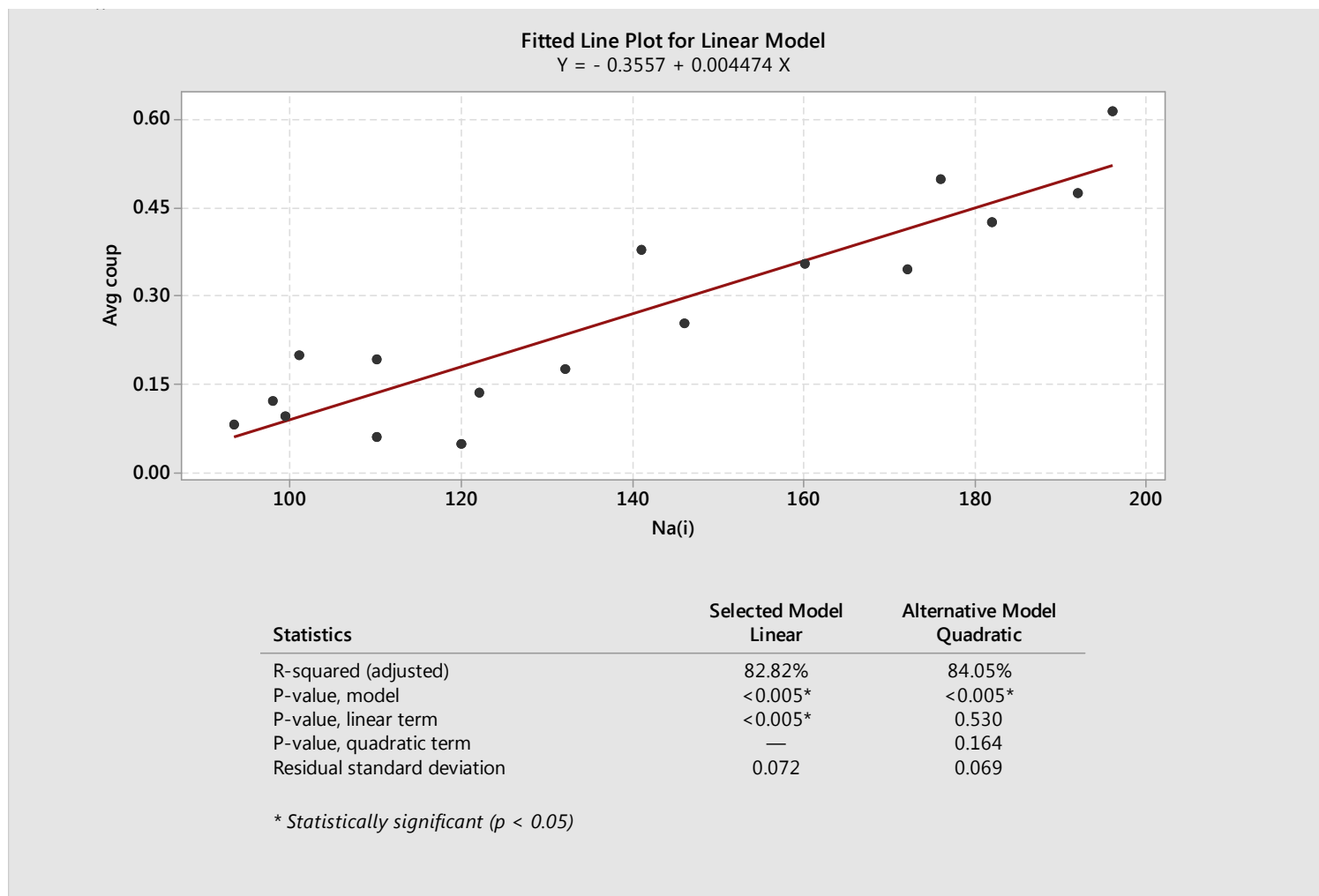


Figure 4-67: Regression for average corrosion rate (Avg coup) versus the initial sodium concentration (Na(i))

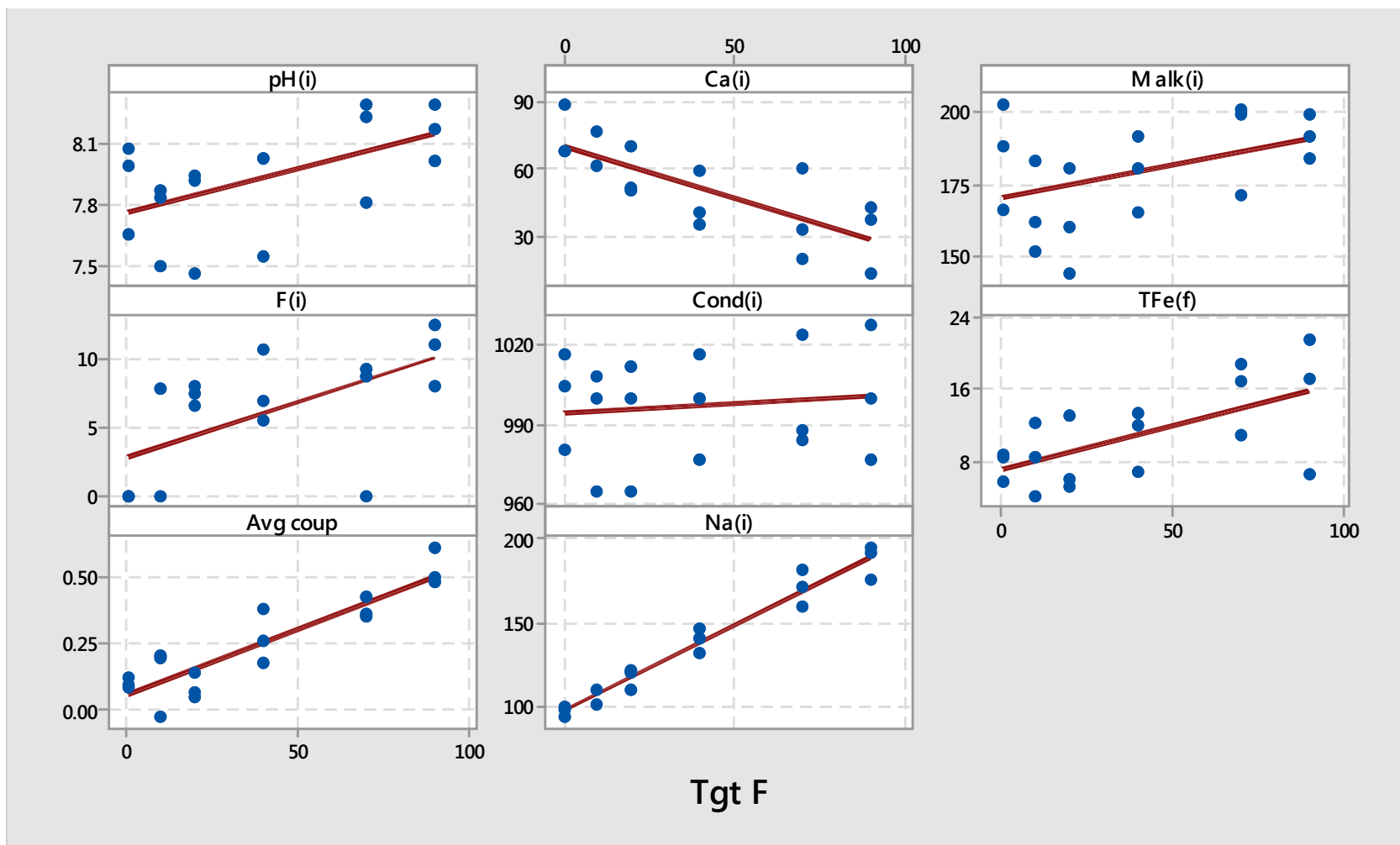


Figure 4-68: Scatterplots of the key variables versus the target fluoride concentration (Tgt F) at a calcium hardness of 120 mg/l as Ca^{2+} and a total alkalinity of 220 mg/l as CaCO_3

The average coupon corrosion rate was found to be moderately strong quadratically related to the initial fluoride concentration ($R^2(\text{adj}) = 43\%$) and extremely well correlated with sodium concentration ($R^2(\text{adj}) = 83\%$). Both ions are directly influenced by the incremental addition of sodium fluoride to the corrosion test solutions. Based on the Pearson correlation coefficients, the average coupon corrosion rate was also influenced by decreases in the calcium concentration and increases in the pH and total alkalinity, which were also associated with the sodium fluoride addition.

The concurrent decreases in the soluble calcium and fluoride levels prior to the corrosion tests, as evident in the low and decreasing residual fluoride levels and the decreasing calcium concentrations relative to the targeted fluoride levels (Table 4-64 and Figure 4-65), indicated the precipitation of calcium fluoride.

A comparison of the trends in the initial pH and initial total alkalinity results in Figures 4-65 and 4-68 indicated that although calcium fluoride precipitated, leaving substantially reduced soluble fluoride concentrations, the soluble fluoride levels and sodium concentrations did however continue to increase linearly with increased sodium fluoride addition. According to these two graphs the initial pH ($\text{pH}(\text{i})$) and initial total alkalinity ($\text{M alk}(\text{i})$) appeared to be correlated more by the sodium concentration ($\text{Na}(\text{i})$) than the soluble fluoride concentration ($\text{F}(\text{i})$) but the regression equations, Equations 4.20 and 4.21, indicated the fluoride had a greater impact than the initial sodium on the resulting initial pH and initial total alkalinity. The impact of the addition of sodium fluoride on the initial pH and total alkalinity, prior to the precipitation of the calcium fluoride, can be attributed to the complete dissociation of the salt into sodium and fluoride ions and the hydrolysis of the fluoride ion, the conjugate base of a weak acid, and the generation of hydroxide ions. Since the sodium ions are not susceptible to precipitation, unlike the fluoride ions, their concentrations remain high in line with the target fluoride concentrations, and they continue to contribute to the ionicity of the test solutions.

4.8.8 Series 8 - Low alkalinity and low calcium with high chloride and high sulphate

Sodium fluoride was added to deionized water with a target calcium hardness of 50 mg/l (as Ca^{2+}), total alkalinity of 55 mg/l (as CaCO_3), chloride concentration of 1000 mg/l (as Cl^-) and a sulphate concentration of 1500 mg/l (as SO_4^{2-}) at the concentrations given in Table 4-67 and the results of the water analyses shown in Table 4-68, along with the coupon corrosion rates in Table 4-69. The fluoride concentrations targeted were between 0 and 90 mg/l.

These corrosion tests, performed with deionized water containing low levels of calcium and alkalinity and high chloride and sulphate concentrations, indicated the following trends with increasing initial fluoride concentrations (Figure 4-69): a decreasing initial calcium concentration and initial pH, and an increasing initial sodium concentration and corrosion rate. Both the initial total alkalinity ($M_{\text{alk}}(i)$) and the final total alkalinity increased with the increasing initial fluoride concentration. It was also evident in Figure 4-69 that the initial fluoride level had decreased relative to the target fluoride concentration.

Regression models were considered to clarify the impacts of: a) only the initial fluoride concentration ($F(i)$) and b) the most significant variables. The following statistically significant equations (Equations 4.22 ($R^2 = 56\%$) and 4.23 ($R^2 = 91\%$) were produced:

$$\text{Average corrosion rate} = 0.3974 + 0.004522 F(i) \dots\dots\dots[4.22]$$

$$\begin{aligned} \text{Average corrosion rate} = & 504 - 0.00698 \times \text{Ca}(i) - 66.4 \times \text{pH}(i) - 0.401 \times \text{Na}(i) \\ & + 0.01481 \times \text{SO}_4(i) + 0.0529 \times \text{pH}(i) \times \text{Na}(i) - 0.000012 \times \text{Na}(i) \times \text{SO}_4(i) \\ & \dots\dots\dots[4.23] \end{aligned}$$

The linear relationship between the average corrosion rate and the initial fluoride concentration, given in Equation, 4.22 is illustrated in Figure 4-70.

Table 4-67: Corrosion tests varying fluoride in low calcium and alkalinity water with high chloride and sulphate concentrations at 45°C – Target and start-up concentrations

Run	Target fluoride (mg/l as F ⁻)	Test solution concentrations at start-up									
		Fluoride (25x diln) ⁽¹⁾ (mg/l as F ⁻)	pH ⁽¹⁾	Calcium ⁽²⁾ (mg/l as Ca ²⁺)	Magnesium ⁽²⁾ (mg/l as Mg ²⁺)	Total alkalinity ⁽¹⁾ (mg/l as CaCO ₃) as	Chloride ⁽²⁾ (mg/l as Cl ⁻)	Sulphate (25x diln) ⁽²⁾ (mg/l as SO ₄ ²⁻) x 10 ³	Sodium ⁽²⁾ (mg/l as Na ⁺)	Conductivity ⁽¹⁾ (µS/cm)	Total iron ⁽¹⁾ (mg/l as Fe ³⁺ (total))
271	0	4.79	7.93	50.7	0.3	60.9	956	1.56	1261	3000	> 0.01
272	10	8.55	7.93	48.2	0.3	56.7	722	1.26	1237	2592	< 0.01
273	20	18.4	7.90	47.3	0.2	59.3	849	1.40	1227	2704	< 0.01
274	40	27.5	7.87	39.4	0.3	58.1	914	1.56	1288	4720	< 0.01
275	70	31.4	7.83	18.1	0.3	62.3	768	1.10	1279	4804	< 0.01
276	90	53.6	7.84	10.9	0.3	60.5	986	1.45	1283	620	< 0.01
277	0	0.0	7.98	47.8	0.4	59.2	920	1.49	1240	5724	< 0.01
278	10	9.3	7.98	47.4	0.4	57.5	822	1.42	1249	5756	< 0.01
279	20	17.5	7.94	47.7	0.3	58.7	865	1.42	1257	5756	< 0.01
280	40	29.0	7.94	37.0	0.4	62.4	878	1.43	1223	5748	< 0.01
281	70	35.0	7.88	17.5	0.5	58.9	817	1.28	1264	5740	< 0.01
282	90	49.6	7.83	9.0	0.3	63.2	897	1.32	1277	5708	< 0.01
283	0	9.4	7.90	49.2	0.3	56.7	894	1.45	1258	5952	< 0.01
284	10	10.0	8.02	48.6	0.3	61.4	798	1.30	1257	5720	< 0.01
285	20	23.9	7.97	48.2	0.3	58.4	843	1.39	1267	5772	< 0.01
286	40	48.6	7.96	46.2	0.3	63.2	861	1.42	1272	5740	< 0.01
287	70	43.1	7.89	18.2	0.3	60.3	821	1.32	1295	5764	< 0.01
288	90	75.8	7.86	9.4	0.2	62.5	827	1.30	1256	5724	< 0.01

Notes: 1. Test conducted in Laboratory B, 2. Test conducted in Laboratory C, nt = not tested.

Table 4-68: Corrosion tests varying fluoride in low calcium and alkalinity water with high chloride and sulphate concentrations at 45°C – Cessation concentrations

Run	Target fluoride (mg/l as F ⁻)	Test solution concentrations at cessation of corrosion tests									
		Fluoride (25x diln) ⁽¹⁾ (mg/l as F ⁻)	pH ⁽¹⁾	Calcium ⁽²⁾ (mg/l as Ca ²⁺)	Magnesium ⁽²⁾ (mg/l as Mg ²⁺)	Total alkalinity ⁽¹⁾ (mg/l as CaCO ₃)	Chloride ⁽²⁾ (mg/l as Cl ⁻)	Sulphate (25x diln) ⁽²⁾ (mg/l as SO ₄ ²⁻) x 10 ³	Sodium ⁽²⁾ (mg/l as Na ⁺)	Conductivity ⁽¹⁾ (µS/cm)	Total iron ⁽¹⁾ (mg/l as Fe ³⁺ (total))
271	0	2.43	8.22	55.0	0.5	55.7	1031	1.78	1500	464	15.7
272	10	11.6	8.23	52.2	0.4	54.8	1039	1.76	1445	3820	16.5
273	20	22.1	8.18	51.6	0.4	55.4	1122	2.03	1462	3548	18.7
274	40	23	8.26	38.7	0.4	62.8	957	1.67	1474	4252	17.2
275	70	40	8.56	12.0	0.3	84.9	1181	1.64	1477	4312	16.5
276	90	49	8.46	5.8	0.3	74.4	933	1.30	1452	1708	13.0
277	0	1.1	8.32	48.4	0.5	54.5	1729	2.84	1430	6756	18.0
278	10	11.1	8.29	50.1	0.5	58.5	1237	2.00	1473	6676	18.6
279	20	25.8	8.22	49.8	0.3	59.2	1603	2.66	1511	6704	18.4
280	40	27.1	8.34	31.8	0.4	63.4	1330	2.19	1489	6640	11.9
281	70	43.8	8.51	11.5	0.4	74.8	1262	2.08	1548	6748	14.6
282	90	58.3	8.49	5.6	0.4	71.4	1182	1.94	1524	6588	9.7
283	0	2.0	8.27	52.4	0.5	53.4	1054	2.02	1535	6816	13.9
284	10	13.2	8.31	50.8	0.4	57.1	969	1.57	1491	6708	16.6
285	20	22.1	8.30	49.5	0.3	57.7	1018	1.57	1478	6724	18.9
286	40	33.0	8.32	31.0	0.4	62.2	933	1.53	1440	6604	17.2
287	70	48.6	8.48	11.8	0.3	68.3	973	1.46	1519	6688	13.7
288	90	68.7	8.50	6.9	0.3	70.1	927	1.50	1524	6620	13.5

Table 4-69: Corrosion coupon readings while varying fluoride in low calcium and alkalinity water with high chloride and sulphate concentrations at 45°C

Run	Target fluoride (mg/l as F ⁻)	Corrosion Coupon Results		
		Coupon 1 (mmpa)	Coupon 2 (mmpa)	Average (mmpa)
271	0	0.41	0.46	0.43
272	10	0.34	0.44	0.39
273	20	0.44	0.41	0.42
274	40	0.45	0.32	0.38
275	70	0.56	0.66	0.61
276	90	0.64	0.66	0.65
277	0	0.39	0.46	0.42
278	10	0.46	0.33	0.40
279	20	0.51	0.58	0.55
280	40	0.56	0.39	0.47
281	70	0.64	0.65	0.65
282	90	0.64	0.70	0.67
283	0	0.51	0.48	0.49
284	10	0.45	0.48	0.46
285	20	0.46	0.53	0.50
286	40	0.53	0.48	0.50
287	70	0.66	0.68	0.67
288	90	0.69	0.68	0.69

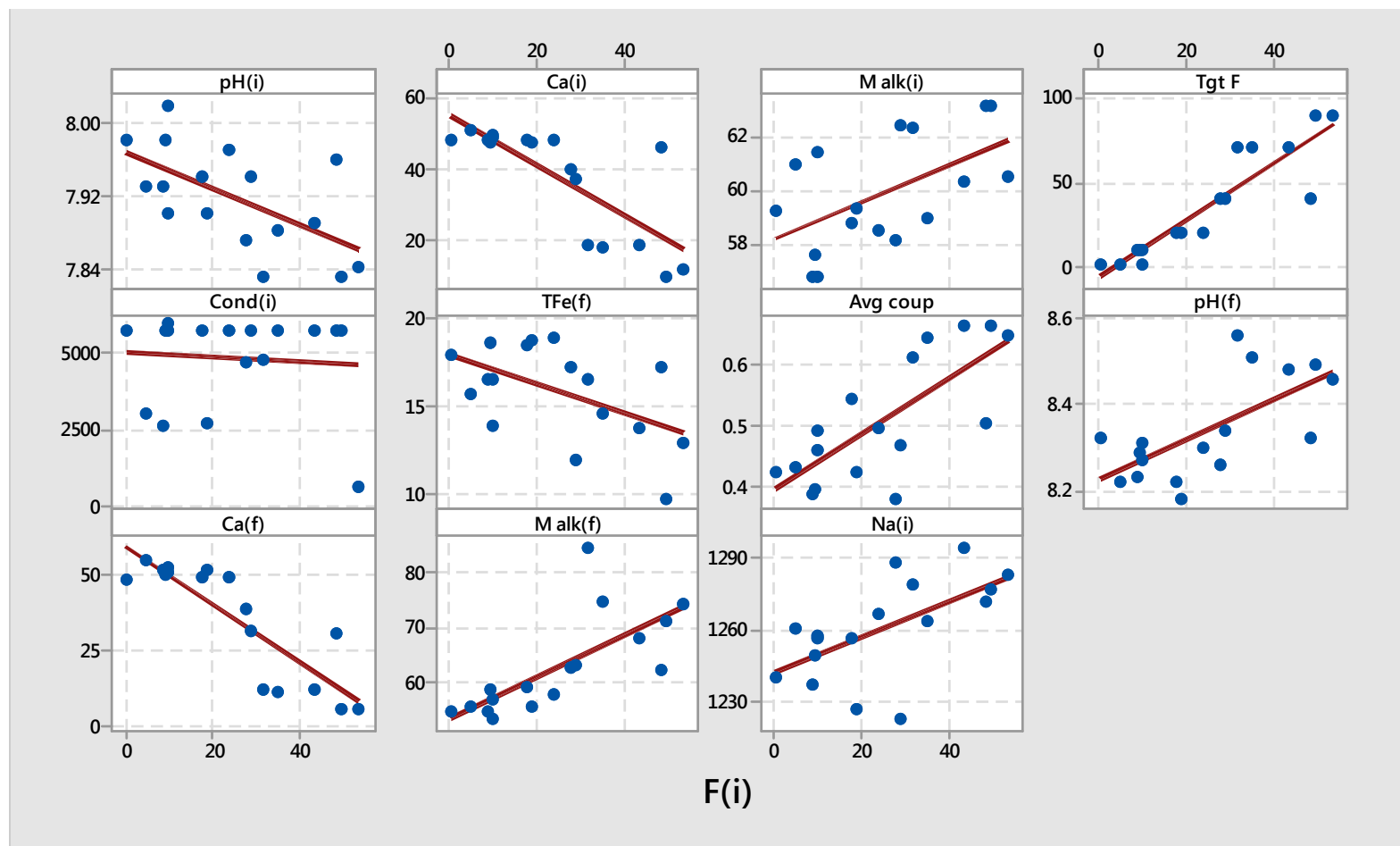


Figure 4-69: Scatterplots of the key variables versus the initial fluoride concentration ($F(i)$) at a calcium hardness of 50 mg/l as Ca^{2+} , total alkalinity of 55 mg/l as CaCO_3 , initial chloride concentration of 1000 mg/l as Cl^- and initial sulphate concentration of 1500 mg/l as SO_4^{2-}

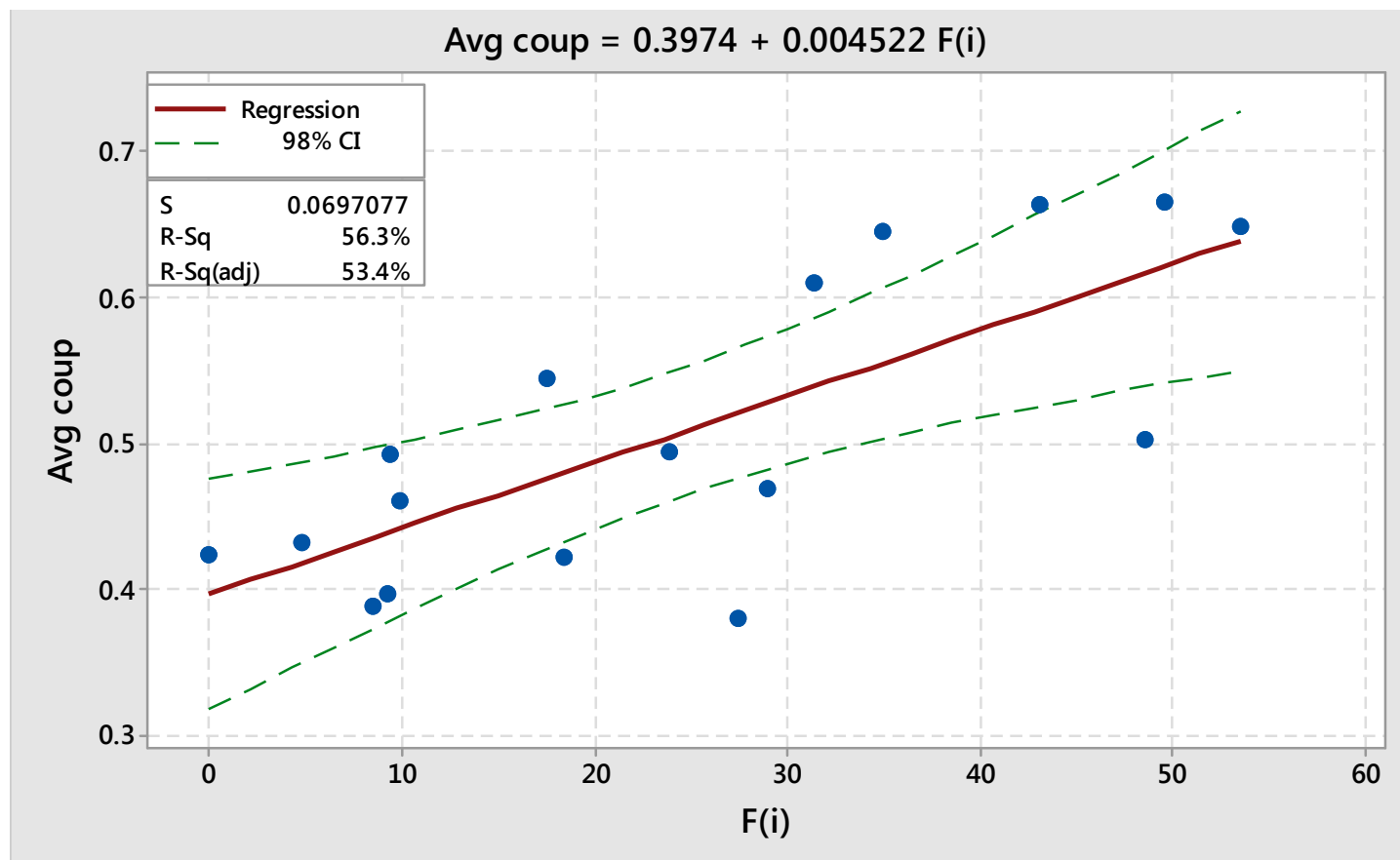


Figure 4-70: Fitted line plot for the average corrosion rate (Avg coup) versus the initial fluoride concentration (F(i)) at a calcium hardness of 50 mg/l as Ca^{2+} , total alkalinity of 55 mg/l as CaCO_3 , initial chloride concentration of 1000 mg/l as Cl^- and initial sulphate concentration of 1500 mg/l as SO_4^{2-}

A comparison of the Pearson correlation coefficients of the statistically significant relationships between the average coupon corrosion rate and initial chemistry variables showed that other than the initial fluoride concentration ($r = 0.75$), there were three other variables, namely the initial calcium ($r = -0.86$), the initial pH ($r = -0.61$), and the initial sodium concentration ($r = 0.59$) that had significant relationships with the corrosion rate. The p values for these variables indicated the lack of statistically significant linear relations between the corrosion rate and the initial total alkalinity and initial conductivity. Regression analyses of the correlation of the initial calcium ($R^2 = 75\%$), initial sodium ($R^2 = 35\%$), initial alkalinity ($R^2 = 19\%$), initial fluoride ($R^2 = 56\%$) and initial conductivity ($R^2 = <1\%$) on the average coupon corrosion rate showed that the initial calcium and initial fluoride concentrations had the largest influence, as individual parameters, on the corrosion rate.

The best fit regression model was however obtained with a different set of parameters (Equation 4.23) ($R^2 = 91\%$), namely the initial sodium, initial pH, initial calcium and initial sulphate concentration. The outcome of this series differed slightly from the previous series, where no chloride and sulphate were added (i.e. series 6), in that the total alkalinity was not considered to be a significant factor in its impact on the average corrosion rate.

4.8.9 Series 9 - High alkalinity and calcium with high chloride and high sulphate

Sodium fluoride was added to deionized water with a target calcium hardness of 120 mg/l (as Ca^{2+}), total alkalinity of 220 mg/l (as CaCO_3), chloride concentration of 1000 mg/l (as Cl^-) and a sulphate concentration of 1500 mg/l (as SO_4^{2-}) at the concentrations given in Table 4-70 and the results of the water analyses shown in Table 4-71, along with the coupon corrosion rates in Table 4-72. The fluoride concentrations targeted ranged between 0 and 90 mg/l.

The results of the corrosion tests performed with deionized water containing high levels of calcium and high total alkalinity with high chloride and indicated a

moderate strong positive correlation ($P = 0.02$, Pearson = 0.690) between the average corrosion rate and the initial sodium concentration (Na(i)) (Figure 4-72). Statistically significant correlations were also detected between the average corrosion rate and the initial fluoride concentration ($P = 0.046$, Pearson = 0.501).

Moderate strong positive correlations were also noted between the initial conductivity (Cond (i)) and the total alkalinity (M alk(i)) ($P = 0.013$, Pearson = 0.573) as well as between the initial conductivity and the initial calcium (Ca(i)) concentration ($P = 0.025$, Pearson = 0.526).

A strong positive linear correlation was noted between the initial calcium and initial total alkalinity ($P = 0.001$ Pearson = 0.812).

The initial pH (pH(i)) was strong negatively correlated with the target fluoride concentration ($P = 0.001$, Pearson = -0.841) and strong positively correlated with the initial calcium ($P = 0.001$, Pearson = 0.849) and initial total alkalinity ($P = 0.001$, Pearson = 0.800).

Strong negative correlations were also apparent between the target fluoride and both the initial calcium concentration ($P = 0.001$, Pearson = -0.987) and the initial total alkalinity ($P = 0.001$, Pearson = -0.789) (Figure 4-71).

Figure 4-72 also indicated the reduced fluoride solubility relative to the target fluoride concentration. Almost all of the fluoride residuals were less than 20 mg/l as F⁻ for the entire targeted fluoride range investigated (i.e. 0 - 90 mg/l F⁻).

A regression analysis for the average corrosion rate led to the linear model (Equation 4.24) with R^2 (adj) value of 77%:

$$\text{Average corrosion rate} = -3.385 + 0.000817 \times \text{Na(i)} + 0.2312 \times \text{F(i)} + 0.01246 \times \text{M alk(i)} - 0.000894 \times \text{F(i)}^2 - 0.0000992 \times \text{F(i)} \times \text{M alk(i)} \dots [4.24]$$

Table 4-70: Corrosion tests varying fluoride in high calcium and alkalinity water with high chloride and sulphate concentrations at 45°C – Target and start-up concentrations

Run	Target Fluoride (mg/l as F ⁻)	Test solution concentrations at start-up									
		Fluoride (25x diln) ⁽¹⁾ (mg/l as F ⁻)	pH ⁽¹⁾	Calcium ⁽²⁾ (mg/l as Ca ²⁺)	Magnesium ⁽²⁾ (mg/l as Mg ²⁺)	Total alkalinity ⁽¹⁾ (mg/l as CaCO ₃)	Chloride ⁽²⁾ (mg/l as Cl ⁻)	Sulphate (25x diln) ⁽²⁾ (mg/l as SO ₄ ²⁻) x 10 ³	Sodium ⁽²⁾ (mg/l as Na ⁺)	Conductivity ⁽¹⁾ (µS/cm)	Total iron ⁽¹⁾ (mg/l as Fe ³⁺ (total))
289	0	1.2	8.46	107.0	0.4	213.2	887	1.43	1277	6196	< 0.01
290	10	8.9	8.48	105.0	0.3	222.8	795	1.29	1322	6224	< 0.01
291	20	13.6	8.30	87.0	0.3	205.0	851	1.38	1264	6220	< 0.01
292	40	12.4	8.35	72.2	0.4	208.4	865	1.31	1321	6152	< 0.01
293	70	17.5	8.34	49.7	0.3	199.6	935	1.39	1333	6104	< 0.01
294	90	20.8	8.24	29.7	0.3	207.3	883	1.30	1332	6024	< 0.01
295	0	< 0.1	8.34	108.0	0.4	216.7	949	1.31	1322	6148	< 0.01
296	10	11.6	8.37	107.0	0.4	211.8	710	1.05	1332	6127	< 0.01
297	20	14.4	8.35	96.7	0.4	212.0	803	1.29	1338	6200	< 0.01
298	40	11.8	8.29	72.9	0.4	215.8	837	1.41	1356	6116	< 0.01
299	70	9.3	8.19	49.1	0.4	206.3	784	1.28	1318	6068	< 0.01
300	90	13.7	8.13	33.2	0.3	191.2	864	1.37	1364	6028	< 0.01
301	0	< 0.1	8.39	98.5	0.5	214.1	947	1.26	1276	5928	< 0.01
302	10	7.1	8.40	94.0	0.4	216.2	796	1.12	1269	5944	< 0.01
303	20	13.8	8.32	86.0	0.4	207.7	873	1.18	1270	5936	< 0.01
304	40	8.3	8.30	64.8	0.4	200.8	851	1.15	1275	5892	< 0.01
305	70	10.7	8.20	44.6	0.3	193.3	875	1.18	1286	5816	< 0.01
306	90	13.4	8.19	28.3	0.4	191.7	812	1.11	1276	5792	< 0.01

Notes: 1. Test conducted in Laboratory B, 2. Test conducted in Laboratory C, nt = not tested.

Table 4-71: Corrosion tests varying fluoride in low calcium and alkalinity water with high chloride and sulphate concentrations at 45°C – Cessation concentrations

Run	Target fluoride (mg/l as F ⁻)	Test solution concentrations at cessation of corrosion tests									
		Fluoride (25x diln) ⁽¹⁾ (mg/l as F ⁻)	pH ⁽¹⁾	Calcium ⁽²⁾ (mg/l as Ca ²⁺)	Magnesium ⁽²⁾ (mg/l as Mg ²⁺)	Total alkalinity ⁽¹⁾ (mg/l as CaCO ₃)	Chloride ⁽²⁾ (mg/l as Cl ⁻)	Sulphate (25x diln) ⁽²⁾ (mg/l as SO ₄ ²⁻) x 10 ³	Sodium ⁽²⁾ (mg/l as Na ⁺)	Conductivity ⁽¹⁾ (µS/cm)	Total iron ⁽¹⁾ (mg/l as Fe ³⁺ (total))
289	0	0.5	8.24	78.3	0.5	131.1	1048	1.68	1529	6728	15.4
290	10	8.7	8.19	73.7	0.4	131.1	905	1.40	1456	7052	19.8
291	20	10.7	8.21	68.1	0.4	129.3	926	1.55	1476	6928	8.9
292	40	12.3	8.26	50.8	0.4	133.2	974	1.54	1470	6868	9.2
293	70	13.9	8.44	24.1	0.4	153.8	904	1.49	1516	7008	13.1
294	90	20.1	8.62	15.2	0.3	184.0	899	1.43	1543	6872	13.3
295	0	< 0.1	8.19	81.0	0.6	124.7	997	1.58	1588	7080	20.2
296	10	9.2	8.17	78.4	0.5	118.6	838	1.30	1586	7052	13.9
297	20	9.5	8.15	73.6	0.5	118.1	957	1.51	1591	7020	17.0
298	40	13.2	8.26	46.9	0.5	136.0	924	1.48	1519	6860	12.4
299	70	13.5	8.45	21.8	0.5	146.8	907	1.66	1627	7004	14.9
300	90	19.6	8.59	14.6	0.4	173.6	965	1.41	1565	6784	20.5
301	0	< 0.1	8.19	81.6	0.5	115.7	1087	1.47	1566	6884	15.7
302	10	7.2	8.17	79.0	0.5	115.7	883	1.17	1537	6820	18.1
303	20	15.4	8.15	74.0	0.5	110.1	1093	1.45	1531	6808	7.5
304	40	9.4	8.24	51.4	0.5	122.5	911	1.20	1519	6660	12.4
305	70	14.1	8.43	22.5	0.4	142.3	1020	1.37	1581	6808	15.8
306	90	17.2	8.58	13.6	0.3	167.6	1069	1.34	1515	6556	13.5

Table 4-72: Corrosion coupon readings while varying fluoride in high calcium and alkalinity water with high chloride and sulphate concentrations at 45°C

Run	Target fluoride (mg/l as F ⁻)	Corrosion Coupon Results		
		Coupon 1 (mmpa)	Coupon 2 (mmpa)	Average (mmpa)
289	0	0.34	0.27	0.31
290	10	0.56	0.49	0.52
291	20	0.55	0.29	0.42
292	40	0.51	0.41	0.46
293	70	0.61	0.39	0.50
294	90	0.59	0.30	0.45
295	0	0.49	0.33	0.41
296	10	0.54	0.41	0.47
297	20	0.48	0.34	0.41
298	40	0.51	0.42	0.46
299	70	0.58	0.39	0.49
300	90	0.49	0.52	0.51
301	0	0.40	0.25	0.32
302	10	0.50	0.29	0.40
303	20	0.32	0.11	0.21
304	40	0.45	0.31	0.38
305	70	0.52	0.26	0.39
306	90	0.37	0.47	0.42

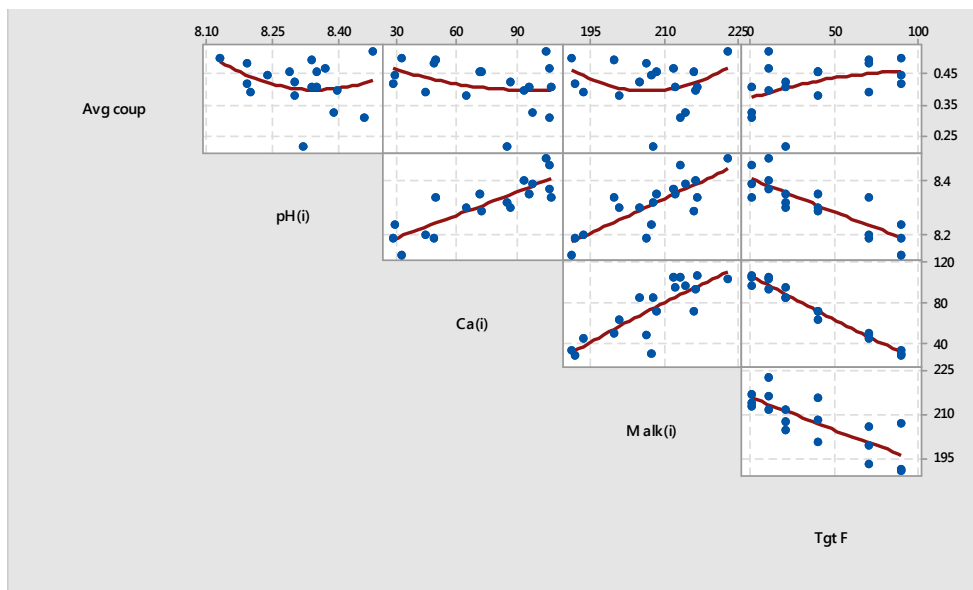


Figure 4-71: First matrix plot of the key variables at a calcium hardness of 120 mg/l as Ca^{2+} , total alkalinity of 220 mg/l as CaCO_3 , initial chloride concentration of 1000 mg/l as Cl^- and initial sulphate concentration of 1500 mg/l as SO_4^{2-}

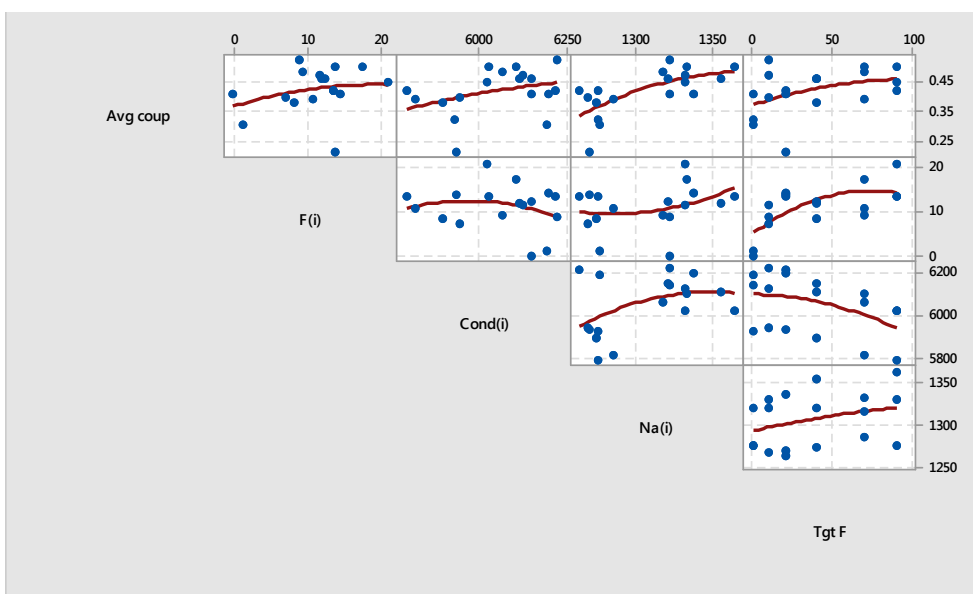


Figure 4-72: Second matrix plot of the key variables at a calcium hardness of 120 mg/l as Ca^{2+} , total alkalinity of 220 mg/l as CaCO_3 , initial chloride concentration of 1000 mg/l as Cl^- and initial sulphate concentration of 1500 mg/l as SO_4^{2-}

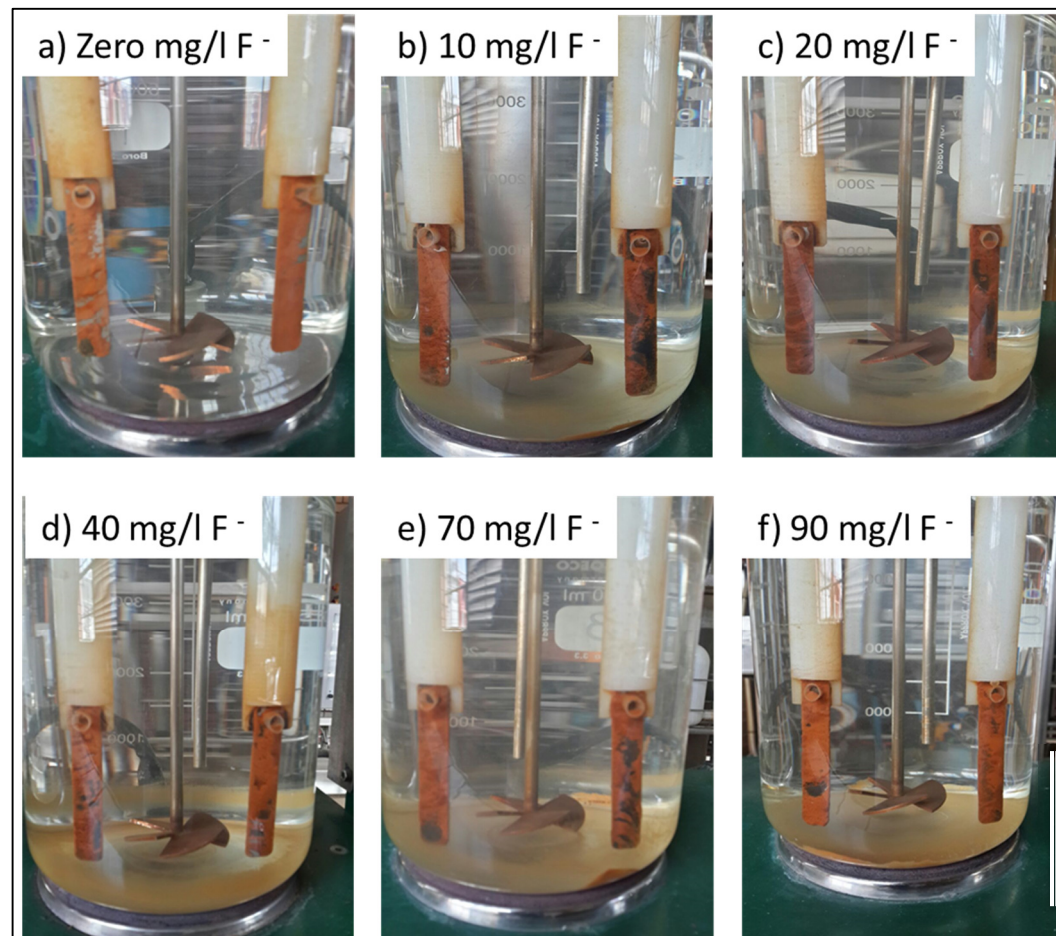


Figure 4-73: Photographs of test solutions illustrating larger volumes of precipitate (calcium fluoride and corrosion products) with increasing fluoride addition (scale bar: 100 mm)

Figure 4-73 illustrates the extent of precipitation of the calcium fluoride and corrosion products with increasing fluoride concentrations. The coupons were not markedly different in appearance.

Based on the linear correlations and the matrix plots it was revealed the average coupon corrosion rate was mostly influenced by the initial sodium, initial fluoride and initial total alkalinity. A regression model with an R^2 (adj) value of 77% was realised (Equation 4.24).

It also became apparent that the initial calcium and initial total alkalinity were very positively correlated with each other and inversely related to the target fluoride concentration. These findings were supported by the perceived increased turbidity and precipitation observed during the experiments with the increased fluoride addition. It was therefore established that the precipitation was attributed to the development of insoluble calcium fluoride.

4.8.10 Regression analysis of the laboratory data generated in section 4.8 (series 1-9)

The data collated in section 4.8 was analysed using the Minitab® software and the results reported below. The main focus of this section was to examine the impact the changes in the parameters had on the average coupon corrosion rate with each series.

The results are summarized in Table 4-73. It was evident that the corrosion rate depended predominantly on the following four parameters: alkalinity, conductivity, fluoride, and sodium. When the test solution contained little to nil calcium hardness that they were more likely to contain a broader range of residual fluoride concentrations (Figures 4-74, 4-77 and 4-81). Test solutions dosed with 50 mg/l of calcium were found to contain no higher than 30 mg/l of fluoride. When chloride (1000 mg/l Cl^-) and sulphate (1500 mg/l SO_4^{2-}) were included, the fluoride solubility increased to 42 mg/l. Similarly with the addition of a high calcium concentration at 120 mg/l as Ca^{2+} , the fluoride residuals reduced to < 10 mg/l

(Figure 4-77). As in the preceding, tests the addition of high concentrations of sulphate and chloride again increased the fluoride solubility, up to 15 mg/l in solution (Figure 4-81). It was observed (Table 4-73) that the series with a low target calcium hardness (50 mg/l as Ca^{2+}) resulted in regression models containing the initial calcium concentration as one of its variables. Often the initial pH, initial total alkalinity and sometimes sodium also featured in these corrosion prediction regression models. In most of the high calcium series sodium was the most dominant parameter to influence corrosion.

From Table 4-73, in the three cases where fluoride featured in corrosion prediction regression models (namely the series with: only fluoride, high total alkalinity or high calcium) only for the first two did the initial fluoride concentration have a significantly strong influence on the coupon corrosion rate.

Although the series with high chloride and sulphate produced the expected highest levels of salinity in terms of conductivity (Figure 4-82) and sodium (Figure 4-83), and their impact on corrosion was highly prominent, they were not the cause of the highest corrosion rates observed amongst the series (Figure 4-75). The low and high total alkalinity series produced the highest corrosion rates.

Table 4-73: Summary of the outcomes of Section 4.8

Series	Key parameters correlating with corrosion
1. Fluoride only	<p>R^2 of 55% for fluoride as a single variable quadratic model.</p> <p>R^2 values for the other variables alone: sodium (73%) > conductivity (56%) > total alkalinity (18%).</p> <p>R^2 of 85% for a calcium, magnesium and fluoride based model. Substituting the fluoride with either sodium, conductivity or total alkalinity produced slightly lower R^2 values.</p>
2. Low M alkalinity	<p>R^2 of 38% for fluoride as a single variable model.</p> <p>R^2 values for the other variables alone: total alkalinity (47%) > conductivity (36%) and sodium (36%).</p> <p>R^2 of 76% for a conductivity and total alkalinity based model.</p>
3. High M alkalinity	<p>Regression analyses for the following as single variables models: conductivity ($R^2 = 62\%$) > fluoride (R^2 of 57%) > sodium ($R^2 = 38\%$).</p> <p>R^2 of 96% for a conductivity, pH and fluoride based model. Substituting the fluoride with sodium in this regression equation did not produce a comparably good fit.</p>
4. Low calcium	<p>The regression model, based on calcium, pH and total alkalinity produced the best fit ($R^2 = 72\%$) but was not statistically significant ($p = 0.162$) due to the limited sample size ($n = 17$).</p>
5. High calcium	<p>R^2 of 45% for a total alkalinity and fluoride based model.</p> <p>Precipitation was observed and indicated to be calcium fluoride on the basis of the low residual fluoride (8 mg/l as F^-) and calcium concentrations (20 mg/l as Ca^{2+}).</p>

continuation of Table 4-73	
6. Low calcium and M alkalinity	<p>R^2 of 87.2% for a total alkalinity, pH, calcium and fluoride based model.</p> <p>R^2 of 87.7% for a total alkalinity, pH, calcium and conductivity based model.</p> <p>R^2 of 94.3% for a total alkalinity, pH, calcium and sodium based model.</p>
7. High calcium and M alkalinity	<p>R^2 of 83% for sodium only based model.</p> <p>Precipitation was observed and indicated to be calcium fluoride on the basis of the lower fluoride and calcium residuals. Sodium and fluoride residuals did however continue to increase with increased sodium fluoride addition.</p>
8. Low calcium and M alkalinity with high sulphate and chloride	<p>R^2 of 75% for calcium and 56% for fluoride as single variable models.</p> <p>R^2 of 91% for a calcium, sodium, pH and sulphate based model. The total alkalinity did not feature in the model.</p>
9. High calcium and M alkalinity with high sulphate and chloride	<p>R^2 of 45% for sodium only based model. Precipitation was observed and attributed to be calcium fluoride precipitation.</p> <p>R^2 of 77% for a sodium, fluoride and total alkalinity based model.</p>

Scatterplots of the average corrosion rate (Avg coup) versus the various parameters at the start-up of the corrosion tests demonstrated there were four main clusters of data and these groups have been described in Table 4-74 and illustrated in Figure 4-74.

Table 4-74: Scatterplots of the clusters and their relative positions

Description of the Cluster	pH range	Calcium range (mg/l as Ca ²⁺)	Total alkalinity range (mg/l as CaCO ₃)	Fluoride range (mg/l as F ⁻)
1. Low pH and moderate corrosion (Black)	4.0 – 6.0	-	0 - 21	-
2. Moderate pH and low corrosion (Yellow)	7.4 – 8.5	20 - 120	143 - 220	0 - 14
3. Moderate pH and high corrosion (Brown)	7.4 - 8.5	0 - 20	52 - 84	0 - 100
4. High pH high corrosion (Red)	8.56 – 9.16	< 4.0	220 - 270	0 - 100

Figure 4-75 shows the average coupon corrosion rate (Avg coup) for the different series allowed for a classification of the series based on the ranges of their corrosion rates, (Table 4-75). Figures 4-76 and 4-77 show the corrosion rates versus the target fluoride concentration and initial fluoride concentration respectively for the entire series, demonstrating the impact of the calcium hardness, alkalinity and the presence of high levels of sulphate and chloride.

To assist in the understanding of the impact of these ions on the average corrosion rate, Figures 4-78 to 4-83 illustrate the impact of the ions on the each other. Unexpectedly, the low and high alkalinity series produced the highest corrosion rates but this occurrence may have been due to the resultant high test solution pH values (Figure 4-78).

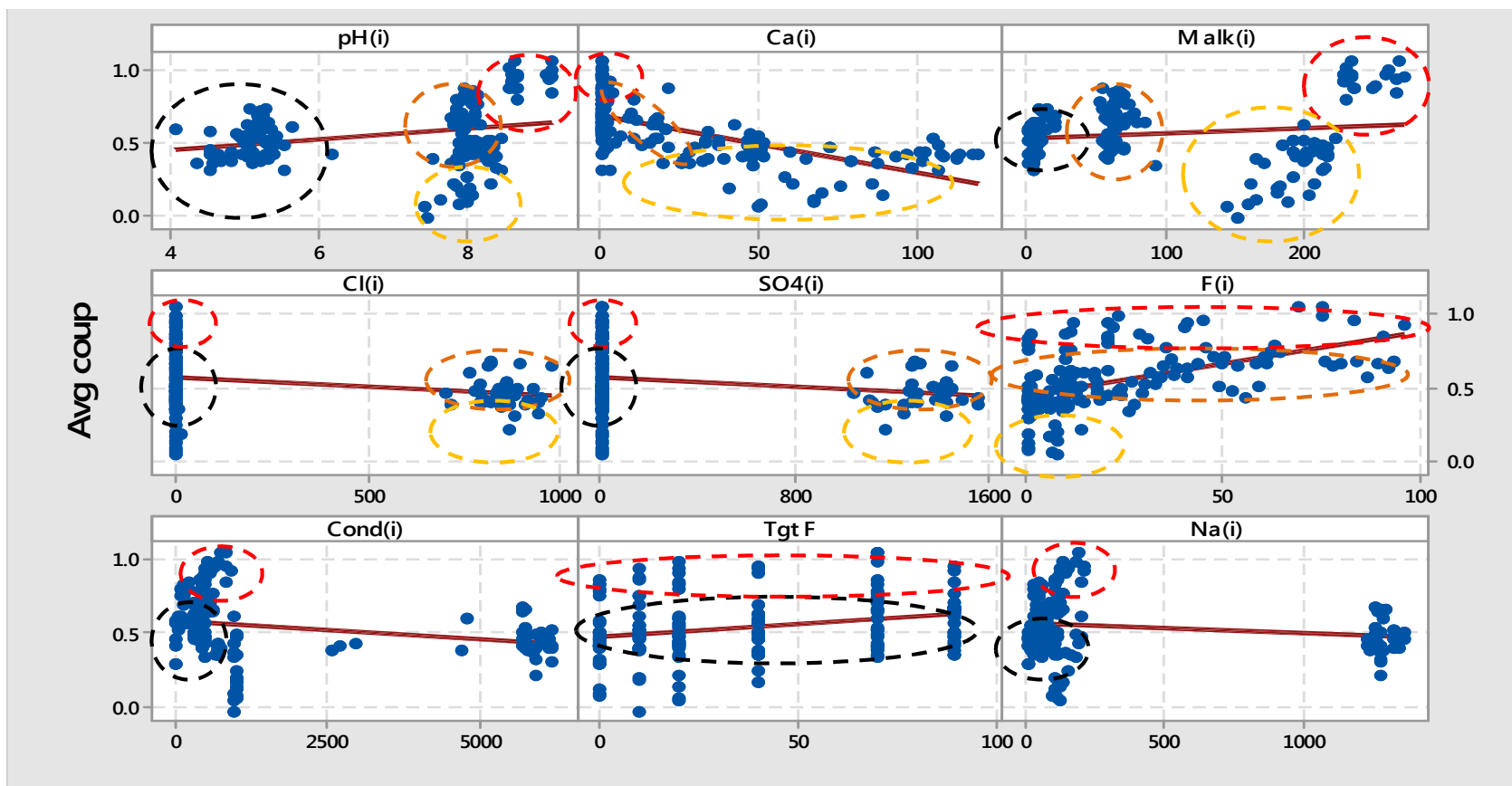


Figure 4-74: Scatterplots of average corrosion rate (Avg coup) in mmpa versus the various parameters at the start-up of the corrosion tests indicating the corresponding clusters

Note: Black. low pH, Yellow. slightly alkaline low corrosion, Brown. slightly alkaline high corrosion, Red. high pH high corrosion.

Table 4-75: Grouping of the series based on the range of their corrosion rates

Description of Corrosion range grouping (based on the average corrosion rate in mmpa)	Fluoride corrosion test series
a) Low (0.1 -0.4)	High calcium and M alkalinity.
b) Moderate (0.4 – 0.7)	Fluoride only Low calcium Low calcium and M alkalinity High calcium Low calcium and M alkalinity with high sulphate and chloride High calcium and M alkalinity with high sulphate and chloride
c) High (0.6 – 0.8)	Low M alkalinity
d) Very high (0.8 – 1.2)	High M alkalinity

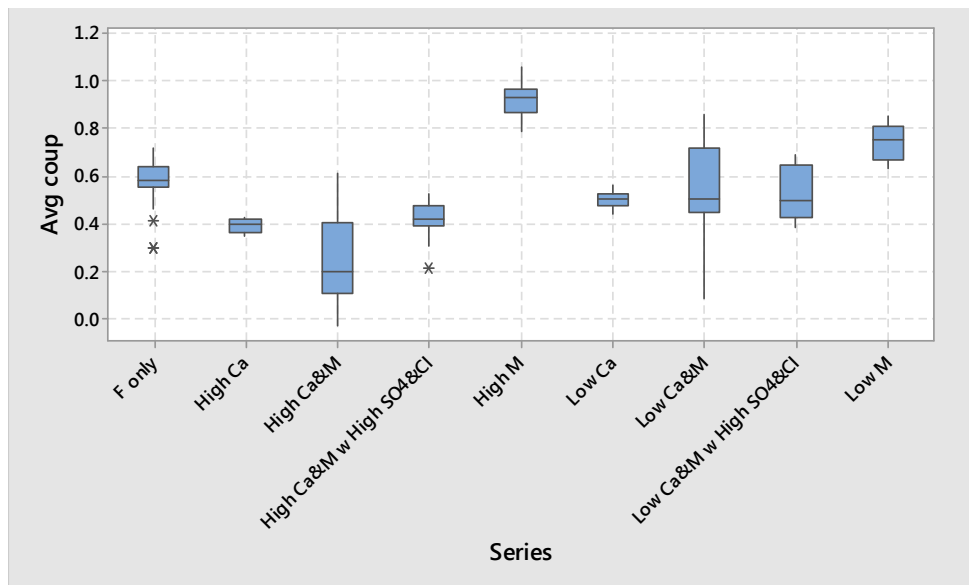


Figure 4-75: Box plot of the average corrosion rate (Avg coup) for the different series

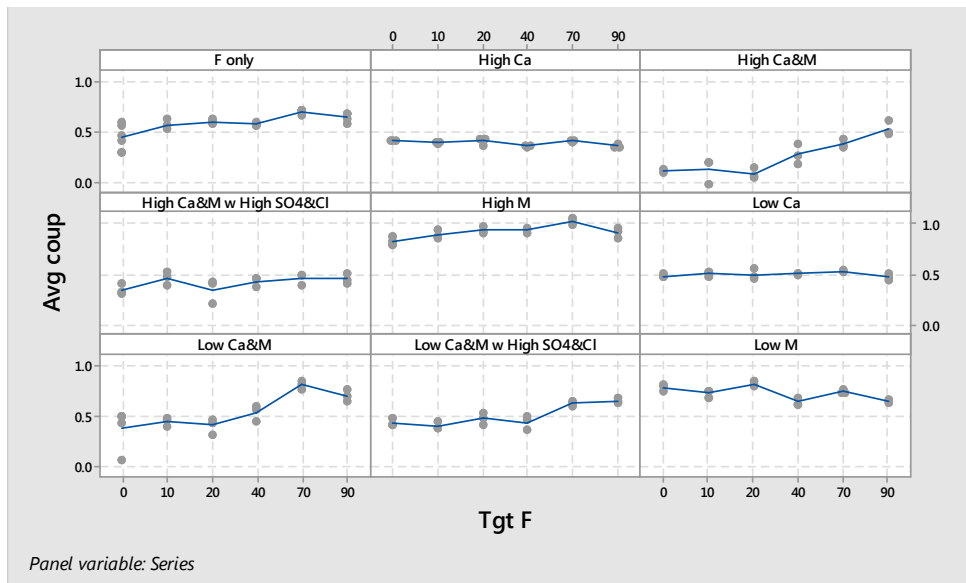


Figure 4-76: Individual value plot of the average corrosion rate (Avg coup) versus the target fluoride concentration (Tgt F) for the series

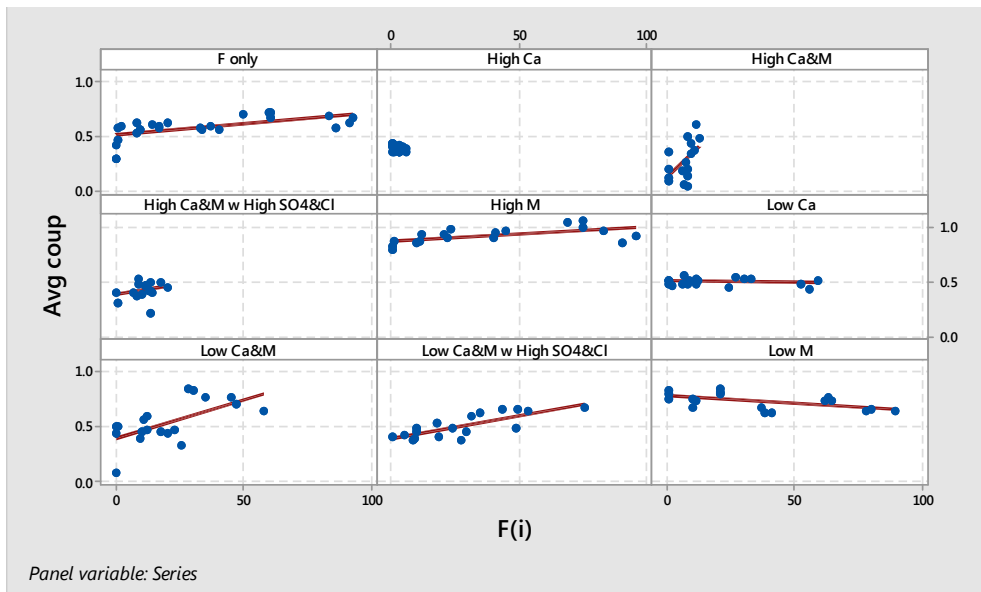


Figure 4-77: Individual value plot of the average corrosion rate (Avg coup) versus the initial fluoride concentration (F(i)) for the series

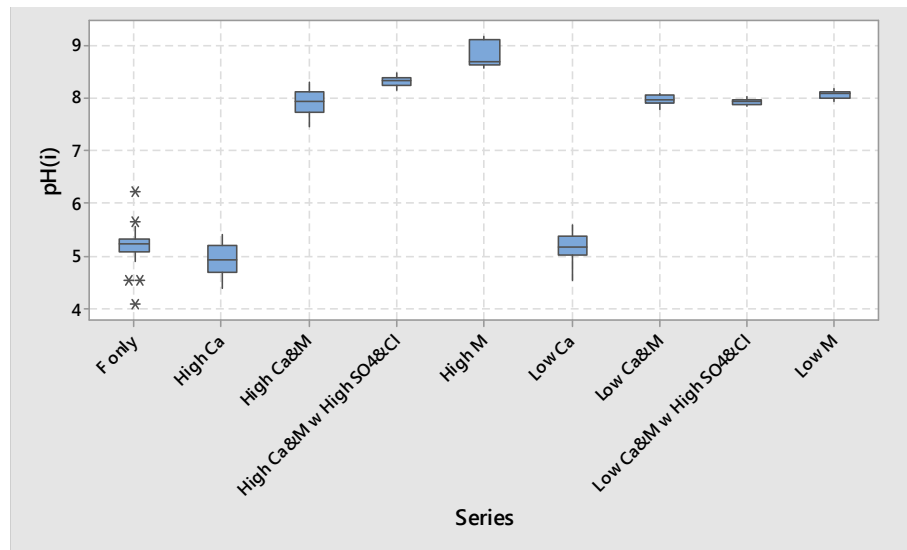


Figure 4-78: Box plot of the initial pH ($\text{pH}(i)$) for the different series

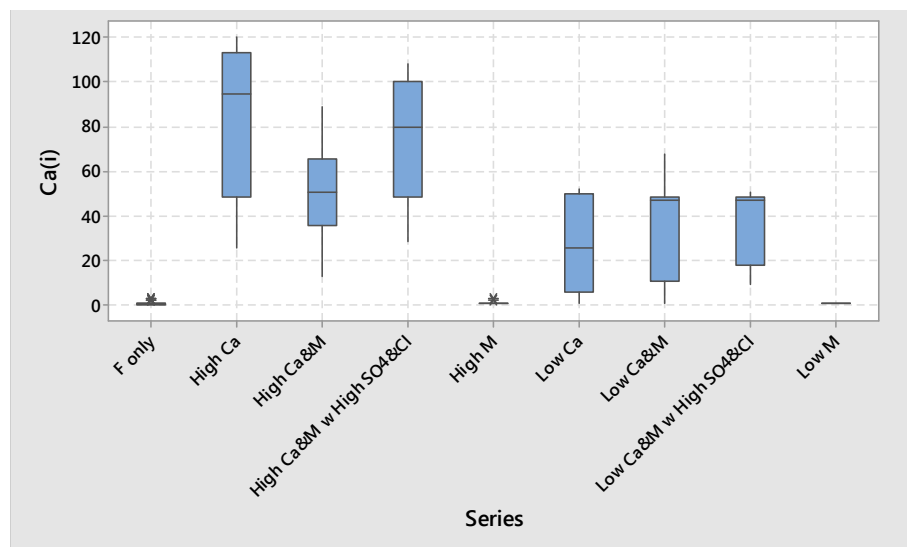


Figure 4-79: Box plot of the initial calcium ($\text{Ca}^{2+}(i)$) for the different series

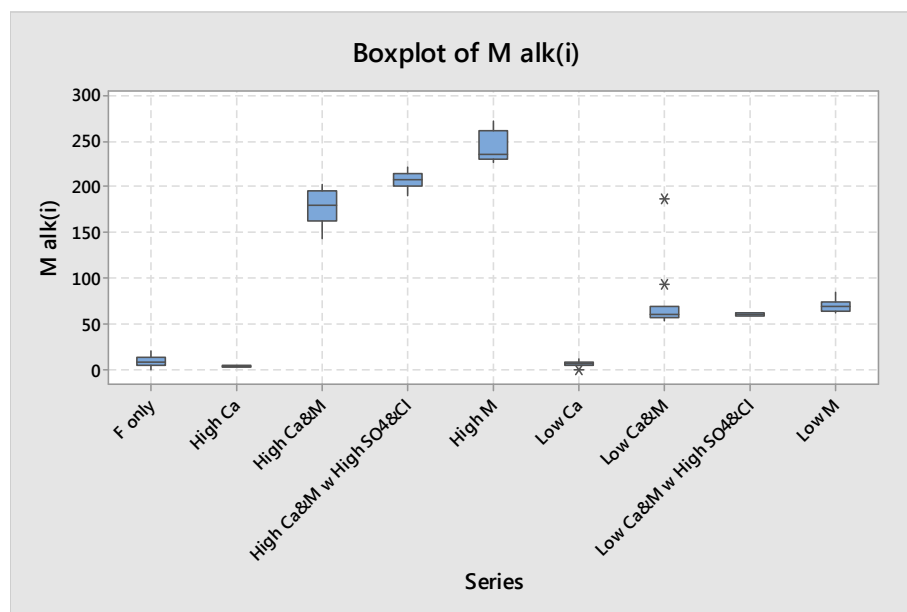


Figure 4-80: Box plot of the initial total alkalinity (M Alk(i)) for the different series

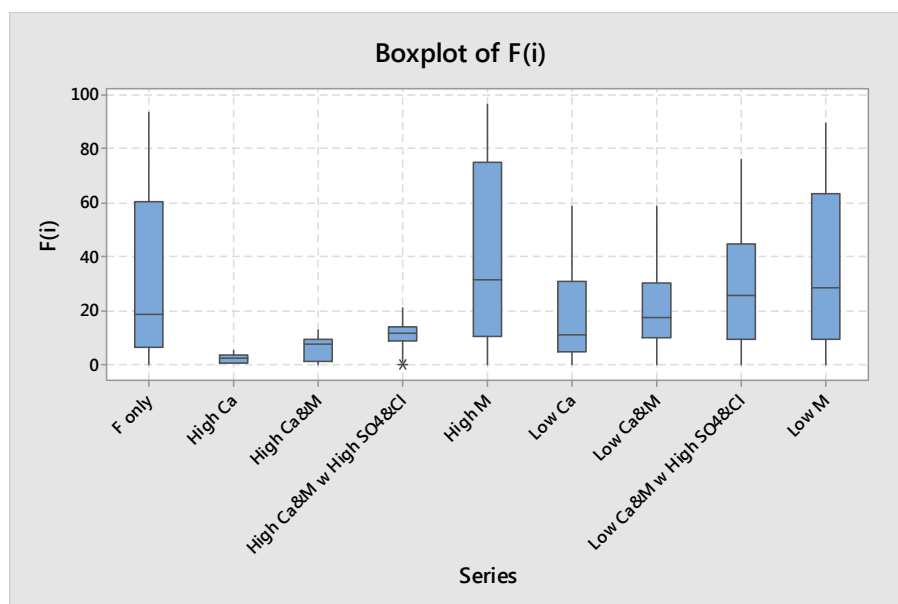


Figure 4-81: Box plot of the initial fluoride (F^- (i)) for the different series

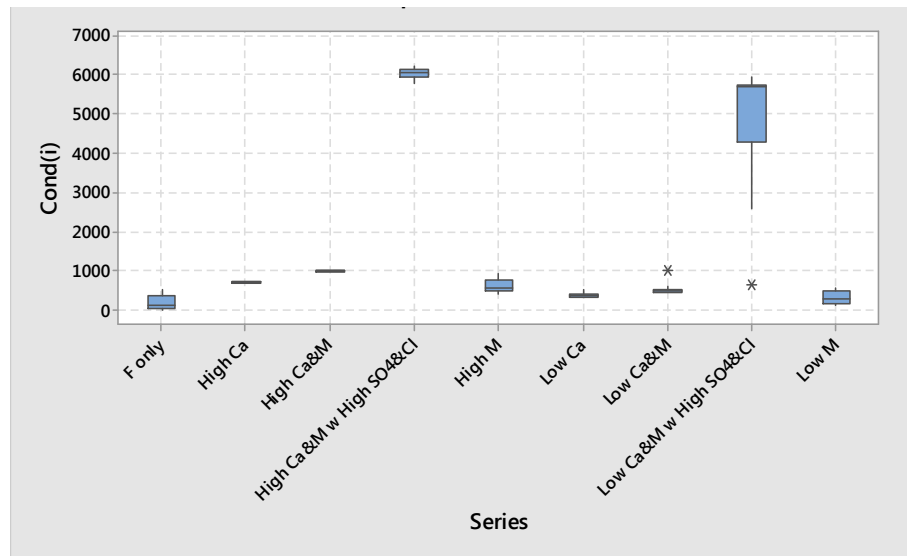


Figure 4-82: Box plot of the initial conductivity (Cond(i)) for the different series

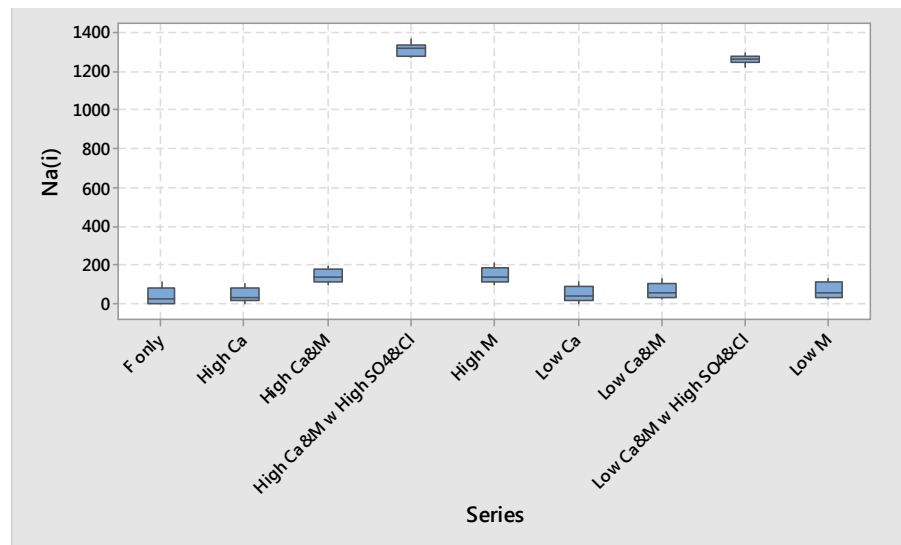


Figure 4-83: Box plot of the initial sodium (Na⁺(i)) for the different series

In order to compare the influence of mainly the sodium ions versus the fluoride ions in terms of their impact on the average corrosion rate, a series of Spearman rho and Pearson correlations were performed. Table 4-76 shows there was no statistically significant monotonic relationship between the average corrosion rate (Avg coup) and the initial sodium concentration (Na(i)). A moderate strong relationship was found between the average corrosion rate and the initial fluoride concentration (F(i)). A particularly strong negative Spearman rho relationship was evident between the average corrosion rate and the initial calcium concentration (Ca(i)).

Table 4-76: Statistically significant Spearman rho correlations between the average corrosion rate (Avg coup) and the various initial test parameters

	Avg coup	Na(i)	Cond(i)	F(i)	pH(i)	Ca(i)
Na(i)	nss	-	-	-	-	-
Cond(i)	-0.406	0.806	-	-	-	-
F(i)	0.573	0.382	-	-	-	-
pH(i)	0.304	0.527	0.381	-	-	-
Ca(i)	-0.744	nss	0.592	-0.526	-	-
Alk (i)	0.222	0.612	0.444	0.214	0.910	nss

Notes: The Spearman Rho coefficient indicates the direction and the intensity of monotonic relationships, that is where both variables increase concurrently, but not at the same rate.

nss. Not statistically significant.

Similar trends were evident with the Pearson linear correlations where the average corrosion rate was correlated against the initial sodium, initial fluoride and initial calcium data, Table 4-77.

Table 4-77: Statistically significant Pearson correlations between the average corrosion rate (Avg coup) and the various initial test parameters

	Avg coup	Na(i)	Cond(i)	F(i)	pH(i)	Ca(i)
Na(i)	nss	-	-	-	-	-
Cond(i)	-0.203	0.961	-	-	-	-
F(i)	0.521	0.003	-	-	-	-
pH(i)	0.265	0.390	0.395	-	-	-
Ca(i)	-0.625	0.298	0.420	-0.507	-	-
Alk (i)	0.157	0.292	0.345	nss	0.788	nss

It was established that the higher the concentration of calcium the lower the solubility of the fluoride ions. At a targeted fluoride concentration range of 0 to 90 mg/l (as F⁻) and the target calcium levels of between 50 and 120 mg/l (as Ca²⁺) it was found that the remaining levels of soluble fluoride ranged between 30 and 10 mg/l, respectively. In the presence of high chloride (1000 mg/l Cl⁻) and sulphate (1500 mg/l SO₄²⁻) the fluoride solubility increased to between 42 and 15 mg/l, respectively. It was only when fluoride was added either to deionized water or to a relatively high total alkalinity water without hardness that the corrosivity of mild steel at 45°C was significantly affected (Table 4-73).

As shown in Figure 4-74, the test solutions with low levels of calcium were corrosive towards mild steel predominantly due to their relatively high pH, sodium and total alkalinity levels.

It was established that for the series where sodium was added, either for the alkalinity (as NaHCO₃), sulphate (as Na₂SO₄) or chloride (as NaCl), generally the resultant models for those series produced corrosion rates which were moderate to strongly correlated with the sodium concentration. This was particularly evident for

series: 8 and 9 and to a lesser extent for series 3 and 7 (Table 4-73 and Figure 4-83).

Both the Spearman (Table 2-84) and Pearson correlation coefficients (Table 4-77) performed on all the results of the fluoride tests indicated a better correlation between the fluoride concentration and the average corrosion rate than the sodium concentration and the average corrosion rate. This therefore implied the greater likelihood of fluoride, rather than sodium, to have influenced the mild steel corrosion. The Spearman and Pearson coefficients also indicated two additional and equally important outcomes: a) the two most dominant factors were the fluoride and calcium concentrations, and b) moderate strong positive correlations existed between the average corrosion rate and the fluoride concentration ($\rho = 0.573$ and $r = 0.521$) and strong negative correlations between the average corrosion rate and the calcium concentration ($\rho = -0.625$ and $r = -0.744$) (Tables 4-76 and 4-77). Strongly positive correlations existed between the sodium concentration and the conductivity ($\rho = 0.806$ and $r = 0.961$).

4.9 Microscopic, Chemical and Electrochemical Studies into the Corrosive Effect of Fluoride on Mild Steel

This section delved into the visual, chemical and electrochemical examination of the effects exhibited during the exposure of mild steel to solutions containing 50 mg/l Ca^{2+} and 55 mg/l CaCO_3 with varying concentrations of fluoride at 45°C. Further to expanding the evaluation of the impact of the fluoride to beyond 90 mg/l it also permitted for a comparison of the data obtained by the previously used weight loss technique (Section 4.8.7) to the electrochemical approach (Section 4.9.4).

Mild steel corrosion coupons were exposed to the 4000 ml test solutions, at atmospheric pressure, and mixed with overhead stirrers at a fluid linear velocity of 1 m/s for 72 h. The coupons were then examined both macroscopically and microscopically, using optical and scanning electron microscopes, and their surface deposits analysed by Energy Dispersive X-ray Spectroscopy (EDS).

The results of the weight loss technique were compared against electrochemical studies performed with similar synthetic solutions, but at the same low fluoride levels as conducted in Section 4.8. These tests were performed at the same temperature and subjected to natural aeration but under static conditions.

4.9.1 Weight loss measurement of the effect of higher fluoride concentrations

This set of experiments was outside of the initial scope of the work relevant to the steel mills, as it extended the evaluation of the impact varying fluoride concentration, beyond the previous maximum of 90 mg/l, had on mild steel corrosion at 45°C. The reason for its inclusion was to discern whether the mild steel corrosion rate continues to increase at fluoride concentrations higher than 90 mg/l. It was included in this section as it permitted for a comparison of the findings of the microscopic and chemical analyses of the coupon and its surface deposits. Other than the higher fluoride concentrations, the remainder of the cations and anions added to the test solutions were the same as in the low calcium hardness and low alkalinity test performed in Section 4.8.7.

The laboratory, equipment, reagents and consumables utilized were the same as those employed in the experiments of Section 4.8. The corrosion tests were performed at the following fluoride concentrations: 0, 70, 100, 130, 170 and 200 mg/l. Unlike previous tests, turbidity measurements were included in order to measure the amount of calcium precipitation.

Table 4-78 summarises the target fluoride concentrations, the test solution start-up concentrations as well as the total iron concentration upon cessation. The corrosion rates are reported in Table 4-79. Illustrations of the trends apparent with the water chemistry and corrosion rates are evident in Figures 4-84 to 4-86.

Table 4-78: Corrosion tests varying fluoride in deionized water with 50 mg/l Ca²⁺ and 55 mg/l CaCO₃ at 45°C – Target, start-up and ending concentrations

Run	Target fluoride (mg/l as F ⁻)	Test solution concentrations						
		Fluoride(i) (25x diln) ⁽¹⁾ (mg/l as F ⁻)	pH(i) ⁽¹⁾	Calcium(i) ⁽²⁾ (mg/l as Ca ²⁺)	Total alkalinity(i) ⁽¹⁾	Cond(i) ⁽¹⁾ (µS/cm)	Turbidity(f) ⁽¹⁾ (NTU)	Total iron(f) ⁽¹⁾ (mg/l as Fe ³⁺ (total))
349	0	0	8.17	35.0	53.6	452	2	2.1
350	70	26	8.12	13.8	64.8	924	13	2.7
351	100	51	8.11	22.7	54.6	636	17	4.1
352	130	79	8.1	18.6	59.9	784	14	0.7
353	160	133	8.09	19.3	63.6	924	14	0.0
354	200	150	8.05	18.3	69.8	1116	15	0.9
355	0	1	8.18	39.3	61.4	388	1	3.2
356	70	26	8.01	24.1	56.6	492	11	2.6
357	100	47	7.97	27.5	62.6	632	13	2.8
358	130	77	7.75	29.8	65.5	776	15	3.0
359	160	107	7.97	31.0	74.0	920	17	2.1
360	200	158	7.94	26.3	81.4	1096	12	3.2

Notes: 1. Test conducted in Laboratory B, 2. Test conducted in Laboratory C, nt = not tested, i. initial (at start-up), f. final (upon cessation).

Table 4-79: Corrosion coupon results while varying fluoride in deionized water with 50 mg/l Ca²⁺ and 55 mg/l CaCO₃ at 45°C

Run	Target fluoride (mg/l as F ⁻)	Corrosion Coupon Results		
		Coupon 1 (mmpa)	Coupon 2 (mmpa)	Average (mmpa)
349	0	0.45	0.51	0.48
350	70	0.66	0.75	0.70
351	100	0.74	0.80	0.77
352	130	0.76	0.73	0.75
353	160	0.82	0.88	0.85
354	200	0.69	0.72	0.70
355	0	0.35	0.38	0.36
356	70	0.60	0.65	0.63
357	100	0.65	0.68	0.66
358	130	0.63	0.63	0.63
359	160	0.71	0.73	0.72
360	200	0.69	0.77	0.73

Figures 4-84 and 4-86 show that the initial total alkalinity continued to rise with sodium fluoride addition, while the initial pH appeared to decrease until it levelled off at the target fluoride concentration of approximately 150 mg/l. The initial calcium concentration followed the same trend as the initial pH and appeared to level off at the target fluoride concentration of approximately 120 mg/l. In Figure 4-84, the average mild coupon corrosion rate followed the same trend as the final solution turbidity and formed a plateau at the target fluoride concentration of approximately 140 mg/l, whereas for the final solution turbidity it was at approximately 130 NTU. Figure 4-85 illustrates the lack of a detectable change in total iron concentration with the change in corrosion rate versus the initial fluoride concentration.

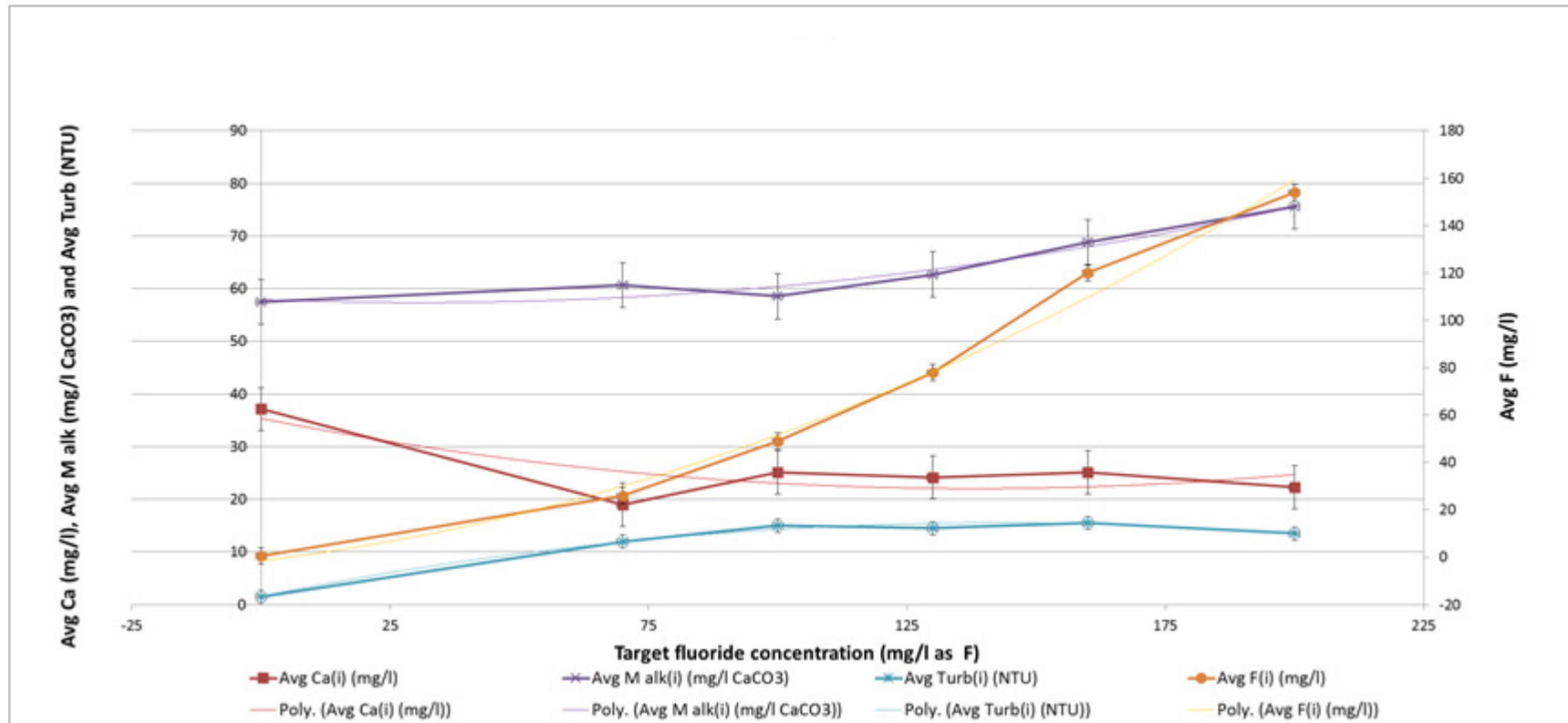


Figure 4-84: Initial calcium (Ca(i)), initial total alkalinity (Talk (i)), initial fluoride (F(i)) and the final turbidity (Turb(f)) versus the target fluoride concentration. Error bars: ± 4.2 Ca mg/l, ± 4.3 mg/l CaCO₃, ± 1.2 NTU and ± 3.4 mg/l

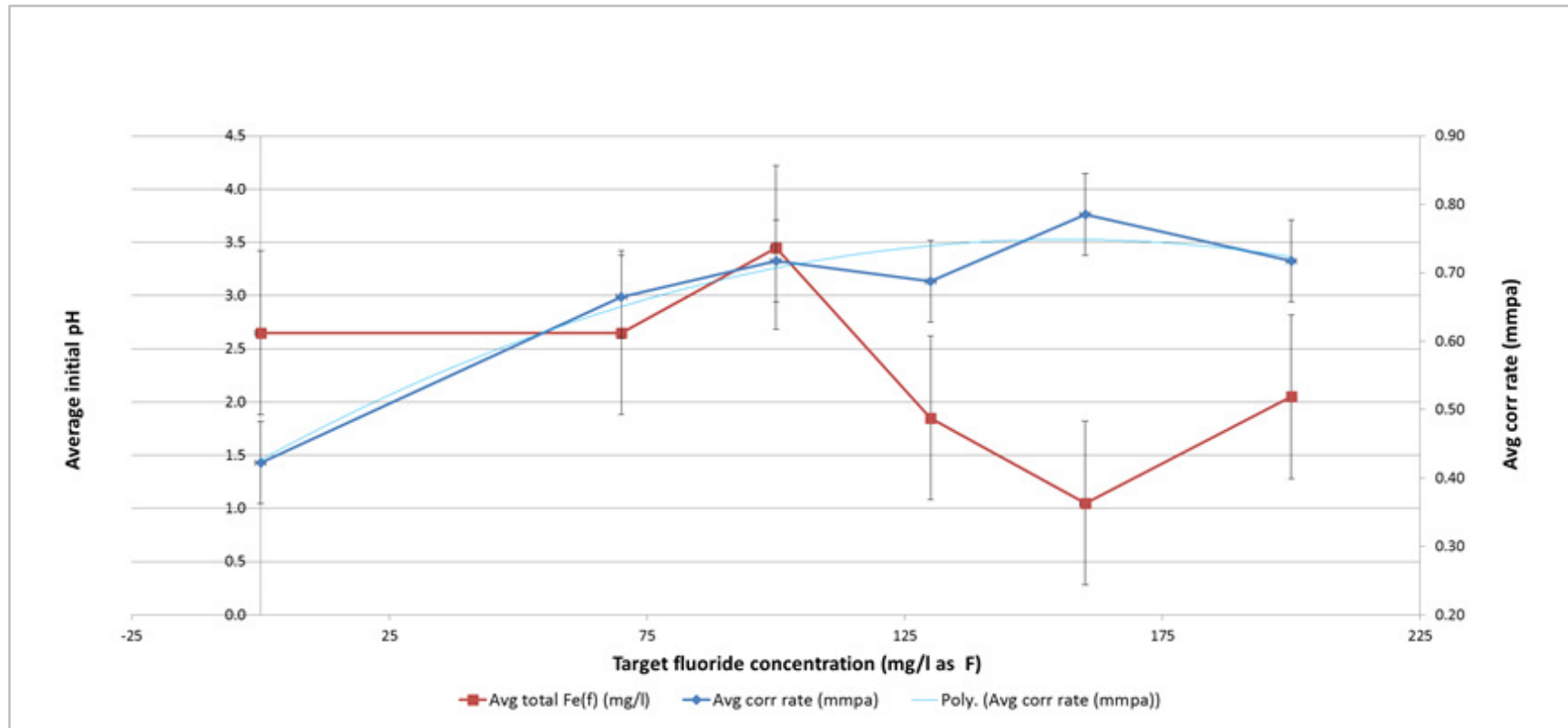


Figure 4-85: Final total iron concentration (Fe(f)) and average coupon corrosion rate (mmpa) versus the target fluoride concentration.
 Error bars: ± 0.8 mg/l Fe and ± 0.06 mmpa

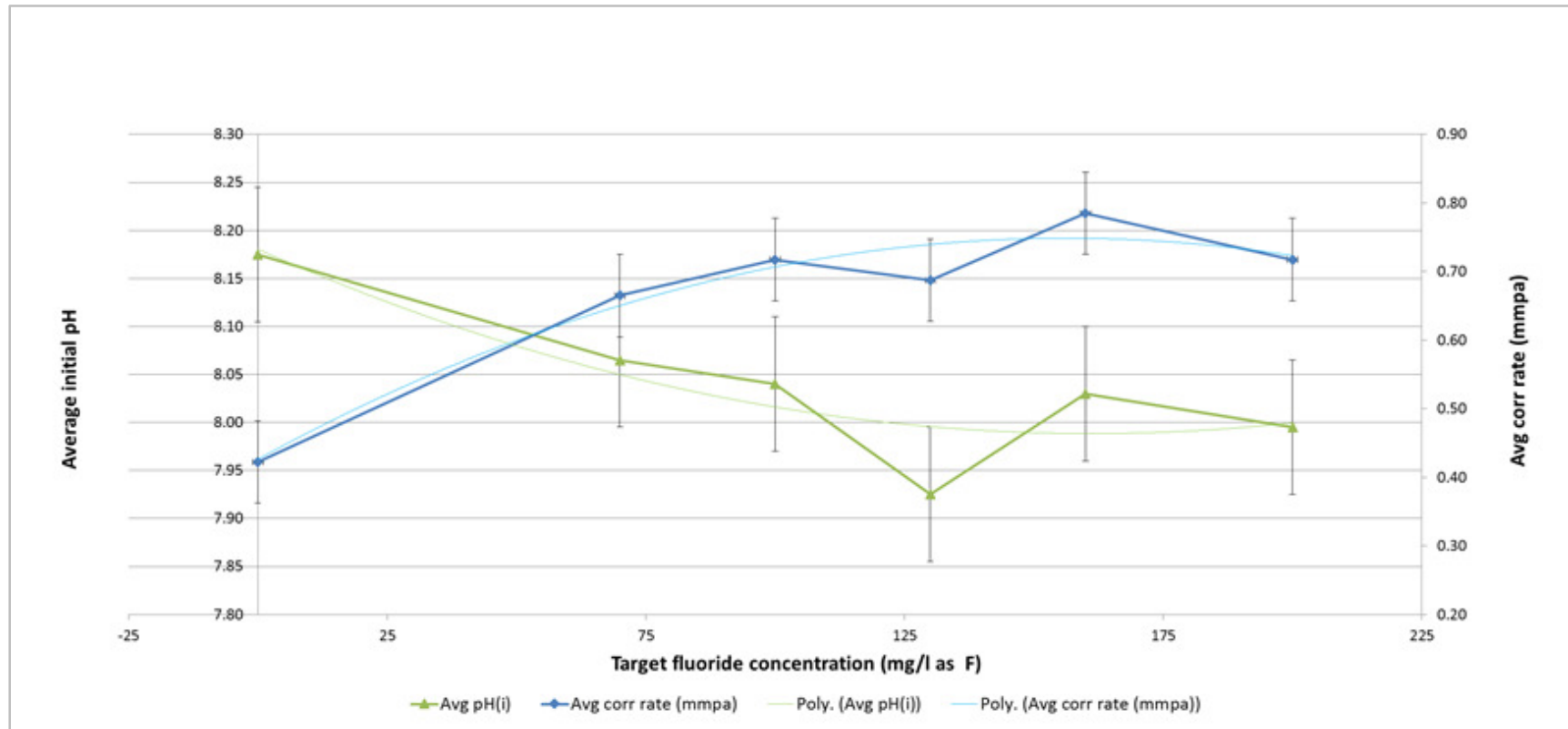


Figure 4-86: Initial pH (pH(i)) and average coupon corrosion rate (mmpa) versus the target fluoride concentration. Error bars: ± 0.07 pH and ± 0.06 mmpa

4.9.2 Macroscopic appearance and low magnification light microscopy

Macroscopic examinations were performed with a low magnification viewing of the coupons after their three day immersion tests at 45°C. A stereomicroscope (Carl Zeiss Stemi SV 6) fitted with a digital camera (Canon Powershot A640) was utilized. The mild steel corrosion coupons removed from position 1 in the corrosion tests of Section 4.9.1 were photographed, after cleaning, and shown in Figure 4-87. The magnitude of uniform corrosion was approximated based on visual examinations of the surfaces of both sides of each coupon.

The corrosion appeared to be mostly uniform corrosion and its severity appeared proportional to the measured fluoride concentrations. The coupons exposed to the test solutions with higher fluoride concentration were found to have a higher ratio of etched metal surface area to darkened and seemingly less affected area.

In the first beaker, to which no fluoride was added, the coupon was mostly uncorroded but had areas that were uniformly corroded and also contained crystalline deposits. The crystals were soluble in dilute hydrochloric acid and produced effervescence, indicative of carbonate (Figures 4-88 to 4-90).

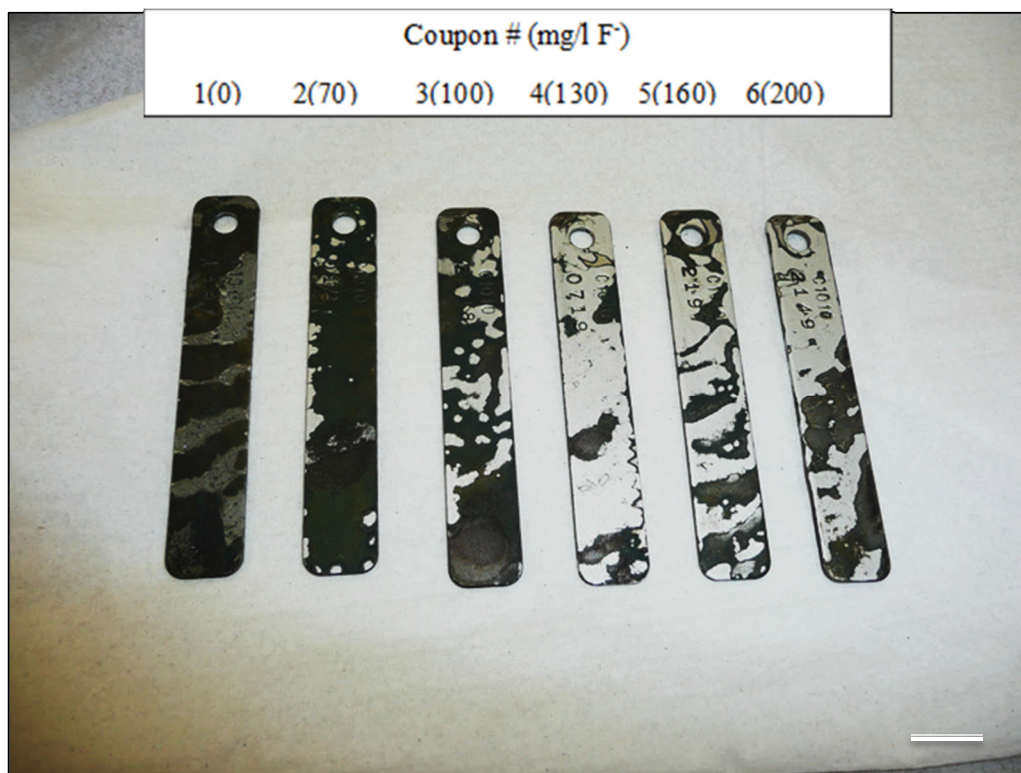


Figure 4-87: Photograph of cleaned mild steel corrosion coupons removed after a 3 day corrosion test performed at 45°C at varying fluoride concentrations in a solution containing 50 mg/l Ca²⁺ and a total alkalinity of 55 mg/l CaCO₃ (scale bar: 1.27 cm)

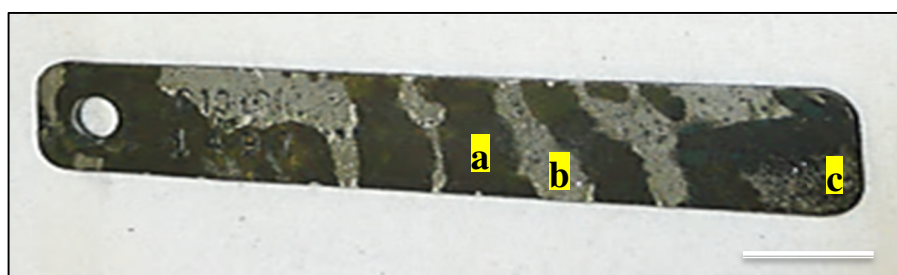


Figure 4-88: Photograph of coupon 1 (0 mg/l F⁻) showing: a) dark apparently unaffected areas, b) uniformly corroded zones and c) “calcium deposit” as indicated by EDS (scale bar: 1.27 cm)

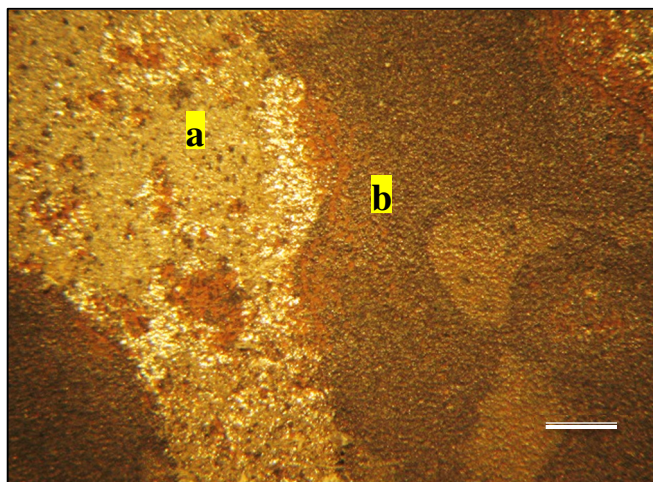


Figure 4-89: Macrograph of coupon 1 (0 mg/l F⁻) showing: a) Shiny etched zones neighbouring b) the darker less corroded zones on coupon 1 (0 mg/l F⁻) (scale bar: 1 mm)

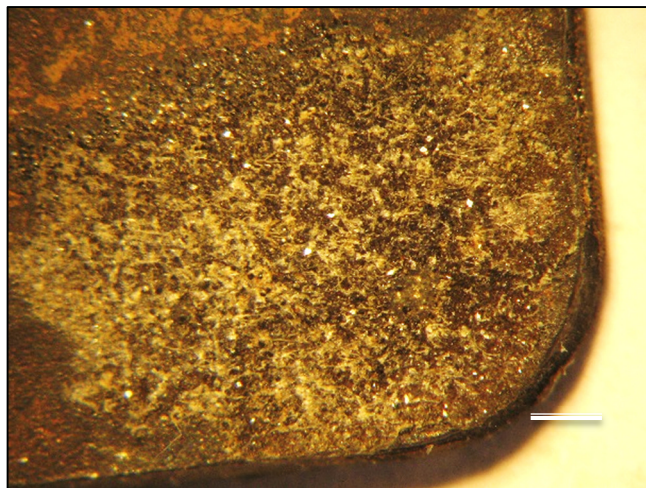


Figure 4-90: Macrograph of coupon 1 (0 mg/l F⁻) showing calcium carbonate crystals deposited on the tip of the coupon (i.e. zone c). Up to 30% of the coupon was covered in crystals (scale bar: 1mm)

The balance of the coupons, from the test solutions with higher fluoride concentrations, only differed from the first coupon in terms of the apparent extent of the corrosion (consistent with the amount of etched surface area). No pitting was evident macroscopically (Figures 4-91 to 4-100).

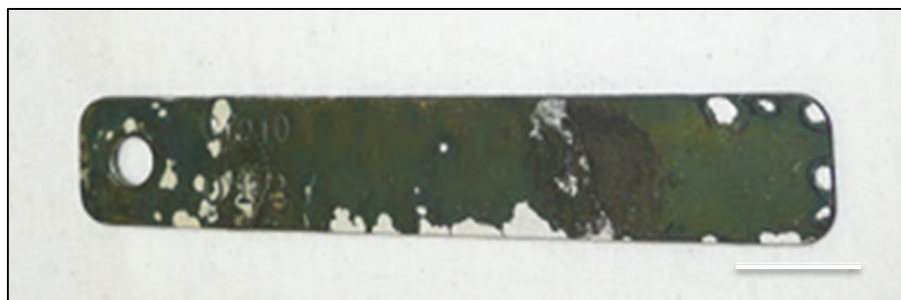


Figure 4-91: Photograph of coupon 2 (70 mg/l F⁻) showing a mostly darkened surface with a small number of corroded areas at the edges of the coupon

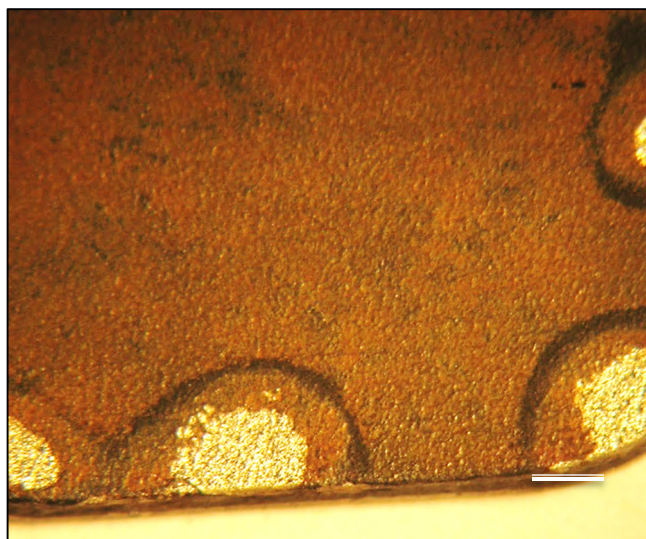


Figure 4-92: Macrograph of coupon 2 (70 mg/l F⁻) showing uniform corrosion zones along edge of coupon (scale bar: 1.mm)

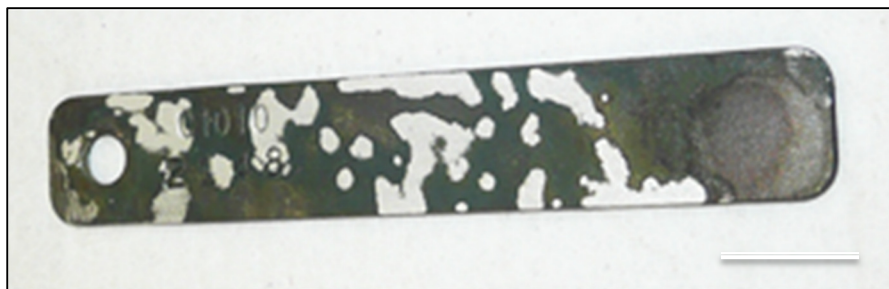


Figure 4-93: Photograph of coupon 3 (100 mg/l F⁻) with up to 45% of the surface showing zones of shallow uniform corrosion (scale bar: 1.27 cm)

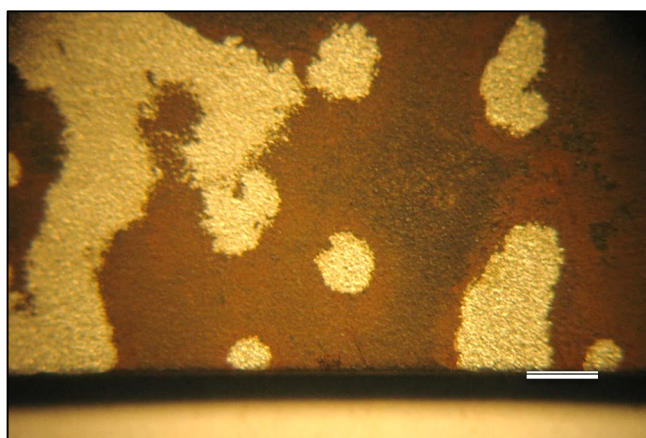


Figure 4-94: Macrograph of coupon 3 (100 mg/l F⁻) showing shallow corroded zones of coupon (scale bar: 1mm)

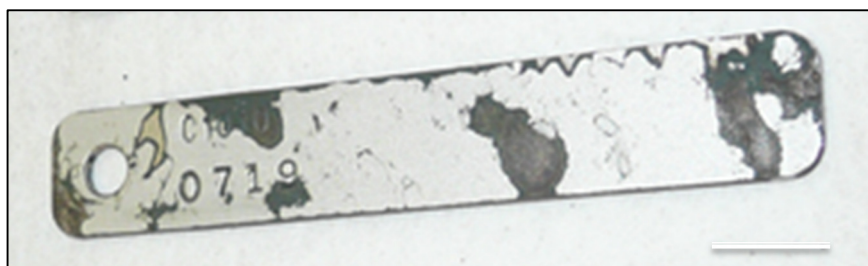


Figure 4-95: Photograph of coupon 4 (130 mg/l F⁻) with approximately 75% uniform corrosion (scale bar: 1.27 cm)

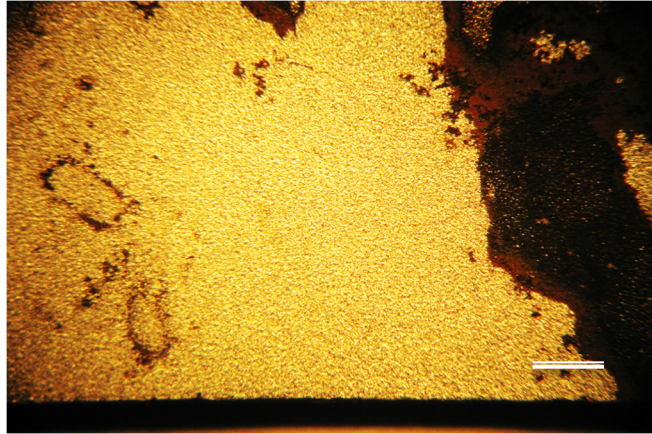


Figure 4-96: Macrograph of coupon 4 (130 mg/l F⁻) showing larger shallow corroded zones relative to the previous coupons (scale bar: 1 mm)



Figure 4-97: Photograph of coupon 5 (160 mg/l F⁻) also with approximately 75% uniform corrosion (scale bar: 1.27 cm)

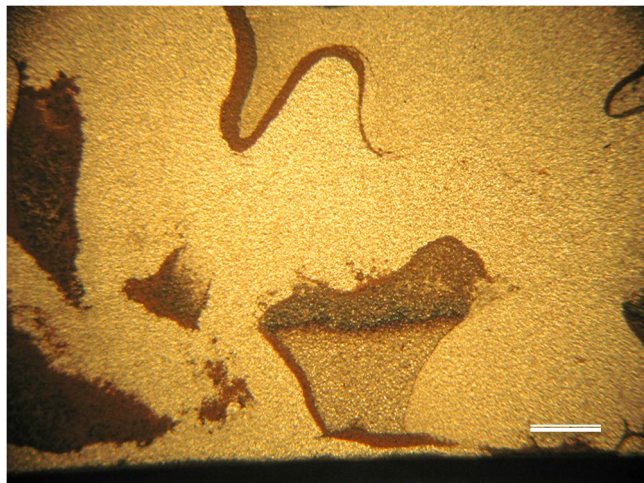


Figure 4-98: Macrograph of coupon 5 (160 mg/l F⁻) showing larger shallow corroded areas similar in appearance to coupon 4 (scale bar: 1 mm)

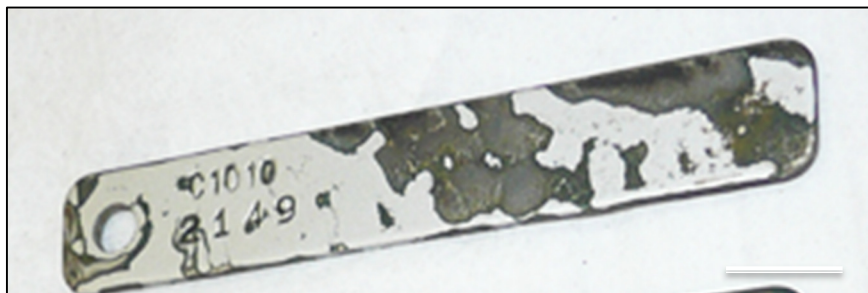


Figure 4-99: Photograph of coupon 6 (200 mg/l F⁻) with approximately 50% uniform corrosion (scale bar: 1.27 cm)

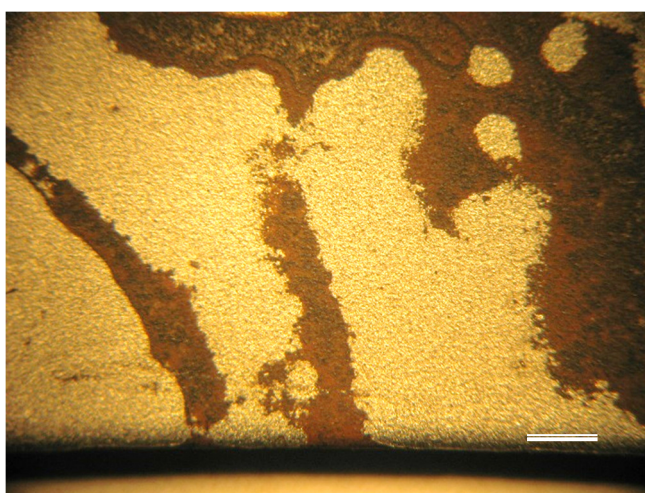


Figure 4-100: Macrograph of coupon 6 (200 mg/l F⁻) showing large shallow corroded areas (scale bar: 1 mm)

4.9.3 Scanning electron microscopy and energy dispersive X-ray analysis

Table 4-80 lists both the standards and equipment utilized when the Scanning Electron Microscopy (SEM) and EDS were performed. The coupons examined were those removed and reported on in Section 4.9.1. The SEM and EDS were performed at an acceleration voltage of 10 kV in order to detect the low atomic number elements, for example fluorine, as well as the metal, for example iron, without compromising image resolution.

Table 4-80: SEM and EDS equipment, software and operating conditions (Location: University of the Witwatersrand)

Equipment, software and operating conditions
<p>Carl Zeiss Sigma Field Emission Scanning Electron Microscope equipped with Smart SEM Version 5.06 software, and Oxford x-act SDD detector with INCA for Windows 7 (Issue 21a SP2 version 5.04)</p> <p>Gun vacuum applied: 4×10^{-9} Torr</p> <p>SEM mode: Secondary electron imaging</p>
<p>Standards :</p> <p>C: CaCO₃ 1-Jun-1999 12:00 AM, O: SiO₂ 1-Jun-1999 12:00 AM, Al: Al₂O₃ 1-Jun-1999 12:00 AM, Ca: Wollastonite 1-Jun-1999 12:00 AM, Fe: Fe 1-Jun-1999 12:00 AM</p>

The scanning electron micrographs are shown in Figures 4-101 to 4-116 and the results of the EDS analyses given in Tables 4-81 and 4-82.

In a surface analysis of the initial set of (un-cleaned) coupons it was revealed that there were crystalline material in most of the coupons examined. The coupon removed from the beaker containing no fluoride (coupon 1) contain carbon and crystalline material that was moderately high in calcium (40%) (Figure 4-101). The deposits on the coupons taken from the test solutions with the intermediate target fluoride concentrations of 70 and 100 mg/l were high in iron (58 - 66%) and contained traces of fluoride (0.5 to 1.1%) (Figures 4-102 to 4-105). The coupon with the highest level of fluoride (Figures 4-106 to 4-109) had residual corrosion products with moderately high levels of iron (23 – 64%) and significantly high levels of calcium (~29%) and fluorine (28- 31%) as F⁻).

After cleaning of the coupons (Table 4-82), it was found that the surface of coupon 1 had calcium (0.4 - 15%) and iron (15 – 92%) (Figure 4-110) whereas the others

that were immersed in fluoride-containing test solutions were mostly high in iron (57 - 91%) (Figure 4-111). EDS analysis of the cleaned coupons produced higher iron concentrations than the pre-cleaned coupons due to larger areas of exposed bare metal. No fluorides were detected on the cleaned coupon surfaces. Apart from coupon 1, all the other coupons had micro-pitting. The pits were estimated to be between: 0.2 and 0.8 μm for coupon 2 (70 mg/l F^-) (Figure 4-112), 0.6 and 1.4 μm for coupon 4 (130 mg/l F^-) (Figure 4-113) and 0.3 and 1.7 μm for coupon 6 (200 mg/l F^-) (Figure 4-115).

Figures 4-112 and 4-113 also show intergranular corrosion, by the intergranular facets. Both the pitting and intergranular corrosion appeared in the shiny areas (Figure 4-114) which had exhibited uniform corrosion, neighbouring the darker less corroded areas (Figures 4-88 and 4-89).

Table 4-81: SEM and EDS of coupon surfaces prior to cleaning

Target Fluoride concentration. (mg/l as F ⁻)	Coupon #	Spot	EDS Results (% (m/m))						
			Carbon (C K)	Oxygen (O K)	Calcium (Ca K)	Iron (Fe L)	Fluoride (F K)	Silicon (Si K)	Sodium (Na K)
0	1	1	12.8	53.5	26.5	7.2	nd	nd	nd
0	1	2	7.1	38.9	40.4	13.6	nd	nd	nd
0	1	3	23.8	32.6	2.2	41.2	nd	0.2	nd
70	2	4	nd	33.8	nd	66.2	nd	nd	nd
70	2	5	nd	32.0	6.4	61.6	nd	nd	nd
70	2	6	7.2	32.0	2.3	58.1	nd	0.5	nd
100	3	7	1.0	27.1	3.6	67.5	0.6	0.2	nd
100	3	8	1.3	33.7	6.3	57.8	nd	0.9	nd
100	3	9	7.1	29.4	3.3	60.1	nd	nd	nd
100	3	10	9.6	29.8	8.7	50.8	1.1	nd	nd
100	3	11	1.5	25.3	40.1	32.3	0.8	nd	nd
100	3	12	nd	7.9	87.3	4.3	0.5	nd	nd
200	6	13	1.5	33.9	nd	62.8	nd	1.8	nd
200	6	14	2.0	13.1	29.1	26.3	28.7	0.2	0.5
200	6	15	1.9	13.1	29.9	23.2	31.1	0.3	0.6
200	6	16	8.9	26.0	1.1	63.6	nd	0.5	nd

Notes: nd. Not detected.

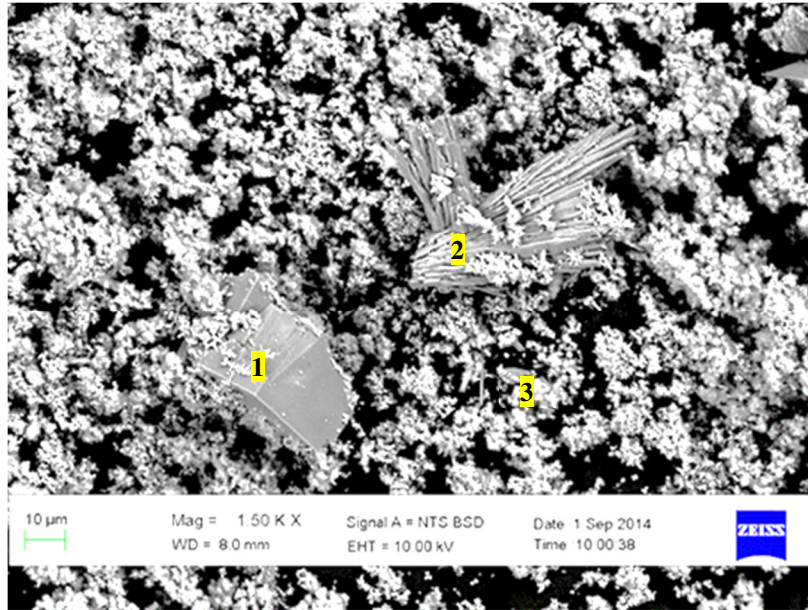


Figure 4-101: SEM image of coupon 1, spots 1-3, showing crystalline material and the areas analysed

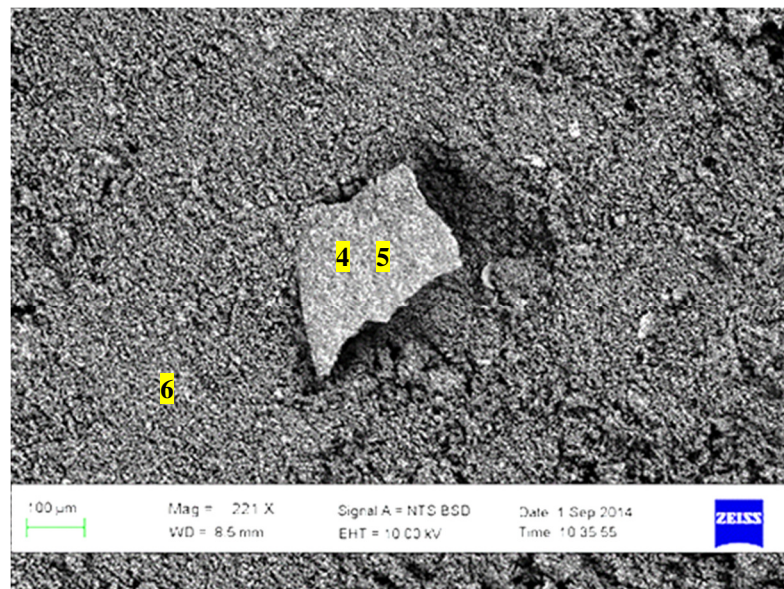


Figure 4-102: SEM image of coupon 2, spots 3-5, showing a flaky particle and the areas analysed

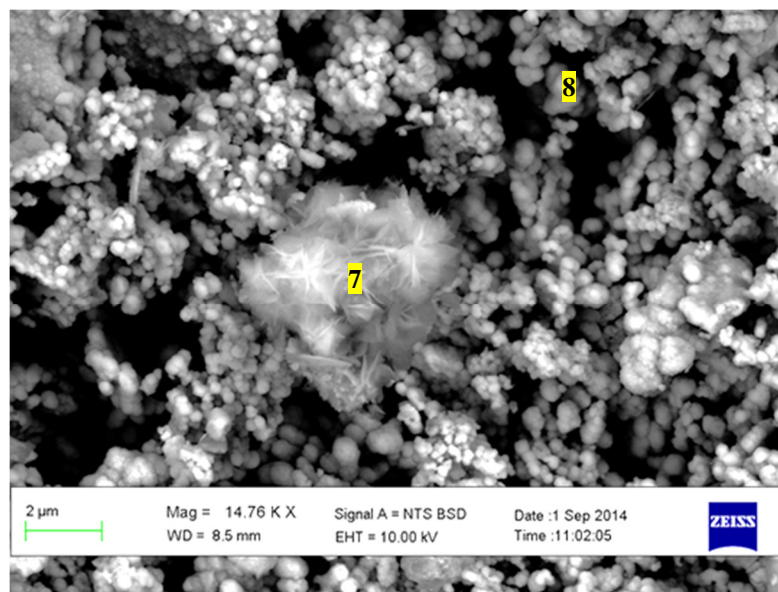


Figure 4-103: SEM image of coupon 3, showing a crystal amongst heterogeneous material and the areas analysed , spots 7 and 8

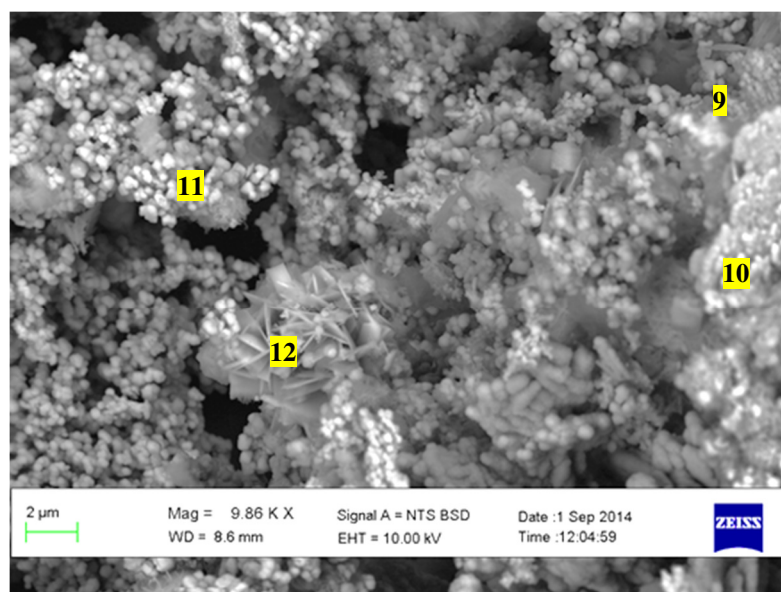


Figure 4-104: SEM image of coupon 3, showing a small rosette aggregate and the areas analysed, spots 9-12

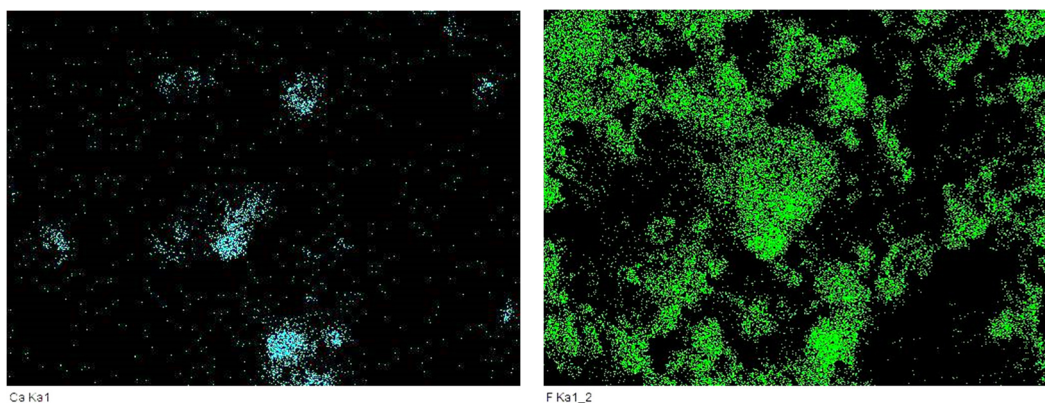


Figure 4-105: Elemental maps of the area shown in Figure 4-104 of coupon 3, calcium(blue) and fluorine (green), spots 9-12

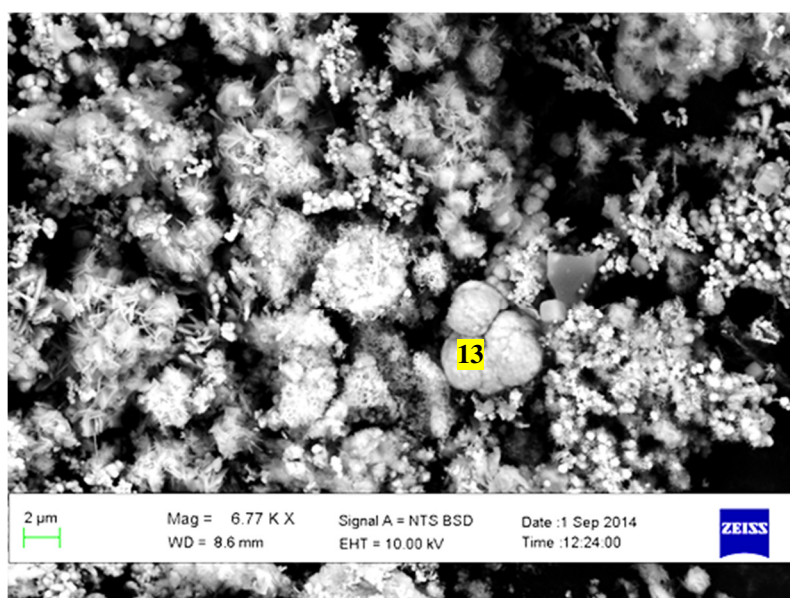


Figure 4-106: SEM image of coupon 6, showing small crystals and the crystal analysed, spot 13

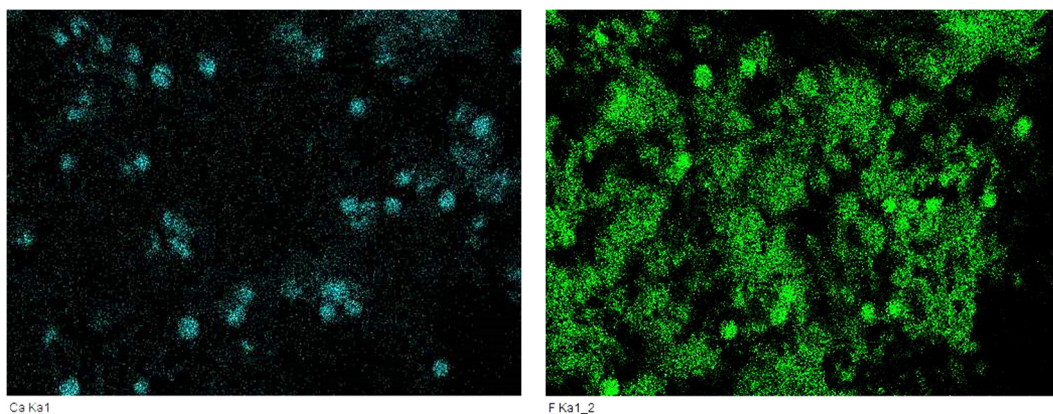


Figure 4-107: Elemental maps of the area shown in Figure 4-106 of coupon 6, spot 13, calcium(blue) and fluorine (green)

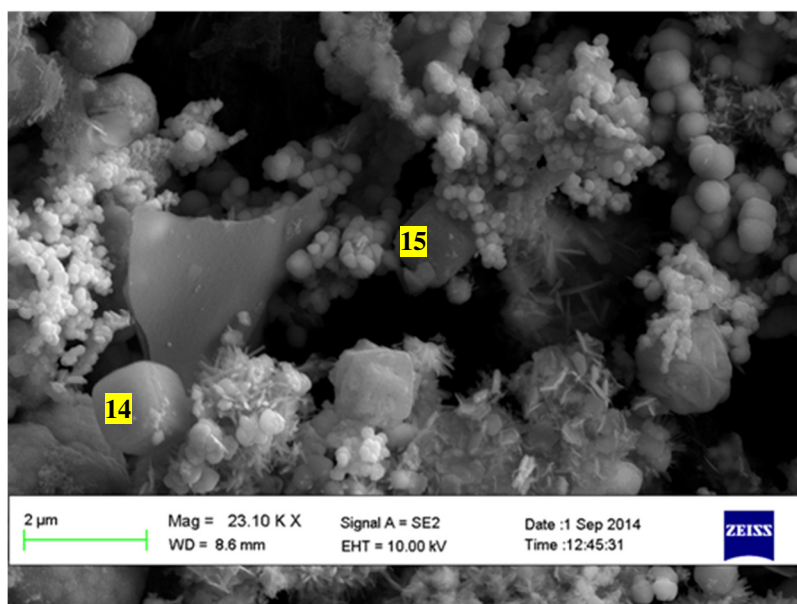


Figure 4-108: SEM of coupon 6, showing crystals high in calcium and fluorine, spots 14 and 15

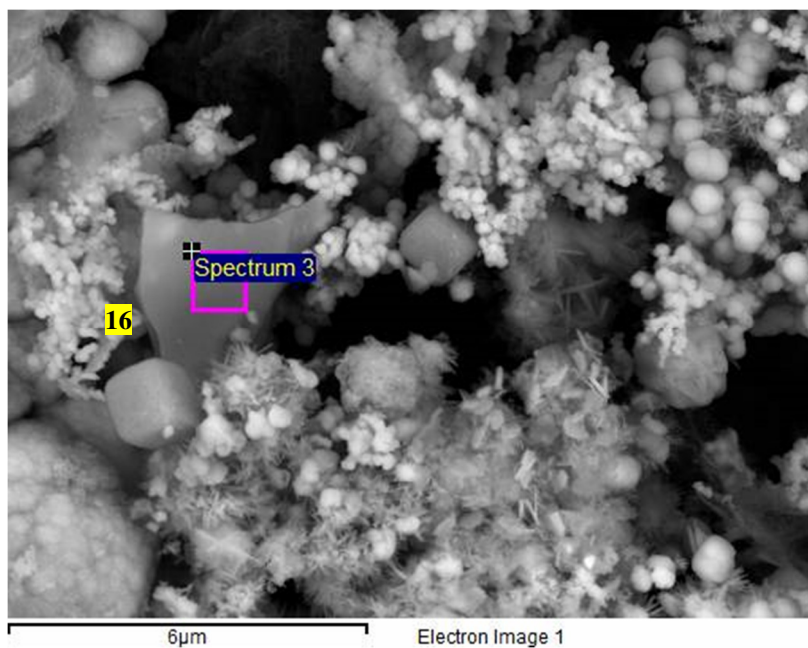


Figure 4-109: SEM image of coupon 6, spot 16 “spectrum 3” showing a flaky particle without calcium and fluorine

Table 4-82: SEM and EDS of coupon surfaces post cleaning

Target Fluoride concentration. (mg/l as F ⁻)	Coupon #	Spot	EDS Results (% (m/m))						
			Carbon (C K)	Oxygen (O K)	Calcium (Ca K)	Iron (Fe L)	Fluoride (F K)	Silicon (Si K)	Sodium (Na K)
0	1	17	26.0	42.5	14.2	15.0	nd	0.3	nd
0	1	18	2.1	5.3	0.4	92.2	nd	nd	nd
0	1	19	8.6	40.6	1.6	49.0	nd	0.2	nd
70	2	20	4.3	35.5	nd	58.1	nd	1.8	nd
70	2	21	5.4	18.0	nd	76.0	nd	0.6	nd
70	2	22	5.4	3.2	nd	91.4	nd	nd	nd
160	5	23	4.4	35.5	nd	57.7	nd	1.5	0.3
160	5	24	8.0	9.5	nd	82.5	nd	nd	nd

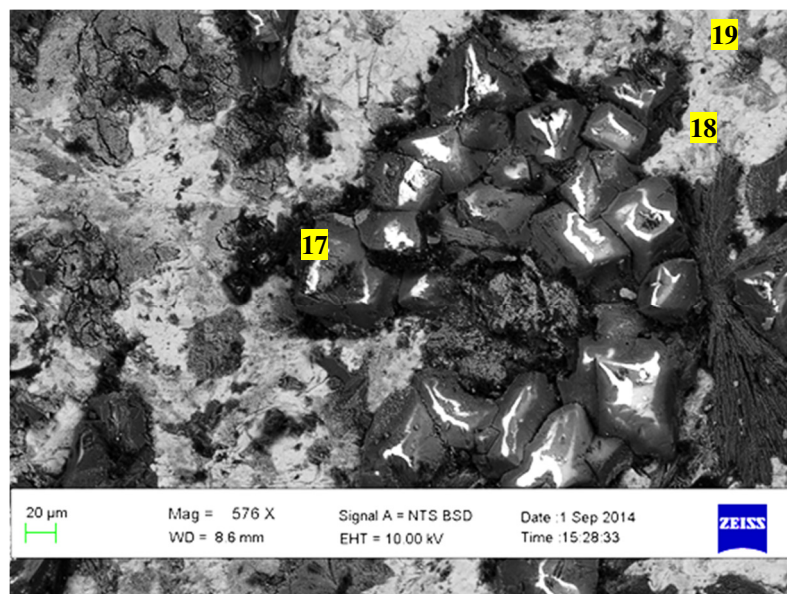


Figure 4-110: Scanning electron micrograph of cleaned coupon 1 showing adherent and dense calcareous surface deposit surrounded by iron oxide/s and the areas analysed, spots 17-19

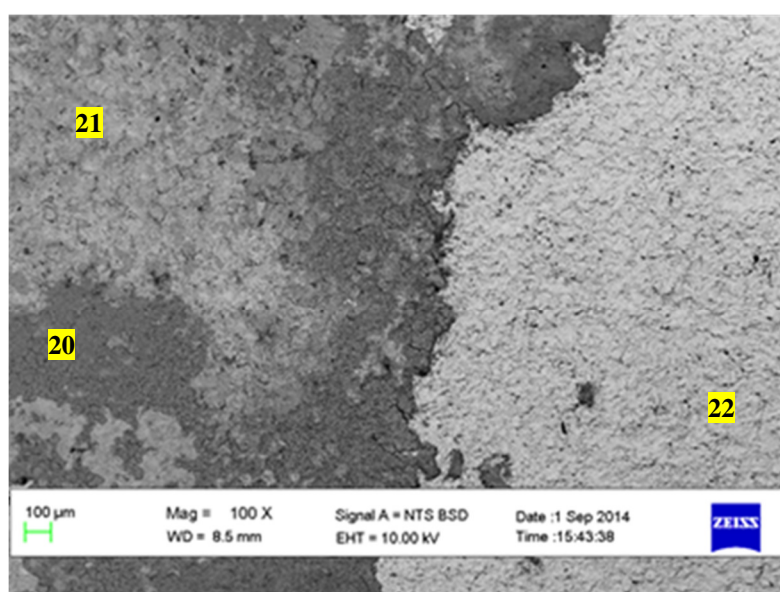


Figure 4-111: SEM image of cleaned coupon 2, showing a dark area covered in corrosion product adjacent to a shiny etched surface and the areas analysed, spots 20-22

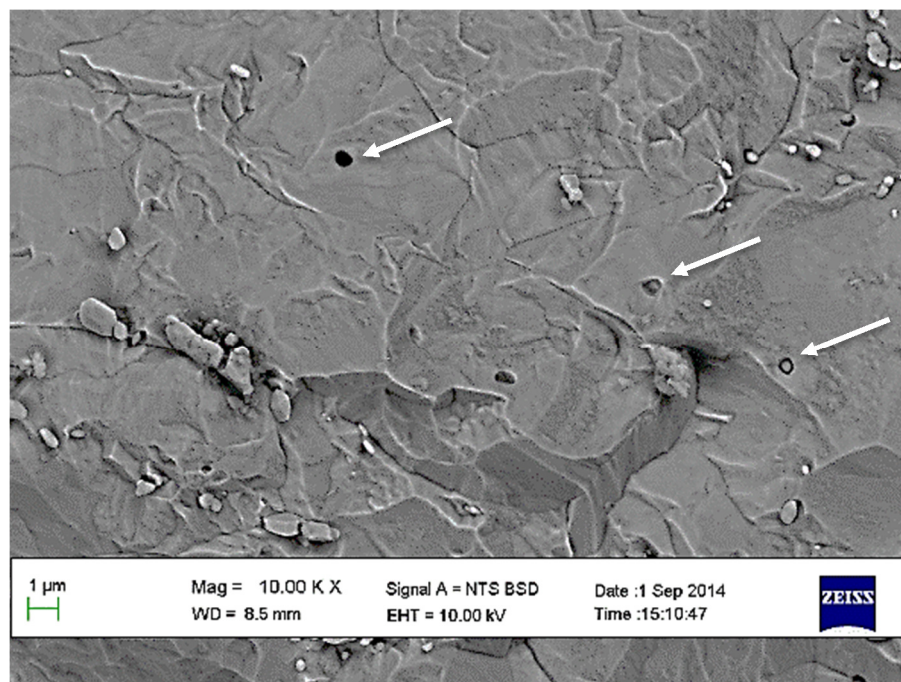


Figure 4-112: SEM image of cleaned coupon 2, spectrum showing numerous micro-pitting in an area that exhibited uniform corrosion, spot 22

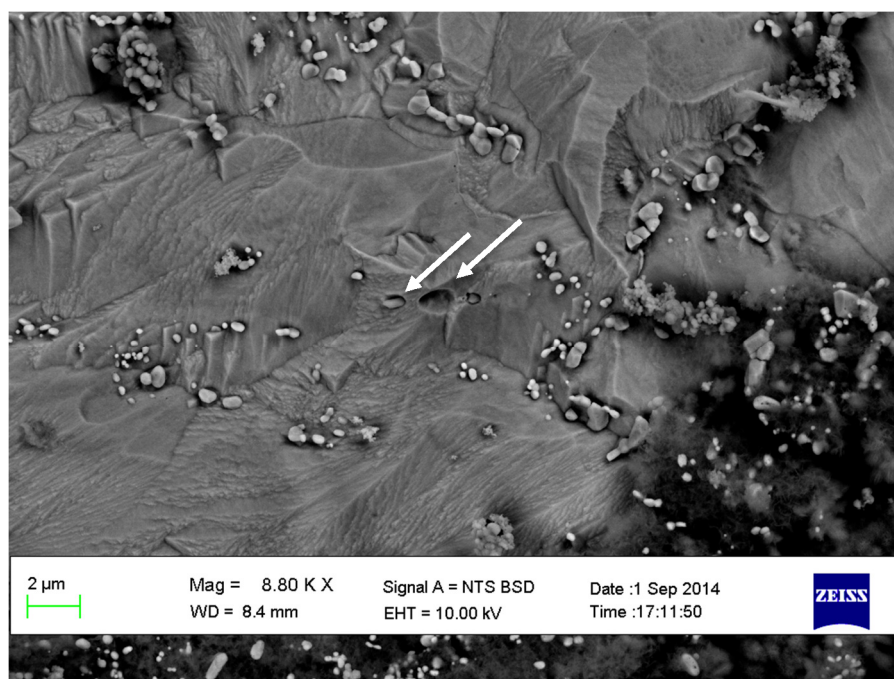


Figure 4-113: SEM image of cleaned coupon 4 (Figures 4-95 and 4-96), showing numerous micro-pitting in an area that exhibited uniform corrosion, as apparent by the irregular surface morphology

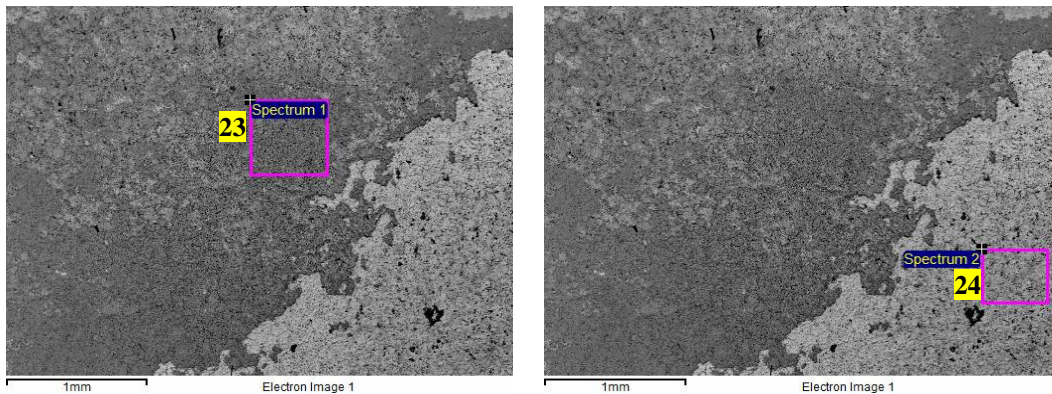


Figure 4-114: SEM images of coupon 5, (Figures 4-97 and 4-98) showing areas of uniformly corroded areas adjacent to a darker area with corrosion product and the areas analysed, spots 23 and 24

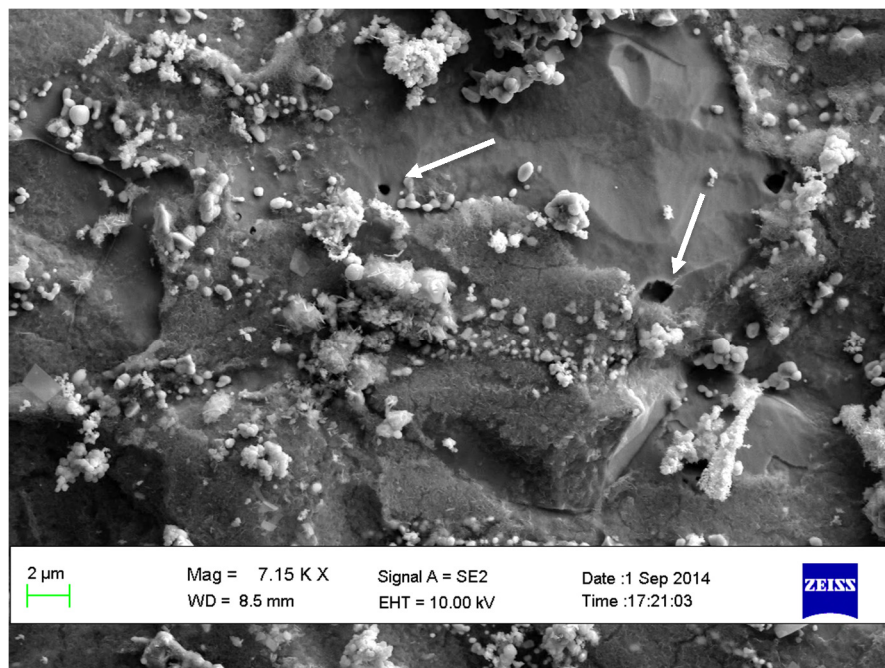


Figure 4-115: SEM image of coupon 6, showing numerous micro-pitting in an area that also appeared macroscopically as uniform corrosion (Figures 4-99 and 4-100)

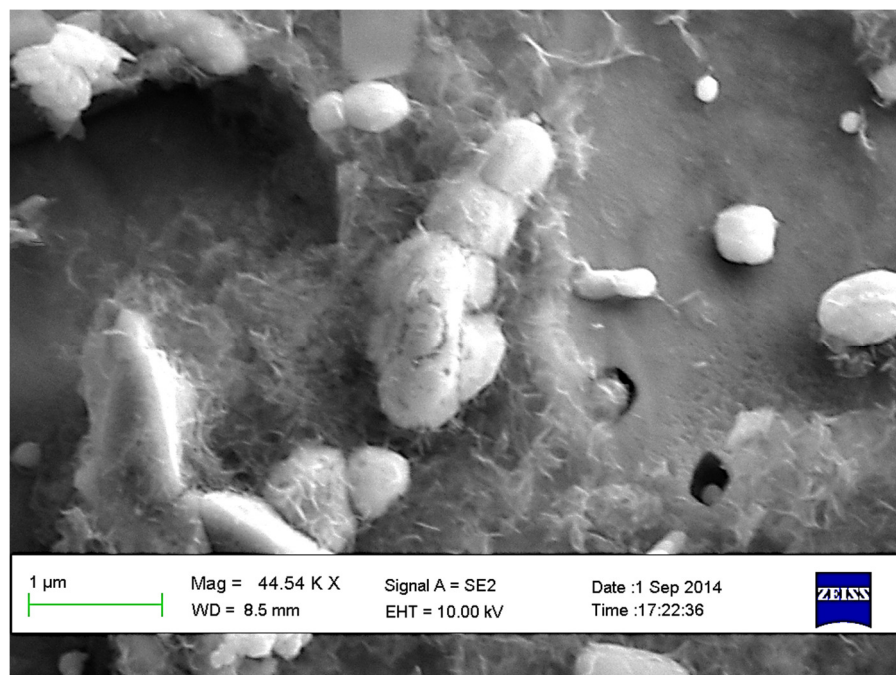


Figure 4-116: SEM image of coupon 6, showing higher magnification of micro pits in an area which exhibited uniform corrosion

4.9.4 Electrochemical studies

Electrochemical measurements were recorded using a Metrohm PGSTAT302N Autolab equipped with Nova 1.10.1.9 data acquisition software and were done against a Ag/AgCl reference electrode. A graphite rod was used as a counter electrode.

Measurements were conducted using a standard three electrode test cell (Figure 4-117) where the working electrodes were prepared by cold mounting a 1 cm² mild steel sample in epoxy resin. Electrical contact was obtained by adhering a piece of copper wire to the back of the metal sample prior to the cold mounting. The working electrodes were all polished to a 600 grit finish just prior to immersion.

The samples were submerged for 90 minutes prior to determining the open circuit potential (OCP). The tests were performed with 500 ml test solutions under natural aeration and non-stirred conditions at $45 \pm 2^\circ\text{C}$. The beaker temperature was

controlled automatically using a Pt100 resistance thermometer and verified against a calibrated alcohol thermometer.

The potentiostat was programmed to apply a continuously varying potential to the sample at a scan rate of 0.5 mV/s. The potentiostatic technique was performed by plotting the resulting log current ($\log(A)$) against the applied potential (V). Scans were from performed for the potentials ranging from ≥ -100 mV to $\leq +100$ mV of the observed corrosion potential. Straight lines were drawn near to the observed corrosion potential and the slopes of the lines determined in order to calculate the Tafel constants which were then used to calculate the corrosion rate, based on an exposed specimen surface area of 1 cm² and the density of the sample (7.87 g/cm³ for mild steel). All the calculations were performed using the using the Nova 1.10.1.9 software, in accordance with ASTM G102-89 (2010) and ASTM G59-97 (2003), and each electrochemical test replicated twice. The total specimen exposure time and the duration of the test was approximately 100 minutes. Essentially the Tafel plot, a plot of the applied current versus the reference potential, allowed for the calculation of the slopes of both the cathodic and anodic polarisation and an extrapolation of the polarisation resistance. The use of these data together with the Stern equation (Champion, 1952) allowed for the calculation of the corrosion current which, together with the known specimen surface area, translated into a corrosion current. The corrosion current was converted into a mass flux, using Faraday's law, and the penetration or corrosion rate then obtained based on the density of the metal specimen being tested.

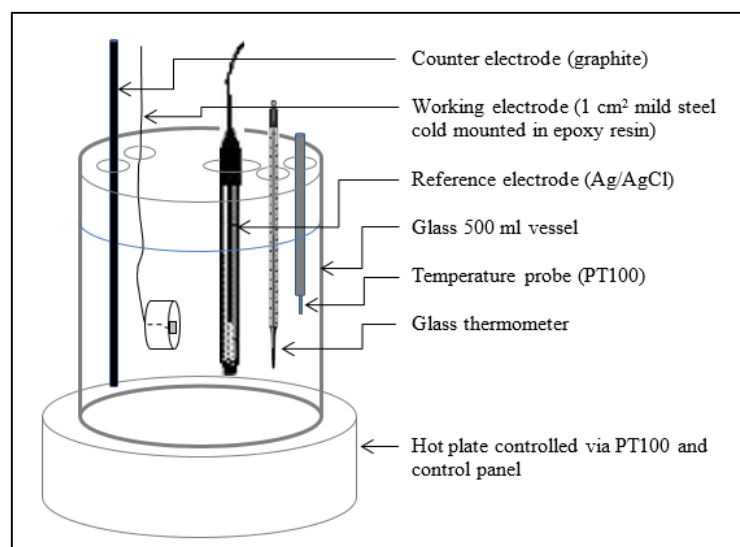


Figure 4-117: Schematic diagram of heated and unaerated three electrode test cell

4.9.4.1 Results

The results of the electrochemical study (Figures 4-118 to 4-129) are summarized in Table 4-83 and were used to show the corrosivity of mild steel in low hardness and alkalinity water with varying fluoride concentrations (0 – 100 mg/l as F^-) at 45°C (Figure 4-130).

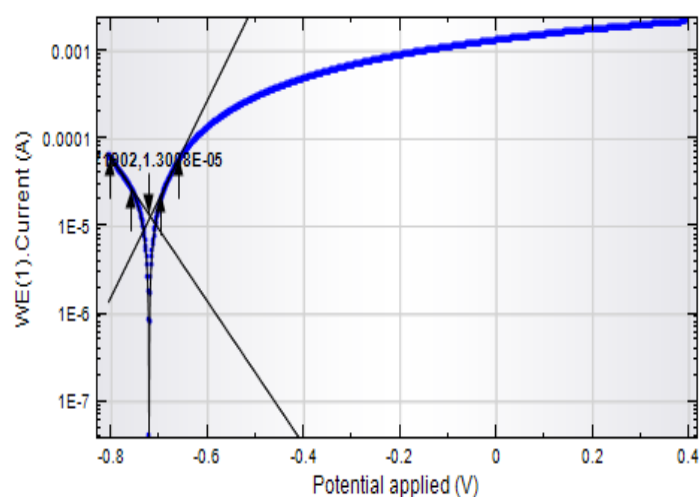


Figure 4-118: Tafel plot of test 1a (0 mg/l F^-)

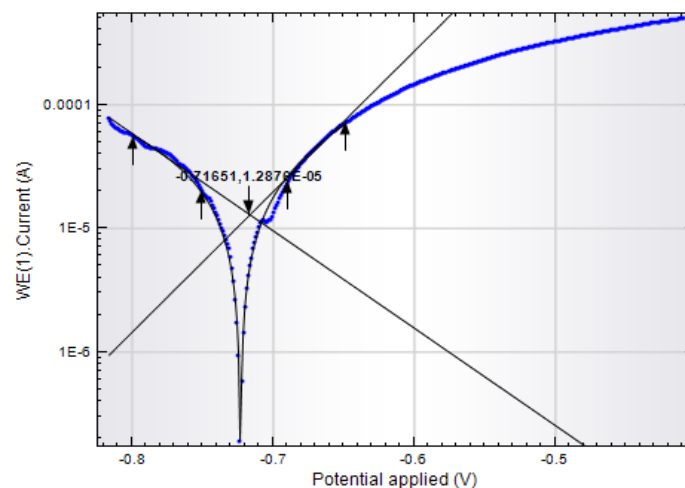


Figure 4-119: Tafel plot of test 1b (0 mg/l F⁻)

Table 4-83: Tafel plots results and calculated corrosion rates in mmpa

Test (Target and actual fluoride concentration (mg/l as F ⁻))	OCP(V)	ba (V/dec)	bc (V/dec)	E _{corr} , Obs (V)	i _{corr} (A) x 10 ⁻⁵	Corrosion rate (mmpa)	Polarization resistance (Ω)
1a (0) (0)	-0.706	0.2653	0.1793	-0.7218	3.58	0.42	1297
1b	-0.716	0.2105	0.1641	-0.7233	2.92	0.34	1373
2a (20) (16)	-0.642	0.2411	0.0827	-0.6384	2.26	0.26	1183
2b	-0.603	0.1840	0.1058	-0.5905	2.08	0.24	1401
3a (40) (36)	-0.422	0.2003	0.1089	-0.4494	2.98	0.35	1029
3b	-0.667	0.2177	0.1180	-0.6737	2.22	0.26	1495
4a (60) (44)	-0.605	0.9307	0.1399	-0.6033	6.42	0.75	823
4b	-0.639	18.372	0.2185	-0.6427	8.54	0.99	1099
5a (80) (51)	-0.361	0.4663	0.3044	-0.3818	6.25	0.73	1279
5b	-0.623	0.3902	0.1636	-0.6231	6.02	0.70	831
6a (100) (69)	-0.570	0.1985	0.2017	-0.5973	4.46	0.52	973
6b	-0.434	0.1838	0.1980	-0.4531	5.88	0.68	704

Note: OCP. Open circuit potential, ba and bc. Anodic and cathodic Tafel constants, E_{corr} (obs). Observed corrosion potential, i_{corr}. Corrosion current

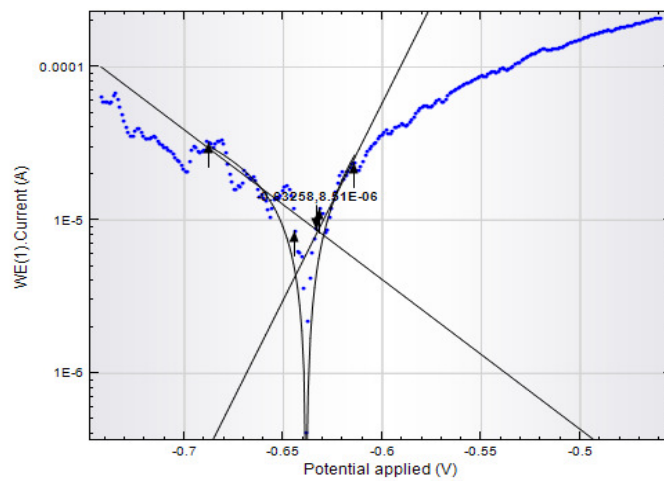


Figure 4-120: Tafel plot of test 2a (20 mg/l F⁻)

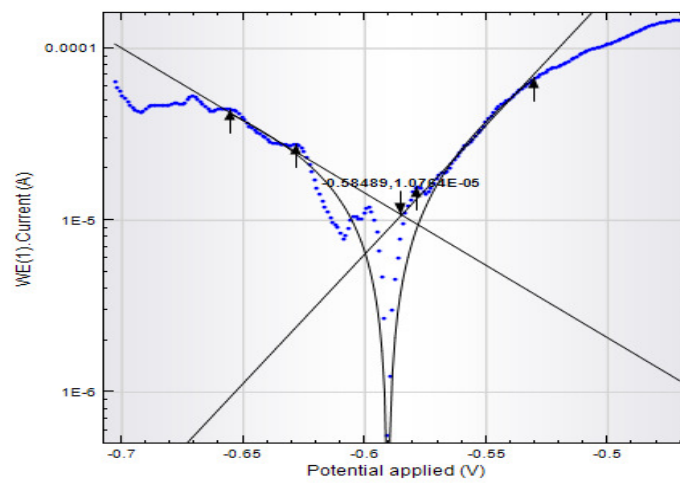


Figure 4-121: Tafel plot of test 2b (20 mg/l F⁻)

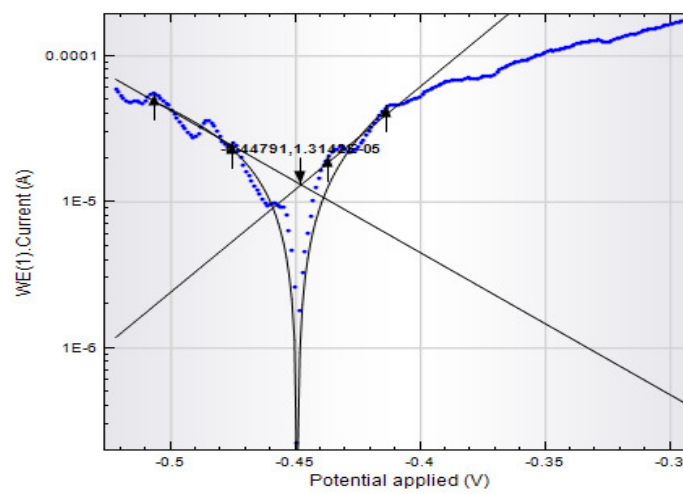


Figure 4-122: Tafel plot of test 3a (40 mg/l F⁻)

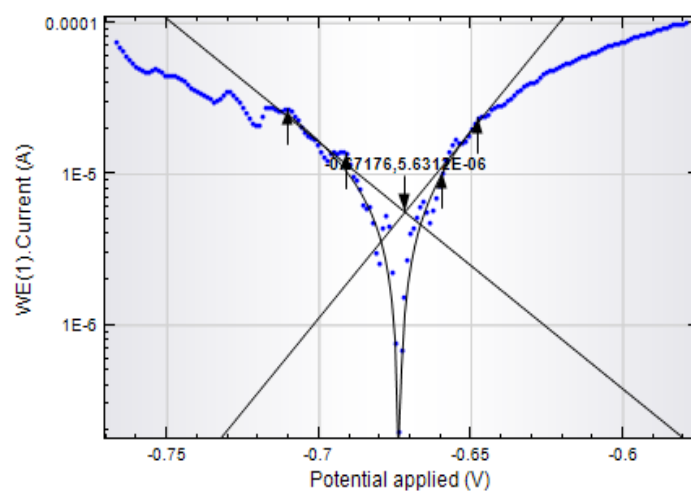


Figure 4-123: Tafel plot of test 3b (40 mg/l F⁻)

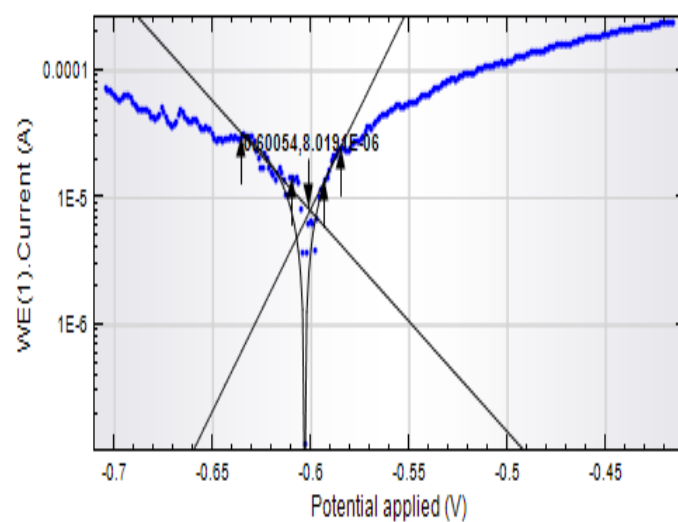


Figure 4-124: Tafel plot of test 4a (60 mg/l F⁻)

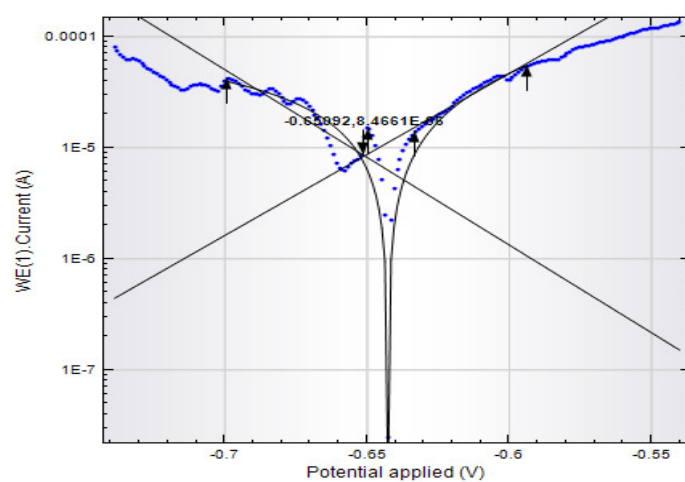


Figure 4-125: Tafel plot of test 4b (60 mg/l F⁻)

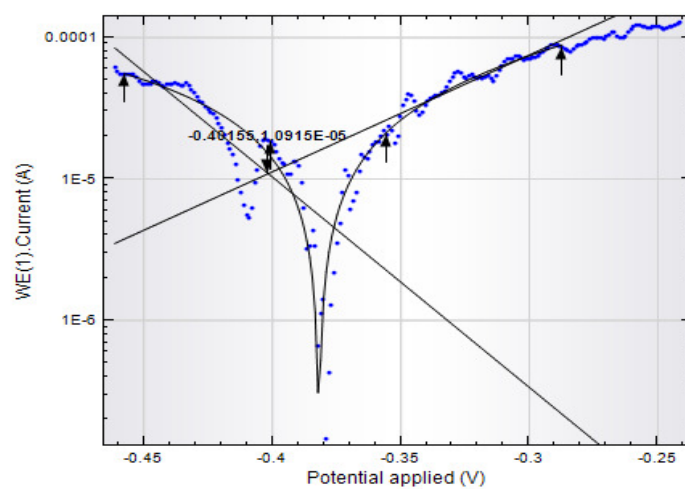


Figure 4-126: Tafel plot of test 5a (80 mg/l F⁻)

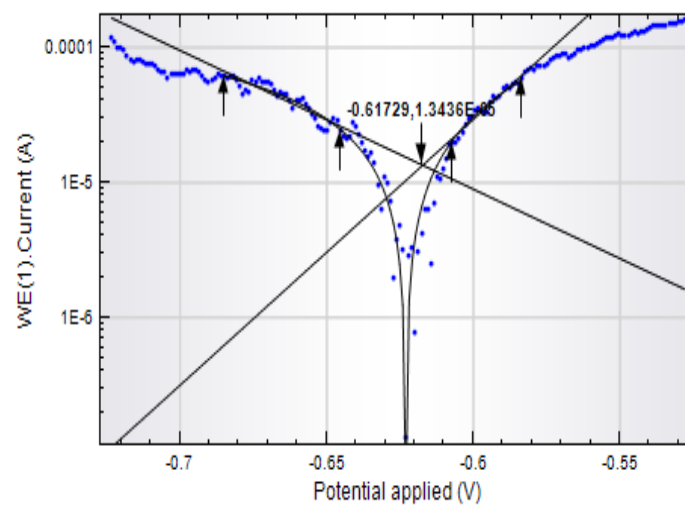


Figure 4-127: Tafel plot of test 5b (80 mg/l F⁻)

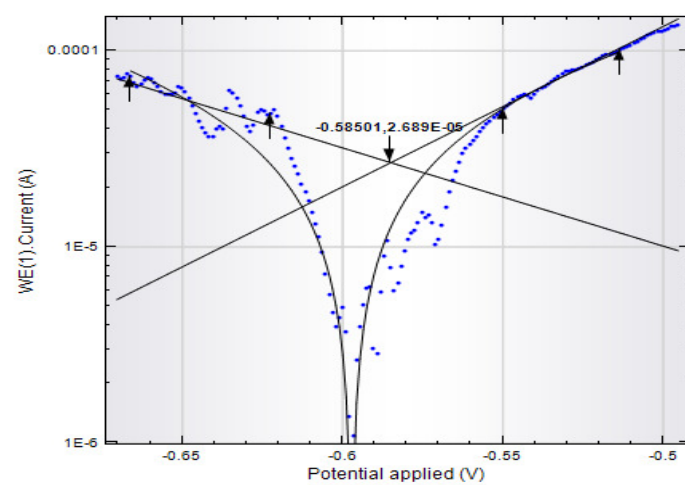


Figure 4-128: Tafel plot of test 6a (100 mg/l F⁻)

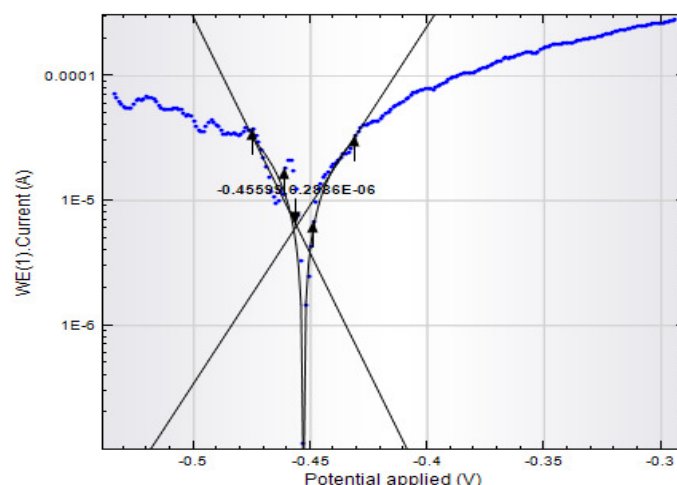


Figure 4-129: Tafel plot of test 6b (100 mg/l F⁻)

According to the plotted calculated corrosion rate versus the target fluoride concentration, it appeared the corrosion rate first decreased from 0.42 mmpa to its minimum value of 0.24 mmpa, at a target fluoride concentration of 20 mg/l (as F⁻), and then it increased to over 0.7 mmpa at the approximate target fluoride concentration of 80 mg/l (Figure 4-130). There then appeared a second, albeit slight decrease, in the corrosion rate at just beyond the 80 mg/l target fluoride concentration. The corrosion results produced by means of this potentiostatic technique compared favourably with the weight loss technique employed in the low alkalinity-low calcium corrosion tests performed in Section 4.8.7 (Figures 4-63 and 4-130). Both techniques first demonstrated an increase in the corrosion rate between 0 and 60 mg/l followed by a levelling off at between 60 and 70 mg/l fluoride. The tests were both performed at similar water chemistries (50 mg/l calcium and a total alkalinity of 55 mg/l (as CaCO₃)). For the target fluoride concentration versus the actual fluoride concentration (Figure 4-130) it was evident there had been a significant reduction in soluble fluoride levels, similar to the tests performed in Section 4.8.7 (Figure 4-65).

The polarization resistance decreased with increasing fluoride whereas the Tafel constants for the anode and cathode varied significantly with fluoride concentration (Figure 4-130). The inverse relationship between the polarisation resistance (slope of voltage versus current curve at the corrosion potential) and the corrosion current

(corrosion rate) is apparent in an almost mirror image of these two curves in Figure 4-130. The corrosion rate is however also a function of the cathodic and anodic Tafel slopes at the corrosion potential. The cathodic Tafel constant first decreased to its minimum value at a fluoride concentration of approximately 20 mg/l and then increased for the remainder of the fluoride range investigated. The anodic Tafel plot initially behaved similarly to the cathode plot for fluoride values up to approximately 20 mg/l but then increased until it reached its maximum at approximately 80 mg/l fluoride.

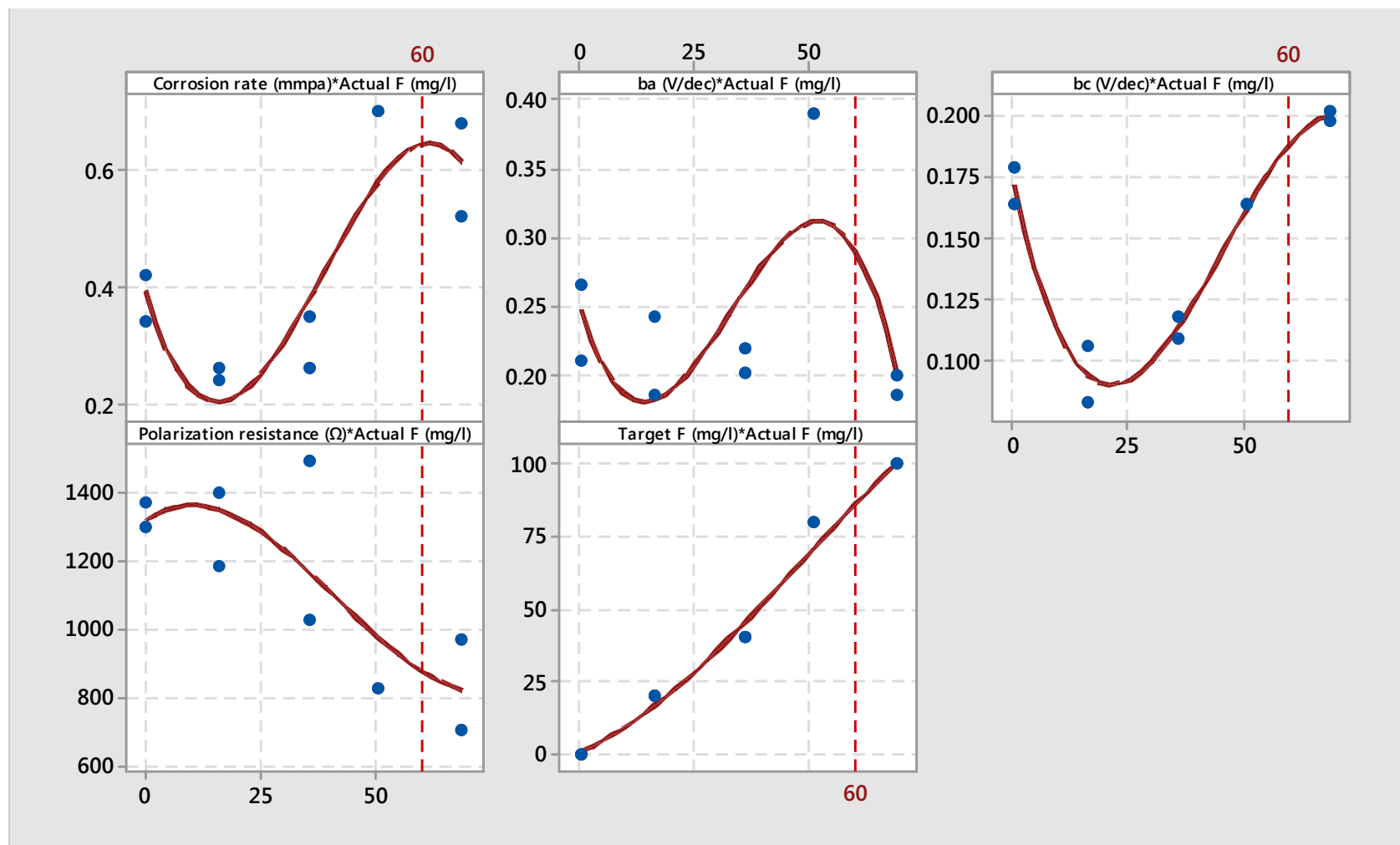


Figure 4-130: Scatterplots of potentiodynamic data versus the actual fluoride concentration

Generally the higher the fluoride concentration (0 to 200 mg/l), the more apparent the extent of the uniform corrosion. No pitting was apparent macroscopically, but was found by scanning electron microscopy in the coupons at fluoride concentrations as low as 70 mg/l. The pits ranged between 0.2 and 1.7 microns in diameter. Coupons immersed in solutions with lower than 70 mg/l fluoride were not examined for microscopic pitting as they were cleaned and used in mass loss corrosion measurements. The SEM observations of the coupons also revealed that after uniform corrosion occurred, intergranular features were also seen on the corroded surface. Due to the higher energy levels of the atoms at the grain boundary, intergranular attack would have been more likely than the corrosion of the grains themselves.

The weight loss and electrochemical techniques both demonstrated that for the lower fluoride concentration range investigated (0 – 90 mg/l), the corrosion rate was related to fluoride concentration. In the Section 4.8.7 series of corrosion tests, performed with low levels of calcium and total alkalinity, the average corrosion rate depended mostly on the initial total alkalinity, initial pH and initial calcium, but was also significantly affected by either the initial fluoride, initial conductivity or initial sodium concentrations. Although the starting calcium concentration and total alkalinity were the same in all the tests performed by either technique, it was inevitable that the measured initial ion concentrations of the ions and the fluoride would have changed as a result of the chemical reactions with the varying fluoride concentrations. A regression model (Equation 4.19) based on sodium as the forth variable produced an R^2 of 94%.

The weight loss corrosion tests performed in this section went beyond the previous target of 90 mg/l fluoride and it was established that the corrosion rate began to plateau at a target fluoride concentration of 150 mg/l, after reaching a peak followed by a trough at the target fluoride concentrations of approximately 100 mg/l and 130 mg/l respectively (Figure 4-86). The addition of sodium fluoride tended to raise the total alkalinity of the test solutions. The final turbidity of the test solutions also increased with sodium fluoride addition but the trend approximated that of the

coupon corrosion rate when plotted against the target fluoride concentration. The initial pH appeared to decrease until it levelled off at the target fluoride concentration of approximately 150 mg/l (Figure 4-86). The initial calcium concentration followed the same trend as the corrosion rate but levelled off at a target fluoride concentration of approximately 120 mg/l (Figure 4-84).

Low magnification optical viewing and EDS analyses of the coupon deposits prior to cleaning revealed that for no fluoride, the coupon was 30% covered in calcium carbonate crystals. The surface deposits contained between 2 and 40% (m/m) calcium. Coupons subjected to between 70 and 200 mg/l fluoride contained deposits with approximately 29% calcium and 28-32% fluoride, an indication that their surface deposits contained precipitated calcium fluoride.

The remainder of the coupons, subjected to between 70 and 200 mg/l fluoride, were found to not contain any calcium or fluorides. This suggested their post cleaning residues primarily comprised iron oxide/hydroxide and were relatively free of calcium carbonate or calcium fluoride deposits.

The 100 minute electrochemical technique, albeit a rather short term exposure, demonstrated a similar trend and similar corrosion rates (0.40 to 0.70 mmpa) to the three day weight loss technique (Figures 4-63 and 4-130). The key findings were that for a low hardness and low alkalinity water, at 45°C, mild steel corrosion increased with the fluoride concentration and then reached a plateau at 60 mg/l. This was supported by the reduction in polarisation resistance with increased fluoride addition (Figure 4-130) due to the increased metal dissolution rate, as inferred by the closely correlated calculated corrosion rate. A drawback of the short run times of both the electrochemical and weight loss techniques were that they were perhaps inadequate for the development of localised corrosion.

CHAPTER 5: APPLICATION OF THE MODELS TO PLANT CONDITIONS

In this chapter the mild steel corrosion coupon data of the two cooling systems reviewed in Chapter 3 were compared against corrosion rates generated with the empirical brackish water mild steel corrosion prediction model derived in Chapter 4.7 (Equation 4.8), referred to as the “Brackish Water Model” (BWM) hereafter. The plant cooling water chemistry data utilized in the calculations are shown in the appendices (Appendices A and B), together with the reported mild steel coupon corrosion rates for each system in Appendix C.

The goodness-of-fit of the BWM to the plant mild steel coupon corrosion rates were analysed visually and quantitatively by means of Pearson correlations. It was also correlated against the indices and the findings discussed.

5.1 Open System One

As apparent in Figure 5-1, the use of the BWM, together with the Open System One water chemistry, produced a statistically significant relationship with the plant mild steel coupon derived corrosion rates ($p < 0.001$). A Pearson correlation coefficient of 0.919 was obtained for the linear relationship between the two variables. A regression analysis of the relationship resulted in a linear fit with an R^2 of 87% (Figure 5-1).

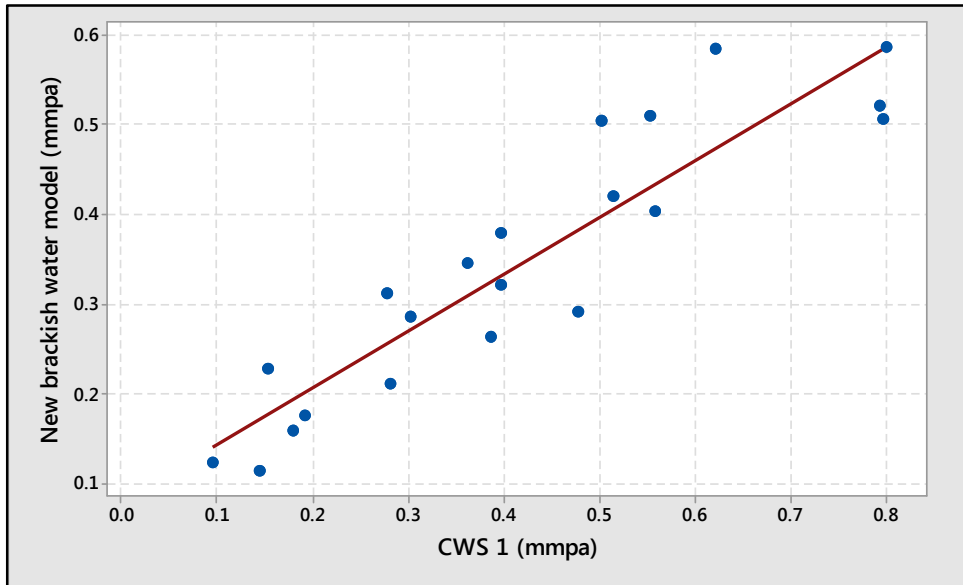


Figure 5-1: Scatterplot comparison of the calculated mild steel corrosion rate (mmpa), based on the BWM and the Open System One water chemistry, versus the measured plant Open System One mild steel coupon corrosion rates (mmpa)

A comparison of the BWM with the previously evaluated indices for the Open System One cooling water, performed in Chapter 3, revealed the significantly improved accuracy of the new model. In Chapter 3, it was found that four indices gave statistically significant correlations with the plant coupon based mild steel corrosion rate (LSI, I_s , SDI and RSI), but none of them predicted corrosive tendency nor gave a reasonably accurate estimate of the corrosion rate on mild steel. Although the buffer capacity produced the expected directional tendency the strength of the relationship was weak and lacked statistical significance.

5.2 Open System Two

The Open System Two corrosion rates (Appendix, Table C1), labelled as CWS 2 in Figure 5-2, were plotted versus the calculated mild steel corrosion rates, where the calculated rates were based on the use of the BWM of Section 4.7 and the water chemistry data given for the Open System Two (Appendix, Table B1). The plots were weakly correlated ($r = -0.104$) and lacked statistical significance ($P = 0.673$). A time series plot was used to demonstrate this lack of correlation, instead of a

scatterplot, as it also revealed the chronological positions of the discrepancies between the CWS2 field data and the new model BWM. In replacing the Open System Two water chemistry data with the Open System One water chemistry data, it was found that the calculated corrosion rates were statistically significantly correlated with the Open System Two plant derived corrosion rates (p value < 0.0001 and r value $= 0.742$). As the two cooling systems utilized the same makeup, they were not expected to have yielded such diverse correlations. It was therefore decided to scrutinize the Open System Two water chemistry data for higher weight factors that may have impacted on the system's actual corrosion data and been excluded from the brackish water model.

Regression analyses were first performed to assess the appropriateness of two of the laboratory derived models reported in Section 4.8, namely the best fit equations of series 6 and 8 (Equations 4.17 and 4.22). The series 6 equation produced a p value of 0.08 and an R^2 of 16%, while the series 8 equation produced a p value of 0.736 and an R^2 of 0.7%, indicating that the predicted mild steel corrosion rates were not statistically significant in their correlations with the plant derived mild steel coupon corrosion results.

Regression analyses were then performed with variables formerly excluded from the laboratory corrosion tests, namely the phosphate, aluminium and oil concentrations. These variables were considered both independently and together with the BWM of Chapter 4.7. The Open System Two water chemistry in Appendix B was used in the corrosion prediction exercise. Table 5-2 show the variables examined and their resulting R^2 values.

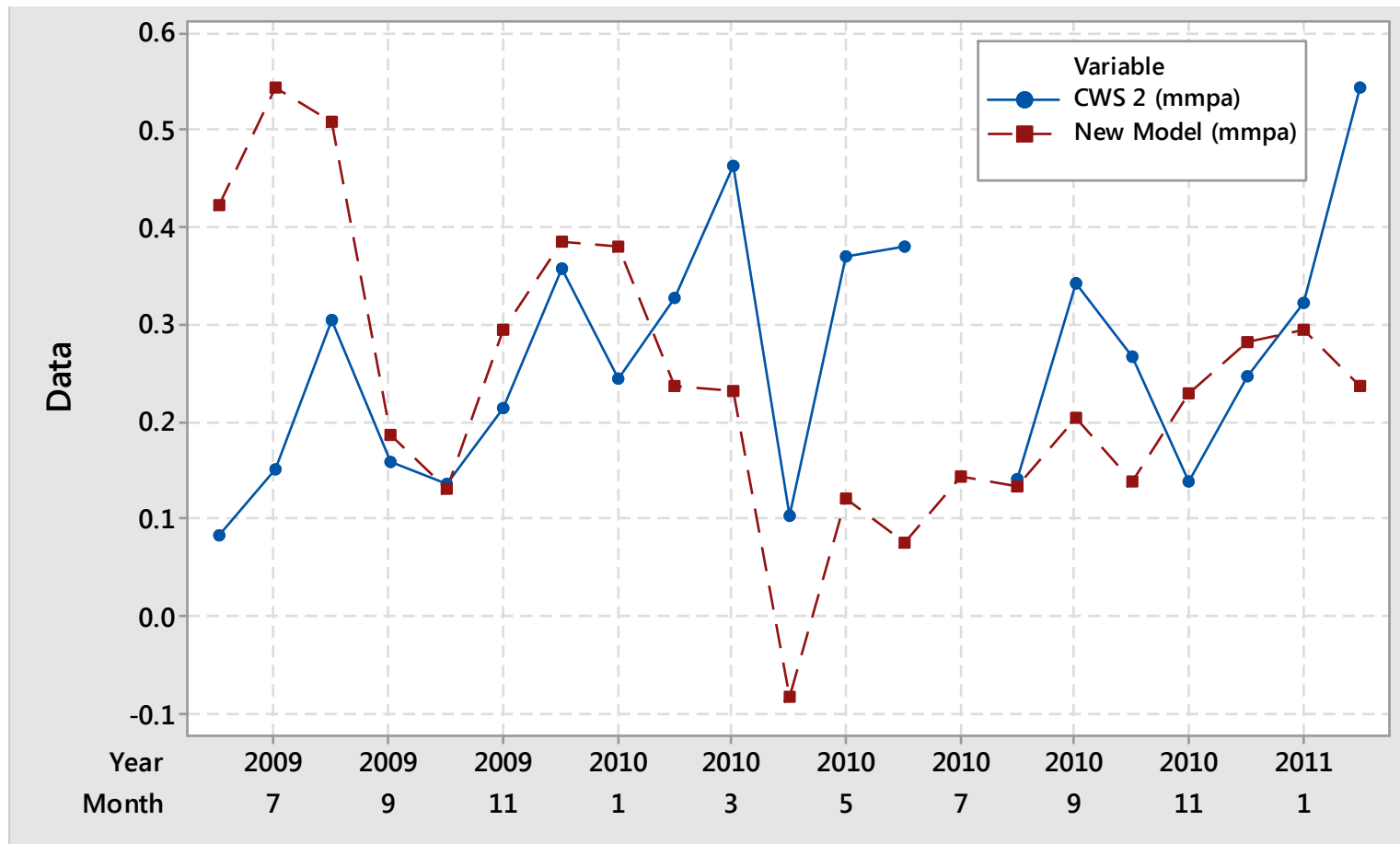


Figure 5-2: Time series plots of the mild steel corrosion rates predicted for CWS 2, based on the new model (i.e. BWM) and CWS2 water chemistry, versus the plant CWS 2 mild steel corrosion rates

Table 5-1: The inclusion of various extraneous variables to improve or supersede the new brackish water model for Open System Two mild steel corrosion prediction

Scenario	Variables considered in regression analyses								% R ²
	pH	Total alkalinity	Aluminium	Phosphate	Fluoride	Oil	Iron	New model	
1				✓				✓	51
2						✓*		✓*	0
3							✓*	✓*	0
4			✓*					✓*	0
6				✓	✓				73
7				✓	✓			✓	85
8	✓			✓	✓				84
9		✓		✓	✓				77
10				✓		✓		✓*	74
11				✓	✓	✓*		✓*	80
12				✓	✓	✓*			80
13						✓	✓		60
14					✓	✓	✓		60
15				✓	✓		✓		90
16			✓	✓	✓				80
17	✓		✓	✓	✓				88
18		✓	✓		✓	✓			92
19		✓	✓	✓	✓				93
20		✓	✓						93

Notes: *. negligible impact.

The R^2 values (Table 5-2) indicated the potential impact the various variables had on the outcome of the corrosion prediction, and from the initial four scenarios it became evident the BWM had minimal, if not nil, correlation with the field corrosion data. It was only once phosphate was included in the BWM that they together resulted in a correlation with an R^2 of 51%. When fluoride was included, together with the BWM and the phosphate, the correlation was improved resulting in an R^2 of 85% (Equation 5.1).

$$\text{Modified BWM} = 0.443 - 0.870 \times \text{PO}_4 + 0.03458 \times \text{F} - 1.801 \times \text{BWM} + 0.2870 \times \text{PO}_4^2 - 0.000507 \times \text{F}^2 + 0.0338 \times \text{F} \times \text{BWM} \dots\dots\dots [5.1]$$

where: Modified BWM corrosion rate (mmpa),

PO₄ = initial phosphate (mg/l as PO₄³⁻),

F = initial fluoride (mg/l as F⁻),

BWM = Brackish water model mild steel corrosion rate (mmpa).

The individual, interactive and collective effects of the variables of Equation 5.1, as applied to Open System Two, are shown in Figure 5-3. The individual effects of the phosphate and fluoride varied with concentration. At lower concentrations, an increase in phosphate tended to decrease corrosion, while an increase in fluoride increased mild steel corrosion. However, at upper concentrations, the reverse was true.

Further refinements in the correlations between the Open System Two water chemistry and its field mild steel corrosion data required a move away from the BWM altogether. Examples of improved correlations were observed for scenarios 15, 18, 19 and 20, where the variables of importance were still mostly: phosphate and fluoride but instead of the new model they included: aluminium, total alkalinity or oil (Table 5-1).

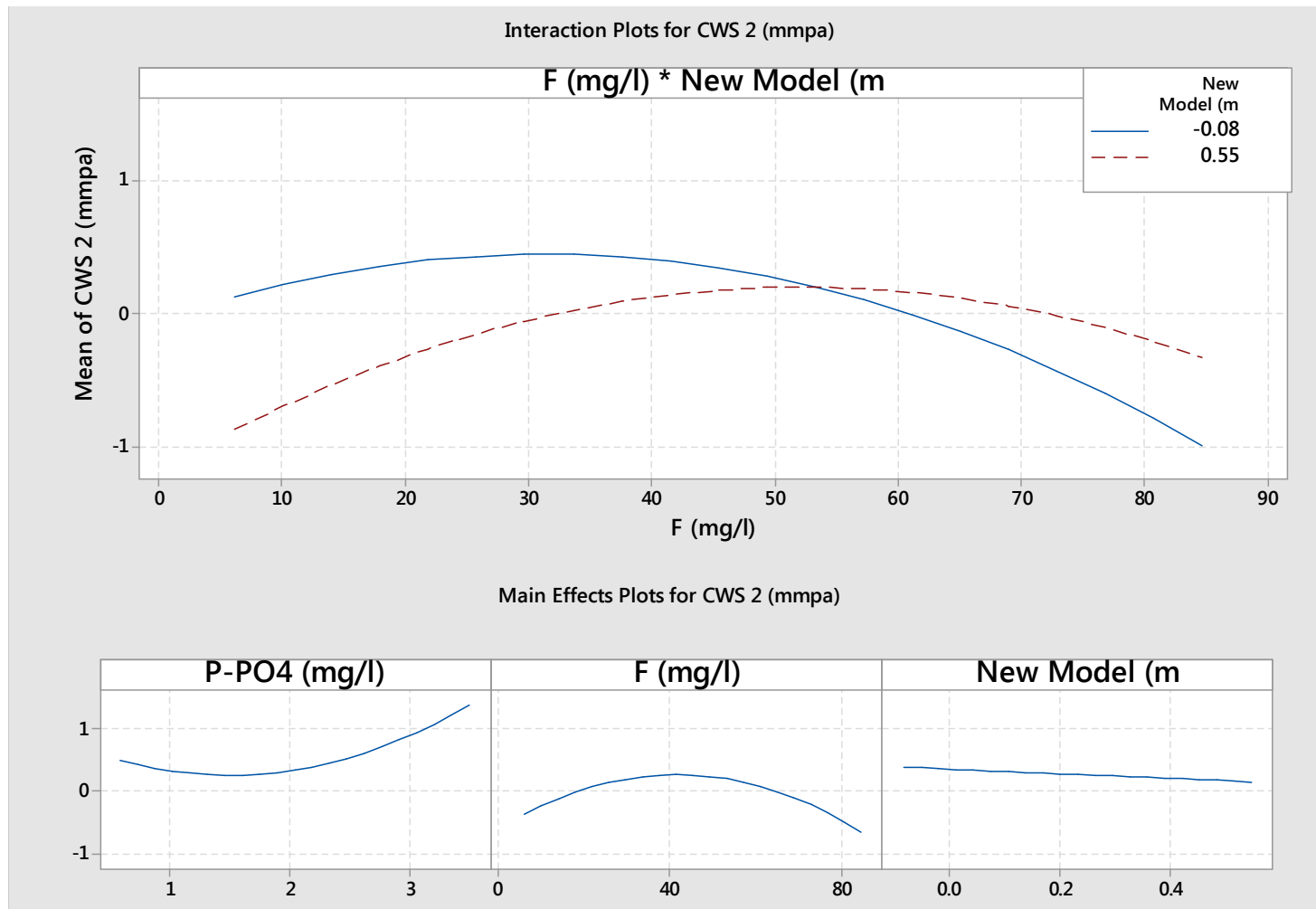


Figure 5-3: Multiple regression for Open System Two showing the fluoride-New Model (i.e. BWM) interaction plot and the effect of the individual variables

Due to the good correlations between both the Open System One and Open System Two field corrosion data and the BWM corrosion results calculated using the Open System One water chemistry, and the fact that a Modified BWM had to be developed in order for there to be a good fit between the Open System Two corrosion and its water chemistry, indicate a possible irregularity with the Open System Two water chemistry data. Although the two cooling systems received the same brackish makeup there were significant differences in their operating conditions, particularly their oil removal rates. The significant difference in the cooling system water chemistries are apparent in the time series comparisons of: pH (Figure H-1), calcium (Figure H-2), total iron (Figure H-7), phosphate (Figure H-8), fluoride (Figure H-9), and oil (Figure H-12). Generally the Open System Two results for oil were higher than Open System One, whereas the opposite was generally apparent for: pH, calcium, phosphate and fluoride.

In order to gain a better understanding of the role of the phosphate, it was decided to review the interaction plot between phosphate and total alkalinity, as well as the impact of the individual variables of scenario 19, Table 5-1. Figure 5-4 shows that individually, the fluoride and total alkalinity had the strongest impacts relative to the aluminium and phosphate concentrations. In the interaction plot between the phosphate and total alkalinity, the higher levels of total alkalinity reversed the reduction in mild steel corrosion imparted by the phosphate.

The different models developed in the various sections (Equations: 3.1, 3.2, 4.3, 4.5, 4.6, 4.8 and 5.1) were tested on the minima and maxima of the combined water chemistry data of One Systems One and Two. The calculated corrosion rates (Table 5-2) were later used to derive hypothetical guideline values for a range of water quality parameters to guide prospective users of brackish waters as cooling water.

Apart from the one exception, where the CWS2 (Equation 3.2) indicated a slight increase in mild steel corrosion with higher total alkalinity, a tendency opposed by both CWS 1 (Equation 3.1) and the laboratory developed equations, generally there was good agreement between the field and laboratory generated models.

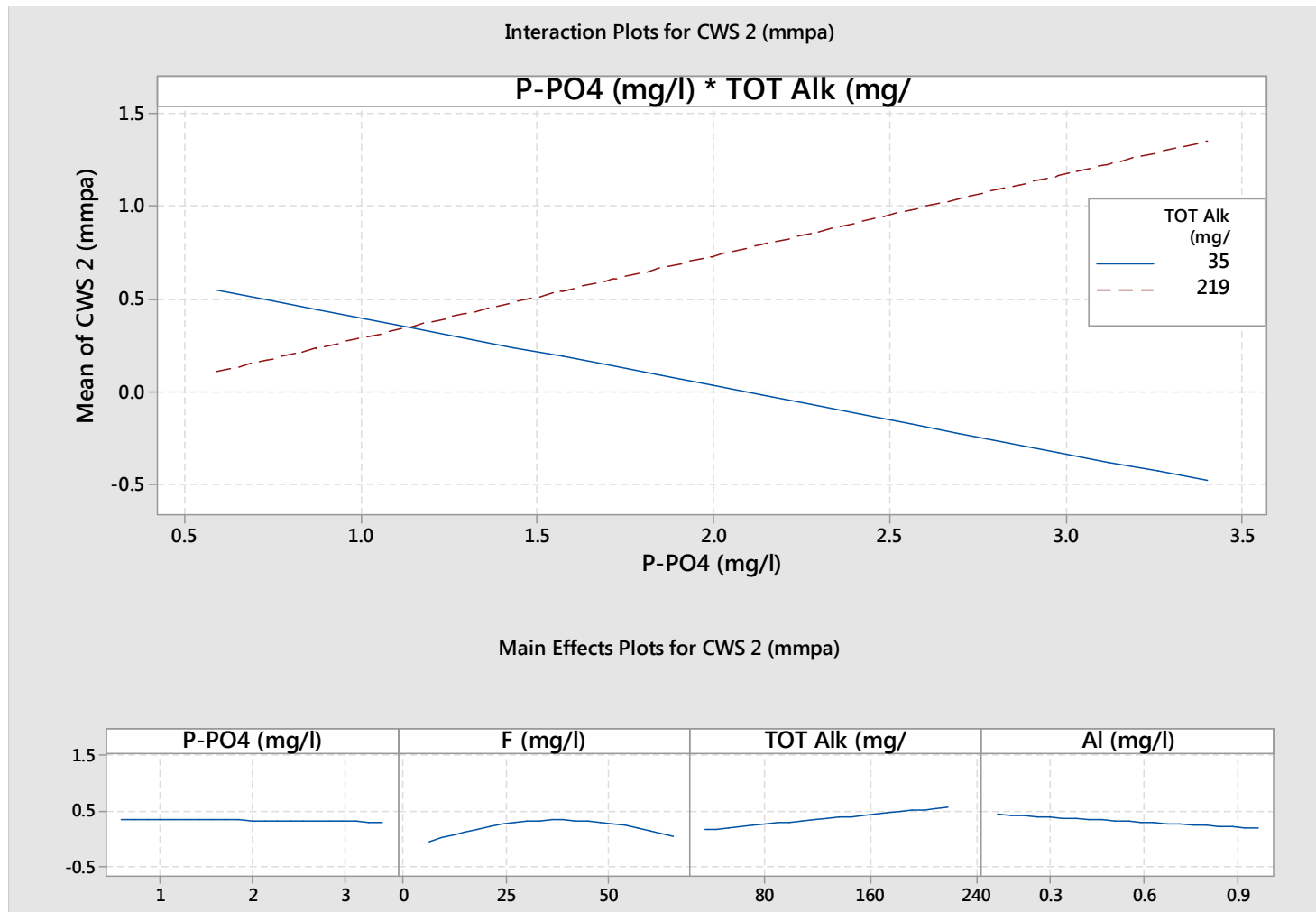


Figure 5-4: Multiple regression for Open System Two showing the phosphate- total alkalinity interaction plot and the effect of the individual variables

Table 5-2: Application of the models to Open Systems One and Two

Equation name:			CWS 1	CWS 2	Ca & alk quadratic	F in brackish	Factorial (brackish)	BWM	Modified BWM	
Equation number:			3.1	3.2	4.3	4.5	4.6	4.8	2.4	
Corrosion rate (mmpa) based on median values ¹ :			0.14	0.32	0.23	0.11	0.12	0.18	0.82	
Statistical Scenarios			Parameter / Scenario	Predicted corrosion rate (mmpa) ¹						
Minimum	Median	Maximum								
6.86	7.69	8.27	pH min	0.14	0.32	0.23	0.42	0.12	0.18	0.82
			pH max	0.15	0.13	0.23	-0.02	-0.01	0.14	0.82
2804	4601	7412	Cond min	-0.91	0.05	0.23	0.11	0.12	0.18	0.82
			Cond max	1.78	0.74	0.23	0.11	0.12	0.18	0.82
502	901	1632	Na min	-2.33	-0.72	0.23	0.11	0.12	0.18	0.82
			Na max	4.66	2.21	0.23	0.11	0.12	0.18	0.82
45	68	120	Ca min	0.33	0.33	0.30	0.14	0.17	0.21	0.82
			Ca max	-0.27	0.29	0.10	-0.30	0.07	0.10	0.81
13	24	46	Mg min	-0.35	0.34	0.23	0.11	0.12	0.18	0.82
			Mg max	1.17	0.27	0.23	0.11	0.12	0.18	0.82
0.2	0.4	1.5	Fe min	0.58	0.32	0.23	0.11	0.12	0.18	0.82
			Fe max	-1.73	0.32	0.23	0.11	0.12	0.18	0.82
35	117	219	Talk min	0.86	0.21	0.50	0.29	0.12	0.46	0.85
			Talk max	-0.76	0.45	0.26	-0.12	0.12	0.23	0.83
400	779	1312	Cl min	2.03	0.93	0.23	0.11	0.13	0.30	0.83
			Cl max	-2.51	-0.53	0.23	0.11	0.10	0.00	0.80
618	1019	1776	SO4 min	1.63	0.85	0.23	0.11	0.27	0.18	0.82
			SO4 max	-2.67	-0.68	0.23	0.11	-0.16	0.18	0.82
6	56	97	F min	0.63	1.17	0.23	0.26	0.12	0.10	0.50
			F max	-0.26	-0.38	0.23	-0.01	0.12	0.15	-0.74

continuation of Table 5-2										
Minimum	Median	Maximum	Parameter	Predicted corrosion rate (mmpa) ¹						
0.6	3.1	9.2	PO4 min	0.08	0.01	0.23	0.11	0.12	0.18	0.39
			PO4 max	0.29	1.11	0.23	0.11	0.12	0.18	17.09
0.35	0.88	2.37	Zn min	0.17	0.32	0.23	0.11	0.12	0.18	0.82
			Zn max	0.07	0.32	0.23	0.11	0.12	0.18	0.82
0.1	0.4	1.0	Al min	0.15	0.50	0.23	0.11	0.12	0.18	0.82
			Al max	0.14	-0.01	0.23	0.11	0.12	0.18	0.82
0.7	1.2	2.8	Oil min	0.12	0.31	0.23	0.11	0.12	0.18	0.82
			Oil max	0.23	0.36	0.23	0.11	0.12	0.18	0.82

Notes:

Bold text. Corrosion is higher than the median value

1. One variable was changed at a time while the others were held constant at the median value.

CHAPTER 6: GENERAL DISCUSSION

As a result of the closing of industrial water loops, or the limited availability of fresh water, industrial facilities have been forced to cascade their inferior water for reuse in their cooling circuits. Furthermore, this water becomes contaminated with materials being used or produced in their processes, as well as concentrate soluble and suspended matter. The main contaminants present in the water in a steel mill are the high levels of suspended solids and mill scale with oil and grease (Christophersen, 2008). Since the advent of the continuous casting machines, steel mills have become more heavily reliant on their cooling water systems (Degrémont, 1991), which has placed additional strain on the efficient operation of these systems. In pursuing ZLD, industrial systems have employed the most advanced wastewater treatment technologies (Siemens, 2012) or resorted to special design requirements in order to manage the associated water types (Maulbetsch and Di Fillippo, 2010).

Additionally effluent streams in steel mills are also high in fluorides, due to the addition of certain alloys and fluxes, and one such material is fluorspar, CaF_2 (Flynn and Nalco Company, 2009). Other industries producing effluent high in fluoride are aluminium smelters, cement production, and ceramic and brick firing (Brindha and Elango, 2011).

This research has shown that a complex series of interactions exist between the various variables used to characterize the corrosive nature of a water used in industry. A range of inorganic cations (sodium, calcium, magnesium, aluminium and iron) and anions (chloride, sulphate, fluoride, phosphate) as well as pH, total alkalinity, conductivity and oil content were measured during the field evaluations in the preamble to the laboratory work.

6.1 Field Data

In an analysis of the monthly mild steel corrosion coupon results of two open cooling systems at a Southern African steel mill, for the period June 2009 to

February 2011, it was realized that it was virtually impossible to predict the corrosivity of the fluoride-containing brackish water solely on the water chemistry data provided. The two systems received the same brackish water as their makeup, but the significant differences in their operating conditions and chemical treatment was sufficient for them to have different mild steel corrosion rates. Matrix scatterplots of the Open System One mild steel coupon corrosion data versus each measured parameter (Figure 3-4) indicated that the coupon corrosion rates increased with increases in pH and phosphate. The Open System Two scatterplot matrix (Figure 3-5) showed that only increases in the levels of calcium, magnesium and silica were very weakly correlated with increases in mild steel corrosion.

In an initial endeavour to investigate the possible combined effect/s or interdependency of the various water chemistry variables, a broad range of scaling and corrosion indices were each compared against the mild steel corrosion coupon data from both cooling systems. Pearson correlations and p values were calculated to determine if there were any correlations between the calculated indices and the field coupon corrosion rates. The results for Open System One indicated that there were statistically significant relationships for (Table 3-5): LSI (Langelier Saturation Index), I_s (O & T scaling Index), SDI (Stiff and Davis Index), and RSI (Ryznar Stability Index), although the Pearson correlation coefficients (r values) contradicted the expectation that higher calcium carbonate scaling tendencies tended to reduce mild steel corrosion. These findings were therefore in agreement with the opinion of several authors who eventually stated that the LSI had no correlation with corrosion rate (Pisigan Jr. and Singley, 1987; Piron *et al.*, 1986; Singley, 1981; Larson and Sollo, 1967; Stumm, 1960; Schock, 1984), and that it should be abandoned (AWWARF and DVGW, 1996).

For Open System One, the buffer capacity was inversely related to the mild steel coupon corrosion rate and agreed with Stumm (1960), who stated that “in waters of high buffer capacity more homogeneous and more protective coatings are formed than in waters of low buffer capacity”. However, the p value for this factor indicated the relationship was not statistically significant.

In a similar study for Open System Two it was found that only the calcium carbonate saturation level produced a statistically significant correlation (i.e. a p value < 0.05). The directional tendency of the correlation was found to be moderate and in line with what was expected, that is, when a water is under-saturated with respect to calcium carbonate, it can be assumed to be corrosive (Langelier, 1936). Similar correlations to the calcium carbonate saturation, but with highly probable chance findings (high p values), were noted for various alternative calcium carbonate based indices: calcium carbonate FIME (Free Ion Momentary Excess), CCPP (Calcium Carbonate Precipitation Potential), RSI (Ryznar Stability Index), I_s (O & T scaling Index), and SDI (Stiff and Davis Index).

Regression analyses of the time plotted corrosion data versus the water quality parameters resulted in an equation per cooling system (Equations 3.1 and 3.2), which were analysed to further understand the impact of the individual variables on field coupon mild steel corrosion data. For Open System One sodium and magnesium were statistically significant and appeared to increase corrosion, whereas all the other variables were either not statistically significant, or appeared to decrease mild steel corrosion. The regression (Equation 3.1) for Open System One generated an R -Sq (adj) value of 88%. The tendencies for either sodium or magnesium to increase corrosion were noted in some of the indices. The former calcium carbonate based indices, such as the LSI, RSI and PSI, all consider magnesium in their calculations of the pH of saturation. Increases in the magnesium concentration increase the pHs, which results in lower LSI or higher RSI and PSI values, indicating increased tendency for the dissolution of the protective layer of calcium carbonate.

For Open System Two, the only statistically significant variable to increase corrosion was fluoride. The regression (Equation 3.2) produced a (R -Sq (adj)) of 41%. This is corroborated by the many authors although this work is differed from that of the referenced articles is in the test conditions (i.e. temperatures), solution chemistry (i.e. pH, alkalinity, calcium hardness) and fluoride concentrations.

Apart from the regression equation produced for the Open System One, the relatively strong and theoretically feasible correlations between the field corrosion coupon data and either the individual water chemistry parameters or the commonly used indices were largely inadequate at providing statistically and scientifically acceptable models for predicting the corrosivity of the brackish water on mild steel at 45°C.

6.2 Laboratory Data

6.2.1 Synthetic brackish water experiments

6.2.1.1 Classical design experiments

a) Low alkalinity tests (18 to 73 mg/l CaCO₃)

The initial series of corrosion tests were conducted in synthetic water with low total alkalinity. The tests performed at 35°C and 45°C both indicated strong negative relationships between the average and individual coupon corrosion rates and the total alkalinity. The scatterplots of the initial and final total alkalinities showed they were approximately similar in their relationship with the average corrosion rate, Tables 4-9 and 4-10, and Figures 4-3 to 4-5 and 4-8. A linear model accounted for 65% of the variances in the average coupon corrosion rate at 45°C (Figure 4-6). Almost all the indices follow these results: LSI, RSI, RCI, CIn, SDI, LR, ME, DFI, CCPP, Y, I_s, PSI and LRM. Some of the indices which do not indicate a decrease in the mild steel corrosion rate with an increase in alkalinity include Stumm's Buffer index (1960) (β) and Pisigan and Singley's (1984) multivariate equations, which also rely on β . Although β is dependent upon the alkalinity, it is also dependent upon the pH. Therefore, where the current findings and most of the previous indices differ from the β based indices is that they may not consider the effect of pH. Most of the indices that do rely on pH assert that increases in pH are likely to cause a decrease in corrosion: LSI, RSI, SDI, I_s and RSI.

A comparison between the coupon data of the corrosion tests at 35°C versus those at 45°C showed the two sets were very similar (Figure 4-7), but due to the limited

number of tests it was not possible to accurately quantify the impact of the temperature difference of 10°C.

b) System equivalent alkalinity tests (55 to 220 mg/l CaCO₃)

Corrosion tests were repeated at the same temperatures, and for a range of total alkalinities equivalent to the field data. The increased temperature from 35°C to 45°C, was enough to produce a slight increase in the corrosivity of the brackish water (at ~pH 7.8) on mild steel if the calcium hardness was < 70 mg/l (as Ca²⁺), and at a moderate alkalinity of 110 mg/l as CaCO₃. When the solution approached calcium carbonate saturation, the impact of temperature diminished (Figure 4-11). As the water became supersaturated, at Ca levels above 75 mg/l and alkalinity of 165 mg/l (as CaCO₃), any increase in temperature led to calcium carbonate precipitation resulting in lower levels of soluble calcium and alkalinity, thereby producing an under-stabilized and more corrosive solution. Although not verified, this trend of an initial decrease in the mild steel corrosion rate, followed by an increase, with increasing alkalinity, is speculated to approximate the trend modelled by the Stumm's Buffer Index (1960). The Buffer Index is a function of pH and alkalinity, and higher β values correlated with lower corrosion rates, while lower β values correlated with higher corrosion rates. For the pH and temperatures considered, the contour plots (Figures 4-14 to 4-17) demonstrated that, as in Figure 4-11, the most suitable calcium hardness and alkalinity were within the narrow middle range, such that the solution was neither very under-saturated nor much supersaturated.

Amongst the indicators of mild steel corrosion at 35°C and 45°C, coupon corrosion rates, Corrater[®] measurements using mild steel tips, test solution final total iron levels and residual oxygen concentration, the only response variable to consistently produce statistically significant strong correlations with any predictor variable was the average coupon corrosion rate. It was only possible to find statistically significant linear correlations, at 95% confidence level, between the average corrosion rate and the Corrater[®] general corrosion readings for the tests at 45°C (Figures 4-12 and 4-13, and Table 4-14). The latter two corrosion measures were

only regarded to be moderately strong and positively correlated. The lack of correlation between the average corrosion rate and the oxygen concentration in Section 4.4.1 (Table 4-9) also lead to a cessation of the oxygen measurements as an indicator of the corrosion rate. The lack of correlation between the average corrosion rate and the total iron levels is attributed to the relatively large standard deviation in the total iron results (~0.8 mg/l, Figure 4-85). This is possibly due to inaccuracies associated with the method of iron re-solubilisation in the sample acid digestion step prior to the analysis.

According to Table 4-14, the only predictor variables to produce relevant statistically significant strong correlations with the average coupon corrosion rates at 35°C were the initial and final calcium, both with negative correlations. At 45°C, moderate negative relationships were apparent for: initial total alkalinity, final pH, and initial calcium. Langelier (1936), Ryznar (1944), Riddick (1944), Stiff and Davis (1952), McCauley (1960) and, Merrill and Sanks (1978) included calcium in their empirically derived predictive models: LSI, RSI, RCI, SDI, DFI, and CCPP. The same is true for the pH of the following indices: LSI, RSI, SDI, β , I_s , PSI and CR13 (Pisigan and Singley, 1984). Linear regression analysis of the correlation between the average coupon corrosion rates and the various predictors confirmed the role of the initial pH and the initial calcium concentration ($R\text{-Sq (adj)} = 54\%$) (Equation 4.2 in Table 4-15).

In the development of the 8-variable empirical model, Pisigan and Singley stated that it was necessary to compensate for the increased corrosion with sodium bicarbonate addition, due to the impact of the sodium ions on the ionic strength of the test solutions. In this work, sodium bicarbonate was used to increase the total alkalinity, and although the sodium levels and ionicity increased with increasing alkalinity, there was no indication of increased corrosion. In fact statistically significant negative correlations were found between the calculated corrosion rate and the ionicity or the total alkalinity (Table 4-16).

The empirically derived non-linear regression (Equation 4.3), based on only initial calcium and initial total alkalinity accounted for 90% of the variations in the average corrosion coupon data. This equation was correlated against the various established indices and their statistically significant linear relationships were only moderate strong, at the 95% confidence level. A review of the formulae of these eight indices and a comparison to the remaining six non-statistically significant and weakly correlated indices revealed that the latter were linearly related to either calcium concentration or total alkalinity whereas the former eight indices are a function of either the log or inverse of either the calcium concentration and/or total alkalinity. The newly proposed empirically derived non-linear regression model differed from both sets of indices in that it was based on a quadratic equation incorporating both the calcium concentration, as Ca^{2+} , and total alkalinity in mg/l as CaCO_3 . A comparison of the contour plot of the new model versus that of other indices for the set of target values considered, revealed the higher impact of calcium concentration on the corrosivity, as from the steeper diagonal contour lines (Figure 4-20).

c) Varying chloride, sulphate, fluoride or magnesium concentrations

There were no statistically significant correlations between the chloride concentration and the corrosion rates measured by either the coupon method or the Corrat[®] (Table G-5). This was supported by the broad and uniform scatter and almost horizontal regression line in Figure 4-29. The findings of these chloride tests contradicted the Cassil Index (CIn) (Loschiavo, 1948), the Larson and Skold Index (LR) and the Modified Larson Ratio (LRM) (Imran *et al.*, Nov 2005). However these indices were devised for the corrosiveness of “soft water supplies” / drinking water systems. The LR was based on water sourced from the Great Lakes (i.e. with a calcium hardness of 25 to 250 mg/l, as CaCO_3 , and total alkalinity of 50 to 250 mg/l, as CaCO_3) (Larson, 1975). Further to being sufficiently different in salinity from the brackish water evaluated, none considered the effect of temperatures above 27°C. Amongst the four equations proposed by Pisigan and Singley (1984), only two were a function of the chloride concentration, and both indicated an increase in

corrosion rate with increases in the chloride concentration. These models were also developed for drinking water systems.

Statistically significant moderate strong positive linear relationships were confirmed between the coupon corrosion rates and the sulphate concentration (Figure 4-30, Table 4-25) and the Pearson correlation coefficients given in Table G-6), and the best fit for the relationship between the average corrosion rate and initial sulphate concentration was a linear equation with an adjusted R^2 of 58 (Figure 4-31). This model differed from that of Larson and Skold (1957) where the chloride and sulphate ions were linearly correlated with the mild steel corrosion rate, in that here, only the sulphate ion was found to be linearly correlated. During these laboratory evaluations of the impact of sulphate it was also noted that the resulting test solution conductivities did not correlate well with the average coupon corrosion rates (Table G-6).

In Section 4.4.4 sodium fluoride was added to chemically comparable synthetic solutions to investigate the impact of fluoride on the corrosivity of a synthetic brackish water on mild steel at 45°C. Table 4-29 and the important statistically significant correlations for the average corrosion rate and key variables show that the addition of sodium fluoride proportionally reduced the soluble calcium levels due to the formation of the sparingly soluble calcium fluoride. The higher the initial fluoride concentration, the lower the resulting final test solution calcium concentration. Higher coupon corrosion rates were associated with these higher fluoride levels and lower soluble calcium levels. Moderate to weak correlations were found between the corrosion rate and the other less prominent variables: pH, total alkalinity and conductivity. Similar findings were obtained by Vasil'eva *et al.* (1986), in tests with solutions of 610 mg/l Ca^{2+} , 15.2 mg/l F^- , 480mg/l SO_4^{2-} , 16.4 mg/l PO_4^{3-} (as P_2O_5), at pH 8.6, and between 30°C and 70°C. The current work differed from these results in that the tests were performed with a phosphorus containing compound, which could have acted as corrosion inhibitor, without magnesium and chloride ions, a significantly higher calcium concentration and significantly lower sulphate concentration. Vasil'eva *et al.* (1986) reported that both

calcium fluoride and calcium phosphate deposited, resulting in a reduction in the corrosion rate of mild steel (St. 3).

Figure 4-34 shows that although high fluoride concentrations of 90 mg/l were targeted, the highest fluoride concentrations attained at 45°C and the initial calcium concentration of 75 mg/l (as Ca^{2+}), was only approximately 34 mg/l (as F^-). This again demonstrated that calcium fluoride precipitation had occurred. Additional support for the reduction of corrosion through the reduction of the fluoride concentration as a result of calcium fluoride precipitation was provided by Macias and Escudero (1994) who established that saturated lime solutions can precipitate CaF_2 to lower the fluoride concentration to below the minimum level that would promote pitting.

A regression analysis for the average coupon corrosion rate versus the test solution initial fluoride concentration for the given range yielded a statistically significant linear model with an R^2 (adj) of 60%. From Figure 4-36, the: pH, calcium, fluoride, and total alkalinity had the most statistically significant relationship with the mild steel coupon corrosion rate. The collective impact of these key variables was more accurately represented by the four variable quadratic regression, Equation 4.5, with an R^2 (adj) of 88%. Figures 4-32 to 4-35 show that the amount of fluoride added had directly impact the test solution residual calcium and fluoride concentrations, and the fluoride concentration was linearly related to the mild steel corrosion rate.

Figure 4-38 and Table 4-33 both indicated statistically significant strong positive correlations between average corrosion rate and magnesium (initial and final) concentrations. This agrees with the LSI, RSI and PSI indices, where an increase in the magnesium concentration results in a higher calculated pH of saturation, a solution with a decreased tendency of being supersaturated with respect to calcium carbonate, and therefore more corrosive towards mild steel.

The regression analysis for the average coupon corrosion rate versus the test solution initial magnesium concentration gave statistically significant linear and

quadratic regression plots, but due to the limited number of samples it was not possible to provide an accurate indication of the strength of the relationship.

6.2.1.2 Factorial design experiments

By combining several variables, instead of creating a separate study for each, the total number of tests (18) were significantly reduced. Further to the previously adopted one-factor-at-a-time (OFAT) classical experimental design approach, the additional benefit of the factorial design approach was to detect the unique effects of the combination of factors.

The factorial design resulted in a four variable main effect regression model (Equation 4.6, $R^2 = 95\%$) with the most influential input variables being: the initial calcium concentration, initial pH, initial chloride concentration and initial sulphate concentration. Figures 4-41 and 4-42 show that the pH and chloride linearly decreased the mild steel coupon corrosion rate, whereas the initial calcium and initial sulphate concentrations first decreased and then increased corrosion.

The trends detected with chloride in this factorial design approach differed from the OFAT approach in that in the former tests the chloride concentration did not have any statistically significant impact on the mild steel corrosion rate. An additional observation, was that the chloride ion reduced the corrosivity of the sulphate ion.

Although sulphate produced a mild steel corrosivity trend that corresponded with conventional opinion, the chloride ion, surprisingly, produced a trend completely contrary to the indices devised for the anion in drinking water systems: CIn, LR, LRM, CR8 and CR13, but agree with Feigenbaum *et al.* (1978) for the saline waters of the Negev desert. The tests by Feigenbaum *et al.* were also for the protection of pipes in contact with natural water, which contained considerably higher concentrations of chloride (202 to 539 mg/l as Cl^-) and sulphate (76 to 875 mg/l as SO_4^{2-}).

6.2.1.3 Evaluation of corrosion inhibitors

The laboratory screening of various commercially available corrosion inhibitors was performed on synthetic fluoride containing brackish water with mild steel over three days at 45°C. The tests served to provide insight into the potential impact of the inhibitors on the corrosion prediction model/s, as well as an indication of their potential to individually minimize the corrosivity of the fluoride containing brackish water at 45°C. The results confirmed the inhibitory nature of zinc and phosphate, and were already in use on the plant. Open System Open contained between 0.35 and 2.37 mg/l Zn^{2+} and between 0.7 and 9.2 mg/l PO_4^{3-} (Table 3-2) while Open System Two contained between 0.6 and 3.4 mg/l PO_4^{3-} (Table 3-3). No zinc was reported for Open System Two.

The concentrations of zinc (2.2 mg/l Zn^{2+}) and phosphate (5.3 mg/l PO_4^{3-}) used in the screening tests were well within the concentration ranges typically used in cooling water systems (Table 2-6 (Buckman, 1981; Flynn and Nalco Company, 2009 and Frayne, 1999)) yet the two corrosion inhibitors only produced minor reductions in mild steel corrosion of 22.7% and 9.7% respectively. Sodium molybdate (5 mg/l as MoO_4^-) alone appeared to have led to an increase in mild steel corrosion by 3.6%, but the corrosion rates obtained were within the range of the error bars of the control tests. Sodium molybdate was also severely under-dosed as a standalone treatment for open cooling systems. Generally, due to cost, the treatment of open cooling systems with molybdate is done in conjunction with other corrosion inhibitors (Frayne, 1999).

6.2.1.4 Regression analysis of all the synthetic brackish water experiments (includes all the classical and factorial data)

This section comprised a statistical analysis of the combined data from all the brackish water related experiments, classical and factorial design experiments. There was insufficient evidence to show that the mean coupon corrosion rate at 35°C was statistically significantly less than at 45°C. This was due to: a) limited number of observations ($n = 20$), and b) in certain cases, e.g. the OFAT brackish water corrosion tests performed at system equivalent alkalinity, the two

temperatures produced identical results at the higher levels of calcium carbonate saturation, Figure 4-11. For the same set of conditions, the higher temperature lead to slightly higher corrosion rates at the lower calcium hardness values (<75 mg/l).

The data allowed for the construction of a five variable equation (Equation 4.8) ($R^2 = 81\%$) for the corrosivity of a fluoride-containing brackish water at 45°C: pH, calcium, total alkalinity, chloride and fluoride. A comparison of these findings with those of each of the experimental design approaches showed that the five variable equation had components from both. The total alkalinity, calcium, pH and chloride ions decreased the mild steel corrosion rate, whereas the fluoride concentration increased the corrosion rate. It was rather unexpected that the sulphate ion did not feature in this equation as it led to moderate strong positive correlations in both the classical and factorial experiments.

According to Pisigan and Singley (1985), the sulphate ion is part of calcium carbonate saturation based indices (LSI, RSI, and PSI), due to the pH of saturation calculation which is common. Increased sulphate concentration resulted in increased pHs, which translates into relatively small reductions in the calcium carbonate scaling tendency, which in turn indicates slightly increased corrosion tendencies. Other indices incorporating the sulphate ion include: LR, CR8 and Y (Yahalom Index) (Feigenbaum *et al.*, 1978). The sulphate ion is very significant component of the LR, with very comparable weightings to the chloride ion and total alkalinity. According to the Larson Ratio (Larson and Skold, 1957) 1 mg/l of sulphate has the equivalent weighting to 1.35 mg/l of chloride and 1.41 mg/l of total alkalinity (as CaCO_3). In the CR8 equation (Pisigan and Singley, 1984), the sulphate ion again has a very small effect on the overall corrosion rate. However, the Y Index (Feigenbaum *et al.*, 1978), originally designed for saline waters, and therefore probably the most fitting for use on brackish waters, indicated that increases in sulphate led to decreased corrosion rate, the chloride and sulphate have the same weighting.

6.2.2 Further experimentation with fluoride

For higher initial calcium concentrations, the fluoride solubility was approximately 40 to 50% higher in the presence of high chloride concentrations (1000 mg/l Cl^-) and sulphate (1500 mg/l SO_4^{2-}), relative to tests performed without the addition of chloride or sulphate ions. Calcium fluoride precipitation resulted in reduced fluoride residuals and the subsequent reduction in mild steel corrosion. This agreed with the work of Vasil'eva *et al.* (1986), Macias and Escudero (1994), Singh *et al.* (2002) and Brell *et al.* (2003). Most of this previous work was performed in significantly different physical or chemical conditions but remained relevant to the similar situations of the current investigation, where calcium fluoride saturation became evident.

Regression analyses performed on the individual nine series of fluoride tests produced a broad spectrum of mathematical models, which at first appeared rather inconsistent in nature. The major findings of the regression analysis of each series are reported in Table 4-73. These results indicated that fluoride was corrosive towards mild steel when it was added to deionized water or to a high total alkalinity water without hardness. The corrosivity for mild steel in test solutions with low levels of calcium was deemed to be predominantly due to their relatively high pH, sodium and total alkalinity levels.

An additional finding of the regression analyses on the individual series was that sodium based laboratory reagents, either for the alkalinity (as NaHCO_3), sulphate (as Na_2SO_4) or chloride (as NaCl) addition, inevitably led to mild steel corrosion rates that were moderate to strongly correlated with the sodium concentration. This is particularly so for series: 7, 8 and 9 which had highest added concentrations of salts, (Table 4-73 and Figure 4-83). It is suggested that apart from the conductivity the sodium concentration most closely correlates with the ionicity of the test solutions, and therefore has the greatest impact on corrosion. This agreed with the modified Larson ratio (LRM) (Imran *et al.*, Nov 2005), where sodium was added to compensate for the increased total dissolved solids.

Spearman (Table 4-76) and Pearson correlation coefficients (Table 4-77) performed on all the results of the fluoride tests indicated there to be less significant relationship between the sodium concentration and the average corrosion rate than between the fluoride concentration and the average corrosion rate. Two additional and equally important outcomes of the statistical correlations were that the two main factors which impacted on the mild steel corrosion rate were the fluoride and calcium concentrations, and that there were moderately strong positive correlations between the average corrosion rate and the fluoride concentration, and strong negative correlations between the average corrosion rate and the calcium concentration, Tables 4-76 and 4-77. Thus both the fluoride and calcium concentrations were the most significant factors impacting the mild steel corrosion rate at 45°C.

6.2.3 Microscopic, chemical and electrochemical studies into the effect of fluoride on mild steel corrosion

This section is based on the optical and elemental analyses of weight loss corrosion coupons exposed to low calcium hardness and low total alkalinity, at higher fluoride concentrations of 70 to 200 mg/l, at 45°C. These conditions were selected because the corrosion tests in Sections 4.4 and 4.8, and shown by Figures: 4-35, 4-50, 4-56, 4-63, 4-66, 4-69 and 4-72, indicated the corrosion rate increased linearly with increasing fluoride concentration and then appeared to plateau at fluoride concentrations between 20 and 65 mg/l. The purpose of this additional test work was to evaluate the impact of fluoride at above 90 mg/l.

The corrosion results of the initial lower fluoride concentrations, 0 to 90 mg/l F⁻, (Section 4.8.7, Figure 4-63), and the higher fluoride tests, 70 to 200 mg/l F⁻ (Figure 4-85) confirmed the plateau in the mild steel corrosion rates at the target fluoride concentration of approximately 70 mg/l. These results differed from the macroscopic examination of the coupons Figure 4-87, where the total area of the corrosion coupons that were etched, and more corroded, were higher for the higher fluoride concentrations (0 to 200 mg/l). A comparison of the results of the combined low (0 to 90 mg/l F⁻) and high fluoride (70 to 200 mg/l F⁻) to those of Singh *et al.*

(2002), albeit in a significantly different environment (i.e. mild steel rebar in contact with 0.01 N NaOH solutions) showed some similarity. Both results confirmed that low fluoride concentrations increased mild steel corrosion (< 25 mg/l (Singh, 2002) or < 40 mg/l in the case of brackish water in the current work) but unlike the previous work (Singh, 2002) higher fluoride concentrations (> 100 mg/l) did not produce inhibition, increasing calcium fluoride precipitation. Corrosion rates were found to plateau between 0.4 and 0.9 mmpa at fluoride concentrations between 20 and 65 mg/l.

Low magnification microscopy, EDS analyses and carbonate spot tests performed on the coupon deposits prior to cleaning, where no fluoride was added to the test solutions, confirmed that up to approximately 30% of the surfaces of the corrosion coupons were covered in calcium carbonate crystals. Coupons subjected to moderately high concentrations of fluoride (70 and 200 mg/l) were found to contain deposits with approximately 30% calcium fluoride. EDS analyses and calcium carbonate spot tests of the cleaned coupons removed from the test solutions without fluoride confirmed the presence of traces of tightly adherent and dense calcium carbonate crystals. At between 70 to 200 mg/l fluoride, the deposits analysed on the cleaned coupons were mainly iron oxide/hydroxide. This indicated that the calcium fluoride deposits formed during the experiment were washed away during the coupon cleaning.

Turbidity measurements of the corrosion test solutions for the 0 to 200 mg/l fluoride range supported the understanding that more calcium fluoride precipitated with higher fluoride concentrations. Unlike calcium carbonate, calcium fluoride had not become firmly attached to the coupon surface, but remained as a suspended solid or formed a sediment.

The addition of sodium fluoride to the low calcium hardness and low total alkalinity test solutions caused a decrease in the initial pH readings, which levelled off at the target fluoride concentration of approximately 150 mg/l (or initial fluoride

concentration of 100 mg/l). The initial calcium concentration followed suite but levelled off at a lower target fluoride concentration of approximately 120 mg/l.

Pitting was found only by scanning electron microscopy in the coupons at fluoride concentrations as low as 70 mg/l. The pits were between 0.2 and 1.7 μm across. Coupons immersed in solutions with lower than 70 mg/l fluoride were not examined for microscopic pitting. The involvement of fluoride in under-deposit or accelerated crevice corrosion or pitting has been recorded by Mayer *et al.*, (1984), Moll *et al.*, (1985) and Dillon and Waltman, (1995).

6.2.4 Application of the models to plant conditions

The combined data from all the brackish water related experiments, utilising the data from both the classical and factorial design experiments, allowed for the construction of a five variable equation (Equation 4.8) ($R^2 = 81\%$) for the corrosivity of a fluoride-containing brackish water at 45°C. The equation included: pH, calcium, total alkalinity, chloride and fluoride. In order to test the accuracy of the empirically derived brackish water mild steel corrosion prediction model, the “Brackish Water Model” (BWM), was applied to the cooling water chemistry of each of the open systems discussed earlier, namely Open Systems One and Two.

The BWM was found to be reasonably accurate in its prediction of the Open System One corrosion, by its statistically significant strong correlation ($r = 0.92$) with the actual plant mild steel coupon data and the linear fit with an R^2 of 87% (Figure 5-1). Although four of the indices found in literature yielded statistically significant correlations with the plant coupon corrosion data (LSI, I_s , SDI and RSI), none of them predicted the correct tendency for corrosion nor accurately estimate the mild steel corrosion rate. The buffer capacity did produce the expected directional tendency, that is its ability to decrease rather than reduce corrosion, but its correlation was not statistically significant.

For Open System Two, the BWM produced a completely deficient fit. Although a weak correlation was apparent between the Open system Two coupon data and the

BWM predicted corrosion rates, the relationship between the two data sets were not statistically significant ($P = 0.673$). In order to account for the poor accuracy of the BWM in its application to the Open System Two the factors initially excluded from the BWM were examined: phosphate, aluminium and oil concentrations. Once phosphate was included, the resulting new model generated a markedly improved correlation with an R^2 of 51%. A second enhancement of the BWM occurred with the inclusion of fluoride ion, which resulted in a Modified BWM with an $R^2 = 85\%$ (Equation 5.1).

To understand the effects imparted by the phosphate and fluoride, the impact of the individual variables, as well as their interactive and collective effects on the BWM were studied. At lower concentrations of either the fluoride or phosphate (Figure 5-3), increased phosphate decreased corrosion, whereas increased fluoride increased mild steel corrosion. The opposite results were evident at higher concentrations. The increased mild steel corrosion at the lower fluoride concentration range ($< 40 \text{ mg/l F}^-$) and decreased corrosivity for higher fluoride (100 mg/l F^-) are in agreed with the earlier findings of this study (Sections 4.4) and Singh *et al.* (2002). It is expected that this model for predicting corrosivity due to the fluoride concentration could vary with the calcium hardness, and should therefore only be used for the range of chemistries considered in this study, that is between 50 and 100 mg/l (as Ca^{2+}). The inhibitory effect of the phosphate on mild steel, at 5 – 20 mg/l as PO_4^{3-} , was as expected and in agreement with Buckman (1981), Flynn and Nalco Company (2009) and Frayne (1999). Figure 5-3 indicated the need to optimize the phosphate dosing in order to maximize its benefit as a corrosion inhibitor, and gave the optimum concentration of $\sim 1.6 \text{ mg/l}$.

Further refinements in the correlations between the Open System Two water chemistry and the field mild steel corrosion data might require moving completely away from the BWM and, while still considering the roles of the phosphate and fluoride, to investigate the potential influence of aluminium cations, total alkalinity and oil. Although good correlations were obtained between both the Open System One and Open System Two field corrosion data and the BWM corrosion results

(calculated using the Open System One water chemistry), whereas for Open System Two a Modified BWM had to be developed to accommodate the inhibitory effect of phosphate and an enhanced corrosivity of the fluoride concentration. These observations indicate that there may have been some irregularities in the Open System Two phosphate and fluoride data, especially since the oil levels were consistently higher and the phosphate and fluoride generally lower in comparison to Open System One water chemistry (Figures H-8, H-9 and H-12).

Figure 5-4 shows that individually fluoride and total alkalinity were the most influential, relative to aluminium and phosphate concentrations. The interaction plot between the phosphate and total alkalinity, also revealed that higher levels of total alkalinity reversed the reduction in mild steel corrosion produced by the phosphates, and that the concentration of phosphate necessary to inhibit mild steel corrosion would also depends on the total alkalinity. The likelihood of increased mild steel corrosion being attributable to high total alkalinity has been already discussed in relation to Stumm's Buffer index (1960) (Section 6.2.1).

A comparison was made of the mild steel corrosion rates calculated using the new models (Equations 3.1, 3.2, 4.3, 4.5, 4.6, 4.8 and 5.1) in Table 5-2, and the combined water chemistry data of Open Systems One and Two. Apart from one exception, generally the field data derived equations, for Open System One (CWS1, Equation 3.1) and Open System Two (CWS2, Equation 3.2) endorsed the laboratory empirically generated models (Equations 4.3, 4.5, 4.6, 4.8 and 5.1).

The equations were then used to derive hypothetical values for a range of water quality parameters guideline for prospective users of brackish waters as cooling water:

- pH: 7.8 to 8.3;
- Conductivity: < 5000 $\mu\text{S}/\text{cm}$;
- Sodium: < 900 mg/l as Na^+ ;
- Calcium: > 70 mg/l as Ca^{2+} , but avoid calcium carbonate supersaturation, optimized in conjunction with the total alkalinity, (Figure 4-16);

- Magnesium: 10 to 35 mg/l as Mg^{2+} ;
- Iron: < 0.5 mg/l as Fe^{3+} ;
- Total Alkalinity: 70 to 200 mg/l as CaCO_3 ;
- Chloride: < 900 as Cl^- ;
- Sulphate: < 1400 mg/l as SO_4^{2-} ;
- Fluoride: < 70 mg/l as F^- ;
- Phosphate: 1 to 4 mg/l as PO_4^{3-} , optimized in conjunction with the total alkalinity and fluoride concentration, (Figures 5-3 and 5-4);
- Aluminium: < 1 mg/l as Al^{3+} ;
- Oil: < 1 mg/l.

CHAPTER 7: CONCLUSIONS

The following conclusions have been made in response to the objectives.

Objective 1: To determine the relationship between the various common water chemistry parameters and the corrosion rate of mild steel in brackish water at elevated temperatures (35 and 45°C)

After attempting an initial statistical correlation of the water chemistry and mild steel corrosion coupon data collected from two open cooling systems (Open Systems One and Two) over 17 months, it was deemed virtually impossible to ascertain any relationship/s between each water chemistry parameter and the measured corrosion rates. It is anticipated that if real time data was used, there would have been significantly stronger correlations between water chemistry and corrosion data.

A broad range of scaling and corrosion indices were then applied to the brackish cooling water of the two systems. For Open System One some indices were statistically significant in their relationship with the field mild steel coupon corrosion rates, but opposite corrosion tendencies were predicted. For Open System Two, only the level of calcium carbonate saturation produced a statistically significant, yet moderate correlation with the field coupon data.

Regression analyses were then employed in a third effort to understand the relationships between the field data water quality parameters and the field corrosion rates. For Open System One, the equation generated indicated that sodium and magnesium were the major species that increased mild steel corrosion ($R\text{-Sq (adj)} = 88\%$). For Open System Two, only a weak correlation between fluoride and the coupon data was found ($R\text{-Sq (adj)} = 41\%$).

Objective 2: To develop mathematical/computer models accurately estimate the corrosion of mild steel utilizing brackish water in industrial cooling systems

Laboratory corrosion tests were performed according to two different approaches. In the first stage a one-factor-at-a-time experimental design was followed and in the second a fractional factorial design.

The initial series of corrosion tests were conducted at 35°C and 45°C in synthetic brackish water with a relatively low total alkalinity (18 to 73 mg/l CaCO₃), with a strong negative relationship between corrosion rate and total alkalinity. A linear model, which agreed with all the indices, accounted for 65% of the variances in the average coupon corrosion rate at 45°C.

A second set of laboratory corrosion tests were performed varying the total alkalinity (55 to 220 mg/l CaCO₃) of the synthetic brackish water at the levels comparable to cooling water chemistry of a steel mill. At 35°C, the only variable with a statistically significant strong correlation with the average mild steel coupon corrosion rate was the calcium concentration, with negative correlation. At 45°C, moderate negative relationships were found for the: initial total alkalinity, final pH, and initial calcium, agreeing with: LSI, RSI, RCI, SDI, DFI, and CCPP. The same was found for the following indices: LSI, RSI, SDI, β , Is, PSI and CR13.

The laboratory corrosion tests gave an empirically derived non-linear regression equation (Equation 4.3), based on only initial calcium and initial total alkalinity, accounting for 90% of the variations in the average mild steel corrosion coupon data. This was a significant improvement over the existing indices, which were at best, only moderately strong correlated with the laboratory corrosion test results. A comparison of the contour plot of the new model versus the previous indices revealed a higher impact of calcium concentration on corrosivity.

The chloride tests indicated that there was no statistically significant correlation between the chloride concentration and the corrosion rates measured by either the coupon method or the Corrat[®] probes. This contradicted CIn, LR and LRM, which were derived for determining the corrosiveness of drinking water systems.

The relationship between the average corrosion rate and initial sulphate concentration was best represented by a quadratic equation with an adjusted R^2 of 61%. This model differed from the model presented by Larson and Skold in which both the chloride and sulphate ions were linearly correlated with the mild steel corrosion rate.

A statistically significant strong positive correlation was obtained between the average corrosion rate and the magnesium concentrations, which agreed with the LSI, RSI and PSI indices, which rely on a calculated pH of saturation. This agreed with the regression analysis of Open System One water chemistry, where magnesium and sodium were the predominant variables for the system's mild steel corrosivity.

In the second stage of the development of mathematical models to explain the impact of the various water chemistry parameters on the mild steel corrosion rate a factorial experimental design was employed, to detect any unique effects attributed to the combination of parameters. This approach yielded a four variable regression model: Average corrosion rate = $2.375 - 0.003575 \times \text{Ca(i)} - 0.000372 \times \text{SO}_4(\text{i}) - 0.000036 \times \text{Cl(i)} - 0.2171 \text{ pH(i)} + 0.000014 \times \text{Ca(i)}^2$, ($R^2 = 95\%$), Surprisingly, the chloride concentration tended to linearly decrease the mild steel corrosion rate by reducing the corrosivity of the sulphate ion, which contradicted the CIn, LR, LRM, CR8 and CR13 indices devised for drinking water systems but agreed with data from saline waters of the Negev desert.

Objective 3: To assess the nature and impact of varying levels of fluoride on mild steel corrosion in brackish water

One-factor-at-a-time laboratory experiments were also performed to investigate the corrosivity of fluoride in the synthetic brackish water at 45°C. The addition of sodium fluoride was proportionally reduced the soluble calcium levels of the synthetic brackish water due to the formation of the sparingly soluble calcium fluoride. Generally, the higher the initial fluoride concentration, the lower the

resulting final test solution calcium concentration, and the higher the associated mild steel coupon corrosion rate.

Although high fluoride concentrations were targeted (90 mg/l as F⁻), the highest fluoride concentrations attained at 45°C and initial calcium concentration of 75 mg/l (as Ca²⁺) was ~34 mg/l (as F⁻). A regression analysis for the average coupon corrosion rate versus the test solution initial fluoride concentration for this fluoride range yielded a statistically significant linear model with an R² (adj) of 60%. By including the pH, calcium hardness and total alkalinity the R² (adj) was raised to 88%: Average corrosion rate = 2.021 - 0.00292 x F(i) – 0.2180 x pH(i) – 0.00225 x M alk(i) + 0.00894 x Ca(i) - 0.00009 Ca(i)².

Optical microscopy, SEM, EDS and additional weight loss corrosion testing to ascertain the effect of higher fluoride concentration (70 to 200 mg/l) on mild steel corrosion coupons at 45°C. The tests were performed for low calcium hardness (50 mg/l Ca²⁺), low total alkalinity (55 mg/l CaCO₃) and without any chloride and sulphate ions. The results of these analyses confirmed the plateau in the mild steel corrosion rate at the target fluoride concentration of ~70 mg/l (corresponding to an initial fluoride concentration of approximately 40 mg/l as F⁻), but also indicated the corrosion rate decreased and then increased to plateau at the target fluoride concentration of 150 mg/l fluoride (i.e. corresponding to an initial fluoride concentration of approximately 100 mg/l as F⁻).

Stereo microscopy, EDS analyses and carbonate spot tests of the mild steel corrosion coupon deposits prior to cleaning showed that where no fluoride was added, up to ~ 30% of the coupon surface area was covered in tightly adhering calcium carbonate crystals. Coupons subjected to relatively high fluoride concentrations (70 and 200 mg/l) had up to 30% of their surface area loosely coated with calcium fluoride.

EDS analyses and carbonate spot tests performed on the traces of tightly bound crystals found on the cleaned coupons confirmed the presence of calcium carbonate.

The corrosion product on the surface of the fluoride free test coupons were mainly iron oxide/hydroxide.

Macroscopic examination of the cleaned coupons showed more surface etching with increasing fluoride concentration. Low concentrations of fluoride were deleterious to mild steel at low concentrations < 40 mg/l for brackish water.

SEM studies of the coupons after cleaning revealed micro-pitting at 70 mg/l fluoride.

Objective 4: To develop additional mathematical models for an accurate estimation of the impact of fluoride on mild steel corrosion in representative raw water and brackish water at temperatures typical of industrial cooling systems

An initial observation made was that the calcium fluoride solubility increased by > 40% in presence of high concentrations of chloride (1000 mg/l Cl^-) and sulphate (1500 mg/l SO_4^{2-}). Calcium fluoride precipitation resulted in reduced fluoride residuals and the subsequent reduction in mild steel corrosion.

Nine series of fluoride tests were performed and each resulted in a mathematical model specific to the particular chemistry employed. The regression analyses revealed that the only prominent role fluoride had in promoting mild steel corrosion was when it was added either to deionized water, or to a relatively high total alkalinity water without hardness. In an analysis of the individual series, sodium featured quite frequently but based on the Spearman and Pearson correlation coefficients there was no statistically significant relationship between it and the corrosion rate. The outcome of this regression analysis confirmed that fluoride was more influential on the mild steel corrosion rate than sodium. The statistical analysis confirmed that both the fluoride and calcium concentrations were the most significant factors impacting on mild steel corrosion rate at 45°C.

Objective 5: To compare the developed model and actual plant data of at least two industrial cooling water systems utilizing brackish water as the cooling medium

The empirically derived brackish water mild steel corrosion prediction model “Brackish Water Model” (BWM) reasonably accurately predicted the Open System One corrosion, as shown by its statistically significant strong correlation ($r = 0.92$) with the actual plant mild steel coupon data and the linear fit with an R^2 of 87%. Only LSI, I_s , SDI and RSI produced statistically significant correlations with the plant coupon corrosion data but none predicted the correct corrosion tendency nor estimated the mild steel corrosion rate. Although β produced the expected directional tendency, its correlation was not statistical significant.

The application of the BWM to Open System Two was totally inadequate. An examination of the factors initially excluded from the BWM: phosphate, aluminium and oil concentrations, revealed that the inclusion of phosphate and fluoride resulted in a modified equation: Modified BWM = $0.443 - 0.870 \times PO_4 + 0.03458 \times F - 1.801 \times BWM + 0.2870 \times PO_4^2 - 0.000507 \times F^2 + 0.0338 \times F \times BWM$, $R^2 = 85\%$. Mill process contaminants such as oil, detected at relatively higher levels in Open System Two, or the difference in side-stream treatment processes may have caused the inaccuracy of BWM on this system water chemistry.

Objective 6: To use the data and models to establish a set of hypothetical guideline values for prospective users of brackish waters as cooling water

The results of this thesis essentially culminated in the following seven main statistically significant models:

- Open System One field water chemistry based regression analysis, R^2 (adj) = 88%
- Open System Two field water chemistry based regression analysis, R^2 (adj) = 41%
- Non-linear regression equation based only on Ca and M alk, R^2 (adj) = 90%
- OFAT Fluoride based regression analysis R^2 (adj) = 88
- Fractional factorial design based regression analysis, (R^2 (adj) = 95%

- Brackish Water Model (BWM), R^2 (adj) = 81%
- Modified BWM (BWM adapted for Open System Two), R^2 (adj) = 85%.

The first two and last models were more suitable to either one cooling system or the other, whereas the rest were generally applicable. Generally, good agreement was obtained between the field and laboratory generated models. There are boundaries pertaining to water chemistry parameters, determined by the specific field or laboratory experimental conditions employed during their derivation.

A set of empirically based guideline water chemistry parameters were proposed. Both the recommended concentrations and the equations serve only to minimize corrosion, and have no bearing on other water related issues, e.g. scaling or fouling. Furthermore, it is also recommended that the individual models are validated by performing field tests, because indices can be completely inappropriate and misleading if applied outside of their boundaries.

Objective 7: To research and evaluate commercially viable options at minimizing the corrosion of mild steel in contact with such aggressive electrolytes at elevated temperatures

Laboratory screening tests confirmed the plants choice of zinc and phosphate as the preferred corrosion inhibitors for Open Systems One and Two.

Although the concentrations of the zinc (2.2 mg/l Zn^{2+}) and phosphate (5.3 mg/l PO_4^{3-}) used in the screening tests were well within the previously reported guidelines only minor reductions in mild steel corrosion of 22.7% and 9.7% respectively were achieved.

CHAPTER 8: RECOMMENDATIONS

Examine mild steel exposed to a lower fluoride concentrations (< 70 mg/l) at 45°C by means of SEM to establish the lowest concentration at which pitting will occur.

Test both the BWM and Modified BWM on other brackish waters used in industry at elevated temperatures and check for their range of applicability and weaknesses and how they may be modified for greater robustness.

To investigate a broader scope of variables, for example the effect of selected hydrocarbons used in steel mills.

Explore broader concentration ranges for the entire range of commercially available corrosion inhibitors evaluated, as well as any other novel corrosion inhibitors.

Explore potential synergies between the various corrosion inhibitors to seek superior and more cost effective solutions at minimising the corrosion of mild steel in brackish water used in industry.

Investigate the effects of different exposure times and flow velocities on the BWM and Modified BWM.

REFERENCES

Abt Associates (Cambridge, MA) and Booz-Allen & Hamilton, Inc. (McLean, VA), (1995). Profile of the Iron and Steel Industry, US EPA, Office of Compliance.

EPA/310-R-95-05, Washington, DC. Available from: <http://www.epa.gov/compliance/resources/publications/assistance/sectors/notebooks/iron-stl.pdf> [Accessed: 30 October 2012].

American Iron and Steel Institute, (1992). Report on Steel Industry Waste Generation, Disposal Practices, and Potential Environmental Impact, Washington DC, 21.

ASTM Standard D2688, 1990 (2011). Standard Methods for Corrosivity of Water in the Absence of Heat Transfer (Weight Loss Methods). ASTM International, West Conshohocken, PA, USA.

ASTM Standard G1, 1990 (1999). Standard Practice for Preparing, Cleaning, and Evaluating Corrosion Test Specimens. ASTM International, West Conshohocken, PA, USA.

ASTM Standard G31, 1972 (1999). Standard Practice for Laboratory Immersion Corrosion Testing of Metals, ASTM International, West Conshohocken, PA, USA.

ASTM Standard G59, 1997 (2003). Standard Test Method for Conducting Potentiodynamic Polarization Resistance Measurements, ASTM International, West Conshohocken, PA, USA.

ASTM Standard G102, 1982 (2010). Standard Practice for Calculation of Corrosion Rates and Related Information from Electrochemical Measurements, ASTM International, West Conshohocken, PA, USA.

Atkinson, J.T.N. and Van Droffellar, H., (1995). Corrosion and its Control: An Introduction to the Subject. Second Edition. NACE International, Houston, Texas.

AWWARF and DVGW-TZW, (1996). Internal Corrosion of Water Distribution Systems, Second Edition. American Water Works Association, Denver, CO, USA, 29-70.

Baylis, J.R., (1926). Prevention of Corrosion and “Red Water”. *Journal of AWWA*, 15, 598-633.

Benfield, L.D. and Morgan, J.M., (1990). Chemical Precipitation. Water Quality and Treatment, A Handbook of Community Water Supplies. Fourth Edition. AWWA. F.W. Pontius, editor. McGraw-Hill, New York, 645.

Brell, S.A., Jaques, T. and Pask, A.J., (2003). Slab Caster Spray Chamber Corrosion. *AISE*, Pittsburg, PA, USA, 1-12.

Brindha, K. and Elango, L., (2011). Fluoride in Groundwater: Causes, Implications and Mitigation Measures. In: Monroy, S.D. editor, Fluoride Properties, Applications and Environmental Management, Nova Science Publishers, USA, 111-136.

Brits, A.J., Geldenhuys, J.C., Kok, A.M., and Baxter, D.A., (1998). The Effect of Water Quality and Chemical Composition of Mild Steel Pipelines. Water Research Commission Report No 259/1/98.

Buckman, (1981). Buckman Cooling Water Treatment Manual, Bulletin No. C1. Buckman Laboratories, Inc. Memphis, Tennessee 38108, USA.

Buckman, (2010). Internal Communications between salesman and customer (27 July 2010).

Buckman, (2011). Internal Communications between salesman and customer (17 August 2011).

Buckman, (2012a). Internal Communications between technical staff and customer (5 January 2012).

Buckman, (2012b). Internal Communications between technical staff and customer 16 March 2012).

Campbell, H.S., (1980). The Effect of Chemical Composition of Water on Corrosion problems. *Anti-Corrosion Methods and Materials*, 27 (3), 4-5.

Campbell, H.S. and Turner, M.E.D., (1983). The Influence of Trace Organics on Scale Formation and Corrosion. *J of Inst. Wat. Eng and Scientists*, 37, 55-72.

Champion, F.A., (1952). Corrosion Testing Procedures. John Wiley and Sons, Inc., New York.

Christophersen, D., (2008). Water Reuse Strategies: Steel Industry Case Studies, *Corrosion*, NACE, 37, 1-15.

Cruse, H., (1971). Dissolved-Copper Effect on Pipe. *Journal of AWWA*, 63(2), 79-81.

Degrémont, (1991). Water Treatment Handbook. 6th ed. New Jersey, USA: Lavoisier Publishing Inc. Secaucus. ISBN: 2950398413, 68-69.

Dillon, J.J. and Waltman, G.B., (1995). The Effect of Mold Powders on Corrosion of Continuous Caster Components. *Corrosion*, NACE, 499, 1-25.

Dye, J.F., (1958). Correlation of the Two Principle Methods of Calculating the Three Kinds of Alkalinity. *Journal of AWWA*, 50(6), 801-820.

Evans, U.R., (1981). An Introduction to Metallic Corrosion. Third Edition, Edward Arnold Publishers, London, UK.

Feigenbaum, C., Gal-Or, L. and Yahalom, J., (1978). Scale Protection Criteria in Natural Waters, *Corrosion*, 34(4), 133-137.

Flynn, D.J., and Nalco Company, (2009). The Nalco Water Handbook. McGraw-Hill, New York.

Frayne, C. (1999). Cooling Water Treatment- Principles and Practice, Chemical Publishing Co., Inc. New York, NY, USA.

Hatch, G.B., (1955). Control of Couples Developed in Water Systems. *Corrosion*, 11(1), 15-22.

Hedberg, T. and Johansson, E., (1987). Protection of Pipes against Corrosion. *Water Supply*, 5(3/4), SS20, 1-7.

Hoyt, B.P., Kirmeyer, G.J., and Courchene, J.E., (1979). Evaluating Home Plumbing Corrosion Problems. *Journal of AWWA*, 71(12), 720-725.

Imran, S.A., Dietz, J.D., Mutoti, G., Taylor, J.S. and Randall, A.A., (Nov 2005). Modified Larsons Ratio Incorporating Temperature, Water Age, and Electroneutrality Effects on Red Water Release, National Research Council of Canada, Ottawa, K1A 0R6, Canada. *Journal of Environmental Engineering (Reston, VA, United States)*, 131(11), 1514-1520.

Imran, S.A., Dietz, J.D., Mutoti, G., Taylor, J.S., Randall, A.A. and Cooper, C.D., (Sept 2005). Red Water Release in Drinking Water Distribution Systems, *Journal of AWWA*, 97(9), 93-100.

Kent, C., (2008). 2008 Sectors Performance Report, US EPA, Office of Policy, Economics and Innovation. Available from: <http://www.epa.gov/sectors/pdf/2008/2008-sector-report-508-full.pdf> [Accessed: 30 October 2012].

Langelier, W.F., (1936). The Analytical Control of Anti-Corrosion Water Treatment. *Journal of AWWA*, 28(10), 1500-1521.

Larson, T.E. and Buswell, A.M., (1942). Calcium Carbonate Saturation Index and Alkalinity Interpretations, *Journal of AWWA*, 34(11), 1667-1679.

Larson, T.E. and Skold, R.V., (1957). Corrosion and Tuberculation of Cast Iron, *Journal of AWWA*, 49(10), 1294-1302.

Larson, T.E. and Skold, R.V., (1958). Laboratory Studies Relating Mineral Water Quality of Water to Corrosion of Steel and Cast Iron, *Corrosion*, NACE, 14, 285-288.

Larson, T.E. and Sollo, Jr., F.W., (1967). Loss in Water Main Carrying Capacity. *Journal of AWWA*, 59(12), 1565-1572.

Larson, T.E., (1975). Corrosion by Domestic waters, Bulletin 59, Illinois State water Survey, Urbana.

Lee, S.H., O'Conner, J.T. and Banerji, S.K., (1980). Biologically Mediated Corrosion and Its Effects on Water Quality in Distribution Systems. *Journal of AWWA*, 72(11), 636-645.

Löchel, B. and Strehblow, H.H., (1983). Breakdown of Passivity of iron by Fluoride, *Electrochimica Acta*, 28(4), 565-571.

Loschiavo, G.P., (1948). Experiences in Conditioning Corrosive Army Water Supplies in New England. *Corrosion*, NACE, 4, 1-14.

Makini, B., (2005). Achieving Zero Liquid Discharge in the Semiconductor Industry, Department of Earth and Environmental Engineering, Columbia University, New York, NY 10025, Available from: http://www.seas.columbia.edu/earth/wtert/sofos/Makini_IETerm.pdf. [Accessed: 6 November 2012].

Marley Cooling Tower, (2001). Electronic Mail from Robert Fleming, Marley Cooling Tower to Ron Rimelman, Tetra Tech, Inc. August 9, 2001. Available from: http://www.swrcb.ca.gov/rwqcb3/water_issues/programs/duke_energy/docs/usepa_efficacy_of_intake_technologies.pdf [Accessed: 3November 2012].

Macias, A. and Escudero, M.L., (1994). The Effect of Fluoride on Corrosion of Reinforcing Steel in Alkaline Solutions, *Corrosion Science*, 36(12), 2169-2180.

Maulbetsch, J.S. and Di Fillippo, M.N., (2010). Performance, Cost, and Environmental Effects of Salt Water Cooling Towers, Pier Final Project Report, Prepared for: California Energy Commission, Public Interest Energy Research Program, CEC-500-2008-043.

Mayer, P., Manolescu, A.V. and Rasile, E.M., (1984). Corrosion of Medium Steel in Aqueous Solutions Containing Fluoride at 300°C. *Corrosion*, 40(4), 186-89.

McCauley, R.F., (1960). Controlled Deposition of Protective Calcite Coatings in Water Mains. *Journal of AWWA*, 52, 1386-1396.

McGannon, H.E., (1971). The Making, Shaping, and Treating of Steel, Tenth Edition, United States Steel Corporation, Pittsburgh, PA, USA, 565.

McNeill, L.S. and Edwards, M., (2001). Iron Pipe Corrosion in Distribution Systems. *Journal of AWWA*, 93(7), 88-100.

Merrill, D.T. and Sanks, R.L., (1978). Corrosion Control by Deposition of CaCO_3 Films: Part 3, a Practical approach for Plant Operators, *Journal of AWWA*, 70(1), 12-18.

Miller, M. and Loewenthal, R.E., (1982). Corrosion of Cast Iron in Aqueous Media: Experimental Investigation. Internal report, Department of Civil Engineering. University of Cape Town.

Millette, J.R., Hammonds, A.F., Pansing, F.J., Hansen, C.E. and Clark, P.J., (1980). Aggressive Water: Assessing the Extent of the Problem. *Journal of AWWA*, 72(5), 262-266.

Moll, V.D., Acosta, C.A., Salvarezza, R.C., Videla H.A. and Arvia, A.J., (1985). The Kinetics and Mechanism of the Localized Corrosion of Mild Steel in Neutral Phosphate-borate Buffer Containing Sodium Fluoride. *Corrosion Science*, 25(4), 239-252.

Nielsen, D.L., Brock, M.A., Rees, G.N. and Baldwin, D.S., (2003). Effects of Increasing Salinity on Freshwater Ecosystem in Australia, *Journal of Botany*, 51, 655-665.

Oddo, J.E., and Tomson, M.B., (1982). Simplified Calculation of CaCO_3 Saturation at High Temperatures and Pressures in Brine Solutions, Society of Petroleum Engineers of AIME, *Journal of Petroleum Technology*, July, 1583-1590.

Oddo, J.E., and Tomson, M.B., (1992). Scale Control, Prediction and Treatment Or How Companies Evaluate A Scaling Problem and What They Do Wrong, *Corrosion* 92(34), NACE, 1-11.

Okereke, A. and Stevens Jr. S.E., (1991). Kinetics of Iron Oxidation by Thiobacillus ferrooxidans. *Applied and Environmental Microbiology*, 57(4), 1952.

Piron, D.L., Desjardins, R., Briere, F. and Ismael, M., (1986). Corrosion Rate of Cast Iron and Copper Pipe by Drinking Water. *Corrosion Monitoring in Industrial Plants Using Nondestructive Testing and Electrochemical Methods*, ASTM STP 908. (G.C. Morgan and P. Labine, editors). American Society. Testing and Materials, Philadelphia.

Pisigan Jr., R.A. and Singley, J.E., (1987). Influence of Buffer Capacity, Chlorine Residual, and Flow Rate on Corrosion of Mild Steel and Copper. *Journal of AWWA*, 79(2), 62-70.

Pisigan, R.A. and Singley, J.E., (1984). Evaluation of the Corrosivity Using the Langelier Index and relative Corrosion rate Models, *Corrosion* 84(149), NACE, 1-24.

Pisigan, R.A. and Singley, J.E., (1985). Experimental Determination of the Calcium Carbonate Saturation States of Water Systems, *Journal of American Water Works Association*, 77(10), 92-94.

Puckorius, P.R. and Brooke, J.M., (1990). A New Practical Index for Calcium Carbonate Scale Prediction in Cooling Tower Systems, *Corrosion* 90(99), NACE.

Raingevars, M.D., Limonova, L.P. and Pomyalova, L.V., (1989). Statistical Model of the Corrosive Behaviour of Carbon Steel in Solutions of Ammonium Fluoride. *Protection of Metals (English translation of Zashita Metallov)*, 24(6), 777-779.

Riddick, T.M., (1944). The Mechanisms of Corrosion of Water Pipes, *Water Works and Sewage*, 91, 133-138.

Rossum, J.R. and Merrill, D.T., (1983). An Evaluation of the Calcium Carbonate Saturation Indexes. *Journal of AWWA*, 75(2), 95-100.

Rostron, A.J., (1979a). The Correlation between Molecular Structure and Tendency to Maintain or to Destroy Iron Passivity in Aqueous Solutions-i. The Electrostatic Hypothesis. *Corrosion Science*, 19(2), 123-130.

Rostron, A.J., (1979b). The Correlation between Molecular Structure and Tendency to Maintain or to Destroy Iron Passivity in Aqueous Solution-ii. Activation Effectiveness of Anions Present Together with a Corrosion Inhibitor and/or an Oxidant. *Corrosion Science*, 19(5), 321-34.

Ryznar, J.W., (1944). A New Index for Determining the Amount of Calcium Carbonate Scale Formed by a Water. *Journal of AWWA*, 36(4), 472-475.

Sander, A. Berghult, B. Elfstrom Broo, A. Lind Johansson, E. Hedberg, T., (1997). Iron Corrosion in Drinking Water Distribution Systems—The Effect of pH, Calcium and Hydrogen Carbonate. *Corrosion Science*, 38(3), 443-445.

Schock, M.R., (1984). Temperature and Ionic Strength Corrections to the Langelier Index Revisited. *Journal of AWWA*, 76(8), 72-76.

Schorsch, L.L., (1996). Why Minimills Give the US Huge Advantages in Steel, *McKinsey Quarterly*, business journal of McKinsey & Company, Available from: http://www.mckinseyquarterly.com/Why_minimills_give_the_US_huge_advantages_in_steel_162 [7 November 2012].

Schott, G.J., (1998). WATERPRO - Corrosion Control and Treatment Process Evaluation Program. *Journal of AWWA*, Proceedings - Water Quality Technology Conference (1998), 765-807.

Shair, S., (1975). Iron Bacteria and Red Water. *Industrial Water Engineering*, 12(2), 16-18.

Siemens, (2012). Available from: http://www.water.siemens.com/en/applications/water_recycle_reuse/zero_liquid_discharge/Pages/default.aspx [Accessed: 3 November 2012].

Silverman, D.C and Puyear R.B., (1987). Effect of environmental variables on aqueous corrosion, *Metals Handbook*, Ninth Edition, Volume 13, Corrosion (Joseph R Davis, Sr., ed.), ASM International, 38-39.

Singh, D.D.N., Ghosh, R. and Singh, B.K., (2002). Fluoride Induced Corrosion of Steel Rebars in Contact with Alkaline Solutions, Cement Slurry and Concrete Mortars. *Corrosion Science*, 44, 1713-1735.

Singh, P.R., Chouthai, S.S., Gadiyar, H.S., (1981). Studies in the Corrosion and Inhibition of Mild Steel in Sodium Fluoride Solutions by Small Amplitude Cyclic Voltammetry. *British Corrosion Journal*, 16(4), 198-201.

Singley, J.E., (1981). The Search for a Corrosion Index. *Journal of AWWA*, 73(11), 579-582.

Sontheimer, H., Kolle, W. and Snoeyink, V.L., (1981). The Siderite Model of Formation of Corrosion Resistant Scales, *Journal of AWWA*, 572-579.

Stiff, Jr., H.A. and Davis, L.E., (1952). A Method For Predicting The Tendency of Oil Field Water to Deposit Calcium Carbonate, *Petroleum Transactions, AIME* 195, 213-216.

Strehblow, H.H., Titze, B. and Loechel, B.P., (1979). Breakdown of Passivity of Iron and Nickel by Fluoride, *Corrosion Science*, 19(12), 1047-1057.

Stumm, W., (1960). Investigation of the Corrosive Behavior of Waters, *Journal American Society of Civil Engineers, Sanitary Engineering Division*, 86(SA6), 27-45.

Tillmans, J. and Heublein, O., (1912). Investigation of the Carbon Dioxide which Attacks Calcium Carbonate in Natural Waters. *Gesundheits Ingenieur (Ger.)* 35(34), 669-677.

Treweek, G.P., Glicker, J., Chow, B., and Sprinker, M., (1985). Pilot-Plant Simulation of Corrosion in Domestic Pipe Materials, *Journal of AWWA*, 77(10), 74-82.

Tuovinen, O.H., Button, K.S., Vuorinen, A., Carlson, L., Mair, D.M. and Yut, L.A., (1980). Bacterial, Chemical, and Mineralogical Characteristics of Tubercles in Distribution pipelines. *Journal of AWWA*, 72(11), 626-635.

Uhlig, H.H., (1963). Corrosion and Corrosion Control: An Introduction to Corrosion Science and Engineering, John Wiley and Sons Inc., New York, NY, USA.

Vasil'eva, V.A., Dudukina, T.A., Dzutsev, V.T., Moskvichev, I.F. and Pavlova, E.M., (1986). Corrosiveness of Clarified Water in a Recycled Fluorine-Containing Water System. *Soviet Journal of Water Chemistry and Technology*, 8(3), 126-127.

Wallis, J. and Aull, R., (2009). Rising Interest in Sea-Water Cooling, *Process Cooling and Equipment*, Process Cooling Trade Publication, 15-18.

WaterCycle, (2012). Available at: <http://www.frenchcreeksoftware.com/WaterCycle/> WaterCycle - Cooling Water Modelling, French Creek Software, Inc. USA.

White, R.T. and Higginson, A., (1985). Factors Affecting the Corrosivity of Underground Minewaters. *Proceedings of Mintek 50: International Conference on Mineral Science and Technology*, Sandton, South Africa, 941-948.

WorldSteel, (2011), Available from:
<http://www.worldsteel.org/dms/internetDocumentList/bookshop/Sustainable-steel-at-the-core-of-a-green-economy/document/Sustainable-steel-at-the-core-of-a-green-economy.pdf> [Accessed: 30 October 2012].

**APPENDIX A: COOLING WATER CHEMISTRY FOR
OPEN COOLING SYSTEM ONE FOR THE
PERIOD 3 MARCH 2009 TO 25 MARCH 2011**

Note: blank or “-“ = no data

Table A-1: Cooling water chemistry (raw data) for Open System One for the period 3 March 2009 to 25 march 2011 (Buckman, 2012b)

Date	Ca (mg/l)	Mg (mg/l)	P-alk (mg/l CaCO ₃)	Total alkalinity (mg/l CaCO ₃)	pH	Cl (mg/l)	S-SO ₄ (mg/l)	Cond (µS/cm)	Suspended solids (mg/l)	F ⁻ (mg/l)	P-P-O ₄ (mg/l)	Na (mg/l)	Fe (mg/l)	Mn (mg/l)	K (mg/l)	Zn (mg/l)	Si-SiO ₂ (mg/l)	Oil (mg/l)	Al (mg/l)
2009/03/0	105	21	0	49	7.4	-	880	3301	12	51	1.9	565	< 0.09	0.42	40	< 0.1	18	1.5	0.4
2009/03/0	92	18	0	45	7.4	-	703	2942	9	47	3.7	416	< 0.09	0.40	32	1.2	20	6.7	1.6
2009/03/0	79	23	0	53	7.2	-	817	3232	15	47	1.1	592	0.52	0.46	41	1.1	20	0.9	0.3
2009/03/1	82	20	0	44	6.9	389	849	3051	24	42	< 0.5	585	1.30	0.41	39	0.3	16	1.4	0.3
2009/03/1	97	23	0	34	7.2	505	915	3480	17	48	< 0.5	662	0.19	0.52	44	0.9	21	3.0	0.6
2009/03/1	77	22	0	38	7.3	445	855	3184	9	48	2.0	620	< 0.09	0.43	42	0.4	21	2.9	0.4
2009/03/1	66	21	0	34	7.2	450	843	3209	12	54	0.6	638	< 0.09	0.35	40	0.9	19	-	0.5
2009/03/1	69	23	0	64	7.5	462	856	3175	10	54	< 0.5	643	< 0.09	0.40	42	0.3	18	0.8	0.4
2009/03/2	60	25	0	87	7.7	412	748	2949	9	39	1.0	555	< 0.09	0.21	42	0.2	16	2.9	0.1
2009/03/2	59	23	0	65	7.6	461	897	3396	18	52	< 0.5	681	0.16	0.25	44	< 0.1	23	1.0	< 0.1
2009/03/2	82	26	0	39	7.3	566	988	3836	12	56	< 0.5	705	0.19	0.45	48	0.5	21	3.1	0.2
2009/03/2	75	27	0	49	7.4	610	1002	3795	11	58	0.6	738	0.33	0.45	49	0.7	24	0.7	0.3
2009/03/3	64	25	0	51	7.4	590	918	3802	5	57	< 0.5	675	< 0.09	0.22	43	0.3	19	0.8	< 0.1
2009/04/0	68	26	0	50	7.5	571	1000	4098	18	49	0.6	744	0.59	0.37	42	0.6	23	1.4	0.2
2009/04/0	64	33	0	60	7.6	661	1249	4658	17	76	1.0	963	< 0.09	0.31	55	0.3	28	1.5	0.2
2009/04/0	55	32	0	58	7.7	671	1254	4737	17	71	0.5	948	< 0.09	0.31	56	0.3	27	0.1	0.2
2009/04/1	75	37	0	89	7.9	704	1314	4773	11	91	< 0.5	1038	< 0.09	0.27	60	0.4	26	0.9	0.1
2009/04/1	94	33	0	43	7.2	780	-	4905	19	71	< 0.5	985	< 0.09	0.46	62	0.8	32	0.5	0.4
2009/04/1	115	32	0	37	7.2	747	1136	4602	18	34	0.7	830	< 0.09	0.49	59	0.6	28	1.1	0.1
2009/04/2	90	29	0	25	6.8	835	1326	4999	22	61	0.6	1057	0.16	0.59	68	1.1	29	7.4	1.0
2009/04/2	111	27	0	26	6.9	659	1232	4451	15	57	< 0.5	848	0.19	0.75	63	1.8	31	0.4	2.7
2009/05/0	69	24	15	135	8.8	517	1035	3889	40	37	< 0.5	749	< 0.09	0.19	56	0.3	18	3.3	0.1
2009/05/0	63	27	0	144	7.9	581	1124	4166	17	54	0.8	844	< 0.09	0.20	61	0.8	17	0.3	< 0.1
2009/05/0	64	25	0	93	7.7	576	1013	4017	16	68	1.3	801	< 0.09	0.20	56	0.3	20	0.8	< 0.1

2009/05/0	99	29	0	75	7.8	640	1190	4407	7	54	0.6	863	< 0.09	0.28	60	0.4	19	1.8	0.2
2009/05/1	95	24	0	65	7.5	590	1028	4061	10	55	< 0.5	739	< 0.09	0.26	53	< 0.1	13	1.3	0.1
2009/05/1	97	28	0	50	7.8	784	1320	5076	43	49	< 0.5	956	< 0.09	0.21	69	< 0.01	20	0.8	0.1
2009/05/1	68	27	0	59	7.8	889	1602	5769	21	67	< 0.5	1189	< 0.09	0.25	79	0.1	21	0.7	0.2
2009/05/2	54	24	0	62	7.7	804	1683	5949	20	75	0.7	1226	< 0.09	0.24	81	0.11	21	2.1	0.4
2009/05/2	40	14	0	105	7.8	767	1663	5849	29	96	0.6	1234	< 0.09	0.13	69	1.2	17	1.1	0.1
2009/05/2	40	13	0	79	7.7	761	1529	5797	25	120	1.1	1166	< 0.09	0.12	65	0.1	17	0.7	0.1
2009/05/2	55	18	6	122	8.6	1033	1619	6473	20	95	4.6	1375	0.58	7.10E-02	72	0.2	20	1.7	0.2
2009/05/2	47	18	2	119	8.5	991	1542	6260	16	62	1.3	1312	1.00	0.16	68	0.3	17	3.0	0.2
2009/06/0	53	17	0	99	7.8	1031	1608	6574	20	72	0.2	1306	0.40	0.17	69	1.2	17	0.5	2.2
2009/06/0	69	19	0	92	8.0	1125	1624	6946	43	81	8.8E-02	1289	0.40	0.18	68	0.6	16	0.5	1.2
2009/06/0	92	28	0	78	7.8	1045	2205	6775	27	84	0.3	1403	1.40	0.31	78	0.4	24	0.8	0.5
2009/06/0	107	30	0	68	7.7	1061	1636	6629	29	70	0.7	1270	9.30E-	0.37	72	0.1	21	0.3	0.2
2009/06/1	103	31	0	70	7.8	1044	1694	6387	27	41	0.5	1324	< 0.09	0.61	76	0.5	20	0.3	0.2
2009/06/1	69	21	0	40	6.8	645	1110	4328	20	42	0.7	877	0.16	0.42	54	0.6	20	0.2	< 0.1
2009/06/1	68	17	0	32	7.2	644	1080	4384	23	63	1.7	862	0.19	0.42	60	0.9	25	2.3	< 0.1
2009/06/1	49	15	0	48	7.0	652	1030	4465	19	57	1.4	849	< 0.09	0.39	63	0.4	20	2.3	< 0.1
2009/06/2	49	18	0	44	7.3	690	1137	4563	13	64	0.49	942	< 0.09	0.51	70	0.3	22	0.4	1.5
2009/06/3	55	22	0	112	7.4	638	1055	4406	19	52	0.5	845	< 0.09	0.29	71	< 0.01	18	0.3	< 0.1
2009/07/0	52	19	0	126	7.9	660	985	4228	22	46	0.3	834	0.83	0.18	66	0.1	17	0.7	< 0.1
2009/07/0	53	22	0	162	7.6	655	1048	3852	18	73	2.2E-02	834	0.44	0.23	68	< 0.1	18	0.8	< 0.1
2009/07/0	59	24	0	121	8.0	623	1043	4211	25	48	0.6	825	0.72	0.27	72	< 0.1	19	0.4	0.2
2009/07/1	59	22	0	124	7.7	602	1169	4555	25	63	1.8	909	0.82	0.33	98	0.4	18	-	< 0.1
2009/07/1	48	17	0	98	7.6	611	1039	4582	20	151	0.5	813	< 0.09	0.14	93	0.1	16	0.7	< 0.1
2009/07/1	49	17	0	115	7.9	510	929	3912	25	56	0.5	735	0.24	0.24	82	< 0.1	13	0.9	0.1
2009/07/1	59	17	0	110	7.3	519	946	3844	22	42	0.5	737	0.81	0.33	92	0.8	16	0.8	0.2
2009/07/2	69	17	0	76	7.2	556	909	3732	19	60	1.9	720	0.26	0.22	92	0.3	14	0.7	0.2
2009/07/2	66	18	0	49	7.2	734	1136	4372	26	53	2.1	950	< 0.09	0.22	100	0.5	17	1.1	0.1
2009/07/2	67	14	0	33	7.1	660	1035	4138	9	56	0.5	829	9.40E-	0.35	84	1.0	19	0.5	0.1
2009/07/2	68	17	0	43	7.2	676	1042	4391	15	53	0.5	878	< 0.09	0.27	88	0.5	13	0.9	0.2
2009/07/3	71	17	0	55	7.3	754	1107	4700	24	42	0.6	943	< 0.09	0.27	90	0.5	14	2.0	0.2
2009/07/3	51	16	0	46	7.4	718	943	4376	20	35	1.2	833	0.09	0.20	86	0.5	14	1.2	0.3
2009/08/0	45	14	0	49	7.3	746	884	4449	23	59	2.2	827	0.36	0.22	84	0.8	17	0.2	0.4
2009/08/0	50	14	0	64	7.1	769	863	4411	38	56	0.61	841	0.34	0.24	87	0.7	17	0.2	0.8
2009/08/1	74	22	0	48	7.0	939	1036	5047	32	66	1.7	934	1.30	0.42	122	0.9	22	0.9	0.7
2009/08/1	87	24	0	80	7.2	921	993	4808	40	58	< 0.5	936	0.85	0.56	112	0.4	21	1.2	0.3
2009/08/1	115	27	0	85	7.4	1052	896	5117	28	45	3.4	970	0.57	0.62	102	0.6	15	0.8	0.2

2009/08/1	93	27	0	78	7.6	1012	897	4898	11	30	0.7	966	0.48	0.49	93	0.7	15	1.5	1.3
2009/08/2	79	27	0	60	7.7	1088	854	5044	20	43	0.7	964	0.28	0.37	90	0.8	12	0.1	0.5
2009/08/2	80	32	0	86	7.8	1145	1060	5707	26	55	0.7	1150	0.35	0.30	108	0.3	15	1.7	0.5
2009/09/0	111	26	0	46	7.1	1019	882	4902	18	45	5.5	855	< 0.09	0.32	135	0.3	17	0.9	0.0
2009/09/0	114	26	0	61	7.0	950	854	4442	28	53	11	802	< 0.09	0.35	128	5.2	12	1.0	0.1
2009/09/0	85	23	0	99	7.8	793	784	4145	19	29	3.7	759	< 0.09	0.22	107	0.8	10	0.9	< 0.1
2009/09/0	63	22	0	141	7.7	725	698	4007	18	25	1.5	724	< 0.09	0.15	94	0.9	6	0.5	< 0.1
2009/09/1	99	24	0	133	7.7	654	930	4028	19	20	1.5	750	0.11	0.83	85	5.7	3.4	0.6	< 0.1
2009/09/1	87	22	0	157	7.8	688	941	4297	12	32	0.5	772	< 0.09	0.56	75	1.4	2.7	0.6	< 0.1
2009/09/1	118	25	0	139	7.9	776	1094	4754	27	34	1.3	854	0.21	0.77	81	1.8	11	0.1	0.4
2009/09/1	101	27	0	185	8.1	753	1170	4833	14	30	1.6	954	< 0.09	0.57	71	0.5	12	0.7	0.5
2009/09/2	91	28	0	199	8.1	872	1265	5496	17	51	0.5	1075	0.51	0.53	78	1.0	8.4	0.2	< 0.1
2009/09/2	92	30	0	198	7.9	993	1359	5656	14	60	0.5	1176	0.22	0.34	84	0.8	9.7	1.1	-
2009/09/2	115	32	0	191	7.9	1159	1269	6130	14	131	1.9	1249	0.20	0.56	83	0.7	10	1.0	0.1
2009/10/0	115	31	0	131	7.8	1121	1248	6006	29	49	0.45	1206	0.84	0.46	82	0.5	9.1	1.2	0.3
2009/10/0	154	33	0	204	8.0	1323	1196	6514	29	58	0.7	1295	< 0.09	0.72	85	0.5	4.3	1.0	< 0.1
2009/10/0	140	30	0	185	7.7	1251	1036	6035	20	44	0.5	1153	0.42	0.72	75	1.0	7.2	1.2	0.0
2009/10/0	117	29	0	199	7.9	1143	1024	5757	17	42	1.7	1169	< 0.09	0.53	75	0.7	8.6	8.8	0.1
2009/10/0	113	30	0	210	7.6	1236	-	5625	16	44	2.9	1175	< 0.09	0.36	77	1.2	10	0.2	0.1
2009/10/1	71	28	0	170	8.1	1033	1090	5331	24	77	2.3	1190	< 0.09	0.26	86	0.7	12	0.8	0.1
2009/10/1	83	30	0	151	8.0	877	1207	5036	27	81	0.5	1260	< 0.09	< 0.01	86	0.2	18	1.1	< 0.1
2009/10/2	73	27	0	149	8.0	854	1041	5070	18	91	1.5	1077	0.24	0.24	74	0.8	17	0.2	< 0.1
2009/10/2	75	21	0	152	8.1	815	936	4793	21	79	4.9	929	< 0.09	0.21	67	0.9	12	0.8	< 0.1
2009/10/2	63	20	0	135	8.1	786	1089	5050	18	71	8.9	1005	< 0.09	0.14	58	0.6	16	0.2	0.1
2009/10/2	56	21	0	147	8.1	806	1101	5070	18	100	4.6	1078	< 0.09	9.70E-02	62	0.4	12	0.4	0.1
2009/10/2	60	21	1	159	8.3	-	1023	5199	23	81	4.3	1073	< 0.09	8.20E-02	59	0.4	13	1.3	0.2
2009/10/3	52	20	2	149	8.4	739	1001	4728	22	95	5.2	1005	< 0.09	0.11	54	0.4	16	0.5	0.0
2009/11/0	56	20	0	115	7.6	743	1062	4739	13	86	4.0	1005	< 0.09	0.19	51	0.7	17	0.8	0.2
2009/11/0	58	21	0	112	7.8	772	1073	4799	15	100	4.9	1043	< 0.09	0.17	60	0.7	18	6.1	< 0.1
2009/11/0	58	21	0	169	8.3	647	925	4446	11	80	3.7	959	0.20	9.70E-02	57	0.6	17	0.6	0.2
2009/11/1	51	19	0	129	8.0	619	696	3773	20	60	2.7	737	0.25	0.16	42	0.6	13	0.9	0.1
2009/11/1	70	20	0	118	7.8	571	850	3980	20	45	7.4	780	0.11	0.22	42	0.8	16	1.4	0.3
2009/11/1	52	18	0	110	7.6	519	751	3675	20	76	4.3	719	0.12	0.19	36	0.5	15	2.4	0.3
2009/11/1	50	19	0	121	8.1	610	767	3925	17	76	5.5	787	0.52	0.15	39	0.6	17	0.2	0.4
2009/11/1	44	18	0	120	7.9	531	627	3428	18	61	2.1	668	< 0.09	< 0.01	33	0.2	12	0.2	1.0
2009/11/2	53	19	0	111	7.8	524	665	3562	15	65	4.9	674	< 0.09	< 0.01	35	0.2	13	4.0	< 0.1
2009/11/2	42	15	0	122	7.9	379	655	3097	9	31	4.6	603	0.31	0.13	29	0.2	9	0.6	0.1

2009/11/2	46	17	0	155	8.0	470	735	3505	16	43	5.2	683	1.2	0.13	32	0.6	10	1.0	0.1
2009/11/2	101	26	0	148	8.0	635	1087	4565	23	55	5.8	892	< 0.09	0.26	46	1.0	16	0.7	0.2
2009/12/0	85	28	0	129	7.8	643	1208	4684	17	49	4.9	988	< 0.09	0.18	47	0.8	17	1.1	0.1
2009/12/0	71	24	0	127	8.0	555	1134	4328	19	45	8.3	950	< 0.09	3.40E-02	44	0.7	15	0.3	< 0.1
2009/12/0	58	20	0	109	7.8	539	1131	4413	19	55	8.0	931	< 0.09	0.10	38	0.6	13	0.1	< 0.1
2009/12/0	50	20	198	489	10.4	632	1173	2945	12	92	3.4	950	< 0.09	< 0.01	40	0.2	12	1.2	< 0.1
2009/12/1	59	25	0	136	8.0	629	1159	4283	23	68	9.2	947	0.70	0.24	40	0.6	17	1.1	0.2
2009/12/1	81	24	0	75	7.6	629	1079	4492	11	91	1.1	953	0.23	0.31	46	0.6	21	0.5	0.2
2009/12/1	87	26	0	86	7.4	729	1426	5490	27	110	4.9	1124	0.11	0.27	55	1.4	29	0.5	0.3
2009/12/2	65	24	0	100	7.5	749	1455	5627	25	101	0.5	1211	< 0.09	0.25	59	0.4	22	0.5	0.2
2010/01/0	60	22	0	104	7.6	628	-	3825	19	84	3.7	905	0.90	0.23	48	0.4	24	1.5	0.4
2010/01/0	61	19	0	94	7.8	627	914	4145	18	66	6.4	873	0.91	0.14	46	0.5	16	0.7	< 0.1
2010/01/0	72	23	0	70	7.5	617	1003	4241	19	81	5.2	885	< 0.09	0.18	45	0.4	18	1.0	0.1
2010/01/0	70	23	0	68	7.3	691	1144	4748	18	93	7	1017	0.53	0.25	50	1.1	21	0.6	0.1
2010/01/1	70	28	0	107	7.5	615	1188	4508	15	86	8.9	949	0.21	0.25	48	1.0	21	1.6	0.3
2010/01/1	70	27	0	109	7.9	598	1141	4565	20	116	2.2	925	< 0.09	0.23	46	0.3	18	0.3	< 0.1
2010/01/1	87	34	0	86	7.4	616	-	4583	18	93	2.4	942	< 0.09	0.26	53	0.8	20	1.2	< 0.1
2010/01/1	85	36	0	67	7.3	611	1280	4456	18	94	5.5	926	< 0.09	0.21	57	0.9	21	0.1	< 0.1
2010/01/2	83	34	0	62	7.2	686	1320	4897	16	105	2.5	994	0.11	0.35	64	1.7	23	1.7	< 0.1
2010/01/2	74	35	0	74	7.5	-	1214	4604	35	107	6.4	926	< 0.09	0.33	68	1.8	27	0.5	0.4
2010/01/2	71	34	0	55	7.1	513	1011	3943	18	106	8.9	794	< 0.09	0.35	60	2.0	27	1.2	0.5
2010/01/2	74	33	0	56	7.1	539	1000	3816	16	117	9.2	782	< 0.09	0.38	63	2.1	30	0.5	1.1
2010/01/2	96	43	0	86	7.4	591	1339	4462	26	119	8.3	950	< 0.09	0.40	97	2.0	32	0.8	0.5
2010/02/0	83	43	0	88	7.5	570	1272	4380	23	105	9.8	889	0.25	0.42	95	2.1	28	-	0.4
2010/02/0	88	39	0	82	7.5	568	1076	3917	22	95	12	738	0.29	0.46	86	1.4	22	1.3	0.3
2010/02/0	86	39	0	69	7.2	548	1174	4378	25	125	8.9	811	< 0.09	0.39	94	1.2	21	0.8	0.3
2010/02/1	100	47	0	72	7.3	813	1591	5269	36	131	3.7	1076	< 0.09	0.70	136	1.8	35	1.3	0.6
2010/02/1	97	47	0	93	7.4	830	1565	5327	2	88	13	1054	0.36	0.59	158	1.1	29	0.9	0.3
2010/02/1	117	57	0	77	7.2	956	1869	5712	32	107	14	1314	< 0.09	0.76	190	1.2	39	1.9	0.4
2010/02/1	105	51	0	82	7.4	864	1636	5414	21	99	9.2	1121	< 0.09	0.71	152	1.1	31	1.0	0.3
2010/02/1	129	52	0	70	7.5	1019	1601	5520	30	70	4.6	1171	0.28	0.86	141	0.8	26	1.0	0.3
2010/02/2	120	52	0	58	7.2	1134	1579	6426	31	78	4.9	1216	< 0.09	0.77	150	1.7	29	1.7	0.7
2010/02/2	98	42	0	66	7.4	779	1248	5143	17	56	5.2	1004	< 0.09	0.58	108	0.9	25	0.2	0.7
2010/02/2	88	37	0	93	7.6	670	1111	4656	22	83	1.5	882	< 0.09	0.42	84	1.6	21	0.3	0.7
2010/03/0	88	41	0	167	7.9	694	1471	5272	16	85	4.6	1118	< 0.09	0.22	93	1.0	20	1.5	< 0.1
2010/03/1	109	40	0	146	8.0	730	1519	5779	22	97	1.3	1105	< 0.09	0.32	99	1.4	21	1.2	< 0.1
2010/03/1	91	36	0	105	7.8	592	1307	4853	20	102	4.3	942	< 0.09	0.28	75	1.0	22	0.4	< 0.1

2010/03/1	89	39	0	120	8.0	601	1401	4777	19	92	2.2	1002	< 0.09	0.29	77	1.4	22	1.3	< 0.1
2010/03/1	113	41	0	137	8.1	629	1546	5001	24	77	5.8	1065	< 0.09	0.31	78	1.3	20	0.4	< 0.1
2010/03/2	145	40	0	142	7.9	791	1420	5340	25	83	< 0.1	1062	< 0.09	0.41	79	0.4	18	1.4	< 0.1
2010/03/2	151	44	0	119	7.8	741	1562	5093	25	83	1.0	1186	< 0.15	0.32	81	1.2	21	2.5	< 0.1
2010/03/2	116	37	0	134	7.9	819	1437	5582	30	67	2.9	1110	0.28	0.31	73	1.6	18	0.1	< 0.1
2010/03/3	92	35	0	243	8.2	722	1376	5783	26	85	8	1155	< 0.15	0.17	67	0.9	17	3.3	< 0.1
2010/04/0	106	36	0	206	8.3	793	1456	5957	26	115	8	1217	< 0.15	0.23	66	1.2	20	1.7	< 0.1
2010/04/0	109	40	0	170	7.9	773	1627	5938	28	116	8.9	1332	0.22	0.28	71	3.5	25	0.7	< 0.1
2010/04/0	102	35	0	174	7.6	829	1444	5425	36	115	14	1165	< 0.15	0.28	62	2.5	25	1.2	< 0.1
2010/04/1	99	35	0	152	7.9	846	1387	5642	29	117	14	1157	< 0.15	0.27	66	2.4	24	-	< 0.1
2010/04/1	112	36	0	167	7.9	910	1430	5707	22	98	16	1190	< 0.15	0.27	71	3.1	23	0.1	< 0.1
2010/04/1	98	37	0	149	8.0	786	1309	5364	22	96	11	1109	< 0.15	0.14	65	3.3	19	0.1	< 0.1
2010/04/2	110	39	0	108	7.8	892	1417	5733	22	101	12	1180	0.18	0.30	73	2.9	21	0.1	< 0.1
2010/04/2	107	41	0	91	7.3	965	1431	5655	32	103	6.4	1165	< 0.15	0.39	76	3.1	24	1.6	< 0.1
2010/04/2	165	54	0	79	7.9	1039	1486	5765	13	89	6.4	1150	< 0.15	0.66	78	1.6	21	0.3	< 0.1
2010/04/2	130	45	0	66	7.6	976	1285	5446	20	59	3.4	1029	< 0.15	0.65	64	1.5	15	0.9	< 0.1
2010/04/3	121	41	0	74	7.6	892	1182	4901	22	48	1.0	954	< 0.15	0.60	58	1.0	13	0.4	< 0.1
2010/05/0	109	38	0	66	7.5	925	1154	5279	10	80	4.3	1010	< 0.15	0.45	54	1.1	15	0.9	< 0.1
2010/05/0	162	50	0	71	7.6	911	1460	5409	24	79	14	1142	0.77	0.96	72	1.5	28	0.8	< 0.1
2010/05/0	163	51	0	59	7.7	821	1416	5207	26	55	8.6	958	< 0.15	0.61	57	0.7	12	0.7	< 0.1
2010/05/1	206	69	0	82	7.8	753	1754	4825	23	65	13	1306	0.35	0.8	72	1.3	26	0.8	< 0.1
2010/05/1	109	42	0	108	7.7	686	1123	4274	27	35	2.4	816	< 0.15	0.32	43	0.9	12	1.1	< 0.1
2010/05/1	100	40	0	112	7.7	581	1091	3896	21	33	9.2	817	< 0.15	0.27	48	0.8	14	0.3	< 0.1
2010/05/1	123	44	0	92	7.8	705	1362	4613	20	56	1.2	1066	< 0.15	0.31	60	0.7	20	3.2	< 0.1
2010/05/2	123	41	0	99	8.1	756	1316	4672	21	52	11	988	0.47	0.35	56	0.5	19	1.2	< 0.1
2010/05/2	94	41	0	86	8.1	784	1433	5326	20	63	1.3	1095	< 0.15	0.27	63	0.2	18	0.6	< 0.1
2010/05/2	88	41	0	96	8.0	768	1505	5427	21	74	7	1150	< 0.15	0.26	66	0.3	21	1.1	< 0.1
2010/05/2	78	40	0	114	8.3	840	1377	6023	22	84	1.0	1120	0.43	0.20	66	0.2	10	0.1	0.2
2010/05/2	84	48	0	164	8.0	972	1739	6406	28	80	1.0	1579	< 0.15	0.15	84	0.6	20	0.6	< 0.1
2010/06/0	83	40	0	156	8.0	1107	1620	6691	29	76	14	1414	0.36	0.2	78	0.6	23	3.0	0.6
2010/06/0	74	37	0	143	7.7	1105	1548	6920	32	88	8.3	1397	< 0.15	0.21	76	0.5	21	0.8	< 0.1
2010/06/0	69	33	0	208	8.1	1079	1724	6892	27	94	1.7	1645	< 0.15	0.17	86	0.4	18	2.2	< 0.1
2010/06/0	59	32	0	204	8.2	1077	1592	6847	28	73	1.0	1451	< 0.15	< 0.01	73	0.1	18	0.1	< 0.1
2010/06/1	64	31	1.7	183	8.4	1007	1589	6741	25	62	1.0	1373	0.28	0.15	87	0.2	20	1.8	< 0.1
2010/06/1	76	31	0	131	8.3	1199	1771	7550	30	129	4.6	1563	< 0.15	0.13	100	0.2	23	2.7	0.4
2010/06/1	117	38	0	140	8.1	1768	1983	8328	32	67	1.0	1785	< 0.15	0.72	91	0.4	18	-	< 0.1
2010/06/1	96	39	2	226	8.4	1525	1879	8326	33	64	5.5	1749	< 0.15	0.22	88	0.3	13	0.2	< 0.1

2010/06/2	102	39	0	212	8.1	1737	1759	8147	38	65	1.0	1683	0.38	0.39	80	0.6	17	0.2	< 0.1
2010/06/2	143	57	0	181	8.3	1801	2503	8791	46	113	4	2432	0.20	0.41	117	0.4	23	1.7	< 0.1
2010/06/2	97	38	0	156	8.0	1225	1687	6990	33	78	13	1610	< 0.15	0.20	87	0.3	20	3.1	0.2
2010/06/2	76	36	0	158	8.2	1113	1660	6724	31	88	1.0	1482	< 0.15	0.15	80	0.1	21	2.1	< 0.1
2010/07/0	64	27	1	132	8.3	932	1180	5623	21	39	3.1	1078	< 0.15	9.60E-02	67	0.2	19	1.1	0.7
2010/07/0	69	30	0	191	8.3	1007	1193	5894	26	87	2.1	1182	< 0.15	0.11	64	0.2	16	1.5	0.7
2010/07/0	79	30	0	199	8.2	973	1072	5538	20	43	1.8	1122	< 0.15	0.17	75	0.2	16	1.5	< 0.1
2010/07/0	71	33	2	192	8.4	1120	1206	6008	19	-	1.0	1214	< 0.15	0.15	110	0.6	21	1.4	< 0.1
2010/07/0	74	31	0	181	8.3	1021	1170	5853	22	68	5.8	1124	< 0.15	0.14	93	0.4	15	1.0	0.6
2010/07/1	85	33	0	285	8.3	1125	1306	6480	21	90	1.0	1299	< 0.15	0.13	95	0.5	20	6.2	< 0.1
2010/07/1	64	28	0	190	7.9	937	1140	5667	29	77	1.0	1155	0.29	3.30E-02	82	0.7	16	1.7	< 0.1
2010/07/1	94	3	2.9	197	8.4	1279	1541	6598	28	93	4.3	1595	< 0.15	1.90E-02	128	0.7	21	1.5	< 0.1
2010/07/2	75	37	3.8	226	8.4	1160	1375	6639	21	74	4.9	1380	< 0.15	0.16	141	0.6	19	3.9	< 0.1
2010/07/2	63	32	0	194	8.3	990	1148	5736	23	98	4.0	1210	< 0.15	0.11	99	0.9	24	2.0	< 0.1
2010/07/2	84	33	2.2	197	8.4	1056	1204	6276	28	91	1.9	1238	< 0.15	0.15	109	0.7	21	1.5	0.7
2010/07/2	87	33	0	181	8.2	1067	1365	6106	27	57	2.1	1230	< 0.15	0.13	99	0.8	19	2.4	0.7
2010/07/2	73	30	0.84	160	8.3	956	1317	5983	29	88	1.4	1164	0.37	0.13	91	< 0.1	21	2.0	0.7
2010/07/3	41	17	0	91	8.1	439	628	3084	14	62	4.6	570	< 0.15	5.40E-02	47	0.3	18	0.4	0.7
2010/08/0	43	17	0	69	7.8	369	551	2770	13	82	0.98	551	< 0.15	0.1	42	1.0	21	4.5	0.7
2010/08/0	48	17	0	86	7.9	390	564	2836	12	54	0.98	541	0.76	0.18	41	1.4	22	6.0	0.7
2010/08/1	66	18	0	75	7.9	512	896	3720	15	64	1.4	791	< 0.15	0.20	56	1.6	26	3.1	0.7
2010/08/1	57	15	0	102	7.6	459	752	3243	18	45	1.0	625	< 0.15	0.36	42	1.9	15	1.8	0.7
2010/08/1	58	21	0	102	8.2	638	1045	4207	19	60	2.9	861	0.2	0.20	69	0.8	19	2.9	0.7
2010/08/1	59	22	0	92	8.0	702	1100	4695	16	93	4.9	979	< 0.15	0.14	66	0.4	19	3.6	0.7
2010/08/1	53	20	0	98	8.0	644	991	4228	20	84	1.0	912	< 0.15	6.90E-02	63	1.2	18	1.4	0.7
2010/08/2	59	21	0	123	7.6	763	1062	5087	27	115	13	956	< 0.15	0.13	75	0.6	19	2.1	0.7
2010/08/2	72	24	0	151	7.7	830	1252	5329	26	93	8.3	1168	< 0.15	0.23	91	0.7	19	3.0	< 0.1
2010/08/2	89	20	0	161	7.9	937	1218	5655	29	91	8.0	1104	< 0.15	< 0.01	89	< 0.1	17	1.1	< 0.1
2010/08/3	98	32	0	189	8.1	1071	1628	6265	29	68	7.4	1502	< 0.15	0.28	110	0.5	16	1.5	< 0.1
2010/09/0	75	25	0	163	8.1	924	1278	5728	32	70	1.0	1143	< 0.15	0.15	81	0.5	19	1.5	< 0.1
2010/09/0	84	25	0	151	7.9	921	1374	5750	27	56	4.3	1230	< 0.15	< 0.01	71	0.1	17	1.3	< 0.1
2010/09/0	83	26	0	160	7.8	974	1434	6052	27	89	1.0	1274	< 0.15	< 0.01	71	0.3	18	2.2	< 0.1
2010/09/1	80	18	0	105	7.6	937	1234	5513	25	56	1.0	1141	< 0.15	< 0.01	58	< 0.1	15	2.6	< 0.1
2010/09/1	70	15	0	93	7.8	783	1034	4708	24	69	1.0	961	< 0.15	< 0.01	52	< 0.1	14	0.9	< 0.1
2010/09/1	83	18	0	93	7.4	937	1038	4887	23	63	1.0	962	< 0.15	< 0.01	68	1.4	20	0.1	< 0.1
2010/09/2	88	20	0	94	7.7	827	1013	4805	21	68	1.0	966	< 0.15	< 0.01	59	0.1	22	0.3	< 0.1
2010/09/2	134	23	0	95	7.5	957	1226	5448	14	43	1.0	1051	< 0.15	< 0.01	66	< 0.1	20	0.9	< 0.1

2010/09/2	126	23	0	86	7.4	1202	1431	6004	28	39	1.0	1223	< 0.15	< 0.01	66	< 0.1	24	0.7	0.7
2010/09/3	99	26	0	86	7.7	1343	1581	6460	25	25	1.5	1334	< 0.15	0.29	65	0.5	20	0.4	0.7
2010/10/0	135	28	0	96	7.5	1253	1381	6205	32	91	11	1308	< 0.15	0.35	60	3.7	20	0.8	0.8
2010/10/0	115	28	0	66	7.7	1091	1262	5657	23	56	2.5	1194	< 0.15	0.37	64	1.6	24	0.8	0.7
2010/10/0	94	28	0	107	7.8	1128	1185	5451	24	36	2.0	1103	< 0.15	0.27	54	0.6	23	0.4	0.7
2010/10/1	97	30	0	96	7.6	1225	1266	6108	24	62	3.7	1181	< 0.15	0.22	59	0.9	27	2.1	0.2
2010/10/1	82	26	0	112	7.6	1035	1000	5141	16	70	7.4	1026	< 0.15	0.09	53	1.4	26	0.1	0.4
2010/10/1	73	22	0	116	7.5	816	855	4396	26	49	11	883	< 0.15	0.11	40	2.8	24	2.0	0.4
2010/10/1	61	19	0	114	7.5	678	758	3865	25	75	11	774	0.21	0.22	36	1.8	24	0.8	0.3
2010/10/2	88	28	0	121	7.8	769	1109	4422	25	120	24	1202	< 0.15	0.20	61	3.8	40	2.8	0.6
2010/10/2	60	19	0	140	7.5	558	783	3254	31	111	3.0	751	< 0.15	0.23	39	1.1	31	3.2	0.6
2010/10/2	43	15	0	147	7.4	459	486	2835	16	77	1.0	566	< 0.15	0.25	27	1.1	26	0.8	2.6
2010/10/2	43	19	0	177	8	658	632	3566	23	88	1.0	815	< 0.15	0.11	39	3.9	28	1.5	0.2
2010/10/2	99	25	0	137	8.1	684	856	3875	17	72	5.5	1063	0.21	0.31	55	0.6	39	2.7	0.3
2010/11/0	76	17	0	100	8	634	708	3721	16	86	3.4	752	0.37	0.16	43	1.0	27	1.7	0.6
2010/11/0	92	20	0	101	7.7	737	776	4169	19	85	6.4	954	< 0.15	0.16	52	1.0	30	2.0	1.0
2010/11/0	63	15	0	101	7.7	703	605	3725	12	66	3.7	682	0.51	0.11	37	0.6	6.8	0.5	0.4
2010/11/1	72	18	0	149	8.1	657	730	3860	12	69	8.6	832	< 0.15	0.11	46	1.4	16	0.4	0.7
2010/11/1	61	14	0	150	8.1	529	572	3013	16	50	3.0	667	0.35	0.12	38	1.4	19	0.5	0.7
2010/11/1	61	14	0	146	8.1	514	529	3126	10	36	1.1	609	< 0.15	9.20E-02	38	1.1	14	0.9	0.7
2010/11/1	52	14	0	139	8	462	469	2838	16	42	1.9	546	0.31	0.11	35	0.5	11	1.1	0.7
2010/11/1	57	17	0	114	8	602	688	3624	24	80	2.5	725	< 0.15	3.20E-02	47	0.5	17	3.1	0.7
2010/11/2	54	18	0	116	7.9	645	788	3961	22	72	7	817	< 0.15	0.13	48	1.1	19	1.7	0.5
2010/11/2	65	20	0	109	7.7	665	998	4180	20	90	9.5	953	0.56	0.20	57	2.0	22	1.5	0.3
2010/11/2	59	19	0	129	8	645	868	4192	20	103	9.5	837	< 0.15	7.30E-02	50	1.7	21	1.0	0.6
2010/11/3	58	21	0	116	7.8	602	840	4024	17	89	12	852	< 0.15	0.16	50	1.9	25	0.1	< 0.1
2010/12/0	57	20	0	123	8.1	553	899	3906	20	90	13	820	0.17	0.15	50	1.8	26	0.5	0.4
2010/12/0	64	23	0	142	8.3	555	932	3793	17	74	11	915	< 0.15	0.11	53	1.6	20	0.6	< 0.1
2010/12/0	46	16	0	179	8.1	429	681	3112	16	27	9.2	632	< 0.15	6.80E-02	36	2.5	14	2.8	0.4
2010/12/1	34	12	5.6	206	8.5	317	489	2599	13	17	1.0	553	< 0.15	< 0.01	25	0.3	9.8	0.1	< 0.1
2010/12/1	32	10	0	228	8	287	421	2340	17	18	5.2	473	< 0.15	< 0.01	21	1.4	7.3	1.8	1.3
2010/12/2	28	10	4.1	220	8.5	299	359	2227	6	14	16	449	< 0.15	1.30E-02	19	2.8	6.4	Nil	0.3
2010/12/2	52	20	0	278	8.1	409	556	2826	23	32	8.3	588	< 0.08	8.10E-02	37	2.0	3.3	0.4	< 0.1
2010/12/3	62	23	6.5	258	8.5	487	607	3193	19	54	4.0	672	0.49	0.16	43	1.3	-	1.0	< 0.1
2011/01/0	73	27	0	138	7.9	596	920	3982	19	95	0.98	843	< 0.08	0.11	55	6.6E-	15	0.3	0.7
2011/01/0	53	25	0	106	7.6	579	959	4018	16	71	0.86	817	< 0.08	0.16	56	0.2	12	0.6	0.7
2011/01/0	68	25	0	99	7.5	569	932	3973	21	84	5.8	799	< 0.08	0.22	57	1.4	16	0.7	0.7

2011/01/1	76	26	0	84	7.3	540	983	4002	22	92	4.3	851	< 0.08	0.31	60	1.8	19	8.0	0.7
2011/01/1	84	27	0	105	7.5	602	1043	4329	22	105	7.7	936	0.69	0.52	67	5.0	28	0.4	0.7
2011/01/1	70	26	0	130	7.6	618	1050	4174	31	100	8.0	873	< 0.08	0.21	66	1.4	-	3.8	0.7
2011/01/1	74	26	0	104	7.6	596	881	4172	27	109	5.5	827	0.20	0.23	66	2.0	-	0.8	0.7
2011/01/2	79	24	0	113	7.6	574	960	4123	25	81	2.6	795	< 0.08	0.18	66	0.7	18	0.8	0.1
2011/01/2	73	23	0	97	7.5	590	979	4154	24	67	2.2	764	0.15	0.26	70	0.5	-	1.4	< 0.1
2011/01/2	66	24	0	140	8	516	839	3580	20	41	2.5	691	< 0.08	0.20	74	0.4	21	1.3	0.1
2011/01/2	68	25	0	112	7.9	605	886	3983	18	83	2.4	764	< 0.08	0.17	90	0.6	24	0.9	< 0.1
2011/01/2	62	21	0	103	7.7	630	839	3891	19	67	2.4	761	0.23	0.28	74	0.5	23	1.7	0.6
2011/02/0	83	20	0	71	7.6	731	1031	4588	19	51	1.3	890	0.16	0.20	87	-	19	1.4	< 0.1
2011/02/0	64	18	0	81	7.7	710	983	4227	19	43	2.0	843	0.32	0.21	81	0.5	14	0.5	0.1
2011/02/0	47	21	0	103	7.9	844	1181	4969	19	69	2.5	1012	< 0.08	0.19	97	0.9	15	1.0	< 0.1
2011/02/0	48	22	0	94	7.8	882	1068	5064	19	91	2.5	1038	< 0.08	0.15	99	0.3	16	Nil	0.3
2011/02/1	49	22	0	114	8.1	1011	1169	5440	20	63	2.5	1122	< 0.08	6.30E-02	105	0.6	17	1.7	0.2
2011/02/1	60	23	0	148	8.1	1028	1309	5691	25	65	2.5	1239	0.25	6.80E-02	92	1.0	15	1.0	0.2
2011/02/1	64	21	0	75	7.3	1066	1302	5928	26	79	2.2	1233	< 0.08	0.22	92	1.1	20	0.3	0.4
2011/02/1	68	22	0	110	7.5	953	1231	5835	28	96	7.4	1204	< 0.08	0.2	90	1.5	25	0.5	< 0.1
2011/02/2	74	23	0	118	7.8	903	1190	5651	37	91	10	1162	< 0.08	0.2	88	2.2	23	0.5	0.4
2011/02/2	79	23	0	134	8	929	1217	5506	27	94	9.5	1129	< 0.08	0.24	92	2.0	26	3.1	0.1
2011/02/2	116	26	0	143	8.0	965	1295	5700	33	79	9.5	1120	0.38	0.37	79	20	22	0.4	0.2
2011/03/0	106	28	0	127	7.6	996	1429	6038	26	82	1.8	1193	< 0.08	0.31	84	0.4	24	0.8	0.2
2011/03/0	80	27	0	103	7.8	882	1392	5729	24	49	2.8	1147	0.14	0.23	82	0.2	23	0.2	< 0.1
2011/03/0	77	34	0	134	7.7	1100	1632	6577	29	39	2.5	1319	0.09	0.29	100	0.5	26	0.2	0.1
2011/03/0	63	31	0	90	7.7	984	1485	5918	23	35	2.5	1172	< 0.08	0.25	90	0.6	27	0.8	< 0.1
2011/03/1	60	23	0	80	7.9	715	995	4349	18	35	2.0	854	< 0.08	0.24	65	0.9	22	1.4	< 0.1
2011/03/1	61	26	0	82	7.4	886	1239	5351	25	38	2.4	1012	< 0.08	0.3	76	0.6	23	0.1	< 0.1
2011/03/1	58	25	0	81	7.4	900	1371	5629	24	26	1.25	1115	< 0.08	0.33	85	0.1	25	0.6	< 0.1
2011/03/1	75	23	0	119	7.5	924	1397	5711	32	47	3.7	1133	0.38	0.27	83	0.3	24	10	0.1
2011/03/2	101	23	0	82	7.6	1047	1795	6851	27	88	5.5	1575	< 0.08	4.70E-02	99	0.4	30	0.9	0.1
2011/03/2	77	18	0	108	7.7	861	1382	5832	25	102	6.7	1240	0.19	0.23	81	1.3	24	0.6	0.1
2011/03/2	51	14	0	76	8.2	597	996	4151	20	66	3.7	852	< 0.08	0.12	55	0.6	24	0.6	0.1

Table A-2: Statistical analysis of the Open System One data

Data	Al (mg/l)	Oil (mg/l)	Si-SiO ₂ (mg/l)	Zn (mg/l)	K (mg/l)	Mn (mg/l)	Fe (mg/l)	Na (mg/l)	P-PO ₄ (mg/l)	F ⁻ (mg/l)	Suspended solids (mg/l)	Cond (µS/cm)	S-SO ₄ (mg/l)	Cl (mg/l)	pH	Total alkalinity (mg/l CaCO ₃)	P-alk (mg/l CaCO ₃)	Mg (mg/l)	Ca (mg/l)
Average	0.4	1.4	19	1.0	70	0.28	0.40	997	4.2	70	22	4867	1153	787	7.8	116	1	27	80
Median	0.3	0.9	19	0.7	67	0.24	0.31	961	2.5	68	21	4754	1131	748	7.8	108	0	25	74
Max	2.7	11	40	5.7	190	0.96	1.40	2432	24	151	46	8791	2503	1801	10.4	489	198	69	206
Min	0.1	0.1	3	0.1	19	0.013	0.09	416	0.0	14	2	2227	359	287	6.8	25	0	10	28

**APPENDIX B: COOLING WATER CHEMISTRY FOR
OPEN COOLLING SYSTEM TWO FOR THE
PERIOD 3 MARCH 2009 TO 25 MARCH 2011**

Table B-1: Cooling water chemistry (raw data) and statistical analysis for Open System Two for the period 1 June 2009 to 28 February 2011 (Buckman, 2012b)

Date	Ca (mg/l)	Mg (mg/l)	P-alk (mg/l CaCO ₃)	Total alkalinity (mg/l CaCO ₃)	pH	Cl (mg/l)	S-SO ₄	Cond (µS/cm)	Suspended solids (mg/l)	F ⁻ (mg/l)	P-PO ₄ (mg/l)	Na (mg/l)	Fe (mg/l)	Mn (mg/l)	K (mg/l)	Zn (mg/l)	Si-SiO ₂ (mg/l)	Oil (mg/l)	Al (mg/l)
2009/06/01								5593	41										
2009/06/03	53	13	0	110	7.6	841	1152	5294	32	23	3.7	855	0.78	0.2	47	0.4	11		0.6
2009/06/04								5048	38										
2009/06/05								4627	40										
2009/06/08								4728	45										
2009/06/11								5492	43										
2009/06/17	45	8.2	0	58	7.0	466	826	3334	45	34	1.2	626	1.6	0.2	53	0.1	13	0.3	0.5
2009/06/18								3886	45										
2009/06/19								4743	34										
2009/06/22								4707	44										
2009/06/24	36	17	0	46	7.3	684	1084	4239	46	71	0.49	891	0.23	0.6	70	0.1	23	0.8	1.0
2009/06/26								5476	49										
2009/06/29								5783	39										
2009/07/01	34	21	0	53	7.1	701	1046	4503	38	58	0.49	788	0.47	0.7	76	0.2	25	0.4	0.7
2009/07/02								3746	51										
2009/07/03								5279	49										
2009/07/06								4590	54										
2009/07/08	47	28	0	56	7.2	838	1405	5772	65	90	1.9	999	1.4	0.7	106	0.3	30	2.6	1.0
2009/07/10								4961	54										
2009/07/13								4748	64										
2009/07/15	57	22	0	34	7.0	781	1467	5518	89	85	0.7	1128	0.15	0.9	137	0.3	34	8.8	3.5

2009/07/16								5764	81										
2009/07/17								7643	56										
2009/07/20								6311	49										
2009/07/22	64	27	0	36	6.7	1110	1695	6072	73	39	0.768	1354	1.3	1.2	159	0.2	38	5	1.0
2009/07/23								5356	56										
2009/07/24								4580	24										
2009/07/27								4525	21										
2009/07/29	55	22	0	23	6.3	957	1223	5486	40	58	1.2	1059	4.2	1	109	0.4	35	3.6	1.5
2009/07/30								5544	37										
2009/08/03								4743	33										
2009/08/05	39	21	0	24	6.6	1064	1032	5490	34	78	0.49	1050	1	0.9	115	1.2	35	1.4	1.8
2009/08/06								5358	53										
2009/08/10								5334	34										
2009/08/12			0	35	7.0	1020		5003	22	35								3.2	
2009/08/13								4688	24										
2009/08/14								5407	42										
2009/08/17								4961	27										
2009/08/19	47	19	0	45	6.8	737	557	3534	9	13	1.6	609	0.52	0.2	64	0.4	6.3	0.5	-
2009/08/20								4855	18										
2009/08/21								4729	47										
2009/08/24								4687	49										
2009/08/26	85	26	0	37	7.1	977	888	4885	41	53	1.9	951	0.9	0.9	96	1.6	27	2.6	0.5
2009/08/27								5564	52										
2009/08/28								4166	19										
2009/08/31								3895	29										
2009/09/02	104	28	0	21	6.4	1002	772	4662	48	50	3	767	1.9	1.3	149	2.6	37	4.6	1.3
2009/09/03								4352	38										
2009/09/04								4526	43										
2009/09/07								5029	42										
2009/09/09	46	30	0	128	7.7	1121	1369	6611	56	119	1.5	1310	0.22	0.4	147	0.9	33	2.9	0.3
2009/09/10								6329	51										
2009/09/11								6492	40										
2009/09/14								6171	32										
2009/09/16	144	20	0	100	7.2	522	881	3225	25	12	0.79	538	< 0.09	1.7	43	9.9	5.7	2	0.8
2009/09/17								4525	47										
2009/09/18								5200	36										
2009/09/21								5834	39										

2009/09/25								5371	27										
2009/09/28								5275	39										
2009/09/30	106	29	0	70	7.6	1436	1197	6288	43	54	0.49	1260	0.56	0.6	79	1.3	24	4.3	0.2
2009/10/02								6208	31										
2009/10/05								5579	44										
2009/10/07	72	26	0	128	7.7	1122	820	5373	52	59	0.49	957	0.71	0.7	66	0.6	18	9.2	0.3
2009/10/08								4714	53										
2009/10/09								5398	30										
2009/10/12								4857	28										
2009/10/14	39	19	0	115	7.7	650	647	3554	22	71	0.49	713	0.19	0.3	47	0.7	21	1.6	0.3
2009/10/15								3511	17										
2009/10/16								3532	21										
2009/10/19								3942	20										
2009/10/21	76	20	62	230	9.4	682	782	5850	18	70	0.89	759	0.28	0.3	55	0.3	19	1.1	0.2
2009/10/22								4544	40										
2009/10/23								4323	18										
2009/10/26								4230	21										
2009/10/28	41	18	0	165	7.9	604	717	3663	25	49	0.49	741	0.24	0.2	42	0.3	12	1.2	0.2
2009/10/29								4045	25										
2009/10/30								3515	31										
2009/11/02								3641	23										
2009/11/04	51	18	0	94	7.3	593	841	3716	40	57	0.49	741	0.22	0.3	54	0.5	19	14	0.4
2009/11/06								3701	20										
2009/11/09								2969	20										
2009/11/11	50	18	0	82	7.4	528	628	3334	26	72	0.49	654	0.61	0.4	35	0.6	27	1.6	0.9
2009/11/12								3789	41										
2009/11/13								3748	44										
2009/11/16								3129	38										
2009/11/18	40	18	0	132	7.6	541	643	3420	22	55	1.2	658	0.7	0.3	30	0.2	23	2.7	0.3
2009/11/19								3415	33										
2009/11/20								3260	22										
2009/11/23								3426	23										
2009/11/25	51	18	0	86	7.3	503	775	3586	35	49	1.9	679	0.7	0.4	31	0.2	22	1.2	0.6
2009/11/26								3697	15										
2009/11/27								3626	24										
2009/11/30								3812	20										
2009/12/02			0	118	7.0	505		3637	24	129							1.3		

2009/12/03								3702	24										
2009/12/04								3791	16										
2009/12/07								3717	23										
2009/12/09	51	21	0	183	6.8	483		3596	32	49	8.6	747	10	0.5	30	0.2	27	1.3	0.6
2009/12/10								3299	49										
2009/12/11								3283	18										
2009/12/16	54	20	0	91	7.1	502	749	3478	35	55	5.2	741	1.5	0.5	31	0.5	25	1.5	0.4
2009/12/17								3300	17										
2009/12/21								3672	18										
2009/12/23	46	19	0	122	7.5	431	830	3425	45	48	1.1	702	0.69	0.3	36	0.1	27	1.1	0.5
2010/01/01								2487	20										
2010/01/04								2501	22										
2010/01/06	45	17	0	100	7.5	436	630	2865	21	25	0.49	576	< 0.09	<	25	0.6	16	2	<
2010/01/07								2885	22										
2010/01/08								3026	26										
2010/01/11								2856	25										
2010/01/13	57	27	0	132	7.7	390	770	2829	26	38	<	568	0.14	0.3	26	0.4	12	1.7	0.2
2010/01/14								3236	27										
2010/01/15								3300	44										
2010/01/18								3416	31										
2010/01/20	62	29	0	111	7.0	398	817	3109	33	43	0.92	588	0.27	0.4	41	0.2	19	2.7	<
2010/01/21								2820	40										
2010/02/08								2775	128										
2010/02/10	68	32	0	136	7.7	435	844	3160	42	27	3.4	529	< 0.09	0.2	84	0.1	13	2.9	0.3
2010/02/12								3934	32										
2010/02/15								3975	59										
2010/02/17	84	37	0	124	7.8	521	976	3579	82	35	2.7	641	< 0.09	0.3	87	0.2	15	2.7	0.1
2010/02/18								3476	31										
2010/02/19								4058	42										
2010/02/22								4110	35										
2010/02/24	70	34	0	93	7.4	735	966	4329	41	37	1.3	822	< 0.09	0.4	81	0.1	18	2.1	0.2
2010/02/26								3213	30										
2010/03/01								3233	23										
2010/03/04								3485	29										
2010/03/05								1479	15										
2010/03/08								3625	19										
2010/03/10	88	31	0	159	7.8	532	1044	3632	32	33	1.6	696	< 0.09	0.3	56	0.1	18	2.1	<

2010/03/11								3451	31										
2010/03/12								2954	14										
2010/03/15								3387	22										
2010/03/17	77	32	0	129	7.8	404	1134	3697	18	32	<	735	< 0.09	0.3	50	0.2	14	0.9	<
2010/03/18								3831	37										
2010/03/22								4672	34										
2010/03/24	95	37	0	54	7.1	815	1228	5067	38	53	2.9	954	< 0.15	0.7	64	0.2	28	3.4	0.7
2010/03/25								4996	30										
2010/03/26								4293	26										
2010/03/29								3767	33										
2010/04/05								3223	26										
2010/04/08								3295	28										
2010/04/09								3764	23										
2010/04/12								3892	19										
2010/04/14	86	33	0	141	7.1	773	1213	5121	69	86	5.5	1018	6.8	0.7	63	0.2	36	1.8	0.4
2010/04/15								5339	69										
2010/04/16								8342	70										
2010/04/19								8788	67										
2010/04/21	51	61	0	60	7.1	1960	2692	10040	54	96	1	2253	0.53	1.7	139	0.3	67	4.8	0.6
2010/04/22								7092	59										
2010/04/23								11280	86										
2010/04/28	109	101	0	29	6.4	3137	3858	13800	103	72	4	3331	1.7	2.9	209	0.4	73	3.4	0.7
2010/05/03								11710	55										
2010/05/06								6032	31										
2010/05/07								4191	28										
2010/05/10								4594	25										
2010/05/12	129	54	0	80	7.6	903	1520	5224	26	33	2.1	1021	< 0.15	0.8	57	0.3	21	2.1	<
2010/05/13								5305	33										
2010/05/14								4443	12										
2010/05/17								3817	18										
2010/05/19	119	43	0	90	7.5	799	1348	4486	22	23	0.98	961	< 0.15	0.4	58	0.3	15	0.3	<
2010/05/21								4416	30										
2010/05/24								4311	22										
2010/05/26	64	34	0	133	7.6	787	1126	4820	22	34	1.2	908	< 0.15	0.2	53	0.2	13	0.5	<
2010/05/27								4759	16										
2010/05/28								4895	22										
2010/05/31								4990	31										

2010/06/02	68	28	0	94	7.3	780	1098	4722	21	23	0.98	933	< 0.15	0.2	55	0.2	16	1.1	<
2010/06/03								5742	28										
2010/06/04								7008	43										
2010/06/07								6184	38										
2010/06/09	60	37	0	180	7.9	1169	1891	7293	44	125	5.2	1551	< 0.15	0.1	88	0.1	18	20	<
2010/06/10								5599	25										
2010/06/11								5806	32										
2010/06/14								6094	32										
2010/06/16	69	30	0	179	7.7	1106	1551	6564	30	46	0.98	1378	< 0.15	0.2	74	0.2	18	0.7	0.7
2010/06/17								6092	25										
2010/06/18								6283	24										
2010/06/21								5964	26										
2010/06/23	96	32	0	146	7.5	1063	1273	5674	27	92	4	1104	0.25	0.5	54	0.6	11	40	0.7
2010/06/24								5365	27										
2010/06/25								4701	22										
2010/06/28								4574	17										
2010/06/30	62	27	0	177	7.7	910	995	5163	23	40	2.1	956	0.66	0.2	58	0.4	17	1.3	0.7
2010/07/01								4946	23										
2010/07/02								4797	23										
2010/07/05								5174	33										
2010/07/07	ICP		0	202	7.6	846		4496	23	5.7								0.4	
2010/07/07	ICP		0	202	7.6	846		4496	23	5.7								0.4	
2010/07/09								5403	24										
2010/07/12								5527	25										
2010/07/14	57	31	0	264	7.9	1135	1151	5907	28	37	5.2	1166	< 0.15	0.3	88	0.4	16	2.2	0.7
2010/07/15								5819	27										
2010/07/16								4990	20										
2010/07/23								4825	25										
2010/07/26								4781	21										
2010/07/28	53	29	0	208	7.7	779	1187	4754	21	20	1.6	925	0.41	0.2	69	0.2	13	0.7	<
2010/07/29								4832	21										
2010/07/30								4579	26										
2010/08/02								5053	29										
2010/08/23								3097	9										
2010/08/25	225	26	0	154	7.7	839	1113	3971	24	6.2	2.7	1026	< 0.15	1.2	85	1.2	13	2.4	<
2010/08/26								4041	21										
2010/08/27								4263	21										

2010/08/30								4231	20										
2010/09/01	96	24	0	148	7.3	771	1094	4505	23	58	2.4	932	0.74	0.5	64	0.7	12	1.1	<
2010/09/02								5034	25										
2010/09/03								4541	44										
2010/09/06								4160	36										
2010/09/08	44	24	0	183	7.6	709	1028	3851	28	28	0.98	960	0.72	<	55	<	9.6	0.8	0.3
2010/09/09								4332	39										
2010/09/10								4890	33										
2010/09/13								4790	22										
2010/09/16								4213	26										
2010/09/20								4977	33										
2010/09/22	53	11	0	61	6.9	862	552	4677	30	37	2.8	499	< 0.15	<	28	<	9.3	1.3	0.5
2010/09/24								3715	16										
2010/09/30								3635	21										
2010/10/01								3969	18										
2010/10/04								4442	22										
2010/10/06	99	27	0	96	7.5	848	931	4219	18	25	0.98	885	< 0.15	0.5	42	0.1	21	1.4	0.8
2010/10/07								4208	21										
2010/10/08								5060	23										
2010/10/11								5123	27										
2010/10/13	65	27	0	111	7.6	1064	1064	5056	30	38	0.98	1073	< 0.15	0.3	43	0.1	22	1.4	0.7
2010/10/14								4625	32										
2010/10/15								4709	27										
2010/10/18								4408	24										
2010/10/21								4367	35										
2010/10/22								3905	25										
2010/10/25								4001	21										
2010/10/27	48	20	0	102	7.7	786	707	3873	15	37	0.98	773	< 0.15	0.2	34	<	13	1.2	0.7
2010/10/28								3655	23										
2010/11/01								4203	20										
2010/11/03	80	11	0	87	7.5	754	468	3809	21	28	0.98	334	< 0.15	0.2	25	<0.1	7.1	1.6	0.5
2010/11/04								3671	17										
2010/11/05								3596	18										
2010/11/08								3435	18										
2010/11/10	65	18	0	108	7.6	583	773	3371	22	22	0.98	619	< 0.15	0.2	43	<	9.5	0.7	0.7
2010/11/11								3237	12										
2010/11/12								3372	22										

2010/11/15								3494	20										
2010/11/17	84	22	0	102	7.6	620	658	3305	17	33	3.4	603	1.6	0.4	48	0.2	18	0.8	0.7
2010/11/18								3530	15										
2010/11/19								3662	15										
2010/11/24	58	20	0	130	7.7	609	1048	3787	33	36	2.5	907	1.1	0.2	47	0.2	19	2.2	0.8
2010/11/25								3323	34										
2010/11/26								3005	17										
2010/11/29								2743	15										
2010/12/02								2549	12										
2010/12/03								3126	18										
2010/12/06								3109	15										
2010/12/08	52	17	0	154	7.9	482	771	3129	18	22	0.98	628	< 0.15	0.2	38	0.5	11	1.5	0.7
2010/12/09								2913	19										
2010/12/10								2543	18										
2010/12/13								2465	16										
2010/12/17								1930	10										
2010/12/20								2084	16										
2010/12/22	66	28	0	82	7.4	452	759	3050	20	54	2.6	615	0.16	0.3	35	0.2	23	1.9	0.7
2010/12/27								3033	13										
2010/12/29	Instrument Failure		0	119	7.8	515		3044	16	35								Nil	
2010/12/31								3472	21										
2011/01/03								2849	16										
2011/01/05	51	20	0	104	7.5	332	652	2448	17	27	0.29	456	0.22	0.2	31	<	8.9	0.8	0.7
2011/01/06								2448	18										
2011/01/07								2641	40										
2011/01/10								2774	26										
2011/01/12	43	18	0	155	7.8	372	571	2731	22	15	<	468	< 0.08	-	36	<0.1	5.8	0.9	0.7
2011/01/13								2525	22										
2011/01/14								2937	24										
2011/01/17								2952	24										
2011/01/19	88	24	0	101	7.4	463	833	3302	29	29	0.46	589	< 0.08	0.2	55	<0.1	ECDev	5	0.7
2011/01/20								3275	38										
2011/01/21								3356	30										
2011/01/24								3294	41										
2011/01/26	74	27	0	185	7.8	432	639	2965	55	33	1.9	494	0.4	0.4	75	<0.1	21	2.3	0.7

2011/01/27								2718	35										
2011/01/28								3993	33										
2011/02/02	72	19	0	93	7.2	786	957	4308	26	25	<	826	0.61	0.4	76	0.2	14	2	0.7
2011/02/03								3979	37										
2011/02/04								3796	30										
2011/02/07								3864	27										
2011/02/09	46	18	0	134	7.6	814	610	3912	36	23	<	764	< 0.08	0.1	55	<0.1	11	1.9	0.7
2011/02/10								4112	34										
2011/02/11								4896	53										
2011/02/14								4559	42										
2011/02/16	64	16	0	91	7.3	751	951	4405	36	40	0.52	863	0.18	0.3	62	<	19	1	0.7
2011/02/17								4149	42										
2011/02/18								3812	29										
2011/02/21								3790	62										
2011/02/23	65	19	0	98	7.4	685	817	4030	31	50	0.67	733	0.29	0.3	51	<	19	1.4	0.7
2011/02/24								3808	32										
2011/02/25								4437	49										
Average	69	26	1	111	7.0	778	1034	4419	32	46	2	883	1	0	65	1	20	3.0	1.0
Median	62	24	0	106	7.5	753	954	4213	28	38	1.2	788	0.61	0.3	55	0.2	18	1.6	0.7
Maximum	225	101	62	264	9.4	3137	3858	15030	128	129	8.6	3331	10	2.9	209	9.9	73	40	3.5
Minimum	34	8.2	0	21	6.3	332	468	1479	9	5.7	0.29	334	0.14	0.1	25	0.1	5.7	0.3	0.1

APPENDIX C: CORROSION RATES FOR OPEN COOLING SYSTEM ONE AND TWO FOR THE PERIOD JUNE 2009 TO FEBRUARY 2011

Table C-1 Mild steel coupon corrosion rates for
Open Systems One and Two for the period June
2009 to February 2011

Year	Month	Open System One (mmpa)	Open System Two (mmpa)
2009	6	0.1450	0.0829
2009	7	0.0964	0.1503
2009	8	0.1533	0.3035
2009	9	0.1926	0.1595
2009	10	0.1801	0.1353
2009	11	0.4439	0.2137
2009	12	0.7974	0.3583
2010	1	0.3977	0.2435
2010	2	0.3628	0.3283
2010	3	0.5535	0.4635
2010	4	0.4785	0.1023
2010	5	0.8003	0.3704
2010	6	0.7928	0.3801
2010	7	0.5034	1.1091
2010	8	0.3873	0.1399
2010	9	0.2791	0.3430
2010	10	0.3024	0.2681
2010	11	0.2819	0.1380
2010	12	0.5579	0.2472
2011	1	0.5145	0.3234
2011	2	0.6226	0.5438

**APPENDIX D: CALCULATED INDICES FOR THE
OPEN SYSTEM ONE COOLING WATER
CHEMISTRY FOR THE PERIOD MARCH 2009 to
MARCH 2011**

Table D-1: Indices calculated for Open System One at 45°C for comparison with the mild steel coupon corrosion rates

Date	Langelier	Larson-Skold Index	RSI at 45°C	PSI at T indicated above	pHs	CR8 Corrosion Index (mmpa)	Buffer Capacity (mg/l as CaCO ₃ /pH)	CR4 Corrosion Index (mmpa)	CCP (mg/l)	I _s (Oddo & T, 1982)	Ionic Strength(M)	Stiff Davis	pHs (S&D eqn)
Mar-09	-0.5	31.7	8.3	7.9	7.8	0.09	9.02	0.084	-4.7	-0.5	0.0460	-0.7	8.1
Apr-09	-0.5	46.5	8.4	8.1	7.9	0.10	8.68	0.092	-4.8	-0.5	0.0642	-0.7	8.1
May-09	0.2	26.7	7.5	7.5	7.7	0.14	6.33	0.084	4.5	0.2	0.0692	0.1	7.9
Jun-09	-0.4	39.3	8.3	7.9	7.9	0.14	9.50	0.094	-3.6	-0.4	0.0731	-0.5	8.0
Jul-09	-0.3	22.1	8.0	7.5	7.7	0.15	12.00	0.086	-3.1	-0.3	0.0553	-0.4	7.9
Aug-09	-0.4	33.8	8.2	7.7	7.8	0.14	11.41	0.092	-4.4	-0.4	0.0614	-0.6	7.9
Sep-09	0.4	16.1	7.0	6.6	7.4	0.13	12.50	0.081	12.1	0.4	0.0624	0.2	7.5
Oct-09	0.6	15.4	6.7	6.5	7.4	0.14	10.76	0.080	20.4	0.7	0.0710	0.5	7.5
Nov-09	0.3	13.2	7.3	7.1	7.6	0.15	8.99	0.078	7.4	0.3	0.0499	0.1	7.8
Dec-09	0.6	13.9	6.8	6.7	7.5	0.14	9.88	0.077	16.4	0.6	0.0651	0.4	7.6
Jan-10	-0.3	25.7	8.0	7.5	7.7	0.12	12.13	0.087	-3.2	-0.3	0.0617	-0.5	7.9
Feb-10	-0.3	33.8	7.9	7.4	7.6	0.11	12.96	0.091	-2.8	-0.3	0.0752	-0.4	7.8
Mar-10	0.6	17.1	6.7	6.5	7.3	0.10	9.89	0.080	19.0	0.6	0.0758	0.5	7.5
Apr-10	0.4	20.7	7.0	6.6	7.4	0.11	10.51	0.083	12.9	0.4	0.0793	0.3	7.5
May-10	0.4	26.8	7.1	6.9	7.5	0.09	7.22	0.082	8.5	0.4	0.0760	0.2	7.6
Jun-10	0.7	21.2	6.8	6.7	7.5	0.17	11.45	0.086	23.2	0.7	0.1021	0.6	7.6
Jul-10	0.8	14.3	6.6	6.6	7.4	0.17	12.54	0.079	26.8	0.9	0.0747	0.7	7.6
Aug-10	0.3	17.5	7.4	7.2	7.6	0.14	8.22	0.080	6.0	0.3	0.0579	0.1	7.8
Sep-10	0.2	24.0	7.4	7.0	7.5	0.14	10.70	0.087	5.6	0.2	0.0735	0.0	7.7
Oct-10	0.2	18.6	7.3	6.9	7.5	0.14	11.68	0.082	5.6	0.2	0.0628	0.0	7.7

Nov-10	0.4	13.2	7.2	7.0	7.5	0.13	8.42	0.076	8.6	0.4	0.0479	0.2	7.8
Dec-10	0.9	6.0	6.5	6.5	7.4	0.15	12.69	0.067	25.0	0.8	0.0391	0.6	7.7
Jan-11	0.1	16.2	7.5	7.1	7.6	0.13	11.33	0.081	2.8	0.1	0.0541	-0.1	7.8
Feb-11	0.1	23.2	7.5	7.3	7.7	0.16	8.74	0.086	4.0	0.1	0.0692	0.0	7.8
Mar-11	0.0	27.4	7.7	7.4	7.7	0.15	9.51	0.090	1.6	0.0	0.0742	-0.2	7.8

Table D-2: Additional indices calculated using WaterCycle™ software (from FrenchCreek Software)

Date	WaterCycle™									
	Saturation (45°C)				Indices (45°C)				FIME (45°C)	
	Calcium carbonate	Calcium fluoride	Iron carbonate	Iron phosphate	Langelier	RSI	PSI	Larson Skold	Calcium carbonate FIME	Calcium fluoride
Mar-09	0.25	2.71	3.25	17.71	-0.45	8.24	8.56	31.96	-0.74	28.72
Apr-09	0.22	3.87	1.90	9.70	-0.47	8.30	8.64	46.86	-0.88	43.46
May-09	1.23	3.35	25.62	17.63	0.31	7.35	7.90	26.64	0.37	36.79
Jun-09	0.33	2.94	4.64	5.75	-0.29	8.05	8.30	39.29	-1.00	33.26
Jul-09	0.42	2.65	7.67	9.76	-0.20	7.89	7.98	22.09	-0.85	28.09
Aug-09	0.34	2.56	5.67	17.67	-0.31	8.01	8.17	33.93	-0.74	28.20
Sep-09	1.83	2.51	9.74	13.61	0.45	6.84	6.88	16.05	0.77	27.00
Oct-09	3.48	5.00	31.00	9.82	0.74	6.53	6.74	15.21	2.69	54.92
Nov-09	1.54	3.22	18.77	39.39	0.37	7.17	7.44	13.24	0.75	33.50
Dec-09	2.76	4.50	20.52	0.67	6.73	7.03	13.00	13.85	2.49	46.81
Jan-10	0.39	8.28	6.23	1.64	-0.22	7.87	7.99	26.15	-0.75	68.63
Feb-10	0.41	9.64	2.77	3.46	-0.19	7.76	7.85	34.61	0.63	84.88
Mar-10	3.01	7.80	13.41	17.55	0.68	6.59	6.84	17.04	2.11	79.20
Apr-10	1.95	10.17	6.87	26.87	0.48	6.84	7.00	20.85	0.97	93.98
May-10	1.74	4.62	14.24	44.16	0.43	6.99	7.41	27.00	0.70	53.23
Jun-10	3.73	4.77	16.82	9.83	0.77	6.62	6.93	20.52	4.74	59.44
Jul-10	4.92	3.72	18.59	4.92	0.87	6.54	6.93	13.97	6.92	46.42
Aug-10	1.17	3.91	16.43	31.44	0.19	7.47	7.78	17.55	0.31	46.52
Sep-10	1.07	2.91	-	-	0.17	7.36	7.50	23.88	0.10	36.55
Oct-10	1.03	4.79	5.44	22.24	0.13	7.41	7.51	18.85	0.04	57.86
Nov-10	1.61	3.80	17.77	35.49	0.31	7.30	7.64	13.22	0.99	45.44
Dec-10	4.14	0.90	22.72	0.75	6.77	7.09	5.98	6.64	1.64	39.15
Jan-11	0.80	5.09	7.61	19.97	0.01	7.61	7.72	16.32	-0.32	58.15
Feb-11	0.99	3.67	7.97	18.55	0.13	7.55	7.83	23.38	-0.02	45.17
Mar-11	0.71	2.06	4.11	8.96	-0.01	7.69	7.91	27.51	-0.50	23.40

**APPENDIX E: CALCULATED INDICES FOR THE
OPEN SYSTEM TWO COOLING WATER
CHEMISTRY FOR THE PERIOD JUNE 2009 to
FEBRUARY 2011**

Table E-1: Indices calculated for Open System Two at 45°C for comparison with the mild steel coupon corrosion rates

Date	Langelier	Larson-Skold Index	RSI at Temp indicated above	PSI at T indicated above	pHs	CR8 Corrosion Index (mmpa)	Buffer Capacity (mg/l as CaCO ₃ /pH)	CR4 Corrosion Index (mmpa)	CCPP (mg/l)	I _s (Odde & T, 1982)	Ionic Strength(M)	Stiff Davis	pH _s (S&D eqn)
Jun-09	-0.70	28.0	8.7	8.1	8.0	0.18	14.06	0.095	-8.9	-0.7	0.0529	-0.9	8.2
Jul-09	-1.36	65.8	9.6	8.8	8.2	0.18	18.73	0.109	-16.7	-1.3	0.0707	-1.5	8.4
Aug-09	-1.34	62.3	9.5	8.9	8.2	0.16	15.89	0.106	-14.1	-1.3	0.0557	-1.5	8.4
Sep-09	-0.41	31.8	8.1	7.4	7.6	0.13	18.27	0.094	-6.3	-0.4	0.0669	-0.6	7.8
Oct-09	0.64	11.6	6.9	6.9	7.5	0.17	10.04	0.076	16.6	0.7	0.0510	0.5	7.7
Nov-09	-0.13	14.3	7.8	7.3	7.7	0.17	13.20	0.081	-1.3	-0.1	0.0452	-0.3	7.9
Dec-09	-0.51	11.7	8.1	7.1	7.6	0.17	37.55	0.086	-16.8	-0.5	0.0465	-0.7	7.8
Jan-10	-0.18	11.8	7.8	7.1	7.6	0.13	18.38	0.078	-3.8	-0.2	0.0403	-0.4	7.8
Feb-10	0.14	15.0	7.3	6.9	7.5	0.12	12.17	0.078	4.5	0.1	0.0501	-0.1	7.7
Mar-10	0.13	17.6	7.3	6.8	7.4	0.11	13.30	0.079	4.5	0.1	0.0582	-0.1	7.7
Apr-10	-1.00	71.1	8.9	7.8	7.9	0.23	35.40	0.113	-22.8	-1.0	0.1419	-1.1	8.0
May-10	0.06	25.3	7.5	7.0	7.5	0.11	11.88	0.087	3.3	0.1	0.0710	-0.1	7.7
Jun-10	0.09	18.3	7.4	6.9	7.5	0.19	16.57	0.089	6.1	0.1	0.0774	0.0	7.7
Jul-10	0.26	11.4	7.2	6.5	7.4	0.23	20.23	0.083	13.0	0.3	0.0673	0.1	7.6
Aug-10	0.78	15.2	6.1	5.7	6.9	0.07	14.20	0.073	33.0	0.7	0.0721	0.5	7.2
Sep-10	-0.29	15.5	7.8	7.0	7.6	0.18	27.43	0.088	-6.8	-0.3	0.0539	-0.5	7.7
Oct-10	-0.02	21.4	7.6	7.2	7.6	0.15	11.36	0.084	1.2	0.0	0.0586	-0.2	7.8
Nov-10	0.07	15.7	7.5	7.0	7.5	0.13	11.72	0.078	2.4	0.1	0.0446	-0.2	7.8
Dec-10	0.18	12.5	7.3	7.0	7.5	0.13	10.89	0.073	4.4	0.1	0.0430	-0.1	7.8
Jan-11	0.18	9.3	7.3	6.7	7.4	0.12	14.25	0.074	5.9	0.2	0.0374	-0.1	7.7
Feb-11	-0.28	18.6	7.9	7.3	7.7	0.16	17.59	0.086	-4.6	-0.3	0.0517	-0.5	7.8

Table E-2: Additional indices calculated using WaterCycle™ software (from French Creek Software)

Date	WaterCycle™												
	Saturation (45°C)							Indices (45°C)				FIME (45°C)	
	Calcium carbonate	Calcium fluoride	Calcium phosphate	Iron carbonate	Iron phosphate	Silica	Magnesium silicate	Langelier	RSI	PSI	Larson Skold	Calcium carbonate FIME	Calcium fluoride
Jun-09	7.76	0.96	1131	0.06	0.01	0.08	0.00	1.60	6.40	8.70	34.40	13.83	-1.11
Jul-09	3.42	2.32	154	0.34	0.08	0.11	8.01	1.10	7.10	9.40	74.60	4.98	23.20
Aug-09	0.04	1.52	0.02	1.24	58	0.12	0.00	-1.30	9.40	9.50	64.40	-1.38	11.28
Sep-09	0.45	4.07	1.22	9.18	72	0.13	0.00	-0.20	7.70	7.80	32.20	-0.51	46.02
Oct-09	1.57	3.01	0.73	19.36	16	0.09	0.01	0.40	7.10	7.10	11.70	0.78	32.05
Nov-09	0.58	2.51	0.46	13.15	41	0.12	0.00	-0.10	7.70	7.80	14.60	-0.61	25.05
Dec-09	0.77	3.41	17.50	128.20	1573	0.40	0.01	0.10	7.50	7.60	12.10	-0.34	33.00
Jan-10	0.72	1.01	0.44	5.96	13	0.08	0.00	0.00	7.50	7.60	11.90	-0.35	0.23
Feb-10	0.92	1.03	8.38	5.59	37	0.08	0.01	0.10	7.30	7.40	15.30	-0.09	0.65
Mar-10	0.91	1.57	7.58	4.85	31	0.11	0.01	0.20	7.30	7.30	18.00	-0.09	12.08
Apr-10	0.21	4.04	0.78	18.55	347	0.09	0.00	-0.40	8.20	8.30	73.00	-1.59	48.89
May-10	0.77	0.98	2.45	50.33	241	0.09	0.01	0.10	7.30	7.40	25.70	-0.23	-0.53
Jun-10	1.36	0.21	15.51	18.20	83	0.08	0.01	0.30	7.10	7.10	18.70	0.55	-30.18
Jul-10	2.55	0.17	25.10	31.56	66	0.08	0.03	0.60	6.70	6.80	11.60	2.80	-33.38
Aug-10	4.62	0.10	283	17.01	53	0.07	0.01	0.90	6.00	6.10	15.50	1.56	-25.00
Sep-10	1.02	1.38	5.41	24.41	108	0.05	0.00	0.20	7.30	7.30	15.70	0.03	8.59
Oct-10	0.64	1.50	0.75	14.44	51	0.10	0.00	0.00	7.00	7.00	21.70	-0.44	10.94
Nov-10	0.77	1.74	5.02	30.99	214	0.10	0.00	0.00	7.50	7.50	15.90	-0.24	14.73
Dec-10	0.08	1.41	3.34	4.62	24	0.09	0.00	0.10	7.50	7.50	12.80	-0.25	8.88
Jan-11	1.32	0.66	1.95	13.13	24	0.06	0.01	0.30	7.10	7.20	9.40	0.33	-8.93
Feb-11	0.60	0.99	0.02	6.62	15	0.08	0.00	-0.10	7.70	7.70	18.80	-0.52	-0.19

APPENDIX F: MATHEMATICAL MODELS USED FOR PREDICTING THE CORROSION RATE OF MILD STEEL

Table F-1: Equations from literature

Reference	Equation and Range of Applicability	Explanation as per the Reference/s
Langelier, 1936	<p>LSI (Langelier Saturation Index) = $\text{pH} - \text{pH}_s$.....[F1.1] (Equation 2.3)</p> <p>Applicable: pH range: 7.0 to 9.5. Temperature range: 25 to 80°C. Ionic strength (salinity) correction holds only to the maximum TDS of 800 mg/l (i.e. to a maximum ionic strength of 0.020). “The LSI is not suitable for use in soft saline waters where a low buffer capacity, ion species such as chlorides, may disrupt the CaCO_3 equilibrium conditions” (Singley, 1981).</p>	<p>Positive: “oversaturation and a tendency to crystallize or lay down a protective coating of CaCO_3” Negative: “indicates under saturation or the tendency to dissolve an existing carbonate coating”.</p>
Ryznar, 1944	<p>RSI (Ryznar Stability Index) = $2\text{pH}_s - \text{pH}$.....[F1.2] (Equation 2.4)</p> <p>Temperature range: up to 93°C. Contact time: 2 hours.</p>	<p>An “index of CaCO_3 saturation” and “of quantitative significance”. “Predict more accurately how badly scaling or corrosive</p>

		a particular water supply may be” Values > 6 and increasingly higher: increasingly severe corrosion. Values < 6 and decreasing: more scale forming.
Riddick, 1944	<p>RCI (Riddick Corrosion Index) = $(75/\text{Alk})[\text{CO}_2 + 0.5 (\text{Hardness} - \text{Alk}) + \text{Cl} + \text{NO}_3^-]\{10/\text{SiO}_2\}\{\text{DO} + 2)/\text{DO}_{\text{sat}}\}$.....[F1.3]</p> <p>Good correlation with the corrosivity of soft water, but less so with hard waters.</p>	<p>RCI ≤ 5: extremely non corrosive</p> <p>RCI: 6-25: non-corrosive</p> <p>RCI: 26-50: moderately corrosive</p> <p>RCI > 50: increasingly corrosive.</p>
Loschiavo, 1948	<p>CIn (Cassil Index) = $\text{Ca} + \text{Mg} + \text{HSiO}_3 - \text{Anions}/2$.....[F1.4]</p> <p>A modification of the calcium carbonate solubility equation to reflect the impact of cations and anions in soft water.</p> <p>Cations decrease corrosion while anions (i.e. chloride and sulphate) increase corrosion.</p>	<p>CIn < 0: very corrosive</p> <p>CIn: 0 – 0.1: “slightly corrosive”</p> <p>CIn > 0.1 “non-corrosive”</p>
Stiff and Davis, 1952	<p>SDI = $\text{pH} - \text{pCa} - \text{pAlk} - \text{K}$.....[F1.5]</p> <p>(Equation 2.14)</p> <p>Applicable to brines and oil fields.</p> <p>Temperature range: tests were performed at 0, 30 and 50°C and</p>	As for the Langelier Saturation Index.

	<p>graphical extrapolations done up to 90°C.</p> <p>Tests were performed with 20% (m/v) sodium chloride solutions.</p> <p>K values are given in graphical form for ionic strength values up to a maximum of 3.6.</p> <p>K depends on the temperature and ionic strength.</p>	
Larson and Skold, 1957, 1958, 1975	<p>Larson-Skold Index, Larson ratio (LR) or Corrosivity Index (CI) = $([Cl^-] + [SO_4^{2-}]) / ([HCO_3^-]) \dots [F1.6]$ (Equation 2.7)</p> <p>“The type of water studied approximates the quality of Great Lakes waters”.</p>	<p>“A higher index indicates a more corrosive water. Several studies qualitatively confirmed these results (although they never directly tested the accuracy of the Larson index)” (McNeill and Edwards, 2001).</p>
Dye, 1958	<p>Momentary Excess (ME)</p> <p>Calculated using nomographs based on temperature, total dissolved solids, initial calcium and carbonate concentrations.</p>	<p>“A more quantitative measure of a water’s degree of supersaturation with respect to calcium carbonate”.</p>
McCauley, 1960	<p>DFI (Driving Force Index) = $[Ca^{2+}][CO_3^{2-}] / K_{sol} \times 10^{10} \dots [F1.7]$</p> <p>Applied to mains and water distribution lines.</p>	<p>DFI: 0.0 – 0.1: slightly corrosive</p> <p>DFI > 0.1: non-corrosive.</p>
Stumm, 1960	<p>β (Buffer Index) = $2.303 \{ ((\alpha_2[H^+][Alk][H^+] + [H^+]^2 - K_w) / (K_1[H^+] + 2K_1K_2)) ([H^+]/K_2 + K_1/[H^+]) + 4 + [OH^-] + [H^+] \} \dots [F1.8]$</p>	<p>“Extent of corrosion is higher the lower the buffer capacity. In waters of high buffer capacity</p>

	<p>(Equation 2.11)</p> <p>Applied to natural waters by sanitary engineers and water supply operators.</p>	<p>more homogeneous and more protective coatings are formed than in waters of low buffer capacity”.</p>
Merrill and Sanks, 1978	<p>CCPP (Calcium Carbonate Precipitation Potential) = $\text{Alkalinity}_{\text{initial}} - \text{Alkalinity}_{\text{saturated}}$ or $\text{Ca}_{\text{initial}} - \text{Ca}_{\text{saturated}}$.....[F1.9]</p> <p>Use of computer program is required.</p> <p>Calculation of the mass of CaCO_3 that will precipitate or dissolve.</p>	<p>“Recommended CCPP values between 4-10 mg/l as CaCO_3 are needed to eliminate aggressive carbon dioxide and to develop and maintain a protective CaCO_3 film...”. “Waters grossly under saturated with respect to CaCO_3....often classified as being corrosive” (Schott, 1998).</p>
Feigenbaum <i>et al.</i> , 1978	<p>Y (Yahalom Index) = $AH + 0.34(\text{Cl}^- + \text{SO}_4^{2-}) \exp(-1/AH) + 19$...[F1.10]</p> <p>(Equation 2.8)</p> <p>$H = ([\text{Ca}^{2+}] \times [\text{HCO}_3^-]^2) / [\text{CO}_2]$[F1.11]</p> <p>A quantitative criterion for the effectiveness of scale as a protector of pipes in contact with natural waters.</p> <p>Calcium range: 78 – 248 mg/l as Ca^{2+}.</p>	<p>$Y < 200$: extremely corrosive</p> <p>Y: 200-500: moderately corrosive</p> <p>$Y > 500$: mildly corrosive</p> <p>“Y holds for a range of salt concentrations”.</p>

	<p>Chlorides range: 202 – 539 mg/l as Cl⁻.</p> <p>Sulphate range: 76 – 875 mg/l as SO₄²⁻.</p> <p>Alkalinity range: 197 – 225 mg/l as CaCO₃.</p>	
Oddo and Tomson, 1982, 1992	<p>I_s (O & T scaling Index) = $\log (T_{Ca} A_{lk}) + pH - 2.78 + 1.143 \times 10^{-2} T - 4.72 \times 10^{-6} T^2 - 4.37 \times 10^{-5} P - 2.05 \times I^{1/2} + 0.727 \times I$.....[F1.12]</p> <p>(Equation 2.15)</p> <p>Calculating the scaling tendency of geopressed energy wells of the U.S. gulf region (i.e. high temperature and pressure aqueous systems).</p>	<p>Positive: “scaling potential” (i.e. precipitate CaCO₃)</p> <p>Negative: “dissolve CaCO₃”</p>
Puckorius and Brooke, 1990	<p>PSI (Puckorius or Practical Scaling Index) = $2pH_s - pH_e$.....[F1.13]</p> <p>(Equation 2.5)</p> <p>pH_e (Equilibrium pH) = $1.465 \log TA + 4.54$.....[F1.14]</p> <p>(Equation 2.6).</p> <p>To provide “a more accurate and practical estimation of calcium carbonate scaling tendency of cooling systems” operating “at a pH above 7.5 and as high as 9 +”</p>	<p>“Supersedes the LSI and RSI, particularly with the new treatment programs where pH’s levels are above 7.5.” Values > 6 and increasingly higher: increasingly tendency to dissolve scale. Values < 6 and decreasing: more scale forming. Value = 6: Stable (i.e. not scaling and no tendency to dissolve scale).</p>

<p>Pisigan and Singley, 1984</p>	<p>SI (Saturation Index) = LSI (Langelier Saturation Index) = pH - pH_s.....[F1.15]</p> <p>pH_s (pH of saturation) = log {K₂/K_s [Ca²⁺][Alk]}[F1.16]</p> <p>CR (Corrosion rate, mpy) = -0.016Ca + 0.073β + 1.719 DO – 1.299Day + 1.178 pH_s.....[F1.17]</p> <p>CR4 (mpy) = ((TDS)^{0.253} (DO)^{0.820}) / ((10^{SI})^{0.0876} (Day)^{0.373}).....[F1.18]</p> <p>CR8 (mpy) = ((Cl)^{0.509} (SO₄)^{0.0249}(Alk)^{0.423}(DO)^{0.780}) / ((Ca)^{0.676}(β)^{0.0304}(Day)^{0.381}(10^{SI})^{0.107})[F1.19]</p> <p>(Equation 2.10)</p> <p>CR13 (mpy) = ((Ca)^{0.221}(Mg)^{1.178}(Na)^{0.363}(Cl)^{6.552}(SO₄)^{0.364} / (TDS)^{5.603}(pH)^{13.350}(Day)^{0.382}) x ((TDS)^{4.179}(β)^{0.053}(DO)^{0.784}(pH_s)^{21.232} (10^{SI})^{0.150}).....[F1.20]</p> <p>Developed for the drinking water industry.</p>	<p>Higher CR values indicate a higher corrosion rate in mpy.</p>
<p>Imran <i>et al.</i>, Nov 2005</p>	<p>LRM (Modified Larson Ratio) = (((Cl⁻ + SO₄²⁻ + Na⁺)^{1/2})/Alk) (T/25)(HRT).....[F1.21]</p>	<p>“Source waters with a value below 0.5 are non-corrosive and those with</p>

	<p>(Equation 2.12)</p> <p>Developed for utilities to respond more rapidly to changing source water changes for the implementation of timely corrosion prevention measures.</p> <p>HRT range: 2 – 5 days.</p> <p>Temperature range: 16.8 - 27.0°C.</p> <p>Chlorides range: 19 – 100 mg/l as Cl^-.</p> <p>Sulphate range: 4 – 232 mg/l as SO_4^{2-}.</p> <p>Alkalinity range: 51 – 210 mg/l as CaCO_3.</p> <p>Conductivity range: 331 – 707 $\mu\text{S/cm}$.</p>	<p>a value above are corrosive.” “The term corrosive in this context refers tocause red water problems.”</p>
--	--	---

Table F-2: Units of equations referred to in Table F-1

Index (Reference)	Units
LSI (Langelier, 1936)	pH: measured pH of the water, pH _s : pH of saturation.
RSI (Ryznar, 1944)	As for Langelier.
RCI (Riddick, 1944)	CO ₂ (carbon dioxide): mg/l as CaCO ₃ , Hardness (total hardness): mg/l as CaCO ₃ , Alk (alkalinity): mg/l as CaCO ₃ , Cl (chloride): mg/l as Cl L, N (nitrate) mg/l as NO ₃ , SiO ₂ (silica): mg/l as SiO ₂ , DO (dissolved-oxygen) and DO _{sat} (saturated oxygen): mg/l as O ₂ .
CIn (Loschiavo, 1948)	All concentrations as equivalents per million (epm).
SDI (Stiff and Davis, 1952)	pH: pH measured, pCa = -log (Ca in mg/l as Ca ²⁺), and pAlk = -log (M alkalinity in mg/l as CaCO ₃), K = constant based on the total ionic strength and temperature.
LR (Larson and Skold, 1957, 1958)	[Cl ⁻], [SO ₄ ²⁻] and [HCO ₃ ⁻]: meq/litre of chloride, sulphate and total alkalinity respectively.
ME (Dye, 1958)	Temperature: °C, Total dissolved solids: mg/l, calcium and carbonate concentrations: mg/l as CaCO ₃ .
DFI (McCauley, 1960)	[Ca ²⁺] (calcium) and [CO ₃ ²⁻] (carbonate): mg/l as CaCO ₃ , K _{sol} (solubility product of CaCO ₃ corrected for temperature and TDS as per the Larson and Buswell nomograph (1942)).
β (Stumm, 1960)	β (Buffer capacity): mole/l /pH, α ₂ : fraction of total carbonate as CO ₃ ²⁻ , [H ⁺] (molar concentration of hydrogen ions): H ⁺ moles/ l, [Alk] (alkalinity): eq/l, (K _w) (dissociation constant of water): 1x10 ⁻¹⁴ , [OH ⁻] (molar concentration hydroxide ions): OH ⁻ mole/l, K ₁ and K ₂ (first and second order

	dissociation constants of H_2CO_3): 4×10^{-7} and 4.6×10^{-11} respectively.
CCPP (Merrill and Sanks, 1978)	CCPP in mg/l as CaCO_3 , calcium in mg/l, alkalinity in mg/l as CaCO_3 , pH, temperature in $^\circ\text{C}$, total dissolved solids in mg/l.
Y (Feigenbaum <i>et al.</i> , 1978)	$A = 3.5 \times 10^{-4}$. Apart from $[\text{HCO}_3^-]$ which is in mg/l as CaCO_3 all the other concentrations are in ppm.
I _s (Oddo and Tomson, 1982, 1992)	I (Ionic strength): moles/l, T _{Ca} (calcium): moles/l as Ca, A _{lk} (alkalinity): moles/l as HCO_3^- , T (temperature): $^\circ\text{F}$, P (pressure): psi.
PSI (Puckorius and Brooke, 1990)	TA (total alkalinity) = Alk (alkalinity): mg/l as CaCO_3 .
CR, CR4, CR8, CR13 (Pisigan and Singley, 1984)	K ₁ and K ₂ (first and second order dissociation constants of H_2CO_3): As in Stumm, 1960. K _s : solubility product constant of CaCO_3 . α_2 (fraction of total carbonate as CO_3^{2-}): As in Stumm, 1960. CR(corrosion rate): mpy (mils per year), TDS(total dissolved solids): mg/l, Ca(calcium): mg/l as Ca, Mg(magnesium): mg/l as Mg, Na(sodium): mg/l as Na, Cl(chloride): mg/l as Cl, SO ₄ (sulphate): mg/l as SO ₄ , Alk(alkalinity): mg/l as CaCO_3 , β (buffer capacity): mg/l as CaCO_3/pH , DO(Dissolved oxygen): mg/l as O ₂ .
LRM Imran <i>et al.</i> , Nov 2005)	Na ⁺ (sodium): mg/l as Na, Cl ⁻ (chloride): mg/l as Cl, SO ₄ ²⁻ (sulphate): mg/l as SO ₄ , Alk (alkalinity): mg/l as CaCO_3 , T (temperature): $^\circ\text{C}$ and HRT (Hydraulic Retention Time): days.

Note: The units are defined in Table F-2.

APPENDIX G: MINITAB® RESULTS

Varying Calcium Hardness and Total Alkalinity

In Section 4.4.1 and 4.4.2 the corrosion rates were obtained for at least five different calcium concentrations while varying the total alkalinity. In the former section the investigation was conducted at relatively low alkalinities (19 and 67.5 mg/l as CaCO₃) whereas in the latter section the tests were performed in line with the two open cooling systems, as given in Table 4-1 (35 to 220 mg/l). G-1 and G-2 list the results of the Minitab linear correlations for Sections 4.4.1 and 4.4.2 respectively.

Varying calcium at the low range of alkalinities (Section 4.4.1)

Table G-1: Minitab® correlations at the low range of alkalinities between parameters at 35°C

Correlations: pH (i)_35, Ca (i) mg/l, Mg (i) mg/l, M alkalinity, ...			
Cell Contents:			
Pearson correlation (r value)			
p value			
	pH (i)_35	Ca (i) mg/l)_35	Mg (i) mg/l)_35
Ca (i) mg/l)_35	0.585		
	0.415		
Mg (i) mg/l)_35	-0.311	-0.296	
	0.689	0.704	
M alkalinity (i)	0.143	0.257	0.557
	0.819	0.743	0.443
Cl (i) (mg/l)_35	0.490	-0.196	0.531
	0.510	0.804	0.469
SO4 (i) mg/l)_35	-0.328	-0.527	0.961
	0.590	0.473	0.039
F (i) (mg/l)_35	-0.327	0.557	-0.549
	0.591	0.443	0.451
Cond. (i) (µS/cm	-0.120	0.295	0.825
	0.848	0.705	0.175
O2 (i) mg/l)_35	-0.077	-0.426	-0.680
	0.902	0.574	0.320
pH (f)_1_35	0.325	-0.984	0.124
	0.594	0.016	0.876
Ca (f) mg/l)_1_3	0.084	1.000	-0.284
	0.893	0.000	0.716
Mg (f) mg/l)_1_3	-0.681	-0.282	0.966
	0.206	0.718	0.034
M alkalinity (f)	-0.410	-0.637	0.512

	0.493	0.363	0.488
Cl (f) (mg/l)_1_	-0.888	-0.030	0.114
	0.044	0.970	0.886
SO4 (f) mg/l)_1_	-0.814	-0.642	-0.355
	0.094	0.358	0.645
F (f) (mg/l)_1_3	0.366	0.261	-0.663
	0.544	0.739	0.337
Cond. (f) (µS/cm	-0.525	-0.467	-0.706
	0.364	0.533	0.294
t Fe (f) (mg/l)_	0.543	0.928	-0.630
	0.344	0.072	0.370
O2 (f) mg/l)_1_3	0.452	-0.448	0.126
	0.548	0.552	0.874
Coupon 1(mmpa)_3	0.162	0.230	-0.757
	0.795	0.770	0.243
Coupon 2(mmpa)_3	0.439	0.788	-0.704
	0.460	0.212	0.296
Average_35	0.290	0.529	-0.775
	0.636	0.471	0.225
Day 1 (mmpa)_35	-0.715	-0.560	-0.497
	0.175	0.440	0.503
M alkalinity (i) Cl (i) (mg/l)_35 SO4 (i) mg/l)_35			
Cl (i) (mg/l)_35	-0.317		
	0.683		
SO4 (i) mg/l)_35	0.171	0.613	
	0.783	0.387	
F (i) (mg/l)_35	0.030	-0.924	-0.650
	0.962	0.076	0.235
Cond. (i) (µS/cm	0.237	0.440	0.647
	0.701	0.560	0.238
O2 (i) mg/l)_35	-0.002	-0.609	-0.514
	0.997	0.391	0.375
pH (f)_1_35	0.564	0.083	0.078
	0.322	0.917	0.901
Ca (f) mg/l)_1_3	-0.251	-0.189	-0.384
	0.684	0.811	0.524
Mg (f) mg/l)_1_3	-0.072	0.295	0.756
	0.909	0.705	0.139
M alkalinity (f)	0.684	-0.293	0.432
	0.202	0.707	0.468
Cl (f) (mg/l)_1_	-0.109	-0.780	0.058
	0.861	0.220	0.927
SO4 (f) mg/l)_1_	-0.606	-0.590	-0.079
	0.278	0.410	0.899
F (f) (mg/l)_1_3	0.704	-0.986	-0.429
	0.185	0.014	0.471
Cond. (f) (µS/cm	-0.877	-0.336	-0.235
	0.051	0.664	0.703
t Fe (f) (mg/l)_	0.020	-0.336	-0.799
	0.975	0.664	0.105
O2 (f) mg/l)_1_3	-0.748	0.841	0.329
	0.252	0.159	0.671
Coupon 1(mmpa)_3	-0.914	0.151	-0.479
	0.030	0.849	0.414
Coupon 2(mmpa)_3	-0.494	-0.087	-0.712
	0.397	0.913	0.178
Average_35	-0.774	0.040	-0.608
	0.125	0.960	0.277
Day 1 (mmpa)_35	-0.555	-0.617	-0.240

	0.332	0.383	0.697
F (i) (mg/l)_35	Cond. (i) (µS/cm	t Fe (i) (mg/l)_	
Cond. (i) (µS/cm	-0.134		
	0.830		
O2 (i) mg/l)_35	0.186	-0.944	*
	0.764	0.016	*
pH (f)_1_35	-0.458	-0.446	*
	0.438	0.452	*
Ca (f) mg/l)_1_3	0.604	0.403	*
	0.281	0.501	*
Mg (f) mg/l)_1_3	-0.068	0.773	*
	0.913	0.125	*
M alkalinity (f)	-0.138	-0.044	*
	0.825	0.944	*
Cl (f) (mg/l)_1_	0.669	0.241	*
	0.217	0.697	*
SO4 (f) mg/l)_1_	0.378	-0.306	*
	0.531	0.617	*
F (f) (mg/l)_1_3	0.165	-0.496	*
	0.790	0.395	*
Cond. (f) (µS/cm	0.289	-0.348	*
	0.637	0.565	*
t Fe (f) (mg/l)_	0.591	-0.093	*
	0.294	0.881	*
O2 (f) mg/l)_1_3	-0.897	-0.113	*
	0.103	0.887	*
Coupon 1(mmpa)_3	0.133	-0.297	*
	0.831	0.627	*
Coupon 2(mmpa)_3	0.433	-0.108	*
	0.467	0.863	*
Average_35	0.283	-0.218	*
	0.645	0.725	*
Day 1 (mmpa)_35	0.400	-0.529	*
	0.505	0.359	*
Day 2 (mmpa)_35	0.352	-0.240	*
	0.561	0.698	*
Day 3 (mmpa)_35	0.099	-0.623	*
	0.901	0.377	*
O2 (i) mg/l)_35	pH (f)_1_35	Ca (f) mg/l)_1_3	
pH (f)_1_35	0.566		
	0.320		
Ca (f) mg/l)_1_3	-0.545	-0.845	
	0.342	0.072	
Mg (f) mg/l)_1_3	-0.652	-0.521	0.161
	0.233	0.368	0.795
M alkalinity (f)	0.354	0.661	-0.731
	0.559	0.224	0.161
Cl (f) (mg/l)_1_	-0.086	-0.597	0.349
	0.891	0.288	0.565
SO4 (f) mg/l)_1_	0.340	-0.416	0.000
	0.575	0.486	1.000
F (f) (mg/l)_1_3	0.618	0.767	-0.377
	0.266	0.130	0.532
Cond. (f) (µS/cm	0.237	-0.557	0.187
	0.701	0.329	0.763
t Fe (f) (mg/l)_	-0.065	-0.306	0.740
	0.918	0.616	0.153
O2 (f) mg/l)_1_3	-0.094	0.417	-0.447
	0.906	0.583	0.553

Coupon 1 (mmpa)_3	0.003	-0.574	0.472
	0.996	0.312	0.422
Coupon 2 (mmpa)_3	-0.162	-0.586	0.802
	0.795	0.299	0.103
Average_35	-0.080	-0.621	0.656
	0.898	0.264	0.229
Day 1 (mmpa)_35	0.563	-0.237	-0.113
	0.323	0.702	0.857
Day 2 (mmpa)_35	0.464	0.003	-0.333
	0.431	0.996	0.584
Day 3 (mmpa)_35	0.828	0.839	-0.773
	0.172	0.161	0.227
Mg (f) mg/l)_1_3 M alkalinity (f) Cl (f) (mg/l)_1_			
M alkalinity (f)	0.154		
	0.805		
Cl (f) (mg/l)_1_	0.630	0.150	
	0.255	0.810	
SO4 (f) mg/l)_1_	0.319	0.005	0.719
	0.600	0.993	0.171
F (f) (mg/l)_1_3	-0.713	0.489	-0.352
	0.176	0.403	0.562
Cond. (f) (µS/cm	0.161	-0.393	0.489
	0.796	0.512	0.403
t Fe (f) (mg/l)_	-0.517	-0.617	-0.116
	0.372	0.268	0.852
O2 (f) mg/l)_1_3	-0.110	-0.335	-0.875
	0.890	0.665	0.125
Coupon 1 (mmpa)_3	-0.205	-0.883	-0.044
	0.741	0.047	0.944
Coupon 2 (mmpa)_3	-0.359	-0.924	-0.081
	0.552	0.025	0.897
Average_35	-0.276	-0.952	-0.054
	0.653	0.013	0.932
Day 1 (mmpa)_35	0.087	0.060	0.602
	0.889	0.924	0.282
Day 2 (mmpa)_35	0.349	0.589	0.742
	0.565	0.296	0.151
Day 3 (mmpa)_35	-0.025	0.700	0.477
	0.975	0.300	0.523
SO4 (f) mg/l)_1_ F (f) (mg/l)_1_3 Cond. (f) (µS/cm			
F (f) (mg/l)_1_3	-0.426		
	0.474		
Cond. (f) (µS/cm	0.904	-0.572	
	0.035	0.314	
t Fe (f) (mg/l)_	-0.325	0.264	-0.110
	0.593	0.668	0.860
O2 (f) mg/l)_1_3	-0.166	-0.779	0.225
	0.834	0.221	0.775
Coupon 1 (mmpa)_3	0.375	-0.510	0.731
	0.534	0.380	0.160
Coupon 2 (mmpa)_3	-0.036	-0.192	0.310
	0.954	0.758	0.612
Average_35	0.212	-0.400	0.582
	0.732	0.504	0.303
Day 1 (mmpa)_35	0.968	-0.215	0.872
	0.007	0.729	0.054
Day 2 (mmpa)_35	0.798	-0.012	0.468
	0.106	0.985	0.426
Day 3 (mmpa)_35	0.978	0.419	0.707

	0.022	0.581	0.293
t Fe (f) (mg/l)_	O2 (f) mg/l)_1_3	Coupon 1 (mmpa)_3	
O2 (f) mg/l)_1_3	-0.381		
	0.619		
Coupon 1 (mmpa)_3	0.373	0.486	
	0.536	0.514	
Coupon 2 (mmpa)_3	0.851	-0.020	0.791
	0.067	0.980	0.111
Average_35	0.612	0.257	0.960
	0.272	0.743	0.010
Day 1 (mmpa)_35	-0.266	-0.149	0.365
	0.666	0.851	0.546
Day 2 (mmpa)_35	-0.527	-0.423	-0.247
	0.362	0.577	0.689
Day 3 (mmpa)_35	-0.580	-0.102	-0.215
	0.420	0.898	0.785
Coupon 2 (mmpa)_3	Average_35	Day 1 (mmpa)_35	
Average_35	0.931		
	0.021		
Day 1 (mmpa)_35	-0.031	0.206	
	0.960	0.740	
Day 2 (mmpa)_35	-0.524	-0.384	0.802
	0.365	0.524	0.103
Day 3 (mmpa)_35	-0.592	-0.421	0.934
	0.408	0.579	0.066

Table G-2: Minitab® correlations at the low range of alkalinities between parameters at 45°C

Correlations: pH (i)_45, Ca (i) mg/l), Mg (i) mg/l), M alkalinity, ...				
Cell Contents:				
Pearson correlation (r value)				
p value				
	pH (i)_45	Ca (i) mg/l)_45	Mg (i) mg/l)_45	
Ca (i) mg/l)_45	-0.231			
	0.278			
Mg (i) mg/l)_45	-0.238	0.282		
	0.262	0.183		
M alkalinity (i)	0.751	-0.148	-0.165	
	0.000	0.490	0.440	
Cl (i) (mg/l)_45	-0.241	0.215	0.177	
	0.268	0.325	0.419	
SO4 (i) mg/l)_45	-0.008	-0.288	0.584	
	0.968	0.173	0.003	
F (i) (mg/l)_45	-0.173	0.047	0.022	
	0.408	0.828	0.920	
Cond. (i) (µS/cm	-0.112	-0.625	0.209	
	0.593	0.004	0.326	
O2 (i) mg/l)_45	-0.095	0.519	-0.221	
	0.652	0.009	0.300	
pH (f)_1_45	0.886	-0.308	-0.277	
	0.000	0.143	0.190	
Ca (f) mg/l)_1_4	-0.330	0.983	0.275	
	0.107	0.000	0.193	
Mg (f) mg/l)_1_4	-0.360	0.273	0.873	
	0.077	0.197	0.000	
M alkalinity (f)	0.725	-0.376	-0.218	
	0.000	0.071	0.306	
Cl (f) (mg/l)_1_	-0.329	0.330	0.338	
	0.109	0.116	0.106	
SO4 (f) mg/l)_1_	-0.256	0.371	0.332	
	0.217	0.075	0.112	
F (f) (mg/l)_1_4	-0.231	0.126	0.300	
	0.266	0.558	0.154	
Cond. (f) (µS/cm	-0.151	0.342	0.469	
	0.471	0.102	0.021	
t Fe (f) (mg/l)_	-0.167	0.722	-0.063	
	0.424	0.000	0.768	
O2 (f) mg/l)_1_4	0.229	-0.082	0.526	
	0.332	0.739	0.021	
Coupon 1(mmpa)_4	-0.486	0.357	0.041	
	0.014	0.087	0.849	
Coupon 2(mmpa)_4	-0.448	0.542	0.176	
	0.025	0.006	0.409	
Average_45	-0.478	0.455	0.111	
	0.016	0.026	0.607	
Day 1 (mmpa)_45	0.158	-0.079	0.517	
	0.452	0.713	0.010	
Day 2 (mmpa)_45	-0.333	0.023	0.235	
	0.104	0.914	0.269	
Day 3 (mmpa)_45	-0.365	-0.079	0.279	
	0.114	0.747	0.248	

	M alkalinity (i)	Cl (i) (mg/l)_45	SO4 (i) mg/l)_45
Cl (i) (mg/l)_45	-0.274		
	0.205		
SO4 (i) mg/l)_45	0.250	-0.110	
	0.228	0.618	
F (i) (mg/l)_45	0.082	0.099	0.232
	0.698	0.653	0.265
Cond. (i) (µS/cm	0.177	0.115	0.407
	0.397	0.601	0.123
O2 (i) mg/l)_45	0.071	0.191	-0.390
	0.737	0.383	0.054
pH (f)_1_45	0.846	-0.367	0.073
	0.000	0.085	0.730
Ca (f) mg/l)_1_4	-0.186	0.258	-0.249
	0.374	0.235	0.229
Mg (f) mg/l)_1_4	-0.129	0.230	0.647
	0.539	0.290	0.000
M alkalinity (f)	0.934	-0.282	0.264
	0.000	0.193	0.202
Cl (f) (mg/l)_1_	0.082	0.248	0.368
	0.698	0.254	0.071
SO4 (f) mg/l)_1_	0.034	0.280	0.311
	0.872	0.196	0.131
F (f) (mg/l)_1_4	0.098	0.180	0.371
	0.640	0.412	0.068
Cond. (f) (µS/cm	0.075	0.238	0.305
	0.722	0.274	0.138
t Fe (f) (mg/l)_	0.039	-0.030	-0.283
	0.852	0.894	0.170
O2 (f) mg/l)_1_4	0.207	0.225	0.370
	0.382	0.369	0.109
Coupon 1(mmpa)_4	-0.769	0.363	-0.491
	0.000	0.088	0.013
Coupon 2(mmpa)_4	-0.768	0.353	-0.453
	0.000	0.099	0.023
Average_45	-0.793	0.360	-0.488
	0.000	0.092	0.013
Day 1 (mmpa)_45	0.191	-0.021	0.601
	0.360	0.925	0.001
Day 2 (mmpa)_45	-0.161	0.083	0.407
	0.443	0.705	0.044
Day 3 (mmpa)_45	-0.182	-0.024	0.449
	0.442	0.923	0.047
	F (i) (mg/l)_45	Cond. (i) (µS/cm	t Fe (i) (mg/l)_
Cond. (i) (µS/cm	0.335		
	0.102		
O2 (i) mg/l)_45	0.073	-0.139	*
	0.728	0.509	*
pH (f)_1_45	-0.163	-0.073	*
	0.437	0.728	*
Ca (f) mg/l)_1_4	0.171	-0.557	*
	0.415	0.016	*
Mg (f) mg/l)_1_4	0.246	0.572	*
	0.236	0.003	*
M alkalinity (f)	0.040	0.065	*
	0.850	0.758	*
Cl (f) (mg/l)_1_	0.255	0.651	*
	0.219	0.000	*
SO4 (f) mg/l)_1_	0.277	0.702	*

	0.180	0.000	*
F (f) (mg/l)_1_4	0.354	0.246	*
	0.083	0.236	*
Cond. (f) (µS/cm	0.084	0.575	*
	0.690	0.003	*
t Fe (f) (mg/l)_	0.177	-0.073	*
	0.396	0.730	*
O2 (f) mg/l)_1_4	-0.191	0.092	*
	0.421	0.699	*
Coupon 1(mmpa)_4	-0.202	0.433	*
	0.333	0.034	*
Coupon 2(mmpa)_4	-0.262	-0.080	*
	0.206	0.703	*
Average_45	-0.247	0.449	*
	0.233	0.028	*
Day 1 (mmpa)_45	-0.104	0.125	*
	0.619	0.553	*
Day 2 (mmpa)_45	0.445	0.454	*
	0.026	0.023	*
Day 3 (mmpa)_45	0.413	0.392	*
	0.070	0.087	*
O2 (i) mg/l)_45 pH (f)_1_45 Ca (f) mg/l)_1_4			
pH (f)_1_45	-0.068		
	0.746		
Ca (f) mg/l)_1_4	0.443	-0.426	
	0.026	0.034	
Mg (f) mg/l)_1_4	-0.148	-0.339	0.327
	0.479	0.097	0.110
M alkalinity (f)	-0.042	0.896	-0.430
	0.844	0.000	0.032
Cl (f) (mg/l)_1_	0.103	-0.173	0.406
	0.624	0.408	0.044
SO4 (f) mg/l)_1_	0.143	-0.206	0.412
	0.495	0.323	0.041
F (f) (mg/l)_1_4	-0.078	-0.148	0.191
	0.711	0.481	0.360
Cond. (f) (µS/cm	0.250	-0.071	0.282
	0.227	0.736	0.172
t Fe (f) (mg/l)_	0.253	-0.184	0.713
	0.222	0.379	0.000
O2 (f) mg/l)_1_4	-0.203	0.324	-0.228
	0.390	0.164	0.335
Coupon 1(mmpa)_4	0.026	-0.668	0.406
	0.903	0.000	0.044
Coupon 2(mmpa)_4	0.044	-0.628	0.477
	0.834	0.001	0.016
Average_45	0.036	-0.666	0.454
	0.865	0.000	0.023
Day 1 (mmpa)_45	-0.104	0.157	-0.155
	0.622	0.453	0.459
Day 2 (mmpa)_45	0.101	-0.331	0.083
	0.632	0.106	0.692
Day 3 (mmpa)_45	0.020	-0.315	-0.009
	0.932	0.177	0.969
Mg (f) mg/l)_1_4 M alkalinity (f) Cl (f) (mg/l)_1_			
M alkalinity (f)	-0.209		
	0.315		
Cl (f) (mg/l)_1_	0.664	0.011	
	0.000	0.959	

SO4 (f) mg/l)_1_	0.618	-0.063	0.737
	0.001	0.764	0.000
F (f) (mg/l)_1_4	0.384	0.010	0.356
	0.058	0.961	0.080
Cond. (f) (µS/cm	0.615	0.026	0.649
	0.001	0.901	0.000
t Fe (f) (mg/l)_	-0.014	-0.163	0.184
	0.947	0.436	0.380
O2 (f) mg/l)_1_4	0.415	0.216	0.066
	0.069	0.360	0.781
Coupon 1(mmpa)_4	0.012	-0.772	0.002
	0.956	0.000	0.992
Coupon 2(mmpa)_4	0.084	-0.809	-0.053
	0.688	0.000	0.801
Average_45	0.047	-0.815	-0.031
	0.822	0.000	0.884
Day 1 (mmpa)_45	0.432	0.189	0.033
	0.031	0.365	0.876
Day 2 (mmpa)_45	0.485	-0.160	0.390
	0.014	0.445	0.054
Day 3 (mmpa)_45	0.497	-0.152	0.298
	0.026	0.522	0.201
SO4 (f) mg/l)_1_ F (f) (mg/l)_1_4 Cond. (f) (µS/cm			
F (f) (mg/l)_1_4	0.184		
	0.378		
Cond. (f) (µS/cm	0.806	0.072	
	0.000	0.731	
t Fe (f) (mg/l)_	0.011	0.258	-0.707
	0.960	0.214	0.000
O2 (f) mg/l)_1_4	-0.089	0.168	0.057
	0.708	0.480	0.812
Coupon 1(mmpa)_4	-0.006	-0.266	-0.092
	0.978	0.199	0.662
Coupon 2(mmpa)_4	0.124	-0.229	0.050
	0.556	0.272	0.811
Average_45	0.056	-0.260	0.187
	0.790	0.209	0.382
Day 1 (mmpa)_45	0.037	-0.001	0.625
	0.860	0.995	0.017
Day 2 (mmpa)_45	0.563	0.169	0.426
	0.003	0.419	0.034
Day 3 (mmpa)_45	0.494	0.356	0.341
	0.027	0.124	0.141
t Fe (f) (mg/l)_ O2 (f) mg/l)_1_4 Coupon 1(mmpa)_4			
O2 (f) mg/l)_1_4	-0.411		
	0.072		
Coupon 1(mmpa)_4	0.185	-0.298	
	0.375	0.202	
Coupon 2(mmpa)_4	0.056	-0.101	0.881
	0.790	0.671	0.000
Average_45	0.128	-0.215	0.971
	0.543	0.362	0.000
Day 1 (mmpa)_45	-0.307	0.561	-0.306
	0.135	0.010	0.137
Day 2 (mmpa)_45	-0.159	-0.160	-0.107
	0.448	0.501	0.610
Day 3 (mmpa)_45	-0.111	-0.085	-0.210
	0.642	0.721	0.375

	Coupon 2 (mpa)_4	Average_45	Day 1 (mpa)_45
Average_45	0.968		
	0.000		
Day 1 (mpa)_45	-0.157	-0.238	
	0.453	0.252	
Day 2 (mpa)_45	-0.037	-0.076	0.306
	0.862	0.717	0.137
Day 3 (mpa)_45	-0.135	-0.180	0.420
	0.572	0.447	0.065

Varying calcium for the full range of total alkalinities (Section 4.4.2)

Table G-3: Varying calcium and alkalinity for the full range of total alkalinities at 35°C

Correlations: Avg coup, t Fe (f), Day 1 (mmpa), Day	
Cell Contents: Pearson correlation (r value)	
p value	
Average coupon corrosion rate	
t Fe (f)	-0.633
	0.367
Day 1 (mmpa)	-0.505
	0.495
Day 2 (mmpa)	-0.356
	0.644
Day 3 (mmpa)	-0.392
	0.608
Day 4 (mmpa)	-0.309
	0.691
pH (i)	0.427
	0.573
Ca (i)	-0.978
	0.022
Mg (i)	0.756
	0.244
T alk (i)	0.252
	0.748
Cl (i)	0.576
	0.424
SO4 (i)	-0.950
	0.050
F (i)	-0.824
	0.176
Cond (i)	0.788
	0.212
pH (f)	0.402
	0.598
Ca (f)	-0.976
	0.024
Mg (f)	0.961
	0.039
T alk (f)	0.320
	0.680
Cl (f)	-0.022
	0.978
SO4 (f)	-0.120
	0.880
F (f)	-0.462
	0.538
Cond (f)	0.743
	0.257
Coup 1	0.904
	0.096
Coup 2	0.972
	0.028

Table G-4: Varying calcium and alkalinity for the full range of total alkalinities at 45°C

Correlations: Avg coup, t Fe (f), Day 1 (mmpa), Day 1, Day 2 (mmpa), ...	
Cell Contents:	
Pearson correlation (r value)	
p value	
Average coupon corrosion rate	
t Fe (f)	0.122
	0.560
Day 1 (mmpa)	0.599
	0.002
Day 2 (mmpa)	0.540
	0.005
Day 3 (mmpa)	0.485
	0.014
Day 4 (mmpa)	0.444
	0.050
pH (i)	0.116
	0.580
Ca (i)	-0.431
	0.032
Mg (i)	0.369
	0.070
T alk (i)	-0.389
	0.054
Cl (i)	0.171
	0.414
SO4 (i)	-0.007
	0.973
F (i)	-0.240
	0.249
Cond (i)	-0.353
	0.084
pH (f)	-0.516
	0.008
Ca (f)	-0.310
	0.132
Mg (f)	0.388
	0.055
T alk (f)	-0.405
	0.045
Cl (f)	0.201
	0.335
SO4 (f)	0.045
	0.832
F (f)	-0.280
	0.175
Cond (f)	-0.145
	0.490
Coup 1	0.955
	0.000
Coup 2	0.962
	0.000

Varying Chloride

Table G-5: Minitab® correlations of the average coupon corrosion with chloride and other parameters

Correlations: Avg Coup, Tgt Cl, etc.	
Cell Contents:	
Pearson correlation (r value)	
p value	
Average coupon corrosion rate	
Tgt Cl	0.020
	0.937
Temp	0.303
	0.221
pH(i)	0.060
	0.814
Ca(i)	-0.534
	0.074
Mg(i)	-0.482
	0.113
T alk(i)	-0.537
	0.021
Cl(i)	-0.011
	0.967
SO4(i)	-0.086
	0.734
F(i)	-0.217
	0.388
Cond(i)	0.196
	0.436
pH(f)	0.234
	0.350
Ca(f)	-0.394
	0.205
Mg(f)	-0.251
	0.432
T alk(f)	0.131
	0.605
Cl(f)	-0.001
	0.996
SO4(f)	-0.052
	0.836
F(f)	-0.532
	0.023
Cond(f)	-0.821
	0.972
tFe(f)	-0.376
	0.125
Coupon 1(mmpa)	0.773
	0.000
Coupon 2(mmpa)	0.898
	0.000
Coupon 3(mmpa)	0.871
	0.024
Avg Coup	1.000

*				
Day 1 (mmpa) *	0.553			
	0.255			
Day 2 (mmpa) *	0.547			
	0.261			
Day 3 (mmpa) *	0.573			
	0.235			
Correlations: Tgt Cl, Cl(i), Cond(i), Cl(f), Cond(f)				
Cell Contents:				
	Tgt Cl	Cl(i)	Cond(i)	Cl(f)
Cl(i)	0.905			
	0.000			
Cond(i)	0.959	0.844		
	0.000	0.000		
Cl(f)	0.892	0.970	0.828	
	0.000	0.000	0.000	
Cond(f)	0.903	0.778	0.818	0.739
	0.000	0.001	0.000	0.002

Note: *. denotes results based only on runs 61-66

Varying Sulphate

Table G-6: Minitab® correlations of the average coupon corrosion with sulphate and other parameters

Correlations: Avg Coup, Tgt SO4, etc.	
Cell Contents:	
Pearson correlation (r value)	
p value	
Average coupon corrosion rate	
Tgt SO4	0.551
	0.027
Temp*	0.379
	0.459
pH(i)	0.186
	0.490
Ca(i)	-0.201
	0.553
Mg(i)	-0.519
	0.102
T alk(i)	0.432
	0.095
Cl(i)	0.284
	0.287
SO4(i)	0.642
	0.007
F(i)	-0.220
	0.412
Cond(i)	0.444
	0.085
pH(f)	-0.171
	0.528
Ca(f)	0.124
	0.716
Mg(f)	-0.289
	0.388
T alk(f)	-0.071
	0.793
Cl(f)	0.206
	0.443
SO4(f)	0.725
	0.001
F(f)	-0.250
	0.351
Cond(f)	0.389
	0.137
tFe(f)	0.625
	0.006
Coupon 1(mmpa)	0.899
	0.000
Coupon 2(mmpa)	0.925
	0.000
Avg Coup	1.000
	*

Day 1 (mmpa) *	0.648			
	0.164			
Day 2 (mmpa) *	0.648			
	0.164			
Day 3 (mmpa) *	0.616			
	0.192			
Day 4 (mmpa) *	0.634			
	0.176			
Correlation: Tgt SO4, SO4(i), Cond(i), SO4(f), Cond(f)				
Cell Contents:				
	Tgt SO4	SO4(i)	Cond(i)	SO4(f)
SO4(i)	0.869			
	0.000			
Cond(i)	0.962	0.781		
	0.000	0.000		
SO4(f)	0.923	0.887	0.839	
	0.000	0.000	0.000	
Cond(f)	0.845	0.687	0.936	0.719
	0.000	0.002	0.000	0.001

Note: *. denotes results based only on runs 67-72

Varying Fluoride

Table G-7: Minitab® correlations of the average coupon corrosion with fluoride and other parameters

Correlations: Avg Coup, Tgt F, Temp, pH(i), Ca(i), Mg(i), T alk(i), Cl(i), ...	
Cell Contents:	
Pearson correlation (r value)	
p value	
Average coupon corrosion rate	
Tgt F	0.703
	0.000
Temp*	0.061
	0.851
pH(i)	-0.182
	0.254
Ca(i)	-0.670
	0.000
Mg(i)	-0.509
	0.003
T alk(i)	-0.311
	0.048
Cl(i)	-0.064
	0.691
SO4(i)	-0.301
	0.055
F(i)	0.540
	0.000
Cond(i)	-0.418
	0.007
pH(f)	0.600
	0.000
Ca(f)	-0.725
	0.000
Mg(f)	-0.542
	0.002
T alk(f)	0.339
	0.030
Cl(f)	-0.429
	0.006
SO4(f)	-0.284
	0.076
F(f)	0.518
	0.001
Cond(f)	-0.486
	0.001
tFe(f)	0.023
	0.887
Day 1 (mmpa)*	-0.704
	0.011
Day 2 (mmpa)*	-0.693
	0.013
Day 3 (mmpa)*	-0.661

	0.019
Day 4 (mmpa) *	-0.645
	0.023
Initial fluoride F(i)	
Cond(i)	0.141
	0.379
tFe(i)	*
	*
pH(f)	0.281
	0.075
Ca(f)	-0.261
	0.635
Mg(f)	0.045
	0.812
T alk(f)	0.353
	0.024
Cl(f)	-0.110
	0.501
SO4(f)	-0.122
	0.453
F(f)	0.969
	0.000
Cond(f)	-0.115
	0.476
tFe(f)	-0.033
	0.836
Day 1 (mmpa) *	-0.416
	0.179
Day 2 (mmpa) *	-0.419
	0.176
Day 3 (mmpa) *	-0.400
	0.198
Day 4 (mmpa) *	-0.394
	0.205

Varying Magnesium

Table G-8: Minitab® correlations of the average coupon corrosion with magnesium and other parameters

Correlations: Avg Coup, Mg(i), pH(i), Ca(i), T	
Cell Contents: Pearson correlation (r value)	
p value	
Average coupon corrosion rate	
Mg(i)	0.991
	0.001
pH(i)	0.296
	0.569
Ca(i)	-0.240
	0.697
T alk(i)	0.966
	0.002
Cl(i)	-0.769
	0.128
SO4(i)	-0.748
	0.128
F(i)	-0.496
	0.317
Cond(i)	0.534
	0.275
pH(f)	0.907
	0.013
Ca(f)	0.305
	0.557
Mg(f)	0.977
	0.001
T alk(f)	0.963
	0.002
Cl(f)	-0.687
	0.131
SO4(f)	-0.871
	0.024
F(f)	0.897
	0.015
Cond(f)	-0.896
	0.016
tFe(f)	0.480
	0.336
Coupon 1 (mmpa)	0.972
	0.001
Coupon 2 (mmpa)	0.980
	0.001
Day 1 (mmpa)	1.000
	*
Day 2 (mmpa)	0.037
	0.944
Day 3 (mmpa)	-0.728
	0.101
Day 4 (mmpa)	-0.394
	0.439

Factorial Design Experiments

Table G-9: Minitab® correlations of the average coupon corrosion with the other parameters based on data obtained per factorial experimental design

Correlations: Avg Coup, Mg(i), pH(i), Ca(i), T alk(i), Cl(i), SO4(i), F(i), ...	
Cell Contents:	
Pearson correlation (r value)	
p value	
Average coupon corrosion rate	
Avg mmpa	-0.252
	0.429
Ca(i)	-0.163
	0.517
Mg(i)	-0.181
	0.472
Na(i)	-0.057
	0.822
Cl(i)	-0.409
	0.092
Ca(f)	-0.154
	0.542
Mg(f)	-0.130
	0.608
Na(f)	-0.173
	0.492
Cl(f)	-0.499
	0.035
pH (i)	-0.411
	0.091
Cond(i)	-0.129
	0.609
M alk(i)	-0.353
	0.151
F(i)	0.090
	0.722
SO4(i)	0.132
	0.602
pH(f)	-0.154
	0.542
Cond(f)	-0.255
	0.308
M alk(f)	-0.235
	0.348
t Fe(f)	0.171
	0.497
F(f)	0.110
	0.665
SO4(f)	0.172
	0.494

APPENDIX H: COMPARISON OF OPEN SYSTEM ONE AND OPEN SYSTEM TWO COOLING WATER CHEMISTRY

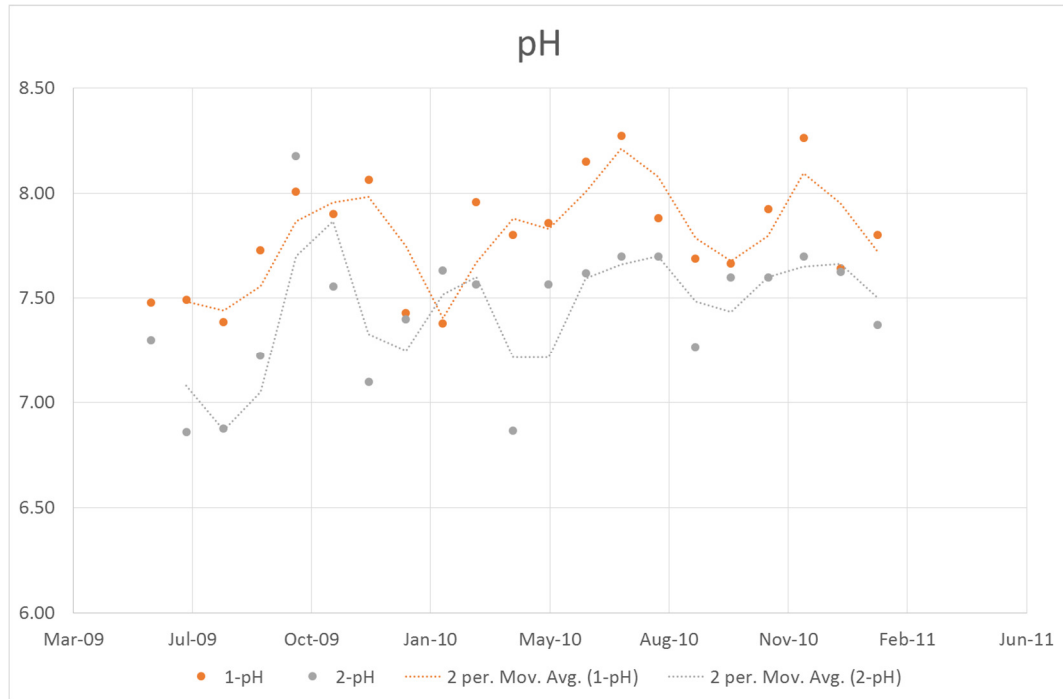


Figure H-1: Open System One versus Open System Two - pH comparison showing a relatively low pH for Open System One for February 2010

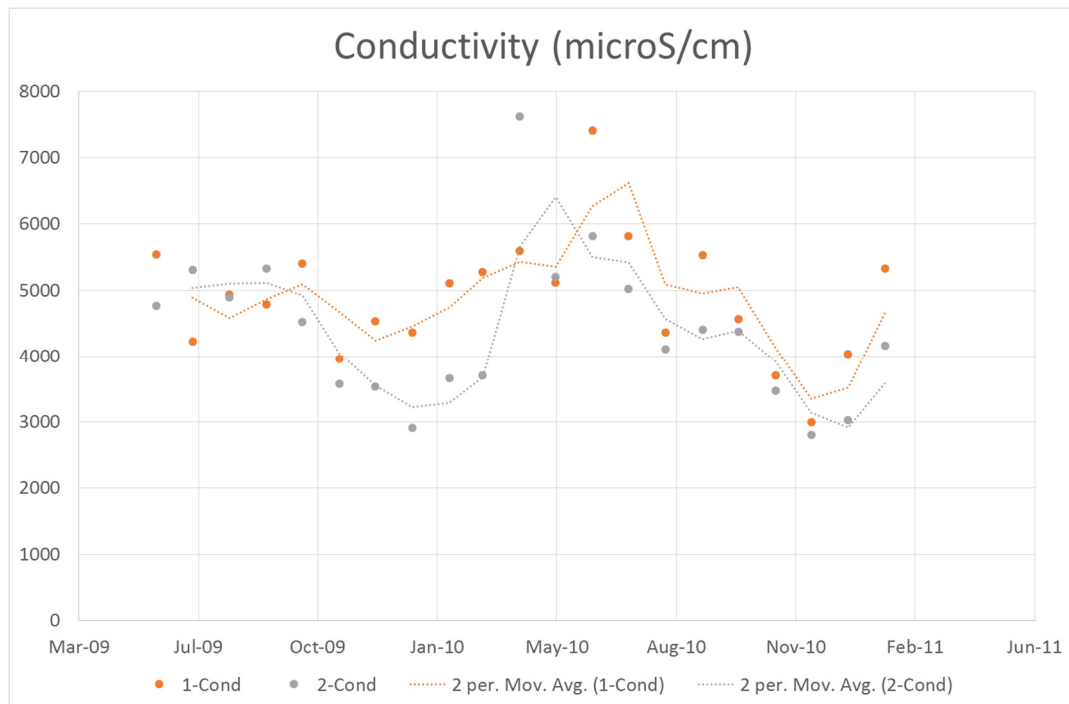


Figure H-2: Open System One versus Open System Two – Conductivity comparison showing spikes for June and May 2010 for Open System One and two respectively

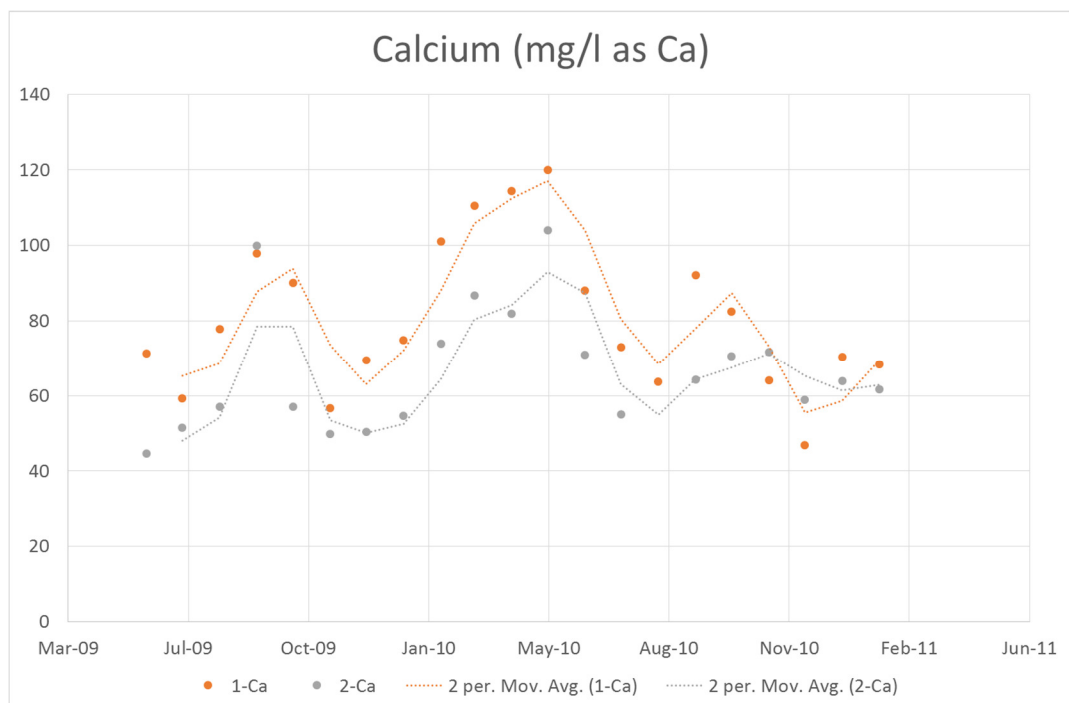


Figure H-3: Open System One versus Open System Two – Calcium comparison

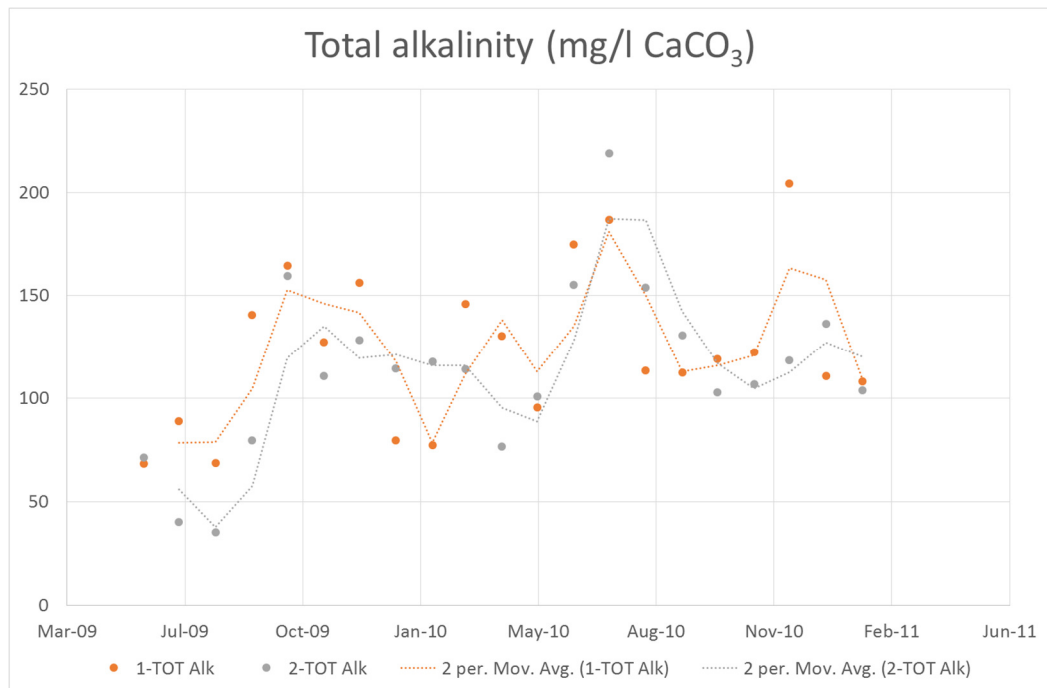


Figure H-4: Open System One versus Open System Two – Total alkalinity comparison showing depressions in the Open System One alkalinity in January and February 2010 and a peak in December 2010

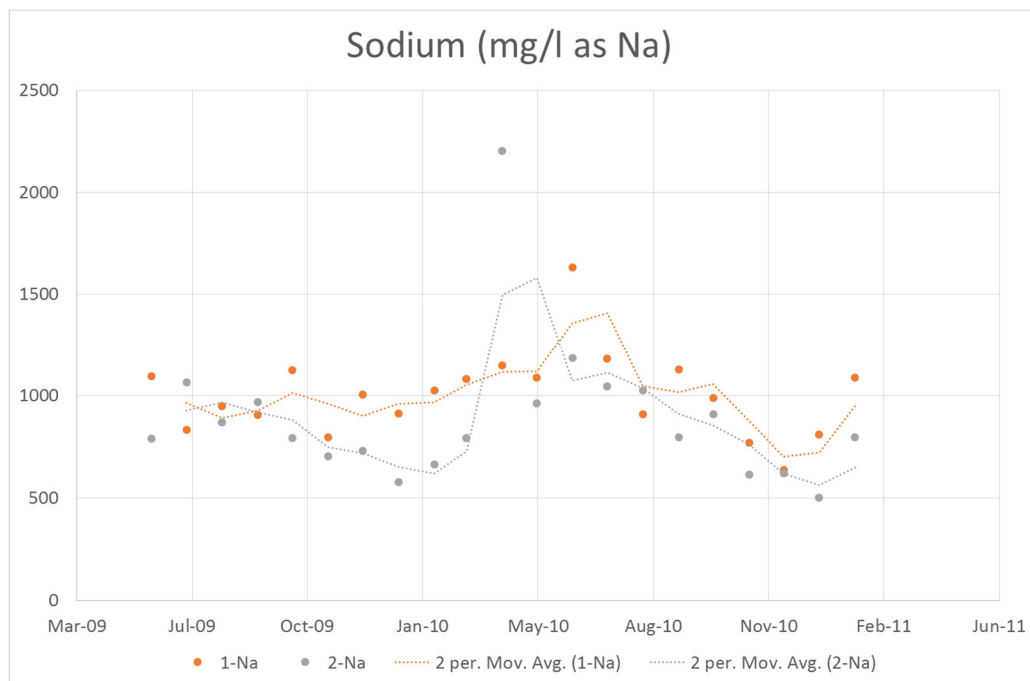


Figure H-5: Open System One versus Open System Two – Sodium comparison showing spikes for June and May 2010 for Open System One and two respectively

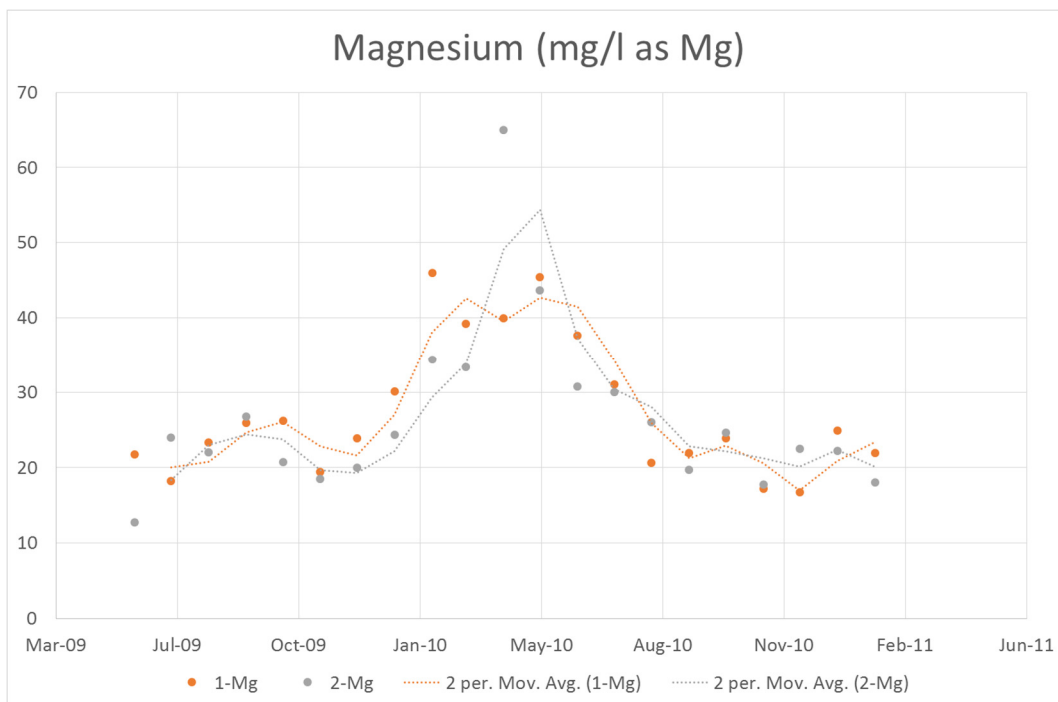


Figure H-6: Open System One versus Open System Two – Magnesium comparison showing a spike for May 2010 for Open System Two

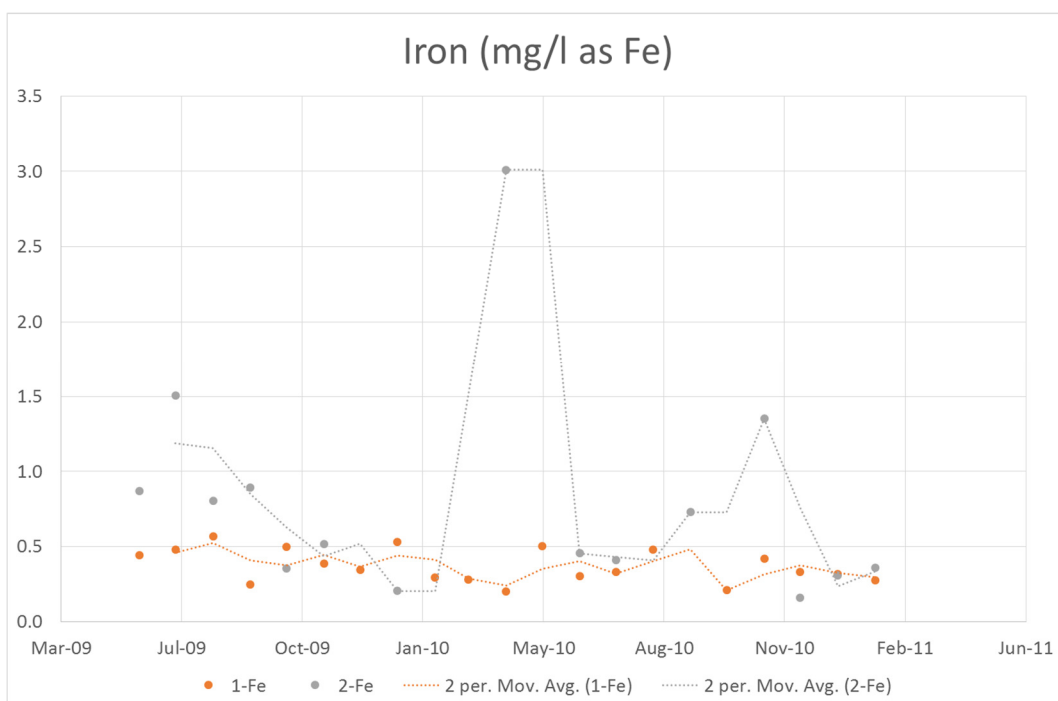


Figure H-7: Open System One versus Open System Two – Iron comparison showing a spike for March 2010 Open System Two

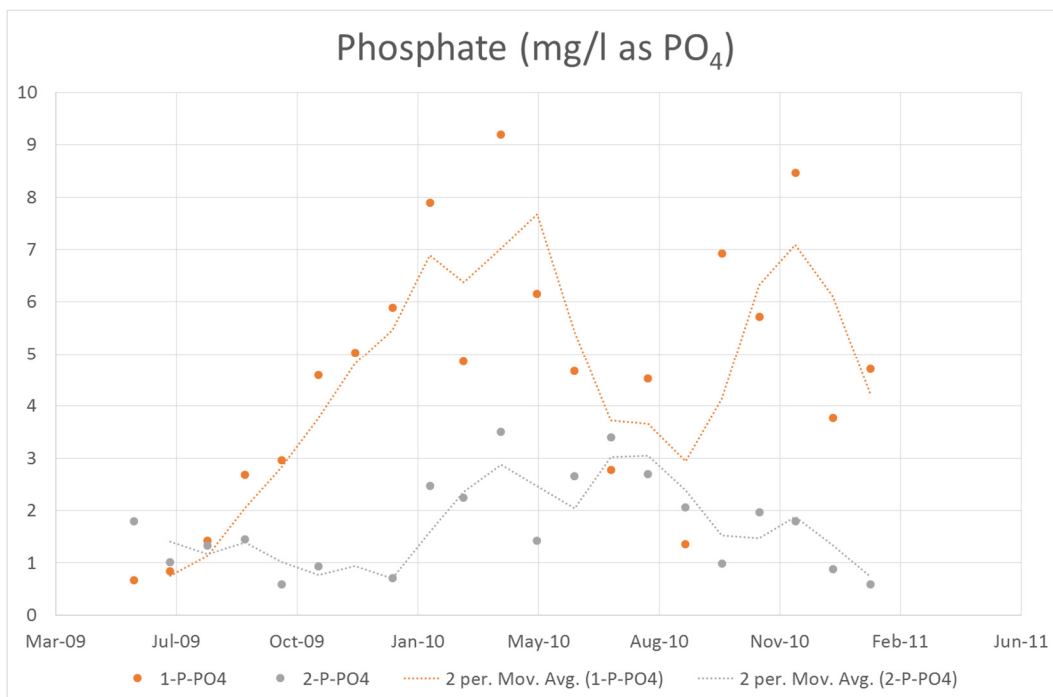


Figure H-8: Open System One versus Open System Two – Iron phosphate comparison showing generally higher levels for Open System One

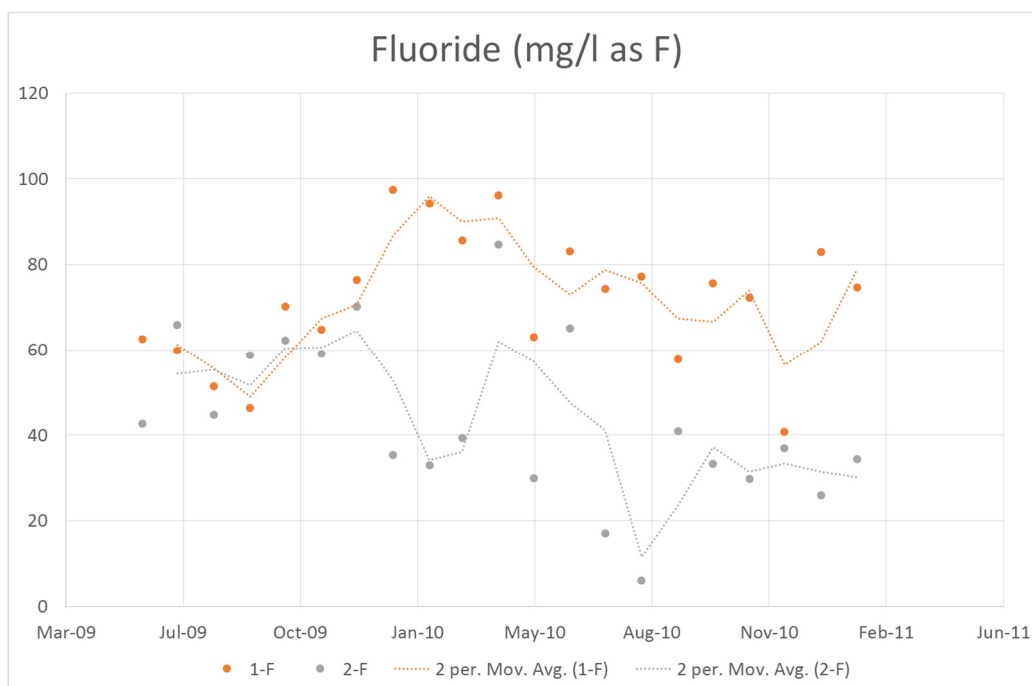


Figure H-9: Open System One versus Open System Two – Fluoride comparison showing generally higher levels for Open System One from November 2009

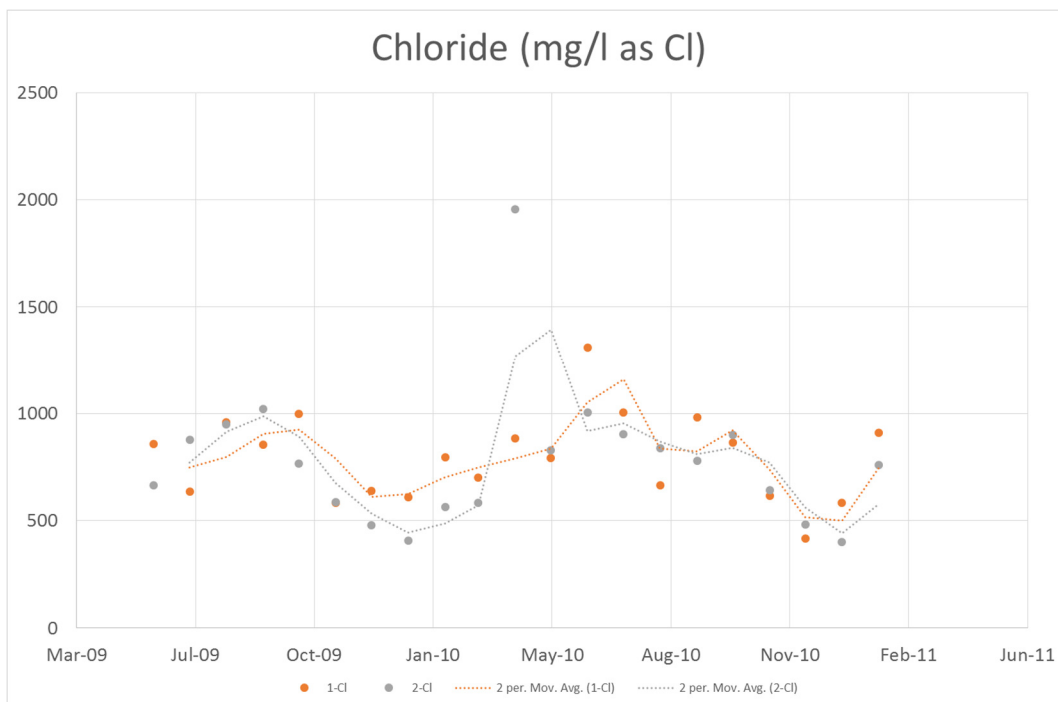


Figure H-10: Open System One versus Open System Two – Chloride comparison showing spikes for June and May 2010 for Open System One and two respectively

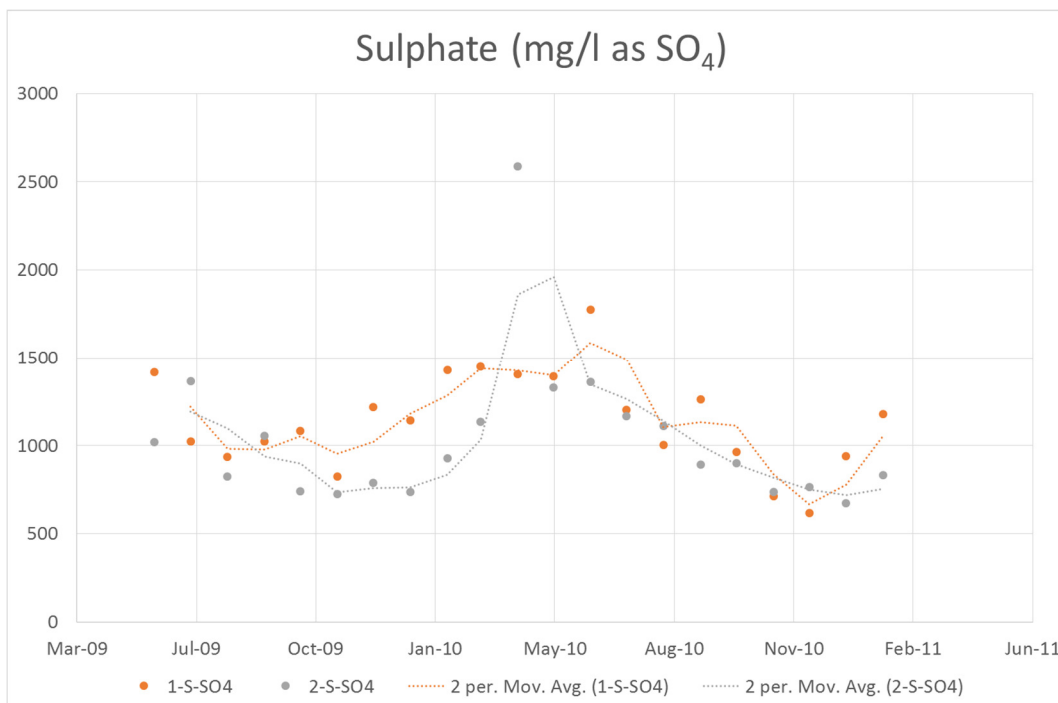


Figure H-11: Open System One versus Open System Two – Sulphate comparison showing spikes for June and May 2010 for Open System One and two respectively

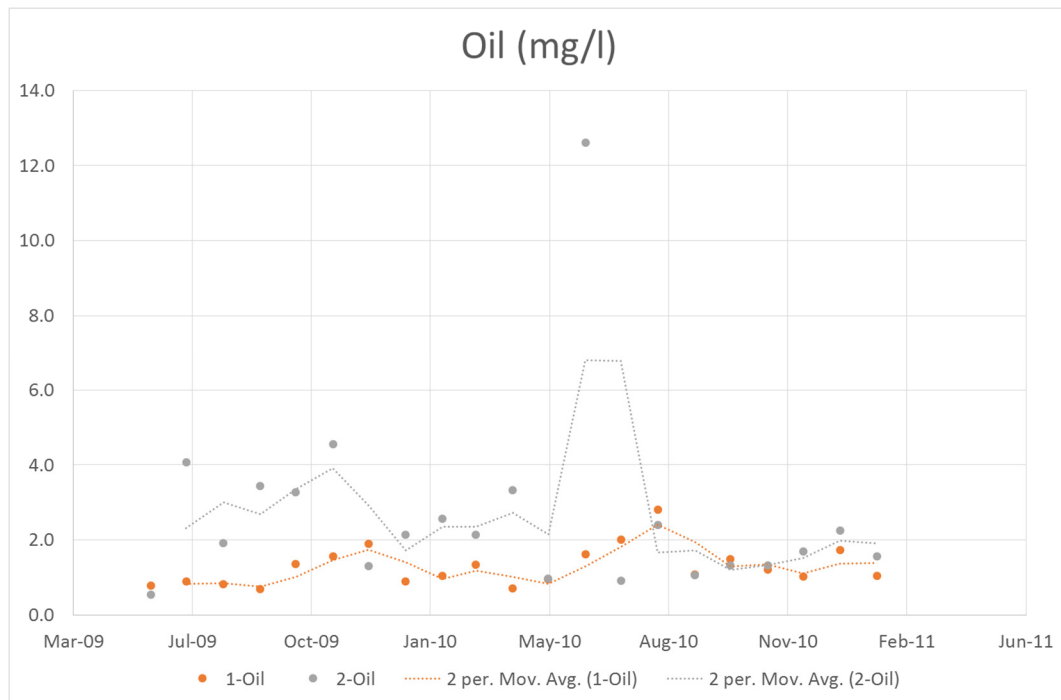


Figure H-12: Open System One versus Open System Two – Oil comparison showing a spike for June 2010 Open System Two